frontiers | Research Topics

Roles of non-coding RNAs in tumor growth and development

Edited by
Giovanni Blandino, Hernandes F. Carvalho, Jawed A. Siddiqui and Valeria Poli

Published in
Frontiers in Oncology
Frontiers in Cell and Developmental Biology

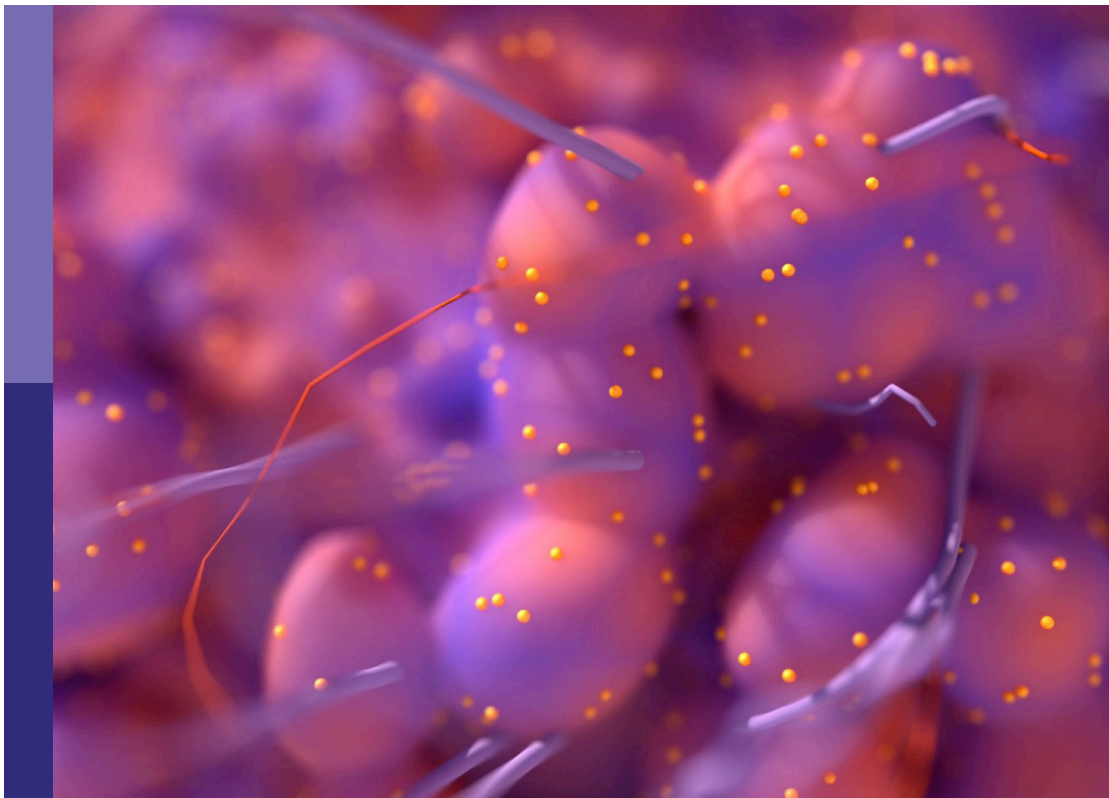

ISSN 1664-8714
ISBN 978-2-83251-066-7
DOI 10.3389/978-2-83251-066-7

About Frontiers

Frontiers is more than just an open access publisher of scholarly articles: it is a pioneering approach to the world of academia, radically improving the way scholarly research is managed. The grand vision of Frontiers is a world where all people have an equal opportunity to seek, share and generate knowledge. Frontiers provides immediate and permanent online open access to all its publications, but this alone is not enough to realize our grand goals.

Frontiers journal series

The Frontiers journal series is a multi-tier and interdisciplinary set of open-access, online journals, promising a paradigm shift from the current review, selection and dissemination processes in academic publishing. All Frontiers journals are driven by researchers for researchers; therefore, they constitute a service to the scholarly community. At the same time, the *Frontiers journal series* operates on a revolutionary invention, the tiered publishing system, initially addressing specific communities of scholars, and gradually climbing up to broader public understanding, thus serving the interests of the lay society, too.

Dedication to quality

Each Frontiers article is a landmark of the highest quality, thanks to genuinely collaborative interactions between authors and review editors, who include some of the world's best academicians. Research must be certified by peers before entering a stream of knowledge that may eventually reach the public - and shape society; therefore, Frontiers only applies the most rigorous and unbiased reviews. Frontiers revolutionizes research publishing by freely delivering the most outstanding research, evaluated with no bias from both the academic and social point of view. By applying the most advanced information technologies, Frontiers is catapulting scholarly publishing into a new generation.

What are Frontiers Research Topics?

Frontiers Research Topics are very popular trademarks of the *Frontiers journals series*: they are collections of at least ten articles, all centered on a particular subject. With their unique mix of varied contributions from Original Research to Review Articles, Frontiers Research Topics unify the most influential researchers, the latest key findings and historical advances in a hot research area.

Find out more on how to host your own Frontiers Research Topic or contribute to one as an author by contacting the Frontiers editorial office: frontiersin.org/about/contact

Roles of non-coding RNAs in tumor growth and development

Topic editors

Giovanni Blandino — Regina Elena National Cancer Institute, Hospital Physiotherapy Institutes (IRCCS), Italy

Hernandes F. Carvalho — State University of Campinas, Brazil

Jawed A. Siddiqui — University of Nebraska Medical Center, United States

Valeria Poli — University of Turin, Italy

Citation

Blandino, G., Carvalho, H. F., Siddiqui, J. A., Poli, V., eds. (2023). *Roles of non-coding RNAs in tumor growth and development*. Lausanne: Frontiers Media SA.

doi: 10.3389/978-2-83251-066-7

Table of contents

frontiers | Frontiers in Oncology

TYPE Editorial
PUBLISHED 01 December 2022
DOI 10.3389/fonc.2022.1098315

OPEN ACCESS

EDITED AND REVIEWED BY
Luisa Lanfrancone,
European Institute of Oncology (IEO), Italy

*CORRESPONDENCE
Jawed Akhtar Siddiqui
jawed.siddiqui@unmc.edu

SPECIALTY SECTION
This article was submitted to Molecular and Cellular Oncology, a section of the journal Frontiers in Oncology

RECEIVED 14 November 2022
ACCEPTED 15 November 2022
PUBLISHED 01 December 2022

CITATION
Sharma G, Barbieri I, Blandino G, Poli V and Siddiqui JA (2022) Editorial: Roles of non-coding RNAs in tumor growth and development.
Front. Oncol. 12:1098315.
doi: 10.3389/fonc.2022.1098315

Editorial: Roles of non-coding RNAs in tumor growth and development

Gunjan Sharma[1], Isaia Barbieri[2], Giovanni Blandino[3], Valeria Poli[2] and Jawed Akhtar Siddiqui[1,4]*

[1]Department of Biochemistry and Molecular Biology, University of Nebraska Medical Center, Omaha, NE, United States, [2]Molecular Biotechnology Center, University of Torino, Torino, Italy, [3]Translational Oncology Research Unit, IRCCS Regina Elena National Cancer Institute, Rome, Italy, [4]Fred and Pamela Buffett Cancer Center, University of Nebraska Medical Center, Omaha, NE, United States

KEYWORDS

non-coding RNAs, microRNAs, cancer, metastasis, enhancer RNAs (eRNAs)

Editorial on the Research Topic
Roles of non-coding RNAs in tumor growth and development

Introduction

In the past two decades, high-throughput sequencing techniques tremendously improved our understanding of the non-coding transcriptome, including the discovery, functions, and regulation of non-coding RNAs (ncRNAs) in normal and pathological conditions. Indeed, only 3% of RNAs are translated into proteins, whereas 75% of the human genome is transcribed. ncRNAs are an extremely diverse class of RNA molecules deeply involved in regulating gene expression, specialized cells functions, proliferation, and differentiation. As such, it is not surprising that their dysregulated expression or mutation can trigger pathological phenomena, including cancer, affecting many different biological processes. Therefore, a more detailed understanding of their regulation, functions, and underlying molecular mechanisms may help in developing novel disease markers and targeted therapies.

This editorial summarizes the recent overview, significant findings, and perspectives provided in 20 research, mini-review, and review articles published over the past few months in the Frontiers Research Topic *Role Of Non-coding RNAs In Tumor Growth And Development*.

MicroRNAs (miRNAs) and long non-coding RNAs (lncRNAs) are the most abundant and best-characterized classes of regulatory RNAs. Briefly, microRNAs are short double-stranded RNAs that down-regulate the expression of sets of target mRNAs, triggering translational repression but also indirectly inducing mRNA degradation. Their expression is driven by RNA Polymerase II as a hairpin-shaped precursor (pri-microRNA) that is processed *via* two consecutive maturation events occurring in the nucleus and in the cytoplasm. They are highly conserved among species and regulate sets

of functionally correlated genes (1). On the other hand, long non-coding (lnc) RNAs, both intra-genic and inter-genic, are defined as nuclear-encoded RNAs longer than 200 bp that lack coding sequences, and they are poorly conserved across species (2). Despite their definition, it has been discovered that a number of lncRNAs contain short Open Reading Frames that are translated into functionally relevant peptides (3). Also, lncRNAs are transcribed by RNA Pol II as polyadenylated, intron-containing RNAs that undergo splicing. They can function both in cis and trans, in the nucleus or in the cytoplasm *via* many different mechanisms dictated by their locus, primary sequence and/or tridimensional structure (4).

Altered expression of both ncRNA classes often occurs in pathological conditions, including tumor onset and progression (5, 6). Here, we divided the contributions into review/minireview articles and research papers and subdivided them according to the class of ncRNA discussed.

Reviews/minireviews

LncRNAs

A number of review articles focus on various aspects of lncRNAs in cancer. In particular, Connerty et al. discuss the general role of lncRNAs in regulating cellular stress in cancer cells. The authors posit that exploiting lncRNAs-mediated regulatory mechanisms may be a quick and efficient way for cancer cells to overcome oxidative, metabolic, and genotoxic stress, one of the most complex challenges for cancer cells. Other authors discuss the roles of specific lncRNAs, such as DRAIRC (Downregulated RNA In Cancer, Yao et al., PCGEM1 (Prostate Gene Expression Marker 1, Su et al., and WT1-AS (Wilms tumor 1 antisense RNA, Zhang et al., in multiple cancer types. DRAIC (Yao et al.) is downregulated in many solid tumors, affecting cancer cell proliferation, autophagy, migration, and invasion. Its expression levels are highly associated with immune cell infiltration, tumor stage, lymph node metastasis, and overall survival of cancer patients, and the authors propose it as an attractive target for both diagnosis and treatment. In contrast, pro-oncogenic PCGEM1 (Su et al.) is consistently up regulated in clinical samples and tumor xenografts compared to normal tissue, affecting cancer cell's motility and metabolism. Interestingly, this lncRNA is able to act both as a competing endogenous RNA (ceRNA) and as a scaffolding RNA to regulate cancer cell's growth and apoptosis. Finally, Zhang et al. describe the role of the WT1-AS, a lncRNA antisense to the WT1 gene, in numerous malignancies and how its expression correlates with clinicopathological features such as tumor size, tumor-node-metastasis stage, and survival.

A peculiar sub-class of long non-coding RNAs is represented by circular RNAs, formed by back-splicing of coding mRNAs. To this end, Liu et al. discuss the regulatory network of circular RNA zinc finger RNA binding protein (CircRNA-ZFR) in cancer onset and progression, highlighting its aberrant expression in numerous solid cancers where it acts *via* multiple mechanisms.

Lnc RNAs and microRNAs

Ghafouri-Fard et al. offer a comprehensive description of the many micro and lncRNAs whose expression is either up- or down-regulated in endometriosis, a disease condition where endometrial-like tissue grows outside the uterus that is known to represent a predisposing factor for the development of many types of cancer. These ncRNAs expression signatures have a strong potential as diagnostic tools in endometriosis, a relevant issue where specific markers are still lacking.

Both coding and non-coding RNAs have been detected in exosomes, where they are believed to play specific roles affecting the gene expression of target cells. Tumor exosomes display indeed highly specific exosome content. Chen et al. provide an overview of tumor-derived exosomal lncRNAs, highlighting their crucial role in mediating direct communication between cancer cells and immune cells, cancer-associated fibroblasts, and endothelial cells in the tumor microenvironment. In this vein, Qiu et al. elaborate on RNA sorting and packaging in secreted exosomes and their roles in cellular communication, discussing the different known mechanisms, biological functions, and potential clinical and therapeutic applications of exosomal microRNAs and lncRNAs.

microRNAs

The oncological role, diagnostic/prognostic values, and molecular mechanisms of the emerging pro-oncogenic microRNAs -1269a and -1269b, essential members of the miRNA 1269 family, are discussed in multiple cancers the review by Xie et al.. The mini-review authored by Ma et al. focuses instead on the significance of miR-1224 in regulating tumor progression, metastasis, invasion, angiogenesis, and drug resistance in multiple solid cancers. Interestingly, while this miRNA is mainly believed to act as a tumor suppressor, it is sometimes involved in tumor progression through metabolic reprogramming of aerobic glycolysis.

Research articles

Most research articles focused on the identification and characterization of different lncRNAs. For example, Congrains et al. characterized and validated a novel sense lncNR4A3 as a regulator of the tumor suppressor gene NR4A3, by modulating the RNA processing machinery components in myeloid

malignancies. Zhang et al. report increased expression of lncRNA TMPO antisense RNA 1 (TMPO-AS1) in bladder cancer patient samples. They show that it acts by facilitating the interaction between the cell cycle regulatory transcription factor E2F1 and OUT domain-containing ubiquitin aldehyde binding 1 (OTUB1), triggering E2F1 deubiquitination and stabilization and promoting bladder cancer malignant features. Their rescue experiments established the essentiality of the TMPO-AS1/E2F1 axis in BC progression.

Enhancer RNAs (eRNAs), i.e., lncRNAs transcribed from enhancers' genomic regions, are crucial in mediating transcriptional regulations usually of their cognate genes. From pancreatic adenocarcinoma (PAAD) transcriptomic data, Tong et al. identified the expression of the LINC00242 eRNA and its cognate gene PHF10 as positively correlating with better prognosis since lower expression correlated with tumor status and grade and low survival rate. LINC00242 and PHF10 expression levels also associated with the quality of the immune infiltrate and allowing to classify PAAD patients into high, medium, and low immune clusters.

The tumor-promoting role of circRNA SSU72 in thyroid malignancies was identified by Zhang et al. *via* CircBank Database bioinformatic analysis. The authors further validated its expression status in papillary thyroid carcinoma (PTC) tissue and cell lines and established the circSSU72/miR-451a/S1PR2 axis as crucial in PTC progression *via* functional *in vitro* experiments.

Despite the definition of lncRNAs as not encoding proteins, open reading frames (ORFs) and short-translated peptides were identified in several of them. Liu et al. developed a comprehensive database of lncRNA-encoded peptides called LncPep. This resource database provides a coding potential assessment for 883,804 lncRNAs across 39 species and represents a valuable tool for discovering and investigating novel functions of lncRNAs in cancer.

Li et al. explored Hox transcript antisense intergenic RNA (HOTAIR) lncRNA and its oncogenic functions in non-small cell lung cancer (NSCLC). They demonstrated that HOTAIR inhibits miR-149-5p-mediated suppression of NSCLC growth and proliferation, acting as an endogenous competing RNA for HNRNPA1 mRNA by sequestering miR-149-5p, thus promoting NSCLC progression.

Naipauer et al. analyzed the host and viral transcriptomes in cells and tumors infected with Kaposi's Sarcoma-associated Herpes Virus (KSHV), to uncover the role of lncRNA-miRNA-mRNA driven networks in KSHV tumorigenesis. Their studies revealed differential expression of the cancer-related lncRNAs Malat1, Neat1, H19, Meg3, and their associated miRNA-target pairs, regulating various hallmarks of tumorigenesis such as cell cycle and p53 signaling.

BRCA1-Associated Protein 1 (BAP1) is known to enhance BRCA1 tumor suppressor potential and its inactivation is associated with various cancers, in particular clear-cell renal cell carcinoma (ccRCC). Liu et al. described a tumor-promoting role for the lncRNA NEAT1in BAP-1 deficient ccRCC, with NEAT1 acting as a ceRNA partner of SERPINE1 *via* shared miR-10a-5p.

In the last study included Moubarak et al. characterized miRNA-124a as a suppressor of brain and lung metastasis in melanoma, showing that its overexpression suppressed metastases formation without affecting primary melanoma growth *in vivo*.

Overall, the collection described here highlights the numerous and heterogeneous functions of ncRNAs in various cancers and their therapeutic potential. Nevertheless, many of the described mechanisms appear to be highly tumor type-specific and/or require further characterization at the molecular level. Further studies will help to draw a complete picture of the roles of ncRNAs in cancer, to be exploited in the clinics with novel diagnostic and therapeutic approaches. The next 10 years will certainly shed considerable light on the complex RNA expression networks contributing to determine many tumors biological and clinical features.

Author contributions

GS and JS wrote the initial draft. All authors listed have revised and approved the final version for publication.

Funding

This work and the authors are, in part, supported by grants from the U.S. Department of Defense (DOD) through the Prostate Cancer Research Program under Award No. W81XWH-21-1-0640 and Fred & Pamela Buffett Cancer Center (FPBCC) Support Grant (P30 CA036727) to JS, Italian Cancer Research Association (AIRC) IG 24851 to VP, AIRC Startup 26505 to IB.

Conflict of interest

The authors declare that the research was conducted in the absence of any commercial or financial relationships that could be construed as a potential conflict of interest.

Publisher's note

References

1. Altuvia Y, Landgraf P, Lithwick G, Elefant N, Pfeffer S, Aravin A, et al. Clustering and conservation patterns of human microRNAs. *Nucleic Acids Res* (2005) 33(8):2697–706. doi: 10.1093/nar/gki567

2. Iyer MK, Niknafs YS, Malik R, Singhal U, Sahu A, Hosono Y, et al. The landscape of long non-coding RNAs in the human transcriptome. *Nat Genet* (2015) 47(3):199–208. doi: 10.1038/ng.3192

3. Ji Z, Song R, Regev A, Struhl K. Many lncRNAs, 5'UTRs, and pseudogenes are translated and some are likely to express functional proteins. *Elife* (2015) 4: e08890. doi: 10.7554/eLife.08890

4. Qian Y, Shi L, Luo Z. Long non-coding RNAs in cancer: Implications for diagnosis, prognosis, and therapy. *Front Med (Lausanne)* (2020) 7:612393. doi: 10.3389/fmed.2020.612393

5. Santarpia L, Nicoloso M, Calin GA. MicroRNAs: a complex regulatory network drives the acquisition of malignant cell phenotype. *Endocr Relat Cancer* (2010) 17(1):F51–75. doi: 10.1677/ERC-09-0222

6. Valastyan S, Weinberg RA. MicroRNAs: Crucial multi-tasking components in the complex circuitry of tumor metastasis. *Cell Cycle* (2009) 8(21):3506–12. doi: 10.4161/cc.8.21.9802

frontiers in Oncology

REVIEW
published: 06 August 2019
doi: 10.3389/fonc.2019.00739

Long Non-coding RNAs as Communicators and Mediators Between the Tumor Microenvironment and Cancer Cells

*Di Chen[1], Tong Lu[2], Junying Tan[1], Hao Li[1], Qiuyue Wang[1] and Liangzhou Wei[1]**

[1] Department of Gastroenterology, Affiliated Hospital of Qingdao University, Qingdao, China, [2] Department of Thoracic Surgery, Affiliated Hospital of Qingdao University, Qingdao, China

Long non-coding RNAs (lncRNAs) are a class of more than 200 nucleotides RNA transcripts which have limited protein coding capacity. They regulate numerous biological processes in cancers through diverse molecular mechanisms. Aberrant expression of lncRNAs has been frequently associated with human cancer. Furthermore, the tumor microenvironment (TME) is composed of different cells such as cancer-associated fibroblasts (CAFs), endothelial cells and infiltrated immune cells, and all of which participate in communication with tumor cells affecting the progression of tumor. LncRNAs are directly and indirectly involved in the crosstalk between stromal cells and tumor cells and dysregulated lncRNAs expression in these cells could drive tumorigenesis. In this review, we explore the influence of aberrantly expressed lncRNAs in tumor progression, clarify the critical roles of lncRNAs in the TME, summarize findings on crosstalk between infiltrated immune cells, CAFs, endothelial cells, and tumor cells via lncRNAs, and discuss the promise of lncRNAs as tumor diagnostic markers and therapeutic targets.

Keywords: long non-coding RNA, tumor microenvironment, stromal cells, exosomes, therapy

OPEN ACCESS

Edited by:
Cecilia Ana Suarez, National Council for Scientific and Technical Research (CONICET), Argentina

Reviewed by:
Xingming Jiang, Second Affiliated Hospital of Harbin Medical University, China
Shao-Chun Wang, China Medical University, Taiwan

***Correspondence:**
Liangzhou Wei
weiliangzhou62@163.com

Specialty section:
This article was submitted to Molecular and Cellular Oncology, a section of the journal Frontiers in Oncology

Received: *09 May 2019*
Accepted: *23 July 2019*
Published: *06 August 2019*

Citation:
Chen D, Lu T, Tan J, Li H, Wang Q and Wei L (2019) Long Non-coding RNAs as Communicators and Mediators Between the Tumor Microenvironment and Cancer Cells. Front. Oncol. 9:739. doi: 10.3389/fonc.2019.00739

INTRODUCTION

Long non-coding RNAs (lncRNAs) are a diverse class of transcribed RNA molecules that are more than 200 nucleotides with limited protein coding potential (1, 2). Current estimates, from the GENCODE database (www.gencodegenes.org), indicate that the human genome contains ∼16,000 lncRNA genes that encode more than 28,000 distinct lncRNAs. Many lncRNAs have emerged as critical players in regulating numerous biological processes in cancer, such as differentiation, cell cycle regulation, and immune response (3–5). They can directly act as tumor suppressors or oncogenes, or are regulated by well-known tumor suppressors or oncogenes, at transcriptional or post-transcriptional levels (6, 7). Furthermore, emerging evidence have shown that dysregulated lncRNAs are greatly involved in various cancers (8–10). For instance, the PCA3 (also called DD3) and PCGEM1 were the first lncRNAs that were associated with cancer because they were overexpressed in prostate cancer (11, 12). PCA3 might be used as a biomarker for the diagnosis of prostate cancer and PCGEM1 involved in c-MYC activation and androgen receptor transcriptional activation was associated with the progression of prostate cancer (13, 14).

Moreover, lncRNA MALAT1 was reported to be overexpressed in multiple cancer types, such as colorectal cancer, non-small cell lung cancer and hepatocellular carcinoma (HCC); its expression was also correlated with tumor progression and poor prognosis (15–18). Importantly, these studies suggested that aberrantly expressed lncRNAs can be used as biomarkers for cancer diagnosis and prognosis as well as potential targets for cancer therapy.

The tumor microenvironment (TME) is a complicated physiological and biochemical system that plays critical functions in tumorigenesis, progression, and metastasis (19–21). In addition to tumor cells, the TME consists mainly of the extracellular matrix (ECM), the tumor vascular system, other non-malignant cells as well as the acidic and hypoxic environment of the tumor (21, 22). With the development of biological technology, different cell types have been identified in the TME, including cancer-associated fibroblasts (CAFs), fat cells, endothelial cells, and infiltrated immune cells such as T lymphocytes, myeloid-derived suppressor cells, and tumor-associated macrophages (22–24). Most of these stromal cells significantly contribute to the initiation and progression of tumors. In recent years, a growing appreciation of the TME indicated that lncRNAs play significant roles in the interactions between tumor cells and stromal cells (25–30). In this review, we discuss the role of lncRNAs in the crosstalk between CAFs, endothelial cells, infiltrated immune cells and tumor cells, and the promise of lncRNAs in cancer treatment, to increase our knowledge of the function of lncRNAs within the TME and lay a foundation for lncRNA-based anti-tumor treatment strategies.

LNCRNAS AND CAFS

CAFs, one of the most abundant stromal cells in the TME, are critically involved in tumor progression (31, 32). CAFs modulate the biology of cancer cells through releasing numerous regulatory factors, such as chemokines, cytokines and growth factors, and thus these cells affect the progression of tumor (31, 33). Transforming growth factor-β1 (TGF-β1), which is secreted by CAFs, is a critical factor promoting the epithelial-mesenchymal transition (EMT) and metastasis of cancer cells such as bladder cancer cells and breast cancer cells (34, 35). And the secretion of TGF-β1 by CAFs induces the metastatic activity of cancer cells by regulating the expression of lncRNAs. For instance, CAFs promoted EMT of bladder cancer cells by activating the transcription of lncRNA-ZEB2NAT via TGF-β1 secretion (34). Similarly, TGF-β1 secreted by CAFs upregualted lncRNA HOTAIR expression to promote EMT and metastasis in breast cancer (35). Furthermore, in oral squamous cell carcinoma, LncRNA-CAF could elevate the expression of cytokine IL-33 to promote the activation of CAFs, leading to proliferation of tumor cells. In return, tumor cells also secreted exosomes including LncRNA-CAF to stroma and increased LncRNA-CAF levels for the activation of CAFs (36).In addition, LINC00092 was found to be upregulated in response to the CAF-secreted chemokine CXCL14 in ovarian cancer cells. Simultaneously, LINC00092, which induced a glycolytic phenotype of ovarian cancer cells, was critical for the maintenance of CAF-like features by interacting with PFKFB2 (37). Therefore, LncRNA-CAF and LINC00092 were served as significant modulators of feedback loop in the cancer cells and CAFs, which were critical for the progression of cancer. Collectively, these studies indicated the importance of lncRNAs in the interaction between the CAFs and cancer cells and provided a potential application for lncRNAs as targets of cancer treatment.

LNCRNAS AND ENDOTHELIAL CELLS

Endothelial cells, which line the interior surface of blood vessels, are important components of stroma in TME (26, 38). They are believed to be critical for angiogenesis and tumor metastasis, and lncRNAs may affect the progression of tumor through modulating the biological behavior of endothelial cells. LncRNA H19, for instance, was reported to be significantly upregulated in glioma-associated endothelial cells cultured in glioma-conditioned medium. Knockdown of H19 inhibited glioma-induced endothelial cell proliferation, migration and tube formation *in vitro*. Mechanistic evidence revealed that H19 modulated the biological behavior of glioma-associated endothelial cells by suppressing miR-29a (39). Furthermore, lncRNA-APC1 played an important tumor-suppressive role in the pathogenesis of colorectal carcinoma. Following mechanism studies showed that lncRNA-APC1 decreased exosome production in colorectal carcinoma cells through reducing the stability of Rab5b mRNA, and this action suppressed tumor angiogenesis through inhibiting the overactivation of the MAPK pathway in endothelial cells (40). In summary, dysregulated lncRNAs affect the biological behavior of endothelial cells by diverse mechanisms, thus modulating specific lncRNA expression in tumor cells or/and endothelial cells may have a significant effect on the progression of cancer.

LNCRNAS INVOLVED IN CROSSTALK BETWEEN INFILTRATED IMMUNE CELLS AND TUMOR CELLS

Tumor-Associated Macrophages (TAMs)

TAMs are important regulators of the TME, and might regulate tumor growth, invasion, and metastasis (41). Two major functional types of macrophages have been identified, including classically activated (M1) and alternatively activated (M2) macrophages (23, 41, 42). M1 macrophages participate in the Th1-type inflammatory response and have anti-tumorigenic functions, while M2 macrophages promote anti-inflammatory responses and have a pro-tumorigenic role (23, 43, 44). Several studies have indicated that lncRNAs could modulate M2 polarization of macrophages to affect tumor cells migration and invasion. For example, lncRNA CCAT1 could modulate the TME of prostate cancer through regulating macrophages polarization. Knockdown of lncRNA CCAT1 enhanced macrophages polarization to M2 through upregulating the expression of miR-148a and further promoted prostate cancer cells migration and invasion (45). LncRNA NIFK-AS1 also played a key

role in modulating the polarization of TAMs in endometrial cancer. It could suppress M2 macrophages polarization by inhibiting miR-146a, thus reducing the endometrial cancer cells proliferation, migration and invasion (46). Moreover, a cell model-based microarray analysis was used to detect lncRNAs involved in M2 polarization and lncRNA-MM2P was found to be upregulated during M2 polarization. In addition, further studies demonstrated that lncRNA-MM2P promoted M2 polarization of macrophages by reducing phosphorylation on STAT6, then affecting macrophage-mediated tumorigenesis and tumor growth (47).

Furthermore, CCL2, which is produced by different tumor types, plays a critical role in tumor metastasis (48, 49). Tumor-derived CCL2 is released into the TME and recruits macrophages to tumor cells, which contribute to tumor cells proliferation, angiogenesis, and immune response evasion (48, 50). It has been demonstrated that lncRNAs could modulate the TME by regulating the expression of CCL2 and further affected metastasis. For example, lncRNA LNMAT1 was greatly upregulated in lymph node-metastatic bladder cancer. The authors showed that LNMAT1 activated the transcription of CCL2 through enhancing hnRNPL-mediated H3K4me3 at the CCL2 promoter. Moreover, LNMAT1-induced CCL2 regulated the TME through recruiting TAMs, ultimately resulting in lymphatic metastasis of bladder cancer (51). Similarly, the expression of lnc-BM was markedly upregulated in breast cancer cells. High expression of lnc-BM also promoted breast cancer brain metastasis in preclinical mouse models. Mechanistically, lnc-BM induced STAT3-dependent expression of CCL2 to attract macrophages to cancer cells, thus enhancing breast cancer brain metastasis (52).

Myeloid-Derived Suppressor Cells (MDSCs)

MDSCs generated in the bone marrow are one of the major components of TME, and these cells play a critical role in cancer progression by suppressing immune responses (53, 54). MDSCs have immunosuppressive activity in pathological conditions through numerous mechanisms involving inducible NO synthase (iNOS), arginase 1 (ARG1), oxygen species (ROS), and nitric oxide (NO) (54, 55). It has been demonstrated that several lncRNAs such as lnc-chop, lnc-C/EBPβ, and lncRNA Pvt1 contributed to the regulation of the immunosuppressive function of MDSCs through modulating the production of ROS and NO or ROS and ARG1.

Notably, lnc-chop interacted with CHOP and the C/EBPβ isoform LIP to increase the activity of C/EBPβ and upregulate target transcripts, such as ARG1, NOS2, COX2, and NOX2. High levels of these target transcripts could result in the production of ROS and NO, thus promoting tumor growth by enhancing the immunosuppression function of MDSCs (56). In contrast, a recent study found that lnc-C/EBPβinhabited the activation of C/EBPβ, decreased the expression of NO and ROS, and further suppressed the immunosuppressive capacity of MDSCs in the tumor environment (57). Granulocytic MDSCs (G-MDSCs) constitute ∼70–80% of MDSCs in cancer patients and tumor-bearing mice (58–60). A recent study showed that LncRNA Pvt1 was critical in modulating the immunosuppressive activity of G-MDSCs. The author found that lncRNA Pvt1 knockdown significantly suppressed G-MDSC-mediated immunosuppression *in vitro* by decreasing the level of ROS and ARG1. In addition, knockdown of lncRNA Pvt1 delayed tumor progression in tumor-bearing mice by inhibiting the function of G-MDSCs (61). These findings suggest that lncRNAs play significant roles in the control of tumor-associated MDSCs and lncRNAs may be potential antitumor immunotherapy targets.

T Cells

T cells, a predominant immune cell type in the TME, can exert both tumor promoting and suppressive functions, as determined by their effector functions (24, 62). LncRNAs have been gradually recognized as modulators of T cell development, activation and differentiation (63). $CD8^+$ T cells, major population of T cells, are prominent anti-tumor cells in TME (60). Recent studies have shown that lncRNAs could modulate the function of $CD8^+$ T cells in the TME through diverse mechanisms, further affecting the progression of cancer. Lnc-Tim3 was found to be upregulated and negatively correlated with the production of IL-2 and IFN-γ in tumor-infiltrating $CD8^+$ T cells of patients with HCC. Mechanistically, lnc-Tim3 bound to Tim-3 and induced nuclear translocation of Bat3 in HCC, which compromised anti-tumor immunity by promoting CD8 + T cell exhaustion (64). Moreover, lnc-sox5 was significantly upregulated in colorectal cancer tissues and lnc-sox5 knockdown promoted the cytotoxicity and infiltration of $CD8^+$T cells. Mechanistic evidence revealed that lnc-sox5 regulated the $CD8^+$T cell infiltration and cytotoxicity through modulating the expression of IDO and therefore affecting the progression of colorectal cancer (65). These data indicate that lnc-Tim3 and lnc-sox5 play different roles in modulating the $CD8^+$T cells to affect the progression of tumor.

Regulatory T cells (Tregs) are an immunosuppressive subset of $CD4^+$ T cells, which may contribute to the suppression of anti-tumor immunity as they frequently accumulate in the TME (66, 67). Several studies have revealed that some lncRNAs such as lnc-EGFR, lncRNA SNHG1, and Flicr modulated the function of Tregs. Among them, lnc-EGFR was found to be overexpressed in Tregs of patients with HCC. It stimulated the differentiation of Tregs and promoted the growth of tumor in an EGFR-dependent manner. Mechanistic evidence revealed that lnc-EGFR specially bound to EGFR and enhanced AP-1/NF-AT1/Foxp3 signaling, leading to Treg differentiation, and HCC progression (68). LncRNA SNHG1 was also reported to promote the differentiation of Tregs. Knockdown of lncRNA SNHG1 could suppress Treg differentiation by increasing the expression of miR-448 and reducing level of IDO, further alleviating the immune escape in breast cancer (69). Moreover, Flicr, a lncRNA, was reported to enhance the immunosuppressive function of Tregs by modulating the expression of Foxp3. So, Flicr might be associated with tumors, but its roles in the TME remains unclear (70). Collectively, these data indicate that the targeting of specific lncRNAs in T cells is promising for tumor therapy. LncRNAs involved in the communication between tumor cells and stromal cells are shown in **Table 1** and **Figure 1**.

TABLE 1 | LncRNAs involved in the crosstalk between stromal cells and tumor cells.

LncRNA	Cancer type	Stromal cells	Mechanisms of action	Reference
LncRNA-CAF	Oral squamous cell carcinoma	CAFs	Lnc-CAF up-regulates IL-33 expression to reprogram CAFs, promoting tumor development.	(36)
LINC00092	Ovarian cancer	CAFs	CAFs-secreted CXCL14 induces LINC00092 upregulation which promotes ovarian cancer metastasis by enhancing PFKFB-2 translation.	(37)
LncRNA-ZEB2NAT	bladder cancer	CAFs	TGFβ1 secreted by CAFs induces epithelial-mesenchymal transition and invasion of bladder cancer cells via lncRNA-ZEB2NAT.	(34)
HOTAIR	Breast cancer	CAFs	TGFβ1 secreted by CAFs induces epithelial-mesenchymal transition and metastasis of breast cancer through HOTAIR.	(35)
LncRNA H19	Glioma	endothelial cells	Knockdown of H19 suppresses proliferation and migration of glioma-associated endothelial cells through upregulating miR-29a.	(39)
LncRNA-APC1	Colorectal carcinoma	endothelial cells	LncRNA-APC1 suppresses the MAPK pathway overactivation in endothelial cells and further inhibits tumor angiogenesis by increasing exosome production in colorectal carcinoma cells.	(40)
LncRNA CCAT1	Prostate cancer	TAMs	LncRNA CCAT1 knockdown enhances macrophages polarization to M2 and promotes prostate cancer cell migration and invasion through upregulating the expression of miR-148a.	(45)
LncRNA NIFK-AS1	Endometrial cancer	TAMs	LncRNA NIFK-AS1 suppresses the M2 macrophages polarization by inhibiting miR-146a, thus reducing the endometrial cancer cell proliferation, migration and invasion.	(46)
LncRNA-MM2P	–	TAMs	LncRNA-MM2P promotes M2 polarization of macrophages via reducing phosphorylation on STAT6, then affecting macrophage- mediated tumorigenesis and tumor growth.	(47)
LncRNA LNMAT1	Bladder cancer	TAMs	LncRNA LNMAT1-induced CCL2 recruits TAMs, leading to lymphatic metastasis of bladder cancer.	(51)
Lnc-BM	Breast cancer	TAMs	Lnc-BM induces STAT3-dependent expression of CCL2 to attract macrophages, thus enhancing breast cancer brain metastasis.	(52)
Lnc-chop	–	MDSCs	Lnc-chop upregulates the production of ROS and NO to enhance immunosuppression and promots tumor growth.	(56)
Lnc-C/EBPβ	–	MDSCs	Lnc-C/EBPβ suppresses the immunosuppressive capacity of MDSCs by suppressing the expression of NO and ROS.	(57)
LncRNA Pvt1	–	MDSCs	LncRNA Pvt1 knockdown suppresses G-MDSC-mediated immunosuppression *in vitro* by decreasing the level of ROS and ARG1, and delays tumor progression in tumor-bearing mice.	(61)
Lnc-Tim3	Hepatocellular carcinoma	$CD8^+$ T cells	Lnc-Tim3 binds to Tim-3 and induces nuclear translocation of Bat3 in hepatocellular carcinoma, which compromises anti-tumor immunity by promoting CD8 + T cell exhaustion.	(64)
Lnc-sox5	Colorectal cancer	$CD8^+$ T cells	Lnc-sox5 regulates the $CD8^+$T cells infiltration and cytotoxicity through modulating the expression of IDO, further affecting the progression of colorectal cancer.	(65)
Lnc-EGFR	Hepatocellular carcinoma	Tregs	Lnc-EGFR specially binds to EGFR, enhances AP-1/NF-AT1/Foxp3 signaling, leading to Treg differentiation, and hepatocellular carcinoma progression	(68)
LncRNA SNHG1	Breast cancer	Tregs	Knockdown of lncRNA SNHG1 suppresses Treg differentiation by increasing the expression of miR-448 and reducing level of IDO, further alleviating the immune escape in breast cancer.	(69)
Flicr	–	Tregs	Flicr modulates the expression of Foxp3 and enhances the immunosuppressive function of Tregs.	(70)

CAFs, cancer-associated fibroblasts; TAMs, tumor-associated macrophages; MDSCs, myeloid-derived suppressor cells; Tregs, regulatory T cells.

EXOSOMAL LNCRNAS-MEDIATED DIRECT COMMUNICATION BETWEEN TUMOR CELLS AND THE TME

Exosomes are critical mediators in intercellular communication through carrying intracellular components including DNA, RNA and protein to the recipient cells (71, 72). Tumor-derived exosomes can be used to change the TME, affect tumor cell proliferation, angiogenesis, and so on (73–75). In recent years, the role of exosomal lncRNAs in the TME has garnered increasing attention (28, 76). Several studies have shown that tumor cell-derived exosomal lncRNAs could affect the function of stromal cells in the TME (**Figure 2**).

Recent studies have revealed that tumor cell-derived exosomal lncRNAs are conveyed to endothelial cells to affect angiogenesis. For instance, lncRNA H19 was found to be highly expressed in CD90+ liver cancer cells. Interestingly, lncRNA H19, which was packed inside exosomes secreted by CD90+

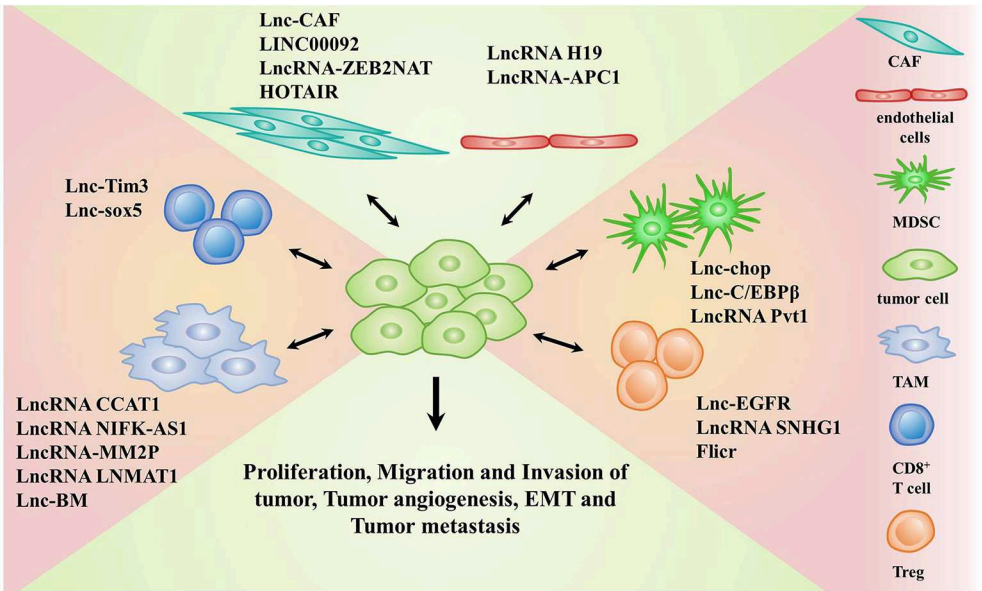

FIGURE 1 | LncRNAs implicated in the crosstalk between stromal cells and tumor cells. Stromal cells include cancer associated fibroblasts (CAFs), endothelial cells, myeloid-derived suppressor cells (MDSCs), tumor-associated macrophages (TAMs), $CD8^{+}$T cells, and regulatory T cells (Tregs).

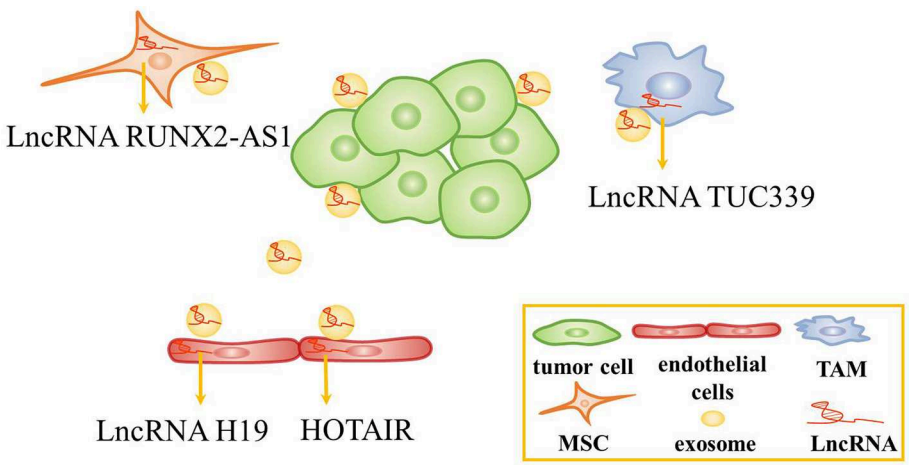

FIGURE 2 | The role of exosomes in the tumor microenvironment. Tumor cells-derived exosomal lncRNAs are transferred to endothelial cells, tumor-associated macrophage (TAMs), and mesenchymal stem cells (MSCs) to alter the function of these cells.

liver cancer cells, was conveyed to and internalized by endothelial cells. Then, lncRNA H19 promoted angiogenesis by increasing VEGF production and release (77). Similarly, HOTAIR was abundant and was packed inside exosomes in glioma cells. Exosomal HOTAIR was transferred to endothelial cells, stimulating angiogenesis by upregulating the expression of VEGFA (78).

In addition, exosomal lncRNAs has been found to be transferred to macrophages and mesenchymal stem cells to alter the function of these cells. In HCC, TUC339 was identified as a kind of lncRNA abundant in tumor-derived exosomes and could be transferred from tumor cells to macrophages. Then, exosomal lncRNA TUC339 regulated macrophage cytokine production, M1/M2 polarization and phagocytosis, while the regulation mechanism needs further investigation (79). Besides, lncRNA RUNX2-AS1 could be packed inside exosomes and transmitted to mesenchymal stem cells. It might suppress the osteogenic differentiation of mesenchymal stem cells by modulating the expression of RUNX2 in multiple myeloma (80). Taken together, several studies revealed that tumor cells-derived exosomes could regulate the TME and affect tumor progression. Thus, tumor cells-derived exosomes containing lncRNAs might be served as biomarkers and therapeutic targets.

LNCRNAS AS POTENTIAL TARGETS FOR THERAPY

Numerous lncRNAs are aberrantly expressed in different cancer types, and their expression levels are associated with the initiation and progression of tumors (81). Recent and ongoing studies have improved our understanding of the role of lncRNAs in tumor biology (82). LncRNAs are emerging as novel molecules involved in tumor progression and are acted as promising biomarkers and therapeutic targets in cancer (83–85).

Due to their physiological and pathological roles in cancer, lncRNAs should be considered as candidates for biomarkers in cancer diagnostics and prognoses (29, 86, 87). For example, serum lncRNA HOTAIR was significantly higher in glioblastoma multiforme patients than in normal controls, which can be served as a novel diagnostic and prognostic biomarker in this disease (88). Similarly, exosomal lncRNA UEGC1 in the plasma was remarkably upregulated in early gastric cancer, indicating it might be a promising biomarker for early gastric cancer diagnosis (89). In a study of 246 subjects including 126 gastric cancer patients and 120 healthy controls, serum exosomal lncRNA HOTTIP was identified as a potential biomarker for diagnosis and prognosis in gastric cancer (90). LncRNAs are also emerging as therapeutic targets for cancer (91). Several features of lncRNAs need to be considered to support lncRNAs as therapeutic targets. First, lncRNAs structural complexity and participation in multicomponent complexes affords few potential targetable key residues to regulate structure-based interactions. Second, lncRNAs can play critical regulatory roles in gene expression and their expression levels are often lower than protein-coding genes. Third, lncRNAs are expressed in a tissue or cell-type specific manner, making them potential efficacious targets for tumor therapy. In addition, lncRNAs may also participate in cell-to-cell communication (84, 86, 92). LncRNAs can be targeted by multiple approaches, such as antisense oligonucleotides (ASOs), short hairpin RNAs (shRNAs), short interfering RNAs (siRNAs), aptamers, and small molecule inhibitor (**Figure 3**). ASOs also have already shown success in modulating coding genes involved in different kinds of solid tumors and other disease (93–96). ASOs are emerging as a potential therapeutic approach for targeting cancer-associated lncRNAs (97). For example, in the MMTV-PyMT mouse mammary carcinoma model, MALAT1 could promote tumor growth and metastasis. Then, in this model, the application of ASOs against MALAT1 resulted in slower tumor proliferation and a reduction in metastasis (98). Moreover, in a mouse xenograft model, MALAT1 ASOs was effective in suppressing lung cancer spreading (99). Thus, MALAT1 may be a potential therapeutic target, and MALAT1 ASOs may be a promising therapy approach for several types of cancer, but further assessment will be needed. A great number of studies have shown that siRNAs are used to against their target mRNAs for different disorders including cancer and metabolic disorders (100, 101). A few lncRNAs were silenced using siRNAs in cell lines (100, 102). However, preclinical studies

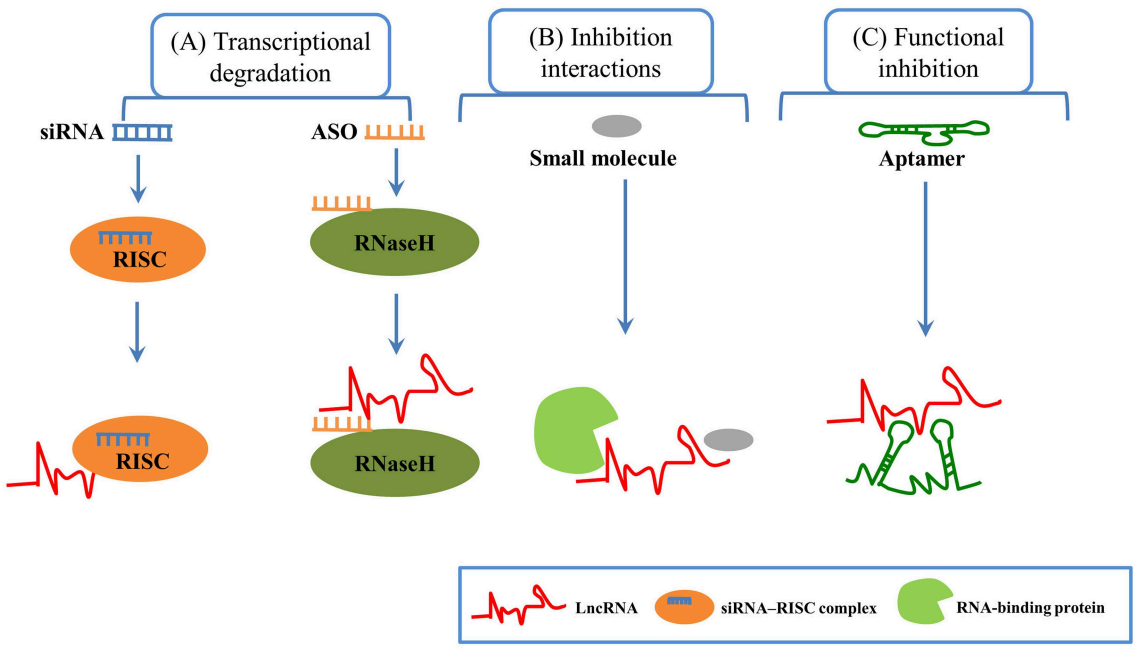

FIGURE 3 | LncRNA-based therapeutic methods in cancer. **(A)** Transcriptional degradation: Short interfering RNAs (siRNAs), which are double-stranded RNAs, can degrade target RNAs through RISC (RNA-induced silencing complex). Antisense oligonucleotides (ASOs), which are single-stranded oligonucleotide sequence, offer specific complementarity, and Rnase H-mediated degradation of target lncRNA. **(B)** Inhibition interactions: Small molecules can inhibit the interaction between lncRNAs and protein. **(C)** Functional inhibition: Aptamers (short RNA or DNA oligonucleotides with 3-dimensional structure) can bind to their target lncRNAs at specific structural regions.

using siRNAs/shRNAs to target lncRNAs were very limited. In human breast cancer cell lines, siRNA-mediated downregulation of HOTAIR inhibited cancer cell viability and matrix invasion (103). In human prostate cancer cell lines, siRNAs directed against MALAT led to suppression of cancer cell growth, migration and invasion (104). Moreover, subcutaneous injection of gastric cancer cell lines transfected with HOTAIR shRNA suppressed engraftment efficiency in nude mice (105). Aptamers can specifically bind to their target lncRNAs depending on the 3-dimensional shape of the lncRNA structures. Several reports have demonstrated promising effects of aptamers to modulate RNA functions, thus aptamers may be potential therapeutic agents to target lncRNAs. For example, Ayatollahi et al. demonstrated the aptamer-targeted Bcl-xL shRNAs delivery into lung cancer cells using alkyl modified PAMAM dendrimers (106). Small molecule inhibitors targeting a unique triple-helical structural element in lncRNAs (such as MALAT1 and NEAT1) are likely to destabilize the transcript to confer a therapeutic effect, although this needs further exploration (107–110).

CONCLUSION

LncRNAs are multifunctional molecules that play critical roles in various biological processes, and dysregulated lncRNAs are often associated with a variety of pathophysiological conditions, such as cancer. We reviewed the recently published studies involving of lncRNAs in the TME. Emerging evidence indicates that lncRNAs play critical roles in modulating the TME and tumor progression. In addition, we described the crosstalk of lncRNAs between immune cells, CAFs, endothelial cells, and tumor cells in the TME and the promise of lncRNAs as tumor diagnostic markers and therapeutic targets.

Finally, tumor cells are thought to produce lncRNA-containing exosomes and tumor-derived exosomal lncRNAs may mediate direct communication between tumor cells and the TME, as illustrated in this review. Further research is still required to better understand the role of lncRNAs in the TME. In the future, lncRNAs may be used in strategies for early cancer detection, monitoring treatment responses and targeted cancer therapy.

AUTHOR CONTRIBUTIONS

DC and LW were the major contributors in writing the manuscript. TL and JT performed the literature search. HL and QW revised the manuscript. All authors read and approved the final manuscript.

REFERENCES

1. Spizzo R, Almeida MI, Colombatti A, Calin GA. Long non-coding RNAs and cancer: a new frontier of translational research? *Oncogene*. (2012) 31:4577–87. doi: 10.1038/onc.2011.621
2. Nagano T, Fraser P. No-nonsense functions for long noncoding RNAs. *Cell*. (2011) 145:178–81. doi: 10.1016/j.cell.2011.03.014
3. Guttman M, Amit I, Garber M, French C, Lin MF, Feldser D, et al. Chromatin signature reveals over a thousand highly conserved large non-coding RNAs in mammals. *Nature*. (2009) 458:223–7. doi: 10.1038/nature07672
4. Qiu M, Xu Y, Wang J, Zhang E, Sun M, Zheng Y, et al. A novel lncRNA, LUADT1, promotes lung adenocarcinoma proliferation via the epigenetic suppression of p27. *Cell Death Dis*. (2015) 6:e1858. doi: 10.1038/cddis.2015.203
5. Bach DH, Lee SK. Long noncoding RNAs in cancer cells. *Cancer Lett*. (2018) 419:152–66. doi: 10.1016/j.canlet.2018.01.053
6. Barsyte-Lovejoy D, Lau SK, Boutros PC, Khosravi F, Jurisica I, Andrulis IL, et al. The c-Myc oncogene directly induces the H19 noncoding RNA by allele-specific binding to potentiate tumorigenesis. *Cancer Res*. (2006) 66:5330–7. doi: 10.1158/0008-5472.CAN-06-0037
7. Huarte M, Guttman M, Feldser D, Garber M, Koziol MJ, Kenzelmann-Broz D, et al. A large intergenic noncoding RNA induced by p53 mediates global gene repression in the p53 response. *Cell*. (2010) 142:409–19. doi: 10.1016/j.cell.2010.06.040
8. Iyer MK, Niknafs YS, Malik R, Singhal U, Sahu A, Hosono Y, et al. The landscape of long noncoding RNAs in the human transcriptome. *Nat Genet*. (2015) 47:199–208. doi: 10.1038/ng.3192
9. Ling H, Vincent K, Pichler M, Fodde R, Berindan-Neagoe I, Slack FJ, et al. Junk DNA and the long non-coding RNA twist in cancer genetics. *Oncogene*. (2015) 34:5003–11. doi: 10.1038/onc.2014.456
10. Tsai MC, Spitale RC, Chang HY. Long intergenic noncoding RNAs: new links in cancer progression. *Cancer Res*. (2011) 71:3–7. doi: 10.1158/0008-5472.CAN-10-2483
11. Bussemakers MJ, van Bokhoven A, Verhaegh GW, Smit FP, Karthaus HF, Schalken JA, et al. DD3: a new prostate-specific gene, highly overexpressed in prostate cancer. *Cancer Res*. (1999) 59:5975–9. PubMed PMID: 10606244.
12. Srikantan V, Zou Z, Petrovics G, Xu L, Augustus M, Davis L, et al. PCGEM1, a prostate-specific gene, is overexpressed in prostate cancer. *Proce Natl Acad Sci USA*. (2000) 97:12216–21. doi: 10.1073/pnas.97.22.12216
13. Hessels D, Klein Gunnewiek JM, van Oort I, Karthaus HF, van Leenders GJ, et al. DD3(PCA3)-based molecular urine analysis for the diagnosis of prostate cancer. *Eur Urol*. (2003) 44:8–15; discussion−6. PubMed PMID: 12814669. doi: 10.1016/S0302-2838(03)00201-X
14. Yang L, Lin C, Jin C, Yang JC, Tanasa B, Li W, et al. lncRNA-dependent mechanisms of androgen-receptor-regulated gene activation programs. *Nature*. (2013) 500:598–602. doi: 10.1038/nature12451
15. Ji P, Diederichs S, Wang W, Boing S, Metzger R, Schneider PM, et al. MALAT-1, a novel noncoding RNA, and thymosin beta4 predict metastasis and survival in early-stage non-small cell lung cancer. *Oncogene*. (2003) 22:8031–41. doi: 10.1038/sj.onc.1206928
16. Amodio N, Raimondi L, Juli G, Stamato MA, Caracciolo D, Tagliaferri P, et al. MALAT1: a druggable long non-coding RNA for targeted anti-cancer approaches. *J Hematol Oncol*. (2018) 11:63. doi: 10.1186/s13045-018-0606-4
17. Schmidt LH, Spieker T, Koschmieder S, Schaffers S, Humberg J, Jungen D, et al. The long noncoding MALAT-1 RNA indicates a poor prognosis in non-small cell lung cancer and induces migration and tumor growth. *J Thorac Oncol*. (2011) 6:1984–92. doi: 10.1097/JTO.0b013e3182307eac
18. Li Q, Dai Y, Wang F, Hou S. Differentially expressed long non-coding RNAs and the prognostic potential in colorectal cancer. *Neoplasma*. (2016) 63:977–83. doi: 10.4149/neo_2016_617
19. Singh SR, Rameshwar P, Siegel P. Targeting tumor microenvironment in cancer therapy. *Cancer Lett*. (2016) 380:203–4. doi: 10.1016/j.canlet.2016.04.009
20. Balkwill FR, Capasso M, Hagemann T. The tumor microenvironment at a glance. *J Cell Sci*. (2012) 125(Pt 23):5591–6. doi: 10.1242/jcs.116392
21. Chen Q, Liu G, Liu S, Su H, Wang Y, Li J, et al. Remodeling the tumor microenvironment with emerging nanotherapeutics. *Trends Pharmacol Sci*. (2018) 39:59–74. doi: 10.1016/j.tips.2017.10.009
22. Jiang X, Wang J, Deng X, Xiong F, Ge J, Xiang B, et al. Role of the tumor microenvironment in PD-L1/PD-1-mediated tumor immune escape. *Mol Cancer*. (2019) 18:10. doi: 10.1186/s12943-018-0928-4

23. Quail DF, Joyce JA. Microenvironmental regulation of tumor progression and metastasis. *Nat Med*. (2013) 19:1423–37. doi: 10.1038/nm.3394
24. Grivennikov SI, Greten FR, Karin M. Immunity, inflammation, and cancer. *Cell*. (2010) 140:883–99. doi: 10.1016/j.cell.2010.01.025
25. Yang N, Zhu S, Lv X, Qiao Y, Liu YJ, Chen J. MicroRNAs: pleiotropic regulators in the tumor microenvironment. *Front Immunol*. (2018) 9:2491. doi: 10.3389/fimmu.2018.02491
26. Kohlhapp FJ, Mitra AK, Lengyel E, Peter ME. MicroRNAs as mediators and communicators between cancer cells and the tumor microenvironment. *Oncogene*. (2015) 34:5857–68. doi: 10.1038/onc.2015.89
27. Rupaimoole R, Calin GA, Lopez-Berestein G, Sood AK. miRNA deregulation in cancer cells and the tumor microenvironment. *Cancer Discov*. (2016) 6:235–46. doi: 10.1158/2159-8290.CD-15-0893
28. Sun Z, Yang S, Zhou Q, Wang G, Song J, Li Z, et al. Emerging role of exosome-derived long non-coding RNAs in tumor microenvironment. *Mol Cancer*. (2018) 17:82. doi: 10.1186/s12943-018-0831-z
29. Lin YH, Wu MH, Yeh CT, Lin KH. Long non-coding RNAs as mediators of tumor microenvironment and liver cancer cell communication. *Int J Mol Sci*. (2018) 19:E3742. doi: 10.3390/ijms19123742
30. Del Vecchio F, Lee GH, Hawezi J, Bhome R, Pugh S, Sayan E, et al. Long non-coding RNAs within the tumour microenvironment and their role in tumour-stroma cross-talk. *Cancer Lett*. (2018) 421:94–102. doi: 10.1016/j.canlet.2018.02.022
31. Chen X, Song E. Turning foes to friends: targeting cancer-associated fibroblasts. *Nat Rev Drug Discov*. (2019) 18:99–115. doi: 10.1038/s41573-018-0004-1
32. Kalluri R. The biology and function of fibroblasts in cancer. *Nat Rev Cancer*. (2016) 16:582–98. doi: 10.1038/nrc.2016.73
33. Gaggioli C, Hooper S, Hidalgo-Carcedo C, Grosse R, Marshall JF, Harrington K, et al. Fibroblast-led collective invasion of carcinoma cells with differing roles for RhoGTPases in leading and following cells. *Nat Cell Biol*. (2007) 9:1392–400. doi: 10.1038/ncb1658
34. Zhuang J, Lu Q, Shen B, Huang X, Shen L, Zheng X, et al. TGFbeta1 secreted by cancer-associated fibroblasts induces epithelial-mesenchymal transition of bladder cancer cells through lncRNA-ZEB2NAT. *Sci Rep*. (2015) 5:11924. doi: 10.1038/srep11924
35. Ren Y, Jia HH, Xu YQ, Zhou X, Zhao XH, Wang YF, et al. Paracrine and epigenetic control of CAF-induced metastasis: the role of HOTAIR stimulated by TGF-ss1 secretion. *Molecul Cancer*. (2018) 17:5. doi: 10.1186/s12943-018-0758-4
36. Ding L, Ren J, Zhang D, Li Y, Huang X, Hu Q, et al. A novel stromal lncRNA signature reprograms fibroblasts to promote the growth of oral squamous cell carcinoma via LncRNA-CAF/interleukin-33. *Carcinogenesis*. (2018) 39:397–406. doi: 10.1093/carcin/bgy006
37. Zhao L, Ji G, Le X, Wang C, Xu L, Feng M, et al. Long noncoding RNA LINC00092 acts in cancer-associated fibroblasts to drive glycolysis and progression of ovarian cancer. *Cancer Res*. (2017) 77:1369–82. doi: 10.1158/0008-5472.CAN-16-1615
38. Junttila MR, de Sauvage FJ. Influence of tumour micro-environment heterogeneity on therapeutic response. *Nature*. (2013) 501:346–54. doi: 10.1038/nature12626
39. Jia P, Cai H, Liu X, Chen J, Ma J, Wang P, et al. Long non-coding RNA H19 regulates glioma angiogenesis and the biological behavior of glioma-associated endothelial cells by inhibiting microRNA-29a. *Cancer Lett*. (2016) 381:359–69. doi: 10.1016/j.canlet.2016.08.009
40. Wang FW, Cao CH, Han K, Zhao YX, Cai MY, Xiang ZC, et al. APC-activated long noncoding RNA inhibits colorectal carcinoma pathogenesis through reduction of exosome production. *J Clin Invest*. (2019) 129:727–43. doi: 10.1172/JCI122478
41. Yang L, Zhang Y. Tumor-associated macrophages, potential targets for cancer treatment. *Biomarker Res*. (2017) 5:25. doi: 10.1186/s40364-017-0106-7
42. Allavena P, Sica A, Garlanda C, Mantovani A. The Yin-Yang of tumor-associated macrophages in neoplastic progression and immune surveillance. *Immunol Rev*. (2008) 222:155–61. doi: 10.1111/j.1600-065X.2008.00607.x
43. Lewis CE, Harney AS, Pollard JW. The multifaceted role of perivascular macrophages in tumors. *Cancer Cell*. (2016) 30:18–25. doi: 10.1016/j.ccell.2016.05.017
44. Biswas SK, Mantovani A. Macrophage plasticity and interaction with lymphocyte subsets: cancer as a paradigm. *Nat Immunol*. (2010) 11:889–96. doi: 10.1038/ni.1937
45. Liu J, Ding D, Jiang Z, Du T, Liu J, Kong Z. Long non-coding RNA CCAT1/miR-148a/PKCzeta prevents cell migration of prostate cancer by altering macrophage polarization. *Prostate*. (2019) 79:105–12. doi: 10.1002/pros.23716
46. Zhou YX, Zhao W, Mao LW, Wang YL, Xia LQ, Cao M, et al. Long non-coding RNA NIFK-AS1 inhibits M2 polarization of macrophages in endometrial cancer through targeting miR-146a. *Int J Biochem Cell Biol*. (2018) 104:25–33. doi: 10.1016/j.biocel.2018.08.017
47. Cao J, Dong R, Jiang L, Gong Y, Yuan M, You J, et al. LncRNA-MM2P identified as a modulator of macrophage M2 polarization. *Cancer Immunol Res*. (2019) 7:292–305. doi: 10.1158/2326-6066.CIR-18-0145
48. Bonapace L, Coissieux MM, Wyckoff J, Mertz KD, Varga Z, Junt T, et al. Cessation of CCL2 inhibition accelerates breast cancer metastasis by promoting angiogenesis. *Nature*. (2014) 515:130–3. doi: 10.1038/nature13862
49. Zhang J, Lu Y, Pienta KJ. Multiple roles of chemokine. (C-C motif) ligand 2 in promoting prostate cancer growth. *J Natl Cancer Institute*. (2010) 102:522–8. doi: 10.1093/jnci/djq044
50. Pena CG, Nakada Y, Saatcioglu HD, Aloisio GM, Cuevas I, Zhang S, et al. LKB1 loss promotes endometrial cancer progression via CCL2-dependent macrophage recruitment. *J Clin Invest*. (2015) 125:4063–76. doi: 10.1172/JCI82152
51. Chen C, He W, Huang J, Wang B, Li H, Cai Q, et al. LNMAT1 promotes lymphatic metastasis of bladder cancer via CCL2 dependent macrophage recruitment. *Nat Commun*. (2018) 9:3826. doi: 10.1038/s41467-018-06152-x
52. Wang S, Liang K, Hu Q, Li P, Song J, Yang Y, et al. JAK2-binding long noncoding RNA promotes breast cancer brain metastasis. *J Clin Invest*. (2017) 127:4498–515. doi: 10.1172/JCI91553
53. Kumar V, Patel S, Tcyganov E, Gabrilovich DI. The nature of myeloid-derived suppressor cells in the tumor microenvironment. *Trends Immunol*. (2016) 37:208–20. doi: 10.1016/j.it.2016.01.004
54. Gabrilovich DI, Nagaraj S. Myeloid-derived suppressor cells as regulators of the immune system. *Nat Rev Immunol*. (2009) 9:162–74. doi: 10.1038/nri2506
55. Bronte V, Zanovello P. Regulation of immune responses by L-arginine metabolism. *Nat Rev Immunol*. (2005) 5:641–54. doi: 10.1038/nri1668
56. Gao Y, Wang T, Li Y, Zhang Y, Yang R. Lnc-chop promotes immunosuppressive function of myeloid-derived suppressor cells in tumor and inflammatory environments. *J Immunol*. (2018) 200:2603–14. doi: 10.4049/jimmunol.1701721
57. Gao Y, Sun W, Shang W, Li Y, Zhang D, Wang T, et al. Lnc-C/EBPbeta negatively regulates the suppressive function of myeloid-derived suppressor cells. *Cancer Immunol Res*. (2018) 6:1352–63. doi: 10.1158/2326-6066.CIR-18-0108
58. Movahedi K, Guilliams M, Van den Bossche J, Van den Bergh R, Gysemans C, Beschin A, et al. Identification of discrete tumor-induced myeloid-derived suppressor cell subpopulations with distinct T cell-suppressive activity. *Blood*. (2008) 111:4233–44. doi: 10.1182/blood-2007-07-099226
59. Lang S, Bruderek K, Kaspar C, Hoing B, Kanaan O, Dominas N, et al. Clinical relevance and suppressive capacity of human myeloid-derived suppressor cell subsets. *Clin Cancer Res*. (2018) 24:4834–44. doi: 10.1158/1078-0432.CCR-17-3726
60. Tian X, Tian J, Tang X, Rui K, Zhang Y, Ma J, et al. Particulate beta-glucan regulates the immunosuppression of granulocytic myeloid-derived suppressor cells by inhibiting NFIA expression. *Oncoimmunology*. (2015) 4:e1038687. doi: 10.1080/2162402X.2015.1038687
61. Zheng Y, Tian X, Wang T, Xia X, Cao F, Tian J, et al. Long noncoding RNA Pvt1 regulates the immunosuppression activity of granulocytic myeloid-derived suppressor cells in tumor-bearing mice. *Molecular Cancer*. (2019) 18:61. doi: 10.1186/s12943-019-0978-2
62. Gonzalez H, Hagerling C, Werb Z. Roles of the immune system in cancer: from tumor initiation to metastatic progression. *Genes Dev*. (2018) 32:1267–84. doi: 10.1101/gad.314617.118

63. Heward JA, Lindsay MA. Long non-coding RNAs in the regulation of the immune response. *Trends Immunol*. (2014) 35:408–19. doi: 10.1016/j.it.2014.07.005
64. Ji J, Yin Y, Ju H, Xu X, Liu W, Fu Q, et al. Long non-coding RNA Lnc-Tim3 exacerbates CD8 T cell exhaustion via binding to Tim-3 and inducing nuclear translocation of Bat3 in HCC. *Cell Death Dis*. (2018) 9:478. doi: 10.1038/s41419-018-0528-7
65. Wu K, Zhao Z, Liu K, Zhang J, Li G, Wang L. Long noncoding RNA lnc-sox5 modulates CRC tumorigenesis by unbalancing tumor microenvironment. *Cell Cycle*. (2017) 16:1295–301. doi: 10.1080/15384101.2017.1317416
66. Togashi Y, Shitara K, Nishikawa H. Regulatory T cells in cancer immunosuppression - implications for anticancer therapy. *Nat Rev Clin Oncol*. (2019). 16:356–71. doi: 10.1038/s41571-019-0175-7
67. Speiser DE, Ho PC, Verdeil G. Regulatory circuits of T cell function in cancer. *Nat Rev Immunol*. (2016) 16:599–611. doi: 10.1038/nri.2016.80
68. Jiang R, Tang J, Chen Y, Deng L, Ji J, Xie Y, et al. The long noncoding RNA lnc-EGFR stimulates T-regulatory cells differentiation thus promoting hepatocellular carcinoma immune evasion. *Nat Commun*. (2017) 8:15129. doi: 10.1038/ncomms15129
69. Pei X, Wang X, Li H. LncRNA SNHG1 regulates the differentiation of Treg cells and affects the immune escape of breast cancer via regulating miR-448/IDO. *Int J Biol Macromolecul*. (2018) 118(Pt A):24–30. doi: 10.1016/j.ijbiomac.2018.06.033
70. Zemmour D, Pratama A, Loughhead SM, Mathis D, Benoist C. Flicr, a long noncoding RNA, modulates Foxp3 expression and autoimmunity. *Proc Natl Acad Sci USA*. (2017) 114:E3472–80. doi: 10.1073/pnas.1700946114
71. Maas SLN, Breakefield XO, Weaver AM. Extracellular vesicles: unique intercellular delivery vehicles. *Trends Cell Biol*. (2017) 27:172–88. doi: 10.1016/j.tcb.2016.11.003
72. Qu L, Ding J, Chen C, Wu ZJ, Liu B, Gao Y, et al. Exosome-transmitted lncARSR promotes sunitinib resistance in renal cancer by acting as a competing endogenous RNA. *Cancer Cell*. (2016) 29:653–68. doi: 10.1016/j.ccell.2016.03.004
73. Zhou R, Chen KK, Zhang J, Xiao B, Huang Z, Ju C, et al. The decade of exosomal long RNA species: an emerging cancer antagonist. *Molecul Cancer*. (2018) 17:75. doi: 10.1186/s12943-018-0823-z
74. Whiteside TL. Tumor-derived exosomes and their role in cancer progression. *Adv Clin Chem*. (2016) 74:103–41. doi: 10.1016/bs.acc.2015.12.005
75. Teng Y, Ren Y, Hu X, Mu J, Samykutty A, Zhuang X, et al. MVP-mediated exosomal sorting of miR-193a promotes colon cancer progression. *Nat Commun*. (2017) 8:14448. doi: 10.1038/ncomms14448
76. Fan Q, Yang L, Zhang X, Peng X, Wei S, Su D, et al. The emerging role of exosome-derived non-coding RNAs in cancer biology. *Cancer Lett*. (2018) 414:107–15. doi: 10.1016/j.canlet.2017.10.040
77. Conigliaro A, Costa V, Lo Dico A, Saieva L, Buccheri S, Dieli F, et al. CD90+ liver cancer cells modulate endothelial cell phenotype through the release of exosomes containing H19 lncRNA. *Molecul Cancer*. (2015) 14:155. doi: 10.1186/s12943-015-0426-x
78. Ma X, Li Z, Li T, Zhu L, Li Z, Tian N. Long non-coding RNA HOTAIR enhances angiogenesis by induction of VEGFA expression in glioma cells and transmission to endothelial cells via glioma cell derived-extracellular vesicles. *Am J Transl Res*. (2017) 9:5012–21.
79. Li X, Lei Y, Wu M, Li N. Regulation of macrophage activation and polarization by HCC-derived exosomal lncRNA TUC339. *Int J Molecul Sci*. (2018) 19:E2958. doi: 10.3390/ijms19102958
80. Li B, Xu H, Han H, Song S, Zhang X, Ouyang L, et al. Exosome-mediated transfer of lncRUNX2-AS1 from multiple myeloma cells to MSCs contributes to osteogenesis. *Oncogene*. (2018) 37:5508–19. doi: 10.1038/s41388-018-0359-0
81. Lin C, Yang L. Long noncoding RNA in cancer: wiring signaling circuitry. *Trends Cell Biol*. (2018) 28:287–301. doi: 10.1016/j.tcb.2017.11.008
82. Evans JR, Feng FY, Chinnaiyan AM. The bright side of dark matter: lncRNAs in cancer. *J Clin Invest*. (2016) 126:2775–82. doi: 10.1172/JCI84421
83. Prensner JR, Chinnaiyan AM. The emergence of lncRNAs in cancer biology. *Cancer Discov*. (2011) 1:391–407. doi: 10.1158/2159-8290.CD-11-0209
84. Fatica A, Bozzoni I. Long non-coding RNAs: new players in cell differentiation and development. *Nat Rev Genet*. (2014) 15:7–21. doi: 10.1038/nrg3606
85. Huarte M. The emerging role of lncRNAs in cancer. *Nat Med*. (2015) 21:1253–61. doi: 10.1038/nm.3981
86. Parasramka MA, Maji S, Matsuda A, Yan IK, Patel T. Long non-coding RNAs as novel targets for therapy in hepatocellular carcinoma. *Pharmacol Therapeut*. (2016) 161:67–78. doi: 10.1016/j.pharmthera.2016.03.004
87. Chen L, Dzakah EE, Shan G. Targetable long non-coding RNAs in cancer treatments. *Cancer Lett*. (2018) 418:119–24. doi: 10.1016/j.canlet.2018.01.042
88. Tan SK, Pastori C, Penas C, Komotar RJ, Ivan ME, Wahlestedt C, et al. Serum long noncoding RNA HOTAIR as a novel diagnostic and prognostic biomarker in glioblastoma multiforme. *Molecul Cancer*. (2018) 17:74. doi: 10.1186/s12943-018-0822-0
89. Lin LY, Yang L, Zeng Q, Wang L, Chen ML, Zhao ZH, et al. Tumor-originated exosomal lncUEGC1 as a circulating biomarker for early-stage gastric cancer. *Molecul Cancer*. (2018) 17:84. doi: 10.1186/s12943-018-0834-9
90. Zhao R, Zhang Y, Zhang X, Yang Y, Zheng X, Li X, et al. Exosomal long noncoding RNA HOTTIP as potential novel diagnostic and prognostic biomarker test for gastric cancer. *Molecul Cancer*. (2018) 17:68. doi: 10.1186/s12943-018-0817-x
91. Schmitt AM, Chang HY. Long noncoding RNAs in cancer pathways. *Cancer Cell*. (2016) 29:452–63. doi: 10.1016/j.ccell.2016.03.010
92. Cabili MN, Trapnell C, Goff L, Koziol M, Tazon-Vega B, Regev A, et al. Integrative annotation of human large intergenic noncoding RNAs reveals global properties and specific subclasses. *Genes Dev*. (2011) 25:1915–27. doi: 10.1101/gad.17446611
93. Buller HR, Bethune C, Bhanot S, Gailani D, Monia BP, Raskob GE, et al. Factor XI antisense oligonucleotide for prevention of venous thrombosis. *N Engl J Med*. (2015) 372:232–40. doi: 10.1056/NEJMoa1405760
94. Gaudet D, Brisson D, Tremblay K, Alexander VJ, Singleton W, Hughes SG, et al. Targeting APOC3 in the familial chylomicronemia syndrome. *N Engl J Med.*. (2014) 371:2200–6. doi: 10.1056/NEJMoa1400284
95. Hong D, Kurzrock R, Kim Y, Woessner R, Younes A, Nemunaitis J, et al. AZD9150, a next-generation antisense oligonucleotide inhibitor of STAT3 with early evidence of clinical activity in lymphoma and lung cancer. *Sci Transl Med*. (2015) 7:314ra185. doi: 10.1126/scitranslmed.aac5272
96. Meng L, Ward AJ, Chun S, Bennett CF, Beaudet AL, Rigo F. Towards a therapy for Angelman syndrome by targeting a long non-coding RNA. *Nature*. (2015) 518:409–12. doi: 10.1038/nature13975
97. Ling H, Fabbri M, Calin GA. MicroRNAs and other non-coding RNAs as targets for anticancer drug development. *Nat Rev Drug Discov*. (2013) 12:847–65. doi: 10.1038/nrd4140
98. Arun G, Diermeier S, Akerman M, Chang KC, Wilkinson JE, Hearn S, et al. Differentiation of mammary tumors and reduction in metastasis upon Malat1 lncRNA loss. *Genes Dev*. (2016) 30:34–51. doi: 10.1101/gad.270959.115
99. Gutschner T, Hammerle M, Eissmann M, Hsu J, Kim Y, Hung G, et al. The noncoding RNA MALAT1 is a critical regulator of the metastasis phenotype of lung cancer cells. *Cancer Res*. (2013) 73:1180–9. doi: 10.1158/0008-5472.CAN-12-2850
100. Vickers TA, Koo S, Bennett CF, Crooke ST, Dean NM, Baker BF. Efficient reduction of target RNAs by small interfering RNA and RNase H-dependent antisense agents. A comparative analysis. *J Biol Chem*. (2003) 278:7108–18. doi: 10.1074/jbc.M210326200
101. Petrocca F, Altschuler G, Tan SM, Mendillo ML, Yan H, Jerry DJ, et al. A genome-wide siRNA screen identifies proteasome addiction as a vulnerability of basal-like triple-negative breast cancer cells. *Cancer Cell*. (2013) 24:182–96. doi: 10.1016/j.ccr.2013.07.008
102. Morrissey DV, Lockridge JA, Shaw L, Blanchard K, Jensen K, Breen W, et al. Potent and persistent in vivo anti-HBV activity of chemically modified siRNAs. *Nat Biotechnol*. (2005) 23:1002–7. doi: 10.1038/nbt1122
103. Gupta RA, Shah N, Wang KC, Kim J, Horlings HM, Wong DJ, et al. Long non-coding RNA HOTAIR reprograms chromatin state to promote cancer metastasis. *Nature*. (2010) 464:1071–6. doi: 10.1038/nature08975
104. Ren S, Liu Y, Xu W, Sun Y, Lu J, Wang F, et al. Long noncoding RNA MALAT-1 is a new potential therapeutic target for castration resistant prostate cancer. *J Urol*. (2013) 190:2278–87. doi: 10.1016/j.juro.2013.07.001
105. Endo H, Shiroki T, Nakagawa T, Yokoyama M, Tamai K, Yamanami H, et al. Enhanced expression of long non-coding RNA HOTAIR is associated

with the development of gastric cancer. *PLoS ONE*. (2013) 8:e77070. doi: 10.1371/journal.pone.0077070
106. Ayatollahi S, Salmasi Z, Hashemi M, Askarian S, Oskuee RK, Abnous K, et al. Aptamer-targeted delivery of Bcl-xL shRNA using alkyl modified PAMAM dendrimers into lung cancer cells. *Int J Biochem Cell Biol*. (2017) 92:210–7. doi: 10.1016/j.biocel.2017.10.005
107. Wilusz JE, JnBaptiste CK, Lu LY, Kuhn CD, Joshua-Tor L, Sharp PA. A triple helix stabilizes the 3' ends of long noncoding RNAs that lack poly(A) tails. *Genes Dev*. (2012) 26:2392–407. doi: 10.1101/gad.204438.112
108. Brown JA, Bulkley D, Wang J, Valenstein ML, Yario TA, Steitz TA, et al. Structural insights into the stabilization of MALAT1 noncoding RNA by a bipartite triple helix. *Nat Struct Molecul Biol*. (2014) 21:633–40. doi: 10.1038/nsmb.2844
109. Zhang B, Mao YS, Diermeier SD, Novikova IV, Nawrocki EP, Jones TA, et al. Identification and Characterization of a Class of MALAT1-like Genomic Loci. *Cell Rep*. (2017) 19:1723–38. doi: 10.1016/j.celrep.2017.05.006
110. Brown JA, Kinzig CG, DeGregorio SJ, Steitz JA. Methyltransferase-like protein 16 binds the 3'-terminal triple helix of MALAT1 long noncoding RNA. *Proc Natl Acad Sci USA*. (2016) 113:14013–8. doi: 10.1073/pnas.1614759113

Conflict of Interest Statement: The authors declare that the research was conducted in the absence of any commercial or financial relationships that could be construed as a potential conflict of interest.

frontiers in Oncology

MINI REVIEW
published: 14 February 2020
doi: 10.3389/fonc.2020.00035

Long Non-coding Wilms Tumor 1 Antisense RNA in the Development and Progression of Malignant Tumors

*Ye Zhang, Lin-Jun Fan, Yi Zhang, Jun Jiang and Xiao-Wei Qi**

Department of Breast and Thyroid Surgery, Southwest Hospital, Third Military Medical University (Army Medical University), Chongqing, China

A growing number of studies have shown that long non-coding RNAs (lncRNAs) play an important role in tumor development and progression and are key molecules affecting tumor progression. The lncRNA Wilms tumor 1 antisense RNA (WT1-AS) is specifically expressed in various malignant tumors. In particular, WT1-AS expression is upregulated in colon cancer and breast cancer but is significantly downregulated in cervical cancer, liver cancer, and kidney cancer. The level of WT1-AS expression is closely related to the size, stage, and patient survival rate of these cancers. In this article, we review the modes of action, expression, function, and mechanisms of WT1-AS in different tumors to provide new targets for tumor diagnosis and treatment.

Keywords: Wilms tumor 1 antisense RNA, tumor, long non-coding RNA, expression, function

OPEN ACCESS

Edited by:
Valeria Poli,
University of Turin, Italy

Reviewed by:
Emanuele Monteleone,
University of Turin, Italy
Mariangela Molando,
Sapienza University of Rome, Italy

****Correspondence:***
Xiao-Wei Qi
qxw9908@foxmail.com

Specialty section:
This article was submitted to Molecular and Cellular Oncology, a section of the journal Frontiers in Oncology

Received: *06 September 2019*
Accepted: *09 January 2020*
Published: *14 February 2020*

Citation:
Zhang Y, Fan L-J, Zhang Y, Jiang J and Qi X-W (2020) Long Non-coding Wilms Tumor 1 Antisense RNA in the Development and Progression of Malignant Tumors. Front. Oncol. 10:35. doi: 10.3389/fonc.2020.00035

INTRODUCTION

Non-coding RNAs (ncRNAs) are a class of non-protein-coding RNAs that mainly include two kinds of RNA: (1) small ncRNAs (sncRNAs) with a length of 21–200 nucleotides such as microRNAs (21–25 nucleotides), transfer RNAs (tRNAs), and small interfering RNAs (siRNA); and (2) long ncRNAs (lncRNAs) with a length of over 200 nucleotides (1, 2). Such ncRNAs play different roles in cells. For example, tRNAs are responsible for carrying and transferring amino acids and are involved in protein translation; sncRNAs are widely used for RNA interference (RNAi), which may act as primers to synthesize double-stranded RNAs (dsRNAs), and then such dsRNAs could serve to amplify siRNA response and allow spreading of RNAi silencing (2).

With the increasing understanding of ncRNAs, multi-faceted, comprehensive, and in-depth studies on their functions, mechanisms of action, and their interactive networks are required to determine their roles under specific conditions, and gain further understanding of various physiological, and pathological processes.

LncRNAs have transcripts of >200 nucleotides (nt) in length. Although lncRNAs barely encode proteins, they can regulate gene expression and participate in various molecular biological processes through mechanisms such as RNAi, gene co-suppression, gene silencing, gene imprinting, and DNA demethylation (2).

LncRNAs are highly diverse and complex endogenous ncRNA molecules involved in the regulation of many biological processes (3, 4). Wilusz et al. and Wang et al. reviewed the function of lncRNAs and proposed that their action can be divided into four modes. (1) Signal: lncRNAs can be activated under specific conditions such as specific expression, DNA damage, and cold condition, and can participate in the regulation of downstream gene expression. (2) Molecular decoy: lncRNAs can form a complex regulatory network directly with proteins or other RNAs once transcribed and can act as molecular blocks to block the translation of target genes. (3) Guide: lncRNAs can bind to proteins and localize the latter to specific DNA sequences to regulate DNA

transcription. The guide role of lncRNAs can be further divided into *cis*-guiding and *trans*-guiding. (4) Scaffold: Protein complexes can bind to lncRNAs and then, through the lncRNAs, can bind to chromatins and DNAs. This enables the regulation of different signaling pathways and the exchange and integration of information (5, 6). Additionally, lncRNAs can also directly participate in protein translation and modification. For example, the antisense RNA of ubiquitin carboxy-terminal hydrolase L1 (*Uchl1*) can participate in the translation and maintain the stability of *Uchl1* mRNA (7). Moreover, overexpressed in colon carcinoma 1 (OCC1) can promote ubiquitination by recruiting the E3 ligase β-TrCP1 and stabilizing its binding to Hu antigen R (HUR) protein (8). Interestingly, Anderson et al. reported that the lncRNA LINC00948 could serve as templates for the translation of functional micropeptides myoregulin (MLN), and MLN was an essential regulator of skeletal muscle activities (9). Similarly, Lu et al. reported the same function of lncRNA and detected 308 lncRNA-encoded new peptides according to shotgun proteomics (10). Those results indicate that lncRNAs are complex and versatile regulators that may be involved in many biological processes. Therefore, great challenges lie in the understanding of the molecular biology of lncRNAs and their uncharted interactions in human disease.

Wilms tumor 1 (*WT1*) is a transcription factor that plays an important role in genitourinary system development and an inhibitory role in the development and progression of Wilms tumor. In addition, *WT1* is widely expressed during fetal spleen, spinal cord, and brain development, suggesting its involvement in the development of these organs (11, 12). The WT1 antisense RNA (WT1-AS) originates from the intron region of WT1 (13). Its expression is regulated by methylation and abnormal splicing and is closely associated with the development and progression of various tumors (14). The function of WT1-AS is highly tissue- and cell-specific and may play distinct roles in different tumors. In-depth research on the roles of WT1-AS in different tumors and its possible mechanisms of action is of great value in cancer diagnosis and treatment. This article provides an overview of the modes of action, expression, and function of WT1-AS in different tumors.

THE MODES OF ACTION OF WILMS TUMOR 1 ANTISENSE RNA IN MALIGNANT TUMORS

As the antisense RNA of *WT1*, WT1-AS primarily acts as a signal and molecular decoy in tumors. Similar to *WT1*, WT1-AS is highly expressed in embryonic kidneys and is highly correlated with *WT1* expression. A subsequent study has demonstrated that WT1-AS can bind to *WT1* mRNA and regulate WT1 protein expression through RNA–RNA interactions (13). Current research shows that the primary modes of action of WT1-AS are signal and molecular decoy. In Wilms tumor and acute myeloid leukemia (AML), a similar mechanism related to WT1-AS–WT1 interaction could regulate the expression of WT1 protein (15). In liver cancer cells, WT1-AS can bind directly to the TATA region of the *WT1* promoter to downregulate *WT1* gene expression (16). Moreover, WT1-AS can bind to microRNAs such as miR-203a-5p and miR-330-5p as a molecular decoy and can inhibit the translation of downstream genes, including *TP53* (tumor protein p53) and *FOXN2* (forkhead box N2) (17, 18), thereby regulating the biological behaviors of tumor cells. Recent studies have found that WT1-AS plays important roles in many tumors, but its role and *WT1* and *TP53* gene expression regulation vary significantly between tumors. Therefore, understanding the specific roles and mechanisms of action of WT1-AS in different tumors can shed new light on comprehensive understanding of the dynamic changes in tumor development and progression and on the search for therapeutic strategies targeting lncRNAs.

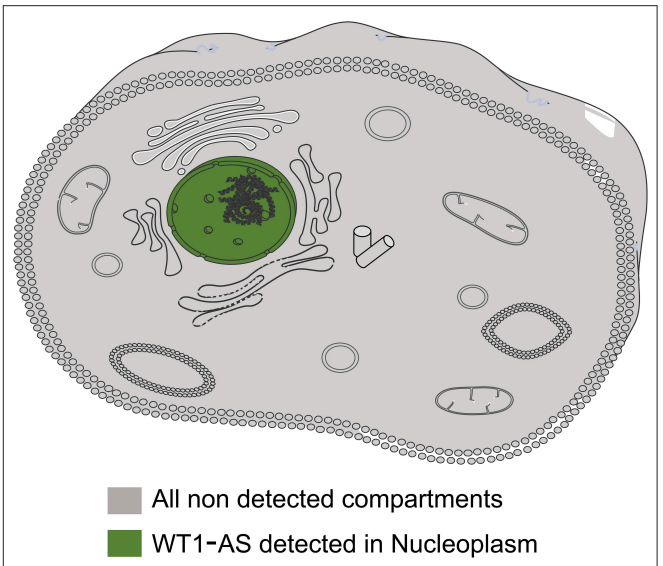

FIGURE 1 | Representative image of cellular localization of Wilms tumor 1 antisense RNA (WT1-AS). The information of WT1-AS cellular localization was derived from RNALocate and lncATLAS; the information provided evidence that WT1-AS is mainly located in the nucleus.

EXPRESSION LEVEL OF WILMS TUMOR 1 ANTISENSE RNA IN MALIGNANT TUMOR CELLS

WT1 is an important transcription factor in various tumors and is mainly located in the nucleus. To identify the subcellular localization of WT1-AS, a search through the RNA localization databases was performed (RNALocate: http://www.rna-society.org/rnalocate/index.html and lncATLAS: http://lncatlas.crg.eu/), which showed that WT1-AS is mainly located in the nucleus, which is similar to WT1 (**Figure 1**).

Numerous studies have shown that WT1-AS expression in tumors is tissue-specific and closely related to tumor development and progression, which is summarized in **Table 1**. Using bioinformatics, Zhang et al. found that WT1-AS expression was upregulated in colon cancer tissue compared with paracancerous tissues, and patients with colorectal cancer with high WT1-AS expression had poorer prognosis (20). Similarly,

TABLE 1 | The association between WT1-AS and the prognosis of patients with malignant tumors.

Tumor type	Expression pattern	Relationship with clinical parameters and prognosis	References
Breast cancer	Upregulated	Patients with high WT1-AS expression had poorer prognosis.	(19)
Colorectal cancer	Upregulated	Patients with high WT1-AS expression had poorer prognosis.	(20)
AML	Upregulated		(15, 21)
Wilms tumor	Upregulated		(15, 21)
Gastric cancer	Downregulated	Low expression was related to clinicopathological parameters such as late staging of the tumor and high degree of infiltration.	(22)
Cervical cancer	Downregulated	Patients with low expression had higher FIGO stage, were more susceptible to lymph node metastasis, and had poorer prognosis.	(17, 18)
Liver cancer	Downregulated	Patients with low WT1-AS expression had lower 5 years survival rates.	(16)
Kidney cancer	Downregulated	WT1-AS expression was an independent predictor of the prognosis of clear cell renal cell carcinoma, and patients with high WT1-AS expression had poorer prognosis.	(23, 24)
Ovarian cancer	Upregulated	Patients with low WT1-AS expression had poor prognosis.	(25–28)

WT1-AS, Wilms tumor 1 antisense RNA; AML, acute myeloid leukemia; FIGO, International Federation of Gynecology and Obstetrics.

Sun et al. screened The Cancer Genome Atlas (TCGA) database for lncRNAs with predictive value for breast cancer prognosis and found that WT1-AS was upregulated in breast cancer. Patients with breast cancer with high WT1-AS expression also had poorer prognosis (19). In addition, others have found that WT1-AS expression is upregulated in AML and Wilms tumor (15, 21). WT1-AS is highly expressed in the aforementioned malignant tumors, and its high expression is significantly associated with late staging and shortened overall survival time. Knocking down WT1-AS expression can significantly reduce tumor cell proliferation and migration.

However, WT1-AS is significantly downregulated in tumors such as gastric cancer, cervical cancer, liver cancer, and kidney cancer; and its biological functions are also quite different. WT1-AS expression is downregulated in gastric cancer tissue compared with that in normal gastric tissue, and its low expression is related to clinicopathological parameters such as late staging of the tumor and high degree of tumor invasion (22). Dai et al. found that WT1-AS expression was downregulated in cervical cancer tissue and that patients with low WT1-AS expression had higher International Federation of Gynecology and Obstetrics (FIGO) stage and were more susceptible to lymph node metastasis (18). Similarly, Cui et al. demonstrated that patients with cervical cancer with low WT1-AS expression had poorer prognosis (17). Lv et al. found lower WT1-AS expression in liver cancer tissue than in cancer-adjacent tissue, and patients with low WT1-AS expression had lower 5 years survival rates (16). Yang et al. compared the lncRNA expression profiles of clear cell renal cell carcinoma (ccRCC) and normal tissue. They found lower WT1-AS expression in ccRCC than in normal tissue, and WT1-AS expression level was significantly correlated with prognosis (23). Moreover, a subsequent study revealed that WT1-AS expression can be used as an independent predictor of ccRCC prognosis and that patients with high WT1-AS expression had poorer prognosis (24).

Interestingly, WT1-AS is differentially expressed in different histological subtypes of ovarian cancer: WT1-AS expression is higher in ovarian cancer tissue than in normal tissue (25). However, CpG island methylation of the *WT1*/*WT1-AS* promoter is higher in ovarian clear cell adenocarcinoma, compared with ovarian serous adenocarcinoma, resulting in the differential expression of WT1-AS between these two tumor types. This may also be the reason why clear cell adenocarcinoma has poorer prognosis than serous adenocarcinoma (26). Similarly, Niskakoski et al. analyzed the differential expression of lncRNAs in various histological subtypes of ovarian cancer and found that non-serous ovarian cancer had a greater degree of epigenetic WT1-AS inactivation than ovarian serous adenocarcinoma (27). In another study, Wang et al. analyzed the competing endogenous RNA (ceRNA) network and found that patients with recurrent ovarian cancer with low WT1-AS expression had poorer prognosis (28).

The above studies demonstrate that WT1-AS expression level is significantly tissue- and cell-specific in different tumors. WT1-AS plays a cancer-promoting role in some tumors but a tumor-suppressing role in others, which may be attributable to the tissue-specific expression of lncRNAs and their complex regulatory network. Therefore, further understanding of the specific roles and mechanisms of action of WT1-AS in different tumors and exploration of the causes of differential WT1-AS expression between tumors is important.

SPECIFIC ROLES AND MECHANISMS OF ACTION OF WILMS TUMOR 1 ANTISENSE RNA IN TUMORS

Wilms Tumor 1 Antisense RNA and Wilms Tumor 1

Although the *WT1* gene plays a tumor-suppressing role in nephroblastoma, it is highly expressed and plays an oncogenic role in breast cancer, lung cancer, and colorectal cancer (29). WT1 has a wide range of biological effects. It not only recognizes and binds to specific target DNAs as a transcription factor and regulates gene transcription but also binds to various growth regulators and the corresponding receptors, thereby playing an important role in cell signal transduction (30). WT1-AS can regulate WT1 protein expression, but its regulatory effects and

mechanisms of action vary between tumors. Dallosso et al. found that AML and Wilms tumor had high *WT1* mutation rates and high *WT1-AS* expression levels (15). WT1-AS may bind to *WT1* mRNA to form a heteroduplex, thereby regulating WT1 protein expression (13). However, how such a heteroduplex is involved in *WT1* expression remains unclear; therefore, the exact mechanism remains to be elucidated. Lv et al. analyzed the correlation between WT1-AS and WT1 in liver cancer and found that WT1-AS was negatively correlated with *WT1* expression. WT1-AS can bind to the TATA region of the WT1 promoter to inhibit WT1 transcription (16).

To determine the correlation between *WT1* mRNA and WT1-AS expression, we performed correlation analysis using Gene Expression Profiling Interactive Analysis (GEPIA; http://gepia.cancer-pku.cn/, an online database based on TCGA), and we found that *WT1* expression is significantly positively correlated with WT1-AS expression in most tumors, which is consistent with the findings of previous studies (including liver cancer) but not with the results of Lv et al. (16) (**Figure 2**). We speculate that this difference is attributable to the fact that the cases collected for the present study were mainly Chinese patients with liver cancer admitted to Nanjing Medical University, whereas the patients included in the TCGA database were mainly from the United States and Europe. Different from those in Asian countries such as China and Japan, where liver cancer is primarily caused by viral hepatitis, cases of liver cancer in the United States and Europe are primarily caused by chronic liver disease resulting from obesity and alcoholism (31, 32). This suggests that WT1-AS and WT1 may have different modes of action under different pathogenic conditions.

The feedback regulatory network of WT1-AS and WT1 may be the key to the different effects of WT1-AS on tumors, but the specific regulatory mechanism remains unclear but is possibly attributable to the methylation level of WT1 sense and antisense strands, histone methylation, and acetylation modifications. At the same time, *WT1* and *WT1-AS* mutations and splice variants may differ between tumors; therefore, these genes may play different roles in various tumors. In-depth study of the WT1–WT1-AS regulatory network in tumors may provide more possibilities for further understanding of the molecular biological characteristics of tumors and for developing new targeted drugs.

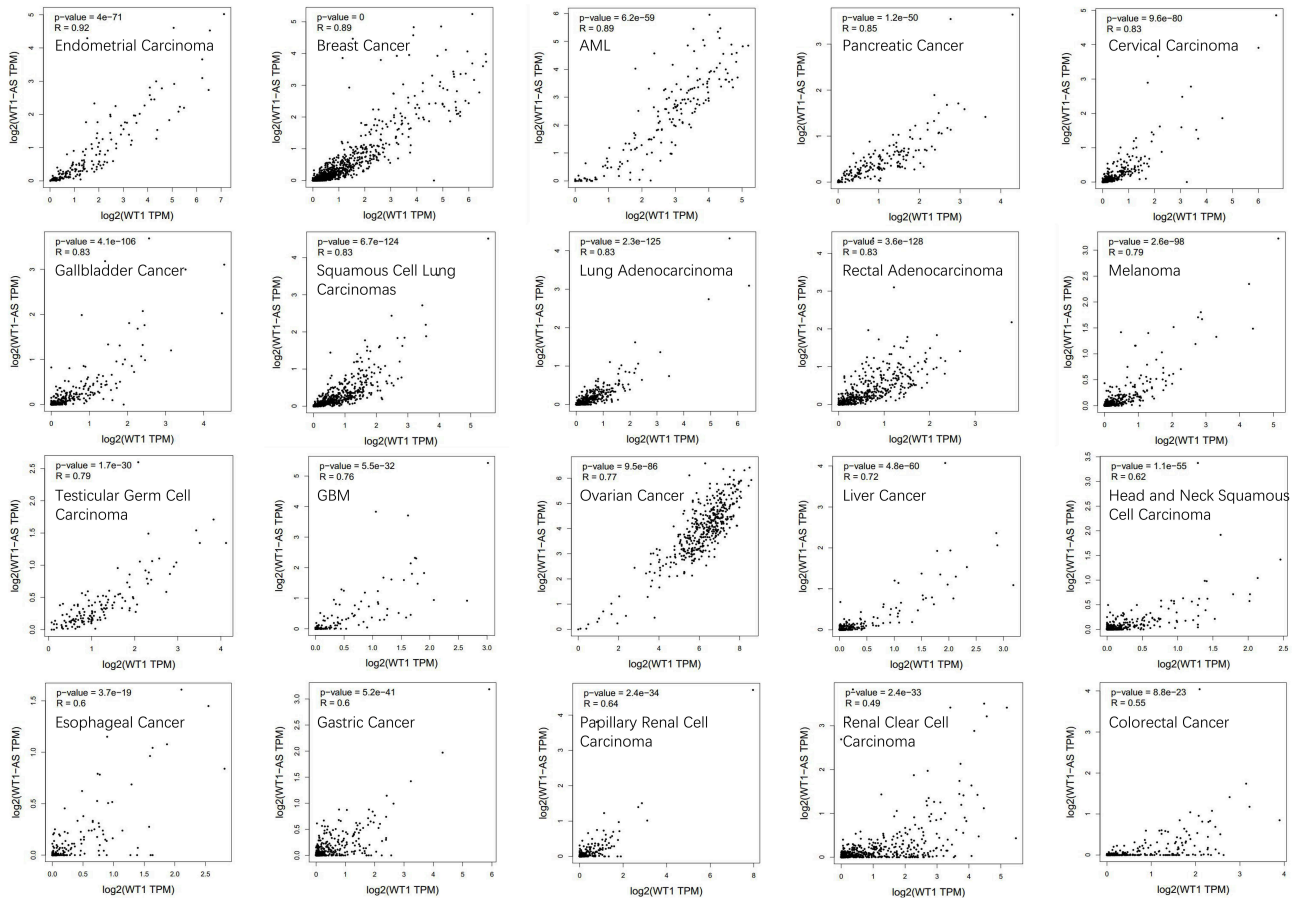

FIGURE 2 | Correlation analysis of Wilms tumor 1 antisense RNA (WT1-AS) and Wilms tumor 1 (*WT1*) mRNA. Data are presented as log scaled, and the correlation analysis was derived from Gene Expression Profiling Interactive Analysis (GEPIA). The correlation coefficient in different cancer types was calculated using the Spearman test. Representative results from 20 common cancers are shown according to their own correlation coefficient. *R*, correlation co-efficient.

Wilms Tumor 1 Antisense RNA and Tumor Cell Proliferation and Apoptosis

The basic biological characteristics of tumor cells are infinite proliferative potential and resistance to death (33). WT1-AS is closely associated with tumor cell proliferation and apoptosis, and its effect on proliferation and apoptosis differs between tumors. Du et al. overexpressed WT1-AS in gastric cancer cell lines and observed slowed cell proliferation and more G1/G0-phase cells. *In vivo* experiments demonstrated that WT1-AS overexpression inhibited tumor formation in mice. The authors also reported that WT1-AS overexpression in gastric cancer cells reduced extracellular signal-regulated kinase (ERK) protein phosphorylation, thereby inhibiting gastric cancer cell proliferation (22). Similar findings have also been observed in cervical cancer (17, 18).

Silencing WT1-AS in ovarian serous adenocarcinoma cell lines can inhibit tumor cell proliferation and downregulate the expression of various oncogenes. In contrast, WT1-AS overexpression can promote tumor cell proliferation (27). Lv et al. found that WT1-AS can downregulate *WT1* expression in liver cancer cells, thereby blocking the JAK/STAT3 (signal transducer and activator of transcription 3) signaling pathway and promoting liver cancer cell apoptosis (16).

The above studies demonstrate that WT1-AS is closely associated with many biological behaviors such as tumor cell proliferation, cell cycle arrest, and resistance to cell death, and that WT1-AS plays different roles in various tumors. Elucidating the regulatory mechanism of WT1-AS in tumor cell proliferation and apoptosis would provide insight in to the development of corresponding diagnostic and treatment strategies to better target and regulate tumor growth.

Wilms Tumor 1 Antisense RNA and Tumor Invasion and Metastasis

The major features of malignant epithelial tumors are invasion and metastasis. They are not only the focus and obstacle of tumor treatment but also complex processes influenced by various regulatory factors, which determine the prognosis of patients with cancer (33). Cui et al. reported that WT1-AS knockdown in the SiHa and CaSKi cervical cancer cell lines increased the invasive and migration abilities of these tumor cells, whereas WT1-AS overexpression attenuated their invasive and migration abilities (17); Dai et al. reported similar results (18). Du et al. found that patients with gastric cancer with low WT1-AS expression were more likely to have local invasion and distant metastasis, whereas WT1-AS overexpression in the HGC7901 and HS-746T gastric cancer cell lines attenuated cell invasion and migration (22). The results of these investigational studies are consistent with the correlation between WT1-AS expression and the clinicopathological parameters of patients with cervical cancer or gastric cancer. However, the specific regulatory mechanism of WT1-AS in the invasion and metastasis of these cancers is still unclear and needs further exploration. Additionally, the regulatory effect of WT1-AS on tumor cell invasion and migration in other cancers remains to be explored further.

Figure 3 summarizes all the reported mechanisms of WT1-AS in malignant tumors.

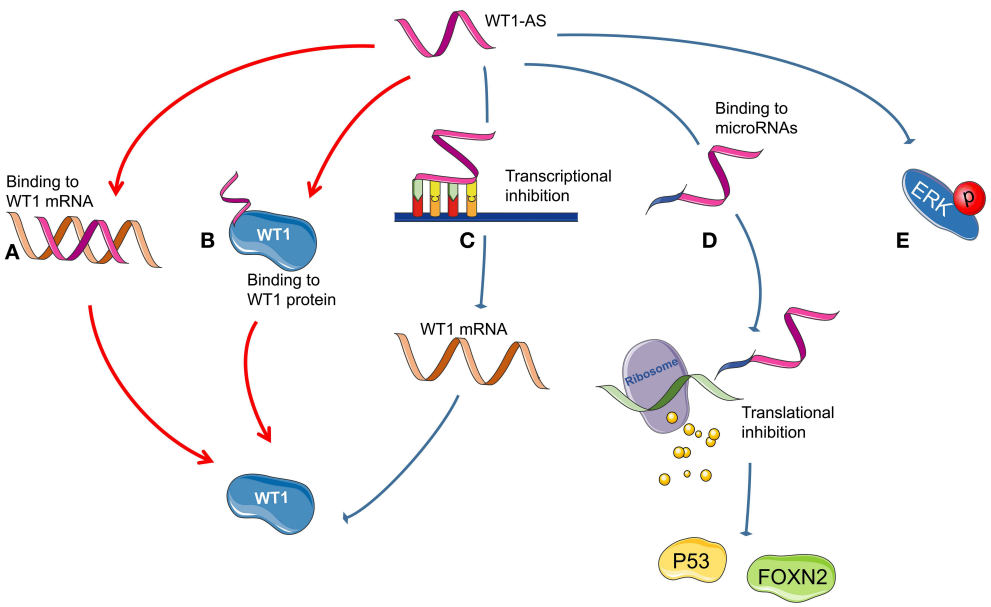

FIGURE 3 | Possible mechanism of Wilms tumor 1 antisense RNA (WT1-AS) functioning. **(A)** A heteroduplex formed by the combination of WT1-AS and Wilms tumor 1 (*WT1*) mRNA could regulate the expression of WT1 protein. **(B)** WT1-AS can bind to WT1 protein to regulate the abundance of WT1 protein. **(C)** WT1-AS can directly bind to the TATA region of the *WT1* promoter, inhibit *WT1* transcription, and downregulate WT1 protein expression, thereby inhibiting the JAK/STAT3 signaling pathway. **(D)** WT1-AS can bind as a molecular decoy to miR-203a-5p and miR-330-5p and can inhibit the translation of downstream genes, including *TP53* and *FOXN2*. **(E)** WT1-AS can reduce extracellular signal-regulated kinase (ERK) phosphorylation.

CONCLUSIONS

As research on the function and mechanisms of action of lncRNAs advances, their role in tumor development and progression has gradually become clearer, and their significance in cancer diagnosis and treatment has attracted increasing research attention. To date, the research progress in WT1-AS appears to clarify that it has some interesting features. Current research indicates that WT1-AS is specifically expressed in malignant tumors, and its expression level is closely related to clinicopathological parameters such as tumor size, tumor-node-metastasis (TNM) stage, and survival, indicating that it plays an important role in such malignant tumors and may serve as a new target for tumor diagnosis and treatment. It is worth noting that WT1-AS plays distinct roles in different tumors, wherein it may be tumor suppressive in some while being cancer promoting in others. Therefore, the specific roles of WT1-AS in different tumors require further validation. As for the antisense RNA of WT1, future progress will be made with the development of new RNA detection technologies to indicate the interaction between WT1 and WT1-AS and its intrinsic mechanisms in different tumors. In addition, the specific regulatory mechanisms of WT1-AS in tumor development and progression remain unclear and require further investigation.

AUTHOR CONTRIBUTIONS

YeZ contributed to the drafting of the manuscript. L-JF and YiZ contributed to the literature search. JJ modified the language. X-WQ contributed to the conception or design of the work. All authors have read and approved the final manuscript.

FUNDING

This study was supported by grants from the National Natural Science Foundation of China (no. 81102030), Biotechnology Innovation Program of Southwest Hospital (no. SWH2016JCYB-39), Talents Training Program of Third Military Medical University (no. 2017MPRC-18), and Military Medical Staff Innovation Plan of Southwest Hospital (no. SWH2018BJLC-04).

REFERENCES

1. Eddy SR. Non-coding RNA genes and the modern RNA world. *Nat Rev Genet.* (2001) 2:919–29. doi: 10.1038/35103511
2. Costa FF. Non-coding RNAs: new players in eukaryotic biology. *Gene.* (2005) 357:83–94. doi: 10.1016/j.gene.2005.06.019
3. St. Laurent G, Wahlestedt C, Kapranov P. The landscape of long noncoding RNA classification. *Trends Genet.* (2015) 31:239–51. doi: 10.1016/j.tig.2015.03.007
4. Li CH, Chen Y. Insight into the role of long non-coding RNA in cancer development and progression. *Int Rev Cell Mol Biol.* (2016) 326:33–65. doi: 10.1016/bs.ircmb.2016.04.001
5. Wilusz JE, Sunwoo H, Spector DL. Long non-coding RNAs: functional surprises from the RNA world. *Genes Dev.* (2009) 23:1494–504. doi: 10.1101/gad.1800909
6. Wang KC, Chang HY. Molecular mechanisms of long non-coding RNAs. *Mol Cell.* (2011) 43:904–14. doi: 10.1016/j.molcel.2011.08.018
7. Carrieri C, Cimatti L, Biagioli M, Beugnet A, Zucchelli S, Fedele S, et al. Long non-coding antisense RNA controls Uchl1 translation through an embedded SINEB2 repeat. *Nature.* (2012) 491:454–7. doi: 10.1038/nature11508
8. Lan Y, Xiao X, He Z, Luo Y, Wu C, Li L, et al. Long non-coding RNA OCC-1 suppresses cell growth through destabilizing HuR protein in colorectal cancer. *Nucleic Acids Res.* (2018) 46:5809–21. doi: 10.1093/nar/gky214
9. Anderson DM, Anderson KM, Chang CL, Makarewich CA, Nelson BR, McAnally JR, et al. A micropeptide encoded by a putative long non-coding RNA regulates muscle performance. *Cell.* (2015) 160:595–606. doi: 10.1016/j.cell.2015.01.009
10. Lu S, Zhang J, Lian X, Sun L, Meng K, Chen Y, et al. A hidden human proteome encoded by "non-coding" genes. *Nucleic Acids Res.* (2019) 47:8111–25. doi: 10.1093/nar/gkz646
11. Pritchard-Jones K, Fleming S, Davidson D, Bickmore W, Porteous D, Gosden C, et al. The candidate Wilms' tumour gene is involved in genitourinary development. *Nature.* (1990) 346:194–7. doi: 10.1038/346194a0
12. Parenti R, Salvatorelli L, Musumeci G, Parenti C, Giorlandino A, Motta F, et al. Wilms' tumor 1 (WT1) protein expression in human developing tissues. *Acta Histochem.* (2015) 117:386–96. doi: 10.1016/j.acthis.2015.03.009
13. Moorwood K, Charles AK, Salpekar A, Wallace JI, Brown KW, Malik K. Antisense WT1 transcription parallels sense mRNA and protein expression in fetal kidney and can elevate protein levels *in vitro*. *J Pathol.* (1998) 185:352–9.
14. Malik K, Salpekar A, Hancock A, Moorwood K, Jackson S, Charles A, et al. Identification of differential methylation of the WT1 antisense regulatory region and relaxation of imprinting in Wilms' tumor. *Cancer Res.* (2000) 60:2356–60.
15. Dallosso AR, Hancock AL, Malik S, Salpekar A, King-Underwood L, Pritchard-Jones K, et al. Alternately spliced WT1 antisense transcripts interact with WT1 sense *RNA* and show epigenetic and splicing defects in cancer. *RNA.* (2007) 13:2287–99. doi: 10.1261/rna.562907
16. Lv L, Chen G, Zhou J, Li J, Gong J. WT1-AS promotes cell apoptosis in hepatocellular carcinoma through down-regulating of WT1. *J Exp Clin Cancer Res.* (2015) 34:119. doi: 10.1186/s13046-015-0233-7
17. Cui L, Nai M, Zhang K, Li L, Li R. lncRNA WT1-AS inhibits the aggressiveness of cervical cancer cell via regulating p53 expression via sponging miR-330–5p. *Cancer Manag Res.* (2019) 11:651–67. doi: 10.2147/CMAR.S176525
18. Dai SG, Guo LL, Xia X, Pan Y. Long non-coding RNA WT1-AS inhibits cell aggressiveness via miR-203a-5p/FOXN2 axis and is associated with prognosis in cervical cancer. *Eur Rev Med Pharmacol Sci.* (2019) 23:486–95. doi: 10.26355/eurrev_201901_16860
19. Sun M, Wu D, Zhou K, Li H, Gong X, Wei Q, et al. An eight-lncRNA signature predicts survival of breast cancer patients: a comprehensive study based on weighted gene co-expression network analysis and competing endogenous RNA network. *Breast Cancer Res Treat.* (2019) 175:59–75. doi: 10.1007/s10549-019-05147-6
20. Zhang H, Wang Z, Wu J, Ma R, Feng J. Long noncoding RNAs predict the survival of patients with colorectal cancer as revealed by constructing an endogenous RNA network using bioinformation analysis. *Cancer Med.* (2019) 8:863–73. doi: 10.1002/cam4.1813
21. Hancock AL, Brown KW, Moorwood K, Moon H, Holmgren C, Mardikar SH, et al. A CTCF-binding silencer regulates the imprinted genes AWT1 and WT1-AS and exhibits sequential epigenetic defects during Wilms' tumourigenesis. *Hum Mol Genet.* (2007) 16:343–54. doi: 10.1093/hmg/ddl478
22. Du T, Zhang B, Zhang S, Jiang X, Zheng P, Li J, et al. Decreased expression of long non-coding RNA WT1-AS promotes cell proliferation and invasion in gastric cancer. *Biochim Biophys Acta.* (2016) 1862:12–9. doi: 10.1016/j.bbadis.2015.10.001
23. Yang K, Lu XF, Luo PC, Zhang J. Identification of six potentially long noncoding RNAs as biomarkers involved competitive endogenous RNA in clear cell renal cell carcinoma. *Biomed Res Int.* (2018) 2018:9303486. doi: 10.1155/2018/9303486

24. Wang J, Zhang C, He W, Gou X. Construction and comprehensive analysis of dysregulated long non-coding RNA-associated competing endogenous RNA network in clear cell renal cell carcinoma. *J Cell Biochem*. (2018) 120:2576–93. doi: 10.1002/jcb.27557
25. Chiu HS, Somvanshi S, Patel E, Chen TW, Singh VP, Zorman B, et al. Pan-cancer analysis of lncRNA regulation supports their targeting of cancer genes in each tumor context. *Cell Rep.* (2018) 23:297–312 e212. doi: 10.1016/j.celrep.2018.03.064
26. Kaneuchi M, Sasaki M, Tanaka Y, Shiina H, Yamada H, Yamamoto R, et al. WT1 and WT1-AS genes are inactivated by promoter methylation in ovarian clear cell adenocarcinoma. *Cancer.* (2005) 104:1924–30. doi: 10.1002/cncr.21397
27. Niskakoski A, Kaur S, Staff S, Renkonen-Sinisalo L, Lassus H, Jarvinen HJ, et al. Epigenetic analysis of sporadic and Lynch-associated ovarian cancers reveals histology-specific patterns of DNA methylation. *Epigenetics.* (2014) 9:1577–87. doi: 10.4161/15592294.2014.983374
28. Wang X, Han L, Zhou L, Wang L, Zhang LM. Prediction of candidate RNA signatures for recurrent ovarian cancer prognosis by the construction of an integrated competing endogenous RNA network. *Oncol Rep.* (2018) 40:2659–73. doi: 10.3892/or.2018.6707
29. Yang L, Han Y, Suarez Saiz F, Minden MD. A tumor suppressor and oncogene: the WT1 story. *Leukemia.* (2007) 21:868–76. doi: 10.1038/sj.leu.2404624
30. Qi XW, Zhang F, Wu H, Liu JL, Zong BG, Xu C, et al. Wilms' tumor 1 (WT1) expression and prognosis in solid cancer patients: a systematic review and meta-analysis. *Sci Rep.* (2015) 5:8924. doi: 10.1038/srep08924
31. Schwaber P. Huston's and Joyce's "The dead". *Psychoanal Study Child.* (1997) 52:332–9. doi: 10.1080/00797308.1997.11822466
32. Fassio E, Diaz S, Santa C, Reig ME, Martinez Artola Y, Alves de Mattos A, et al. Etiology of hepatocellular carcinoma in Latin America: a prospective, multicenter, international study. *Ann Hepatol.* (2010) 9:63–9. doi: 10.1016/S1665-2681(19)31681-3
33. Hanahan D, Weinberg RA. Hallmarks of cancer: the next generation. *Cell.* (2011) 144:646–74. doi: 10.1016/j.cell.2011.02.013

Conflict of Interest: The authors declare that the research was conducted in the absence of any commercial or financial relationships that could be construed as a potential conflict of interest.

frontiers in Oncology

MINI REVIEW
published: 20 March 2020
doi: 10.3389/fonc.2020.00285

Long Non-coding RNAs: Major Regulators of Cell Stress in Cancer

Patrick Connerty, Richard B. Lock and Charles E. de Bock**

Children's Cancer Institute, School of Women's and Children's Health, Lowy Cancer Centre, University of New South Wales (UNSW), Sydney, NSW, Australia

Cellular stress can occur in many forms; oxidative stress caused by reactive oxygen species (ROS), metabolic stress from increased metabolic programs and genotoxic stress in the form of DNA damage and disrepair. In most instances, these different types of cell stress initiate programmed cell death. However, in cancer, cells are able to resist cellular stress and by-pass growth limiting checkpoints. Recent findings have now revealed that the large and heterogenous RNA species known as long non-coding RNAs (lncRNAs) are major players in regulating and overcoming cancer cell stress. lncRNAs constitute a significant fraction of the genes differentially expressed in response to cell stress and contribute to the management of downstream cellular processes, including the regulation of key stress responses such as metabolic stress, oxidative stress and genotoxic stress. This review highlights the complex regulatory role of lncRNAs in the cell stress response of cancer by providing an overview of key examples from recent literature.

Keywords: lncRNA, metabolism, cell stress, oxidative stress, cancer, tumor suppressor gene, genotoxic stress

OPEN ACCESS

Edited by:
Sergio Giannattasio, Istituto di Biomembrane, Bioenergetica e Biotecnologie Molecolari (IBIOM), Italy

Reviewed by:
Graziano Pesole, University of Bari Aldo Moro, Italy
Claudia Cava, National Research Council, Italy

****Correspondence:***
Patrick Connerty
PConnerty@ccia.org.au
Charles E. de Bock
Cdebock@ccia.org.au

Specialty section:
This article was submitted to Molecular and Cellular Oncology, a section of the journal Frontiers in Oncology

Received: *02 December 2019*
Accepted: *18 February 2020*
Published: *20 March 2020*

Citation:
Connerty P, Lock RB and de Bock CE (2020) Long Non-coding RNAs: Major Regulators of Cell Stress in Cancer. Front. Oncol. 10:285. doi: 10.3389/fonc.2020.00285

INTRODUCTION

When the first draft of the Human Genome Project was completed in 2001 it came as a major surprise that protein-coding genes accounted for as little as 1–2% of the human genome (1). Initial thoughts were that this non-coding element of our DNA was merely genetic noise, left over DNA with no function or role and was therefore colloquially named "junk DNA." However, it is now appreciated that most of the genome, while non-protein coding, is transcribed into RNA and these transcripts appear to be functionally different RNA species (2).

It has since been identified that our genome encodes for both long (>200 nucleotide) and short (<200 nucleotide) non-coding RNA species. Short-RNA species include microRNAs, short interfering RNAs, Piwi-interacting, and small nucleolar RNAs. All of these have distinct roles in either positively or negatively regulating gene expression via epigenetic and post-transcriptional regulation of target mRNAs (3). Long non-coding RNAs (lncRNAs), loosely described as non-protein-coding transcripts of >200 nucleotides, are a diverse group of RNA molecules which have been discovered to promote and inhibit gene expression via a variety of mechanisms (4).

Recently, considerable research has now shown that lncRNAs are important regulators of the cellular stress response and thereby implicated in the maintenance of human cancer. The aim of this review is to highlight some of the recent key developments for the role of lncRNAs in cellular stress in cancer.

LONG NON-CODING RNAS

lncRNAs are broadly defined as non-protein coding transcripts longer than 200 nucleotides. Similar to protein coding mRNA, the majority of lncRNAs are transcribed by RNA polymerase II, with some exceptions transcribed by RNA Pol III (5). These lncRNAs can also be poly-adenylated, spliced, expressed stably and localized in the nucleus, cytosol or mitochondria (6).

CLASSIFICATION

There is wide literature on the classification of non-coding RNAs which is constantly being updated as new discoveries are made about this extensive RNA species. lncRNAs can be classified by a diverse range of features such as genomic location and biogenesis, lncRNA structure, protein binding motif (k-mers) and mechanism of action (7, 8). At their simplest level, however, lncRNAs can be classified by their location relative to coding loci along the genome into 5 main categories: (1) sense; (2) antisense; (3) bi-directional; (4) intergenic; and, (5) intronic (**Figures 1A–E**). Sense lncRNA are transcribed from the sense strand of protein-coding genes and contain exons from protein coding genes. They sometimes overlap with part of the protein-coding gene or cover the entire sequence of a protein coding gene through an intron. Anti-sense lncRNAs, as their name suggests, are the opposite of sense lncRNAs and are transcribed from the anti-sense strand of protein coding genes. Bi-directional lncRNAs are similar to anti-sense lncRNAs but located in close proximity (within 1 kb) to the transcriptional start site of a protein coding gene and do not overlap, or only partially overlap, with their paired protein coding gene. Intergenic lncRNAs (lincRNAs) do not intersect with any protein-coding gene annotations and are located in the long stretches of intergenic space present in the human genome. Finally, intronic lncRNAs are restricted to protein coding gene introns and are either independent unique transcripts or created as a by-product of the pre-mRNA splicing.

FUNCTION

lncRNAs have diverse roles in cellular process such as acting as epigenetic modulators, promoting or inhibiting transcription, splicing, translation, and modulating protein function. lncRNAs achieve this through four main mechanisms (**Figures 1F–I**):

Guidance: lncRNAs can act as guides for specific proteins and facilitate their localization within the cell or to a specific genetic locus to enable their action. For example, one of the first lncRNAs documented, Xist, is able to accumulate on the entire length of the X chromosome and induce heterochromatin formation via recruiting components of the PRC2 polycomb protein complex. This results in X chromosome inactivation in humans and mice (9).

Decoy: lncRNAs can bind to and inhibit a protein target or titrate out protein or other non-coding RNA (such as a miRNA). Examples of this include the lncRNA GAS5 which contains hairpin structures which function as glucocorticoid receptor mimics, sequestering activated glucocorticoid receptor (10), or lncRNA-PAGBC which competitively binds miRNA to alleviate mRNA repression (11).

Scaffold: lncRNAs that serve as a central platform to recruit multiple proteins into ribonucleoprotein complexes. For example, HOTAIR, which acts as modular scaffold of histone modification complexes (12).

Signal: lncRNAs which may not necessarily have a direct biological function but can act as a cellular signal because their transcription occurs at a very specific time and cellular location—related to developmental cues or stimuli response. For example the lncRNA linc-p21 acts as a transcriptional repressor in the *p53* pathway and is upregulated directly in response to DNA damage (13).

It should be noted that these functions are not mutually exclusive, and some lncRNAs such as HOTAIR, have been documented to regulate gene expression through a combination of the above functional mechanisms. By facilitating the binding of histone modification complexes, HOTAIR acts as a modular scaffold, and by targeting the PRC2 complex to specific genomic locations, it serves as a guide. Furthermore, lncRNAs utilize the mechanisms of action outlined above to function as lncRNA oncogenes or lncRNA tumor suppressors in a cancer specific context. These two functional groups can be defined as a gene that encodes a lncRNA with the ability to directly promote tumorigenesis or a gene that encodes a lncRNA with the ability to directly inhibit tumorigenesis respectively. As our knowledge of lncRNAs role in oncogenic gene regulation widens so too does our understanding on the key roles these RNA molecules play in a cancer cells ability to survive cell stresses.

THE CANCER SPECIFIC ROLE OF LONG NON-CODING RNAS IN CELLULAR STRESS

In order for a cell to develop into a cancer it must overcome a number of anti-oncogenic checkpoints originally referred to as the "hallmarks" of cancer. Historically there were six hallmarks needed to be overcome for a cell to develop into a cancer. This list included; a cell to develop insensitivity to anti-growth signals, sustained angiogenesis, limitless replication potential, self-sufficiency in growth signals, and evasion of apoptosis (14). Recently, the list was updated to include immune system evasion and importantly, deregulation of metabolism (15) a central process in cellular stress responses.

A key feature of cancer cells is their ability overcome environmental stresses including but not limited to hypoxia, nutrient deprivation, and exposure to DNA-damaging agents (16). To survive these stressful conditions, cancer cells utilize the hallmarks of cancer and alter gene expression, reprogram metabolic pathways and evade growth inhibition signaling. lncRNAs have now been implicated in both positively and negatively regulating, metabolic stress, oxidative stress and genotoxic stress of cancer cells (**Table 1**) as well as an appreciable number of cancer-related cell signaling pathways (35).

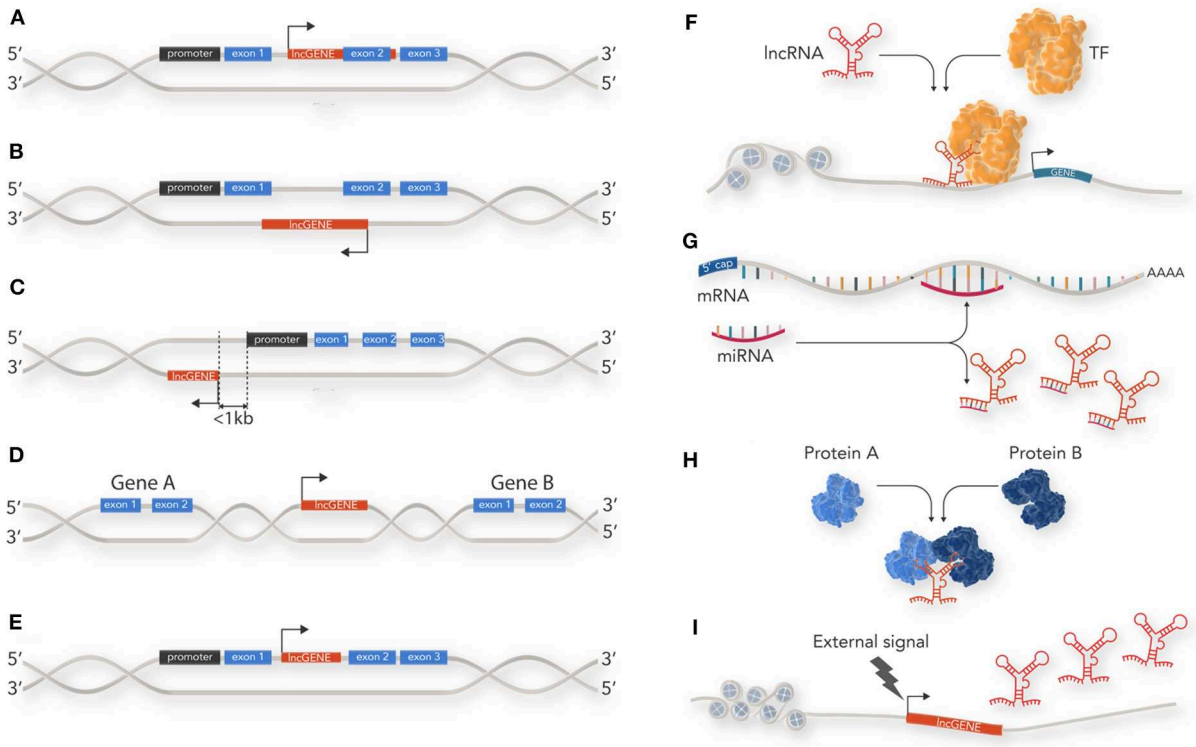

FIGURE 1 | Classification and cellular function of lncRNAs: lncRNAs are classified by their location relative to coding loci along the genome. **(A)** sense lncRNAs are transcribed from the sense strand of protein-coding genes and contain exons from protein coding genes. **(B)** Antisense lncRNAs are the opposite of sense lncRNAs and are transcribed from the anti-sense strand of protein coding genes. **(C)** Bi-directional lncRNAs are similar to anti-sense lncRNAs but located in close proximity (within 1 kb) to the transcriptional start site of a protein coding gene and do not overlap, or only partially overlap, with their paired protein coding gene. **(D)** Intergenic lncRNAs (lincRNAs) do not intersect with any protein-coding gene annotations and are located in the long stretches of intergenic space present in the human genome. **(E)** Intronic lncRNAs are restricted to protein coding gene introns. **(F)** lncRNAs can act as guides for specific proteins and facilitate their localization within the cell or to a specific genetic locus to enable their action. For example, recruitment of transcription factor (TF) to a gene promotor. **(G)** lncRNAs can act as decoys by sequestering inhibitory RNAs, such as miRNAs, and prevent mRNA degradation. **(H)** lncRNAs can act as scaffolds for proteins within a larger protein complex. **(I)** lncRNAs can act as a cellular signal by which lncRNA transcription occurs at a very specific time and cellular location related to developmental cues or stimuli response.

METABOLIC STRESS

The reprogramming of metabolism is now recognized as one of the hallmarks of cancer. Most cancers utilize an inefficient aerobic glycolysis pathway in favor of oxidative phosphorylation for their energy production (termed the Warburg effect) (36). This abnormal metabolic program allows cancer cells to produce the high levels of cellular energy needed for rapid proliferation. However, inefficient metabolic processing can also lead to an increase in stress as the cancer cells attempt to overwork metabolic networks. In order to deal with this increased stress burden cancer cells often over express key enzymatic proteins of cellular energy production pathways (such as AMPK, PKM2, MYC) or downregulate metabolic suppressors (such as p53). It is now becoming apparent that lncRNAs are key players in enabling cancer cells to reprogram metabolism and deal with metabolic stress (**Figure 2**) (37).

Some lncRNAs are able to act as oncogenes and enable cells to overcome metabolic stress loads through promoting the expression of key genes that facilitate metabolic plasticity. In gastric cancer cells the lncRNA MACC1-AS1, is able to stabilize its sense MACC1 RNA and post-transcriptionally increase MACC1 expression. MACC1 upregulation then mediates metabolic plasticity through the AMPL/Lin28 pathway and maintains the expression of key metabolic enzymes GLUT1, HK2, and LDH throughout glucose deprivation (17). Similarly, in colorectal cancer cells, the lncRNA GLCC1 is expressed in response to glucose starvation. GLCC1 then stabilizes the oncogenic transcription factor C-MYC from ubiquitination mediated degradation by directly binding with HSP90. This in turn allows the cells to survive high rates of glycolysis and lactate generation (18). Finally, in melanoma, the lncRNA SAMMSON was found to promote mitochondrial stability via sequestering p32, a key regulator of mitochondrial homeostasis and metabolism, in the cytoplasm where it stabilized mitochondria and promoted proliferation. Depletion of SAMMSON directly resulted in structurally aberrant mitochondria which were sensitive to accumulation of mitochondrial peptide precursors and mitochondrial import defects, collectively known as mitochondrial precursor-over-accumulation stress (mPOS) (19).

In contrast, other lncRNAs can act as tumor supressors to inhibit tumor cell survival and are often down regulated

TABLE 1 | List of lncRNAs implicated in cancer cells in response to different stress types.

lncRNA	lncRNA alias	Cancer	Stress type	Role	Reference
MACC1-AS1	MACC1-AS1	Gastric	Metabolic	Pro-Oncogenic	(17)
GLCC1	AF339830	Colorectal	Metabolic	Pro-Oncogenic	(18)
SAMMSON	SAMMSON	Melanoma	Metabolic	Pro-Oncogenic	(19)
FILNC1	FILNC1	Renal	Metabolic	Anti-Oncogenic	(20)
IDH1-AS1	IDH-AS1	Colon/Cervical	Metabolic	Anti-Oncogenic	(21)
NBR2	NBR2	Breast	Metabolic	Anti-Oncogenic	(22)
HAND2-AS1	HAND2-AS1	Osteosarcoma	Metabolic	Anti-Oncogenic	(23)
H19	H19	Cholangiocarcinoma/ Pituitary	Metabolic/Oxidative	Both Pro and Anti Oncogenic	(24, 25)
HULC	HULC	Cholangiocarcinoma	Oxidative	Pro-Oncogenic	(25)
NLUCAT1	Lnc-ARRDC3-1	Lung adenocarcinoma	Oxidative	Pro-Oncogenic	(26)
NONHSAT1010169	NOAT113026	Breast	Genotoxic	Pro-Oncogenic	(27)
GUARDIN	LNCTAM34A	Breast	Genotoxic	Pro-Oncogenic	(28)
NEAT1	NEAT1	Multiple Myeloma	Genoxtoxic	Pro-Oncogenic	(29)
BORG	BMP/OP-responsive gene	Breast	Genotoxic	Pro-Oncogenic	(30)
PRAL	PRAL	Hepatocellular Carcinoma	Genotoxic	Anti-Oncogenic	(31)
LOC572558	HSALNT0149810	Bladder	Genotoxic	Anti-Oncogenic	(32)
LincRNA-p21	TP53COR1	Lung/Sarcoma/Lymphoma	Genotoxic	Anti-Oncogenic	(13, 33)
PANDA	PANDAR	Bone	Genotoxic	Anti-Oncogenic	(34)

in cancer cells. In renal cancer cells, the lncRNA FILNC1 is significantly down regulated compared to healthy kidney cells. FILNC1 can directly bind with AUF1, a C-MYC mRNA binding protein and inhibits C-MYC mRNA processing resulting in the downregulation of C-MYC protein and altered metabolic plasticity (20). Similarly, the lncRNA IDH1-AS1 is transcriptionally repressed by C-MYC to promote the Warburg effect via HIF1α. Overexpression of IDH1-AS1 in colon and cervical cancer cells resulted in decreased cell proliferation and cancer xenograft growth. IDH1-AS1 was found to promote homodimerization of IDH1, a key protein of the TCA cycle, and decreased glycolysis (21). In breast cancer cells, the lncRNA NBR2 was found to be directly induced by the LKB1-AMPK pathway under energy stress. It in turn regulates AMPK, a critical sensor of cellular energy status, and promotes its kinase activity thus keeping the metabolic pathways of the cell in check. Depletion of NBR2 increased cell proliferation, decreased apoptosis and allowed breast cancer cells to continue cycling under high levels of energy stress (22). Finally, in osteosarcoma, the lncRNA HAND2-AS1 inhibited glucose uptake, lactate production and expression of metabolic enzymes via sequestering FBP1, an inhibitory enzyme of the metabolic gene HIF1α. Furthermore, expression of HAND2-AS1 was directly increased after metabolic stress within the cell. RNAi induced knockdown of HAND2-AS1 relieved the metabolic energy stress induced apoptosis, resulting in cancer cell survival and promoted osteosarcoma progression (23).

However, it should be noted that lncRNAs can act as both tumor suppressors and oncogenes in regulating the cell stress response. For example, whilst overexpression of the lncRNA H19 promotes cholangiocarcinoma cell growth under oxidative stress conditions, in pituitary tumors H19 has been found to act as a tumor suppressor lncRNA and inhibits the ability of cells to respond to metabolic stress. In the pituitary tumor context, H19 directly binds with 4E-BP1 and competitively inhibits it binding to the key energy sensing protein mTORC1, resulting in reduced 4E-BP1 signaling. When H19 is downregulated, 4E-BP1 is able to re-bind mTOR subunits, increasing phosphorylation to prevent its interaction with translation factor elF4E, resulting in increased protein translation, metabolic flexibility, and tumorigenesis. Significantly, over expression of H19 was more effective than the dopamine agonist cabergoline, the first-line treatment for pituitary tumors, at inhibiting tumor cell growth in *in vivo* models (24). Taken together, this highlights that importance of cellular context for lncRNA function and has implications on targeting lncRNAs as part of any future therapeutic strategy.

OXIDATIVE STRESS

Reactive oxygen species (ROS), are the natural by-products of aerobic metabolism in the cell. Mitochondria are the primary source of endogenous ROS. These metabolic molecules play an important role in the physiological function of cells, as both effectors and as signaling molecules. Due to their central role and their potential toxic impact on cellular components, ROS production and removal are tightly controlled processes (38). Cancer cells are often present in hypoxic microenvironments that promote an accelerated metabolism that demands high ROS concentrations for increased proliferation. Different mechanisms are employed by cancer cells to facilitate the high levels of oxidative stress, such as utilization of the pentose phosphate pathway and deregulation of key antioxdative proteins such

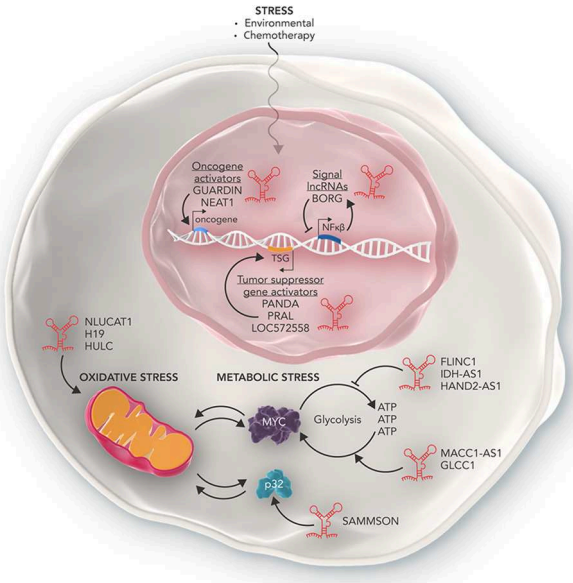

FIGURE 2 | The many roles of lncRNAs in regulating cellular stress. Some lncRNAs such as NLUCAT1, H19, and HULC can promote the ability of cancer cells to overcome oxidative stress in the mitochondria. Other lncRNAs such as MACC1-AS1, GLCC1, and SAMMSON promote the ability of cancer cells to deal with increased metabolic stress and enables cancer cells to produce high amounts of metabolic energy required to rapidly proliferate. Conversely, lncRNAs such as FLINC1, IDH-AS1, and HAND2-AS1 act in an anti-oncogenic manner and inhibit the ability of cancer cells to tolerate metabolic stress via mechanisms such as inhibiting transcription of oncogenic metabolic proteins such as MYC. Furthermore, lncRNAs can also regulate the response of cancer cells to genotoxic stress as a result of chemotherapy. Some lncRNAs can activate oncogenes conferring resistance to genotoxic stress, while others activate tumor suppressor genes and inhibit cancer cell development. Other lncRNAs such as BORG are part of complex feedback loops which help maintain homeostasis of cancer cells in response to genotoxic stress.

as NRF2 (39). However, two recent studies have highlighted roles for lncRNAs in the ability of cancer cells to respond to oxidative stress. In cholangiocarcinoma the lncRNAs H19 and HULC are upregulated in cells as a direct response to exposure to oxidative stress factors such as hydrogen peroxide. These then in turn act as miRNA sponges and sequester let-7a, let-7b and miR-372/miR-373 thereby up-regulating the expression of the cytokine IL-6 that promotes migration and cell invasion in *in vitro* assays (25). In a second study on lung adenocarcinoma, lncRNA NLUCAT1 expression directly promoted the expression of key oxidative homeostasis genes *ALDH3A1*, *GPX2*, *GLRX*, and *PDK4* and therefore the ability of lung cancer cells to resist ROS-induced apoptosis. Consequently depletion of NLUCAT1 could re-sensitize cells to ROS-dependent apoptosis induced by hydrogen peroxide (26).

GENOTOXIC STRESS

Cells undergo genotoxic stress as a result of damage to DNA structure and genome instability (40). The cellular mechanisms of DNA-damage prevention, such as DNA repair, cell cycle checkpoints and apoptosis, all protect cells from acquiring deleterious genetic mutations. However, genotoxic stress often induces carcinogenesis through dysregulating key regulatory pathways of the cell (41). Remarkably in fully established cancer cells, the properties of genotoxic stress are used to treat the disease. The basis of many chemotherapeutic agents is to induce DNA damage and use genotoxic stress responses to induce cell death in cancer cells. However, in therapy-resistant cases, cancer cells can adapt to resist, and overcome genotoxic stress. Cancer cells can resist treatment and genotoxic stress through a variety of mechanisms such as inhibiting tumor suppressor genes, up regulating cellular growth factors and skipping cell cycle checkpoints (42). lncRNAs also play a key role in the ability of cancer cells to overcome genotoxic stress and directly contribute to carcinogenesis, therapy resistance and aggressiveness of cancers (**Figure 2**).

As the fundamental basis of many current chemotherapeutic therapies is to induce genotoxic stress to kill cancer cells, drug resistance and acquired chemoresistance have been identified to be closely associated with genotoxic stress resistance. The altered expression of lncRNAs has now also been identified as an important mechanism to directly promote drug resistance in cancer cells (43). For example, over expression of the lncRNA NONHSAT1010169 in breast cancer tumors, induced resistance to the anthracycline epirubicin, a first-line treatment for metastatic breast cancer. Moreover, forced expression of NONHSAT101069 stimulated the migration and invasion of breast cancer cells, while its depletion re-sensitized resistant breast cancer cells to epirubicin. At the molecular level, it was found that NONHSAT101069 drove epirubicin resistance via sequestering miR-129 which in turn relieved miRNA-inhibition of the oncogenic protein Twist1, increasing drug resistance (27). Another newly described and annotated lncRNA in breast cancer is GUARDIN, a p53-responsive lncRNA, that can sustain cancer cell growth via two key mechanisms; sequestering miR-23a which in turn stabilizes *TRF2* and acting as an RNA scaffold for the oncoprotein BRCA1. Through these interactions GUARDIN is able to protect cells from apoptosis induced by genotoxic stress and drive cancer cell resistance to chemotherapies (28). In multiple myeloma cells, the lncRNA NEAT1 upregulates DNA-repair proteins and enables multiple myeloma cells to resist massive amounts of genotoxic stress. As anticipated, knockdown of NEAT1 results in a downregulation of DNA-repair processes and re-sensitizes multiple myeloma cells to common chemotherapeutic agents (29).

In other cases, lncRNAs are able to be directly induced by genotoxic stress and provide resistance to cancer cells as a type of pro-cancer cell-stress response. One example is the lncRNA BORG. BORG is induced within breast cancer cells which have been exposed to environmental and chemotherapeutic stresses commonly faced by cancer cells undergoing treatment. Exposure of breast cancer cells to doxorubicin results in a rapid and marked increase in the expression of BORG. This expression is driven by NF-kB, which in a feed-forward loop manner drives NF-kB activity and provides breast cancer cells with chemoresistance

properties reducing the extent of DNA damage caused by chemotherapeutic agents. Knockdown of BORG results in re-sensitization of breast cancer cells. BORG provides a great example of how the synthesis of lncRNAs is extremely rapid, compared to protein synthesis, and thus how lncRNAs are ideal genetic tools that can be readily deployed when cells are subject to stress (30).

Alternatively, lncRNAs can also inhibit the ability of cancer cells to respond to genotoxic stress. This is often through enhancing DNA-damage response pathways and promoting genotoxic induced cell cycle arrest and apoptosis. One of the most well-studied and iconic enzymes of the DNA-damage response pathway is the tumor suppressor gene *TP53*. The p53 protein regulates the expression of hundreds of genes that are involved in multiple biological processes, including DNA damage repair, cell cycle arrest and apoptosis. In the case of genotoxic stress, p53 is considered the key "decision making" transcription factor that determines cellular outcomes (44). lncRNAs are now found to be positively promoted or associated with p53 and the DNA-damage pathway. PRAL is one such p53 associated lncRNA. PRAL is a hepatocellular carcinoma related lncRNA whose genomic alterations are significantly associated with hepatocellular carcinoma patient survival. PRAL can inhibit the growth of hepatocellular carcinoma and induce apoptosis via p53 in both *in vitro* and *in vivo* settings. It achieves this by facilitating the combination of HSP90 and p53 through RNA-scaffolding and thereby inhibiting p53 ubiquitination and subsequent degradation (31). Another example of p53 enhancing lncRNAs is LOC572558. Over expression of the lncRNA LOC572558, which is found to be down regulated in bladder cancer, is able to enhance the phosphorylation of p53. This in turn enhances p53 signaling to inhibit bladder cancer cell proliferation (32). Furthermore, the LincRNA-p21 is a vital enabler of p53. LincRNA-p21 is essential to p53-mediated apoptosis in response to DNA damage. It does this by recruiting hnRNP-K to increase p53-dependent transcription of p21 (a key checkpoint protein in the p53 pathway). After lincRNA-p21 depletion, hnRNP-K binds to the promoters of p53-repressed genes, this results in increased proliferation rates and faulty G1/S check points (33, 45). Many lncRNAs have documented supportive effects on p53 activity and stability, however, the exact mechanisms by which this is achieved remains unknown. For example, the lncRNA PANDA stabilizes p53 protein, not mRNA, expression and protects it from proteasome degradation via an as yet, unknown mechanism (34). The role of lncRNAs in regulating the p53 signaling network is such an extensive and emerging field in the space of lncRNA biology that a dedicated database TP53LNC-DB has been recently created which annotates currently available information of lncRNAs in human p53 signaling (46).

Together this highlights the ability of lncRNA in cancer cells to resist genotoxic stress, their ever-growing value as biomarkers for diagnosing cancer, and as therapeutic targets for developing new treatments for drug resistant cancers or inhibiting cancer cell progression (47, 48).

CONCLUDING REMARKS

In conclusion, the ability of cancer cells to survive and react to cellular stresses is one of the key features which defines their capacity to cause disease and evade therapy. We are now appreciating that there is a secondary "non-coding" level of complexity which governs cancer stress responses to a range of diverse pressures. The key RNA species, lncRNAs, are able to modulate genetic regulation and cellular pathways in an oncogenic manner allowing cancer cells to survive high levels of cellular stress that would otherwise kill healthy cells. Importantly, lncRNAs are also able to act as tumor suppressors in regulating cellular stress, with the same lncRNA performing opposite roles in different tissues, highlighting the tissue-specific complexity of these RNA molecules. While this review is far from an exhaustive list of lncRNAs in regulating cancer cell stress, the studies highlighted in this review exemplify the pleiotropic effects of lncRNAs on cell stress in cancer. Future studies will continue to elucidate more functions of lncRNAs in cancer-stress responses that will help provide important insight into lncRNA action, allowing us to harness them for therapeutic strategies and proving that this "junk" isn't junk at all.

AUTHOR CONTRIBUTIONS

PC, RL, and CB all made substantial, direct and intellectual contributions to this manuscript, and approved it for publication.

REFERENCES

1. Lander ES, Linton LM, Birren B, Nusbaum C, Zody MC, Baldwin J, et al. Initial sequencing and analysis of the human genome. *Nature*. (2001) 409:860–921. doi: 10.1038/35057062
2. Birney E, Stamatoyannopoulos JA, Dutta A, Guigó R, Gingeras TR, Margulies EH, Weng Z, Snyder M, Dermitzakis ET, Thurman RE, et al. Identification and analysis of functional elements in 1% of the human genome by the ENCODE pilot project. *Nature*. (2007) 447:799–816. doi: 10.1038/nature05874
3. Svoboda P. Renaissance of mammalian endogenous RNAi. *FEBS Lett*. (2014) 588:2550–6. doi: 10.1016/j.febslet.2014.05.030
4. Rinn JL, Chang HY. Genome regulation by long noncoding RNAs. *Annu Rev Biochem*. (2012) 81:145–66. doi: 10.1146/annurev-biochem-051410-092902
5. Massone S, Ciarlo E, Vella S, Nizzari M, Florio T, Russo C, et al. NDM29, a RNA polymerase III-dependent non coding RNA, promotes amyloidogenic processing of APP and amyloid β secretion. *Biochim Biophys Acta*. (2012) 1823:1170–7. doi: 10.1016/j.bbamcr.2012.05.001
6. Zhao Y, Liu S, Zhou L, Li X, Meng Y, Li Y, et al. Aberrant shuttling of long noncoding RNAs during the mitochondria-nuclear crosstalk in hepatocellular carcinoma cells. *Am J Cancer Res*. (2019) 9:999–1008.
7. Dahariya S, Paddibhatla I, Kumar S, Raghuwanshi S, Pallepati A, Gutti RK. Long non-coding RNA: classification, biogenesis and functions in blood cells. *Mol Immunol*. (2019) 112:82–92. doi: 10.1016/j.molimm.2019.04.011
8. Kirk JM, Kim SO, Inoue K, Smola MJ, Lee DM, Schertzer MD, et al. Functional classification of long non-coding RNAs by k-mer content. *Nat Genet*. (2018) 50:1474–82. doi: 10.1038/s41588-018-0207-8
9. Maenner S, Blaud M, Fouillen L, Savoye A, Marchand V, Dubois A, et al. 2-D structure of the a region of Xist RNA and its implication for PRC2 association. *PLoS Biol*. (2010) 8:107. doi: 10.1371/journal.pbio.1000276

10. Kino T, Hurt DE, Ichijo T, Nader N, Chrousos GP. Noncoding RNA Gas5 is a growth arrest- and starvation-associated repressor of the glucocorticoid receptor. *Sci Signal*. (2010) 3:ra8. doi: 10.1126/scisignal.2000568
11. Wu X, Wang F, Li H, Hu Y, Jiang L, Zhang F, et al. Lnc RNA - PAGBC acts as a micro RNA sponge and promotes gallbladder tumorigenesis. *EMBO Rep*. (2017) 18:1837–53. doi: 10.15252/embr.201744147
12. Tsai MC, Manor O, Wan Y, Mosammaparast N, Wang JK, Lan F, et al. Long noncoding RNA as modular scaffold of histone modification complexes. *Science*. (2010) 329:689–93. doi: 10.1126/science.1192002
13. Hall JR, Messenger ZJ, Tam HW, Phillips SL, Recio L, Smart RC. Long noncoding RNA lincRNA-p21 is the major mediator of UVB-induced and p53-dependent apoptosis in keratinocytes. *Cell Death Dis*. (2015) 6:e1700. doi: 10.1038/cddis.2015.67
14. Hanahan D, Weinberg RA. The hallmarks of cancer. *Cell*. (2000) 100:57–70. doi: 10.1016/S0092-8674(00)81683-9
15. Hanahan D, Weinberg RA. Hallmarks of cancer: the next generation. *Cell*. (2011) 144:646–74. doi: 10.1016/j.cell.2011.02.013
16. Fulda S, Gorman AM, Hori O, Samali A. Cellular stress responses: cell survival and cell death. *Int J Cell Biol*. (2010)1687–8876. doi: 10.1155/2010/214074
17. Zhao Y, Liu Y, Lin L, Huang Q, He W, Zhang S, et al. The lncRNA MACC1-AS1 promotes gastric cancer cell metabolic plasticity via AMPK/Lin28 mediated mRNA stability of MACC1. *Mol Cancer*. (2018) 17:69. doi: 10.1186/s12943-018-0820-2
18. Tang J, Yan T, Bao Y, Shen C, Yu C, Zhu X, et al. LncRNA GLCC1 promotes colorectal carcinogenesis and glucose metabolism by stabilizing c-Myc. *Nat Commun*. (2019) 10:3499. doi: 10.1038/s41467-019-11447-8
19. Leucci E, Vendramin R, Spinazzi M, Laurette P, Fiers M, Wouters J, et al. Melanoma addiction to the long non-coding RNA SAMMSON. *Nature*. (2016) 531:518–22. doi: 10.1038/nature17161
20. Xiao ZD, Han L, Lee H, Zhuang L, Zhang Y, Baddour J, et al. Energy stress-induced lncRNA FILNC1 represses c-Myc-mediated energy metabolism and inhibits renal tumor development. *Nat Commun*. (2017) 8:783. doi: 10.1038/s41467-017-00902-z
21. Xiang S, Gu H, Jin L, Thorne RF, Zhang XD, Wu M. LncRNA IDH1-AS1 links the functions of c-Myc and HIF1α via IDH1 to regulate the Warburg effect. *Proc Natl Acad Sci USA*. (2018) 115:E1465–74. doi: 10.1073/pnas.1711257115
22. Liu X, Xiao ZD, Han L, Zhang J, Lee SW, Wang W, et al. LncRNA NBR2 engages a metabolic checkpoint by regulating AMPK under energy stress. *Nat Cell Biol*. (2016) 18:431–42. doi: 10.1038/ncb3328
23. Kang Y, Zhu X, Xu Y, Tang Q, Huang Z, Zhao Z, et al. Energy stress-induced lncRNA HAND2-AS1 represses HIF1α-mediated energy metabolism and inhibits osteosarcoma progression. *Am J Cancer Res*. (2018) 8:526–37.
24. Wu ZR, Yan L, Liu YT, Cao L, Guo YH, Zhang Y, et al. Inhibition of mTORC1 by lncRNA H19 via disrupting 4E-BP1/Raptor interaction in pituitary tumours. *Nat Commun*. (2018) 9:4624. doi: 10.1038/s41467-018-06853-3
25. Wang WT, Ye H, Wei PP, Han BW, He B, Chen ZH, et al. LncRNAs H19 and HULC, activated by oxidative stress, promote cell migration and invasion in cholangiocarcinoma through a ceRNA manner. *J Hematol Oncol*. (2016) 9:1–12. doi: 10.1186/s13045-016-0348-0
26. Moreno Leon L, Gautier M, Allan R, Ilié M, Nottet N, Pons N, et al. The nuclear hypoxia-regulated NLUCAT1 long non-coding RNA contributes to an aggressive phenotype in lung adenocarcinoma through regulation of oxidative stress. *Oncogene*. (2019) 38:7146–65. doi: 10.1038/s41388-019-0935-y
27. Yao N, Fu Y, Chen L, Liu Z, He J, Zhu Y, et al. Long non-coding RNA NONHSAT101069 promotes epirubicin resistance, migration, and invasion of breast cancer cells through NONHSAT101069/miR-129-5p/Twist1 axis. *Oncogene*. (2019) 38:7216–33. doi: 10.1038/s41388-019-0904-5
28. Hu WL, Jin L, Xu A, Wang YF, Thorne RF, Zhang XD, et al. GUARDIN is a p53-responsive long non-coding RNA that is essential for genomic stability. *Nat Cell Biol*. (2018) 20:492–502. doi: 10.1038/s41556-018-0066-7
29. Taiana E, Favasuli V, Ronchetti D, Todoerti K, Pelizzoni F, Manzoni M, et al. Long non-coding RNA NEAT1 targeting impairs the DNA repair machinery and triggers anti-tumor activity in multiple myeloma. *Leukemia*. (2020) 34:234–44. doi: 10.1038/s41375-019-0542-5
30. Gooding AJ, Zhang B, Gunawardane L, Beard A, Valadkhan S, Schiemann WP. The lncRNA BORG facilitates the survival and chemoresistance of triple-negative breast cancers. *Oncogene*. (2019) 38:2020–41. doi: 10.1038/s41388-018-0586-4
31. Zhou CC, Yang F, Yuan S, Ma JZ, Liu F, Yuan JH, et al. Systemic genome screening identifies the outcome associated focal loss of long noncoding RNA PRAL in hepatocellular carcinoma. *Hepatology*. (2016) 63:850–63. doi: 10.1002/hep.28393
32. Zhu Y, Dai B, Zhang H, Shi G, Shen Y, Ye D. Long non-coding RNA LOC572558 inhibits bladder cancer cell proliferation and tumor growth by regulating the AKT–MDM2–p53 signaling axis. *Cancer Lett*. (2016) 380:369–74. doi: 10.1016/j.canlet.2016.04.030
33. Dimitrova N, Zamudio JR, Jong RM, Soukup D, Resnick R, Sarma K, et al. LincRNA-p21 Activates p21 in cis to promote polycomb target gene expression and to enforce the G1/S checkpoint. *Mol Cell*. (2014) 54:777–90. doi: 10.1016/j.molcel.2014.04.025
34. Kotake Y, Kitagawa K, Ohhata T, Sakai S, Uchida C, Niida H, et al. Long non-coding RNA, panda, contributes to the stabilization of p53 tumor suppressor protein. *Anticancer Res*. (2016) 36:1605–11.
35. Fu P, Zheng X, Fan X, Lin A. Role of cytoplasmic lncRNAs in regulating cancer signaling pathways. *J Zhejiang Univ Sci B*. (2019) 20:1–8. doi: 10.1631/jzus.B1800254
36. Weinhouse S, Warburg O, Burk D, Schade AL. On respiratory impairment in cancer cells. *Science*. (1956) 124:267–72. doi: 10.1126/science.124.3215.267
37. Jia D, Lu M, Jung KH, Park JH, Yu L, Onuchic JN, Kaipparettu BA, Levine H. Elucidating cancer metabolic plasticity by coupling gene regulation with metabolic pathways. *Proc Natl Acad Sci USA*. (2019) 116:3909–18. doi: 10.1073/pnas.1816391116
38. Murphy MP. How mitochondria produce reactive oxygen species. *Biochem J*. (2009) 417:1–13. doi: 10.1042/BJ20081386
39. Rojo de la Vega M, Chapman E, Zhang DD. NRF2 and the hallmarks of cancer. *Cancer Cell*. (2018) 34:21–43. doi: 10.1016/j.ccell.2018.03.022
40. Campisi J, D'Adda Di Fagagna F. Cellular senescence: when bad things happen to good cells. *Nat Rev Mol Cell Biol*. (2007) 8:729–40. doi: 10.1038/nrm2233
41. Nohmi T. Thresholds of genotoxic and non-genotoxic carcinogens. *Toxicol Res*. (2018) 34:281–90. doi: 10.5487/TR.2018.34.4.281
42. Ji X, Lu Y, Tian H, Meng X, Wei M, Cho WC. Chemoresistance mechanisms of breast cancer and their countermeasures. *Biomed Pharmacother*. (2019) 114:108800. doi: 10.1016/j.biopha.2019.108800
43. Velegzhaninov IO, Ievlev VA, Pylina YI, Shadrin DM, Vakhrusheva OM. Programming of cell resistance to genotoxic and oxidative stress. *Biomedicines*. (2018) 6:5. doi: 10.3390/biomedicines6010005
44. Hafner A, Bulyk ML, Jambhekar A, Lahav G. The multiple mechanisms that regulate p53 activity and cell fate. *Nat Rev Mol Cell Biol*. (2019) 20:199–210. doi: 10.1038/s41580-019-0110-x
45. Huarte M, Guttman M, Feldser D, Garber M, Koziol MJ, Kenzelmann-Broz D, et al. A large intergenic noncoding RNA induced by p53 mediates global gene repression in the p53 response. *Cell*. (2010) 142:409–19. doi: 10.1016/j.cell.2010.06.040
46. Khan MR, Bukhari I, Khan R, Hussain HMJ, Wu M, Thorne RF, et al. TP53LNC-DB, the database of lncRNAs in the p53 signalling network. *Database*. (2019) 2019:bay136. doi: 10.1093/database/bay136
47. Qi P, Zhou X yan, Du X. Circulating long non-coding RNAs in cancer: current status and future perspectives. *Mol Cancer*. (2016) 15:39. doi: 10.1186/s12943-016-0524-4
48. Jiang M-C, Ni J-J, Cui W-Y, Wang B-Y, Zhuo W. Emerging roles of lncRNA in cancer and therapeutic opportunities. *Am J Cancer Res*. (2019) 9:1354–66.

Conflict of Interest: The authors declare that the research was conducted in the absence of any commercial or financial relationships that could be construed as a potential conflict of interest.

frontiers in Oncology

REVIEW
published: 04 August 2020
doi: 10.3389/fonc.2020.01370

Role of Non-coding RNAs in the Pathogenesis of Endometriosis

Soudeh Ghafouri-Fard[1], *Hamed Shoorei*[2] *and Mohammad Taheri*[3]*

[1] Department of Medical Genetics, Shahid Beheshti University of Medical Sciences, Tehran, Iran, [2] Department of Anatomical Sciences, Faculty of Medicine, Birjand University of Medical Sciences, Birjand, Iran, [3] Urogenital Stem Cell Research Center, Shahid Beheshti University of Medical Sciences, Tehran, Iran

Endometriosis is a disorder characterized by the presence of endometrial glands and stroma like lesions outside of the uterus. Although several hypothesis have tried to explain the underlying cause of endometriosis, yet the main cause remained obscure. Recent studies have shown contribution of non-coding RNAs in the pathogenesis of endometriosis. Two classes of these transcripts namely long non-coding RNAs (lncRNAs) and microRNAs (miRNAs) have mostly attracted attention of researchers. Several studies have reported aberrant expression of these transcripts in affected tissues from patients as well as animal models. Modulation of important signaling pathways such as PI3K/AKT, P38-MAPK, ERK1/2-MAPK and Wnt-β catenin by miRNAs and lncRNAs have potentiated these molecules as biomarkers or therapeutic agents in endometriosis. Single nucleotide polymorphisms with miR-126, miR-143 and miR-146b have been associated with risk of endometriosis. Moreover, miRNAs and lncRNAs control inflammatory responses, cell proliferation, angiogenesis and tissue remodeling, thus understanding the role of these transcripts in endometriosis is a possible way to develop novel diagnostic tests and therapeutic targets for this disorder.

Keywords: miRNA, lncRNA, endometriosis, non-coding RNA, inflammation

OPEN ACCESS

Edited by:
Jawed Akhtar Siddiqui, University of Nebraska Medical Center, United States

Reviewed by:
Felice Petraglia, University of Florence, Italy
Kai Fu, Central South University, China

***Correspondence:**
Mohammad Taheri
mohammad_823@yahoo.com

Specialty section:
This article was submitted to Molecular and Cellular Oncology, a section of the journal Frontiers in Oncology

Received: *03 April 2020*
Accepted: *29 June 2020*
Published: *04 August 2020*

Citation:
Ghafouri-Fard S, Shoorei H and Taheri M (2020) Role of Non-coding RNAs in the Pathogenesis of Endometriosis. Front. Oncol. 10:1370. doi: 10.3389/fonc.2020.01370

INTRODUCTION

Endometriosis is a condition that endometrial glands and stroma like lesions are detected in organs outside of the uterus (1). These lesions can involve the peritoneum or being presented as superficial implants or cysts on the ovary, or deep infiltrating lesions (2). Although the main etiology of endometriosis is not clear, numerous hypotheses have tried to explain the development of this disorder. Among the most appreciated hypotheses is the retrograde menstruation which can be accompanied by possible hematogenous or lymphatic circulation, thus leading to seeding of endometrial tissue in ectopic places. Yet, this phenomenon is much more prevalent than the occurrence of endometriosis. Hence, other hormonal or immune-related factors contribute in implantation and persistence of lesions in the pelvic cavity (3). Imperfect differentiation or migration of Müllerian residues during fetal period or transdifferentiate of circulating blood cells are other popular hypotheses regarding development of endometriosis (3). Notably, several genomics studies have shown remarkable alterations in gene profile in endometriosis (4). The genetics basis of this condition is complex and has not been explored yet, though, most studies

have reported a polygenic/multifactorial mode for its inheritance (4). Most recently, non-coding RNAs have been demonstrated to contribute in the pathogenesis of endometriosis (5). These transcripts have regulatory roles on expression of protein-coding genes, thus regulate several signaling pathways. They are classified into two main classes according to their length: long non-coding RNAs (lncRNAs) with sizes more than 200 nucleotides and microRNAs (miRNAs) with sizes about 20 nucleotides. LncRNAs can regulate the genetic information flow, through modulating chromatin structure, transcription, splicing, mRNA stability, mRNA accesibility, and post-translational alterations. They have interaction domains for DNA, mRNAs, miRNAs, and proteins which are specified by nucleotide sequence and secondary structure (6). NONCODE database has indicated the presence of at least 100,000 lncRNAs in the human genome (7) which significantly surpluses the number of protein coding genes. There are complex interaction networks between lncRNAs and miRNAs. While certain miRNAs can regulate the stability and half-life of lncRNA, lncRNAs can compete with miRNAs for binding with the mRNA target sites (6). Being mostly located in the cytoplasm, miRNAs constitute critical regulators of gene expression. They mostly exert their effects at post-transcriptional level through binding with their targets and subsequent mRNA degradation and/or translational repression. In addition, miRNAs have been shown to exert specific nuclear functions being emphasized by the miRNA-guided transcriptional regulation of gene expression (8). The regulatory roles of miRNAs and lncRNAs in the expression of genes indicate their participation on the pathogenesis of human disorders. In the current study, we summarize the role of these transcripts in the pathophysiology of endometriosis.

MIRNAS AND ENDOMETRIOSIS

Several studies have reported aberrant expression of miRNAs in affected tissues or peripheral blood samples of patients. Zhang et al. have extracted exosomes from the serum of patients with endometriosis and healthy subjects, then assessed expression miRNAs by miRNA microarrays. They reported differential expression of 24 miRNAs between these two sets of samples. As confirmed by qPCR, expression of miR-22-3p and miR-320a was increased in serum exosomes of patients compared with controls (9). Another study has shown that exosomal miR-22-3p isolated from peritoneal macrophages increases proliferation, migration, and invasion of ectopic endometrial stromal cells via modulation of the SIRT1/NF-κB signaling pathway (10). Others have assessed expression profile of miRNAs peritoneal or tissue samples obtained from these patients. For instance, Zhou et al. have used miRNA microarray technique to identify miRNA signature in the ectopic endometrium samples. They reported over-expression of miR-3154 and miR-3926 in theses tissues compared with normal endometrium (11). Zhang et al. have isolated mononuclear cells from peritoneal fluid of patients with endometriosis and assessed expression of miRNAs in the supernatant of peritoneal fluid. They also purified human endometrial stromal cells from both endometrial and endometriotic tissues of these patients. They reported up-regulation of miR-146b peritoneal fluid supernatant and CD14 + monocytes/Macrophages of peritoneal fluid in endometriosis patients. This miRNA could inhibit the M1 polarization of endometrial stromal cells co-cultured macrophages (12). **Table 1** shows the list of up-regulated miRNAs in samples obtained from patients with endometriosis.

Several miRNAs have been shown to be down-regulated during the pathogenic process of endometriosis. Rekker et al. have used fluorescence-activated cell sorting to endometrial stromal cells from paired endometrial and endometrioma biopsies. Subsequently, they profiled miRNAs in endometriotic stroma using high-throughput sequencing method. They reported downregulation of miR-375 in these cells compared to eutopic cells. This miRNA has been shown to regulate expression of the endothelin 1 (EDN1) gene (30). Yang et al. have shown down-regulation of miR-200b, miR-15a-5p, miR-19b-1-5p, miR-146a-5p, and miR-200c while up-regulation of VEGFA in endometriotic tissues. They have speculated that the higher angiogenic and proteolytic activities observed in the eutopic endometrium could assist the implantation of these cells at ectopic regions (39). **Table 2** summarizes the function and characteristics of miRNAs that are down-regulated in samples obtained from patients with endometriosis.

Diagnostic power of several miRNAs has been assessed in endometriosis. Maged et al. have shown that serum miR-122 and miR-199a had a sensitivity of 95.6 and 100.0% and a specificity of 91.4 and 100%, respectively, for diagnosis of disease status in women. Thus, these miRNAs are putative serum biomarkers for endometriosis (24). Moustafa et al. have shown up-regulation of miR-125b-5p, miR-150-5p, miR-342-3p, and miR-451a, while down-regulation of miR-3613-5p and let-7b in serum samples of patients with endometriosis compared with controls. The area under curve (AUC) values in receiver operating characteristic (ROC) curves ranged from 0.68 to 0.92 for these miRNAs. Notably, a classifier combining these miRNAs provided an AUC of 0.94 as verified in the independent set of individuals not included in the training set. Importantly, neither phase of menstrual cycle nor use of hormonal medicines affected the expression levels in these miRNAs. Thus, authors concluded the potential of the miRNAs panel in detection of endometriosis in clinical setting (13). **Table 3** summarizes the results of studies which reported diagnostic value of miRNAs in endometriosis.

Few studies have reported association between single nucleotide polymorphisms (SNPs) within miRNA coding genes and risk of endometriosis. For instance, Sepahi et al. have genotyped the rs4636297 of miR-126 in 157 endometriosis patients and 252 healthy subjects. G allele of this SNP has been shown to protect against endometriosis. Moreover, significant association has also been detected between the A allele and severity of endometriosis (72). Zhang et al. have shown association between the CT/CC genotypes of miR-146b rs1536309 and the risk of pain symptom of endometriosis. Moreover, they detected lower levels of the miR-146b and higher pro-inflammatory functions in macrophages from CT/CC genotype carriers (12). Nimi-Hoveidi et al. have genotyped miR-143 rs41291957 and rs4705342 SNPs in infertile women with endometriosis and matched healthy subjects. They

TABLE 1 | Up-regulated miRNAs in endometriosis.

MicroRNA	Species	Numbers of clinical samples	Assessed cell line	Targets/ Regulators	Signaling Pathways	Function	References
miR-197-5p, miR-22-3p, miR-320a, miR-320b, miR-3692-5p, miR-4476, miR-4530, miR-4532, miR-4721, miR-4758-5p, miR-494-3p, miR-6126, miR-6734-5p, miR-6776-5p, miR-6780b-5p, miR-6785-5p, miR-6791-5p, miR-939-5p	Human	Isolated-exosome from serum samples of endometriosis patients ($n = 20$) and normal controls ($n = 20$)	–	–	–	Mentioned-microRNAs could be considered as potential biomarkers for endometriosis diagnosis.	(9)
miR-22-3p	Human	Peritoneal fluid samples from endometriosis patients ($n = 20$) and normal controls ($n = 20$)	HESCs	SIRT1	NF-κB	Exosomal miR-22-3p derived from pMϕ by regulating the SIRT1/NF-κB pathway could promote proliferation, migration, and invasion of human ectopic endometrial stromal cells (eESCs).	(10)
miR-92a	Human, mouse	Endometrial samples from women with progesterone-resistant endometriosis ($n = 12$) and with progesterone-responsive endometriosis ($n = 11$)	SHT290	PTEN	AKT	The expression of miR-92a is increased in progesterone resistant endometriosis samples. miR-92a via targeting PTEN/AKT signaling pathway could promote progesterone resistance in endometriosis.	(13)
miR-125b, miR-150, miR-342, miR-451a,	Human	Serum samples from endometriosis patients ($n = 41$) and normal controls ($n = 59$)	–	–	–	Mentioned-microRNAs could be considered as potential biomarkers for endometriosis diagnosis.	(13)
miR-342-3p	Human, mouse	Fat specimens from endometriosis patients ($n = 10$) and normal controls ($n = 10$)	Primary adipocyte cells	Cebpa, Cebpb, Ppar-γ, leptin, adiponectin, IL-6, HSL	–	miR-342-3p could affect the expression of metabolic genes in adipocytes of women with endometriosis. Therefore, it has a direct effect on fat metabolism.	(14)
miR-3154	Human, mouse	Ectopic endometrial tissues and serum from endometriosis patients ($n = 68$) and normal controls ($n = 23$)	EC109, EC520, EN211, EN307	–	–	This miRNA could be considered as a potential biomarker for endometriosis diagnosis.	(11)
miR-3926	Human, mouse	Ectopic endometrial tissues and serum from endometriosis patients ($n = 68$) and normal controls ($n = 23$)	EC109, EC520, EN211, EN307	–	–	This miRNA could be considered as a potential biomarker for endometriosis diagnosis.	(11)
miR-146b	Human	Peritoneal fluid samples from endometriosis patients ($n = 74$) and normal controls ($n = 23$)	ESCs, THP-1, PBMC	IRF5/IL-12p40	NF-kB	miR-146b via IRF5/IL-12p40/NF-kB axis is involved in the negative regulation of inflammation.	(12)
miR-33b	Rat	–	ESCs	ZEB1	Wnt/β-catenin	Overexpression of miR-33b via inhibiting ZEB1/Wnt/β-catenin signaling pathway could promote endometriosis.	(15)

(Continued)

TABLE 1 | Continued

MicroRNA	Species	Numbers of clinical samples	Assessed cell line	Targets/ Regulators	Signaling Pathways	Function	References
miR-142-5p, miR-146a-5p, miR-1281, miR-940, miR-4634	Human	Eutopic endometrium samples from endometriosis patients (*n* = 38), normal controls (*n* = 38)	–	–	–	These miRs could be considered as potential biomarkers for endometriosis diagnosis.	(16)
miR-210-3p	Human, mouse	Normal endometria (*n* = 27), eutopic endometria (*n* = 57), ectopic lesions (*n* = 57)	HESCs, hEM15A, ISK, 293T	BARD1	–	Knockdown of miR-210-3p could induce a G2/M arrest of Ishikawa cells and ESCs under hypoxia. Therefore, miR-210-3p by targeting BARD1 could protect endometriotic cells from oxidative stress-induced cell cycle arrest.	(17)
miR-17-5p	Human	51 endometriosis patients and 51 controls	Endometrial tissue	–	–	There is a positive relationship between intrauterine bacterial colonization and increased levels of miR-17-5p. Therefore, it could be a biomarker of endometriosis.	(18)
miR-200b	Human	3 endometriotic and 3 nonendometriotic eutopic endometrium	Endometriotic mesenchymal stem cells (EMSCs)	–	–	In endometriosis, regulation of miR-200b may have a role in the modulating proliferation and differentiation of stem cells.	(19)
miR-451a, miR-486-5p, miR-130-3p	Human	Endometriosis patients (*n* = 54) and normal controls (*n* = 13)	–	–	–	Exosomal microRNAs could be involved in the progression of endometriosis.	(20)
miR-150-5p, miR-451a	Baboon	–	–	–	–	In the baboon model of endometriosis, the expression of these miRNAs is increased in response to simvastatin treatment. Therefore, it could be considered as a potential biomarker for endometriosis diagnosis.	(21)
miR-451a	Mouse	–	–	YWHAZ, CAB39, MAPK1, β-catenin, IL-6	–	Inhibition of miR-451a could reduce the established-lesion in an animal model of endometriosis.	(22)
miR-27a-3p, miR-451a, miR-144-5p, miR-1266-5p, miR-200c-3p, miR-200a-3p, miR-20b-5p, miR-200a-5p, miR-96-5p	Human	Endometrium (*n* = 6), endometriotic lesions (*n* = 6), PF (*n* = 6), and plasma (*n* = 6) from endometriosis patients	12Z, EEC-1, HUVEC	–	–	Mentioned-microRNAs could be considered as potential biomarkers for endometriosis diagnosis.	(23)
miR-122, miR-199a	Human	Endometriosis patients (*n* = 45) and normal controls (*n* = 35)	–	IL-6	–	Mentioned-microRNAs could be considered as biomarkers for the diagnosis of endometriosis.	(24)

(Continued)

TABLE 1 | Continued

MicroRNA	Species	Numbers of clinical samples	Assessed cell line	Targets/ Regulators	Signaling Pathways	Function	References
miR-145	Human	Plasma samples of 55 patients with endometriosis and 23 normal controls	–	–	–	The mentioned-miR could be considered as a biomarker for the diagnosis of endometriosis.	(25)
miR-126, miR-145	Human	47 infertile patients with endometriosis, 47 normal controls	–	–	–	Overexpression of miR-126 and miR-145 in the mid-luteal phase of patients with endometriosis could play an important role in infertility due to endometriosis.	(26)
miR-106b-3p, miR-451a, miR-486-5p	Human	Peritoneal fluid (PF) samples form endometriosis patients ($n = 60$), normal control ($n = 60$)	–	–	–	Mentioned-microRNAs could be considered as a biomarker for the diagnosis of endometriosis.	(27)
miR-106b-3p, miR-130a-3p, miR-150-5p, miR-451a, miR-486-5p	Human	Endometriosis patients in the menstrual phase of the cycle ($n = 12$), normal control in the menstrual phase of the cycle ($n = 4$)	–	–	–	Analysis of microRNAs according to the phase of the menstrual cycle could be useful for the diagnosis of endometriosis.	(27)
miR-29c-3p, miR-185-5p, miR-195-5p	Human	Peritoneal fluid (PF) samples. Endometriosis samples ($n = 126$), 45 normal controls. (Based on the menstrual phase)	–	–	–	Analysis of microRNAs according to the phase of the menstrual cycle could be useful for the diagnosis of endometriosis.	(27)
miR-194-3p	Human	Midsecretory phase of the eutopic endometrium of women with endometriosis ($n = 19$), normal controls ($n = 14$)	HESCs	Progesterone receptor	–	In eutopic endometrium from women with endometriosis, mir-194-3p could repress the progesterone receptor and decidualization.	(28)
miR-33a-5p	Human	Plasma samples of endometriosis patients ($n = 51$), normal controls ($n = 41$)	–	–	–	The mentioned-miRNAs could be considered as a biomarker for the diagnosis of endometriosis	(29)
miR-139-5p, miR-139-3p, miR-202-5p, miR-506-3p, miR-150-5p, miR-202-3, miR-150-3p, miR-513c-5p, miR-193a-5p, miR-584-5p, miR-371a-5p, miR-216b-5p	Human	Paired samples of endometriomas ($n = 4$) and eutopic endometrium ($n = 4$)	HESCs, ST-T1b	HOXA9, HOXA10 for miR-139-5p	–	miR-139-5p by regulating HOXA9 and HOXA10 genes could be involved in endometriosis-associated infertility	(30)
miR-615-3p	Human	60 tissue samples (30 paired EC and EU) from patients with endometriosis ($n = 30$)	–	–	–	The mentioned-miR could be considered as a biomarker for the diagnosis of endometriosis	(31)
miR-29c, miR-200a, miR-145	Human	Tissues of 56 female patients with endometriosis, 38 normal controls	–	HOXA-10, HOXA-11, integrin αvβ3, IGFBP-1, CD44V6, N-cadherin, FAK	–	Mentioned-microRNAs via targeting several pathways could influence the endometrial receptivity in infertile patients with endometriosis	(32)

(Continued)

TABLE 1 | Continued

MicroRNA	Species	Numbers of clinical samples	Assessed cell line	Targets/ Regulators	Signaling Pathways	Function	References
miR-29c	Human, baboon	Tissues: ectopic ($n = 15$) and normal controls ($n = 11$)	HuFs, HESCs,	FKBP4	–	miR-29c via targeting FKBP4 could modulate progesterone resistance in endometriosis	(33)
miR-451a	Human, baboon	41 endometriosis, 40 without visible signs of endometriosis	–	–	–	The level of miR-451a in serum is positively correlated with endometriotic lesion content.	(34)
miR-325, miR-492, miR-520e, miR-203a-3p, miR-93	Human	28 ovarian cancer samples, 17 normal samples, 33 endometriosis samples and	–	–	–	Mentioned-microRNAs could be considered as biomarkers for the diagnosis of endometriosis.	(35)
miR-27b-3p	Human	21 patients with endometriosis and 15 normal controls	HESCs, ISK	Ki-67, col-1, CTGF, fibronectin, TGF-β1, MMP2, MMP9	–	miR-27b-3p is upregulated in patients with endometriosis. Ginsenoside Rg3 extract (Rg3E) by modulating miR-27b-3p could decreases fibrotic and invasive nature of endometriosis	(36)
miR-29a, miR-148a, miR-100, let-7g	Human	Ectopic endometriotic tissues ($n = 4$), eutopic control endometrium	ISK, HESCs	BCL2, DNMT3B, OPRM1, Mip1α	–	The redox-sensitive microRNAs could be useful in the treatment of endometriosis-associated pain	(37)
miR-1304-3p, miR-544b, miR-3684, miR-494-5p, miR-4683, miR-6747-3p	Human	Eight patients with endometriosis and six normal controls	–	–	–	Mentioned-microRNAs could be used as a diagnostic biomarkers for endometriosis	(38)
miR-16-5p, miR-106b-5p, miR-145-5p	Human	Endometriotic tissues ($n = 32$), normal controls ($n = 19$)	–	EGFR2, PTEN, CXCR4	–	Mentioned-microRNAs could be used as a diagnostic biomarkers for endometriosis	(39)
miR-210	Human	Ectopic endometrial tissues ($n = 10$), eutopic endometrial tissues ($n = 10$)	CRL-7566	HIF-1α, Bcl-2, Beclin-1	–	The hypoxia-induced higher miR-210 expression through promoting autophagy and enhancing cell survival by Bcl2/Beclin-1 axis could contribute to pathological development of endometriosis	(40)
miR-122	Human	25 healthy women, 25 endometriosis patients	–	MCP-1, TGF-β1	–	Serum miR-122 could be useful in the evaluation of patients with endometriosis	(41)
miR-125b-5p, miR-150–5p, miR-342-3p, miR-143-3p, miR-145-5p, miR-500a-3p, miR-451a, miR-18a-5p	Human	24 endometriosis patients, 24 normal controls	–	–	–	Serum microRNAs could be considered as diagnostic markers of endometriosis	(42)

TABLE 2 | List of down-regulated miRNAs in endometriosis.

microRNA	Species	Numbers of clinical samples	Assessed cell line	Targets/ Regulators	Signaling Pathways	Function	References
miR-141	Human	Endometriotic tissue samples ($n = 32$), normal controls ($n = 17$)	ISK	–	TGF-β1/ SMAD2	miR-141 via inhibiting the TGF-β1/SMAD2 signaling pathway could inhibit TGF-β1-induced EMT in endometriosis.	(9)
miR-3613-5p, miR-6755-3p	Human	24 endometriosis patients, 24 normal controls	–	–	–	Serum microRNAs could be considered as diagnostic markers of endometriosis.	(42)
miR-200b	Human	Three endometriosis patients, three normal controls	12Z, ST-T1b, HESCs	ZEB1, ZEB2, KLF4	–	miR-200b by targeting ZEB1, ZEB2, and KLF4 could affect the proliferation, invasiveness, and stemness of endometriotic cells.	(43)
miR-15a-5p	Human	31 patients with endometriosis and 31 normal controls	HESCs	VEGFA	–	miRNA-15a-5p by regulating VEGFA in endometrial mesenchymal stem cells could contribute to the pathogenesis of endometriosis.	(44)
miR-503	Human	Endometriotic tissues were from patients with ovarian endometriotic cysts ($n = 32$), normal control (eutopic, $n = 8$)	endometriotic cyst stromal cells (ECSCs), NESCs	VEGF-A, cyclin D1, Bcl-2, Rho A	–	miR-503 via targeting key molecules could induce apoptosis and cell-cycle arrest and could inhibit cell proliferation and angiogenesis in endometriosis.	(45)
miR-200b, miR-15a-5p, miR-19b-1-5p, miR-146a-5p, miR-200c	Human	Endometriotic tissues ($n = 32$), normal controls ($n = 19$)	–	VEGF-A	–	Mentioned-microRNAs could be used as a diagnostic biomarkers for endometriosis.	(39)
miR-3935, miR-4427, miR-652-5p miR-205-5	Human	Eight patients with endometriosis and 6 normal controls	–	–	–	Mentioned-microRNAs could be used as a diagnostic biomarkers for endometriosis.	(38)
miR-34a-5p	Human	Tissues: eutopic endometrial ($n = 10$) and ectopic endometrial ($n = 10$)	hEnSCs	VEGF-A	–	Overexpression of miR-34a-5p via targeting VEGFA could suppress the proliferation of endometrial-derived stem cells (EnSCs).	(46)
Let-7b-5p, Let-7c-5p, Let-7e-5p	Mouse	–	–	–	–	The family of let-7 in the serum shows a dysregulation in endometriosis.	(47)
miR-548l	Human	Ectopic endometriotic tissues ($n = 4$), eutopic control endometrium	ISK, HESCs	–	–	The mentioned-redox-sensitive miR could be useful in the treatment of endometriosis-associated pain.	(37)
miR-200c	Human, rat	normal endometrial ($n = 12$) and ectopic endometrial ($n = 27$) tissues	HESCs	MALAT1, ZEB1, ZEB2	–	miR-200c by targeting MALAT1/ZEB1/ZEB2 could suppress endometriosis.	(48)
miR-33b	Human	Tissues of 20 female patients with endometriosis, 15 normal controls	Endometrial tissue	VEGF, MMP-9	–	miR-33b via mediating apoptosis and altering VEGF or MMP-9 expression could affect proliferation and apoptosis of endometrial cells.	(49)

(Continued)

TABLE 2 | Continued

microRNA	Species	Numbers of clinical samples	Assessed cell line	Targets/ Regulators	Signaling Pathways	Function	References
miR-30c	Human	Patients with endometriosis ($n = 20$), normal endometrial tissues ($n = 18$)	HESCs	PAI-1	–	Overexpression of miR-30c by targeting PAI-1 could repress the invasion, migration, proliferation, and adhesion of HESCs.	(50)
miR-424-5p	Human	Patients with endometriosis ($n = 26$), normal endometrial tissues ($n = 26$)	CRL-7566	FGFR1	STAT3	miR-424-5p by negatively regulating FGFR1 through STAT3 signaling expression could promote apoptosis and inhibit proliferation in CRL-7566 cells.	(51)
miR-34c-5p, miR-106a-5p, miR-182-5p, miR-200a-3p, miR-449b-5p	Human	60 tissue samples (30 paired EC and EU) from patients with endometriosis ($n = 30$)	–	FOXC1, FOXO1, CEBPA	–	Mentioned-microRNAs could be considered as biomarkers for the diagnosis of endometriosis.	(31)
miR-105-5p, miR-141-3p, miR-375, miR-429, miR-675-3p, miR-767-5p, miR-873-5p, miR-1298-5p, miR-6507-5p,	Human	Paired samples of endometriomas ($n = 6$) and eutopic endometrium ($n = 6$)	HESCs, ST-T1b	EDN1 for miR-375	–	miR-375 by targeting EDN1 could be involved in the regulation of invasive growth and cell proliferation in endometriosis development.	(30)
miR-134-5p, miR-3141, miR-4499, miR-6088, miR-6165, miR-6728-5p	Human	Isolated-exosome from serum samples of endometriosis patients ($n = 20$) and normal controls ($n = 20$)	–	–	–	Mentioned-microRNAs could be considered as potential biomarkers for endometriosis diagnosis.	(10)
miR-138	Rat, mouse	–	HESCs, THP-1	VEGF	NF-κB,	miR-138 via the VEGF/NF-κB signaling pathway could induce inflammation and apoptosis in endometriosis.	(52)
miR-451	Human	Tissue samples from endometriosis patients ($n = 40$) and normal controls ($n = 20$)	HESCs	YWHAZ, OSR1, TTN, CDKN2D	–	Downregulation of miR-451 could contribute to the pathogenesis of endometriosis by reducing apoptosis and promoting cell proliferation in the eutopic endometrium.	(53)
miR-543	Human	Eutopic endometrium samples from endometriosis patients ($n = 38$), normal controls ($n = 38$)	–	HOX10, ITGAV, ITGB3, OPN, ESR, PGR, CDH1, MMP	–	miR-543 is downregulated in patients with endometriosis and also is downregulated at the phase of implantation window. Therefore, it could affect embryo implantation in women with endometriosis-related infertility.	(16)
Let-7b, miR-6313	Human	Serum samples from endometriosis patients ($n = 41$) and normal controls ($n = 59$)	–	–	–	Mentioned-microRNAs could be considered as potential biomarkers for endometriosis diagnosis.	(13)
miR-202-3p	Human	Tissue samples from endometriosis patients ($n = 27$) and normal controls ($n = 31$)	HESCs	ROCK1	–	Suppression of miR-202-3p via targeting ROCK1 could enhance cell viability, invasion, and migration in ESCs.	(54)

(Continued)

TABLE 2 | Continued

microRNA	Species	Numbers of clinical samples	Assessed cell line	Targets/ Regulators	Signaling Pathways	Function	References
miR-199a-5p	Human, rat	Control endometrial stromal cells (CSCs, $n = 15$), eESCs ($n = 15$)	HESCs, CSCs	ZEB1	PI3K/Akt/mTOR	miR-199a-5p via ZEB1/PI3K/Akt/mTOR signaling pathway could Inhibit the EMT of ovarian ectopic ESCs.	(55)
miR-20a	Human, mouse	Endometriosis patients ($n = 60$) and normal controls ($n = 25$)	PBMCs, NKCs, NK-92	ERG, HLX, perforin	STAT4	miR-20a via ERG/HLX/STAT4/perforin axis could mediate the cytotoxicity of natural killer (NK) cells in endometriosis.	(56)
Let-7b	Human, mouse	Fat specimens from endometriosis patients ($n = 10$) and normal controls ($n = 10$)	Primary adipocyte cells	Cebpa, Cebpb, Ppar-γ, leptin, adiponectin, IL-6, HSL	–	Let-7b could affect the expression of metabolic genes in adipocytes of women with endometriosis. Therefore, it has a direct effect on fat metabolism.	(14)
miR-205-5p	Human, mouse	Ectopic endometrial tissues and serum from endometriosis patients ($n = 68$) and normal controls ($n = 23$)	EC109, EC520, EN211, EN307	ANGPT2	ERK/AKT	miR-205-5p via ANGPT2/ ERK/AKT axis in endometrial stromal cells could inhibit human endometriosis progression.	(11)
miR-4497	Human, mouse	Ectopic endometrial tissues and serum from endometriosis patients ($n = 68$) and normal controls ($n = 23$)	EC109, EC520, EN211, EN307	–	–	This miR could be considered as a potential biomarker for endometriosis diagnosis.	(11)
miR-141-3p	Human	20 pairs of ectopic endometrial (EC) samples and eutopic endometrial (EU) samples, normal controls ($n = 20$)	HESCs	KLF-12	–	miR-141-3p via targeting KLF-12 could promote apoptosis and suppress cell proliferation and migration in ectopic ESCs.	(57)
miR-135a/b	Human	Samples of ectopic endometriosis lesions and eutopic endometrium tissue ($n = 23$)	–	–	–	Mentioned-microRNAs could be considered as potential biomarkers for endometriosis diagnosis.	(58)
miR-145, Let-7b	Human	3 endometriotic and 3 non-endometriotic eutopic endometrium	EMSCs	–	–	In endometriosis, regulation of miR-145 and let-7b may have a role in the modulating proliferation and differentiation of stem cells.	(19)
miR-451	Human, mouse	Endometriosis patients ($n = 30$) and normal controls ($n = 30$)	–	AXIN1, CDX2, CTNNB1	Wnt	miR-451 is downregulated in follicular fluid samples extracted from endometriosis patients. Downregulation of miR-451 by suppressing the Wnt signaling pathway in mouse and human oocytes could affect preimplantation embryogenesis.	(59)
miR-142-3p	Human	20 ectopic endometrial tissue samples, 20 eutopic endometrial tissues	CRL-7566, hEM15A, ECSCs, NESCs	KLF9	VEGFA	miR-142-3p by regulating KLF9-mediated autophagy could suppress endometriosis *in vitro* and *in vivo*.	(60)

(Continued)

TABLE 2 | Continued

microRNA	Species	Numbers of clinical samples	Assessed cell line	Targets/ Regulators	Signaling Pathways	Function	References
miR-142-3p	Human	Serum samples from endometriosis patients ($n = 41$) and normal controls ($n = 44$)	12Z, ST-T1b, ECSCs	IL6ST, ITGAV, RAC1, WASL, ROCK2	STAT3	Downregulation of miR-142-3p via upregulating the expression of proinflammatory signaling receptors and cytoskeletal elements could promote the pathogenesis of endometriosis.	(61)
miR-375, miR-27a-3p, miR-30d-5p	Human	Endometrium ($n = 6$), endometriotic lesions ($n = 6$), PF ($n = 6$), and plasma ($n = 6$) from endometriosis patients	12Z, EEC-1, HUVEC	–	–	Mentioned-microRNAs could be considered as potential biomarkers for endometriosis diagnosis.	(23)
miR-488	Human, mouse	GSE5108 and GSE23339 chips	Endometrial tissues	FZD7	Wnt	Overexpression of miR-488 via inhibiting FZD7/Wnt pathway could reduce the proliferation, migration, and invasion of endometrial glandular epithelial cells.	(62)
miR-31	Human	Plasma samples of 55 patients with endometriosis and 23 normal controls	–	–	–	The mentioned-miR could be considered as a biomarker for the diagnosis of endometriosis.	(25)
miR-370-3p	Human	Sera and tissue from endometriosis patients ($n = 20$) and normal controls ($n = 26$)	HESCs	SF-1	–	miR-370-3p by regulating SF-1 could suppress proliferation in endometriotic cells.	(63)
miR-126-5p	Human	32 cases of ectopic endometrium and eutopic endometrium, 31 normal controls	EECs, ESCs, NESCs, 293T	BCAR3	–	Downregulation of miR-126-5p via negatively regulating BCAR3 could promote cell migration and invasion in endometriosis.	(64)
miR-3613-5p	Baboon	–	–	–	–	In the baboon model of endometriosis, the expression of miR-150-5p and miR-451a is decreased in response to simvastatin treatment. Therefore, they could be considered as potential biomarkers for endometriosis diagnosis.	(21)
miR-29c-3p, miR-1343-5p	Human	Peritoneal fluid (PF) samples form endometriosis patients ($n = 60$), normal control ($n = 60$)	–	–	–	Mentioned-microRNAs could be considered as potential biomarkers for endometriosis diagnosis.	(27)
miR-214	Human, mouse	Endometriosis patients ($n = 24$), normal control ($n = 8$)	Endometrial epithelial cells (EECs), HESCs	CTGF	–	miR-214-enriched exosomes could inhibit fibrogenesis in endometriosis.	(65)
miR-148a	Human	Endometriosis patients ($n = 7$), patients with endometriosis-associated ovarian cancer (EAOC, $n = 7$), normal controls ($n = 6$)	Hs 832(C).T	HLA-G, Caspase-3, Caspase-9, GPER	–	GPER/miR-148a/HLA-G signaling could mediate cell apoptosis in endometriosis.	(66)
miR-381	Human	Endometriosis patients ($n = 6$), patients with ovarian cancer ($n = 3$), normal control ($n = 3$)	TOV21G, TOV112D	PIK3CA	–	In endometriosis-associated clear cell and endometrioid ovarian cancer, miR-381 via targeting PIK3CA could regulate cell motility, growth, and colony formation.	(67)

(Continued)

TABLE 2 | Continued

microRNA	Species	Numbers of clinical samples	Assessed cell line	Targets/ Regulators	Signaling Pathways	Function	References
miR-203	Human	Endometriosis patients ($n = 6$), patients with ovarian cancer ($n = 3$), normal control ($n = 3$)	TOV21G, TOV112D	–	–	The mentioned-miRNA could be considered as a biomarker for the diagnosis of endometriosis.	(67)
Let-7b	Mouse	–	–	ER-α, ER-ß, Cyp19a, KRAS, 4A, KRAS-4B, IL-6	–	Let-7b treatment of endometriosis could decrease inflammatory signaling (IL-6), decreased estrogen signaling (ER and Cyp19A1), and also decrease KRAS.	(68)
miR-21-5p, miR-181b-5p, miR-503-5p, miR-642a-3p, miR-3180-3p, miR-3180, miR-3937, miR-4498, miR-4690-5p, miR-6075, miR-6080, miR-6802-5p, miR-6820-5p, miR-7110-5p,	Human	Endometriosis patients ($n = 16$), normal control ($n = 16$)	HESCs	Caspase-3 for miR-21-5p	–	The extract of saponin via decreasing the expression miR-21-5p could induced apoptosis of endometrial cells in women with endometriosis.	(69)
miR-449b-3p	Human	Ectopic (endometrioma; $n = 19$), eutopic ($n = 19$), and normal ($n = 35$) endometrial tissues	HESCs, HUVECs	–	–	The aberrant expression of miR-449b-3p by effecting on endometrial stromal cell proliferation and angiogenesis could be involved in the development and progression of endometriosis.	(70)
miR-17	Human	Serum samples of endometriosis patients ($n = 80$), normal control ($n = 60$)	–	IL-4, IL-6	–	Investigating the expression of miR-17 could be considered as a noninvasive diagnostic test for the detection of endometriosis.	(71)
miR-154-5p, miR-196b-5p, miR-378a-3p	Human	Plasma samples of endometriosis patients ($n = 51$), normal controls ($n = 41$)	–	–	–	Mentioned-microRNAs could be considered as biomarkers for the diagnosis of endometriosis.	(29)

reported association between the C allele of rs4705342 and increased risk of endometriosis. In addition, the A allele of rs41291957 polymorphism was associated with susceptibility to endometriosis (73). **Table 4** shows the results of studies which assessed association between miRNA SNPs and endometriosis.

LNCRNAS AND ENDOMETRIOSIS

Expression levels of lncRNAs have been assessed in different samples obtained from patients with endometriosis or animal models of endometriosis. Cai et al. have assessed expression profiles of these transcripts in the uterus of rats with endometriosis and reported differential expression of a number of lncRNAs between endometriosis group and controls. They concluded that differentially expressed genes influence endometrial receptivity in rats with endometriosis during the implantation window which results in implantation failure (74). Using a high throughput method, Sun et al. have reported dysregulation of 948 lncRNA and 4,088 mRNA transcripts in ectopic endometrial tissue compared with paired eutopic endometrial tissue. These lncRNAs were mostly enriched in biological pathways associated with endometriosis, thus were thought to regulate expression of associated protein coding genes in cis- and/or trans (75). Huang et al. have assessed expression of the lncRNA UCA1 in ectopic and eutopic endometrium tissues of ovarian endometriosis patients and controls. They reported over-expression of this lncRNA in ectopic endometrium tissues

TABLE 3 | Diagnostic value of miRNAs in endometriosis.

Sample number	Area under curve	Sensitivity	Specificity	References
Isolated-exosome from serum samples of endometriosis patients ($n = 20$) and normal controls ($n = 20$)	0.855 for miR-22-3p, 0.827 for miR-320a			(10)
Serum samples from endometriosis patients ($n = 41$) and normal controls ($n = 59$)	0.84 for miR-451a, 0.78 for Let-7b, 0.73 for miR-125b, 0.92 for miR-342, 0.76 for miR-3613	82.5% for Let-7b, 90% for miR-451a, 56.1% for miR-125b, 90% for miR-342, 92.7% for miR-3613	67.8% for Let-7b, 72.9% for miR-451a, 78% for miR-125b, 91.2% for miR-342, 61% for miR-3613	(13)
51 endometriosis patients and 51 controls		90%	76.5%	(18)
Serum samples from endometriosis patients ($n = 45$) and normal controls ($n = 35$)	0.963 for miR-122, 1.000 for miR-199a	95.6% for miR-122, 100.0% for miR-199a	91.4% for miR-122, 100.0% for miR-199a	(24)
Serum samples of endometriosis patients ($n = 80$), normal control ($n = 60$)	0.84			(71)
Plasma samples of endometriosis patients ($n = 51$), normal controls ($n = 41$)	0.72 for miR-154-5p	67% for miR-154-5p	68% for miR-154-5p	(29)
Patients with endometriosis ($n = 41$), individuals without visible signs of endometriosis ($n = 40$)	0.8599	85.37%	84.62%	(34)
Ovarian cancer samples ($n = 28$), normal samples (n17), endometriosis samples ($n = 33$)	0.775 for miR-492			(35)
Endometriosis patients ($n = 24$), normal controls ($n = 24$)	0.974 for miR-125b-5p, 0.808 for miR-150-5p, 0.760 for miR-342-3p, 0.926 for miR-143-3p, 0.901 for miR-500a-3p, 0.835 for miR-451a, 0.797 for miR-18a-5p, 0.718 for miR-6755-3p, 0.862 for miR-3613-5p	100% for miR-125b-5p	96% for miR-125b-5p	(42)

TABLE 4 | Association between polymorphisms with SNPs and risk of endometriosis.

Number of cases and controls	Variant	References
Endometriosis patients ($n = 157$) and healthy controls ($n = 252$)	miR-126 rs4636297 is associated with endometriosis risk and its severity. For ir-126 rs4636297 in allele (G vs. A) and genotype (GG vs. AA genotype), there was significant protection against endometriosis	(72)
Endometriosis patients ($n = 74$) and healthy controls ($n = 23$)	miR-146b rs1536309 C > T polymorphism is associated with the risk of pain symptom of endometriosis. rs1536309 CT/CC frequency is involved in increased pain susceptibility. miR-146b rs1536309 C > T polymorphism by regulating miR-146b expression was associated with the M1 polarization of macrophages	(12)
Infertile women ($n = 77$) with endometriosis and healthy controls ($n = 226$)	Among the groups of the study, there was a significant difference in the genotype distribution and allele frequency of miR-143 rs41291957 and miR-143 rs4705342 polymorphism. C allele and TC genotype were associated with an increased risk of endometriosis	(73)

compared with paired eutopic endometrium tissues in the majority of patients. They also demonstrated higher serum levels of this lncRNA after treatment. Notably, serum levels of UCA1 on the day of discharge were remarkably lower in patients with recurrence compared with patients without recurrence. Based on these results, authors concluded that UCA1 participates in the pathogenesis of ovarian endometriosis and may be a putative diagnostic and prognostic marker for this condition (76). **Tables 5**, **6** show up- and down-regulated lncRNAs in the endometriotic samples, respectively.

Among down-regulated lncRNAs is H19 whose role in the pathogenesis of endometriosis has been shown in **Figure 1**.

TABLE 5 | Up-regulated lncRNAs in endometriosis.

lncRNA	Species	Numbers of clinical samples	Assessed cell line	Targets/ Regulators	Signaling Pathways	Function	References
TC0101441	Human	10 pairs of ectopic and eutopic endometria from patients with ovarian endometriotic cysts, normal endometrium tissue ($n = 10$)	ECSCs	N-cadherin, snail, slug, TCF8/ZEB1	–	Extracellular vesicle-mediated transfer of the lncRNA-TC0101441 could enhance the migration and invasion of endometriosis	(77)
UCA1	Human	98 patients with endometriosis, 28 normal controls (serum samples)	–	–	–	LncRNA-UCA1 could be used as a diagnostic and prognostic biomarker for ovarian endometriosis	(76)
MALAT1	Human	Endometrial tissues from patients with endometriosis ($n = 15$), normal controls ($n = 7$)	Endometrial cells	MMP-9, caspase-3	NF-κB/iNOS	LncRNA-MALAT1 via NF-κB/iNOS pathway could facilitate endometrial cell apoptosis and also via targeting MMP-9 could suppress endometrial cell proliferation and invasion.	(78)
	Human	Paired eutopic and ectopic endometrium samples from patients with endometriotic ($n = 30$), normal controls ($n = 30$)	HESCs	HIF-1α, 3-MA, Beclin1	–	LncRNA-MALAT1 via targeting HIF-1α/3-MA/Beclin1 could mediate hypoxia-induced pro-survival autophagy of HESCs in endometriosis.	(79)
CCDC144NL-AS1	Human	Paired ectopic and eutopic endometria from patients with endometriotic ($n = 34$), normal controls ($n = 27$)	hEM15A, HUVECs	Vimentin, MMP-9	–	lncRNA-CCDC144NL-AS1 knockdown could decrease migration and invasion phenotypes in endometrial stromal cells from endometriosis	(80)
BANCR	Rat	–	–	VEGF, MMP-2, MMP-9	ERK/MAPK	lncRNA-BANCR inhibitor via inhibiting ERK/MAPK signaling pathway could repress the development of ectopic endometrial tissues	(81)
SNORD3A, TCONS_00006582	Human	Eutopic endometrium samples ($n = 17$), normal samples ($n = 17$)	–	–	–	lncRNAs could be considered as novel diagnostic biomarkers and therapeutic targets for endometriosis	(82)
NONRATT006252, gi|672027621| ref|XR_592747.1|, gi|672045999 |ref|XR_591544.1|, gi|672066614| ref|XR_594547.1, NONRATT006252, gi|672045999| ref|XR_591544.1|	Rat	–	–	Dlx3, P2ry6, Adamts7	–	During the implantation window process, changes in the expression of lncRNAs could affect endometrial receptivity in rats with endometriosis.	(74)

(Continued)

TABLE 5 | Continued

lncRNA	Species	Numbers of clinical samples	Assessed cell line	Targets/ Regulators	Signaling Pathways	Function	References
AFAP1-AS1	Human, mouse	Paired eutopic and ectopic endometrium samples from patients with ovarian endometriotic cysts ($n = 18$), normal controls ($n = 10$)	HESCs, ISK	ZEB1, E-cadherin	–	lncRNA-AFAP1-AS1 by targeting ZEB1 could promote EMT of endometriosis. Knockdown of AFAP1-AS1 could inhibit the growth of endometrial epithelial cells through inhibiting E2-induced activity of promoter site pGL3-P886 of transcription factor ZTB1.	(83)
LINC01279, MSC-AS1	Human	GSE7305, GSE7846, GSE29981 and E-MTAB-694 datasets	–	–	–	LINC01279 and MSC AS1 could be associated with the pathogenesis of endometriosis.	(84)
CHL1-AS2	Human	Paired eutopic and ectopic endometrium samples from patients with endometriotic ($n = 31$), normal controls ($n = 30$)	HL-60, Jurkat	–	–	lncRNA-CHL1-AS2 could be involved in the endometriosis development.	(85)
H19	Human	Eutopic endometrial tissues from patients with endometriosis ($n = 23$), normal controls ($n = 23$)	HESCs, 293T	miR-216a-5p, ACTA2	–	The estrogen-regulated lncRNA-H19/ACTA2/miR-216a-5p axis could mediate the invasion and migration of eutopic endometrial stromal cells (euESCs) in women with endometriosis.	(78)
HOXA11-AS1	Human	Paired eutopic and ectopic endometrium samples from patients with endometriotic ($n = 30$), normal controls ($n = 15$)	–	HOXA9, HOXA10, HOXA11, HOXA13		Although lncRNA-HOXA11-AS1 had no role on endometrial receptivity in endometriosis-associated infertility, it could influence the development of peritoneal endometriosis.	(86)
AC068282.3, RP11-369C8.1, RP11-432J24.5, GBP1P1	Human	Eutopic endometrial tissues from patients with endometriosis ($n = 40$), normal controls ($n = 28$)	–	–	–	lncRNAs could be considered as novel diagnostic biomarkers and therapeutic targets for endometriosis.	(87)
CHL1-AS2, XLOC_009813, LOC643650, XLOC_009813, LOC255167, LOC400043, XLOC_012904, XLOC_l2_009510, AFAP1-AS1, XR_113107, XLOC_002900, LOC284576, XLOC_002900, XLOC_004907, XLOC_009813, XLOC_l2_008976, XLOC_006043, LOC100128893, XLOC_002900, XR_110229	Human	Paired eutopic and ectopic endometrium samples from patients with endometriotic ($n = 25$)	–	–	–	lncRNAs could be considered as novel diagnostic biomarkers and therapeutic targets for endometriosis.	(75)

(Continued)

TABLE 5 | Continued

lncRNA	Species	Numbers of clinical samples	Assessed cell line	Targets/ Regulators	Signaling Pathways	Function	References
PRKAR2B	Human	Paired eutopic and ectopic endometrium samples from patients with endometriotic ($n = 3$), normal controls ($n = 3$)	–	–	PI3K-Akt, NF-κB, TGF-β, MAPK	lncRNA could be considered as a novel diagnostic biomarker and therapeutic target for endometriosis.	(88)
NONHAT076754	Human	Paired eutopic and ectopic endometrium samples from patients with ovarian endometriotic cysts ($n = 92$)	HESCs	ZO-1, E-cadherin, N-cadherin	–	Exosomal lncRNA-NONHAT076754 could facilitate endometriosis invasion.	(89)
aHIF	Human	Ectopic ($n = 30$) and normal ($n = 16$) endometrium samples	ECSCs, HUVECs	VEGF-A, VEGF-D	–	Exosomal lncRNA-aHIF could Promote angiogenesis in endometriosis.	(90)

The expression pattern of MALAT1 has been assessed in a number of studies among them is the study by Liang et al. that reported down-regulation of this lncRNA in the endometriosis (48). **Figure 2** depicts the molecular mechanism of involvement of MALAT1 in this disorder.

INTERACTION BETWEEN MIRNAS AND LNCRNAS IN THE PATHOGENESIS OF ENDOMETRIOSIS

Based on the significant roles of lncRNAs and miRNAs in the pathogenesis of endometriosis and the presence of functional interactions between these two sets of transcripts, it is expected that lncRNA/miRNA pairs could regulate certain aspects of endometriosis. LncRNAs can act as a competing endogenous RNA (ceRNA) for miRNAs to affect their bioavailability of these transcripts. Assessments in the endometrial tissues have led to identification of a number of miRNAs that are inhibited by the lncRNA H19. For instance, Ghazal et al. have shown that H19 serves as a molecular sponge to decrease the availability of let-7. This interaction leads to over-expression of the downstream target of let-7, IGF1R, thus increasing the proliferation of endometrial stroma cells. They also demonstrated down-regulation of H19 in the eutopic endometrium of patients with endometriosis and speculated that the subsequent decrease in the IGF1R activity might diminish endometrial stromal cell proliferation and negatively influence the endometrial receptivity for pregnancy (92). In addition, Xu et al. have demonstrated the role of the estrogen-modulated H19/ACTA2/miR-216a-5p axis in the regulation of invasion and migration of eutopic endometrial stromal cells in subjects with endometriosis (78). Liu et al. have reported the significance of H19/miR-342-3p/IER3 axis in suppression of Th17 cell differentiation and decreasing the risk of endometriosis (93). A recent high throughput study of RNA profile of the ectopic and eutopic endometrium of patients has led to construction of the ceRNA network. Assessment of the RNA interaction network in endometriosis has resulted to identification of the role of miRNAs and lncRNAs that are associated with cyclin-dependent kinase 1 (CDK1) and proliferating cell nuclear antigen (PCNA). These genes regulate the growth and apoptosis of endometrial stromal cells, thus are involved in the pathophysiology of endometriosis. Taken together, the RNA interactive network has critical role in this disorder (102).

DISCUSSION

Several studies have assessed expression profile of lncRNAs and miRNAs in tissues/blood samples obtained from patients with endometriosis. Association between genomic variants of miRNAs and endometriosis has also been another research avenue. However, the latter field has been less explored for lncRNAs. Considering the presence of myriads of SNPs within lncRNA coding genes that modulate their expression and regulatory functions on their targets, assessment of their association with the risk of endometriosis is a necessary step for identification of the role of these transcripts. Non-coding RNAs have fundamental roles in the development of endometriosis. Their role in this process has been highlighted not only by the studies which reported their aberrant expression in patients' samples, but also by the investigations which showed modulation of their expression by therapeutic agents. For instance, Quercetin (3,3′,4′,5,7-pentahydroxyflavone) as a phytochemical agent with antioxidant, anti-inflammatory and antiangiogenic characteristics has been shown to suppress the proliferation and induce cell cycle arrest in VK2/E6E7 and End1/E6E7 cells. Moreover, it has exerted antiproliferative and anti-inflammatory impacts on endometriosis autoimplanted mouse models. This effect has been accompanied by induction of miR-503-5p, miR-1283, miR-3714 and miR-6867-5p in both cell lines and stimulation of miR-503-5p and miR-546 expression in the animal model (103). Saponin extract, as another natural therapeutic agent has been shown to reduce expression of miR-21-5p in the human endometrial stromal cells from patients with endometriosis. Suppression of this miRNA could induce apoptosis in these cells. These results imply that he therapeutic

TABLE 6 | Down-regulated lncRNAs in endometriosis.

lncRNA	Species	Numbers of clinical samples	Assessed cell line	Targets/ Regulators	Signaling Pathways	Function	References
CLEC2D	Human	Paired eutopic and ectopic endometrium samples from patients with endometriotic ($n = 3$), normal controls ($n = 3$)	–	–	PI3K-Akt, NF-κB, TGF-β, MAPK	This lncRNA could be considered as a novel diagnostic biomarker and therapeutic target for endometriosis.	(88)
ABO, TCONS_08347373	Human	Eutopic endometrium samples ($n = 17$), normal samples ($n = 17$)	–	–	–	lncRNAs could be considered as novel diagnostic biomarkers and therapeutic targets for endometriosis.	(82)
MALAT1	Human	Granulosa cells (GCs) from endometriosis patients ($n = 52$) and controls ($n = 52$)—(follicles ≥10)	KGN	p21, CDK2, cyclin D1	ERK/MAPK	Downregulation of lncRNA-MALAT1 by upregulating p21 via activation of the ERK/MAPK pathway could inhibit granulosa cell proliferation in endometriosis.	(91)
H19	Human	Eutopic endometrial tissues from endometriosis patients ($n = 10$), normal controls ($n = 10$)	HESCs	Let-7, IGF1R	–	lncRNA-H19 via IGF signaling pathway could alter the growth of stromal cells in the endometrium of women with endometriosis.	(92)
	Human	Endometriosis patients ($n = 20$), controls ($n = 16$) (peritoneal fluid samples)	HESCs	miR-342-3p, IER3	–	The level of IL-17 and the percentage of Th17 cells/CD4+ T cells are decreased when lncRNA-H19 overexpressed. Therefore, upregulated-lncRNA-H19 through miR-342-3p/IER3 pathway could inhibit Th17 cell differentiation to relieve endometriosis.	(93)
NONRATT003997, gi|672033904|ref| XR_589853.1|	Rat	–	–	Dlx3, P2ry6, Adamts7	–	During the implantation window process, changes in the expression of lncRNAs could affect endometrial receptivity in rats with endometriosis.	(74)
SRA	Human	Endometriotic samples from women with endometriosis ($n = 24$), normal controls ($n = 24$)	HESCs	Estrogen receptor	–	Silencing of SRA1 via regulating ER expression could decrease stromal cells growth in ovarian endometriosis.	(94)
AC002454.1, RP11-403H13.1	Human	Eutopic endometrial tissues from patients with endometriosis ($n = 40$), normal controls ($n = 28$)	–	–	–	LncRNAs could be considered as novel diagnostic biomarkers and therapeutic targets for endometriosis.	(87)
LOC100505776, UCA1, LOC100506860, XLOC_012981, LINC00261, LOC100507043, LOC100507218, LOC440335, XLOC_l2_013295, LINC00116, MSX2P1, XLOC_l2_013295, KLKP1, XLOC_005677, XLOC_l2_013295, XLOC_001243, XLOC_003147, LOC100507043	Human	Paired eutopic and ectopic endometrium samples from patients with endometriotic ($n = 25$)	–	–	–	LncRNAs could be considered as novel diagnostic biomarkers and therapeutic targets for endometriosis.	(75)
LINC00261	–	–	CRL-7566	–	–	LINC00261 could inhibit endometriosis cell growth and migration.	(95)

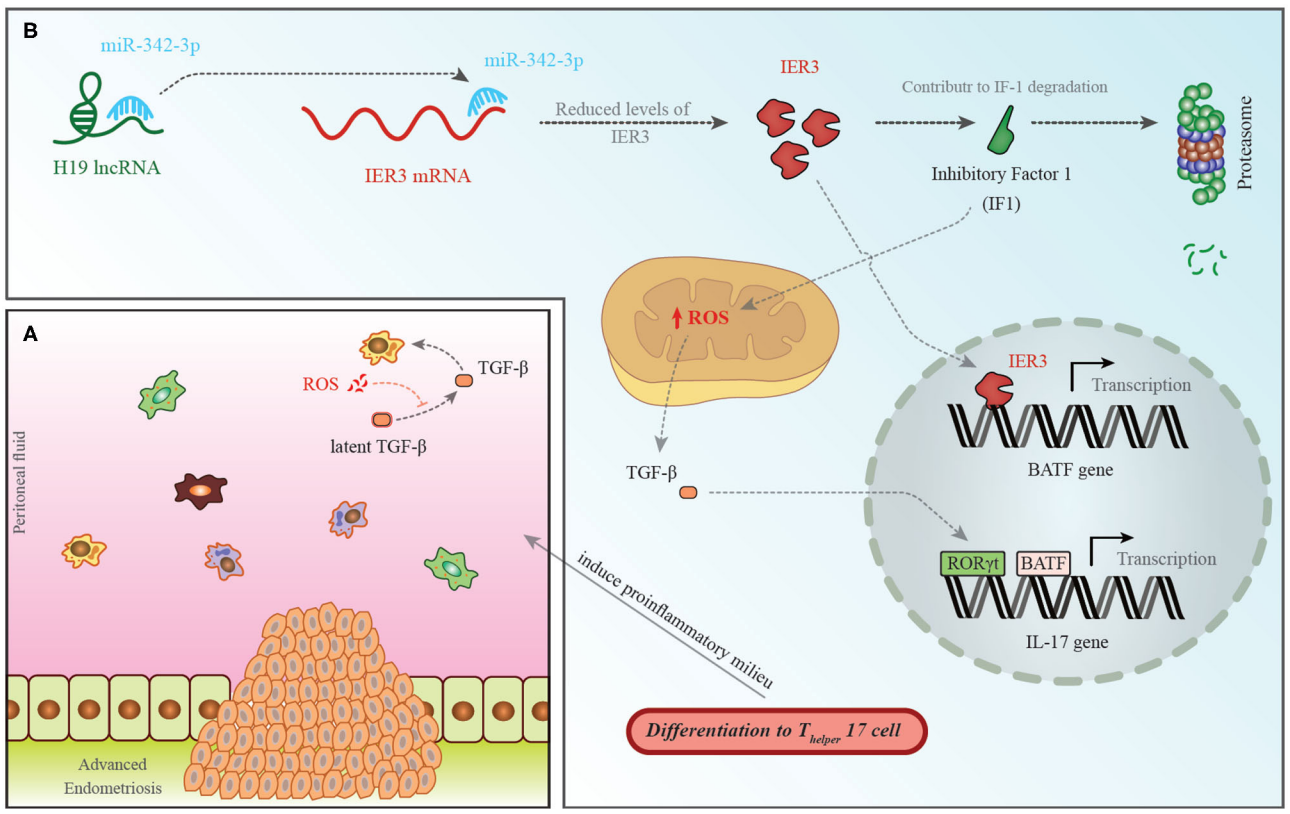

FIGURE 1 | (A) A pro-endometriotic microenvironment produced by an existing endometriotic lesion provides the appropriate micro-environment for the progression of this disorder. After the buildup of cells by a previously established lesion, these elements show distinctive features that destroy immune surveillance (96). **(B)** H19 levels have been shown to be decreased in the PBMCs of patients with endometriosis. This is accompanied with an increase in miR-342-3p levels. This miRNA binds with the 3′ UTR of IER3, thus inhibiting its expression (93). IER3 participates in proteasomal degradation of IF-1. Decrease in the levels of IF-1 leads to increase in reactive oxygen species (ROS) levels (97). ROS increases active extracellular TGF-β levels. This cytokine influences RORγt, thus activating transcription of IL-17 and leading to differentiation of TH17 cells (98).

effect of saponin is exerted through modulation of specific miRNAs (69).

Expressions of miRNAs have been assessed in different samples from patients with endometriosis such as endometrium, peripheral blood and peritoneal fluid. There are some cases of inconsistency between these studies. For instance, expression of miR-451a has been shown to be up-regulated in serum (13), exosomes (20) and endometriosis lesions of patients with endometriosis (23) as well as samples obtained from mouse models of endometriosis (22). However, another study has reported downregulation of miR-451 in the eutopic endometrial tissues of patients with endometriosis compared with control tissues (53). The lncRNA UCA1 has been reported to be up-regulated in ectopic endometrium tissues compared with paired eutopic endometrium tissues in the majority of patients using qRT-PCR (76). On the other hand, a microarray analysis showed down-regulated of this lncRNA in ovarian ectopic endometrial tissue compared with paired eutopic endometrial tissue (75). Similar discrepancy has been observed for MALAT1. While it has been upregulated in endometrial tissues from patients with endometriosis compared with normal controls (78), it was downregulated in granulosa cells from endometriosis patients compared with controls (91). The heterogeneity of samples and the method of expression analysis can partly explain the inconsistency of these results.

Mechanistically, lncRNAs can sponge miRNAs, regulate expression of inflammatory factors, alter cell proliferation, migration and apoptosis of endometrial cells. They might also affect implantation process (104, 105). Several transcription factors and signaling pathways have been regulated by lncRNAs in the endometrial tissues. Examples are HOX genes, N-cadherin, snail, slug, TCF8/ZEB1, matrix metalloproteinase, apoptosis related genes such as caspases and autophagy-related genes such as Beclin1.

The advent of next generation sequencing has enhanced the pace of identification of dysregulated non-coding RNAs in all human diseases including endometriosis. This technique has been applied by Khalaj et al. to identify signature of these transcripts in extracellular vesicles (EVs) obtained from endometriosis patient tissues and plasma samples compared with controls. Authors have demonstrated the presence of distinctive signatures of miRNAs and lncRNAs indicating their participation in the pathogenesis of endometriosis. Dysregulated transcripts were enriched in the pathways related to immune and

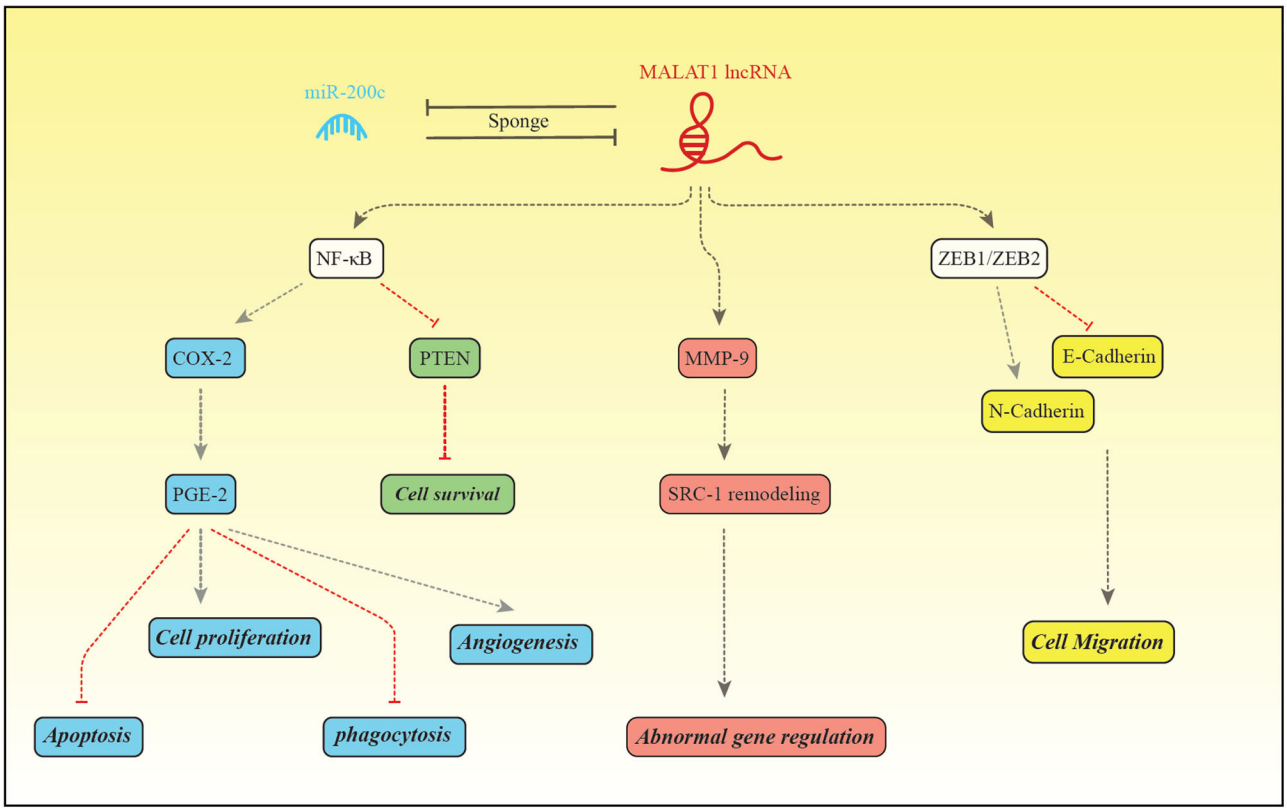

FIGURE 2 | MALAT1 and miR-200c regulate expression of each other through the sponging mechanism. Liang et al. have reported down-regulation of MALAT1 and up-regulation of miR-200c in patients with endometriosis (48). MALAT1 increase expression of NF-κB which in turn binds with PGE-2 to enhance its expression (99). PGE-2 activates BCL2/BAX through interaction with EP2/EP4 receptor and suppresses intrinsic apoptotic pathway (100). PGE2 also activates cell proliferation through EP2/EP3 (101). In addition, PGE-2 suppresses MMP2, CD36 and annexin A2 in macrophages, thus inhibits phagocytic activity of macrophages. These effects facilitate implantation and growth of endometrial tissue in the peritoneum (101). PGE-2 influences angiogenic activity and cell cycle progression through increasing expression of VEGF and inhibiting PTEN, respectively (99). MALAT1 can enhance MMP9 levels. MMP9 increases production of the truncated isoform of Steroid receptor coactivator-1. MALAT1 also increases transcription of ZEB1/ZEB2, therefore induces mesenchymal cell phenotype which is accompanied by enhancement of cell migration (48).

metabolic functions. Their results indicated that endometriosis-associated EVs transport distinctive cargo and influence the disease course by modulation of inflammation, angiogenesis and proliferation (23). Moreover, exosomal miRNAs isolated from peritoneal macrophages have been shown to increase proliferation, migration, and invasion of ectopic endometrial stromal cells (10). Thus, these transcripts have fundamental roles in the pathogenesis of endometriosis. Taken together, these studies have opened a new research era for identification of the pathophysiology of endometriosis. Another technical development which has facilitated identification of this process has been the cell sorting technique. This technique has paved the way for cell-type-specific analysis of ectopic tissues to recognize the interactions between different cell types during the course of disease (30).

Considering the unavailability of affected tissues in the endometriosis except through invasive methods, identification of biomarkers in the serum of patients has a practical significance. Recent studies have demonstrated appropriate diagnostic power and sensitivity and specificity values for several miRNAs in this regard. Several miRNAs panels are expected to be applied in the clinical settings with high diagnostic power values. In spite of the presence of these supporting results, there is no consensus on a panel for the diagnosis of endometriosis, since most of studies have been conducted in small samples sizes of patients and their results have not been verified in independent samples. Besides, based on the differences in the source of controls, the applied techniques and the biological sources, meta-analysis of the obtained data is complicated. The diagnostic power of lncRNAs in the endometriosis has been less studied. Thus, future studies are needed to assess this aspect as well.

Taken together, based on the results of human and animal investigation, both miRNAs and lncRNAs participate in the pathogenesis of endometriosis. A more comprehensive assessment of these transcripts using the high throughput methods and identification of the functional links between these two sets of transcripts would facilitate identification of

the pathogenesis of endometriosis and recognition of possible therapeutic targets in this regard.

AUTHOR CONTRIBUTIONS

HS performed the data collection. MT and SG-F wrote the draft and revised it. MT designed the hypothesis. All authors contributed to the article and approved the submitted version.

FUNDING

This study was financially supported by Shahid Beheshti University of Medical Sciences.

REFERENCES

1. Giudice LC. Endometriosis. *New Engl J Med.* (2010) 362:2389–98. doi: 10.1056/NEJMcp1000274
2. Nisolle M, Donnez J. Peritoneal endometriosis, ovarian endometriosis, and adenomyotic nodules of the rectovaginal septum are three different entities. *Fertil Steril.* (1997) 68:585–96. doi: 10.1016/S0015-0282(97)00191-X
3. Parasar P, Ozcan P, Terry KL. Endometriosis: epidemiology, diagnosis and clinical management. *Curr Obstet Gynecol Rep.* (2017) 6:34–41. doi: 10.1007/s13669-017-0187-1
4. Hansen KA, Eyster KM. Genetics and genomics of endometriosis. *Clin Obstet Gynecol.* (2010) 53:403–12. doi: 10.1097/GRF.0b013e3181db7ca1
5. Panir K, Schjenken JE, Robertson SA, Hull ML. Non-coding RNAs in endometriosis: a narrative review. *Human Reprod Update.* (2018) 24:497–515. doi: 10.1093/humupd/dmy014
6. Fernandes JCR, Acuña SM, Aoki JI, Floeter-Winter LM, Muxel SM. Long non-coding RNAs in the regulation of gene expression: physiology and disease. *Noncoding RNA.* (2019) 5:17. doi: 10.3390/ncrna5010017
7. Zhao Y, Li H, Fang S, Kang Y, Wu W, Hao Y, et al. NONCODE 2016: an informative and valuable data source of long non-coding RNAs. *Nucleic Acids Res.* (2016) 44(D1):D203–8. doi: 10.1093/nar/gkv1252
8. Catalanotto C, Cogoni C, Zardo G. MicroRNA in control of gene expression: an overview of nuclear functions. *Int J Mol Sci.* (2016) 17:1712. doi: 10.3390/ijms17101712
9. Zhang L, Li H, Yuan M, Li D, Sun C, Wang G. Serum exosomal microRNAs as potential circulating biomarkers for endometriosis. *Dis Mark.* (2020) 2020:2456340. doi: 10.1155/2020/2456340
10. Zhang L, Li H, Yuan M, Li D, Wang G. Exosomal miR-22-3p derived from peritoneal macrophages enhances proliferation, migration, and invasion of ectopic endometrial stromal cells through regulation of the SIRT1/NF-κB signaling pathway. *Eur Rev Med Pharmacol Sci.* (2020) 24:571–80. doi: 10.26355/eurrev_202001_20033
11. Zhou C-F, Liu M-J, Wang W, Wu S, Huang Y-X, Chen G-B, et al. miR-205-5p inhibits human endometriosis progression by targeting ANGPT2 in endometrial stromal cells. *Stem Cell Res Ther.* (2019) 10:287. doi: 10.1186/s13287-019-1388-5
12. Zhang Z, Li H, Zhao Z, Gao B, Meng L, Feng X. miR-146b level and variants is associated with endometriosis related macrophages phenotype and plays a pivotal role in the endometriotic pain symptom. *Taiw J Obstetr Gynecol.* (2019) 58:401–8. doi: 10.1016/j.tjog.2018.12.003
13. Moustafa S, Burn M, Mamillapalli R, Nematian S, Flores V, Taylor HS. Accurate diagnosis of endometriosis using serum microRNAs. *Am J Obstetr Gynecol.* (2020). doi: 10.1016/j.ajog.2020.02.050
14. Zolbin MM, Mamillapalli R, Nematian SE, Goetz L, Taylor HS. Adipocyte alterations in endometriosis: reduced numbers of stem cells and microRNA induced alterations in adipocyte metabolic gene expression. *Reprod Biol Endocrinol.* (2019) 17:36. doi: 10.1186/s12958-019-0480-0
15. Zhang H, Li G, Sheng X, Zhang S. Upregulation of miR-33b promotes endometriosis via inhibition of Wnt/β-catenin signaling and ZEB1 expression. *Mol Med Rep.* (2019) 19:2144–52. doi: 10.3892/mmr.2019.9870
16. Yang P, Wu Z, Ma C, Pan N, Wang Y, Yan L. Endometrial miR-543 is downregulated during the implantation window in women with endometriosis-related infertility. *Reprod Sci.* (2019) 26:900–8. doi: 10.1177/1933719118799199
17. Dai Y, Lin X, Xu W, Lin X, Huang Q, Shi L, et al. MiR-210-3p protects endometriotic cells from oxidative stress-induced cell cycle arrest by targeting BARD1. *Cell Death Dis.* (2019) 10:1–15. doi: 10.1038/s41419-019-1395-6
18. Nabiel Y, ELshahawy H, Mosbah A. Intrauterine bacterial colonization and endometrial microRNA-17-5p levels in association to endometriosis: a study in an egyptian population. *Immunol Investig.* (2019). doi: 10.1080/08820139.2019.1693592. [Epub ahead of print].
19. Mashayekhi P, Noruzinia M, Zeinali S, Khodaverdi S. Endometriotic mesenchymal stem cells epigenetic pathogenesis: deregulation of miR-200b, miR-145, and let7b in a functional imbalanced epigenetic disease. *Cell J.* (2019) 21:179. doi: 10.22074/cellj.2019.5903
20. Chen Y, Wang K, Xu Y, Guo P, Hong B, Cao Y, et al. Alteration of myeloid-derived suppressor cells, chronic inflammatory cytokines, and exosomal miRNA contribute to the peritoneal immune disorder of patients with endometriosis. *Reprod Sci.* (2019) 26:1130–8. doi: 10.1177/1933719118808923
21. Cosar E, Mamillapalli R, Moridi I, Duleba A, Taylor HS. Serum microRNA biomarkers regulated by simvastatin in a primate model of endometriosis. *Reprod Sci.* (2019) 26:1343–50. doi: 10.1177/1933719118765971
22. Li M, Zhou Y, Taylor HS. miR-451a inhibition reduces established endometriosis lesions in mice. *Reprod Sci.* (2019) 26:1506–11. doi: 10.1177/1933719119862050
23. Khalaj K, Miller JE, Lingegowda H, Fazleabas AT, Young SL, Lessey BA, et al. Extracellular vesicles from endometriosis patients are characterized by a unique miRNA-lncRNA signature. *JCI Insight.* (2019) 4:e128846. doi: 10.1172/jci.insight.128846
24. Maged AM, Deeb WS, El Amir A, Zaki SS, El Sawah H, Al Mohamady M, et al. Diagnostic accuracy of serum miR-122 and miR-199a in women with endometriosis. *Int J Gynecol Obstetr.* (2018) 141:14–9. doi: 10.1002/ijgo.12392
25. Bashti O, Noruzinia M, Garshasbi M, Abtahi M. miR-31 and miR-145 as potential non-invasive regulatory biomarkers in patients with endometriosis. *Cell J.* (2018) 20:1–131. doi: 10.22074/cellj.2018.4915
26. Cheng F, Lu L, Wang H, Cheng H, Zhang D. Expression and significance of miR-126 and miR-145 in infertility due to endometriosis. *J Coll Phys Surg Pak.* (2019) 29:585–7. doi: 10.29271/jcpsp.2019.06.585
27. Marí-Alexandre J, Barceló-Molina M, Belmonte-López E, García-Oms J, Estellés A, Braza-Boïls A, et al. Micro-RNA profile and proteins in peritoneal fluid from women with endometriosis: their relationship with sterility. *Fertil Steril.* (2018) 109:675–84. e2. doi: 10.1016/j.fertnstert.2017.11.036
28. Pei T, Liu C, Liu T, Xiao L, Luo B, Tan J, et al. miR-194-3p represses the progesterone receptor and decidualization in eutopic endometrium from women with endometriosis. *Endocrinology.* (2018) 159:2554–62. doi: 10.1210/en.2018-00374
29. Pateisky P, Pils D, Szabo L, Kuessel L, Husslein H, Schmitz A, et al. hsa-miRNA-154-5p expression in plasma of endometriosis patients is a potential diagnostic marker for the disease. *Reprod Biomed Online.* (2018) 37:449–66. doi: 10.1016/j.rbmo.2018.05.007

30. Rekker K, Tasa T, Saare M, Samuel K, Kadastik Ü, Karro H, et al. Differentially-expressed miRNAs in ectopic stromal cells contribute to endometriosis development: the plausible role of miR-139-5p and miR-375. *Int J Mol Sci.* (2018) 19:3789. doi: 10.3390/ijms19123789
31. Zhao L, Gu C, Ye M, Zhang Z, Fan W, Meng Y. Integration analysis of microRNA and mRNA paired expression profiling identifies deregulated microRNA-transcription factor-gene regulatory networks in ovarian endometriosis. *Reprod Biol Endocrinol.* (2018) 16:4. doi: 10.1186/s12958-017-0319-5
32. Shu X-M. Assessment of the expression of mir-29c, mir-200a and mir-145 in endometrial tissue and the downstream molecules in infertile patients with endometriosis. *J Hain Med Univ.* (2017) 23:97–100.
33. Joshi NR, Miyadahira EH, Afshar Y, Jeong J-W, Young SL, Lessey BA, et al. Progesterone resistance in endometriosis is modulated by the altered expression of microRNA-29c and FKBP4. *J Clin Endocrinol Metab.* (2017) 102:141–9. doi: 10.1210/jc.2016-2076
34. Nothnick WB, Falcone T, Joshi N, Fazleabas AT, Graham A. Serum miR-451a levels are significantly elevated in women with endometriosis and recapitulated in baboons (Papio anubis) with experimentally-induced disease. *Reprod Sci.* (2017) 24:1195–202. doi: 10.1177/1933719116681519
35. Braicu O-L, Budisan L, Buiga R, Jurj A, Achimas-Cadariu P, Pop LA, et al. miRNA expression profiling in formalin-fixed paraffin-embedded endometriosis and ovarian cancer samples. *OncoTargets Ther.* (2017) 10:4225. doi: 10.2147/OTT.S137107
36. Kim MK, Lee SK, Park JH, Lee JH, Yun BH, Park JH, et al. Ginsenoside Rg3 decreases fibrotic and invasive nature of endometriosis by modulating miRNA-27b: *in vitro* and *in vivo* studies. *Sci Rep.* (2017) 7:1–14. doi: 10.1038/s41598-017-17956-0
37. Wright KR, Mitchell B, Santanam N. Redox regulation of microRNAs in endometriosis-associated pain. *Redox Biol.* (2017) 12:956–66. doi: 10.1016/j.redox.2017.04.037
38. Xu X, Li Z, Liu J, Yu S, Wei Z. MicroRNA expression profiling in endometriosis-associated infertility and its relationship with endometrial receptivity evaluated by ultrasound. *J X Ray Sci Technol.* (2017) 25:523–32. doi: 10.3233/XST-17286
39. Yang R, Teng H, Xu X, Liu S, Wang Y, Guo F, et al. Microarray analysis of microRNA deregulation and angiogenesis-related proteins in endometriosis. *Genet Mol Res.* (2016) 15:1–8. doi: 10.4238/gmr.15027826
40. Xu T, Zhao S, Dong M, Yu X. Hypoxia responsive miR-210 promotes cell survival and autophagy of endometriotic cells in hypoxia. *Eur Rev Med Pharmacol Sci.* (2016) 20:399–406.
41. Falih ES, Aubaid SH, Yousif WaT. The role of microRNA 122, MCP-1 and TGF-β1 as diagnostic biomarkers for endometriosis. *Indian J Public Health Res Dev.* (2019) 10:2652–6. doi: 10.5958/0976-5506.2019.03267.4
42. Cosar E, Mamillapalli R, Ersoy GS, Cho S, Seifer B, Taylor HS. Serum microRNAs as diagnostic markers of endometriosis: a comprehensive array-based analysis. *Fertil Steril.* (2016) 106:402–9. doi: 10.1016/j.fertnstert.2016.04.013
43. Eggers JC, Martino V, Reinbold R, Schäfer SD, Kiesel L, Starzinski-Powitz A, et al. microRNA miR-200b affects proliferation, invasiveness and stemness of endometriotic cells by targeting ZEB1, ZEB2 and KLF4. *Reprod Biomed Online.* (2016) 32:434–45. doi: 10.1016/j.rbmo.2015.12.013
44. Liu X, Bai X, Teng Y, Song L, Lu N, Yang R. miRNA-15a-5p regulates VEGFA in endometrial mesenchymal stem cells and contributes to the pathogenesis of endometriosis. *Eur Rev Med Pharmacol Sci.* (2016) 20:3319–26.
45. Hirakawa T, Nasu K, Abe W, Aoyagi Y, Okamoto M, Kai K, et al. miR-503, a microRNA epigenetically repressed in endometriosis, induces apoptosis and cell-cycle arrest and inhibits cell proliferation, angiogenesis, and contractility of human ovarian endometriotic stromal cells. *Human Reprod.* (2016) 31:2587–97. doi: 10.1093/humrep/dew217
46. Ma Y, Huang YX, Chen YY. miRNA-34a-5p downregulation of VEGFA in endometrial stem cells contributes to the pathogenesis of endometriosis. *Mol Med Rep.* (2017) 16:8259–64. doi: 10.3892/mmr.2017.7677
47. Seifer BJ, Su D, Taylor HS. Circulating miRNAs in murine experimental endometriosis: decreased abundance of let-7a. *Reprod Sci.* (2017) 24:376–81. doi: 10.1177/1933719116667228
48. Liang Z, Chen Y, Zhao Y, Xu C, Zhang A, Zhang Q, et al. miR-200c suppresses endometriosis by targeting MALAT1 *in vitro* and *in vivo*. *Stem Cell Res Ther.* (2017) 8:251. doi: 10.1186/s13287-017-0706-z
49. Yang W, Hong L, Xu X, Wang Q, Huang J, Jiang L. Regulation of miR-33b on endometriosis and expression of related factors. *Eur Rev Med Pharmacol Sci.* (2017) 21:2027−33.
50. Chen X, Jiang Y, Pan D. miR-30c may serve a role in endometriosis by targeting plasminogen activator inhibitor-1. *Exp Ther Med.* (2017) 14:4846–52. doi: 10.3892/etm.2017.5145
51. Yang W, Hong L, Xu X, Wang Q, Huang J, Jiang L. MiR-424-5p regulates proliferation and apoptosis by targeting FGFR1 in endometriosis cells. *Int J Clin Exp Med.* (2017) 10:666–74.
52. Zhang A, Wang G, Jia L, Su T, Zhang L. Exosome-mediated microRNA-138 and vascular endothelial growth factor in endometriosis through inflammation and apoptosis via the nuclear factor-κB signaling pathway. *Int J Mol Med.* (2019) 43:358–70. doi: 10.3892/ijmm.2018.3980
53. Gao S, Liu S, Gao Z-M, Deng P, Wang D-B. Reduced microRNA-451 expression in eutopic endometrium contributes to the pathogenesis of endometriosis. *World J Clin Cases.* (2019) 7:2155. doi: 10.12998/wjcc.v7.i16.2155
54. Zhang M, Zhang Y, Li L, Ma L, Zhou C. Dysregulation of miR-202-3p affects migration and invasion of endometrial stromal cells in endometriosis via targeting ROCK1. *Reprod Sci.* (2020) 27:731–42. doi: 10.1007/s43032-019-00079-4
55. Liu Y, Lu C, Fan L, Wang J, Li T, Liu Z, et al. MiR-199a-5p targets ZEB1 to inhibit the epithelial-mesenchymal transition of ovarian ectopic endometrial stromal cells via PI3K/Akt/mTOR signal pathway *in vitro* and *in vivo*. *Reprod Sci.* (2020) 27:110–8. doi: 10.1007/s43032-019-00016-5
56. Chen L-J, Hu B, Han Z-Q, Ni J, Zhou Y-M, Chen X-X, et al. MicroRNA-20a mediates the cytotoxicity of natural killer cells in endometriosis via ERG/HLX/STAT4/perforin axis. *Preprint.* (2020). doi: 10.21203/rs.2.17459/v1
57. Zhang Y, Yan J, Pan X. miR-141-3p affects apoptosis and migration of endometrial stromal cells by targeting KLF-12. *Pflügers Archiv Eur J Physiol.* (2019) 471:1055–63. doi: 10.1007/s00424-019-02283-2
58. Petracco R, Dias ACdO, Taylor HS, Petracco Á, Badalotti M, Michelon JdR, et al. Evaluation of miR-135a/b expression in endometriosis lesions. *Biomed Rep.* (2019) 11:181–7. doi: 10.3892/br.2019.1237
59. Li X, Zhang W, Fu J, Xu Y, Gu R, Qu R, et al. MicroRNA-451 is downregulated in the follicular fluid of women with endometriosis and influences mouse and human embryonic potential. *Reprod Biol Endocrinol.* (2019) 17:96. doi: 10.1186/s12958-019-0538-z
60. Ma L, Li Z, Li W, Ai J, Chen X. MicroRNA-142-3p suppresses endometriosis by regulating KLF9-mediated autophagy *in vitro* and *in vivo*. *RNA Biol.* (2019) 16:1733–48. doi: 10.1080/15476286.2019.1657352
61. Kästingschäfer CS, Schäfer SD, Kiesel L, Götte M. miR-142-3p is a novel regulator of cell viability and proinflammatory signalling in endometrial stroma cells. *Reprod Biomed Online.* (2015) 30:553–6. doi: 10.1016/j.rbmo.2015.01.002
62. Zhu H, Cao XX, Liu J, Hua H. MicroRNA-488 inhibits endometrial glandular epithelial cell proliferation, migration, and invasion in endometriosis mice via Wnt by inhibiting FZD7. *J Cell Mol Med.* (2019) 23:2419–30. doi: 10.1111/jcmm.14078
63. Hu Z, Mamillapalli R, Taylor HS. Increased circulating miR-370-3p regulates steroidogenic factor 1 in endometriosis. *Am J Physiol Endocrinol Metab.* (2019) 316:E373–82. doi: 10.1152/ajpendo.00244.2018
64. Meng X, Liu J, Wang H, Chen P, Wang D. MicroRNA-126-5p downregulates BCAR3 expression to promote cell migration and invasion in endometriosis. *Mol Cell Endocrinol.* (2019) 494:110486. doi: 10.1016/j.mce.2019.110486
65. Wu D, Lu P, Mi X, Miao J. Exosomal miR-214 from endometrial stromal cells inhibits endometriosis fibrosis. *MHR Basic Sci Reprod Med.* (2018) 24:357–65. doi: 10.1093/molehr/gay019
66. He SZ, Li J, Bao HC, Wang MM, Wang XR, Huang X, et al. G protein-coupled estrogen receptor/miR-148a/human leukocyte antigen-G signaling pathway mediates cell apoptosis of ovarian

endometriosis. *Mol Med Rep.* (2018) 18:1141–8. doi: 10.3892/mmr.2018.9039
67. Hsu CY, Hsieh TH, Er TK, Chen HS, Tsai CC, Tsai EM. MiR-381 regulates cell motility, growth and colony formation through PIK3CA in endometriosis-associated clear cell and endometrioid ovarian cancer. *Oncol Rep.* (2018) 40:3734–42. doi: 10.3892/or.2018.6779
68. Sahin C, Mamillapalli R, Yi KW, Taylor HS. micro RNA Let-7b: a Novel treatment for endometriosis. *J Cell Mol Med.* (2018) 22:5346–53. doi: 10.1111/jcmm.13807
69. Park JH, Lee SK, Kim MK, Lee JH, Yun BH, Park JH, et al. Saponin extracts induced apoptosis of endometrial cells from women with endometriosis through modulation of miR-21-5p. *Reprod Sci.* (2018) 25:292–301. doi: 10.1177/1933719117711263
70. Liu Y, Chen J, Zhu X, Tang L, Luo X, Shi Y. Role of miR-449b-3p in endometriosis via effects on endometrial stromal cell proliferation and angiogenesis. *Mol Med Rep.* (2018) 18:3359–65. doi: 10.3892/mmr.2018.9341
71. Wang F, Wang H, Jin D, Zhang Y. Serum miR-17, IL-4, and IL-6 levels for diagnosis of endometriosis. *Medicine.* (2018) 97:e10853. doi: 10.1097/MD.0000000000010853
72. Sepahi N, Kohan L, Jahromi AR, Daneshbod Y, Hoveidi EN. mir-126 rs4636297 and TGF β RI rs334348 functional gene variants are associated with susceptibility to endometriosis and its severity. *Gynecol Endocrinol.* (2017) 33:429–32. doi: 10.1080/09513590.2017.1290064
73. Nimi-Hoveidi E, Kohan L, Hashemi SS. Association of miR-143 rs41291957 and rs4705342 genetic variants with endometriosis risk in infertile women. *KAUMS J.* (2016) 20:441−6.
74. Cai H, Zhu X, Li Z, Zhu Y, Lang J. lncRNA/mRNA profiling of endometriosis rat uterine tissues during the implantation window. *Int J f Mol Med.* (2019) 44:2145–60. doi: 10.3892/ijmm.2019.4370
75. Sun P-r, Jia S-z, Lin H, Leng J-H, Lang J-H. Genome-wide profiling of long noncoding ribonucleic acid expression patterns in ovarian endometriosis by microarray. *Fertil Steril.* (2014) 101:1038-46. e7. doi: 10.1016/j.fertnstert.2013.12.035
76. Huang H, Zhu Z, Song Y. Downregulation of lncrna uca1 as a diagnostic and prognostic biomarker for ovarian endometriosis. *Rev Assoc Méd Bras.* (2019) 65:336–41. doi: 10.1590/1806-9282.65.3.336
77. Qiu J-J, Lin Y-Y, Tang X-Y, Ding Y, Yi X-F, Hua K-Q. Extracellular vesicle-mediated transfer of the lncRNA-TC0101441 promotes endometriosis migration/invasion. *Exp Cell Res.* (2020) 388:111815. doi: 10.1016/j.yexcr.2020.111815
78. Xu Z, Zhang L, Yu Q, Zhang Y, Yan L, Chen Z-J. The estrogen-regulated lncRNA H19/miR-216a-5p axis alters stromal cell invasion and migration via ACTA2 in endometriosis. *Mol Hum Reprod.* (2019) 25:550–61. doi: 10.1093/molehr/gaz040
79. Liu H, Zhang Z, Xiong W, Zhang L, Du Y, Liu Y, et al. Long non-coding RNA MALAT 1 mediates hypoxia-induced pro-survival autophagy of endometrial stromal cells in endometriosis. *J Cell Mol Med.* (2019) 23:439–52. doi: 10.1111/jcmm.13947
80. Zhang C, Wu W, Zhu H, Yu X, Zhang Y, Ye X, et al. Knockdown of long noncoding RNA CCDC144NL-AS1 attenuates migration and invasion phenotypes in endometrial stromal cells from endometriosis. *Biol Reprod.* (2019) 100:939–49. doi: 10.1093/biolre/ioy252
81. Zhu M, Chen L, Hu M, Shi Z, Liu Y. Effects of lncRNA BANCR on endometriosis through ERK/MAPK pathway. *Eur Rev Med Pharmacol Sci.* (2019) 23:6806–12. doi: 10.26355/eurrev_201908_18719
82. Cui D, Ma J, Liu Y, Lin K, Jiang X, Qu Y, et al. Analysis of long non-coding RNA expression profiles using RNA sequencing in ovarian endometriosis. *Gene.* (2018) 673:140–8. doi: 10.1016/j.gene.2018.06.046
83. Lin D, Huang Q, Wu R, Dai S, Huang Z, Ren L, et al. Long non-coding RNA AFAP1-AS1 promoting epithelial-mesenchymal transition of endometriosis is correlated with transcription factor ZEB1. *Am J Reprod Immunol.* (2019) 81:e13074. doi: 10.1111/aji.13074
84. Liu J, Wang Q, Zhang R, Zhang C, Lin J, Huang X. Identification of LINC01279 as a cell cycle-associated long non-coding RNA in endometriosis with GBA analysis. *Mol Med Rep.* (2018) 18:3850–8. doi: 10.3892/mmr.2018.9387
85. Zhang C, Wu W, Ye X, Ma R, Luo J, Zhu H, et al. Aberrant expression of CHL1 gene and long non-coding RNA CHL1-AS1, CHL1-AS2 in ovarian endometriosis. *Eur J Obstetr Gynecol Reprod Biol.* (2019) 236:177–82. doi: 10.1016/j.ejogrb.2019.03.020
86. Wang M, Hao C, Huang X, Bao H, Qu Q, Liu Z, et al. Aberrant expression of lncRNA (HOXA11-AS1) and homeobox A (HOXA9, HOXA10, HOXA11, and HOXA13) genes in infertile women with endometriosis. *Reprod Sci.* (2018) 25:654–61. doi: 10.1177/1933719117734320
87. Wang Y, Li Y, Yang Z, Liu K, Wang D. Genome-wide microarray analysis of long non-coding RNAs in eutopic secretory endometrium with endometriosis. *Cell Physiol Biochem.* (2015) 37:2231–45. doi: 10.1159/000438579
88. Liu S-P, Tian X, Cui H-Y, Zhang Q, Hua K-Q. The messenger RNA and long non-coding RNA expression profiles in ectopic and eutopic endometrium provide novel insights into endometriosis. *Reprod Dev Med.* (2019) 3:11. doi: 10.4103/2096-2924.255992
89. Qiu J, Hua K. Exosomal long noncoding RNA-NONHAT076754 faciliates endometriosis invasion and predicts endometriosis recurrence. *J Minim Invasive Gynecol.* (2019) 26:S12. doi: 10.1016/j.jmig.2019.09.044
90. Qiu J-J, Lin X-J, Zheng T-T, Tang X-Y, Zhang Y, Hua K-Q. The exosomal long noncoding RNA aHIF is upregulated in serum from patients with endometriosis and promotes angiogenesis in endometriosis. *Reprod Sci.* (2019) 26:1590–602. doi: 10.1177/1933719119831775
91. Li Y, Liu Y-D, Chen S-L, Chen X, Ye D-S, Zhou X-Y, et al. Down-regulation of long non-coding RNA MALAT1 inhibits granulosa cell proliferation in endometriosis by up-regulating P21 via activation of the ERK/MAPK pathway. *MHR Basic Sci Reprod Med.* (2019) 25:17–29. doi: 10.1093/molehr/gay045
92. Ghazal S, McKinnon B, Zhou J, Mueller M, Men Y, Yang L, et al. H19 lncRNA alters stromal cell growth via IGF signaling in the endometrium of women with endometriosis. *EMBO Mol Med.* (2015) 7:996–1003. doi: 10.15252/emmm.201505245
93. Liu Z, Liu L, Zhong Y, Cai M, Gao J, Tan C, et al. LncRNA H19 over-expression inhibited Th17 cell differentiation to relieve endometriosis through miR-342-3p/IER3 pathway. *Cell Bioscience.* (2019) 9:84. doi: 10.1186/s13578-019-0346-3
94. Lin K, Zhan H, Ma J, Xu K, Wu R, Zhou C, et al. Silencing of SRA1 regulates ER expression and attenuates the growth of stromal cells in ovarian endometriosis. *Reprod Sci.* (2017) 24:836–43. doi: 10.1177/1933719116670036
95. Sha L, Huang L, Luo X, Bao J, Gao L, Pan Q, et al. Long non-coding RNA LINC00261 inhibits cell growth and migration in endometriosis. *J Obstetr Gynaecol Res.* (2017) 43:1563–9. doi: 10.1111/jog.13427
96. Liang Y, Wu J, Wang W, Xie H, Yao S. Pro-endometriotic niche in endometriosis. *Reprod Biomed Onl.* (2019) 38:549–59. doi: 10.1016/j.rbmo.2018.12.025
97. García-Bermúdez J, Cuezva JM. The ATPase inhibitory factor 1 (IF1): A master regulator of energy metabolism and of cell survival. *Biochim Biophys Acta Bioenerget.* (2016) 1857:1167–82. doi: 10.1016/j.bbabio.2016.02.004
98. Zhang D, Jin W, Wu R, Li J, Park S-A, Tu E, et al. High glucose intake exacerbates autoimmunity through reactive-oxygen-species-mediated TGF-β cytokine activation. *Immunity.* (2019) 51:671–81. e5. doi: 10.1016/j.immuni.2019.08.001
99. Kaponis A, Iwabe T, Taniguchi F, Ito M, Deura I, Decavalas G, et al. The role of NF-kappaB in endometriosis. *Front Biosci.* (2012) 4:1213–34. doi: 10.2741/s327
100. Cho YJ, Lee SH, Park JW, Han M, Park MJ, Han SJ. Dysfunctional signaling underlying endometriosis: current state of knowledge. *J Mol Endocrinol.* (2018) 60:R97–113. doi: 10.1530/JME-17-0227
101. Hsiao K-Y, Wu M-H, Tsai S-J. *Roles of Prostaglandin E 2 in Endometriosis. Endometriosis:* Tokyo: Springer (2014). p. 125–46.
102. Zhang M, Li J, Duan S, Fang Z, Tian J, Yin H, et al. Comprehensive characterization of endometrial competing endogenous RNA network in infertile women of childbearing age. *Aging.* (2020) 12:4204–21. doi: 10.18632/aging.102874

103. Park S, Lim W, Bazer FW, Whang K-Y, Song G. Quercetin inhibits proliferation of endometriosis regulating cyclin D1 and its target microRNAs *in vitro* and *in vivo*. *J Nutr Biochem.* (2019) 63:87–100. doi: 10.1016/j.jnutbio.2018.09.024
104. Gao W-l, Liu M, Yang Y, Yang H, Liao Q, Bai Y, et al. The imprinted H19 gene regulates human placental trophoblast cell proliferation via encoding miR-675 that targets Nodal Modulator 1 (NOMO1). *RNA Biol.* (2012) 9:1002–10. doi: 10.4161/rna.20807
105. Keniry A, Oxley D, Monnier P, Kyba M, Dandolo L, Smits G, et al. The H19 lincRNA is a developmental reservoir of miR-675 that suppresses growth and Igf1r. *Nat Cell Biol.* (2012) 14:659–65. doi: 10.1038/ncb2521

Conflict of Interest: The authors declare that the research was conducted in the absence of any commercial or financial relationships that could be construed as a potential conflict of interest.

frontiers in Oncology

ORIGINAL RESEARCH
published: 25 September 2020
doi: 10.3389/fonc.2020.528520

Long Non-coding RNA HOTAIR Function as a Competing Endogenous RNA for miR-149-5p to Promote the Cell Growth, Migration, and Invasion in Non-small Cell Lung Cancer

Hang Li[1,2,3], *Zhigang Cui*[4], *Xiaoting Lv*[1,2], *Juan Li*[1,2,5], *Min Gao*[1,2], *Zitai Yang*[1,2], *Yanhong Bi*[1,2], *Ziwei Zhang*[1,2], *Shengli Wang*[1,2], *Sixuan Li*[1,2], *Baosen Zhou*[1,2] *and Zhihua Yin*[1,2*]

[1] Department of Epidemiology, School of Public Health, China Medical University, Shenyang, China, [2] Key Laboratory of Cancer Etiology and Intervention, University of Liaoning Province, Shenyang, China, [3] Department of Clinical Epidemiology, Shengjing Hospital of China Medical University, Shenyang, China, [4] School of Nursing, China Medical University, Shenyang, China, [5] College of Medicine, The First Affiliated Hospital, Zhejiang University, Hangzhou, China

Lung cancer is a leading cause of cancer death all around the world. Long non-coding RNAs (lncRNAs) have been confirmed to be involved in carcinogenesis of malignancies. However, the molecular mechanism of most lncRNAs in various kinds of cancers remains unclear. LncRNA HOTAIR and HNRNPA1 are reported to play an oncogenic role in non-small cell lung cancer, and the overexpression of HNRNPA1 is shown to promote the proliferation of lung adenocarcinoma cells. In our study, we find that the overexpression of HOTAIR could promote the proliferation and overexpression of miR-149-5p could inhibit the proliferation of lung cancer cells. Flow cytometric analysis determines that overexpression of miR-149-5p induces cell cycle arrest in the G0/G1 phases, whereas overexpression of HOTAIR decreases the proportion of G0/G1phase cells. Also, overexpression of HOTAIR promotes the migration and invasion ability of lung cancer cells, confirmed by the wound-healing and transwell assays, which are suppressed by overexpression of miR-149-5p. Furthermore, the dual-luciferase reporter assay indicates that miR-149-5p could bind both HOTAIR and the 3′UTR of HNRNPA1. In summary, we find that HOTAIR can regulate HNRNPA1 expression through a ceRNA mechanism by sequester miR-149-5p, which post-transcriptionally targets HNRNPA1, thus promoting lung cancer progression.

Keywords: non-small cell lung cancer, HOTAIR, miR-149-5p, HNRNPA1, ceRNA

OPEN ACCESS

Edited by:
Giovanni Blandino, Regina Elena National Cancer Institute (IRCCS), Italy

Reviewed by:
Chicca Lo Sardo, Regina Elena National Cancer Institute (IRCCS), Italy
Arunkumar Ganesan, National Cancer Institute (NCI), United States

***Correspondence:**
Zhihua Yin
zhyin@cmu.edu.cn

Specialty section:
This article was submitted to Molecular and Cellular Oncology, a section of the journal Frontiers in Oncology

Received: *01 March 2020*
Accepted: *19 August 2020*
Published: *25 September 2020*

Citation:
Li H, Cui Z, Lv X, Li J, Gao M, Yang Z, Bi Y, Zhang Z, Wang S, Li S, Zhou B and Yin Z (2020) Long Non-coding RNA HOTAIR Function as a Competing Endogenous RNA for miR-149-5p to Promote the Cell Growth, Migration, and Invasion in Non-small Cell Lung Cancer. Front. Oncol. 10:528520. doi: 10.3389/fonc.2020.528520

INTRODUCTION

Lung cancer is the most lethal and frequently diagnosed malignant tumor. Approximately 2.09 million new cases were diagnosed, and 1.76 million died of lung cancer around the world in 2018 (1). In China, lung cancer remains the most common cancer with the highest incidence and mortality rate in 2015 (2). Given that the symptoms of lung cancer are not obvious in the early stage, the majority of lung cancer patients are diagnosed in the middle and late stages when they lose the best chance for treatment. Therefore, the overall 5-year survival rate of lung cancer is unfavorable (3). To protect the high-risk population and improve the prognosis of lung cancer, the development of effective screening biomarkers and potential therapy targets are important. Although considerable efforts are made to study the carcinogenesis of lung cancer, the underlying molecular mechanism is still unclear.

Tobacco smoking is an acknowledged environmental risk factor for lung cancer, nonetheless, it is estimated that 25% of lung cancer patients have no exposure to smoking, which suggests that genetically predisposed risk factors may play an important role in the carcinogenesis of lung cancer (4, 5). In recent years, a lot of evidence has shown that the non-coding RNAs such as microRNAs (miRNAs), and long non-coding RNAs (LncRNAs) play an important role in various kinds of cancers (6).

Long non-coding RNAs are a class of RNAs with no function of protein coding and are expressed uniquely in different tissues and cancers. Mounting evidence demonstrates that lncRNAs can exert on various cellular processes of carcinogenesis, such as cell differentiation, proliferation, apoptosis, and metastasis (6). LncRNAs function as an oncogene or tumor suppressor in various kinds of malignancies. Hox transcript antisense intergenic RNA (HOTAIR) is reported to play a role in carcinogenesis of various malignant tumors, including lung cancer (7–12).

Competing endogenous RNAs (ceRNAs) are transcripts that regulate each other at the post-transcriptional stage due to the shared miRNA response elements (MREs) (13). LncRNAs can function as ceRNAs to regulate the levels of miRNAs by competing for shared miRNAs binding to target genes, which results in the upregulation of the mRNA level of target genes. LncRNAs can play roles in regulating the expression level of target genes in a variety of malignant tumors, including lung cancer that has been reported in a large number of studies (14–20). Zhao et al. (21) find that lncRNA GMDS-AS1 could act as ceRNA to upregulate the mRNA of CYLD by sponging miR-96-5p. In addition, the intervention of the GMDS-AS1/miR-96-5p/CYLD axis could regulate the growth and apoptosis of lung adenocarcinoma cells (21). Yang et al. (18) find that LCAT1 function as a ceRNA for miR-4715-5p, which leads to the upregulation of the activity of the endogenous target of miR-4715-5p, Rac family small GTPase 1 (RAC1).

In the present study, we investigate the effect of miR-149-5p, HNRNPA1, and HOTAIR on lung cancer cells. We find that HOTAIR may act as a competing endogenous RNAs (ceRNAs) for miR-149-5p to upregulate the expression of HNRNPA1.

MATERIALS AND METHODS

Cell Culture and Transfection

Human lung adenocarcinoma cell lines (A549, SPC-A-1) and normal lung bronchus epithelial cell line (HBE) were purchased from the Academy of Sciences of China (Shanghai, China). The cells were cultured in RPMI 1640 medium (Biological Industries, Israel) supplemented with 10% fetal bovine serum (Biological Industries, Israel) and 100 U/mL penicillin and 100 U/mL streptomycin (Biological Industries, Israel) and incubated in a 37°C cell incubator with a humidified atmosphere of 5% CO_2. The cell transfection was performed with jetPRIME (Polyplus, France) for the dual luciferase reporter gene assay and INTERFERin (Polyplus, France) for siRNA-HOTAIR.

Bioinformatics Analysis

LncRNA HOTAIR expression profiles of 91 lung adenocarcinoma and 65 normal lung tissues (GSE19188) were downloaded from Gene Expression Ominibus (GEO, https://www.ncbi.nlm.nih.gov/geo/). The data were analyzed with the GEO2R online tools developed by the National Center for Biotechnology Information (https://www.ncbi.nlm.nih.gov/geo/geo2r/, NCBI). The effect of expression of HOTAIR on prognosis of non-small cell lung cancer patients was analyzed by using online tools GEPIA (http://gepia.cancer-pku.cn/) (22). The MiRWalk2.0 (23) (http://zmf.umm.uni-heidelberg.de/apps/zmf/mirwalk2/), miRTarBase (http://mirtarbase.mbc.nctu.edu.tw/), and RNA22 V2 (https://cm.jefferson.edu/rna22/Interactive/RNA22Controller) were applied to predict the binding sites of microRNA on HOTAIR and mRNA of HNRNPA1.

Quantitative Real-Time Polymerase Chain Reaction

The total RNA was isolated from cells by using RNAIso plus according to the protocol of the manufacturer (Takara, Japan). The concentration of the RNA samples was measured by using Nanodrop 2000 (Thermo Fisher Scientific, USA), and immediately, the RNA samples were reverse transcribed to cDNA utilizing the PrimeScript^{TM} RT reagent Kit with gDNA Eraser (Takara, Japan). MicroRNAs were reverse-transcribed by using stem-loop primers, which were specifically designed and synthesized by Sangon (China). Quantitative real-time polymerase chain reaction (qRT-PCR) was performed by using 2×SG Fast qPCR Master Mix (Sangon, China) on an Applied Biosystems 7500 Real-Time PCR System (Applied Biosystems, USA) according to the manufacturers' protocol. $2^{-\Delta\Delta CT}$ methods were performed to calculate the relative gene expression. The expression of lncRNA and mRNA was normalized to GAPDH, and the expression of microRNA was normalized to U6 small nuclear RNA. The sequences of the primers used in the present study are showed in **Table 1**.

Lentivirus Packaging and Transfection

The overexpression vector of HOTAIR and its control were named HOTAIR and HOTAIR-NC. The overexpression of miR-149-5p and its control were named miR-149 and miR-NC. The small interfering RNA (siRNA) for HOTAIR silencing and

TABLE 1 | Primers sequences.

Gene	Sequences (5′-3′)
miR-149-5p forward	5′-CGUCUGGCUCCGUGUCUUC-3′
miR-149-5p reverse	5′-AGUGCAGGGUCCGAGGUAUU-3′
miR-149-5p RT primer	5′-GUCGUAUCCAGUGCAGGGUCCGA GGUAUUCGCACUGGAUACGACGGGAGU-3′
U6 forward	5′-AGAGAAGAUUAGCAUGGCCCCUG-3′
U6 reverse	5′-AGUGCAGGGUCCGAGGUAUU-3′
U6 RT primer	5′-GUCGUAUCCAGUGCAGGGUCCGA GGUAUUCGCACUGGAUACGACAAAAUA-3′
HOTAIR forward	5′-UCAGCACCCACCCAGGAAUC-3′
HOTAIR reverse	5′-AGAGUUGCUCUGUGCUGCCA-3′
GAPDH forward	5′-CAGGAGGCAUUGCUGAUGAU-3′
GAPDH reverse	5′-GAAGGCUGGGGCUCAUUU-3′

control were named siHOTAIR and siNC. Plasmid of HOTAIR overexpression, miR-149 mimics, and siHOTAIR were designed and constructed by GenePharma company (GenePharma, China). The lentiviral expression construct and the packaging plasmid were co-transfected to 293T to package the lentiviral particles. HOTAIR and miR-149-5p were packaged to lentivirus by the Genepharma company (GenePharma, China). We performed a preliminary experiment of lentivirus transfection to select the approximate transducing units of lentivirus for transfection in the next step, and 48 h after transfection, transfection efficiency was estimated by taking photos on the inverted fluorescence microscope. The fluorescence intensity of green fluorescent protein indicates the efficiency of transfection (Leica, Germany).

Small Interfering RNA Synthesis for HOTAIR Knockdown and Transfection

To investigate the function of HOTAIR, three types of small interfering RNAs against HOTAIR (siHOTAIR) were synthesized by GenePharma Technologies (Shanghai, China). Transfection was performed with INTERFERin (Polyplus, France), and the efficiency of knockdown was examined by quantitative real-time PCR (qRT-PCR). The siHOTAIR with the highest knockdown efficiency was used for further study.

Cell Proliferation Assay and Cell Confluence Determination

Cell proliferation was detected by using Celigo Imaging Cytometer (Nexcelom, USA). A549 and SPC-A-1 cells transfected with HOTAIR, miR-149, or siHOTAIR and their controls were counted by a Countstar IC1000 cell counter (Countstar, China) and seeded on a 6-well plate (Corning, USA) at a density of 5×10^4 cells/well and incubated in the 37°C cell incubator with a humidified atmosphere of 5% CO_2. After incubation for 24, 48, 72, and 96 h, cell confluence was measured by using a Celigo Imaging Cytometer (Nexcelom, USA).

Transwell Assay

Upper chambers (Corning, USA) for transwell were placed in a 24-well plate, and A549 cells transfected with HOTAIR or HOTAIR-NC, SPC-A-1 cells transfected with siHOTAIR or siNC, and miR-149-5p or miR-NC were suspended in serum-free RPMI 1640 medium at a density of 2.5×10^5 cells/ml. The upper chambers were seeded with cell suspensions (200 μl), and the bottom chambers were filled with 500 μl RPMI 1640 containing 10% FBS. After 36 h of incubating, cells migrated to the bottom chambers, and the chambers were washed three times with cold PBS buffer, then soaked in ice-bath methanol 15 min for fixing the cells. PBS buffer containing 1% crystal violet was used to stain the cells. The number of migrated cells were counted from five randomly selected fields under a light microscope.

Wound-Healing Assay

Cell migration was also detected by wound-healing assay. Transfected A549 cells and SPC-A-1 cells were seeded in 12-well plates (Corning, USA), and artificial scratches were made by sterile pipette tips along the center of each well. When the cells reached over 90% confluence and the cell debris were removed by washing the cells three times with PBS buffer, photos were taken by using an inverted microscope (Nikon, Japan) in bright field instantly (0 h). After the cells were incubated in 37°C with serum-free RPMI 1640 for 24 h, photos were taken again using the identical method. The data was analyzed by using Image J 1.8.0 software (Bethesda, USA).

Cell Cycle Analysis

Cell cycle analysis was performed by using flow cytometry. Transfected cells were harvested and washed twice with cold PBS buffer, and then 70% ethanol was added to fix the cells at 4°C overnight. The cells were stained with PI in the dark at room temperature for 30 min. The proportion of cells in each phase of the cell cycle was measured by Guava® easyCyte 12 (Millipore, USA) according to the manufacturer's protocol. The data was analyzed by ModFit LT 5.0 (Verity Software House).

Western Blot

Cells were harvested and lysed by using the RIPA buffer containing protease inhibitors (Solarbio, China), and subsequently, the concentration of the protein samples were quantified by using the Enhanced BCA Protein Assay Kit (Beyotime, China). Protein samples were loaded and separated by 10% SDS-PAGE, and subsequently, they were transferred onto 0.45 μm PVDF membranes (Millipore, USA). The membranes were soaked in PBST buffer containing 5% skim milk at 37°C for 1 h, and then washed with PBST buffer thrice for 10 min. Subsequently, the membranes were incubated with the primary antibodies specific for HNRNPA1 (1:1,500, Proteintech, China) and β-actin (1:2,000, Bioss, China) at 4°C overnight, respectively. The membranes were washed three times with PBST buffer and were incubated with HRP-conjugated secondary antibody for 1 h at room temperature. Signals of the protein bands were detected by utilizing Immobilon ECL substrate (Millipore, Germany) and Azure Gel Imaging Systems C500 (Azure Biosystems, USA). Band intensity of western blot was measured by Image J 1.8.0 software (Bethesda, USA). The β-actin protein was selected as loading control.

Cell Apoptosis Analysis

Cell apoptosis analysis was also performed utilizing flow cytometry. Transfected cells were harvested and washed twice with cold PBS buffer and were then stained with Annexin V-APC /7-AAD in the dark for 15 min. The cells were detected on Guava® easyCyte 12 (Millipore, USA) according to the manufacturer's protocol.

Luciferase Reporter Assay

The luciferase reporter vectors were designed and manufactured by RioBio (Guangzhou, China). Cells (293 T) were seeded at 5×10^4 cells/well in 24-well plates and were allowed to settle overnight. The next day, cells were co-transfected with pmir-h-HOTAIR-WT, pmir-h-HOTAIR-MUT, pmir-h-HNRNPA1-WT, or pmir-h-HNRNPA1-MUT reporter plasmids and mimics NC, miR-149-5p mimics accordingly; 24 h after transfection, cells were lysed using passive lysis buffer (Promega, USA), and the luciferase activity was measured by Synergy H1 Multi-Mode Reader (Biotek, USA) using the Dual-Glo Luciferase Assay System (Promega, USA) and normalized to renilla luciferase activity, respectively. Experiments were performed in triplicate.

Statistical Analysis

Statistical analysis was performed using SPSS 21.0 software (SPSS Inc, USA) and GraphPad Prism 6.0 (GraphPad Software, USA). Two independent sample *t*-tests was performed to assess significant differences in measured variables among groups. All the experiments were performed in triplicate, and the data were presented as mean ± standard deviation (SD). A $P < 0.05$ was considered statistically significant.

RESULTS

LncRNA HOTAIR Is Aberrantly Highly Expressed in Lung Adenocarcinoma

We analyzed the gene expression data from GEO (GEO series accession No. GSE19188), and the results show that HOTAIR is aberrantly upregulated in 91 non-small cell lung cancer tissues compared with 65 adjacent normal lung tissues (**Figure 1A**).

Aberrantly High Expression of LncRNA HOTAIR May Have an Unfavorable Prognosis

We analyzed the prognosis of lung cancer patients by using the GEPIA online tools, and the results of Kaplan-Meier analysis show that, compared with patients with high HOTAIR expression, disease-free survival (DFS) of patients with low HOTAIR expression was more favorable (HR = 1.4, $P = 0.043$; logrank $P = 0.042$) (**Supplementary Figure 3**).

Background Expression of miR-149-5p and HOTAIR in Lung Cancer Cell Lines

The background expression level of miR-149-5p and HOTAIR in A549, SPC-A-1, and HBE cell lines were quantified by qRT-PCR (**Figure 1B**). The upregulated expression of HOTAIR was detected by using RT-qPCR in the SPC-A-1 cell line compared with A549 and HBE cell line (**Figure 1C**). The expression of miR-149-5p was lower in the SPC-A-1 cell line compared to that in A549 and HBE, and therefore, SPC-A-1 was chosen to perform miR-149-5p overexpressed lentivirus transfection, and the overexpression level of miR-149-5p was detected by qRT-PCR (**Figure 1D**). The background expression of HOTAIR in the A549 cell line was lower than that in the HBE cell line so that the A549 cell line was chosen to perform HOTAIR overexpressed lentivirus transfection (**Figure 1E**). Background expression of HOTAIR in the SPC-A-1 cell line was higher than that in HBE cell line; therefore, siHOTAIR and siNC were transfected to SPC-A-1 cell line to knock down HOTAIR expression to perform the gain- and loss-of-function experiments for investigating the effect of HOTAIR on lung cancer cells. The knockdown efficiency of HOTAIR was detected and quantified by qRT-PCR, and the result showed that siHOT-1597 had the highest knockdown efficiency (**Figure 1F**).

miR-149-5p Inhibits the Proliferation of Lung Cancer Cells

To investigate the effect of miR-149-5p on the proliferation of SPC-A-1 cells, transfected SPC-A-1 cells were planted on 6-well plates and photographed to measure the cell confluence by using Celigo Imaging Cytometer at 24, 48, 72, and 96 h after the cells were planted on 6-well plates. The cell growth activity of SPC-A-1 cells transfected with miR-149-5p overexpression lentivirus were suppressed compared with SPC-A-1 cells transfected with miR-NC (**Figure 2A**).

LncRNA HOTAIR Promotes Cell Proliferation of Lung Cancer Cells

To elucidate the effect of HOTAIR on the proliferation of A549 cells, transfected A549 cells were planted on 6-well plates. After 24, 48, 72, and 96 h, the cells were photographed to measure the cell confluence by using a Celigo Imaging Cytometer. The cell proliferation was promoted in A549 cells transfected with HOTAIR overexpression lentivirus when compared to cells transfected with HOTAIR-NC (**Figure 2B**). Cell proliferation of SPC-A-1 cells transfected with siHOT-1597 was also detected, and results show that knockdown of HOTAIR could inhibit cell proliferation (**Figure 2C**).

HOTAIR and miR-149-5p Play Roles in Cell Cycle of Lung Cancer Cell Line

To investigate whether HOTAIR and miR-149-5p have an effect on the cell cycle of the lung cancer cell line, flow cytometry was performed. The percentage of cells in the G0/G1 phase of A549 cells transfected with HOTAIR was less than that of A549 cells transfected with HOTAIR-NC. The percentage of cells in the S phase of A549 transfected with HOTAIR was more than that of A549 transfected with HOTAIR-NC (**Figure 3A**). The percentage of cells in the G0/G1 phase of SPC-A-1 cells transfected with miR-149-5p was more than that of SPC-A-1 transfected with miR-NC. The S phase of SPC-A-1 transfected with miR-149-5p was less than that of SPC-A-1 transfected with miR-NC (**Figure 3A**). The percentage of cells in the G0/G1 phase of SPC-A-1 cells transfected with siHOTAIR-1597 was less than that of SPC-A-1

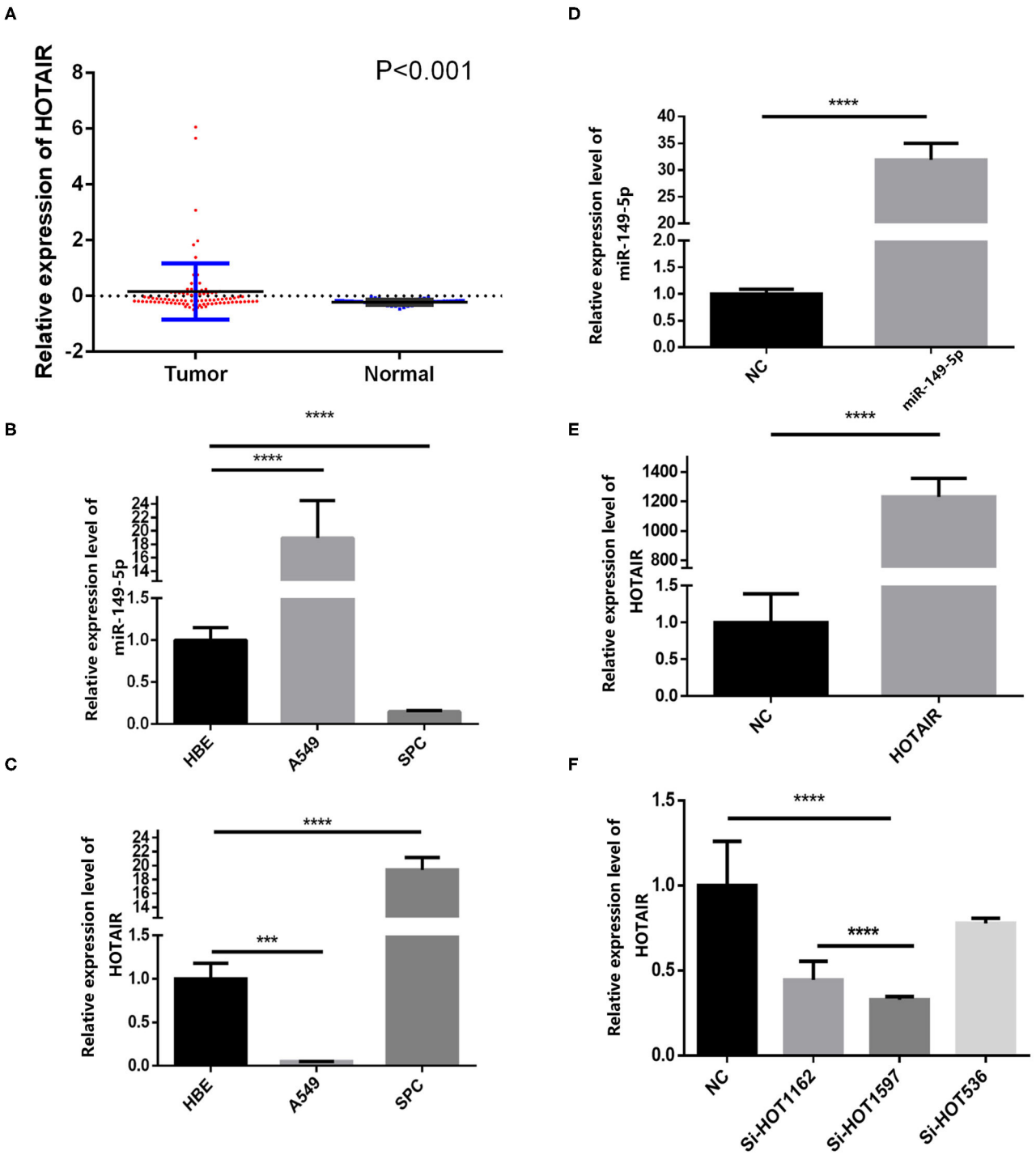

FIGURE 1 | Relative expression of HOTAIR in non-small cell lung cancer tissues and normal lung tissues and QRT-PCR results of HOTAIR and miR-149-5p in A549 and SPCA1 cell lines and transfected cells. **(A)** Relative expression of HOTAIR in non-small cell lung cancer tissues and normal lung tissues from the GEO data set. **(B)** Background expression of miR-149-5p in HBE, A549, and SPC-A-1 cell lines. **(C)** Background expression of HOTAIR in HBE, A549, and SPC-A-1 cell lines. **(D)** Relative expression of miR-149-5p in SPC-A1 cells transfected by miR-149-5p overexpression lentivirus. **(E)** Relative expression of HOTAIR in A549 cells transfected by HOTAIR overexpression lentivirus. **(F)** Relative expression of HOTAIR in SPC-A-1 cells after transfection by small inferring RNAs (siHOT-1162, siHOT-1597, and siHOT-536). ***$P < 0.01$; ****$P < 0.05$.

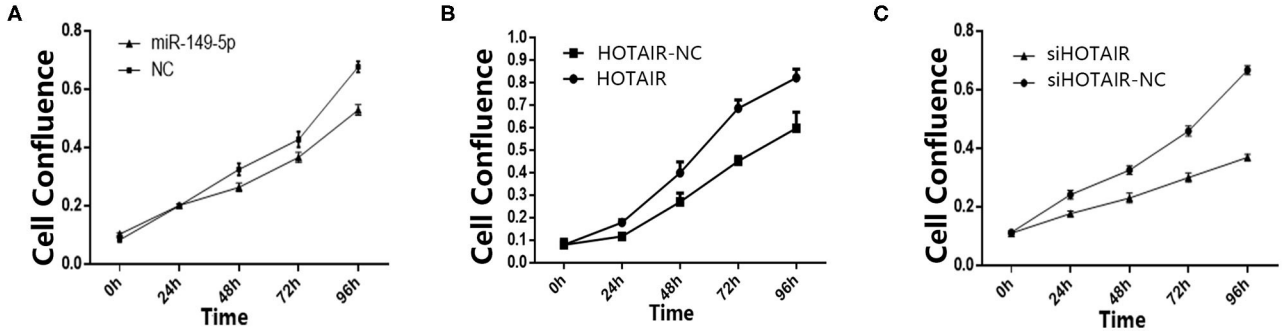

FIGURE 2 | (A) Cell confluence of SPC-A-1 cells transfected by miR-149-5p overexpressed lentivirus after 24, 48, 72, and 96 h detected by Celligo. **(B)** Cell confluence of A549 cells transfected by HOTAIR overexpressed lentivirus after 24, 48, 72, and 96 h detected by Celligo. **(C)** Cell confluence of SPC-A-1 cells transfected by siHOT-1597 after 24, 48, 72, and 96 h detected by Celligo.

cells transfected with siNC. The percentage of cells in the S phase of SPC-A-1 transfected with siHOTAIR-1597 was less than that of SPC-A-1 transfected with siNC (**Figure 3A**). The results of cell cycle analysis suggest that HOTAIR may promote cell division and miR-149-5p may cause G0/G1 phase arrest.

HOTAIR and miR-149-5p Have No Effect on Apoptosis of Lung Cancer Cell Line

To investigate whether HOTAIR and miR-149-5p have an effect on the apoptosis of lung cancer cell lines, flow cytometry was performed to estimate the percentage of apoptotic cells. A549 transfected with HOTAIR and HOTAIR-NC, SPC-A-1 cells transfected with miR-149-5p and miR-NC and cells transfected with siHOT-1597 and siNC were tested for apoptosis percentage. The results show that there is no statistically significant difference in the percentage of apoptotic cells between A549 cells transfected with the HOTAIR and HOTAIR-NC group (**Figure 3B**). No statistically significant difference was observed in the percentage of apoptotic cells between the SPC-A-1 cells transfected with miR-149-5p and cells transfected with miR-NC (**Figure 3B**). There was also no statistically significant difference in the percentage of apoptotic cells between the SPC-A-1 cells transfected with siHOTAIR and siNC (**Figure 3B**), indicating that HOTAIR or miR-149-5p may have no effect on the apoptosis of lung cancer cell lines.

miR-149-5p Inhibited the Migration and Invasion Ability of the SPC-A-1 Cells

To investigate the potential effect of miR-149-5p on the migration and invasion ability of lung cancer cells, we performed wound-healing and transwell assays. The results of the wound-healing assay showed that the migration ability of SPC-A-1 cells transfected with miR-149-5p was inhibited compared with SPC-A-1 cells transfected with miR-NC (**Figure 4A**). Results of the transwell assay showed that invasion ability of SPC-A-1 cells transfected with miR-149-5p was inhibited compared with SPC-A-1 cells transfected with miR-NC (**Figure 4B**). The results suggest that miR-149-5p may inhibit the migration and invasion ability of SPC-A-1 cells.

HOTAIR Can Promote the Migration and Invasion Ability of Lung Cancer Cells

To determine whether HOTAIR could affect the migration and invasion ability of A549, we performed wound-healing and transwell assays in transfected A549 cells. The results of the wound-healing assay show that the migration ability of A549 transfected with HOTAIR was promoted compared with group of A549 transfected with HOTAIR-NC (**Figure 4A**). The result of the transwell assay showed that the invasion ability of A549 transfected with HOTAIR was promoted compared with the group of A549 transfected with HOTAIR-NC (**Figure 4B**). The migration and invasion ability of SPC-A-1 cells transfected with siHOT-1597 was also detected by wound-healing and transwell assays, and results show that knockdown of HOTAIR could inhibit the migration and invasion ability of SPC-A-1 cells (**Figures 4A,B**).

HOTAIR and HNRNPA1 Were Targeted by miR-149-5p

Results of bioinformatics analysis to predict miR-149-5p binding sites show the potential binding sites of miR-149-5p on HOTAIR and mRNA of HNRNPA1. Subsequently, we performed a dual-luciferase reporter assay in the 293T cell line to determine the direct binding between HOTAIR and miR-149-5p and the direct binding between HNRNPA1 and miR-149-5p. The results show that a significant reduction in luciferase reporter activity was observed in group of cells co-transfected with pmir-h-HOTAIR-WT and miR-149-5p mimics and group of cells co-transfected with pmir-h-HNRNPA1-WT and miR-149-5p mimics (**Figure 4C**).

HNRNPA1 Protein Expression Is Promoted by HOTAIR and Inhibited by miR-149-5p

Results of the Western blot assay showed that HNRNPA1 protein expression is downregulated in SPC-A-1 cells transfected with miR-149-5p compared with the control group (**Figure 4D**). In A549 cells transfected with HOTAIR, HNRNPA1 protein expression is elevated compared with A549 cells that are transfected with HOTAIR-NC (**Figure 4D**). The HNRNPA1

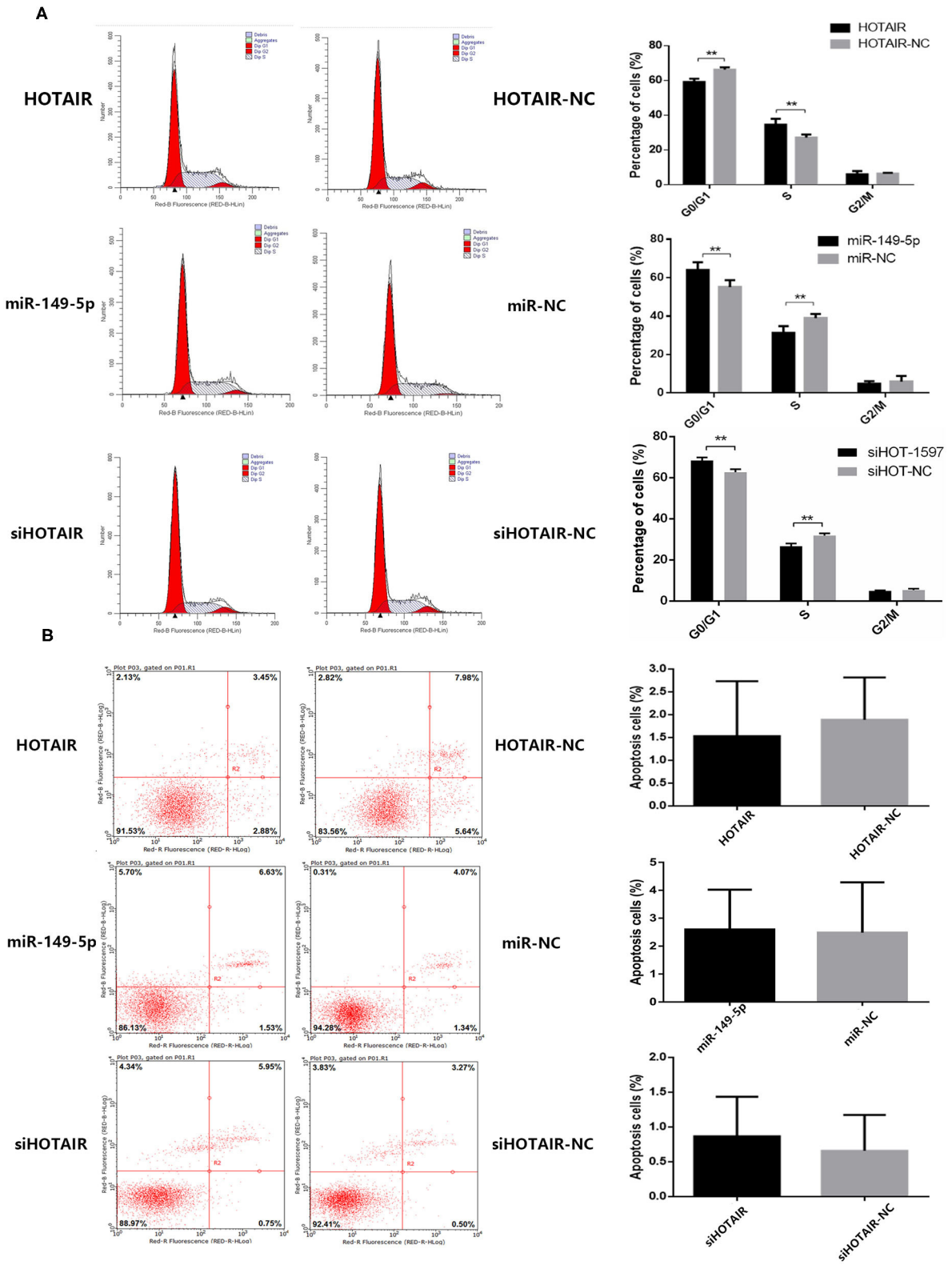

FIGURE 3 | (A) Flow cytometry analysis of cell cycle distribution of lung cancer cells transfected with HOTAIR, miR-149-5p, and siHOTAIR. HOTAIR-transfected A549 cells show a decreased percentage of G0/G1-phase cells and increased S-phase cells ($p < 0.05$). miR-149-5p-transfected SPC-A-1 cells show an increased percentage of G0/G1-phase cells and decreased S-phase cells ($p < 0.05$). siHOTAIR-transfected SPC-A-1 cells show an increased percentage of G0/G1-phase cells and decreased S-phase cells ($p < 0.05$). **(B)** Flow cytometry analysis of apoptosis of lung cancer cells transfected with HOTAIR, miR-149-5p, and siHOTAIR. HOTAIR, miR-149-5p, or siHOTAIR have no effect on percentage of apoptosis apoptotic lung cancer cells ($p > 0.05$). $^{**}P < 0.05$.

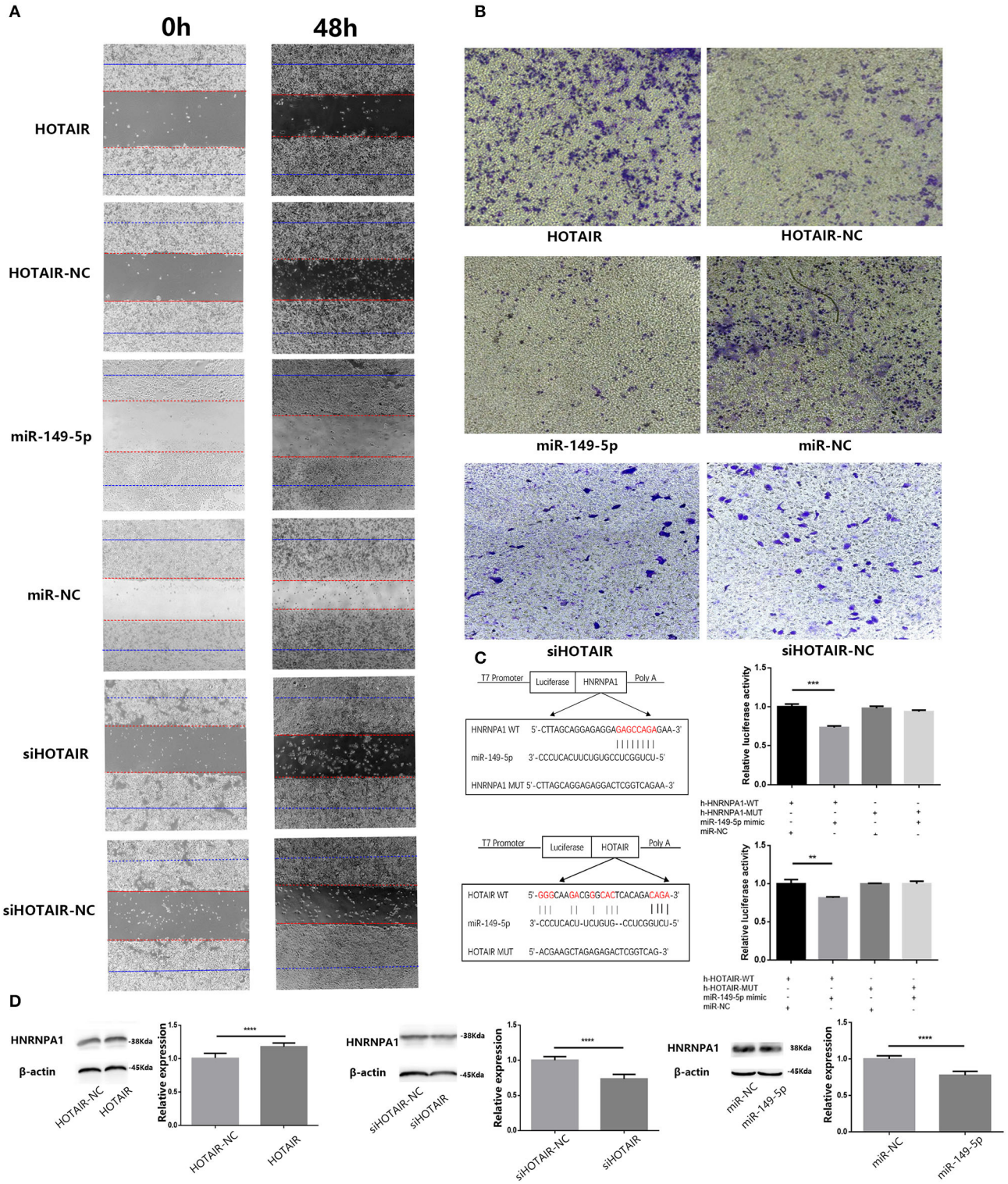

FIGURE 4 | (A) Wound-healing assay was performed to analyze the migratory abilities of lung cancer cells (A549 and SPC-A-1) transfected with HOTAIR, miR-149-5p, and siHOTAIR for 0 and 48 h. Results show that HOTAIR can promote cell migration of A549 cells, miR-149-5p, can inhibit cell migration of SPC-A-1 cells and silencing HOTAIR can inhibit cell migration of SPC-A-1 cells. **(B)** Transwell assay was performed to analyze the invasion abilities of lung cancer cells (A549 and SPC-A-1) transfected with HOTAIR, miR-149-5p, and siHOTAIR. Results show that HOTAIR can promote cell invasion of A549 cells, miR-149-5p can inhibit cell invasion of SPC-A-1 cells, and silencing HOTAIR can inhibit cell invasion of SPC-A-1 cells. **(C)** Predicted binding site between HNRNPA1 and miR-149-5p and

(Continued)

FIGURE 4 | predicted binding site between HOTAIR and miR-149-5p. Luciferase activity in 293T cells of dual-luciferase reporter gene assay show that miR-149-5p can bind to HOTAIR and 3′UTR of HNRNPA1 ($p < 0.05$). **(D)** The protein level of HNRNPA1 in lung cancer cells (A549 and SPC-A-1) transfected with HOTAIR, miR-149-5p, and siHOTAIR detected by western blot analysis. $^{**}P < 0.01$, $^{***}P < 0.001$, $^{****}P < 0.05$.

protein expression is suppressed in SPC-A-1 cells transfected with siHOTAIR compared with SPC-A-1 cells transfected with siNC (**Figure 4D**). The results suggest that HNRNPA1 is elucidated to be targeted by miR-149-5p and HNRNPA1 expression is positively correlated with HOTAIR expression. The ceRNA axis of HOTAIR/miR-149-5p/HNRNPA1 may exist.

DISCUSSION

Cancer is considered to be a genetic disease traditionally, and recent research has demonstrated that epigenetic regulation, such as DNA methylation, histone deacetylation, chromatin remodeling, gene imprinting, and non-coding RNA (ncRNA) regulation, play indispensable roles in cancer development. Non-coding RNAs, such as microRNAs, long non-coding RNAs, and circRNAs, constitute more than 90% of the human transcripts. It has been demonstrated that non-coding RNAs exert an important functional role in carcinogenesis of malignant tumors (6, 24). In the present study, our results show that HOTAIR forms a competitive endogenous RNA mechanism with miR-149-5p and HNRNPA1. HOTAIR can inhibit the binding of miR-149-5p to HNRNPA1 mRNA by competitively sequestering miR-149-5p, and thereby decreasing the degradation of HNRNPA1 mRNA. Overexpression of HOTAIR could promote the migration and invasion of lung cancer cells and improve cell proliferation ability. Overexpression of miR-149-5p could inhibit the migration and invasion of lung cancer cells and cell proliferation. Overexpression of miR-149-5p arrests the cell cycle of lung cancer cells in the G0/G1 phase. The dual luciferase reporter gene assay showed that miR-149-5p binds to HOTAIR, and miR-149-5p also has a targeted binding relationship with HNRNPA1.

MicroRNA plays an important role in proto-oncogenes or tumor suppressor genes in malignant tumors and can regulate the occurrence and progression of malignant tumors. It has been demonstrated that miR-149 plays a role as a proto-oncogene or a tumor suppressor gene in a variety of malignant tumors (25–29). A study on colorectal cancer finds that the expression level of miR-149 in colorectal cancer tissues is significantly lower than that in adjacent normal tissues, and the expression level of miR-149 is inversely proportional to the expression level of FOXM1. Patients with low expression levels of miR-149 are more likely to present with a poor prognosis, such as lymph node metastasis, distant metastasis, or more malignant TNM grades, and miR-149 could bind to mRNA of FOXM1 and then suppress its expression, thereby inhibiting the proliferation, metastasis, and invasiveness of colorectal cancer cells, which suggests that miR-149 could play a role as a tumor suppressor gene in colorectal cancer (30). Aberrant expression of miR-149 is found in non-small cell lung cancer cells and is associated with invasive properties of lung cancer cells and increased epithelial-mesenchymal transition as reported by the study of Ke et al. (25) The researchers demonstrate that miR-149 could inhibit the expression of FOXM1 and reduce the FOXM1 protein level and inhibit the EMT process in non-small cell lung cancer by miR-149 overexpression and knockout of FOXM1 gene. HNRNPA1 is reported to be overexpressed in lung adenocarcinoma tissues and may play an oncogenic role in lung adenocarcinoma. In research by Liu et al. lentivirus-mediated RNA interference of HNRNPA1 was conducted in the A549 cell line, and expression of HNRNPA1 protein was successfully suppressed. They find that reduction of HNRNPA1 could inhibit cell proliferation of A549 cells partly by inducing cell cycle arrest in the G0/G1 phase and possibly acting by affecting the expression of telomerase and NF-κB activation. It is suggested that HNRNPA1 acted as an oncogene in lung adenocarcinoma (31). In our study, we find that HNRNPA1 is a downstream target gene of miR-149-5p, and miR-149-5p could inhibit the protein expression of HNRNPA1 in a lung cancer cell line. miR-149-5p could inhibit the proliferation of lung cancer cells, and high expression levels of miR-149-5p could lead to cell cycle arrest in the G0/G1 phase. Overexpression of miR-149-5p could inhibit the migration and invasion ability of lung cancer cells elucidated by the results of wound-healing and transwell assays. Results of the dual-luciferase reporter assay show that, miR-149-5p could bind to 3′UTR of mRNA of HNRNPA1, thus inhibiting the protein expression of HNRNPA1, which provided a biological plausible evidence for tumor suppressor role of miR-149-5p in lung cancer.

HOTAIR is a long-chain non-coding RNA of about 2.2 kb in length. Transcribed to the HOXC region, it could bind to the PRC2 and LSD1 complexes (32). The abnormally expressed HOTAIR is closely related to the occurrence of various malignant tumors, including breast cancer (33), colorectal cancer (34), lung cancer (35), and gastric cancer (36). It has been reported that HOTAIR indirectly regulates the expression of proto-oncogenes through acting as the miRNA sponge (8, 37). In a study on gastric cancer, HOTAIR could indirectly regulate the expression of HER2 by binding to miR-331-3p (8). A study of pancreatic cancer finds that HOTAIR could indirectly regulate NOTCH3 by binding to miR-613 (37). Our study elucidates the target binding of HOTAIR to miR-149-5p and the results of the dual luciferase reporter gene also validate the existence of competitive endogenous RNA mechanisms of miR-149-5p with HOTAIR and HNRNPA1.

CONCLUSION

HOTAIR could promote the migration, invasion ability, and cell proliferation of lung cancer cells. miR-149-5p could inhibit the migration, invasion ability, and cell proliferation of lung cancer cells. HOTAIR may act as a competing endogenous

RNAs (ceRNAs) for miR-149-5p to upregulate the expression of HNRNPA1.

DATA AVAILABILITY STATEMENT

The datasets generated for this study are available on request to the corresponding author.

AUTHOR CONTRIBUTIONS

HL performed the molecular biology studies and drafted the manuscript. ZYi participated in the design of the study. HL, ZC, ZYa, JL, XL, MG, ZZ, SW, YB, SL, and BZ performed the statistical analysis. All authors read and approved the final manuscript.

FUNDING

This study was supported by National Natural Science Foundation of China (No. 81673261).

SUPPLEMENTARY MATERIAL

The Supplementary Material for this article can be found online at: https://www.frontiersin.org/articles/10.3389/fonc.2020.528520/full#supplementary-material

REFERENCES

1. Bray F, Ferlay J, Soerjomataram I, Siegel RL, Torre LA, Jemal A. Global cancer statistics 2018: GLOBOCAN estimates of incidence and mortality worldwide for 36 cancers in 185 countries. *CA Cancer J Clin.* (2018) 68:394–424. doi: 10.3322/caac.21492
2. Chen WQ, Zheng RS, Baade PD, Zhang SW, Zeng HM, Bray F, et al. Cancer statistics in China, 2015. *CA Cancer J Clin.* (2016) 66:115–32. doi: 10.3322/caac.21338
3. Carr SR, Akerley W, Hashibe M, Cannon-Albright LA. Evidence for a genetical contribution to non-smoking-related lung cancer. *Thorax.* (2015) 70:1033–9. doi: 10.1136/thoraxjnl-2014-206584
4. Subramanian J, Govindan R. Lung cancer in never smokers: a review. *J Clin Oncol.* (2007) 25:561–70. doi: 10.1200/JCO.2006.06.8015
5. Sun S, Schiller JH, Gazdar AF. Lung cancer in never smokers–a different disease. *Nat Rev Cancer.* (2007) 7:778–90. doi: 10.1038/nrc2190
6. Huarte M. The emerging role of lncRNAs in cancer. *Nat Med.* (2015) 21:1253–61. doi: 10.1038/nm.3981
7. Huang L, Liao LM, Liu AW, Wu JB, Cheng XL, Lin JX, et al. Overexpression of long noncoding RNA HOTAIR predicts a poor prognosis in patients with cervical cancer. *Arch Gynecol Obstet.* (2014) 290:717–23. doi: 10.1007/s00404-014-3236-2
8. Liu XH, Sun M, Nie FQ, Ge YB, Zhang EB, Yin DD, et al. Lnc RNA HOTAIR functions as a competing endogenous RNA to regulate HER2 expression by sponging miR-331-3p in gastric cancer. *Mol Cancer.* (2014) 13:92. doi: 10.1186/1476-4598-13-92
9. Ono H, Motoi N, Nagano H, Miyauchi E, Ushijima M, Matsuura M, et al. Long noncoding RNA HOTAIR is relevant to cellular proliferation, invasiveness, and clinical relapse in small-cell lung cancer. *Cancer Med.* (2014) 3:632–42. doi: 10.1002/cam4.220
10. Wu ZH, Wang XL, Tang HM, Jiang T, Chen J, Lu S, et al. Long non-coding RNA HOTAIR is a powerful predictor of metastasis and poor prognosis and is associated with epithelial-mesenchymal transition in colon cancer. *Oncol Rep.* (2014) 32:395–402. doi: 10.3892/or.2014.3186
11. Zhao W, An Y, Liang Y, Xie XW. Role of HOTAIR long noncoding RNA in metastatic progression of lung cancer. *Eur Rev Med Pharmacol Sci.* (2014) 18:1930–6.
12. Li H, Tang XM, Liu Y, Li W, Chen Q, Pan Y. Association of functional genetic variants of HOTAIR with hepatocellular carcinoma (HCC) susceptibility in a Chinese population. *Cell Physiol Biochem.* (2017) 44:447–54. doi: 10.1159/000485011
13. Salmena L, Poliseno L, Tay Y, Kats L, Pandolfi PP. A ceRNA hypothesis: the Rosetta Stone of a hidden RNA language? *Cell.* (2011) 146:353–8. doi: 10.1016/j.cell.2011.07.014
14. Wang H, Huo X, Yang XR, He J, Cheng L, Wang N, et al. STAT3-mediated upregulation of lncRNA HOXD-AS1 as a ceRNA facilitates liver cancer metastasis by regulating SOX4. *Mol Cancer.* (2017) 16:136. doi: 10.1186/s12943-017-0680-1
15. Cui D, Qian R, Li Y. Circular RNA circ-CMPK1 contributes to cell proliferation of non-small cell lung cancer by elevating cyclin D1 via sponging miR-302e. *Mol Genet Genomic Med.* (2019) 8:e999. doi: 10.1002/mgg3.999
16. Qi H, Xiao Z, Wang Y. Long non-coding RNA LINC00665 gastric cancer tumorigenesis by regulation miR-149-3p/RNF2 axis. *Onco Targets Ther.* (2019) 12:6981–90. doi: 10.2147/OTT.S214588
17. Xia W, Mao Q, Chen B, Wang L, Ma W, Liang Y, et al. The TWIST1-centered competing endogenous RNA network promotes proliferation, invasion, and migration of lung adenocarcinoma. *Oncogenesis.* (2019) 8:62. doi: 10.1038/s41389-019-0167-6
18. Yang J, Qiu Q, Qian X, Yi J, Jiao Y, Yu M, et al. Long noncoding RNA LCAT1 functions as a ceRNA to regulate RAC1 function by sponging miR-4715-5p in lung cancer. *Mol Cancer.* (2019) 18:171. doi: 10.1186/s12943-019-1107-y
19. Yang Y, Li S, Cao J, Li Y, Hu H, Wu Z. RRM2 regulated by LINC00667/miR-143-3p signal is responsible for non-small cell lung cancer cell progression. *Onco Targets Ther.* (2019) 12:9927–39. doi: 10.2147/OTT.S221339
20. Tiansheng G, Junming H, Xiaoyun W, Peixi C, Shaoshan D, Qianping C. lncRNA metastasis-associated lung adenocarcinoma transcript 1 promotes proliferation and invasion of non-small cell lung cancer cells via down-regulating miR-202 expression. *Cell J.* (2020) 22:375–85. doi: 10.22074/cellj.2020.6837
21. Zhao M, Xin XF, Zhang JY, Dai W, Lv TF, Song Y. LncRNA GMDS-AS1 inhibits lung adenocarcinoma development by regulating miR-96-5p/CYLD signaling. *Cancer Med.* (2019) 9:1196–208. doi: 10.1002/cam4.2776
22. Tang Z, Li C, Kang B, Gao G, Li C, Zhang Z. GEPIA: a web server for cancer and normal gene expression profiling and interactive analyses. *Nucleic Acids Res.* (2017) 45:W98–102. doi: 10.1093/nar/gkx247
23. Dweep H, Gretz N. miRWalk2.0: a comprehensive atlas of microRNA-target interactions. *Nat Methods.* (2015) 12:697. doi: 10.1038/nmeth.3485
24. Santosh B, Varshney A, Yadava PK. Non-coding RNAs: biological functions and applications. *Cell Biochem Funct.* (2015) 33:14–22. doi: 10.1002/cbf.3079
25. Ke Y, Zhao W, Xiong J, Cao R. miR-149 inhibits non-small-cell lung cancer cells EMT by targeting FOXM1. *Biochem Res Int.* (2013) 2013:506731. doi: 10.1155/2013/506731
26. Chan SH, Huang WC, Chang JW, Chang KJ, Kuo WH, Wang MY, et al. MicroRNA-149 targets GIT1 to suppress integrin signaling and breast cancer metastasis. *Oncogene.* (2014) 33:4496–507. doi: 10.1038/onc.2014.10
27. Qian B, Zhao L, Wang X, Xu J, Teng F, Gao L, et al. miR-149 regulates the proliferation and apoptosis of cervical cancer cells by targeting GIT1. *Biomed Pharmacother.* (2018) 105:1106–16. doi: 10.1016/j.biopha.2018.06.075
28. Wang AL, Li Y, Zhao Q, Fan LQ. Formononetin inhibits colon carcinoma cell growth and invasion by microRNA149mediated EphB3 downregulation and inhibition of PI3K/AKT and STAT3 signaling pathways. *Mol Med Rep.* (2018) 17:7721–9. doi: 10.3892/mmr.2018.8857
29. Feng Q, Zhang H, Nie X, Li Y, Chen WD, Wang YD. miR-149* suppresses liver cancer progression by down-regulating tumor necrosis factor receptor 1-associated death domain protein expression. *Am J Pathol.* (2019) 190:469–83. doi: 10.1016/j.ajpath.2019.10.010

30. Xu K, Liu X, Mao X, Xue L, Wang R, Chen L, et al. MicroRNA-149 suppresses colorectal cancer cell migration and invasion by directly targeting forkhead box transcription factor FOXM1. *Cell Physiol Biochem.* (2015) 35:499–515. doi: 10.1159/000369715
31. Liu X, Zhou Y, Lou Y, Zhong H. Knockdown of HNRNPA1 inhibits lung adenocarcinoma cell proliferation through cell cycle arrest at G0/G1 phase. *Gene.* (2016) 576(2 Pt 2):791–7. doi: 10.1016/j.gene.2015.11.009
32. Gupta RA, Shah N, Wang KC, Kim J, Horlings HM, Wong DJ, et al. Long non-coding RNA HOTAIR reprograms chromatin state to promote cancer metastasis. *Nature.* (2010) 464:1071–6. doi: 10.1038/nature08975
33. Collina F, Aquino G, Brogna M, Cipolletta S, Buonfanti G, De Laurentiis M, et al. LncRNA HOTAIR up-regulation is strongly related with lymph nodes metastasis and LAR subtype of triple negative breast cancer. *J Cancer.* (2019) 10:2018–24. doi: 10.7150/jca.29670
34. Lin K, Jiang H, Zhang LL, Jiang Y, Yang YX, Qiu GD, et al. Down-regulated LncRNA-HOTAIR suppressed colorectal cancer cell proliferation, invasion, and migration by mediating p21. *Dig Dis Sci.* (2018) 63:2320–31. doi: 10.1007/s10620-018-5127-z
35. Liu XH, Liu ZL, Sun M, Liu J, Wang ZX, De W. The long non-coding RNA HOTAIR indicates a poor prognosis and promotes metastasis in non-small cell lung cancer. *BMC Cancer.* (2013) 13:464. doi: 10.1186/1471-2407-13-464
36. Xu Z, Chen H, Yang B, Liu X, Zhou X, Kong H. The association of HOTAIR with the diagnosis and prognosis of gastric cancer and its effect on the proliferation of gastric cancer cells. *Can J Gastroenterol Hepatol.* (2019) 2019:3076345. doi: 10.1155/2019/3076345
37. Cai H, Yao J, An Y, Chen X, Chen W, Wu D, et al. LncRNA HOTAIR acts a competing endogenous RNA to control the expression of notch3 via sponging miR-613 in pancreatic cancer. *Oncotarget.* (2017) 8:32905–17. doi: 10.18632/oncotarget.16462

Conflict of Interest: The authors declare that the research was conducted in the absence of any commercial or financial relationships that could be construed as a potential conflict of interest.

frontiers in Oncology

ORIGINAL RESEARCH
published: 23 November 2020
doi: 10.3389/fonc.2020.569668

Novel Non-Coding Transcript in *NR4A3* Locus, LncNR4A3, Regulates RNA Processing Machinery Proteins and *NR4A3* Expression

Ada Congrains, Fernanda Soares Niemann, Adriana Da Silva Santos Duarte, Karla Priscila Vieira Ferro and Sara Teresinha Olalla-Saad*

Hematology and Transfusion Medicine Center, University of Campinas, Campinas, Brazil

OPEN ACCESS

Edited by:
Jawed Akhtar Siddiqui, University of Nebraska Medical Center, United States

Reviewed by:
Alexander Deutsch, Medical University of Graz, Austria
Jian Pan, Soochow University, China
Shenglai Li, University of Chicago, United States

***Correspondence:**
Ada Congrains
adacongrains@hotmail.com

Specialty section:
This article was submitted to Molecular and Cellular Oncology, a section of the journal Frontiers in Oncology

Received: *04 June 2020*
Accepted: *19 October 2020*
Published: *23 November 2020*

Citation:
Congrains A, Niemann FS, Duarte ADSS, Ferro KPV and Olalla-Saad ST (2020) Novel Non-Coding Transcript in NR4A3 Locus, LncNR4A3, Regulates RNA Processing Machinery Proteins and NR4A3 Expression. Front. Oncol. 10:569668. doi: 10.3389/fonc.2020.569668

NR4A3 is a key tumor suppressor in myeloid malignancy, mice lacking both *NR4A1* and family member *NR4A3* rapidly develop lethal acute myeloid leukemia (AML). We identified a long non-coding transcript in the *NR4A3* locus and pursued the characterization of this anonymous transcript and the study of its role in leukemogenesis. We characterized this novel long non-coding transcript as a sense polyadenylated transcript. Bone marrow cells from AML patients expressed significantly reduced levels of lncNR4A3 compared to healthy controls (controls = 15, MDS= 20, p=0.05., AML= 21, p<0.01). Expression of *NR4A3*, as previously reported, was also significantly reduced in AML. Interestingly, the expression of both coding and non-coding transcripts was highly correlated (Pearson R = 0.3771, P<0.01). Transient over-expression of LncNR4A3 by nucleofection led to an increase in the RNA and protein level of *NR4A3*, reduction of proliferation in myeloid cell lines K-562 and KG1 (n=3 and 2 respectively, p<0.05) and reduced colony formation capacity in primary leukemic cells. A mass spectrometry-based quantitative proteomics approach was used to identify proteins dysregulated after lncNR4A3 over-expression in K-562. Enrichment analysis showed that the altered proteins are biologically connected (n=4, p<0.001) and functionally associated to RNA binding, transcription elongation, and splicing. Remarkably, we were able to validate the most significant results by WB. We showed that this novel transcript, lncNR4A3 regulates *NR4A3* and we hypothesize this regulatory mechanism is mediated by the modulation of the RNA processing machinery.

Keywords: NR4A3, RNA processing, long non-coding RNA, myeloid malignancy, acute myeloid leukemia

INTRODUCTION

NR4A3/NOR-1 is a member of the NR4A orphan nuclear receptor subfamily. This subfamily comprises three closely related members: *NR4A1* (also known as Nur77, TR3, or NGFI-B), *NR4A2* (also known as Nurr1, RNR-1, or TONOR), and *NR4A3* (also known as NOR-1 or MINOR). NR4As dysregulation has been associated with a wide range of conditions including atherosclerosis, diabetes, and several malignancies (1–7).

The role of *NR4A1* and *NR4A3* in myeloid malignancy is particularly relevant. *NR4A1/NR4A3* knock-out mice rapidly develop lethal acute myeloid leukemia (AML) (8, 9) and reduced dosage of these genes, in mice, leads to a phenotype that recapitulates myelodysplastic syndrome (MDS), a hematologic disorder with increased susceptibility to AML. Additionally, leukemic blasts from AML patients have reduced expression of *NR4A1/NR4A3* genes (9). This evidence strongly supports the hypothesis that the loss of tumor suppressors *NR4A1/3* is a key initiating step in leukemic transformation. Strategies aiming to block the inactivation of these transcription factors would hold great potential in the treatment of AML and MDS. However, the mechanisms that lead to their inactivation remain elusive.

Long non-coding RNAs are increasingly recognized as master regulators of cellular function in health and disease (10–14). These non-coding transcripts are involved in virtually all steps of genetic regulation. They recruit chromatin modifying proteins (15) and transcription factors (16), hijack the splicing (17) and translation machinery (11), sequester miRNAs (18), among other functions. Previous work of our group identified a long non-coding RNA in the *NR4A3* locus expressed in hematopoietic stem cells from myelodysplastic syndrome patients (19). Due to the important role of *NR4A3* gene in myeloid malignancy, we pursued the functional characterization of this transcript.

A long non-coding RNA encoded in the *NR4A3* locus is an interesting candidate to explore cis regulation upon *NR4A3*. Here, we characterized this hitherto unknown transcript, evaluated its expression in patient samples, functionally studied its role in NR4A3 locus regulation and used a mass-spectrometry-based proteomics approach to identify the targets of lncNR4A3.

TABLE 1 | Clinical characteristics of patients and healthy controls.

Characteristics patients and healthy controls		**Number**
Controls		15
Sex (male/female)		12/3
Age median [range]		30 [15–47]
MDS cases		20
Sex (male/female)		12/8
Age median [range]		59 [31–86]
% of blasts in BM, mean		5.9
FAB classification		
Low risk (RA/RARS)		4/4
High risk (RAEB/RAEB-t)		11/1
AML cases		21
Sex (male/female)		12/9
Age median [range]		59 [22–88]
% of blasts in BM, mean		77.6
FAB classification		
M0		1
M1		6
M2		5
M3		2
M4		4
M5		2
AML-MRC (secondary to MDS)		1
AML cases for nucleofection		2
	FAB classification	% of blasts in BM
Case 1	M3	95
Case 2	M4	59.6

RA, refractory anemia; RARS, refractory anemia with ringed sideroblasts; RAEB, refractory anemia with excess blasts; RAEB-t, refractory anemia with excess blasts in transformation; M0, undifferentiated acute myeloblastic leukemia; M1, acute myeloblastic leukemia with minimal maturation; M2, acute myeloblastic leukemia with maturation; M3, acute promyelocytic leukemia; M4, acute myelomonocytic leukemia; M5, acute monocytic leukemia; AML-MRC, acute myeloid leukemia with myelodysplasia-related changes.

PATIENTS, MATERIALS, AND METHODS

Patients

Samples from patients with previously untreated AML and MDS by World Health Organization (WHO) criteria, were used in this study. Diagnosis was confirmed by cytologic examination of blood and bone marrow (patient characteristics shown in **Table 1**). Mononuclear cells were isolated by Ficoll-Hypaque separation of total bone marrow (BM). Samples from MDS patients (12 males, 8 females, median age: 74, range: 31–86 years) and AML patients (12 males, 9 females, median age, 59 years, range, 22–88 years) were collected at the time of diagnosis and BM mononuclear cells of 15 controls (12 males, 3 females, median age, 30 years, range, 15–47 years) were obtained from bone marrow donors. French-American-British (FAB) classification of the patients is presented in **Table 1**. All patients were diagnosed between 2009 and 2014 at the hematology and transfusion medicine center, University of Campinas. Bone marrow mononuclear cells for the nucleofection experiments were obtained from BM aspirates of two AML patients. The mononuclear cell fraction was separated as described above. One patient had more than 80% CD34+ cells and cells were directly used for the experiments and for the other patient, CD34+ cells were separated using Indirect CD34 MicroBead Kit, Miltenyi Biotech GmbH, Germany. All participants gave written informed consent to the study; procedures were approved by the University Ethics Committee (number CEP1209/2011) and all methods were in accordance with the relevant guidelines and regulations.

Nucleofection

After full characterization of lncNR4A3, we successfully cloned the transcript in pcDNA^{TM}3.1 (+) (Invitrogen) expression vector. The lncNR4A3 and empty vector were delivered into k-562, KG1 cells, and CD34+ hematopoietic cells by nucleofection using AMAXA nucleofector device (Lonza, Switzerland) and SF Cell Line Kit (for K-562 and KG1) and P3 Primary Cell Kit (for CD34 +cells), (Lonza, Switzerland). 10^6 cells were nucleofected with 2 μg of vector for K-562 and CD34+ cells and 4 μg for KG1 cells according to the optimized protocol provided by the manufacturer. After nucleofection cells CD34+ cells were resuspended in expansion medium StemSpan^{TM}, Stemcell Technologies (supplemented with 10ng/ml of IL3, IL6, FLT3, TPO), or methylcellulose medium (MethoCult^{TM} Stemcell). Nucleofection efficiency was evaluated using 2μg of pmax-GFP and results are shown in **Supplementary Results**.

Quantitative RT-PCR (qRT-PCR)

RNA was isolated from k-562, KG1, CD34+ cells and total bone marrow samples using Illustra RNAspin Mini Kit (GE Healthcare Life Sciences) following the manufacturer's instructions. RNA quantification was performed in a NanoDrop spectrophotometer (ND-1000 Spectrophotometer). A total of 1 µg of RNA from each sample (except for CD34+ cells, from which samples less than 1µg RNA were obtained) was reverse transcribed into complementary DNA (cDNA) (RevertAid First Strand cDNA Synthesis Kit, Thermo Scientific) using random primers. For strand-specific PCR we used sequence specific primers for reverse transcription (complementary to positive and negative strands respectively), instead of dT oligos or random primers. These primers were designed near the expected ends of lncNR4A3.

Real-time PCR amplifications were performed on the ABI 7500 Sequence Detector System (Applied Biosystems) using SybrGreen PCR Master Mix (Applied Biosystems). Primers sequences are provided in **Supplementary Methods**.

Viability Assay—CCK-8

For proliferation analysis, cell counting kit, CCK-8 (Dojindo Molecular Technologies, Inc.) assay was used. This viability assay uses a water-soluble tetrazolium salt, 2-(2-methoxy-4-nitrophenyl)-3-(4-nitrophenyl)-5-(2,4-disulfophenyl)-2H tetrazolium, monosodium salt (WST-8), which has been shown to have greater sensitivity than traditional assays such as MTT (20). Cells were seeded in 96-well plates at a density of $2x10^5$ cells/ml after nucleofection and were incubated at 37°C for further 48 and 72 h for K-562 and KG1 respectively. After that time, CCK-8 reagent was added to the well, following manufacturer's instruction and cell viability was assessed by measurement of absorbance at 450nm, expressed relative to control empty-vector-nucleofected cells.

Proteomic Analysis

Protein was extracted as described above and concentrations were determined by Bradford protein quantification assay. A total of 50 µg of protein were run in a sodium dodecyl sulfate-polyacrylamide gel electrophoresis (SDS-PAGE) and undergo reduction, alkylation, and in-gel digestion with trypsin (details in **Supplementary Methods**). Peptides were separated by C18 (100 mm 6,100 mm) RP-nanoUPLC (nanoACQUITY, Waters) coupled with a Q-Tof Premier Mass Spectrometer (Waters) with nanoelectrospray source at a flow rate of 0.6 ml/min.

For protein quantification, data was analyzed by Scaffold Q+ (version 4.4.3; Proteome Software, Inc., Portland, OR, USA) and set to a false discovery under 1%. Gene ontology enrichment was carried out using String software V10.5. Details of analysis in **Supplementary Methods**.

Western Blotting

Cells were lysed in a buffer containing 100 mM Tris (pH 7.6), 1% Triton X-100, 150 mM NaCl, 0.1 mg aprotinin, 35 mg/ml PMSF 10 mM Na3VO4, 100 mM NaF, 10 mM Na4P2O7, and 4 mM EDTA (approximately 5×10^6 cells). Samples were centrifuged at 4°C for 20 min to remove cell debris. Protein concentration was measured using the Bradford Assay (Bio-Rad). Laemmli buffer containing 100 mmol/L of dithiothreitol was added to the protein extracts and heated at 100°C for 5 min. Samples were run on a 10% SDS-PAGE. After the run, the proteins were transferred to nitrocellulose membranes (Millipore). Membranes were immunoblotted with NR4A3 (Abcam, ab41918), HnRNPK (Abcam, ab32969), SF3B2 (ProteinTech, 10919-1-AP), HnRNPA1 (ProteinTech, 11176-1-AP), PARP1 (Santa Cruz, sc-56197), Lamin B1 (Santa Cruz, sc-6127), and GAPDH (Santa Cruz, sc-32233) antibodies. K-562 protein samples were obtained from three independent experiments, all bands are shown in the **Supplementary Material**; however, only one patient sample of HSC CD34+ cells (which is a rare population of hematopoietic progenitors) was available for protein extraction. Band intensity was quantified using UVITEC alliance software.

Statistical Analysis

Statistical analysis of the data was performed using R version 3.5.1 and GraphPad prism software. The patient's data was analyzed by Student's t-test (two-way) and statistical significance between two groups (controls *vs*. MDS, and controls *vs*. AML) is shown in the graphs. To measure correlation between lncNR4A3 and NR4A3, the Pearson coefficient was calculated, Pearson r and P-value are shown in the corresponding figure. For the functional experiments the significance of differences between two groups (empty vector and lncNR4A3) was estimated with Student's t test and differences were considered statistically significant at the level of $P < 0.05$. Figures were plotted using "R" programing language ("ggplot2," "cowplot," "gridextra" packages). For screening of differently expressed proteins from the proteomic analysis, we used an in-house program developed in "R" 3.5.1 to apply ANOVA built-in function to all proteins detected; however, proteins with more than three missing spectrometry readings were excluded from the analysis.

RESULTS

lncNR4A3 Characterization

To characterize lncNR4A3, we based on a partial sequence identified by Nakaya *et al.* and deposited in a dataset for partially intronic non-coding RNAs (21). Additionally, we performed a search for ESTs (expressed sequence tags) in the UCSC database in this region, identifying several human ESTs (Accession: BG539866, BG546553, BG570616, BF105874, BE502919, BE219816, AW204232, see **Supplementary Figure 1**). Since most PCR approaches are not direction-sensitive, we used strand-specific PCR to identify the orientation of the transcript, which is based on synthesis of cDNA using specific primers complementary to positive and negative strands of DNA near the expected ends of the transcript from both strands. This assay revealed that lncNR4A3 is transcribed in the same orientation than NR4A3, hence considered a sense transcript

(**Figure 1B**). To characterize the complete sequence of lncNR4A3, we used primers near the putative 5′ and 3′ ends to perform rapid amplification of cDNA ends. Due to the difficulty to amplify the 3′end of this transcript, we suspected it did not have a poly A tail. We used oligo dT beads to enrich RNAs with poly A tails and collected RNA not bound to the beads as RNA depleted of polyadenylated transcripts. Unexpectedly, LncNR4A3 only amplified in the poly A enriched fraction for cDNA from K-562, suggesting LncNR4A3 is polyadenylated (see **Supplementary Figure 2**). After several attempts and methods (see **Supplementary Methods**) LncNR4A3 full sequence (deposited under NCBI GeneBank accession number MK510719) was identified by RACE. This sequence also matches the alignment of ESTs found in the region, supporting MK510719 is the full sequence of the transcript (see **Supplementary Figure 1**). LncNR4A3 was characterized as a polyadenylated, 1,214 bp transcript overlapping the second intron, and an alternative exon of the NR4A3 gene, see **Figure 1A**.

Expression of lncNR4A3 and *NR4A3* Is Suppressed in Acute Myeloid Leukemia

The novel non-coding transcript, lncNR4A3 was significantly reduced in cells from the bone marrow of AML patients (controls= 15, MDS=20, AML=21), see **Figure 1D**. As previously reported (9), *NR4A3* is also reduced in bone marrow cells from MDS and AML patients (**Figure 1C**). Expression of lncNR4A3 and *NR4A3* were positively correlated (Pearson R = 0.3771, P<0.01, **Figure 1E**), supporting involvement of one in the expression of the other.

We also characterized the expression of lncNR4A3 in several myeloid and lymphoid cell lines, CD34+ hematopoietic stem cells, and non-hematopoietic cells lines HS5 and Hela (see **Supplementary Figure 4**). LncNR4A3 was detected in all cell types evaluated, but expression in myeloid malignant cell lines was extremely low compared to CD34+ HSCs (a normal hematopoietic progenitor cell population from umbilical cord blood) and HS5 (stromal cell line).

LncNR4A3 Over-Expression Modulates the Expression of RNA-Binding Proteins and Particularly Members of the hnRNP Family

We investigated the global effects of lncNR4A3 over-expression among the entire proteome of lncNR4A3 over-expressing K-562 cells compared to controls. Whole-cell lysates were processed and analyzed by Q-tof mass spectrometry as described in methods. A total of over 400 proteins were identified (see complete list in **Supplementary Data File**). Enrichment analysis using STRING software showed that the altered proteins are biologically connected (n=4, p<0.001, see protein-protein interaction network, **Figure 2A**) and functionally associated to RNA binding and processing and cellular components including the spliceosome (**Figure 2B**).

Pathways analysis rendered similar results, KEGG pointed to protein processing in endoplastic reticulum and spliceosome as second most significantly associated pathway, "Reactome" gave metabolism of RNA as most associated metabolic pathway and "Local String network cluster" pointed to messenger RNA (mRNA) splicing as associated pathway. The association of these pathways support the role of lncNR4A3 in RNA processing.

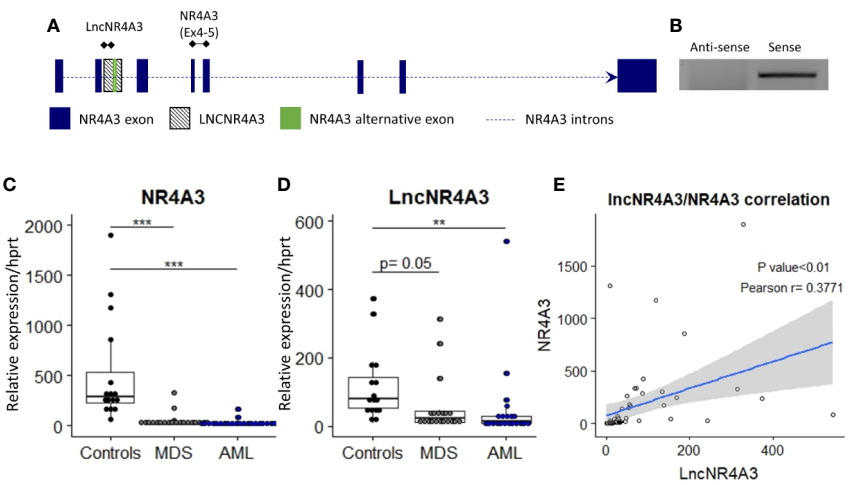

FIGURE 1 | **(A)** Transcriptional map of the NR4A3 locus showing position of LncNR4A3 and primers used in this work. **(B)** EtdBr-staining bands in agarose gel electrophoresis from strand-specific PCR to identify the orientation of the transcript, lncNR4A3 is transcribed in the same orientation than NR4A3. **(C, D)** Quantitative RT-PCR (QRT-PCR) quantification of NR4A3 and long non-coding transcript, LncNR4A3, in normal bone marrow cells (NBM) of 15 controls, 20 myelodysplastic syndrome patients (MDS), and 21 acute myeloid leukemia patients bone marrows (AML). **(E)** Linear regression of the expression of LncNR4A3 plotted against NR4A3 expression and correlation analysis results (Pearson correlation P value, R coefficient). ** : <0.01, *** : <0.001.

From this analysis 22 proteins were significantly up-regulated and 19 down-regulated ($p<0.05$). Among the regulated proteins there are four members of the hnRNP (heterogeneous nuclear ribonucleoproteins) family and three of them up-regulated (**Table 2**, **Figure 2C**). The most significantly enriched protein in the lncNR4A3-K-562 cells was the heterogeneous nuclear ribonucleoprotein K (p-value = 0.00058). We validated the upregulation of *hnRNPK* in K-562 cells and AML patient cells; however, no effect was detected in KG1 cell line (see **Supplementary Figure 9**). Heterogeneous nuclear ribonucleoproteins (hnRNPs) are involved in RNA translocation and processing, also considered splicing switches (22, 23). Poly (ADP) ribose polymerase (*PARP1*) upregulation was also validated, while this protein is most known for its role in DNA damage repair, it is also involved in alternative splicing and RNA elongation (24, 25). Among up-regulated proteins, western blotting confirmed increased expression of splicing factor 3 B2 (*SF3B2*), a component of the spliceosome machinery that promotes splicing. Remarkably, splicing defects are key in leukemogenesis and mutations in the genes encoding the splicing machinery proteins are common in hematologic malignancy (26, 27). Lamin B1 was also among the proteins up-regulated by LncNR4A3 over-expression, this protein is an important structural component of the nucleus and evidence shows it is crucial for RNA synthesis and proliferation (28, 29). And more interestingly, expression of NR4A3 is known to be regulated by RNA splicing and elongation (30).

Artificial Re-Expression of lncNR4A3 Leads to Increased Expression of NR4A3 Messenger RNA and NR4A3 Protein Level and Reduction of Proliferation in Myeloid Cell Lines K-562, KG1, and Primary Leukemic Cells

The endogenous expression of both *NR4A3* (data not shown) and lncNR4A3 in myeloid cell lines is almost completely abrogated (see **Supplementary Figure 4**), therefore we sought to determine if the inactivation of *NR4A3* could be reversed by lncNR4A3 artificial re-expression. Transient over-expression of lncNR4A3 led to a more than 2-fold increase of *NR4A3* mRNA (**Figure 3A** for K-562 and **Supplementary Figure 8** for KG1) and more importantly, this regulatory effect translated into an increased NR4A3 protein level (**Figure 3D**). Levels of lncNR4A3 and NR4A3 mRNA were evaluated by qRT-PCR. Efficiency of the over-expression was verified by qRT-PCR, which showed that all nucleofections rendered more than 500-fold over-expression of lncNR4A3 compared to controls (see **Supplementary Figure 7**).

Consistent with this reactivation of *NR4A3*, the proliferation of K-562 and KG1 cells was reduced as shown by cell viability assay CCK-8 (**Figure 3B** and **Supplementary Figure 8**, K-562 and KG1 respectively). We also examined the effects of lncNR4A3 in CD34+ hematopoietic cells from two acute

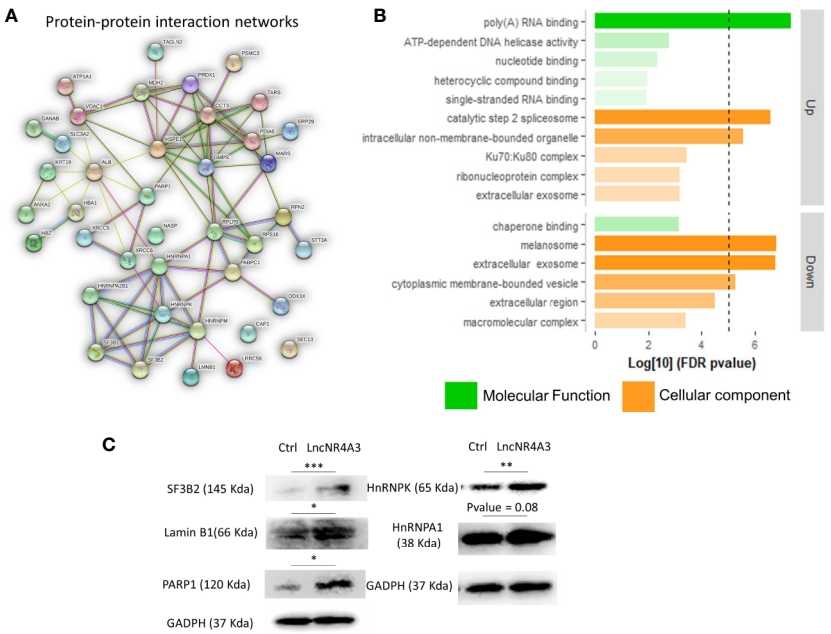

FIGURE 2 | **(A)** Protein–protein interaction network, a weighted linkage graph constructed using STRING software, inputting the differentially expressed proteins identified in the proteomics analysis. **(B)** Histogram plotting the Log[10] of the p-values obtained from the gene ontology enrichment analysis, cellular component, and molecular function ontology Log[10]p-values were plotted for up-regulated and down-regulated proteins obtained from proteomics analysis, threshold of 5 is denoted by the dashed line. **(C)** Immunoblots confirming regulation of several target proteins identified by the MS-proteomics analysis in K-562 controls and lncNR4A3 over-expressing cells, blots from three independent experiments shown in **Supplementary Figure 10**, paired t-test was applied to stablish significant differences between optical density of the blots (*: <0.05, **: <0.01, ***<0.001).

TABLE 2 | MS-proteomics analysis results.

Up-regulated				
Protein name	**Control (mean)**	**LncNR4A3 (mean)**	**P-value (ANOVA)**	**Gene symbol**
Heterogeneous nuclear ribonucleoprotein K	8	14.25	0.00058	HNRNPK
Isoform of O00571, ATP-dependent RNA helicase DDX3X	4.5	10.75	0.003531	DDX3X
Poly[ADP-ribose] polymerase 1	1	10.5	0.005331	PARP1
Isoform of P12956, X-ray repair cross-complementing protein 6	6	20.75	0.005752	XRCC6
GMP synthase [glutamine-hydrolyzing]	3.75	10	0.006819	GMPS
Isoform of P52272, heterogeneous nuclear ribonucleoprotein M	2.75	8.5	0.010682	HNRNPM
Isoform of P09651, heterogeneous nuclear ribonucleoprotein A1	2.5	6	0.011724	HNRNPA1
Isoform of Q06830, peroxiredoxin-1 (fragment)	10.33	14.33	0.013235	PRDX1
Leucine-rich repeat-containing protein 59	5.25	6.67	0.017570	LRRC59
Nuclear autoantigenic sperm protein	3	7.25	0.017570	NASP
Lamin-B1	2	5.5	0.020311	LMNB1
Splicing factor 3B subunit 1	0.75	3	0.0388027	SF3B1
X-ray repair cross-complementing protein 5	3.75	9	0.040405	XRCC5
Hemoglobin subunit zeta	4	8.33	0.040642	HBZ
Isoform of P49368, T-complex protein 1 subunit gamma	9.75	14.75	0.042462	CCT3
Isoform of P11940, polyadenylate-binding protein	2.75	7.75	0.0424626	PABPC1
Threonine–tRNA ligase, cytoplasmic	5.75	9.75	0.043422	TARS
Isoform of P17980, 26S proteasome regulatory subunit 6A (fragment)	1.5	3.67	0.044629	PSMC3
Isoform of Q13435, splicing factor 3B subunit 2	0.25	2.25	0.0446904	SF3B2
Transgelin-2 OS=homo sapiens	22	29.67	0.0452401	TAGLN2
Keratin, type I cytoskeletal 19	1	3.67	0.045318	KRT19
Adenylyl cyclase-associated protein 1	7.5	8.5	0.049825	CAP1
Downregulated				
Exosome RNA helicase MTR4	1	0	1,24E–29	MTREX
Isoform of P55735, protein SEC13 homolog	4	0.33	0.001222	SEC13
60S acidic ribosomal protein P0	13.75	9.67	0.003655	RPLP0
Methionine–tRNA ligase, cytoplasmic	9	4.75	0.00414	MARS
Protein disulfide-isomerase A6	27.75	12.5	0.004389	PDIA6
Isoform of Q14697, neutral alpha-glucosidase AB	21.25	5.25	0.0053375	GANAB
Annexin A2 OS=homo sapiens	10	2.67	0.006343	ANXA2
Sodium/potassium-transporting ATPase subunit alpha-1	11	1.75	0.010610	ATP1A1
Isoform of P62249, 40S ribosomal protein S16	5.33	4	0.016130	RPS16
Malate dehydrogenase, mitochondrial	54	34.33	0.018010	MDH2
Isoform of P02768, serum albumin	11.25	1.75	0.018507	ALB
Endoplasmic reticulum resident protein 29	14	6	0.020775	ERP29
Isoform of P08195, 4F2 cell-surface antigen heavy chain	6	1	0.0221184	SLC3A2
Hemoglobin subunit alpha	6	2.5	0.027172	HBA1
Heterogeneous nuclear ribonucleoproteins A2/B1	6.25	4	0.02933	HNRNPA2B1
Dolichyl-diphosphooligosaccharide–protein glycosyltransferase subunit 2	15.75	4.5	0.029406	RPN2
Dolichyl-diphosphooligosaccharide–protein glycosyltransferase subunit STT3A	3.75	1.25	0.030766	STT3A
Voltage-dependent anion-selective channel protein 1	12.75	2.75	0.0336062	VDAC1
10 kDa heat shock protein, mitochondrial	7.67	2.33	0.0474206	HSPE1

myeloid leukemia patients. Expression of NR4A3 mRNA was increased in both samples after lncNR4A3 over-expression (38% and 68% increase in mRNA level) and due to sample availability, only one patient sample was analyzed by western blot, confirming upregulation of *NR4A3* (**Figure 3C**). Nucleofection-mediated transient over-expression of lncNR4A3 in these cells caused an important reduction in their colony formation capacity (15-days methylcellulose CFU assay) when compared to empty-vector nucleofected cells (**Figure 3D**). Methylcellulose colony-forming unit (CFU) assay shows that the over-expression of lncNR4A3 compromised the proliferation capacity of these cells, evidenced by the reduced number of colonies as well as colony size in lncNR4A3-nucleofected cells after 15 days in semi-solid culture (control-1: 7 clusters, 5 colonies, lncNR4A3-1: 5 clusters, 0 colonies; control-2: 19 clusters, 13 colonies, lncNR4A3-2: 2 clusters, 1 colony) see **Figure 3D** and **Supplementary Figures 8** and **9**.

DISCUSSION

Despite the advancements in therapeutic interventions, acute myeloid leukemia (AML) patients have limited treatment options and mortality remains high. Myelodysplastic syndromes (MDS) are a group of pre-leukemic conditions, associated to aging, characterized by inefficient hematopoiesis and accumulation of genetic lesions (31). There is a diversity of genetic abnormalities associated with leukemogenesis, and targeting a mechanism common to myeloid malignancy is a

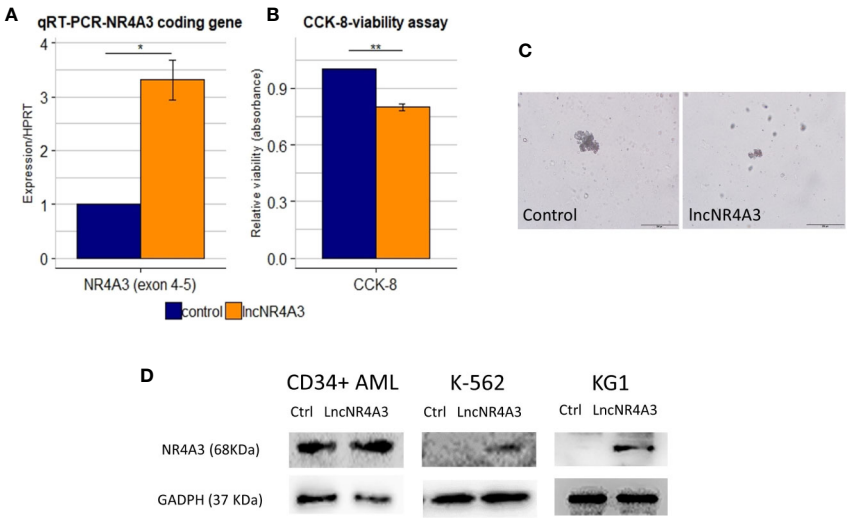

FIGURE 3 | **(A)** Relative quantification by quantitative RT-PCR (qRT-PCR) of NR4A3 expression in LncNR4A3 over-expressing K-562 and empty vector control cells shows significant modulation of NR4A3 at mRNA level in K-562 (mean ± SEM, n=3), similar results for KG1 cells are shown in **Supplementary Figure 8**. **(B)** CCK-8 viability assay results showing reduced viability after lncNR4A3 over-expression in k-562, results for KG1 are shown in **Supplementary Figure 8**. **(C)** Photographs of human hematopoietic CFUs in semi-solid culture (bar: 200µm), see additional colonies in supplementary information. Left: representative colony from control CD34+ cells after 15 day in culture. Right: representative cluster from LncNR4A3 over-expressing cells 15 days in culture. **(D)** Immunoblots showing the reactivation of NR4A3 protein in AML CD34+ cells, KG1 and K-562 cells. * : <0.05, *** : <0.001.

challenge to the development of efficient therapies. The suppression of NR4As nuclear receptors is a common feature of AML irrespective of subtype and cytogenetics, and the loss of these nuclear receptors leads to rapid development of AML in mice. All these characteristics make the reactivation of *NR4A1/3* an appealing treatment approach. However, the mechanisms that regulate *NR4A1/3* repression during myeloid malignization are not well-understood.

Heterogeneous nuclear ribonucleoproteins (HnRNP) comprise a family of multifunctional RNA binding proteins involved in different levels of transcriptional and post-transcriptional regulation including pre-mRNA processing, mRNA stability, and translation (32–36). Several members of this family have been associated with RNA elongation and splicing (32, 34, 36). Moreover, *HnRNPK* has been characterized as a tumor suppressor in myeloid malignancy (37). This protein family, as well as other proteins identified in this study as targets of lncNR4A3, are associated with RNA synthesis, elongation and splicing (25, 27, 28, 32, 34).

Here, we identified a novel sense non-coding transcript in the *NR4A3* locus. The expression of this transcript is abrogated in myeloid malignancy patients, and myeloid malignant cell lines. Finally, the artificial re-expression of lncNR4A3 caused the re-activation of *NR4A3* in leukemic cells and modulation of several proteins associated to RNA processing in K-562.

Although, we embarked on the characterization of lncNR4A3 under the hypothesis of a cis-regulatory role of lncNR4A3 upon *NR4A3*. Our results provide evidence of a broader reach of this transcript in the regulation of a set of proteins involved in RNA processing. Unfortunately, proteomics approaches are not as comprehensive as transcriptomic ones and due to sensitivity limitations of the technique and equipment, we cannot infer that these proteins are directly regulated or the only ones regulated by lncNR4A3. We also cannot conclude that the dysregulated proteins are cause or consequence of NR4A3 dysregulation. Despite the numerous reported cases of local regulation by long non-coding RNAs (12, 38–41), results from global transcription analysis reveal that long non-coding RNAs act as global expression regulators, modulating, not only one, but many distant loci (15, 38, 41–43). Moreover, there are several cases of lncRNAs acting through cis- and trans-mechanisms simultaneously (38, 40, 41). Deeper analysis of several cases of reportedly cis-acting lncRNAs revealed a wider set of genome-wide targets from which the locally regulated gene was merely a part or an indirect product of a *trans*-mechanism (38, 40, 43). All these are possible scenarios of the regulatory landscape of the *NR4A3* locus. In this study we have pointed to a completely new player in the regulation of NR4A3 and the association of this lncRNA with RNA processing machinery. However, future work is necessary to identify direct targets of this transcript and precise regulatory mechanisms of this important locus in the light of these new findings.

Another technical limitation of the study of LncNR4A3 is the fact that primer design cannot exclude immature forms of *NR4A3* as contaminants in the qRT-PCR quantification. We performed an amplification using primers spanning exon 3 and adjacent intron to quantify the influence of non-processed *NR4A3* RNA (**Supplementary Figure**). We were able to detect the immature *NR4A3* RNA (exon-intron primers); however, close to the limit of reliable detection and in significantly less abundance (~3 cycles) than lncNR4A3.

Despite these limitations, the strong functional association between the up-regulated proteins, suggests a role of lncNR4A3 in RNA processing. We reviewed the literature to understand the nature of the mechanisms that regulate *NR4A3* expression. Although some reports suggested that epigenetic modification is involved in the silencing of *NR4A3* in some cancer models (1, 44), solid evidence from a recent study demonstrated that the abrogation of *NR4A3* expression in myeloid malignization was mediated by the blockade of transcriptional processing rather than epigenetic silencing (30). They showed that *NR4A3* promoter region of AML blasts lacks common epigenetic markers of repression compared to normal cells, and their repression during malignization depends on RNA processing defects (30). Here, we present evidence of the role of this novel long non-coding RNA, lncNR4A3 in *NR4A3* regulation and the modulation of a set of RNA processing related proteins. This study focused on the effect of this new regulatory transcript in myeloid malignancy; however, *NR4A3* plays important roles in lymphopoiesis (9) and its suppression is associated to lymphomagenesis (6). The reactivation of *NR4A3* by lncNR4A3 could have similar tumor suppressor effect in the context of lymphoma and other malignancies.

Our results suggest that the re-expression of lncNR4A3 is able to revert, to some extent, the loss of *NR4A3* in leukemic cells. This enhanced synthesis of *NR4A3* leads to the expected reduction in cell viability. Although, it is likely that lncNR4A3 is a fine tuner of expression for several targets, far beyond *NR4A3*, we present evidence of a tumor suppressor role of this transcript in myeloid leukemia through the regulation of *NR4A3*.

DATA AVAILABILITY STATEMENT

Proteomics quantitative data is available in a **Supplementary Material**, and raw spectra for the proteomic analysis is available upon request. Novel LncNR4A3 sequence was deposited in the NCBI database under the accession number MK510719.

ETHICS STATEMENT

The studies involving human participants were reviewed and approved by Campinas State University Ethics Committee (number CEP1209/2011). The patients/participants provided their written informed consent to participate in this study.

AUTHOR CONTRIBUTIONS

AC designed and performed the research, analyzed data and wrote the paper. FN contributed in performing the research. AD contributed in performing the research. KF contributed in performing the research. SO-S contributed in the design of the research, data analysis, and interpretation. All authors contributed to the article and approved the submitted version.

FUNDING

This work was supported by the Fundação de Amparo à Pesquisa do Estado de São Paulo (FAPESP) and carry out in the Hematology and Transfusion Medicine Centre – UNICAMP. The authors would like to gratefully acknowledge Romenia Ramos Domingues, Dr. Bianca Alves Pauletti and Dr. Adriana Franco Paes Leme at the Brazilian Biosciences National Laboratory CNPEM (Campinas, Brazil) for providing technical support, and the Brazilian Biosciences National Laboratory (LNBio, CNPEM), for their support with the use of the Q-tof spectrometer for the proteomics analysis.

SUPPLEMENTARY MATERIALS

The Supplementary Material for this article can be found online at: https://www.frontiersin.org/articles/10.3389/fonc.2020.569668/full#supplementary-material.

REFERENCES

1. Yeh C-M, Chang L-Y, Lin S-H, Chou J-L, Hsieh H-Y, Zeng L-H, et al. Epigenetic silencing of the NR4A3 tumor suppressor, by aberrant JAK/STAT signaling, predicts prognosis in gastric cancer. *Sci Rep* (2016) 6 (August):31690. doi: 10.1038/srep31690
2. Rodrıguez-Calvo R, Guadall A, Calvayrac O, Navarro MA, Alonso J, Ferran B, et al. Over-expression of Neuron-derived Orphan Receptor-1 (NOR-1) exacerbates neointimal hyperplasia after vascular injury. *Hum Mol Genet* (2013) 22(10):1949–59. doi: 10.1093/hmg/ddt042
3. Nagaoka M, Yashiro T, Uchida Y, Hara M, Arai H, Ogawa H, et al. The Orphan Nuclear Receptor NR4A3 Is Involved in the Function of Dendritic Cells. *J Immunol* (2017) 199(8):2958–67. doi: 10.4049/jimmunol.1601911
4. Tessem JS, Moss LG, Chao LC, Arlotto M, Lu D, Jensen MV. Nkx6.1 regulates islet β-cell proliferation via Nr4a1 and Nr4a3 nuclear receptors. *PNAS* (2014) 111(14):5242–7. doi: 10.1073/pnas.1320953111
5. Fu Y, Luo L, Luo N, Zhu X, Garvey WT. NR4A Orphan Nuclear Receptors Modulate Insulin Action and the Glucose Transport System. *J Biol Chem* (2007) 282(43):31525–33. doi: 10.1074/jbc.M701132200
6. Deutsch AJA, Rinner B, Pichler M, Prochazka K, Bischof M, Fechter K, et al. NR4A3 suppresses lymphomagenesis through induction of pro-apoptotic genes. *Cancer Res* (2017) 77(9):2375–86. doi: 10.1158/0008-5472.CAN-16-2320
7. Haller F, Bieg M, Will R, Körner C, Weichenhan D, Bott A, et al. Enhancer hijacking activates oncogenic. *Nat Commun* (2019) 10(368):3–13. doi: 10.1038/s41467-018-08069-x
8. Ramirez-Herrick AM, Mullican SE, Sheehan AM, Conneely OM. Reduced NR4A gene dosage leads to mixed myelodysplastic/myeloproliferative neoplasms in mice. *Blood* (2011) 117(9):2681–90. doi: 10.1182/blood-2010-02-267906
9. Mullican SE, Zhang S, Konopleva M, Ruvolo V, Andreeff M, Milbrandt J, et al. Abrogation of nuclear receptors Nr4a3 and Nr4a1 leads to development of acute myeloid leukemia. *Nat Med* (2007) 13(6):730–5. doi: 10.1038/nm1579
10. Lee JT, Bartolomei MS. X-inactivation, imprinting, and long noncoding RNAs in health and disease. *Cell* (2013) 152(6):1308–23. doi: 10.1016/j.cell.2013.02.016
11. Carrieri C, Cimatti L, Biagioli M, Beugnet A, Zucchelli S, Fedele S, et al. Long non-coding antisense RNA controls Uchl1 translation through an embedded SINEB2 repeat. *Nature* (2012) 491(7424):454–7. doi: 10.1038/nature11508
12. Congrains A, Kamide K, Oguro R, Yasuda O, Miyata K, Yamamoto E, et al. Genetic variants at the 9p21 locus contribute to atherosclerosis through

modulation of ANRIL and CDKN2A/B. *Atherosclerosis* (2012) 220(2):449–55. doi: 10.1016/j.atherosclerosis.2011.11.017
13. Congrains-Castillo A, Niemann FS, Santos AS, Saad STO. LEF1 - AS1 , long non - coding RNA , inhibits proliferation in myeloid malignancy. *J Cell Mol Med* (2019) 23(4):3021–5. doi: 10.1111/jcmm.14152
14. Cardamone G, Paraboschi EM, Soldà G, Cantoni C, Supino D, Piccio L. Not only cancer: the long non-coding RNA MALAT1 affects the repertoire of alternatively spliced transcripts and circular RNAs in multiple sclerosis. *Hum Mol Genet* (2019) 28(9):1414–28. doi: 10.1093/hmg/ddy438
15. Khalil AM, Guttman M, Huarte M, Garber M, Raj A, Rivea Morales D, et al. Many human large intergenic noncoding RNAs associate with chromatin-modifying complexes and affect gene expression. *Proc Natl Acad Sci U States America* (2009) 106(28):11667–72. doi: 10.1073/pnas.0904715106
16. Ng S, Johnson R, Stanton LW. Human long non-coding RNAs promote by association with chromatin modifiers and transcription factors. *EMBO J* (2011) 31(3):522–33. doi: 10.1038/emboj.2011.459
17. Tripathi V, Ellis JD, Shen Z, Song DY, Pan Q, Watt AT, et al. The Nuclear-Retained Noncoding RNA MALAT1 Regulates Alternative Splicing by Modulating SR Splicing Factor Phosphorylation. *Mol Cell* (2010) 39(6):925–38. doi: 10.1016/j.molcel.2010.08.011
18. Du Z, Sun T, Hacisuleyman E, Fei T, Wang X, Brown M, et al. Integrative analyses reveal a long noncoding RNA-mediated sponge regulatory network in prostate cancer. *Nat Commun* (2016) 7:10982. doi: 10.1038/ncomms10982
19. Baratti MO, Moreira YB, Traina F, Costa FF, Verjovski-Almeida S, Olalla-Saad ST. Identification of protein-coding and non-coding RNA expression profiles in CD34+and in stromal cells in refractory anemia with ringed sideroblasts. *BMC Med Genomics* (2010) 3(30):1–15. doi: 10.1186/1755-8794-3-30
20. Tominaga H, Ishiyama M, Ohseto F, Sasamoto K. A water-soluble tetrazolium salt useful for colorimetric cell viability assay. *Analyt Commun* (1999) 36):47–50. doi: 10.1039/a809656b
21. Nakaya HII, Amaral PP, Louro R, Lopes A, Fachel AA, Moreira YB, et al. Genome mapping and expression analyses of human intronic noncoding RNAs reveal tissue-specific patterns and enrichment in genes related to regulation of transcription. *Genome Biol* (2007) 8(3):R43. doi: 10.1186/gb-2007-8-3-r43
22. Okunola HL, Krainer AR. Cooperative-Binding and Splicing-Repressive Properties of hnRNP A1. *Mol Cell Biol* (2009) 29(20):5620–31. doi: 10.1128/MCB.01678-08
23. Glinka M, Herrmann T, Funk N, Havlicek S, Rossoll W. The heterogeneous nuclear ribonucleoprotein-R is necessary for axonal b -actin mRNA translocation in spinal motor neurons. *Hum Mol Genet* (2010) 19 (10):1951–66. doi: 10.1093/hmg/ddq073
24. Matveeva EA, Tinawi QMH, Rouchka EC, Fondufe-Mittendorf YN. Coupling of PARP1 – mediated chromatin structural changes to transcriptional RNA polymerase II elongation and cotranscriptional splicing. *Epigenet Chromatin* (2019) 12(15):1–18. doi: 10.1186/s13072-019-0261-1
25. Matveeva E, Maiorano J, Zhang Q, Eteleeb AM, Convertini P, Chen J, et al. Involvement of PARP1 in the regulation of alternative splicing. *Cell Discovery* (2016) 2:1–19. doi: 10.1038/celldisc.2015.46
26. Crews LA, Balaian L, De los Santos NP, Leu HS, C.Court A, Lazzari E, et al. RNA splicing modulation selectively impairs leukemia stem cell maintenance in secondary human AML. *Cell Stem Cell* (2017) 19(5):599–612. doi: 10.1002/jmri.25711.PET/MRI
27. Wang L, Lawrence MS, Wan Y, Stojanov P, Sougnez C, Stevenson K, et al. SF3B1 and Other Novel Cancer Genes in Chronic Lymphocytic Leukemia. *New Engl J Med* (2011) 365(26):2497–506. doi: 10.1056/nejmoa1109016
28. Tang CW, Maya-mendoza A, Martin C, Zeng K, Chen S, Feret D, et al. The integrity of a lamin-B1-dependent nucleoskeleton is a fundamental determinant of RNA synthesis in human cells. *J Cell Sci* (2008) 121:1014–24. doi: 10.1242/jcs.020982
29. Shimi T, Butin-israeli V, Adam SA, Hamanaka RB, Goldman AE, Lucas CA, et al. The role of nuclear lamin B1 in cell proliferation and senescence. *Genes Dev* (2011) 25(24):2579–93. doi: 10.1101/gad.179515.111.polymerase
30. Boudreaux SP, Duren RP, Call SG, Nguyen L, Freire PR, Narayanan P, et al. Drug targeting of NR4A nuclear receptors for treatment of acute myeloid leukemia. *Leukemia* (2018) 33 (1):22–4. doi: 10.1038/s41375-018-0174-1
31. Löwenberg B, Downing JR, Burnett A. Acute myeloid leukemia. *New Engl J Med* (1999) 341(14):1051–62. doi: 10.1056/NEJM199909303411407
32. König J, Zarnack K, Rot G, Curk T, Kayikci M, Zupan B. iCLIP reveals the function of hnRNP particles in splicing at individual nucleotide resolution. *Nat Struct Mol Biol* (2010) 17(7):909–15. doi: 10.1038/nsmb.1838.iCLIP
33. Michelotti EF, Michelotti GA, Aronsohn AII, Levens D. Heterogeneous Nuclear Ribonucleoprotein K Is a Transcription Factor. *Mol Cell Biol* (1996) 16(5):2350–60. doi: 10.1128/MCB.16.5.2350
34. Lemieux B, Blanchette M, Monette A, Mouland AJ, Wellinger RJ, Chabot B. A Function for the hnRNP A1 / A2 Proteins in Transcription Elongation. *PloS One* (2015) 10(5):1–20. doi: 10.1371/journal.pone.0126654
35. Lai C, Huang Y, Lee J, Tseng JT, Chang K, Chen Y, et al. Translational upregulation of Aurora-A by hnRNP Q1 contributes to cell proliferation and tumorigenesis in colorectal cancer. *Cell Death Dis* (2017) 8:1–12. doi: 10.1038/cddis.2016.479
36. Kim MK, Nikodem VM. hnRNP U Inhibits Carboxy-Terminal Domain Phosphorylation by TFIIH and Represses RNA Polymerase II Elongation. *Mol Celullar Biol* (1999) 19(10):6833–44. doi: 10.1128/MCB.19.10.6833
37. Gallardo M, Lee HJ, Zhang X, Bueso-ramos C, Pageon LR, Mcarthur M, et al. hnRNP K is a haploinsufficient tumor suppressor that regulates proliferation and differentiation programs in hematologic malignancies. *Cancer Cell* (2016) 28(4):486–99. doi: 10.1016/j.ccell.2015.09.001.hnRNP
38. Vance KW, Sansom SN, Lee S, Chalei V, Kong L, Cooper SE, et al. The long non-coding RNA Paupar regulates the expression of both local and distal genes. *EMBO J* (2014) 33(4):296–311. doi: 10.1002/embj.201386225
39. Beltran M, Aparicio-Prat E, Mazzolini R, Millanes-Romero A, Massó P, Jenner RG, et al. Splicing of a non-coding antisense transcript controls LEF1 gene expression. *Nucleic Acids Res* (2015) 43(12):5785–97. doi: 10.1093/nar/gkv502
40. Holdt LM, Hoffmann S, Sass K, Langenberger D, Scholz M, Krohn K, et al. … Alu Elements in ANRIL Non-Coding RNA at Chromosome 9p21 Modulate Atherogenic Cell Functions through Trans-Regulation of Gene Networks. *PloS Genet* (2013) 9(7):1–12. doi: 10.1371/journal.pgen.1003588
41. Johnsson P, Ackley A, Vidarsdottir L, Lui W, Grandér D, Morris KV. A pseudogene long noncoding RNA network regulates PTEN transcription and translation in human cells. *Nat Struct Mol Biol* (2013) 20(4):440–6. doi: 10.1038/nsmb.2516.A
42. Guttman M, Donaghey J, Carey BW, Garber M, Grenier JK, Munson G, et al. lincRNAs act in the circuitry controlling pluripotency and differentiation. *Nature* (2011) 477:295–300. doi: 10.1038/nature10398
43. Rinn J, Guttman M, Rinn JL. Modular regulatory principles of large non-coding RNAs. *Nature* 482 (2012), 339–46. doi: 10.1038/nature10887
44. Zhao Y, Nomiyama T, Findeisen HM, Qing H, Aono J, Jones KL, Bruemmer D. Epigenetic regulation of the NR4A orphan nuclear receptor NOR1 by histone acetylation. *FEBS Lett* (2014) 588(24):4825–30. doi: 10.1016/j.febslet.2014.11.017

Conflict of Interest: The authors declare that the research was conducted in the absence of any commercial or financial relationships that could be construed as a potential conflict of interest.

frontiers in Oncology

ORIGINAL RESEARCH
published: 18 March 2021
doi: 10.3389/fonc.2021.643163

The Long Non-coding RNA TMPO-AS1 Promotes Bladder Cancer Growth and Progression *via* OTUB1-Induced E2F1 Deubiquitination

*Yeyu Zhang[1], Yuxing Zhu[1], Mengqing Xiao[1], Yaxin Cheng[1], Dong He[2], Jianye Liu[3], Liang Xiang[1], Lian Gong[1], Zhanwang Wang[1], Liping Deng[1] and Ke Cao[1]**

[1] Department of Oncology, The Third Xiangya Hospital of Central South University, Changsha, China, [2] Department of Respiratory, The Second People's Hospital of Hunan Province, Changsha, China, [3] Department of Urology, The Third Xiangya Hospital of Central South University, Changsha, China

OPEN ACCESS

Edited by:
Chien-Feng Li,
National Health Research Institutes, Taiwan

Reviewed by:
Wei-Ming Li,
Kaohsiung Medical University, Taiwan
Wanshan Li,
Chi Mei Medical Center, Taiwan
Hong-Yue Lai,
Chi Mei Medical Center, Taiwan

***Correspondence:**
Ke Cao
csucaoke@163.com

Specialty section:
This article was submitted to Molecular and Cellular Oncology, a section of the journal Frontiers in Oncology

Received: *17 December 2020*
Accepted: *08 February 2021*
Published: *18 March 2021*

Citation:
Zhang Y, Zhu Y, Xiao M, Cheng Y, He D, Liu J, Xiang L, Gong L, Wang Z, Deng L and Cao K (2021) The Long Non-coding RNA TMPO-AS1 Promotes Bladder Cancer Growth and Progression via OTUB1-Induced E2F1 Deubiquitination. Front. Oncol. 11:643163. doi: 10.3389/fonc.2021.643163

Background: Increasing evidence indicates that long non-coding RNAs (lncRNAs) play crucial roles in cancer tumorigenesis and progression. TMPO antisense RNA 1 (TMPO-AS1) has been found to be involved in several cancers by acting as a competing endogenous RNA. However, the potential roles of TMPO-AS1 in bladder cancer (BC) and the potential interactions with proteins remain poorly understood.

Methods: The expression of the lncRNA TMPO-AS1 was evaluated *via* bioinformatic analysis and further validated by quantitative real-time PCR (qRT-PCR). Loss- and gain-of-function assays were performed to determine the biological functions of TMPO-AS1 in BC cell proliferation, migration, and invasion. Moreover, chromatin immunoprecipitation, Western blotting, and fluorescence *in situ* hybridization, as well as RNA pull-down, RNA immunoprecipitation, and luciferase reporter assays, were conducted to explore the upstream and downstream molecules interacting with TMPO-AS1.

Results: TMPO-AS1 is upregulated in BC. Functional experiments demonstrated that TMPO-AS1 promotes cell proliferation, migration, and invasion in BC and inhibits cell apoptosis *in vivo* and *in vitro*. Mechanically, E2F1 is responsible for TMPO-AS1 upregulation. Additionally, TMPO-AS1 facilitates the interaction of E2F1 with OTU domain-containing ubiquitin aldehyde binding 1 (OTUB1), leading to E2F1 deubiquitination and stabilization; therefore, TMPO-AS1 promotes BC malignant phenotypes. Furthermore, rescue experiments showed that TMPO-AS1 promotes BC growth in an E2F1-dependent manner.

Conclusions: Our study is the first to uncover the novel TMPO-AS1/E2F1 positive regulatory loop important for the promotion of BC malignant behaviors. The TMPO-AS1/E2F1 loop should be considered in the quest for new BC therapeutic options.

Keywords: long non-coding RNA, bladder cancer, TMPO-AS1, E2F1, OTUB1

INTRODUCTION

Bladder cancer (BC) is the most common malignant tumor of the urinary system worldwide (1); about 549,393 new cases and 199,922 cancer-related deaths were reported in 2018 (2). The majority of BC cases are urothelial cell carcinomas. Of note, urothelial BC can be categorized into non-muscle-invasive BC (NMIBC) and muscle-invasive BC (MIBC). Approximately 75% of patients with BC exhibit NMIBC with high recurrence and progression, while the remaining 25% of patients with BC present with MIBC and have a poor prognosis (3). Although therapies, including transurethral resection, cystectomy, chemotherapy, radiation, and immunotherapy, have contributed to the reduction of BC-associated morbidity/mortality, the 5-years survival rate of patients with BC have hardly improved (4). Therefore, it is urgent to explore the molecular mechanisms and biomarkers of BC to develop better diagnostic, monitoring, and therapeutic approaches and reduce the disease burden.

Long non-coding RNAs (lncRNAs) are a class of non-coding RNAs longer than 200 nucleotides with limited protein-coding potential (5). LncRNAs are known to influence several biological and pathological processes, such as cell proliferation, metastasis, drug resistance, and metabolism and are involved in multiple diseases, particularly in cancer (6–8). Previous studies have suggested that numerous lncRNAs are involved in BC (9). Recent studies have demonstrated that TMPO antisense RNA 1 (TMPO-AS1) serves as a competing endogenous RNA to sponge microRNAs (miRNAs) in multiple carcinomas, including hepatocellular carcinoma, thyroid cancer, lung adenocarcinoma, and breast cancer (10–13). However, whether TMPO-AS1 interacts with other molecules and plays a role in BC is still unknown.

Besides regulating the transcription of mRNAs, transcription factors (TFs) are also involved in the regulation of the transcription of lncRNAs (14). E2F1, a member of the E2F transcription factor family consisting of eight proteins, is a transcription activator essential for the regulation of cell cycle, apoptosis, cell proliferation, and DNA damage response (15). Studies have demonstrated that E2F1 can modulate the expression of lncRNAs (16). However, little is known on the E2F1-mediated regulation of lncRNAs in BC. Of note, the stabilization of TFs can be modulated by ubiquitination and deubiquitination (17). However, no lncRNAs have been linked to E2F1 deubiquitination.

Here, we focus on the roles of TMPO-AS1 in BC carcinogenesis and investigate the protein upstream and downstream of TMPO-AS1. We demonstrate that E2F1 activates the transcription of TMPO-AS1, which, in turn, facilitates the interaction of E2F1 with OTU domain-containing ubiquitin aldehyde binding 1 (OTUB1), a deubiquitinase; consequently, the E2F1 protein levels are increased *via* stabilization, promoting BC malignant phenotypes. Therefore, the TMPO-AS1/E2F1 positive feedback loop should be considered as a novel target for the treatment of BC.

MATERIALS AND METHODS

Bioinformatic Analysis

The expression data on lncRNA TMPO-AS1 in 33 types of human cancers were obtained from the Gene Expression Display Server GEDS (http://bioinfo.life.hust.edu.cn/web/GEDS/) (18). The expression of TMPO-AS1 in BC tissues and in normal tissues was analyzed using The Cancer Genome Atlas (TCGA) BLCA RNA-seq data retrieved from the UCSC XENA (https://xena.ucsc.edu), TANRIC (https://ibl.mdanderson.org/tanric/_design/basic/analysis.html) (19), and Gene Expression Omnibus (GEO, www.ncbi.nlm.nih.gov, GSE133624 and GSE120736 datasets) databases. The prognostic value of TMPO-AS1 was evaluated using GEPIA 2 (http://gepia2.cancer-pku.cn/#index). Additionally, hTFtarget (http://bioinfo.life.hust.edu.cn/hTFtarget#!/) and ChIPBase v2.0 (http://rna.sysu.edu.cn/chipbase/index.php) were used to find out the potential TFs of TMPO-AS1 (20, 21). The JASPAR (http://jaspar.genereg.net) 2018 database was used to identify the E2F1-TMPO-AS1 binding profile (22). Genes co-expressed with TMPO-AS1 (TCGA-BLCA dataset) were defined as those with the correlation coefficients $\geq$0.6 and p-values $<$0.01 using Co-LncRNA (http://bio-bigdata.hrbmu.edu.cn/Co-LncRNA/). (23). A pathway enrichment analysis was conducted using Metascape (https://metascape.org/gp/index.html#/main/step1) (24). The interactions between E2F1, OTUB1, and TMPO-AS1 were predicted *via* Agostini et al. introduced catRAPID (http://s.tartaglialab.com/page/catrapid_group), a server to identify the interaction of RNA and protein (25) and Tuvshinjargal et al. developed a web server named PRIdictor (http://bclab.inha.ac.kr/pridictor) to reveal mutual binding in protein and RNA (26). Additionally, the protein interactions between E2F1 and OTUB1 were predicted using HDOCK (http://hdock.phys.hust.edu.cn) (27). Last but not least, the ubiquitination sites of E2F1 were predicted using UbPred (http://www.ubpred.org) (28).

Clinical Samples

Resected BC and normal adjacent specimens were collected from patients with BC admitted to the Third Xiangya Hospital, Central South University, Hunan, China, from 2016 to 2018; all patients provided written informed consent. Six pairs of BC and paired adjacent normal tissues were stored in liquid nitrogen at −80°C. This study was approved by the ethics committee of the Third Xiangya Hospital, Central South University, Hunan, China.

Cell Culture and Treatments

The human BC cell lines, namely 5637, T24, and RT4, were obtained from American Type Culture Collection (ATCC; Rockville, MD, USA). BIU87 and EJ were purchased from the Advanced Research Center of Central South University (Changsha, China). Cells were cultured in Dulbecco's modified Eagle's medium (DMEM; Invitrogen, Carlsbad, CA, USA) containing 10% fetal bovine serum (FBS; Gibco, Thermo Fisher Scientific, Waltham, MA, USA), 1 mmol/L glutamine, and 100 U/ml penicillin at 37°C in an incubator with 5% CO_2. The protein synthesis inhibitor cycloheximide (10 μg/ml, C1998; Millipore, Sigma-Aldrich, St Louis, MO, USA) and

TABLE 1 | Primers used for qRT-PCR, siRNAs oligonucleotides, shRNA oligonucleotides and ChIP.

Primers used for qRT-PCR	
TMPO-AS1-F	AGAGCCGAACTACGAACCAA
TMPO-AS1-R	CTGTCCCTTATCGGCGTCT
E2F1-F	ACGTGACGTGTCAGGACCT
E2F1-R	GATCGGGCCTTGTTTGCTCTT
β-actin-F	CATGTACGTTGCTATCCAGGC
β-actin-R	CTCCTTAATGTCACGCACGAT
U1-F	GGGAGATACCATGATCACGAAGGT
U1-R	CCACAAATTATGCAGTCGAGTTTCCC
siRNAs oligonucleotides	
TMPO-AS1-F	GAGCCGAACUACGAACCAACU
TMPO-AS1-R	UUGGUUCGUAGUUCGGCUCUG
E2F1-F	ACCUCUUCGACUGUGACUUUG
OTUB1-F	AGCGACUCCGAAGGUGUUAAC
OTUB1-R	GUUAACACCUUCGGAGUCGCU
Negative control-F	UUCUCCGAACGUGUCACGUTT
Negative control-R	ACGUGACACGUUCGGAGAATT
shRNA oligonucleotides	
TMPO-AS1-F	GAGCCGAACTACGAACCAACT
TMPO-AS1-R	TTGGTTCGTAGTTCGGCTCTG
ChIP	
TMPO-AS1-F	CAACAAGTGCGACACTCCAT
TMPO-AS1-R	GTGTGGAGGGCTTTTTGAAC
GAPDH-F	TACTAGCGGTTTTACGGGCG
GAPDH-R	TCGAACAGGAGGAGCAGAGAGCGA

BC, bladder cancer; lncRNAs, long non-coding RNAs; TMPO-AS1, TMPO antisense RNA 1; E2F1, E2F transcription factor 1; OTUB1, OTU domain-containing ubiquitin aldehyde binding 1; NMIBC, non-muscle-invasive bladder cancer; MIBC, muscle-invasive bladder cancer; miRNA, microRNA; TF, transcription factor; TCGA, The Cancer Genome Atlas; ChIP, chromatin immunoprecipitation; FISH, fluorescence in situ hybridization; IHC, immunohistochemistry; qRT-PCR, quantitative real-time PCR; RIP, RNA immunoprecipitation; Co-IP, co-immunoprecipitation.

proteasome inhibitor MG132 (20 μM, S2619; Selleck, Houston, TX, USA) were used to examine the ubiquitin proteasome-related protein degradation.

Quantitative Real-Time PCR

Total RNA was extracted from BC tumor tissues, the paired adjacent normal tissues, and BC cells (T24 and RT4) using TRIzol (Invitrogen, Carlsbad, CA, USA) according to the instructions in the PrimeScript RT Reagent Kit (TaKaRa, Dalian, China). The quantitative real-time PCR (qRT-PCR) was performed using the SYBR Green PCR Master Mix (Toyobo, Osaka, Japan) as per the instructions of the manufacturer. The relative expression of genes was determined using the $2^{-\Delta\Delta CT}$ method, and the expression was normalized to that of β-actin. All experiments were performed in triplicate. The primer sequences used in this study are listed in **Table 1**.

Cell Transfection

For *in vitro* functional assays, TMPO-AS1, E2F1, and OTUB1 overexpression plasmids and small interfering RNAs, as well as the empty vectors, were designed by GeneChem Co., Ltd (Shanghai, China) and transfected into T24 and RT4 cells using the Lipofectamine 3000 Reagent (Invitrogen, Carlsbad, CA, USA). For *in vivo* xenograft experiments, RT4 cells were stably transfected with empty lentiviral vectors, sh-TMPO-AS1 (designed according to the sequence of si-TMPO-AS1) or sh-TMPO-AS1, together with E2F1 overexpressing lentiviral vectors purchased from GeneChem Co., Ltd. (Shanghai, China) according to the protocol of the manufacturer. The empty vectors were used as the negative control. The transfection efficiency was determined *via* qRT-PCR.

Methyl Thiazolyl Tetrazolium Assay

The methyl thiazolyl tetrazolium (MTT) assay was conducted according to the instructions of the manufacturer. Briefly, the BC cells were plated into 96-well plates at a density of 1×10^4 cells/well and incubated for 24 h. Later, 10 μl of the MTT Solution (Sigma Chemicals, St. Louis, MO, USA) was added to each well, and the cells were cultured at 37°C for 4 h. Furthermore, cell viability/proliferation was estimated *via* the measurement of the absorbance at 570 nm with the Epoch Microplate Spectrophotometer (BioTek Instruments Inc., Winooski, VT, USA).

Colony Formation Assay

The colony formation assay was performed as previously described in a study of Zeng et al. (29). Briefly, T24 and RT4 cells, treated as described in the abovementioned study, were seeded into 6-well plates at a density of 1,000 cells/well and cultured for 2–3 weeks. Then, the cells were washed with FBS, fixed with 4% paraformaldehyde, stained with 1% crystal violet, and counted. Only colonies with more than 50 cells were considered.

Cell Apoptosis Analysis

The cell apoptosis in BC cells (T24 and RT4 cells) was investigated *via* flow cytometry using the Annexin V-PE/7-AAD Kit (KA3809; Abnova, Wuhan, China) according to the protocol of the manufacturer.

Wound Healing Assay

The wound healing assay was conducted as previously described (30). Briefly, cells were seeded into 6-well plates at a density of 1×10^5 cells/well. Then, a sterile 200 μl pipette tip was used to scratch a straight line in the cell monolayer. Later, the cells were washed with FBS and cultured for 48 h. The scratch width was measured 48 h later.

Transwell Assay

The transwell assay was conducted to evaluate cell migration and invasion. Briefly, 5×10^4 BC cells (T24 and RT4) were suspended in the serum-free medium and seeded into the upper chamber of the Transwell Plates (8 μm pore; Corning, Corning, NY, USA) with Matrigel (BD Biosciences, San Jose, CA, USA), while the complete medium with 10% FBS was added to the lower chamber. After a 48-h incubation, the migrating cells were fixed with 4% paraformaldehyde, stained with 0.1% crystal violet (Sigma-Aldrich, St. Louis, MO, USA), and photographed under a microscope (DMB5-2231P1, DMB HK Ltd., Hong Kong, China).

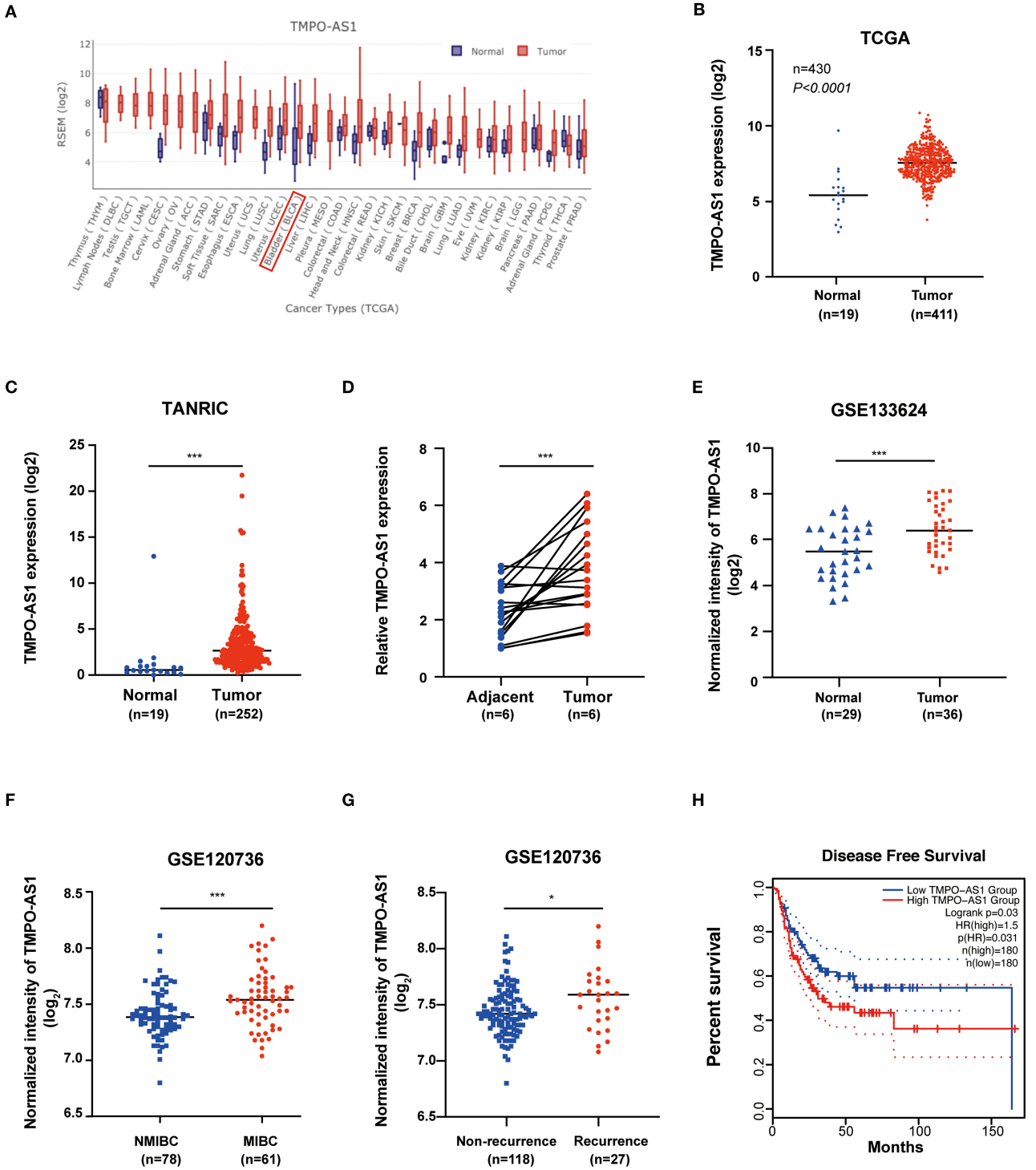

FIGURE 1 | TMPO antisense RNA 1 (TMPO-AS1) is upregulated in bladder cancer (BC) tissues. **(A)** TMPO-AS1 is highly expressed in the majority of cancers according to the Gene Expression Display Server (GEDS). **(B,C)** The expression of TMPO-AS1 in BC vs. normal tissues was verified in data retrieved from TCGA and the TANRIC databases. **(D)** Quantitative real-time PCR (qRT-PCR) was conducted to validate the expression of TMPO-AS1 in six pairs of BC tissues and adjacent normal tissues collected in this study (replicates = 3). **(E–G)** The expression profile of TMPO-AS1 in BC as per two datasets retrieved for the GEO database: GSE133624 and GSE120736. **(H)** The disease-free survival curve shows that high levels of TMPO-AS1 expression are associated with poor prognosis of patients with BC (GEPIA). $^{*}p < 0.05$, $^{***}p < 0.001$.

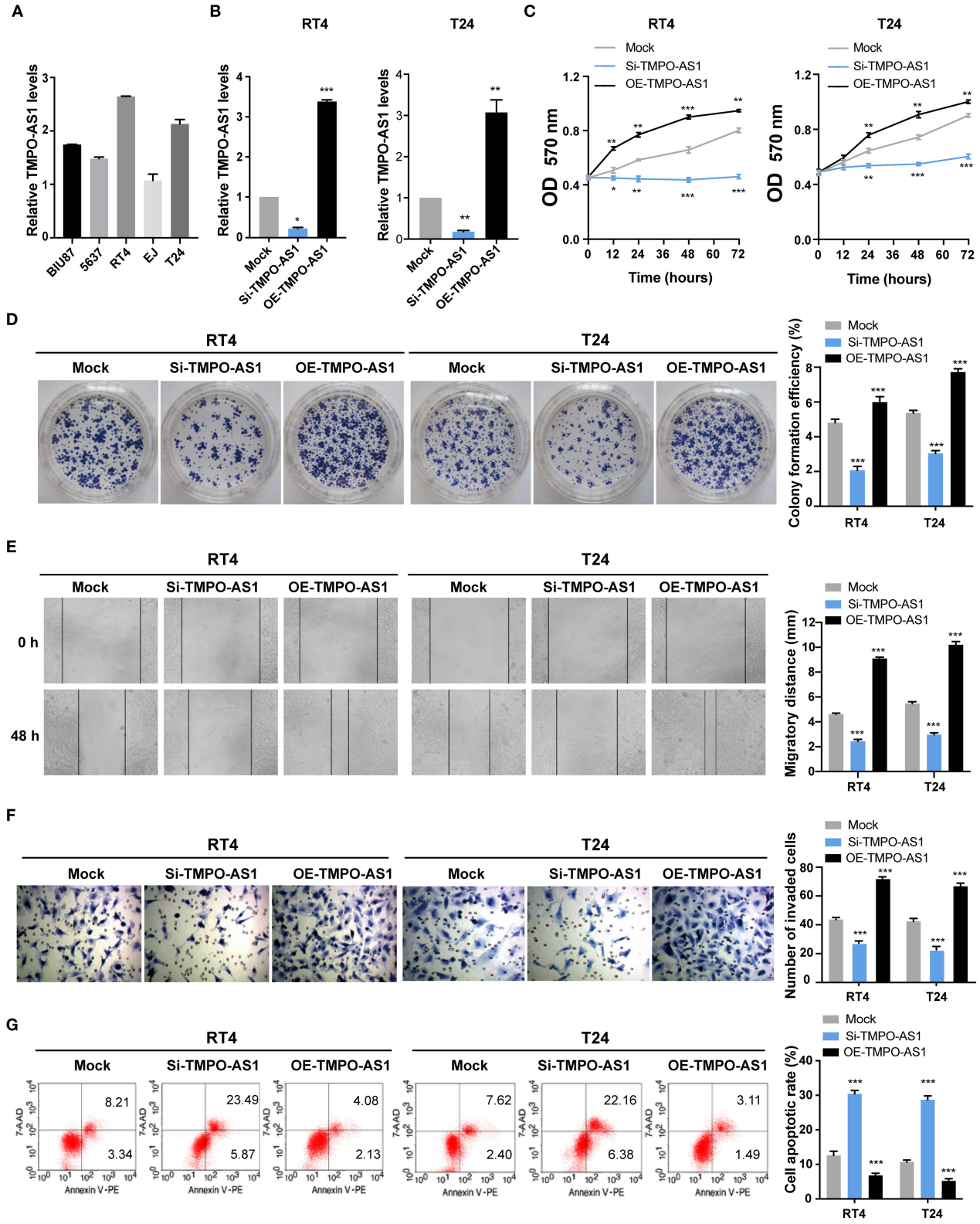

FIGURE 2 | TMPO-AS1 promotes the proliferation, migration, invasion, and survival of BC cells *in vitro*. **(A)** The qRT-PCR show the mRNA levels of TMPO-AS1 in five BC cell lines (BIU87, 5637, T24, EJ, and RT4). **(B)** The efficiencies of TMPO-AS1 knockdown or overexpression in RT4 and T24 cells were examined by qRT-PCR.

(Continued)

FIGURE 2 | Mock, the negative control; Si-TMPO-AS1, siRNA targeting TMPO-AS1; OE-TMPO-AS1, ectopic expression of TMPO-AS1. **(C,D)** The effect of TMPO-AS1 knockdown and overexpression on the cell proliferation was measured using methyl thiazolyl tetrazolium (MTT) and colony formation assays. **(E,F)** The effect of TMPO-AS1 knockdown or overexpression on the migration and invasion of RT4 and T24 cells was evaluated *via* wound healing and transwell assays. **(G)** Cell apoptosis was analyzed by flow cytometry in TMPO-AS1 knockout or overexpressing RT4 and T24 cells, stained with Annexin V-PE/7-AAD. Error bars represent the mean ± SD from three independent experiments. $*p < 0.05$, $**p < 0.01$, $***p < 0.001$.

Western Blotting

Total proteins were extracted using the radioimmunoprecipitation assay (RIPA) buffer (Beyotime Biotechnology Inc., Shanghai, China) with the Protease Inhibitor Cocktail (Roche, Basel, Switzerland). The protein concentration was measured using a bicinchoninic acid (BCA) kit (Thermo Fisher Scientific, Waltham, MA, USA). The protein samples were resolved *via* sodium dodecyl sulfate polyacrylamide gel electrophoresis (SDS-PAGE) and transferred onto polyvinylidene fluoride (PVDF) membranes. Later, the membranes were blocked in *phosphate-buffered saline* (PBS) containing 5% skim milk powder at room temperature for 1 h and incubated with the primary antibodies at 4°C overnight, followed by the secondary antibodies. The protein bands were visualized using the Pierce® ECL Western Blotting Substrate Kit (32106; Thermo Fisher Scientific, Waltham, MA, USA) and normalized to the levels of β-actin as reference. The antibodies used in this study are listed in **Supplementary Table 1**.

Luciferase Reporter Assay

Wild-type or mutant sequences of the E2F1 binding sites for the promoter of TMPO-AS1 were synthesized and inserted into the pGL3 vector (Promega, Madison, WI, USA). T24 and RT4 cells were seeded into 48-well plates and cotransfected with the above vectors along with E2F1 expression or control plasmids. About 48 h later, the luciferase activity was measured and analyzed using the Luciferase Reporter Assay System (Promega, Madison, WI, USA).

Chromatin Immunoprecipitation Assay

The chromatin immunoprecipitation (ChIP) was performed using the EZ Magna ChIP™ Kit (Millipore, Burlington, MA, USA) according to the instructions of the manufacturer. Briefly, 1×10^7 cells (T24 and RT4) were fixed with 1% formaldehyde and treated with 10% glycine. Later, the cross-linked chromatin was broken into small DNA fragments *via* sonication. The sonicated DNA was immunoprecipitated using antibodies against E2F1 or control rabbit immunoglobulin G (IgG) (Bioss Antibodies Inc., Woburn, MA, USA). qRT-PCR was performed to quantify the precipitated chromatin using the specific primers listed in **Table 1**.

RNA Pull-Down Assay

TMPO-AS1 was transcribed *in vitro* and labeled *via* 3′-end biotinylation. The RNA pull-down assay was performed using the Pierce™ Magnetic RNA-Protein Pull-Down Kit (Thermo Fisher Scientific, Waltham, MA, USA). Briefly, the lysates of control or TMPO-AS1 overexpressing T24 and RT4 cells were incubated with control or biotinylated TMPO-AS1 at room temperature for 4 h, followed by the addition of streptavidin magnetic beads (Thermo Fisher Scientific, Waltham, MA, USA) at 4°C for 60 min with rotation. After three washing steps with washing buffer, the RNA-binding proteins were eluted using 50 μl elution buffer and analyzed *via* Western blotting.

RNA Immunoprecipitation

RNA immunoprecipitation was performed using the EZ-Magna RIP™ RNA-Binding Protein Immunoprecipitation Kit (Millipore, Burlington, MA, USA) based on the instructions of the manufacturer. Briefly, cell extracts were incubated with magnetic beads conjugated with antibodies against SNRNP70 (Cat.# CS203216) and anti-E2F1 (Cat.# OM250777) or with normal rabbit IgG (Cat.# PP64B). Anti-SNRNP70 and normal rabbit IgG antibodies were used as positive and negative controls, respectively. The relative abundance of TMPO-AS1 was normalized to the amount of enriched U1snRNA *via* qRT-PCR.

Co-immunoprecipitation

Cell lysates were incubated with primary antibodies against E2F1 (1:80, OM250777; Omnimabs, Alhambra, CA, USA) at 4°C overnight. Rabbit IgG antibodies (1:150, Bioss Antibodies Inc., Woburn, MA, USA) were used as the negative control. Later, the cell lysates were mixed with the protein A/G agarose (Cat.# P1012, Beyotime Biotechnology Inc., Jiangsu, China) at 4°C for 2 h, followed by centrifugation and washing steps. The precipitated complex was separated using the SDS-PAGE and analyzed *via* a Western blotting.

Fluorescence *in situ* Hybridization

Fluorescence *in situ* hybridization (FISH) was performed using the Ribo™ Fluorescent *in situ* Hybridization Kit (RiboBio Co. Ltd., Guangzhou, China) following the instructions of the manufacturer. The TMPO-AS1 and 18S probes were synthesized and labeled with the Cy3 fluorescent dye. Fluorescence was detected under a Confocal Laser Microscope (SP5; Leica Microsystems, Wetzlar, Germany).

Immunohistochemistry

The tissue sections obtained from paraffin-embedded tissues were dewaxed in xylene and rehydrated in an ethanol gradient. Later, tissues were incubated in 1% hydrogen peroxide and boiled in citrate buffer (10 mM, pH = 6.0) for 15 min. Subsequently, tissues were incubated with the primary antibodies against Ki-67 (1:1,000, 27309-1-AP; Proteintech, Chicago, IL, USA), E2F1 (1:200, OM250777; Omnimabs, Alhambra, CA, USA), and caspase-3 (1:200, 19677-1-AP; Proteintech, Chicago, IL, USA) at 4°C overnight, followed by incubation with horseradish peroxidase (HRP)-conjugated goat anti-rabbit secondary antibody (SP-9000, zsbio, Beijing, China)

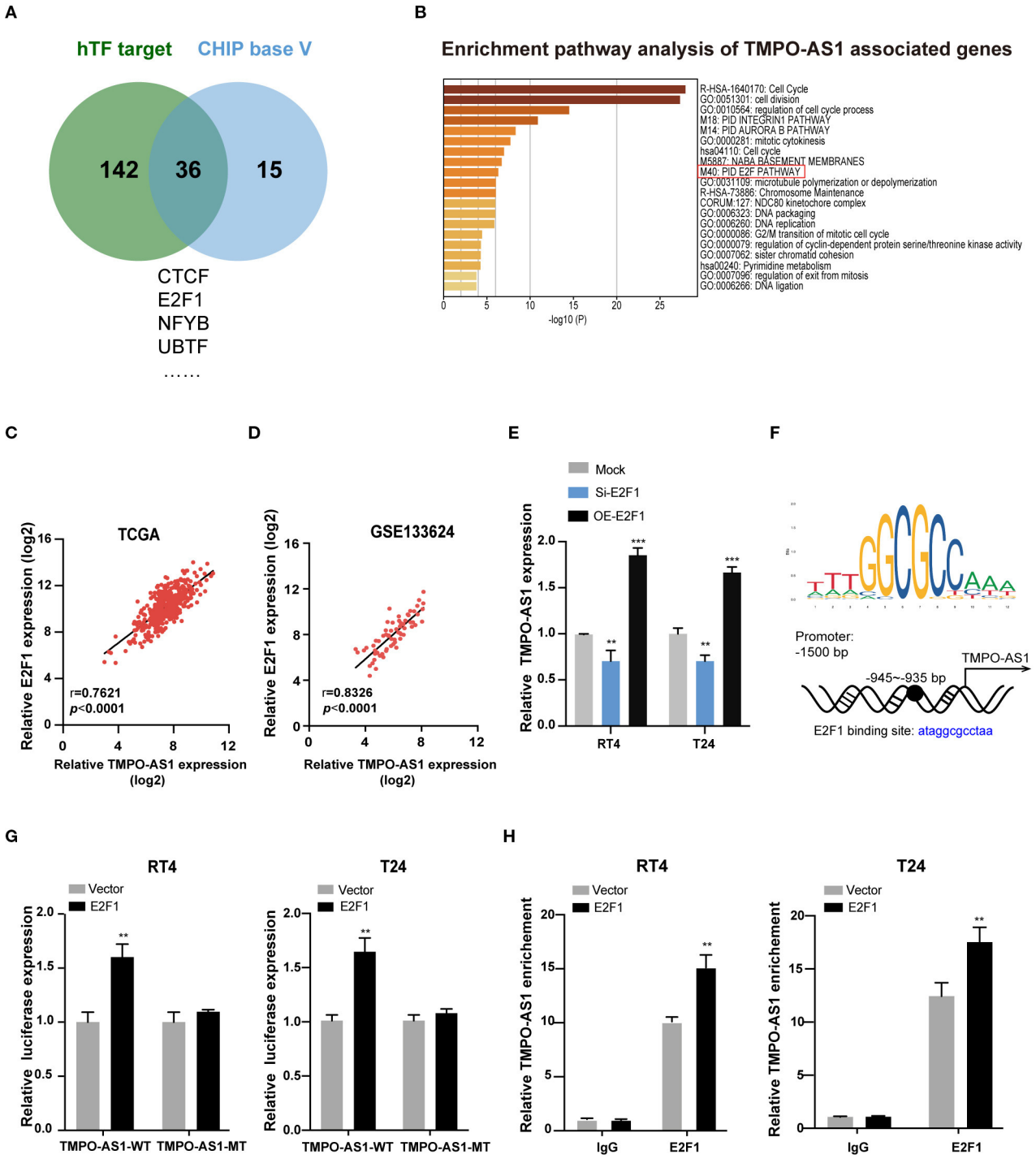

FIGURE 3 | E2F1 binds to the promoter of TMPO-AS1 and activates its transcription. **(A)** The potential transcription factors of TMPO-AS1 were predicted using the ChIPBase v2.0 and hTFtarget. **(B)** The pathway enrichment analysis of genes co-expressed with TMPO-AS1 was obtained using Metascape. **(C,D)** The correlation between TMPO-AS1 and E2F transcription factor 1 (E2F1) mRNA expression in BC tissues was assessed using the Pearson's correlation analysis in datasets retrieved from TCGA and the GEO (GSE133624) databases. **(E)** The expression of TMPO-AS1 was evaluated using qRT-PCR in E2F1 silenced or overexpressing RT4 and T24 cells. Mock, the negative control; Si-E2F1, siRNA targeting E2F1; OE-E2F1, ectopic expression of E2F1. **(F)** The binding sites between E2F1 and the TMPO-AS1 promoter region were predicted using JASPAR. **(G)** Luciferase reporter assays were conducted to measure the TMPO-AS1 promoter luciferase activity in RT4 and T24 cells overexpressing E2F1. Vector, the negative control. **(H)** The ChIP assay demonstrates the binding between E2F1 and the TMPO-AS1 promoter. Error bars represent the mean ± SD from three independent experiments. $^{**}p < 0.01$, $^{***}p < 0.001$.

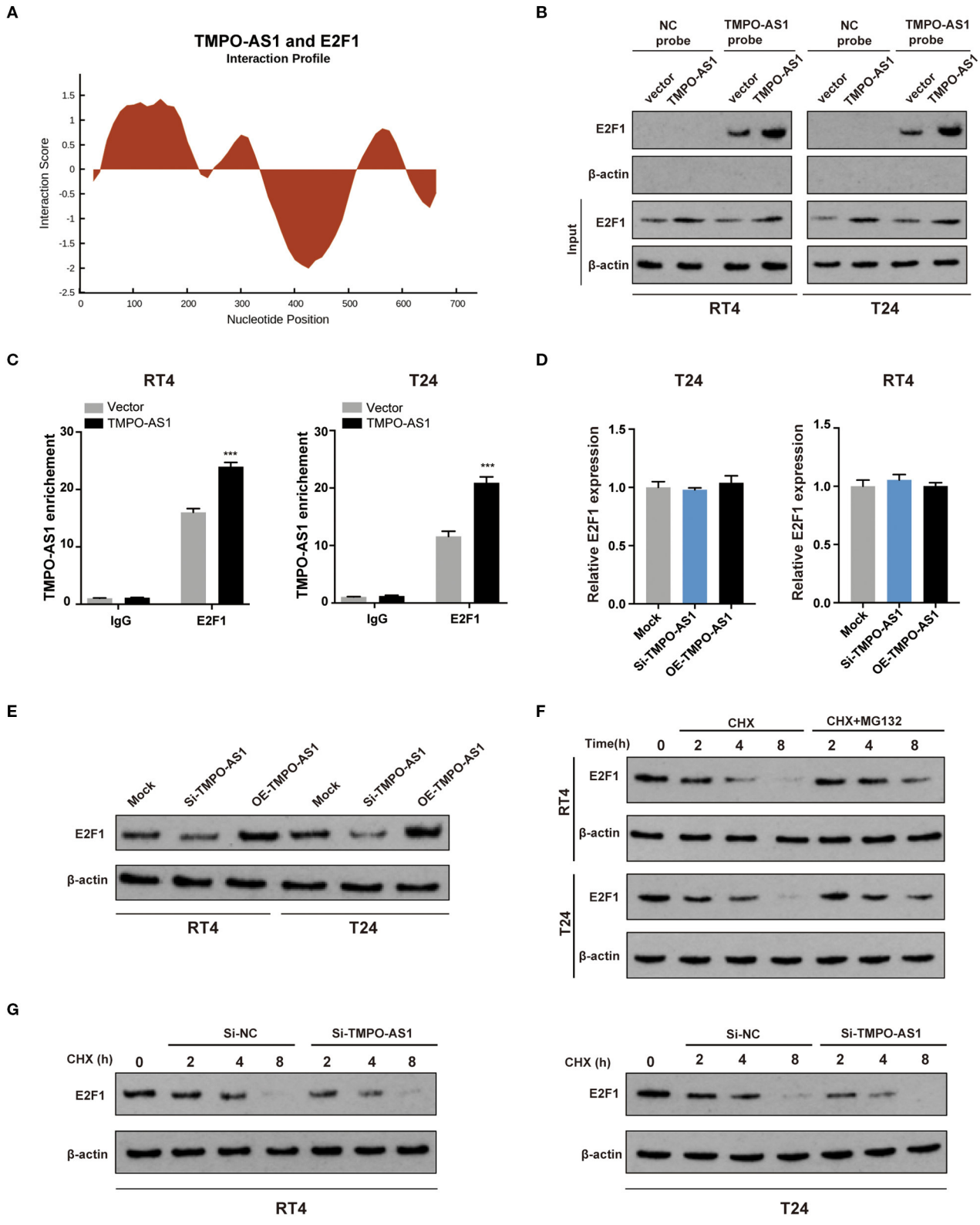

FIGURE 4 | TMPO-AS1 upregulates the protein levels of E2F1 *via* the promotion of protein stability. **(A)** The interaction between TMPO-AS1 and E2F1 was predicted using catRAPID. **(B)** An RNA pull-down assay was performed to validate the potential interaction between TMPO-AS1 and E2F1 in RT4 and T24 cells overexpressing

(Continued)

FIGURE 4 | TMPO-AS1. **(C)** A radioimmunoprecipitation assay (RIPA) was performed to further confirm the interaction between E2F1 and TMPO-AS1 in TMPO-AS1 overexpressing RT4 and T24 cells; immunoglobulin G (IgG) was used as the negative control. Error bars represent the mean ± SD from three independent experiments. **(D)** *E2F1* mRNA expression was assessed using qRT-PCR in TMPO-AS1 knockout or overexpressing BC cells. **(E)** The E2F1 protein expression was evaluated *via* Western blotting in TMPO-AS1 knockout or overexpressing RT4 and T24 cells. **(F)** Western blotting show that the proteasome inhibitor MG132 protein increased the stability of E2F1 in cycloheximide-treated RT4 and T24 cells. **(G)** Western blotting showing the decreased E2F1 stability in TMPO-AS1 knockdown RT4 and T24 cells. CHX, cycloheximide. ***$p < 0.001$.

at room temperature for 30 min. Diaminobenzidine was used as chromogen; hematoxylin was used as the nuclear counterstain.

Xenograft Mouse Model

All animal experiments were approved by the Animal Care and Use Committee of the Central South University. The 1×10^6 RT4 cells transfected with empty vector, sh-TMPO-AS1, or sh-TMPO-AS1 together with E2F1-expressing lentiviral vectors were injected subcutaneously into the flanks of 4- to 6-week-old male BALB/c nude mice ($n = 4$ per group) obtained from the Shanghai Experimental Laboratory Animal Center (Shanghai, China). Tumor volumes were measured every 3 days and calculated as follows: tumor volume $= (D \times d^2)/2$, where D and d refer to the longest and shorter diameters, respectively. Mice were euthanized after 25 days.

Statistical Analysis

All statistical analyses were performed using the GraphPad Prism Software, Version 8 (GraphPad Software, San Diego, CA, USA). Data are presented as the mean ± SD of at least three independent experiments. The relationship between E2F1 and TMPO-AS1 was analyzed using the Pearson's correlation coefficient. Significant differences were analyzed using the Student's *t*-test or the one-way ANOVA. Values of $p < 0.05$ were considered statistically significant.

RESULTS

TMPO-AS1 Is Upregulated in Bc Tissues

To evaluate the expression of TMPO-AS1 in tumor and normal tissues, we used the online database GEDS; interestingly, we found that TMPO-AS1 is upregulated in multiple tumor tissues vs. normal tissues (**Figure 1A**). Consistently, the expression of TMPO-AS1 was upregulated in BC tissues compared with the normal tissues according to TCGA (**Figure 1B**) and TANRIC databases (**Figure 1C**). We further confirmed that the expression of TMPO-AS1 was higher in six BC tissues compared with that in the corresponding normal tissues *via* qRT-PCR (**Figure 1D**). Moreover, the integrative analysis of GSE133624 and GSE120736 showed that TMPO-AS1 was not only highly expressed in BC tissues (**Figure 1E**) but also exhibited higher levels in MIBC vs. NMIBC samples (**Figure 1F**). Of note, the higher expression of TMPO-AS1 was associated with the recurrence of BC (**Figure 1G**) and the advanced tumor stage (**Supplementary Figure 1A**). Furthermore, patients with BC of higher TMPO-AS1 expression levels were associated with shorter disease-free survival times (**Figure 1H**). Taken together, these data suggest that TMPO-AS1 is highly expressed in BC tissues, and it may serve as a potential prognostic biomarker in patients with BC.

TMPO-AS1 Promotes the Proliferation, Migration, Invasion, and Survival of BC Cells *in vitro*

Since the expression of TMPO-AS1 was the highest in T24 and RT4 cells among five BC cell lines (BIU87, 5637, T24, EJ, and RT4) as per qRT-PCR (**Figure 2A**), these two cell lines were selected for the following experiments. To investigate the effects of TMPO-AS1 on the proliferation, migration, and apoptosis of BC cells, loss- and gain-of-function assays were performed. First, si-RNA targeting TMPO-AS1 or a TMPO-AS1-overexpression plasmid was transfected into T24 and RT4 cells. The transfection efficacy was examined using qRT-PCR (**Figure 2B**). Importantly, TMPO-AS1 knockdown significantly inhibited cell viability/proliferation (**Figures 2C,D**), migration (**Figure 2E**), and invasion (**Figure 2F**), whereas the overexpression of TMPO-AS1 resulted in the opposite effects. Additionally, cell apoptosis was induced in TMPO-AS1-silenced T24 and RT4 cells, whereas the overexpression of TMPO-AS1 inhibited cell apoptosis (**Figure 2G**). Overall, these findings suggest that TMPO-AS1 plays an oncogenic role in BC cells, promoting their proliferation, migration, invasion, and survival *in vitro*.

E2F1 Activates the Transcription of TMPO-AS1 in BC Cells

To figure out the underlying mechanism of TMPO-AS1-mediated carcinogenesis in BC, we investigated the upstream and downstream targets of TMPO-AS1. We screened out the potential TFs of TMPO-AS1 using hTFtarget and ChIPBase v2.0 (**Figure 3A**). Interestingly, we obtained 36 candidate TFs for TMPO-AS1; of note, E2F1 had the highest positive correlation with TMPO-AS1 among the 36 TFs (**Supplementary Table 2**). Importantly, a previous study reported that the overexpression of E2F3 induced the promoter activity of TMPO-AS1/LAP2, an antisense transcript (31). Additionally, we analyzed the genes co-expressed with TMPO-AS1 (correlation coefficient ≥ 0.6 and $p < 0.01$) in BC using Co-LncRNA (**Supplementary Table 3**) and used them in the context of pathway analysis *via* Metascape. Remarkably, we found that TMPO-AS1 is involved in the E2F pathway (**Figure 3B**). Thus, we focused on E2F1 in the following experiments, and we examine its transcriptional expression among five BC cell lines (**Supplementary Figure 1B**). Importantly, E2F1 was positively correlated with TMPO-AS1 in BC as evidenced by TCGA and GSE133624 datasets (**Figures 3C,D**). Furthermore, the expression of TMPO-AS1

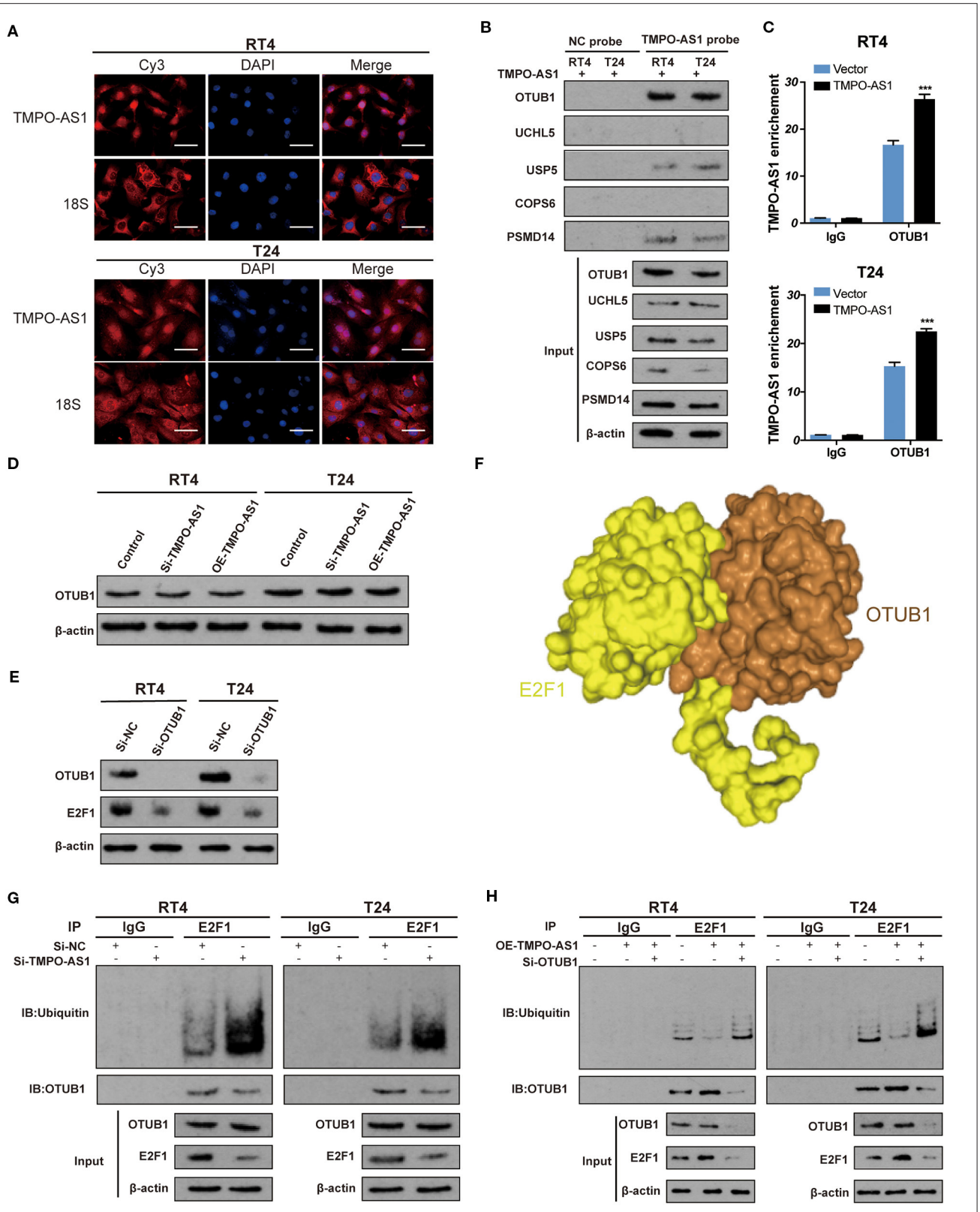

FIGURE 5 | TMPO-AS1 stabilizes E2F1 *via* OTUB1-mediated deubiquitination. **(A)** The TMPO-AS1 cellular localization was evaluated using FISH. **(B)** RNA pull-down assays demonstrated that OTUB1 is the deubiquitinase that most likely binds to TMPO-AS among a group of deubiquitinases (OTUB1, UCHL5, USP5, COPS6, and PSMD14). **(C)** RIP assays were performed to validate the interaction between TMPO-AS1 and OTUB1, in the context of TMPO-AS1 overexpressing RT4 and T24

(Continued)

FIGURE 5 | cells; IgG was used as the negative control. Error bars represent the mean ± SD from three independent experiments. **(D)** Western blotting images show that TMPO-AS1 silencing has no effect on the OTUB1 protein levels in RT4 and T24 cells. **(E)** Western blotting images showing that the knockdown of OTUB1 leads to the decrease in the E2F1 protein levels in RT4 and T24 cells. Si- OTUB1, siRNA targeting OTUB1. **(F)** E2F1 (yellow) and OTUB1 (brown) are very likely to bind to each other as per HDOCK predictions. **(G)** Co-IP assays were performed in control or si-TMPO-AS1-treated RT4 and T24 cells using an anti-E2F1 antibody, followed by Western blotting to analyze the ubiquitin levels of E2F1. **(H)** RT4 and T24 cells transfected with the empty vector, and the construct for the overexpression of TMPO-AS1, alone, or together with si-OTUB1 were subjected to immunoprecipitation with an anti-E2F1 antibody, followed by Western blotting to analyze the ubiquitin levels of E2F1. $^{***}p < 0.001$.

was downregulated after E2F1 silencing and upregulated in E2F1-overexpressing BC cells (**Figure 3E**). Of note, the putative binding site between TMPO-AS1 and E2F1 was located at around −945 to −935 bp, upstream of the transcription start site, as predicted by JASPAR (http://jaspar.genereg.net), a collection of transcription factor binding site profiles (22) (**Figure 3F**). Importantly, this prediction was validated *via* luciferase reporter assays. The overexpression of E2F1 dramatically enhanced the luciferase activity of the wild-type TMPO-AS1 promoter but did not affect the transcriptional activity of the mutant TMPO-AS1 promoter (**Figure 3G**). Moreover, the results of ChIP assays demonstrated that E2F1 was remarkably enriched in the TMPO-AS1 promoter region relative to the observed in the context of control IgG (**Figure 3H**). Overall, these results indicate that E2F1 binds to the promoter of TMPO-AS1 and its transcription.

TMPO-AS1 Regulates the Protein Levels of E2F1 *via* Protein Stabilization

Given that lncRNAs have been reported to interact with E2F1 (32), we investigated whether TMPO-AS1 could interact with E2F1. As shown in **Figure 4A**, a possible interaction between TMPO-AS1 and E2F1 was predicted by catRAPID. Consequently, we conducted RNA pull-down assays to validate the prediction. The results showed that E2F1 was abundantly enriched in the context of the TMPO-AS1 probe compared with the oligo control, especially in TMPO-AS1 overexpressing RT4 and T24 cells (**Figure 4B**). Similarly, RIP results demonstrated that E2F1 remarkably immunoprecipitated TMPO-AS1, particularly after the TMPO-AS1 overexpression in RT4 and T24 cells (**Figure 4C**). The interaction between TMPO-AS1 and E2F1 prompted us to further investigate whether TMPO-AS1 influenced the expression of E2F1. Interestingly, the overexpression or knockdown of TMPO-AS1 had no significant impact on the E2F1 mRNA expression (**Figure 4D**), but it either increased or decreased the protein levels of E2F1 in RT4 and T24 cells (**Figure 4E**), respectively. These results suggest that the TMPO-AS1-mediated E2F1 regulation occurs at the posttranscriptional level. Of note, we found that the proteasome inhibitor MG132 markedly increased the stability of E2F1 in cycloheximide-treated RT4 and T24 cells (**Figure 4F**), implying that the turnover of E2F1 is dependent on the ubiquitin-proteasome system. Importantly, TMPO-AS1 silencing significantly shortened the half-life of E2F1 (**Figure 4G**). Altogether, our data demonstrate that TMPO-AS1 directly interacts with E2F1 and regulates its protein levels *via* protein stabilization.

TMPO-AS1 Stabilizes E2F1 *via* OTUB1-Mediated Deubiquitination

Later, we aimed to understand the underlying mechanism of TMPO-AS1-mediated E2F1 stabilization. First, using FISH, we found that TMPO-AS1 is predominantly distributed in the cytoplasm in both T24 and RT4 cells (**Figure 5A**), indicating that TMPO-AS1 might be involved in translational regulation. Of note, it was predicted that E2F1 has four potential ubiquitination sites, as per UbPred (**Supplementary Figure 2A**). Therefore, we hypothesized that TMPO-AS1 may associate with a specific ubiquitinase/deubiquitinase to regulate E2F1 ubiquitination. Since we have previously studied a group of deubiquitinases (OTUB1, UCHL5, USP5, COPS6, and PSMD14) in BC (unpublished data), we evaluated their binding potential to TMPO-AS1 using PRIdictor. The results highlighted OTUB1 as the deubiquitinase that most likely associates with TMPO-AS1 (**Supplementary Figure 2B**), and the transcriptional expression of OTUB1 was evaluated by qRT-PCR (**Supplementary Figure 1C**). To validate this prediction, we conducted RNA pull-down assays and found that TMPO-AS1 precipitated more OTUB1 than the other deubiquitinases (**Figure 5B**). Similarly, RIP assays showed that TMPO-AS1 was obviously immunoprecipitated by the anti-OTUB1 antibody (vs. IgG; **Figure 5C**). Furthermore, catRAPID showed that a region of TMPO-AS1 (located at 76–127 nt) exhibits a high potential of interaction with some of the OTUB1 amino acid residues (51–152; **Supplementary Figure 2C**), further supporting the association between TMPO-AS1 and OTUB1. Of note, despite the direct association between TMPO-AS1 and OTUB1, TMPO-AS1 failed to alter the OTUB1 protein expression (**Figure 5D**). Importantly, the OTUB1 knockdown led to a decrease in the E2F1 protein levels in RT4 and T24 cells (**Figure 5E**), suggesting an interaction between these two proteins. Such interaction was further supported by the prediction by HDOCK; OTUB1 is very likely to bind to E2F1 (**Figure 5F**). Importantly, the results of co-immunoprecipitation (Co-IP) assays showed that silencing TMPO-AS1 not only increased E2F1 ubiquitination but also mitigated the interaction between OTUB1 and E2F1 (**Figure 5G**); importantly, this phenotype was rescued after the TMPO-AS1 overexpression. Furthermore, the OTUB1 knockdown significantly reversed the decreased ubiquitination of E2F1 induced by the overexpression of TMPO-AS1 in RT4 and T24 cells (**Figure 5H**). Taken together, these results

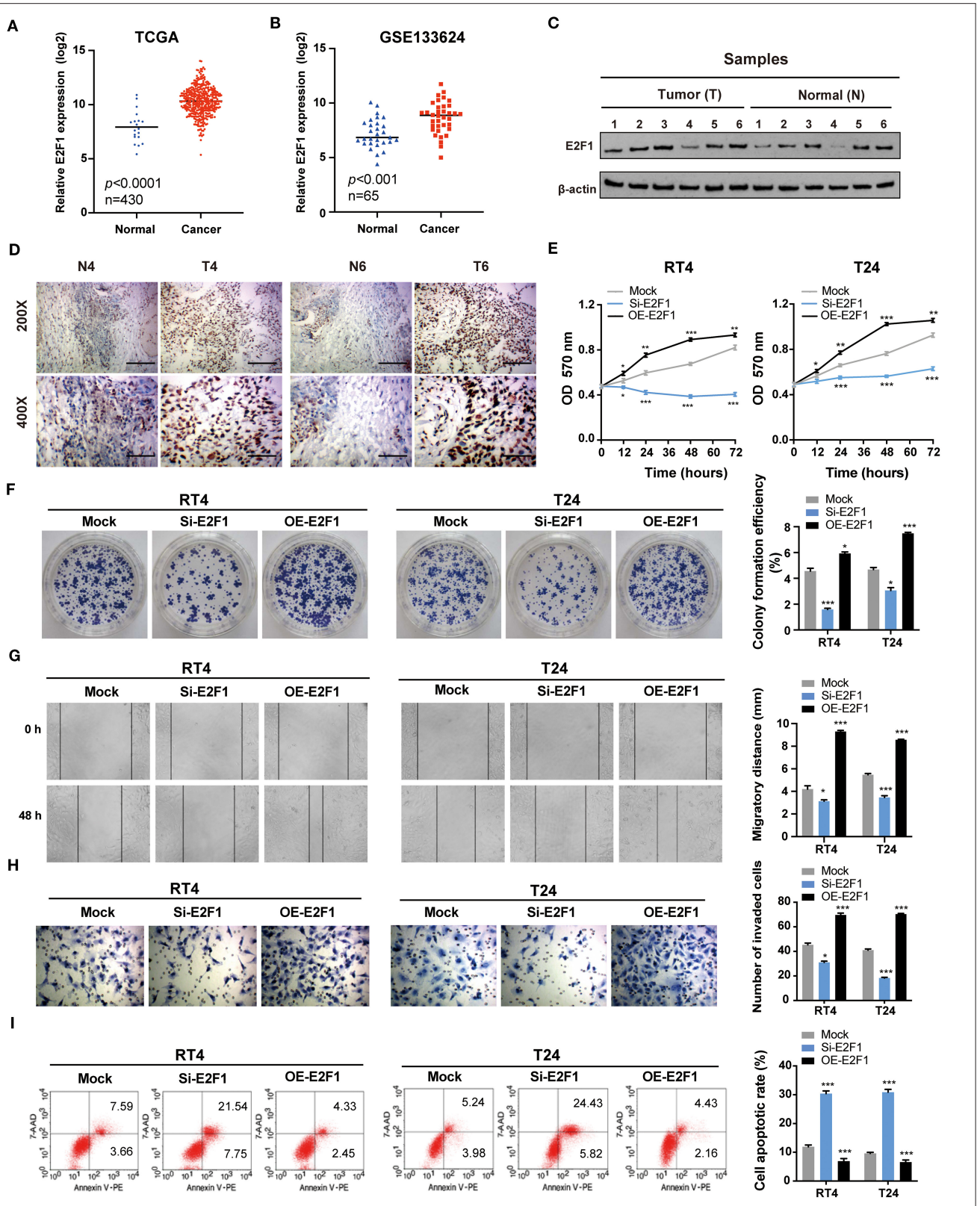

FIGURE 6 | E2F1 promotes the proliferation, migration, and invasion and inhibits the apoptosis of BC cells *in vitro*. **(A,B)** The expression of *E2F1* is upregulated in BC tissues compared with that in normal tissues based on data retrieved from TCGA and the GEO (GSE133624) databases. **(C)** The protein expression of E2F1 was

(Continued)

FIGURE 6 | assessed *via* Western blotting in six paired BC and adjacent normal tissue samples. **(D)** The protein expression of E2F1 was also assessed using immunohistochemistry in six paired BC and adjacent normal tissue samples. **(E)** The MTT assay was performed to determine the viability/proliferation of E2F1 knockdown and overexpressing RT4 and T24 cells. **(F)** The effects of E2F1 knockdown and overexpression on BC cell proliferation were assessed *via* colony formation assays. **(G,H)** The migratory and invasive capacities of E2F1 knockdown and overexpressing RT4 and T24 cells were evaluated *via* wound healing and transwell assays. **(I)** Cell apoptosis was analyzed by flow cytometry. Error bars represent the mean ± SD from three independent experiments. $^{*}p < 0.05$, $^{**}p < 0.01$, $^{***}p < 0.001$.

indicate that TMPO-AS1 upregulates E2F1 protein levels *via* OTUB1-mediated deubiquitination and the consequent protein stabilization.

E2F1 Promotes the Proliferation, Migration, and Invasion and Inhibits the Apoptosis of BC Cells *in vitro*

E2F1 is associated with cell proliferation, apoptosis, metastasis, and invasiveness (33). Hence, we speculated that E2F1 would promote BC tumorigenesis and development. According to the data retrieved from TCGA and the GEO (GSE133624) databases, the expression of E2F1 was remarkably higher in BC tissues than that in normal tissues (**Figures 6A,B**). Furthermore, Western blotting and immunohistochemistry (IHC) analyses showed that the expression of E2F1 protein was upregulated in six paired BC tissues compared with the adjacent normal tissues (**Figures 6C,D**). As anticipated, further functional experiments demonstrated that the E2F1 knockdown significantly inhibited cell proliferation (**Figures 6E,F**), migration (**Figure 6G**), and invasion (**Figure 6H**), and induced apoptosis (**Figure 6I**), whereas the overexpression of E2F1 led to the opposite effects. Altogether, these results reveal that E2F1 promotes malignant phenotypes in BC cells.

TMPO-AS1 Regulates Malignant Phenotypes in BC Cells *via* E2F1 *in vitro*

Since the overexpression of either E2F1 or TMPO-AS1 enhanced the proliferation, migration, and invasion of BC cells, and TMPO-AS1 upregulated the protein levels of E2F1, we hypothesized that TMPO-AS1 would promote BC progression *via* E2F1. To prove this theory, we restored the expression of E2F1 in TMPO-AS1-silenced BC cells (**Figure 7A**) and performed MTT, colony formation, wound healing, and transwell assays. As expected, the restoration of E2F1 in BC cells significantly reversed the inhibition of cell proliferation (**Figures 7B,C**), migration (**Figure 7D**), and invasion (**Figure 7E**) induced by TMPO-AS1 silencing. Furthermore, the TMPO-AS1 silencing-mediated promotion of apoptosis could be abrogated by the E2F1 overexpression (**Figure 7F**). Therefore, our data demonstrate that TMPO-AS1 promotes cell proliferation, migration, invasion, and survival of BC *via* E2F1 *in vitro*.

TMPO-AS1 Regulates BC Growth *via* E2F1 *in vivo*

Stably transfected RT4 cells were subcutaneously inoculated into nude mice to explore whether TMPO-AS1 would promote BC growth *via* E2F1 *in vivo*; every 5 days, the tumor volumes were measured. Results showed that the knockout of TMPO-AS1 significantly suppressed tumor growth compared to the control group, whereas the overexpression of E2F1 abolished the inhibitory effect on tumor growth induced by the knockout of TMPO-AS1 (**Figures 8A,B**). Furthermore, the IHC staining showed that the depletion of TMPO-AS led to a substantial decrease of the protein levels of Ki-67 and E2F1 and to a notable increase in the expression of caspase-3. Of note, this phenotype was reversed by the overexpression of E2F1 (**Figure 8C**). Collectively, the above findings demonstrate that TMPO-AS1 regulates the BC-associated tumor growth through E2F1 *in vivo*.

DISCUSSION

Bladder cancer is the most common urinary system malignancy, with a heavy burden worldwide. Therefore, it is imperative to elucidate the mechanisms of carcinogenesis in BC. An increasing number of studies have demonstrated that lncRNAs play a vital role in tumor initiation, development, and progression in the context of numerous cancers, including BC (34). In our study, we investigated the biological roles of the lncRNA TMPO-AS1 in BC. Functional experiments demonstrated that TMPO-AS1 could promote the proliferation, migration, and invasion of BC cells and could inhibit apoptosis in BC cells *via* the stabilization of E2F1.

Here, we found that TMPO-AS1 is highly expressed in BC and correlates with poor prognoses. Importantly, we performed *in vitro* experiments and proved that TMPO-AS1 functions as an oncogene, consistent with the reported in previous studies (35). In fact, thousands of abnormally expressed lncRNAs have been reported in BC (36). However, little is known about their upstream regulation and downstream targets. In the present study, we showed that TMPO-AS1 positively correlates with the expression of E2F1; moreover, we show that E2F1 activates the transcription of TMPO-AS1. Therefore, our data, showing that TMPO-AS1 is upregulated in BC due to E2F1, contribute to a better understanding of the upstream regulatory mechanisms in the context of lncRNAs.

LncRNAs may be oncogenes or tumor suppressors *via* the regulation of gene expression (e.g., epigenetic regulation, transcriptional activation or repression, or posttranscriptional modulation) or even *via* protein modification (6, 37). Our data demonstrated that TMPO-AS1 directly binds to E2F1, increasing its stability. The knockdown of TMPO-AS1 resulted in higher E2F1 ubiquitination levels. Interestingly, we demonstrated that OTUB1, a deubiquitinase, is responsible for the TMPO-AS1-mediated E2F1 stabilization. In line with our results, a previous

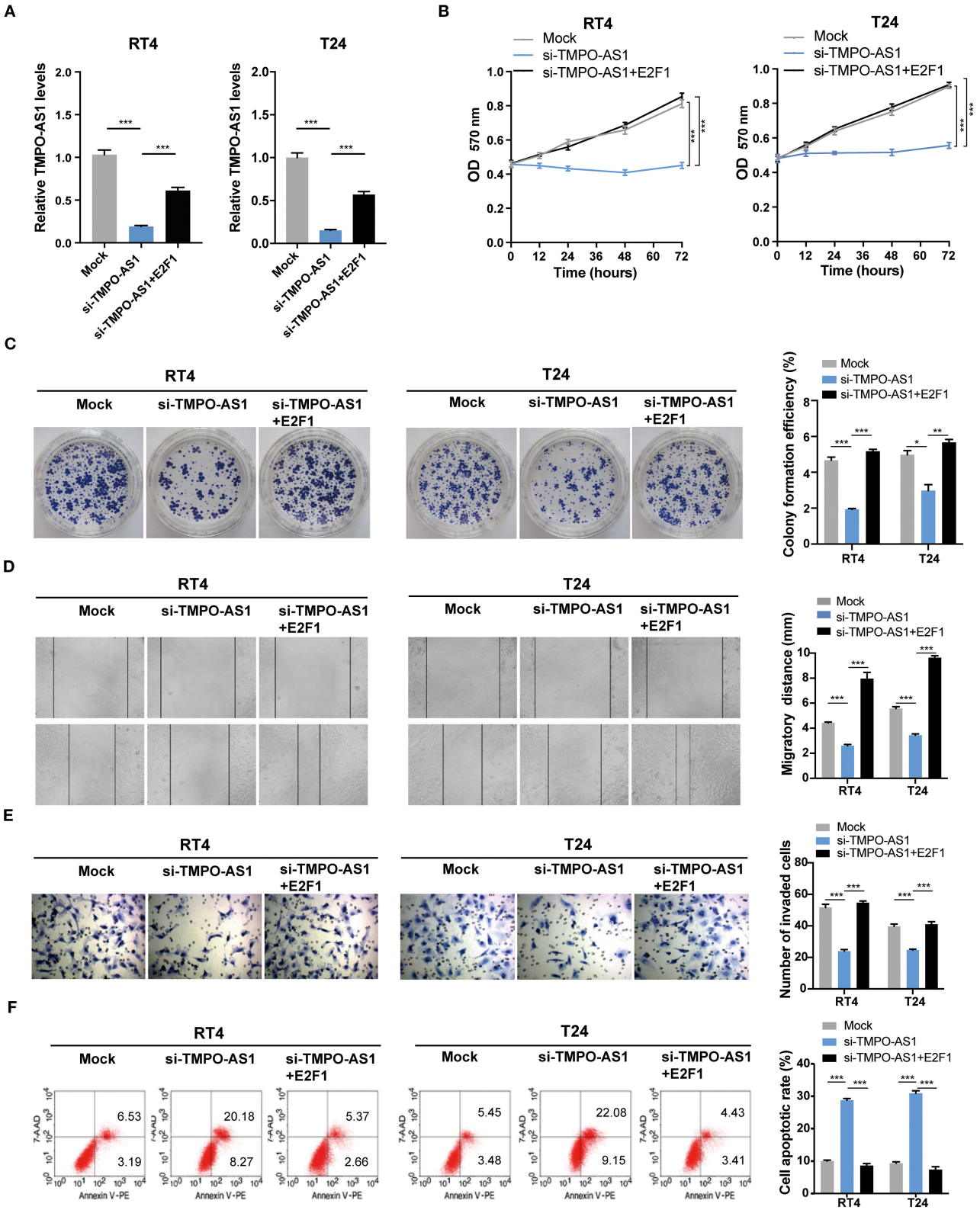

FIGURE 7 | TMPO-AS1 promotes BC malignant phenotypes *via* E2F1 *in vitro*. **(A)** The TMPO-AS1 expression was evaluated using qRT-PCR in RT4 and T24 cells transfected with an empty vector, sh-TMPO-AS1, or co-transfected with sh-TMPO-AS1 and E2F1-ectopic expression vector. **(B,C)** MTT and colony formation assays were performed to assess the proliferative ability of transfected cells. **(D,E)** The cell migration and invasion were estimated using wound healing and transwell assays. **(F)** The apoptosis in transfected BC cells stained with Annexin V-PE/7-AAD was evaluated *via* flow cytometry analysis. Error bars represent the mean ± SD from three independent experiments. $^{*}p < 0.05$, $^{**}p < 0.01$, $^{***}p < 0.001$.

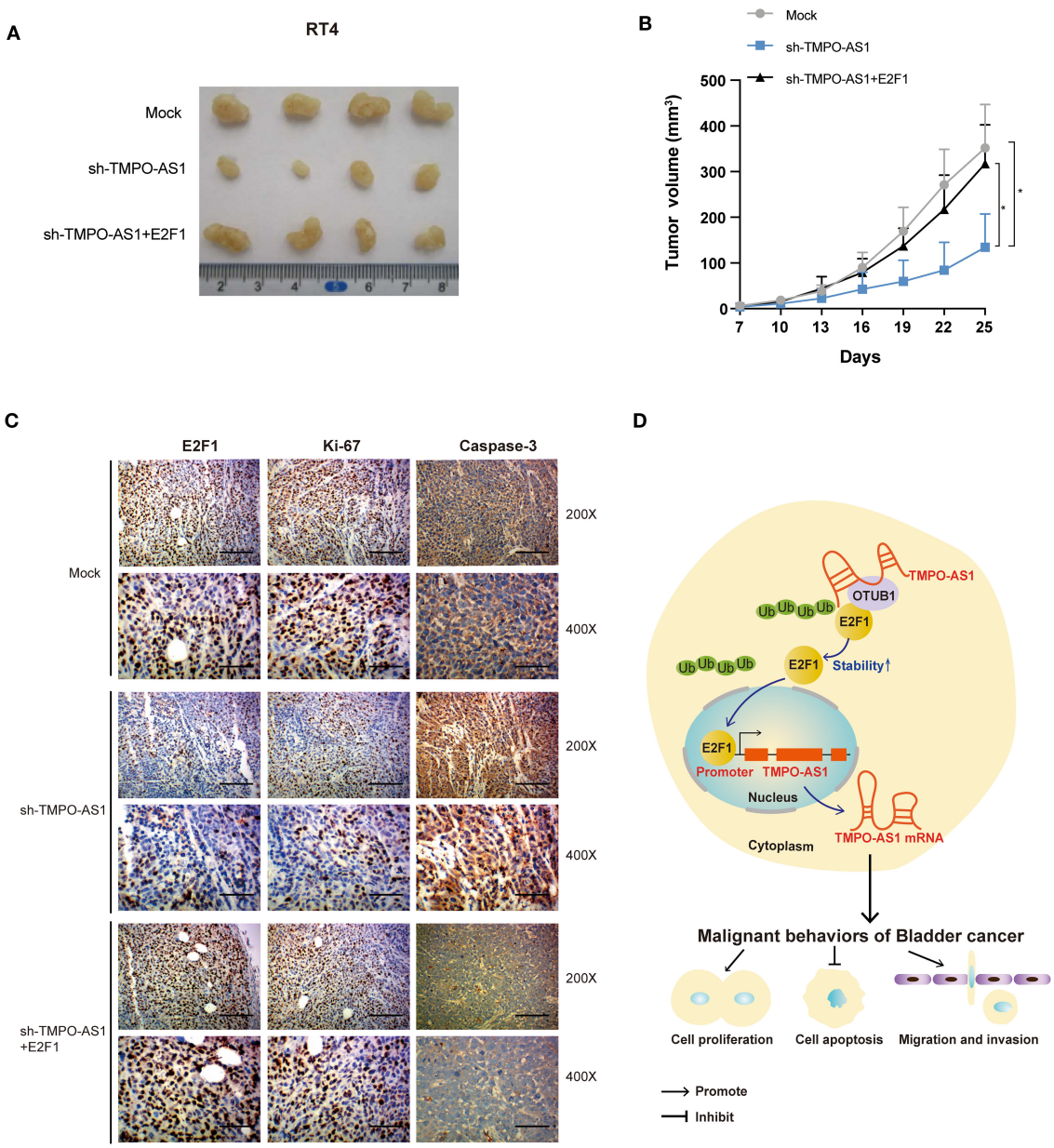

FIGURE 8 | TMPO-AS1 regulates BC growth *in vivo via* E2F1. **(A)** Representative images of the tumor xenografts 25 days after the subcutaneous injection of RT4 cells transfected with empty vector, sh-TMPO-AS1, and sh-TMPO-AS1 along with an E2F1-overexpression construct into the flanks of nude mice. **(B)** The tumor volumes were measured every 3 days in the three groups. Three independent experiments were performed. **(C)** The expression of E2F1, Ki-67, and caspase-3 in xenografts was evaluated using immunohistochemistry. Representative images are shown. **(D)** A schematic diagram illustrating the role and mechanism of TMPO-AS1 in BC tumorigenesis and progression is illustrated. *$p < 0.05$.

study revealed that POH1, a deubiquitinase, binds to and deubiquitinates E2F1, contributing to its stabilization (38).

Most studies suggest that TMPO-AS1 contributes to tumorigenesis through TMPO-AS1–miRNA–mRNA axes (39), whereas others propose that TMPO-AS1 forms RNA–RNA complexes to regulate the gene expression (40). In fact, very recently, a study has shown that TMPO-AS1 promotes BC cell growth *via* the TMPO-AS1/miR-98-5p/EBF1 positive feedback loop (41). However, this study only elucidated the function of TMPO-AS1 as a miRNA "sponge" for *EBF1* mRNA *in vitro*; the roles of TMPO-AS1 in BC, *in vivo*, are still unknown. Therefore, our study highlights, for the first time, that TMPO-AS1, to act as a "sponge" for mRNAs, interacts directly with proteins and, thereby, influences protein–protein interactions, revealing a novel regulatory mechanism of TMPO-AS1.

Additionally, in the current study, we found that the overexpression of either E2F1 or TMPO-AS1 boosts the proliferation, migration, and invasion and inhibits apoptosis of BC cells. Moreover, we verified that TMPO-AS1 promotes BC growth and progression in an E2F1-dependent manner. In fact, numerous studies have shown that lncRNAs can target E2F1 in cancers, such as lung carcinoma (42), breast cancer (32), and BC (43). Moreover, it is well acknowledged that E2F1 can promote tumor carcinogenesis, development, and progression *via* the facilitation of cell proliferation (44) and migration (45, 46). Of note, upregulated E2F1 is a strong predictor of the BC progression (33). Together with these previous studies, our data support the notion that that the positive feedback loops are extremely important for the regulation of carcinogenesis and cancer progression (43, 47). Particularly, our data highlight a mutual regulatory pattern between lncRNAs and TFs, which may lead to increased oncogenic activity in cancer development.

However, our study is not without limitations. Due to the low number of available clinical BC samples, we validated the clinical significance of TMPO-AS1 using the online software. In addition, the specific mechanistic sequence behind the TMPO-AS1-induced OTUB1-mediated E2F1 deubiquitination, as well as the structure of the possible complex formed, remains unknown. We plan to investigate the abovementioned detail in a follow-up study.

In summary, our study uncovers the upstream and downstream partners of TMPO-AS1 in the context of BC, proposing a new positive feedback loop that contributes to BC tumorigenesis, involving TMPO-AS1 and E2F1 (**Figure 8D**). Therefore, the TMPO-AS1/E2F1 loop should be considered in the development of new therapeutic approaches for BC.

DATA AVAILABILITY STATEMENT

The original contributions presented in the study are included in the article/**Supplementary Material**, further inquiries can be directed to the corresponding author/s.

ETHICS STATEMENT

The studies involving human participants were reviewed and approved by ethics committee of the Third Xiangya Hospital, Central South University. The patients/participants provided their written informed consent to participate in this study. The animal study was reviewed and approved by Animal Care and Use Committee of the Central South University. Written informed consent was obtained from the individual(s) for the publication of any potentially identifiable images or data included in this article.

AUTHOR CONTRIBUTIONS

KC and YYZ designed this study. JL and MX collected the clinical samples. JL and YYZ contributed to the experiments implementation. YC, DH, and LX analyzed the data. KC, YYZ, and YXZ drafted the manuscript. LG, ZW, and LD edited the manuscript. All authors read and approved the final manuscript.

FUNDING

This work was financially supported by the National Natural Science Foundation of China (81874137), the Outstanding Youth Foundation of Hunan Province (2018JJ1047), the Huxiang Young Talent Project (2016RS3022), the Hunan Province Science and Technology Talent Promotion Project (2019TJ-Q10), and the Independent Exploration and Innovation Project of Central South University (2019zzts825).

ACKNOWLEDGMENTS

We thank all our colleagues for their efforts and valuable feedback.

SUPPLEMENTARY MATERIAL

The Supplementary Material for this article can be found online at: https://www.frontiersin.org/articles/10.3389/fonc.2021.643163/full#supplementary-material

Supplementary Figure 1 | The expression of TMPO-AS1, E2F1, and OTUB1 in bladder cancer (BC). **(A)** The expression of TMPO-AS1 in BC samples in the context of different clinical stages. **(B)** The mRNA levels of E2F1 in five BC cell lines (BIU87, 5637, T24, EJ, and RT4). **(C)** Quantitative real-time PCR (qRT-PCR) showing the mRNA levels of OTUB1 in five BC cell lines (BIU87, 5637, T24, EJ, and RT4).

Supplementary Figure 2 | E2F1 ubiquitination sites and the interactions between TMPO-AS1 and five deubiquitinases. **(A)** The potential ubiquitination sites in E2F1. **(B)** The interaction between TMPO-AS1 and five deubiquitinases (UCHL5, USP5, COPS6, PSMD14, and OTUB1) predicted by PRIdictor. **(C)** CatRAPID was used to predict the interaction pattern between TMPO-AS1 and OTUB1.

Supplementary Table 1 | List of antibodies used in this study.

Supplementary Table 2 | The 36 overlapping transcription factors (TFs) revealed by the hTFtarget and ChIPBase v2.0 and the correlation analysis between their expression and TMPO-AS1.

Supplementary Table 3 | Genes co-expressed with TMPO-AS1 as per Co-lncRNA.

REFERENCES

1. Kamat AM, Hahn NM, Efstathiou JA, Lerner SP, Malmstrom PU, Choi W, et al. Bladder cancer. *Lancet.* (2016) 388:2796–810. doi: 10.1016/S0140-6736(16)30512-8
2. Bray F, Ferlay J, Soerjomataram I, Siegel RL, Torre LA, Jemal A. Global cancer statistics 2018: GLOBOCAN estimates of incidence and mortality worldwide for 36 cancers in 185 countries. *CA Cancer J Clin.* (2018) 68:394–424. doi: 10.3322/caac.21492
3. Robertson AG, Kim J, Al-Ahmadie H, Bellmunt J, Guo G, Cherniack AD, et al. Comprehensive molecular characterization of muscle-invasive bladder cancer. *Cell.* (2018) 174:1033. doi: 10.1016/j.cell.2018.07.036
4. Berdik C. Unlocking bladder cancer. *Nature.* (2017) 551:S34–5. doi: 10.1038/551S34a

5. Ponting CP, Oliver PL, Reik W. Evolution and functions of long noncoding *RNAs*. *Cell.* (2009) 136:629–41. doi: 10.1016/j.cell.2009.02.006
6. Gupta RA, Shah N, Wang KC, Kim J, Horlings HM, Wong DJ, et al. Long non-coding RNA HOTAIR reprograms chromatin state to promote cancer metastasis. *Nature.* (2010) 464:1071–6. doi: 10.1038/nature08975
7. Chen C, He W, Huang J, Wang B, Li H, Cai Q, et al. LNMAT1 promotes lymphatic metastasis of bladder cancer via CCL2 dependent macrophage recruitment. *Nat Commun.* (2018) 9:3826. doi: 10.1038/s41467-018-06152-x
8. Wang CJ, Zhu CC, Xu J, Wang M, Zhao WY, Liu Q, et al. The lncRNA UCA1 promotes proliferation, migration, immune escape and inhibits apoptosis in gastric cancer by sponging anti-tumor miRNAs. *Mol Cancer.* (2019) 18:115. doi: 10.1186/s12943-019-1032-0
9. Martens-Uzunova ES, Bottcher R, Croce CM, Jenster G, Visakorpi T, Calin GA. Long noncoding RNA in prostate, bladder, and kidney cancer. *Eur Urol.* (2014) 65:1140–51. doi: 10.1016/j.eururo.2013.12.003
10. Peng F, Wang R, Zhang Y, Zhao Z, Zhou W, Chang Z, et al. Differential expression analysis at the individual level reveals a lncRNA prognostic signature for lung adenocarcinoma. *Mol Cancer.* (2017) 16:98. doi: 10.1186/s12943-017-0666-z
11. Mitobe Y, Ikeda K, Suzuki T, Takagi K, Kawabata H, Horie-Inoue K, et al. ESR1-Stabilizing long noncoding RNA TMPO-AS1 promotes hormone-refractory breast cancer progression. *Mol Cell Biol.* (2019) 39:e00261-19. doi: 10.1128/MCB.00261-19
12. Guo X, Wang Y. LncRNA TMPO-AS1 promotes hepatocellular carcinoma cell proliferation, migration and invasion through sponging miR-329-3p to stimulate FOXK1-mediated AKT/mTOR signaling pathway. *Cancer Med.* (2020) 9:5235–46. doi: 10.1002/cam4.3046
13. Li Z, Feng Y, Zhang Z, Cao X, Lu X. TMPO-AS1 promotes cell proliferation of thyroid cancer via sponging miR-498 to modulate TMPO. *Cancer Cell Int*. (2020) 20:294. doi: 10.1186/s12935-020-01334-4
14. Huarte M, Guttman M, Feldser D, Garber M, Koziol MJ, Kenzelmann-Broz D, et al. A large intergenic noncoding RNA induced by p53 mediates global gene repression in the p53 response.*Cell.* (2010) 142:409–19. doi: 10.1016/j.cell.2010.06.040
15. Tsantoulis PK, Gorgoulis VG. Involvement of E2F transcription factor family in cancer. *Eur J Cancer.* (2005) 41:2403–14. doi: 10.1016/j.ejca.2005.08.005
16. Xu TP, Wang YF, Xiong WL, Ma P, Wang WY, Chen WM, et al. E2F1 induces TINCR transcriptional activity and accelerates gastric cancer progression via activation of TINCR/STAU1/CDKN2B signaling axis. *Cell Death Dis*. (2017) 8:e2837. doi: 10.1038/cddis.2017.205
17. Mofers A, Pellegrini P, Linder S, D'Arcy P. Proteasome-associated deubiquitinases and cancer. *Cancer Metastasis Rev.* (2017) 36:635–53. doi: 10.1007/s10555-017-9697-6
18. Xia M, Liu CJ, Zhang Q, Guo AY. GEDS: a gene expression display server for mRNAs, miRNAs and proteins. *Cells.* (2019) 8:675. doi: 10.3390/cells8070675
19. Li J, Han L, Roebuck P, Diao L, Liu L, Yuan Y, et al. TANRIC: an interactive open platform to explore the function of lncRNAs in Cancer. *Cancer Res.* (2015) 75:3728–37. doi: 10.1158/0008-5472.CAN-15-0273
20. Zhou KR, Liu S, Sun WJ, Zheng LL, Zhou H, Yang JH, et al. ChIPBase v2.0: decoding transcriptional regulatory networks of non-coding RNAs and protein-coding genes from ChIP-seq data. *Nucleic Acids Res.* (2017) 45:D43–D50. doi: 10.1093/nar/gkw965
21. Zhang Q, Liu W, Zhang HM, Xie GY, Miao YR, Xia M, et al. hTFtarget: a comprehensive database for regulations of human transcription factors and their targets. *Genomics Proteomics Bioinformatics.* 18:120-128. doi: 10.1016/j.gpb.2019.09.006
22. Khan A, Fornes O, Stigliani A, Gheorghe M, Castro-Mondragon JA R, et al. JASPAR 2018: update of the open-access database of transcription factor binding profiles and its web framework. *Nucleic Acids Res.* (2018) 46:D260–6. doi: 10.1093/nar/gkx1188
23. Zhao Z, Bai J, Wu A, Wang Y, Zhang J, Wang Z, et al. Co-LncRNA: investigating the lncRNA combinatorial effects in GO annotations and KEGG pathways based on human RNA-Seq data. *Database (Oxford).* (2015) 2015:bav082. doi: 10.1093/database/bav082
24. Zhou Y, Zhou B, Pache L, Chang M, Khodabakhshi AH, Tanaseichuk O, et al. Metascape provides a biologist-oriented resource for the analysis of systems-level datasets. *Nat Commun.* (2019) 10:1523. doi: 10.1038/s41467-019-09234-6
25. Agostini F, Zanzoni A, Klus P, Marchese D, Cirillo D, Tartaglia GG. catRAPID omics: a web server for large-scale prediction of protein-RNA interactions. *Bioinformatics.* (2013) 29:2928–30. doi: 10.1093/bioinformatics/btt495
26. Tuvshinjargal N, Lee W, Park B, Han K. PRIdictor: Protein-RNA Interaction predictor. *Biosystems.* (2016) 139:17–22. doi: 10.1016/j.biosystems.2015.10.004
27. Yan Y, Zhang D, Zhou P, Li B, Huang SY. HDOCK: a web server for protein-protein and protein-DNA/RNA docking based on a hybrid strategy. *Nucleic Acids Res.* (2017) 45:W365–W373. doi: 10.1093/nar/gkx407
28. Radivojac P, Vacic V, Haynes C, Cocklin RR, Mohan A, Heyen JW, et al. Identification, analysis, and prediction of protein ubiquitination sites. *Proteins.* (2010) 78:365–80. doi: 10.1002/prot.22555
29. Zeng Q, Liu J, Cao P, Li J, Liu X, Fan X, et al. Inhibition of REDD1 sensitizes bladder urothelial carcinoma to paclitaxel by inhibiting autophagy. *Clin Cancer Res.* (2018) 24:445–59. doi: 10.1158/1078-0432.CCR-17-0419
30. Liu JY, Zeng QH, Cao PG, Xie D, Yang F, He LY, et al. SPAG5 promotes proliferation and suppresses apoptosis in bladder urothelial carcinoma by upregulating Wnt3 via activating the AKT/mTOR pathway and predicts poorer survival. *Oncogene.* (2018) 37:3937–52. doi: 10.1038/s41388-018-0223-2
31. Parise P, Finocchiaro G, Masciadri B, Quarto M, Francois S, Mancuso F, et al. Lap2alpha expression is controlled by E2F and deregulated in various human tumors. *Cell Cycle.* (2006) 5:1331–41. doi: 10.4161/cc.5.12.2833
32. Yu L, Fang F, Lu S, Li X, Yang Y, Wang Z. lncRNA-HIT promotes cell proliferation of non-small cell lung cancer by association with E2F1. *Cancer Gene Ther.* (2017) 24:221–6. doi: 10.1038/cgt.2017.10
33. Lee JS, Leem SH, Lee SY, Kim SC, Park ES, Kim SB, et al. Expression signature of E2F1 and its associated genes predict superficial to invasive progression of bladder tumors. *J Clin Oncol.* (2010) 28:2660–7. doi: 10.1200/JCO.2009.25.0977
34. Mercer TR, Dinger ME, Mattick JS. Long non-coding RNAs: insights into functions. *Nat Rev Genet.* (2009) 10:155–9. doi: 10.1038/nrg2521
35. Cui H, Zhao J. LncRNA TMPO-AS1 serves as a ceRNA to promote osteosarcoma tumorigenesis by regulating miR-199a-5p/WNT7B axis. *J Cell Biochem.* (2020) 121:2284–93. doi: 10.1002/jcb.29451
36. Bhan A, Soleimani M, Mandal SS. Long noncoding RNA and cancer: a new paradigm. *Cancer Res.* (2017) 77:3965–81. doi: 10.1158/0008-5472.CAN-16-2634
37. Tsai MC, Manor O, Wan Y, Mosammaparast N, Wang JK, Lan F, et al. Long noncoding RNA as modular scaffold of histone modification complexes. *Science.* (2010) 329:689–93. doi: 10.1126/science.1192002
38. Wang B, Ma A, Zhang L, Jin WL, Qian Y, Xu G, et al. POH1 deubiquitylates and stabilizes E2F1 to promote tumour formation. *Nat Commun.* (2015) 6:8704. doi: 10.1038/ncomms9704
39. Hu Y, Zhang Y, Ding M, Xu R. LncRNA TMPO-AS1/miR-126-5p/BRCC3 axis accelerates gastric cancer progression and angiogenesis via activating PI3K/Akt/mTOR pathway. *J Gastroenterol Hepatol.* doi: 10.1111/jgh.15362. [Epub ahead of print].
40. Qin Z, Zheng X, Fang Y. Long noncoding RNA TMPO-AS1 promotes progression of non-small cell lung cancer through regulating its natural antisense transcript TMPO. *Biochem Biophys Res Commun.* (2019) 516:486–93. doi: 10.1016/j.bbrc.2019.06.088
41. Luo H, Yang L, Liu C, Wang X, Dong Q, Liu L, et al. TMPO-AS1/miR-98-5p/EBF1 feedback loop contributes to the progression of bladder cancer. *Int J Biochem Cell Biol.* (2020) 122:105702. doi: 10.1016/j.biocel.2020.105702
42. Lu G, Li Y, Ma Y, Lu J, Chen Y, Jiang Q, et al. Long noncoding RNA LINC00511 contributes to breast cancer tumourigenesis and stemness by inducing the miR-185-3p/E2F1/Nanog axis. *J Exp Clin Cancer Res.* (2018) 37:289. doi: 10.1186/s13046-018-0945-6
43. Su F, He W, Chen C, Liu M, Liu H, Xue F, et al. The long non-coding RNA FOXD2-AS1 promotes bladder cancer progression and recurrence through a positive feedback loop with Akt and E2F1. *Cell Death Dis.* (2018) 9:233. doi: 10.1038/s41419-018-0275-9
44. Wang H, Yu S, Peng H, Shu Y, Zhang W, Zhu Q, et al. Long noncoding RNA Linc00337 functions as an E2F1 co-activator and promotes cell

proliferation in pancreatic ductal adenocarcinoma. *J Exp Clin Cancer Res.* (2020) 39:216. doi: 10.1186/s13046-020-01725-5

45. Chen HZ, Tsai SY, Leone G. Emerging roles of E2Fs in cancer: an exit from cell cycle control. *Nat Rev Cancer.* (2009) 9:785–97. doi: 10.1038/nrc2696
46. Li H, Tong F, Meng R, Peng L, Wang J, Zhang R, et al. E2F1-mediated repression of WNT5A expression promotes brain metastasis dependent on the ERK1/2 pathway in EGFR-mutant non-small cell lung cancer. *Cell Mol Life Sci.* doi: 10.1007/s00018-020-03678-6. [Epub ahead of print].
47. Xu MD, Wang Y, Weng W, Wei P, Qi P, Zhang Q, et al. A positive feedback loop of lncRNA-PVT1 and FOXM1 facilitates gastric cancer growth and invasion. *Clin Cancer Res*. (2017) 23:2071–80. doi: 10.1158/1078-0432.CCR-16-0742

Conflict of Interest: The authors declare that the research was conducted in the absence of any commercial or financial relationships that could be construed as a potential conflict of interest.

frontiers in Oncology

REVIEW
published: 27 April 2021
doi: 10.3389/fonc.2021.664904

Insights Into Exosomal Non-Coding RNAs Sorting Mechanism and Clinical Application

Yi Qiu[1,2], *Peiyao Li*[1,3], *Zuping Zhang*[1,2*] *and Minghua Wu*[1,2*]

[1] *Hunan Cancer Hospital and the Affiliated Cancer Hospital of Xiangya School of Medicine, Central South University, Changsha, China,* [2] *Cancer Research Institute, School of Basic Medical Science, Central South University, Changsha, China,* [3] *Key Laboratory of Carcinogenesis and Cancer Invasion of Ministry of Education, China National Health Commission Key Laboratory of Carcinogenesis, Xiangya Hospital, Central South University, Changsha, China*

OPEN ACCESS

Edited by:
Marco Tafani,
Sapienza University of Rome, Italy

Reviewed by:
Muhammad Nawaz,
University of Gothenburg, Sweden
Weifeng He,
Army Medical University, China
Reza Rahbarghazi,
Tabriz University of Medical Sciences, Iran

***Correspondence:**
Minghua Wu
wuminghua554@aliyun.com
Zuping Zhang
zhangzp74@126.com

Specialty section:
This article was submitted to Molecular and Cellular Oncology, a section of the journal Frontiers in Oncology

Received: *06 February 2021*
Accepted: *07 April 2021*
Published: *27 April 2021*

Citation:
Qiu Y, Li P, Zhang Z and Wu M (2021) Insights Into Exosomal Non-Coding RNAs Sorting Mechanism and Clinical Application. Front. Oncol. 11:664904. doi: 10.3389/fonc.2021.664904

Exosomes are natural nanoscale bilayer phospholipid vesicles that can be secreted by almost all types of cells and are detected in almost all types of body fluids. Exosomes are effective mediators of cell–cell signaling communication because of their ability to carry and transfer a variety of bioactive molecules, including non-coding RNAs. Non-coding RNAs have also been found to exert strong effects on a variety of biological processes, including tumorigenesis. Many researchers have established that exosomes encapsulate bioactive non-coding RNAs that alter the biological phenotype of specific target cells in an autocrine or a paracrine manner. However, the mechanism by which the producer cells package non-coding RNAs into exosomes is not well understood. This review focuses on the current research on exosomal non-coding RNAs, including the biogenesis of exosomes, the possible mechanism of sorting non-coding RNAs, their biological functions, and their potential for clinical application in the future.

Keywords: exosome, extracellular vesicles, non-coding RNAs, sorting mechanism, cell-cell communication, ncRNAs

INTRODUCTION

Since the discovery of extracellular vesicles (EVs), researchers have found EVs in almost all biological fluids. EVs have received unprecedented attention owing to their key roles, such as their potential as biomarkers for liquid biopsies and therapeutic applications (1, 2). Based on their formation, typical EVs are roughly divided into three categories: microvesicles (also called outer membrane vesicles, ectosomes, or shedding vesicles), exosomes, and apoptotic bodies. Microvesicles (100–1000-nm diameter) are released from the cell membrane through the blebbing and fission of the plasma membrane. Apoptotic bodies (50–5000-nm diameter) fall off during the process of cell apoptosis (3–6). Exosomes derived from the endosomal compartment are phospholipid bilayer vesicles with a diameter of 50–150 nm, generated by sequential invagination of the plasma membrane and endomembrane (7–9). They are specifically loaded with cargos, depending on the producer cell type and its homeostatic state. This review focuses on exosomes, which are the most studied type of EVs. Exosomes contain a variety of bioactive substances, including DNA, RNA, proteins, and lipids, which are secreted into the extracellular space and absorbed by target cells to

change their phenotype. Functional exosomes can protect packaged cargos from being destroyed by various biological enzymes, extending the circulating half-life and enhancing exosomal RNA biological effects (10).

Accumulating evidence suggests that most pluricellular organisms sustain exosome-based communications *via* the intercellular exchange of non-coding RNAs (ncRNAs) between cells. Valadi et al. first reported exosomes containing mRNAs and microRNAs (miRNAs) (11). Subsequently, a large number of studies have confirmed the existence of many other ncRNA species in exosomes (12–15). More than 98% of the human genome is composed of ncRNAs that are involved in a broad range of physiological or pathophysiological processes in humans (16). NcRNAs play an indispensable role in genetic expression, epigenetic regulation, RNA splicing and translation processes, protein degradation, and transport, among others. Exosomal ncRNAs, especially those derived from tumors, are highly enriched and stable and act as messengers in cell–cell communications (17, 18). This review mainly focuses on three types of ncRNAs: miRNAs (average length of 22 nucleotides), long ncRNA (lncRNA) (>200 nucleotides in length), and circular RNA (circular molecule that has a covalently closed loop structure, lacking a poly A tail or 5′→3′ polarity) (19–21).

To advance the field of exosomal biology and understand the roles of exosomal ncRNAs, this review focuses on the cellular machinery and processes of exosome formation, sorting of ncRNAs into the exosome pathway, and biological roles of the three types of exosomal ncRNAs. The application of exosomal ncRNAs as biomarkers and the potential roles of exosomal ncRNAs as therapeutic agents are also discussed.

BIOGENESIS OF EXOSOMES

Exosome biogenesis is closely related to the cellular endocytosis pathway. Endocytosis of the plasma membrane leads to the formation of early endosomes, which then bud inward and mature into late endosomes (LE). In turn, LEs develop into multivesicular bodies (MVBs) containing intraluminal vesicles (ILVs). Most MVBs fuse with lysosomes to degrade the contained cargo, whereas some bud and divide from the endosomal membrane to produce ILVs, which are released into the extracellular space when the endosomal membrane fuses with the cytoplasmic membrane, namely exosomes (22, 23). The biogenesis of exosomes has often been described to involve an endosomal sorting complex required for transport (ESCRT)-dependent or ESCRT-independent mechanism, although the pathways may not be entirely separated. In fact, the pathways may work synergistically, and different subpopulations of exosomes could depend on different machineries (**Figure 1**) (24–26).

ESCRT-Dependent Mechanism in the Biogenesis of Exosomes

The ESCRT pathway was initially defined in yeast genetic screens to identify the factors necessary to sort membrane proteins into intraluminal endosomal vesicles. ESCRT-dependent exosome biogenesis includes ubiquitin-dependent and ubiquitin-independent ESCRT sorting signals. The canonical mechanism by which ESCRT is activated is initiated by the recognition of ubiquitinated membrane proteins on cell membranes. Ubiquitinated endosomal proteins that are deposited into the lumens of MVBs are either sorted for lysosomal-mediated degradation or secreted as exosomes into the extracellular milieu. The ESCRT system includes four protein complexes: ESCRT-0, ESCRT-I, ESCRT-II, and ESCRT-III (26, 27). The ESCRT-0 complex is first activated by phosphatidylinositol 3-phosphate PI (3)P and ubiquitinated molecules on the multivesicular membrane (28). Subsequently, the ESCRT-I complex is recruited by ESCRT-0 with the help of the hepatocyte growth factor-regulated tyrosine kinase substrate prosaposin (HRS PSAP) subunits, which can be promoted by heparanase (endosomal enzyme) (29). The interaction between ESCRT-I and ESCRT-II is mediated through VPS28 and EAP45 (Vps36) subunits, which are essential for sorting cargo in the MVBs and deforming the membrane, resulting in bud formation (30–32). ESCRT-III aggregates at the neck of the bud and causes the sprout to shear, thereby releasing ILVs and driving vesicle scission from MVBs. The VPS4/VTAL complex is hydrolyzed by ATPase, which provides energy to depolymerize the polymerized ESCRT-III for recycling to complete further budding processes (33). The membrane protein syntenin combines with the cytoplasmic protein syndecan and ALIX accessory protein to form a ternary complex. This complex can interact with the TSG101 domain of ESCRT I and the CHMP4 domain of ESCRT III and participate in the ESCRT-dependent pathway for exosome secretion (34–36).

Other groups of researchers recently reported that some ESCRT-related proteins can be recruited independently of ubiquitination to promote exosome secretion by cargos. The post-translational attachment of small ubiquitin-like modifier (SUMO) to proteins plays a vital role in mediating ESCRT-dependent sorting into EVs. SUMO is a small ubiquitin-like protein consisting of more than 100 amino acid residues with a molecular weight of approximately 12 kDa. It is named after ubiquitin, with which it shares a similar mode of action and spatial structure. SUMOylation is a covalent modification similar to ubiquitination in which the terminal diglycine configuration of SUMO forms an isopeptide bond with the E-amino group of the substrate protein lysine. Unlike ubiquitination, which often mediates the degradation of target proteins, SUMOylation modification is thought to enhance the stability of target proteins (37, 38). SUMO is recruited to ESCRT formation sites by interacting with phosphoinositols and requires the ESCRT subunits Tsg101 and VPS4, as well as the ESCRT-associated protein Alix. Furthermore, the release of the cytosolic protein α-synuclein within EVs in human cerebrospinal fluid is SUMO-dependent (39, 40). Liu et al. demonstrated the existence of a ubiquitin-independent pathway; for example, the COP9 signalosome (CSN)-associated protein CSN5 can regulate the sorting of exosomal proteins (such as HSP70 and HIV Gag protein) in both a deubiquitinating activity-dependent and -independent manner (41).

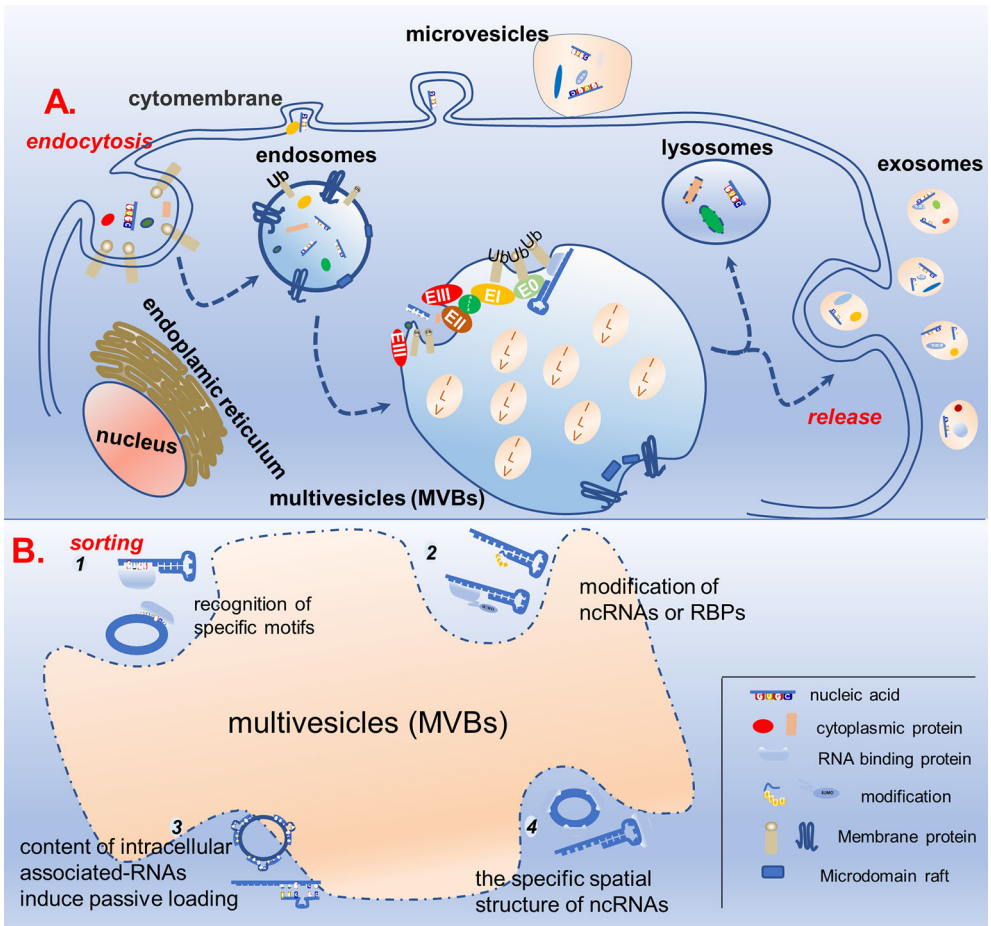

FIGURE 1 | Schematic diagram of exosome biogenesis and potential mechanisms for sorting non-coding RNA. **(A)** Proteins and nucleic acids are secreted into extracellular vesicles through budding and fission of the cell membrane, while others enter the cell through the endocytosis pathway to form endosomes, which further mature into multivesicles bodies. In the multivesicles, membrane invagination, budding, and fission results in the formation of ILVs in ESCRT-dependent and ESCRT-independent manners. ILVs either fuse with lysosomes to degrade the cargos or dock with the cell membrane to be released, forming biological exosomes. **(B)** In the process of ILVs formation, specific non-coding RNAs are specifically sorted into ILVs. There are four possible mechanisms, as follows: (1) recognition of specific motifs on non-coding RNAs by RBP; (2) modification of non-coding RNAs or RBPs capable of binding to them to help them wrapped in ILVs; (3) the content of intracellular associated-RNAs modulate ncRNAs' sorting into ILV; (4) the specific spatial structure of non-coding RNAs also affects its ability to enter ILVs.

ESCRT-Independent Mechanism in the Biogenesis of Exosomes

Katarina et al. were the first to discover an ESCRT-independent exosome formation mechanism. They provided evidence that intracellular ceramide was deposited with the depletion of the neutral sphingomyelinase enzyme, which induces the coalescence of small raft-based microdomains into larger domains, promoting domain-induced budding (42). Subsequently, Aude et al. revealed the presence of lipid raft microdomains in exosomal membranes and indicated their possible involvement in vesicle formation and structure (43). Tetraspanins, a family of four transmembrane proteins, were shown to be responsible for exosome formation (44). Similarly, Van Niel found that tetraspanin CD63 directly participates in ESCRT-independent biogenesis of the PMEL (a component of melanocyte lysosome-related organelles) luminal domain, rather than traditional ESCRT-dependent cargoes, to ILVs (45). CD82 and CD9, which are also tetraspanin membrane proteins, induce beta-catenin export *via* exosomes, which are blocked by a sphingomyelinase inhibitor (46). Other tetraspanin membrane proteins, such as Tspan8, including CD106 and CD49d, as well as CD81 (RacGTPase), are also considered to be involved in the ESCRT-independent pathway (47, 48). Exosomal cholesterol secretion depends on the presence of flotillin protein (49). Many other molecules are also involved in the formation of exosomes, and further details need to be explored (50–52).

Another ESCRT-independent mechanism is RAB GTPase-dependent exosome generation. RAB GTPases are positioned on the surface of a specific membrane structure and regulate the vesicle transport of the corresponding membrane structure by recruiting effector factors. For example, RAB5 regulates the formation and mutual fusion of the endoplasmic reticulum.

The transition from RAB5 to RAB7 on the endosome membrane regulates the transition from the early endosome to the late endosome. RAB7 regulates the fusion of late endosomes and lysosomes to degrade ILVs, whereas RAB27 regulates the docking and fusion of MVBs and membranes to release ILVs to form exosomes. The membrane proteins of endocytosis, especially the receptor tyrosine kinase family epidermal growth factor receptor (EGFR), are located in the endosome and MVBs and initiate lysosomal degradation through the fusion of MVBs and lysosomes. Kang et al. conducted experiments to knock down the ESCRT components HRS and TSG101 as well as the related protein Alix. As a result, they found that these were not involved in the formation of EGFR exosomes driven by $RAB31^{Q65L}$. Active RAB31 drove EGFR into MVBs to form ILVs and exosomes, whereas EGFR phosphorylated RAB31 to drive homologous exosomes. Flotillin protein in the lipid raft microdomain was involved in the formation of ILVs driven by active RAB31, which was independent of the ESCRT mechanism. It was further proved that RAB31 recruited TBC1D2B to inactivate RAB7, inhibit the fusion of MVBs and lysosomes, and further promote the production of exosomes (53–55).

POSSIBLE SORTING MECHANISM OF EXOSOMAL NCRNAS

The higher enrichment of certain ncRNAs in exosomes secreted by cells in specific states indicates that exosomal ncRNA encapsulation is an intense biological process that initiates exosomal ncRNA signaling. However, the exact cellular process responsible for selective specific exosomal ncRNA enrichment has not been well established in eukaryotic cells (**Table 1**).

RNA-Binding Proteins Mediate ncRNAs Sorting Depending on Their Characteristic Motif

It is worth noting that almost all RNAs in cells exists as ribonucleoprotein (RNP) complexes. As such, proteins capable of interacting with RNA (i.e., RBPs) can be critical factors for the promotion of ncRNA transmission in the parent cells and can serve as the intracellular inducers of ncRNA loading in exosomes in the recipient cell (76). It has also been reported that short nucleotide sequences on RNA can guide its transport to different subcellular compartments, including exosomes (77–80).

Proteomic analyses have detected the specific binding of heterogeneous nuclear RNP A2B1 (hnRNPA2B1) to exosomal miR-198 with the RTS motifs. hnRNPA2B1, which is present in exosomes, binds to exosomal miRNA directly and controls its loading into these microvesicles. Moreover, hnRNPA2B1 in exosomes is SUMOylated, and SUMOylation controls the binding of hnRNPA2B1 to miRNAs (77, 79, 81, 82). Another recent study found that epirubicin-treated endothelial cells specifically regulated the extracellular separation of miR-503 by disrupting hnRNPA2B1 (83). In addition to miRNAs, hnRNPA2B1 has been found to specifically regulate lncRNAs. There is a special motif at the 5′ end of lncARSR that can bind to the RBP hnRNPA2B1 and has been sorted into exosomes together with the target miR-198 of lncARSR (15). Lei et al. identified that the expression of lncRNA H19 was upregulated in gefitinib-resistant non-small cell lung cancer (NSCLC) cells and that there was a GGAG substrate in the 5′ terminal region, which was bound to hnRNPA2B1 protein to be specifically sorted into exosomes (73). In trastuzumab-resistant breast cancer cells, hnRNPA2B1 is overexpressed or silenced, and exosome AGAP2AS1 expression is upregulated or downregulated (74). Moreover, lncRNA LNMAT2 specifically binds to hnRNPA2B1 and is packaged into exosomes through its specific sequence of GGAG in the 1930–1960-nt region and the stem-loop structure in this region (75).

Serine and arginine rich splicing factor 1 has been identified as a mediator of exosomal miRNA enrichment in pancreatic cancer cells by binding to a specific miRNA sequence motif (64). Major vault protein can selectively enrich miR-193a to exosomes and reduce its intracellular content; however, this specific interaction region has not been studied. In turn, MiR-193a can affect its target GTPase Rab27B and exosome production (65, 66, 84, 85). Zhang et al. suggested that exosomes package circular RNAs (circRNAs) containing the purine-rich 5′-GMWGVWGRAG-3′ motif, with the characteristic "garbage dumping" and "intercellular signaling" functions (72). Zietzer et al. confirmed that the export of miRNAs into EVs depends on the binding efficiency of the respective miRNAs to hnRNPU. miR-30c-5p, the most significant miRNA regulated by hnRNPU, retains a significant enrichment of the sequence motif AAMRUGCU as a transport signal (56). Wozniak et al. identified a common short sequence of the "AAUGC" motif present in miRNAs that are selectively loaded into exosomes after RILP cleavage, which promotes the movement of MVBs toward the cell periphery and induces selective exosomal miRNA cargo loading. This motif binds the RBP FMR1 and directs miRNA loading into exosomes by interacting with components of the ESCRT pathway (57, 86). Syncrip/hnRNPQ, a highly conserved RBP, can identify hEXO (GGCU/A) sequences in target miRNAs and mediate exosome enrichment through the collaboration of the non-canonical N-terminal RNA recognition region NURR domain and the classical RRM domain (61, 62). Additionally, miR-133 was specifically sorted into H/R-induced EPC-derived exosomes *via* YBX-1 to increase fibroblast angiogenesis and MEndoT (87). Recent discoveries have indicated that circulating Ago2 complexes are responsible for the stability of plasma miRNAs through the KRAS-MEK-ERK signaling pathway, protecting miRNAs contained within EVs from RNase degradation (67, 88, 89). Considering RNA-binding ubiquitin E3 ligase (MEX3C) associates with Ago2 and the adaptor-related protein complex 2 (AP-2), which is involved in miRNA sorting, containing a C-terminal RING finger domain and the hnRNP K homology (KH) domain, miR-451a is specifically sorted into exosomes *via* a ceramide-dependent pathway (90, 91) In general, the concept that specific ncRNA motif binding to RBP is involved in exosomal ncRNA sorting has been confirmed in different types of cells.

TABLE 1 | Summary of non-coding RNAs and their possible sorting mechanism.

RNA Type	Disease/ source	Molecular partner	Sorting mechanism	Reference
miRNA	Endothelial cell	RBP: hnRNPU	Exosomal miR-30c-5p is selected through its motif AAMRUGCU binding to hnRNPU.	(56)
miRNA	Inflammation	RBP: FMR1	FMR1 and lysosomal protein cRILP co-ordinate the loading of miRNAs with AAUGC motif into exosomes.	(57)
miRNA	Cutaneous injury	RBP: hnRNPA2B1	SUMOylated hnRNPA2B1 directs the loading of certain miRNAs through the recognition of specific short motifs, such as the GGAG tetraloop.	(58, 59)
miRNA	Epithelial cells	RBP: hnRNPA2B1	Membrane protein cav-1 tyrosine 14 (Y14) phosphorylation interacts with the O-GlcNAcylated hnRNPA2B1, leading to a change in miRNA-17/93 expression bound to hnRNPA2B1.	(60)
miRNA	Hepatocyte	RBP: Syncrip/ hnRNPQ	Syncrip identifies hEXO (GGCU/A) sequences in target miRNAs through the collaboration of the non-canonical N-terminal RNA recognition region NURR domain and the classical RRM domain.	(61, 62)
miRNA	HEK293T cells	RBP: YBX1	YBX1 interacts with miR-223 through its internal cold shock domain to form hairpin-loop secondary structure, rather than specific recognition motif, which promotes the separation of miR-223 into exosomes.	(63)
miRNA	Pancreatic cancer cells	RBP: SRSF1	SRSF1 mediates enrichment in exosomes of miRNAs with a specific common short motif (e.g., miR-1246) with a motif length of 6 bp and GG bases at positions 3 and 4.	(64)
miRNA	Colon cancer cell	Major vault protein (MVP)	MVP can selectively enrich miR-193a to exosomes and reduce its intracellular content, however, the specific interaction region has not been studied. MiR-193a in turn can affect its target GTPase Rab27B and affect exosome production.	(65, 66)
miRNA	Colon cancer cell	AGO	Ago2 complexes are responsible for the stability of plasma miRNAs, such as miR-16. However, the exact mechanism underlying this interaction remains clear.	(67)
miRNA	Human colonic NCM460 epithelial cells	SP/NK-1R signaling	SP/NK-1R signaling increased the production of exosomes and the level of miR-21 in the exosome cargo.	(68)
miRNA	Human B cells	3' uridylation/ uridinetransferase	MiRNAs with 3' uridylation were more likely to be secreted into exosomes. This may underlie the mechanism by which cells regulate specific miRNAs functions: either the 3' uridylation of miRNAs may destabilize RNA, or there is a uridinetransferase in the exocrine (e.g., ZCCHC11 mediates the addition of uracil at the miR-26a terminal).	(69)
miRNA	Prostate cancer cells	3'-end uridylation	Post-transcriptional 3'-end uridylation of miR-2909 can drive the recruitment of this miRNA for sorting into exosomes.	(70)
circRNA	Platelets	—	Platelets selectively encapsulate shorter size circRNA into exosomes, which may also be related to the RBP binding of circRNA.	(71)
circRNA	HepG2 cells	—	circRNAs with a common 5'-GMWGVWGRAG-3' motif appear to be more likely to be sorted into exosomes.	(72)
lncRNA	Renal cell carcinoma cell	hnRNPA2B1	There is a special motif at the 5'-end of lncARSR that is able to bind to the RNA-binding protein hnRNPA2B1 and has been sorted into exosomes together with the target miR-198 of lncARSR.	(15)
lncRNA	Human NSCLC cell	hnRNPA2B1	The expression of lncRNA H19 was upregulated in gefitinib-resistance cells of NSCLC. There was also a GGAG substrate in the 5' terminal region, which was bound to hnRNPA2B1 protein, allowing for its specific sorting into exosomes	(73)
lncRNA	Human breast cancer cell	hnRNPA2B1	In trastuzumab-resistant breast cancer cells, hnRNPA2B1 is overexpressed or silenced, and exosome AGAP2AS1 expression is correspondingly up-regulated or decreased.	(74)
lncRNA	Bladder cancer cell	hnRNPA2B1	lncRNA LNMAT2 specifically binds to hnRNPA2B1 and is packaged into exosomes through its specific sequence of GGAG on the 1930-1960 nt region and the stem-loop structure in this region.	(75)

— No specific molecules were found.

Modification of ncRNAs or RBPs Guide Their Sorting Into Exosomes

Collectively, current research is beginning to uncover new mechanisms by which exosomes are involved in the post-transcriptional modification of ncRNA (92). Reports have shown that miRNAs are modified through a series of processing events after transcription, such as 5′-end phosphorylation, 3′-end adenylation or uridylation, and terminal nucleotide deletion. Khan et al. attempted to develop a method for competence-mass spectrometry, which can be used to perform a multiplex, direct analysis of miRNAs from biological samples, and revealed modifications of miRNAs in serum samples (93). Koppers et al. performed RNA sequencing and bioinformatics analysis and found a non-random distribution of miRNAs between B cells and exosomes. Subsequently, in the urine samples, the 3′-terminal adenylation miRNAs were relatively enriched in the cells, whereas the 3′-end uridine subtypes were found in excess in the exosomes, suggesting that post-transcriptional modifications, especially 3′-end adenylation and uridylation, play the opposite role and may at least partially guide the entry of ncRNAs into exosomes (69). Wani et al. revealed that post-transcriptional modifications, especially 3′-end adenylation and uridylation of miR-2909, exert opposing effects that may contribute to its sorting into exosomes secreted by cancer cells (70).

Emerging evidence suggests that the post-translational modification of RBPs also has a considerable influence on the sorting of specific ncRNAs. Lee et al. showed that cav 1 14 (Y14)-tyrosine phosphorylation leads to interactions between caveolin 1 (cav 1) and hnRNPA2B1. Cav 1, as a lipid-raft scaffolding protein,

has been proposed to induce local membrane composition and curvature, constitutes a complex with HNRNPA2B1-miRNAs, subsequently directs theirs their routing towards exosomes in lung epithelial cells. Oxidative stress induces the O-GlcNAcylation of hnRNPA2B1, resulting in a robustly altered hnRNPA2B1-bound miRNA repertoire. Notably, cav-1 pY14 also promoted hnRNPA2B1 O-GlcNAcylation. Functionally, macrophages serve as the principal recipients of epithelial EVs in the lungs. EV-containing cav-1/hnRNPA2B1 complex-bound miR-17/93 activates tissue macrophages (60). Furthermore, hnRNPA2B1 in exosomes is SUMOylated, which controls the binding of hnRNPA2B1 to miRNAs (58). The KRAS-MEK-ERK pathway-dependent phosphorylation of Ago2 has been demonstrated to exert specific control over the sorting of let-7a, miR-100, and miR-320a into exosomes (94).

Content of Intracellular Associated RNAs Modulates the Sorting of ncRNAs Into Exosomes

It has been reported that ncRNAs can be modulated by their upstream or downstream RNAs, thus being packaged into exosomes either *via* passive leakage or in an active secretion manner. The most classical is the RNA processing of miRNA, which affects miRNA enrichment in exosomes. It is known that miRNA maturation in the cytoplasm requires a type II endoribonuclease known as the Dicer enzyme. It cleaves the stem loop structure of pre-miRNA and produces ~22-nt miRNA double strands, which are unwound into mature single-stranded miRNAs and combined with RNA-induced silencing complex (RISC). The co-localization and accumulation or relocalization of miRISC components in MVBs is thought to facilitate the sorting of miRNAs into exosomes (95, 96).

It has been proven that ncRNAs can interact with their target RNAs to regulate the content of their own or target RNAs in cells, after which they are sorted into exosomes passively or actively. Squadrito et al. suggested that the occurrence of physiological (cell-activation-dependent) or artificial overexpression of miRNA target sequences (mRNA) in macrophages contributes to the enrichment of the corresponding miRNA exosomes and P-bodies. Perhaps, through such a mechanism, the miRNA loading in the producer cells can be reduced; however, through this mechanism, the activity of miRNA can be affected and cell homeostasis can be successfully achieved (97). In renal cell cancer cells, Qu et al. found a new lncRNA, lncARSR, which has a specific GGAG/CCCU at its 5′-end and can bind to the RBP hnRNPA2B1 and is selected as an exosome. Interestingly, the target of lncARSR, miR-198, rather than the target miR-18a, can be secreted into the exosomes along with the lncARSR-hnRNPA2B1 complex (15, 58). In HEK293T and MCF-7 cells, miR-7, the target of CDR1as, was artificially upregulated. Subsequently, Li et al. observed that CDR1as circRNA levels in exosomes were significantly downregulated. This result indicates that the sorting of circRNA to exosomes may be regulated by the level of related miRNAs in the production cells and may transfer biological activity to the recipient cells (98).

Secondary/Tertiary Structure of ncRNAs Regulates Their Sorting

These interactions could occur because the secondary/tertiary structures of ncRNAs, as opposed to those of other nucleic acid sequences, partially result in a greater protein binding capacity. Shurtleff et al. discovered that RBP Y-box protein I (YBX1) binds to and is required for the sorting of miR-223 in HEK293T cells. YBX1 interacts with miR-223 through its internal cold shock domain to form a hairpin-loop secondary structure, rather than a specific recognition motif, which promotes the separation of miR-223 into exosomes (63). Platelets are rich in circRNAs and seem to be more inclined to secrete smaller-sized circRNAs into exosomes than larger ones. It is reasonable to speculate that the mechanism by which circRNAs are sorted into exosomes is related to their circular tertiary structure, which needs to be further characterized (71).

CLINICAL APPLICATION OF EXOSOMAL NCRNAS

Biological Effects of Exosomal ncRNAs

Exosomes are known to be rich in biological information (proteins, nucleic acids, etc.). They are not only acting as tissue sampling to reflect the state of parent cells, but also representative tools to transmit cell-to-cell communication information. Exosomes play a vital role in mediating cell–cell communication and transporting cargo from donor cells to recipient cells, regardless of whether the recipient cells are located in distant or nearby tissues (7, 99). Bidirectional cell–cell communication involving exosome-borne cargos, such as ncRNAs, has emerged as a critical mechanism. As natural intercellular shuttles of ncRNAs, exosomes influence an array of developmental, physiological, and pathological processes in the recipient cell or tissue to which they can be selectively targeted (**Figure 2**) (100). For example, Exosomal ncRNAs could interact with many inflammatory factors and inflammatory cells to influence the progression of inflammatory diseases. The exosomes promoted macrophage M1 differentiation at least partially *via* transferring pro-inflammatory miRNAs, such as miR-155. Moreover, exosome-mediated miR-155 inhibitor delivery significantly prevented DSS-induced colitis (101). Hepatocyte exosomes induced by lipotoxic injury are rich in miR-192-5p. It can regulate the Rictor/Akt/FoxO1 signaling pathway, induce an increase in the expression of M1 macrophages and inflammatory factors, and affect the progression of steatohepatitis (102). Exosomes from patients with septic shock convey miRNAs and mRNAs related to inflammatory response for intercellular communication (103). In general, exosomal ncRNAs are essential as a major contributor that regulates delivery and reduces inflammatory response (59). The ncRNAs content of exosomes could be regulated by the physiological state of cells and may play a role in maintaining tissue homeostasis and synchronizing the functional state of cells. For example, miRNAs transferred from mother's milk to the infant may play a crucial role in the development of the

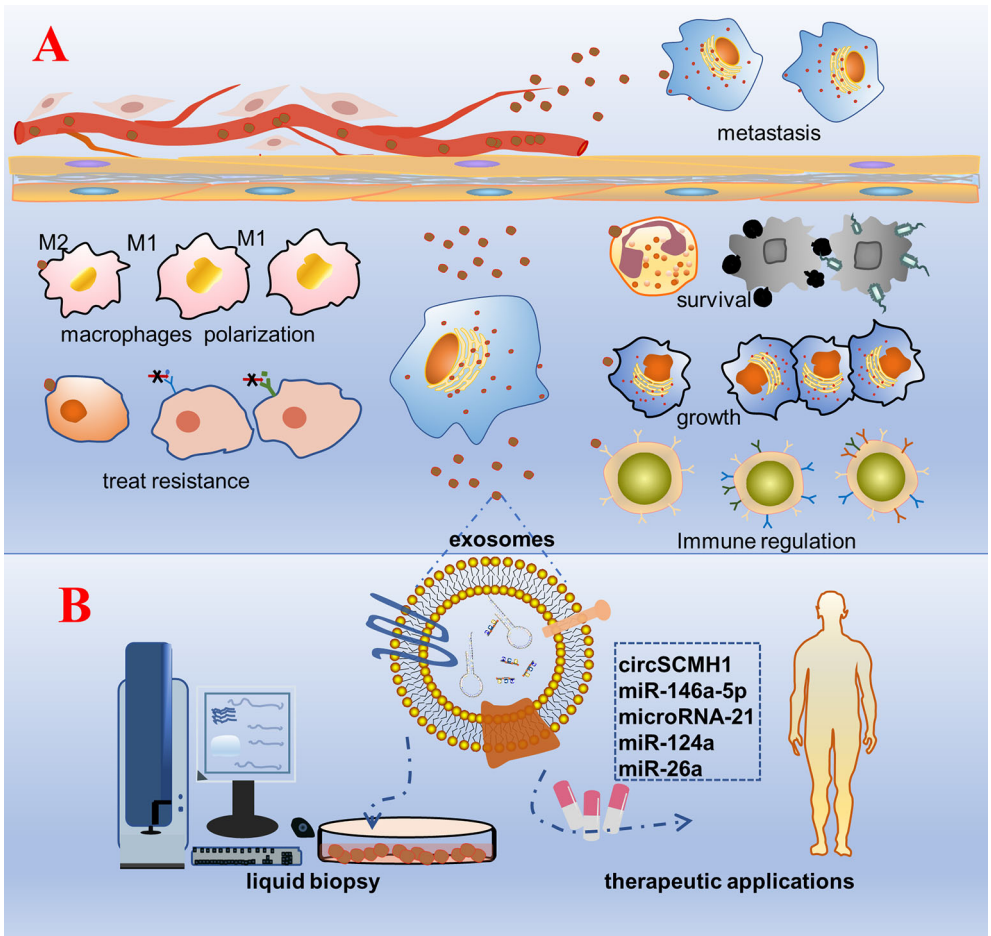

FIGURE 2 | Schematic diagram of the biological function and clinical application prospects of exosomal non-coding RNAs. **(A)** Biological function: cells are stimulated by factors, such as tumorigenesis, secrete exosomes wrapped with bioactive non-coding RNAs, and are accepted by the recipient cell. As a result, a series of phenotypic changes occur: pathogenic microorganisms escape the body's immune surveillance to survive; growth of specific recipient cells; regulation of the number and functions of immune cells, such as T cells and NK cells; polarization of macrophages and the inflammatory response; change in the tolerance of the recipient cells to treatment; transmission to distant tissue cells through body fluids inducing cancer metastasis. **(B)** Clinical application: purification, separation, and detection of exosomes in various body fluids, construction of a platform for rapid detection and analysis of diseases, and engineering of exosomal non-coding RNAs that are promising for treatment.

infant's immune system (104). Exosomal miRNAs have been proven to act as regulators of neuron- astrocyte crosstalk, osteoblast differentiation, myoblast differentiation, and so on (105–108). Exosomal ncRNAs play a key role in premetastatic niche formation and metastasis (109, 110). Zhang et al. observed that the expression of circSATB2 in serum exosomes of patients with NSCLC was higher than that in non-cancerous donors, which was related to lymph node metastasis of lung cancer and could promote the proliferation of normal bronchial epithelial cells. This suggests that exosomal circSATB2 can transmit cell communication and promote the metastasis of tumor cells (111). Exosomes imposed by pathogenic microorganisms, such as viruses, bacteria, and parasites, may be exploited for the superior delivery of ncRNAs to evade host immune surveillance *in vivo* (112–114). *Schistosoma japonicum* egg-derived exosomal Sja-miR-71a attenuated pathological progression and liver fibrosis in *S. japonicum* infection (115). Adult *Schistosoma* secretes exosomal miRNAs that are internalized by Th cells to evade immune surveillance (116). Exosomes are soluble biological mediators obtained from mesenchymal stem cells (MSCs) cultured *in vitro*. MSC-derived exosomes produced under physiological or pathological conditions are central mediators of intercellular communication by transporting proteins, lipids, mRNAs, siRNA, rRNAs, and ncRNAs to neighboring or distant cells.

Exosomal ncRNA as a Specific Biomarker for Liquid Biopsy

Liquid biopsy is a minimally invasive method for analyzing solid tissues, blood, and other body fluids. Exosomes can be conveniently detected in almost all human body fluids, making them an ideal indicator for liquid biopsy. Exosomes derived from

different cell types and statuses have been shown to possess distinct RNA profiles, particularly ncRNAs. These new analytes represent an alternative tool to complement the diagnosis, monitoring, and prediction of response to treatment of tumor processes, as well as other human disease processes, such as those in viral and parasitic infections (117, 118). ncRNAs are important regulators of cellular signaling that can be detected and released into circulation with high stability *via* packing in exosomes (119–122). Therefore, the use of exosomal ncRNAs has promising prospects in liquid biopsy in case of diseases and may continue to be an exciting focus of research in the field.

Owing to the rapid development of various exosome detection technologies in recent years, exosomal ncRNAs have become a specific and effective biomarker for clinical liquid biopsy (123–125). Methods of exosome isolation to date include ultracentrifugation (mostly approved for exosome purity), ultrafiltration, size-exclusion chromatography, polymer precipitation, immunoaffinity chromatography, and microfluidics-based techniques (126–128). Wang et al. described the construction and testing of an electrochemical biosensor for the sensitive detection of exosomal miRNAs. The electrochemical biosensor exhibited good selectivity for miR-21 detection; showed benefits of simple operation, low cost, and portability; and provided a promising platform for the early diagnosis and screening of tumor biomarkers and the development of devices for point-of-care testing (129). Wu et al. established a platform for the simultaneous multiplex analysis of multiple exosome biomarkers (such as proteins and miRNAs) in clinical biological fluids, which not only allows for the observation of the tissue status of biomarkers in clinical samples but also shows that exosome subsets can more accurately distinguish the prognosis of patients (130). Zabegina et al. isolated exosomes with thyroid-specific surface molecules by immunobeads followed by miRNA analysis, demonstrating possibly improved diagnostic potency (130). Serum exosomal miRNA profiles of steroid-induced osteonecrosis of the femoral head (SONFH) and hsa-miR-135b-5p may be a unique diagnostic biomarker for SONFH (131). Zheng et al. found that the expression level of exosomal lnc-SLC2A12-10:1 was significantly correlated with tumor size, TNM stage, lymph node metastasis, and degree of differentiation, suggesting that exosomal lnc-SLC2A12-10:1 may be a potential noninvasive biomarker for the diagnosis and prognosis monitoring of gastric cancer (132). In summary, ncRNAs derived from exosomes are considered potential new biomarkers for various diseases, especially cancer, and can be easily detected in liquid biopsies.

Therapeutic Applications of Engineered Exosomal ncRNAs

A variety of ncRNA molecules are known to function in human diseases. However, safety issues with delivery systems have limited the exploration of the potential therapeutic roles of ncRNAs. Engineered EVs carrying therapeutic molecules are promising candidates for disease therapy. In recent years, exosomes have been discovered with low immunogenicity, positive safety in clinical trials, and the ability of selectively homing to inflammation and tumor sites. Therefore, engineered exosomal ncRNAs have great therapeutic potential (133–137).

Yang et al. found that in an ischemic stroke model, the engineered extracellular vesicular rabies virus glycoprotein-circSCMH1 selectively transmits circSCMH1 to the brain and mechanically binds to the transcription factor MeCP2, thus resulting in the inhibition of MeCP2 target gene transcription and promoting the functional recovery of stroke in animals (138). Exosomal miRNAs and proteins isolated from hiPSC-NSC cultures have many functions, such as neuroprotection and anti-inflammation. The intranasal administration of exosomes can be absorbed by a variety of nerve cells, which is beneficial for brain repair after injury or disease (139). A separate study showed that secreted exosomes coated with miR-146a-5p from MSCs relieved Group 2 innate lymphoid cells (ILC2s) in innate airway inflammation, showing significant advantages of low immunogenicity and high biosafety (140). Engineered exosomes loaded with anti-inflammatory agents, such as miRNA-21, could be used to target macrophages in the inflammatory region to regulate inflammatory responses for achieving the ability to regulate inflammatory responses when needed (141). Engineered exosomal ncRNAs have also shown great advantages in the treatment of tumors. In addition to the unique properties of MSCs, MSC-derived exosomal ncRNAs exert desirable therapeutic effects (142). Lang et al. reported that bone marrow-derived MSCs could encapsulate miRNAs, such as miR-124a, into exosomes, and these engineered exosomes could be used to treat mice harboring intracranial glioma stem cell. It was found that engineered exosomes could systematically transmit anti-glioma miRNAs to glioblastomas for longer survival (143). Liang et al. introduced a new approach for the targeted delivery of exosomes loaded with functional miR-26a to scavenger receptor class B type 1-expressing liver cancer cells, resulting in decreased rates of cell migration and proliferation (144).

CONCLUSION

Nanoscale exosomes encapsulating a variety of cargos, including ncRNAs, which protect the cargo from degradation by various enzymes in the extracellular space, are vital for intracellular and intercellular communication. Exosomes can be selectively secreted *via* ESCRT-dependent or ESCRT-independent pathways. Exosomes have multiple functions in physiological and pathological processes, and ncRNAs can also play an important regulatory role in these processes. The relationship between them has attracted great research interest in recent years. Subsequently, an increasing number of studies have revealed that exosomal ncRNAs are involved in pathogenic microbial infection and inflammatory disease, tumor invasion and metastasis, immunoregulation and immunotherapy, and resistance to treatment. However, how ncRNAs in exosomes are selectively packaged and then transported to target cells remains unclear, which hinders the prospects of clinical

applications of exosomal ncRNAs as biomarkers. Elucidating the mechanism by which cells sort specific ncRNAs into the circulation will aid in the selection of more representative exosomal RNAs and pave the way for advances in the early diagnosis of diseases. Exosomal ncRNAs can transmit signals, such as those involved in growth promotion, invasion, metastasis, and angiogenesis. Moreover, animal experiments have confirmed their effect on the disease phenotype. Thus, we believe that understanding how these disease-causing or disease-suppressing exosomal ncRNAs are sorted, secreted, and spread to adjacent or distant cells in the initial stages of a disease will underlie the development of timely, accurate, and effective early intervention measures.

Although plenty of methods have been developed to isolate exosomes, it has been found that extracellular ncRNAs could be mixed with a variety of exosomal vectors such as lipoprotein and Argonaute protein, which obviously interferes with the accuracy of studies on exosomal ncRNAs. Therefore, researchers are making unremitting efforts to improve the technology of exosome purification and separation. In addition, exosomes have been recognized as a class of aggregated nanoparticles with different properties of extracellular vesicles. Currently, there is a lack of specific characterization of the heterogeneity of different exosome subtypes. Significant differences of the proteins, lipids, and nucleic acids contained in different exosome subtypes have been demonstrated. The heterogeneity of secreted nanoparticles is increasingly recognized. Numerous studies have exploited new technologies to characterize EV subtypes. Ayuko Hoshino and his team deconvolved the heterogeneity of extracellular nanoparticles and defined three distinct subsets: small exosomes (Exo-S, 50–70 nm), large exosomes (Exo-L, 90–120 nm) and exomeres. The exomeres obtained through sequential ultracentrifugation (SUC) were non-membranous particles (<50 nm). Many of the most abundant miRNAs are more associated with extracellular exomeres than parent cells or Exo-S components. Furthermore, some RBPs proved to be related to the mechanism of sorting ncRNA, such as YBX1 and MVP protein, were also strongly correlated with exomeres components. Therefore, there is an urgent need to identify signature proteins that can more effectively distinguish EV subtypes (145–149). Therefore, the application of the enriched ncRNAs in different exosome subtypes in liquid biopsy or clinical treatment also needs further study.

Technological advances have enabled researchers to opt for more effective methods for the separation of high-purity exosomes, allowing for the in-depth study of the mechanism underlying the non-random distribution of functional molecules to exosomes in cells. It is reasonable to speculate that hundreds of millions of patients, especially those with poor treatment outcomes, will greatly benefit from the in-depth study of the mechanism and role of exosomal ncRNAs.

AUTHOR CONTRIBUTIONS

YQ and MW conceived, wrote, and edited the manuscript. YQ and PL designed figures and wrote and edited the manuscript. MW and ZZ wrote and edited the manuscript. All authors contributed to the article and approved the submitted version.

FUNDING

This work is supported by grants from the National Science Foundation for Young Scientists of China (Grant 81802871); Graduate Scientific Research and Innovation Project of Central South University (No. 1053320192778).

ACKNOWLEDGMENTS

We are very grateful to the many researchers working in this field.

REFERENCES

1. Hoshino A, Kim HS, Bojmar L, Gyan KE, Cioffi M, Hernandez J, et al. Extracellular Vesicle and Particle Biomarkers Define Multiple Human Cancers. *Cell* (2020) 182(4):1044–61.e18. doi: 10.1016/j.cell.2020.07.009
2. de Jong OG, Kooijmans SAA, Murphy DE, Jiang L, Evers MJW, Sluijter JPG, et al. Drug Delivery With Extracellular Vesicles: From Imagination to Innovation. *Acc Chem Res* (2019) 52(7):1761–70. doi: 10.1021/acs.accounts.9b00109
3. Mateescu B, Kowal EJ, van Balkom BW, Bartel S, Bhattacharyya SN, Buzas EI, et al. Obstacles and Opportunities in the Functional Analysis of Extracellular Vesicle RNA - an ISEV Position Paper. *J Extracell Vesicles* (2017) 6(1):1286095. doi: 10.1080/20013078.2017.1286095
4. Anand S, Samuel M, Kumar S, Mathivanan S. Ticket to a Bubble Ride: Cargo Sorting Into Exosomes and Extracellular Vesicles. *Biochim Biophys Acta Proteins Proteom* (2019) 1867(12):140203. doi: 10.1016/j.bbapap.2019.02.005
5. Janas T, Janas MM, Sapon K, Janas T. Mechanisms of RNA Loading Into Exosomes. *FEBS Lett* (2015) 589(13):1391–8. doi: 10.1016/j.febslet.2015.04.036
6. Villarroya-Beltri C, Baixauli F, Gutierrez-Vazquez C, Sanchez-Madrid F, Mittelbrunn M. Sorting it Out: Regulation of Exosome Loading. *Semin Cancer Biol* (2014) 28:3–13. doi: 10.1016/j.semcancer.2014.04.009
7. O'Brien K, Breyne K, Ughetto S, Laurent LC, Breakefield XO. RNA Delivery by Extracellular Vesicles in Mammalian Cells and its Applications. *Nat Rev Mol Cell Biol* (2020) 21(10):585–606. doi: 10.1038/s41580-020-0251-y
8. Kalluri R, LeBleu VS. The Biology, Function, and Biomedical Applications of Exosomes. *Science* (2020) 367(6478):eaau6977. doi: 10.1126/science.aau6977
9. Battaglia R, Musumeci P, Ragusa M, Barbagallo D, Scalia M, Zimbone M, et al. Ovarian Aging Increases Small Extracellular Vesicle CD81(+) Release in Human Follicular Fluid and Influences miRNA Profiles. *Aging (Albany NY)* (2020) 12(12):12324–41. doi: 10.18632/aging.103441
10. Mathieu M, Martin-Jaular L, Lavieu G, Thery C. Specificities of Secretion and Uptake of Exosomes and Other Extracellular Vesicles for Cell-to-Cell Communication. *Nat Cell Biol* (2019) 21(1):9–17. doi: 10.1038/s41556-018-0250-9
11. Valadi H, Ekstrom K, Bossios A, Sjostrand M, Lee JJ, Lotvall JO. Exosome-Mediated Transfer of mRNAs and microRNAs is a Novel Mechanism of

Genetic Exchange Between Cells. *Nat Cell Biol* (2007) 9(6):654–9. doi: 10.1038/ncb1596
12. Yin Y, Cai X, Chen X, Liang H, Zhang Y, Li J, et al. Tumor-Secreted miR-214 Induces Regulatory T Cells: A Major Link Between Immune Evasion and Tumor Growth. *Cell Res* (2014) 24(10):1164–80. doi: 10.1038/cr.2014.121
13. Yin J, Zeng A, Zhang Z, Shi Z, Yan W, You Y. Exosomal Transfer of miR-1238 Contributes to Temozolomide-Resistance in Glioblastoma. *EBioMedicine* (2019) 42:238–51. doi: 10.1016/j.ebiom.2019.03.016
14. Shao N, Xue L, Wang R, Luo K, Zhi F, Lan Q. Mir-454-3p Is an Exosomal Biomarker and Functions as a Tumor Suppressor in Glioma. *Mol Cancer Ther* (2019) 18(2):459–69. doi: 10.1158/1535-7163.mct-18-0725
15. Qu L, Ding J, Chen C, Wu ZJ, Liu B, Gao Y, et al. Exosome-Transmitted Lncarsr Promotes Sunitinib Resistance in Renal Cancer by Acting as a Competing Endogenous Rna. *Cancer Cell* (2016) 29(5):653–68. doi: 10.1016/j.ccell.2016.03.004
16. Slack FJ, Chinnaiyan AM. The Role of Non-coding Rnas in Oncology. *Cell* (2019) 179(5):1033–55. doi: 10.1016/j.cell.2019.10.017
17. Hong BS, Cho JH, Kim H, Choi EJ, Rho S, Kim J, et al. Colorectal Cancer Cell-Derived Microvesicles are Enriched in Cell Cycle-Related mRNAs That Promote Proliferation of Endothelial Cells. *BMC Genomics* (2009) 10:556. doi: 10.1186/1471-2164-10-556
18. Spinelli C, Adnani L, Choi D, Rak J. Extracellular Vesicles as Conduits of Non-Coding Rna Emission and Intercellular Transfer in Brain Tumors. *Noncoding RNA* (2018) 5(1):1. doi: 10.3390/ncrna5010001
19. Geng X, Lin X, Zhang Y, Li Q, Guo Y, Fang C, et al. Exosomal Circular RNA Sorting Mechanisms and Their Function in Promoting or Inhibiting Cancer. *Oncol Lett* (2020) 19(5):3369–80. doi: 10.3892/ol.2020.11449
20. Zhang WL, Liu Y, Jiang J, Tang YJ, Tang YL, Liang XH. Extracellular Vesicle Long non-Coding RNA-mediated Crosstalk in the Tumor Microenvironment: Tiny Molecules, Huge Roles. *Cancer Sci* (2020) 111 (8):2726–35. doi: 10.1111/cas.14494
21. Vignard V, Labbé M, Marec N, André-Grégoire G, Jouand N, Fonteneau JF, et al. MicroRNAs in Tumor Exosomes Drive Immune Escape in Melanoma. *Cancer Immunol Res* (2020) 8(2):255–67. doi: 10.1158/2326-6066.cir-19-0522
22. Hanson PI, Cashikar A. Multivesicular Body Morphogenesis. *Annu Rev Cell Dev Biol* (2012) 28:337–62. doi: 10.1146/annurev-cellbio-092910-154152
23. Bebelman MP, Bun P, Huveneers S, van Niel G, Pegtel DM, Verweij FJ. Real-Time Imaging of Multivesicular Body-Plasma Membrane Fusion to Quantify Exosome Release From Single Cells. *Nat Protoc* (2020) 15(1):102–21. doi: 10.1038/s41596-019-0245-4
24. Palmulli R, van Niel G. To be or Not to be... Secreted as Exosomes, a Balance Finely Tuned by the Mechanisms of Biogenesis. *Essays Biochem* (2018) 62 (2):177–91. doi: 10.1042/EBC20170076
25. Hessvik NP, Llorente A. Current Knowledge on Exosome Biogenesis and Release. *Cell Mol Life Sci* (2018) 75(2):193–208. doi: 10.1007/s00018-017-2595-9
26. Vietri M, Radulovic M, Stenmark H. The Many Functions of Escrts. *Nat Rev Mol Cell Biol* (2020) 21(1):25–42. doi: 10.1038/s41580-019-0177-4
27. Han Q, Lv L, Wei J, Lei X, Lin H, Li G, et al. Vps4A Mediates the Localization and Exosome Release of β-Catenin to Inhibit Epithelial-Mesenchymal Transition in Hepatocellular Carcinoma. *Cancer Lett* (2019) 457:47–59. doi: 10.1016/j.canlet.2019.04.035
28. Tamai K, Tanaka N, Nakano T, Kakazu E, Kondo Y, Inoue J, et al. Exosome Secretion of Dendritic Cells is Regulated by Hrs, an ESCRT-0 Protein. *Biochem Biophys Res Commun* (2010) 399(3):384–90. doi: 10.1016/j.bbrc.2010.07.083
29. David G, Zimmermann P. Heparanase Involvement in Exosome Formation. *Adv Exp Med Biol* (2020) 1221:285–307. doi: 10.1007/978-3-030-34521-1_10
30. Schoneberg J, Lee IH, Iwasa JH, Hurley JH. Reverse-Topology Membrane Scission by the ESCRT Proteins. *Nat Rev Mol Cell Biol* (2017) 18(1):5–17. doi: 10.1038/nrm.2016.121
31. Kostelansky MS, Sun J, Lee S, Kim J, Ghirlando R, Hierro A, et al. Structural and Functional Organization of the ESCRT-I Trafficking Complex. *Cell* (2006) 125(1):113–26. doi: 10.1016/j.cell.2006.01.049
32. Hierro A, Sun J, Rusnak AS, Kim J, Prag G, Emr SD, et al. Structure of the ESCRT-II Endosomal Trafficking Complex. *Nature* (2004) 431(7005):221–5. doi: 10.1038/nature02914
33. Larios J, Mercier V, Roux A, Gruenberg J. ALIX- and ESCRT-III-dependent Sorting of Tetraspanins to Exosomes. *J Cell Biol* (2020) 219(3):e201904113. doi: 10.1083/jcb.201904113
34. Sun R, Liu Y, Lu M, Ding Q, Wang P, Zhang H, et al. ALIX Increases Protein Content and Protective Function of iPSC-derived Exosomes. *J Mol Med (Berl)* (2019) 97(6):829–44. doi: 10.1007/s00109-019-01767-z
35. Ghossoub R, Lembo F, Rubio A, Gaillard CB, Bouchet J, Vitale N, et al. Syntenin-ALIX Exosome Biogenesis and Budding Into Multivesicular Bodies are Controlled by ARF6 and PLD2. *Nat Commun* (2014) 5:3477. doi: 10.1038/ncomms4477
36. Baietti MF, Zhang Z, Mortier E, Melchior A, Degeest G, Geeraerts A, et al. Syndecan-syntenin-ALIX Regulates the Biogenesis of Exosomes. *Nat Cell Biol* (2012) 14(7):677–85. doi: 10.1038/ncb2502
37. Isik S, Sano K, Tsutsui K, Seki M, Enomoto T, Saitoh H, et al. The SUMO Pathway is Required for Selective Degradation of DNA Topoisomerase IIbeta Induced by a Catalytic Inhibitor ICRF-193(1). *FEBS Lett* (2003) 546 (2-3):374–8. doi: 10.1016/s0014-5793(03)00637-9
38. Matic I, van Hagen M, Schimmel J, Macek B, Ogg SC, Tatham MH, et al. In Vivo Identification of Human Small Ubiquitin-Like Modifier Polymerization Sites by High Accuracy Mass Spectrometry and an In Vitro to In Vivo Strategy. *Mol Cell Proteomics* (2008) 7(1):132–44. doi: 10.1074/mcp.M700173-MCP200
39. Kunadt M, Eckermann K, Stuendl A, Gong J, Russo B, Strauss K, et al. Extracellular Vesicle Sorting of α-Synuclein is Regulated by Sumoylation. *Acta Neuropathol* (2015) 129(5):695–713. doi: 10.1007/s00401-015-1408-1
40. Chang HM, Yeh ETH. Sumo: From Bench to Bedside. *Physiol Rev* (2020) 100 (4):1599–619. doi: 10.1152/physrev.00025.2019
41. Liu Y, Shah SV, Xiang X, Wang J, Deng ZB, Liu C, et al. COP9-Associated CSN5 Regulates Exosomal Protein Deubiquitination and Sorting. *Am J Pathol* (2009) 174(4):1415–25. doi: 10.2353/ajpath.2009.080861
42. Trajkovic K, Hsu C, Chiantia S, Rajendran L, Wenzel D, Wieland F, et al. Ceramide Triggers Budding of Exosome Vesicles Into Multivesicular Endosomes. *Science* (2008) 319(5867):1244–7. doi: 10.1126/science.1153124
43. de Gassart A, Geminard C, Fevrier B, Raposo G, Vidal M. Lipid Raft-Associated Protein Sorting in Exosomes. *Blood* (2003) 102(13):4336–44. doi: 10.1182/blood-2003-03-0871
44. Rana S, Zoller M. Exosome Target Cell Selection and the Importance of Exosomal Tetraspanins: A Hypothesis. *Biochem Soc Trans* (2011) 39(2):559–62. doi: 10.1042/BST0390559
45. van Niel G, Charrin S, Simoes S, Romao M, Rochin L, Saftig P, et al. The Tetraspanin CD63 Regulates ESCRT-independent and -Dependent Endosomal Sorting During Melanogenesis. *Dev Cell* (2011) 21(4):708–21. doi: 10.1016/j.devcel.2011.08.019
46. Chairoungdua A, Smith DL, Pochard P, Hull M, Caplan MJ. Exosome Release of Beta-Catenin: A Novel Mechanism That Antagonizes Wnt Signaling. *J Cell Biol* (2010) 190(6):1079–91. doi: 10.1083/jcb.201002049
47. Nazarenko I, Rana S, Baumann A, McAlear J, Hellwig A, Trendelenburg M, et al. Cell Surface Tetraspanin Tspan8 Contributes to Molecular Pathways of Exosome-Induced Endothelial Cell Activation. *Cancer Res* (2010) 70 (4):1668–78. doi: 10.1158/0008-5472.CAN-09-2470
48. Perez-Hernandez D, Gutierrez-Vazquez C, Jorge I, Lopez-Martin S, Ursa A, Sanchez-Madrid F, et al. The Intracellular Interactome of Tetraspanin-Enriched Microdomains Reveals Their Function as Sorting Machineries Toward Exosomes. *J Biol Chem* (2013) 288(17):11649–61. doi: 10.1074/jbc.M112.445304
49. Strauss K, Goebel C, Runz H, Mobius W, Weiss S, Feussner I, et al. Exosome Secretion Ameliorates Lysosomal Storage of Cholesterol in Niemann-Pick Type C Disease. *J Biol Chem* (2010) 285(34):26279–88. doi: 10.1074/jbc.M110.134775
50. Sahu R, Kaushik S, Clement CC, Cannizzo ES, Scharf B, Follenzi A, et al. Microautophagy of Cytosolic Proteins by Late Endosomes. *Dev Cell* (2011) 20(1):131–9. doi: 10.1016/j.devcel.2010.12.003
51. Zhu H, Guariglia S, Yu RY, Li W, Brancho D, Peinado H, et al. Mutation of SIMPLE in Charcot-Marie-Tooth 1C Alters Production of Exosomes. *Mol Biol Cell* (2013) 24(11):1619–37. doi: 10.1091/mbc.E12-07-0544
52. Laulagnier K, Grand D, Dujardin A, Hamdi S, Vincent-Schneider H, Lankar D, et al. PLD2 is Enriched on Exosomes and its Activity is Correlated to the

Release of Exosomes. *FEBS Lett* (2004) 572(1-3):11–4. doi: 10.1016/j.febslet.2004.06.082
53. Worst TS, Meyer Y, Gottschalt M, Weis CA, von Hardenberg J, Frank C, et al. Rab27a, RAB27B and VPS36 are Downregulated in Advanced Prostate Cancer and Show Functional Relevance in Prostate Cancer Cells. *Int J Oncol* (2017) 50(3):920–32. doi: 10.3892/ijo.2017.3872
54. Wei D, Zhan W, Gao Y, Huang L, Gong R, Wang W, et al. RAB31 Marks and Controls an ESCRT-independent Exosome Pathway. *Cell Res* (2020) 31 (2):157–77. doi: 10.1038/s41422-020-00409-1
55. Kenific CM, Zhang H, Lyden D. An Exosome Pathway Without an ESCRT. *Cell Res* (2020) 31(2):105–6. doi: 10.1038/s41422-020-00418-0
56. Zietzer A, Hosen MR, Wang H, Goody PR, Sylvester M, Latz E, et al. The RNA-binding Protein hnRNPU Regulates the Sorting of microRNA-30c-5p Into Large Extracellular Vesicles. *J Extracell Vesicles* (2020) 9(1):1786967. doi: 10.1080/20013078.2020.1786967
57. Wozniak AL, Adams A, King KE, Dunn W, Christenson LK, Hung WT, et al. The RNA Binding Protein FMR1 Controls Selective Exosomal miRNA Cargo Loading During Inflammation. *J Cell Biol* (2020) 219(10):e201912074. doi: 10.1083/jcb.201912074
58. Villarroya-Beltri C, Gutierrez-Vazquez C, Sanchez-Cabo F, Perez-Hernandez D, Vazquez J, Martin-Cofreces N, et al. Sumoylated hnRNPA2B1 Controls the Sorting of miRNAs Into Exosomes Through Binding to Specific Motifs. *Nat Commun* (2013) 4:2980. doi: 10.1038/ncomms3980
59. Zhou X, Brown BA, Siegel AP, El Masry MS, Zeng X, Song W, et al. Exosome-Mediated Crosstalk Between Keratinocytes and Macrophages in Cutaneous Wound Healing. *ACS Nano* (2020) 14(10):12732–48. doi: 10.1021/acsnano.0c03064
60. Lee H, Li C, Zhang Y, Zhang D, Otterbein LE, Jin Y. Caveolin-1 Selectively Regulates microRNA Sorting Into Microvesicles After Noxious Stimuli. *J Exp Med* (2019) 216(9):2202–20. doi: 10.1084/jem.20182313
61. Santangelo L, Giurato G, Cicchini C, Montaldo C, Mancone C, Tarallo R, et al. The RNA-Binding Protein SYNCRIP is a Component of the Hepatocyte Exosomal Machinery Controlling MicroRNA Sorting. *Cell Rep* (2016) 17(3):799–808. doi: 10.1016/j.celrep.2016.09.031
62. Hobor F, Dallmann A, Ball NJ, Cicchini C, Battistelli C, Ogrodowicz RW, et al. A Cryptic RNA-binding Domain Mediates Syncrip Recognition and Exosomal Partitioning of miRNA Targets. *Nat Commun* (2018) 9(1):831. doi: 10.1038/s41467-018-03182-3
63. Shurtleff MJ, Temoche-Diaz MM, Karfilis KV, Ri S, Schekman R. Y-Box Protein 1 is Required to Sort microRNAs Into Exosomes in Cells and in a Cell-Free Reaction. *Elife* (2016) 5:e19276. doi: 10.7554/eLife.19276
64. Xu YF, Xu X, Gin A, Nshimiyimana JD, Mooers BHM, Caputi M, et al. SRSF1 Regulates Exosome microRNA Enrichment in Human Cancer Cells. *Cell Commun Signal* (2020) 18(1):130. doi: 10.1186/s12964-020-00615-9
65. Teng Y, Ren Y, Hu X, Mu J, Samykutty A, Zhuang X, et al. MVP-Mediated Exosomal Sorting of miR-193a Promotes Colon Cancer Progression. *Nat Commun* (2017) 8:14448. doi: 10.1038/ncomms14448
66. Statello L, Maugeri M, Garre E, Nawaz M, Wahlgren J, Papadimitriou A, et al. Identification of RNA-binding Proteins in Exosomes Capable of Interacting With Different Types of RNA: RBP-Facilitated Transport of RNAs Into Exosomes. *PloS One* (2018) 13(4):e0195969. doi: 10.1371/journal.pone.0195969
67. McKenzie AJ, Hoshino D, Hong NH, Cha DJ, Franklin JL, Coffey RJ, et al. Kras-Mek Signaling Controls Ago2 Sorting Into Exosomes. *Cell Rep* (2016) 15(5):978–87. doi: 10.1016/j.celrep.2016.03.085
68. Bakirtzi K, Man Law IK, Fang K, Iliopoulos D, Pothoulakis C. MiR-21 in Substance P-Induced Exosomes Promotes Cell Proliferation and Migration in Human Colonic Epithelial Cells. *Am J Physiol Gastrointest Liver Physiol* (2019) 317(6):G802–10. doi: 10.1152/ajpgi.00043.2019
69. Koppers-Lalic D, Hackenberg M, Bijnsdorp IV, van Eijndhoven MAJ, Sadek P, Sie D, et al. Nontemplated Nucleotide Additions Distinguish the Small RNA Composition in Cells From Exosomes. *Cell Rep* (2014) 8(6):1649–58. doi: 10.1016/j.celrep.2014.08.027
70. Wani S, Kaul D. Cancer Cells Govern miR-2909 Exosomal Recruitment Through its 3'-End Post-Transcriptional Modification. *Cell Biochem Funct* (2018) 36(2):106–11. doi: 10.1002/cbf.3323
71. Preußer C, Hung LH, Schneider T, Schreiner S, Hardt M, Moebus A, et al. Selective Release of circRNAs in Platelet-Derived Extracellular Vesicles. *J Extracell Vesicles* (2018) 7(1):1424473. doi: 10.1080/20013078.2018.1424473
72. Zhang J, Zhang X, Li C, Yue L, Ding N, Riordan T, et al. Circular RNA Profiling Provides Insights Into Their Subcellular Distribution and Molecular Characteristics in HepG2 Cells. *RNA Biol* (2019) 16(2):220–32. doi: 10.1080/15476286.2019.1565284
73. Lei Y, Guo W, Chen B, Chen L, Gong J, Li W. Tumorreleased Lncrna H19 Promotes Gefitinib Resistance Via Packaging Into Exosomes in Nonsmall Cell Lung Cancer. *Oncol Rep* (2018) 40(6):3438–46. doi: 10.3892/or.2018.6762
74. Zheng Z, Chen M, Xing P, Yan X, Xie B. Increased Expression of Exosomal Agap2-AS1 (Agap2 Antisense Rna 1) In Breast Cancer Cells Inhibits Trastuzumab-Induced Cell Cytotoxicity. *Med Sci Monit* (2019) 25:2211–20. doi: 10.12659/MSM.915419
75. Chen C, Luo Y, He W, Zhao Y, Kong Y, Liu H, et al. Exosomal Long Noncoding RNA LNMAT2 Promotes Lymphatic Metastasis in Bladder Cancer. *J Clin Invest* (2020) 130(1):404–21. doi: 10.1172/JCI130892
76. Zang J, Lu D, Xu A. The Interaction of circRNAs and RNA Binding Proteins: An Important Part of circRNA Maintenance and Function. *J Neurosci Res* (2020) 98(1):87–97. doi: 10.1002/jnr.24356
77. Hoek KS, Kidd GJ, Carson JH, Smith R. Hnrnp A2 Selectively Binds the Cytoplasmic Transport Sequence of Myelin Basic Protein Mrna. *Biochemistry* (1998) 37(19):7021–9. doi: 10.1021/bi9800247
78. Wang G, Chen HW, Oktay Y, Zhang J, Allen EL, Smith GM, et al. : PNPASE Regulates RNA Import Into Mitochondria. *Cell* (2010) 142(3):456–67. doi: 10.1016/j.cell.2010.06.035
79. Hwang HW, Wentzel EA, Mendell JT. A Hexanucleotide Element Directs microRNA Nuclear Import. *Science* (2007) 315(5808):97–100. doi: 10.1126/science.1136235
80. Groot M, Lee H. Sorting Mechanisms for MicroRNAs Into Extracellular Vesicles and Their Associated Diseases. *Cells* (2020) 9(4):1044. doi: 10.3390/cells9041044
81. Michlewski G, Caceres JF. Antagonistic Role of Hnrnp A1 and KSRP in the Regulation of let-7a Biogenesis. *Nat Struct Mol Biol* (2010) 17(8):1011–8. doi: 10.1038/nsmb.1874
82. Li T, Evdokimov E, Shen RF, Chao CC, Tekle E, Wang T, et al. Sumoylation of Heterogeneous Nuclear Ribonucleoproteins, Zinc Finger Proteins, and Nuclear Pore Complex Proteins: A Proteomic Analysis. *Proc Natl Acad Sci USA* (2004) 101(23):8551–6. doi: 10.1073/pnas.0402889101
83. Pérez-Boza J, Boeckx A, Lion M, Dequiedt F, Struman I. hnRNPA2B1 Inhibits the Exosomal Export of miR-503 in Endothelial Cells. *Cell Mol Life Sci* (2020) 77(21):4413–28. doi: 10.1007/s00018-019-03425-6
84. Pu Y, Zhao F, Cai W, Meng X, Li Y, Cai S. MiR-193a-3p and miR-193a-5p Suppress the Metastasis of Human Osteosarcoma Cells by Down-Regulating Rab27B and SRR, Respectively. *Clin Exp Metastasis* (2016) 33(4):359–72. doi: 10.1007/s10585-016-9783-0
85. Ostrowski M, Carmo NB, Krumeich S, Fanget I, Raposo G, Savina A, et al. Rab27a and Rab27b Control Different Steps of the Exosome Secretion Pathway. *Nat Cell Biol* (2010) 12(1):19–30. doi: 10.1038/ncb2000
86. Willson J. RILP Gets Cleaved and Exosomes Leave. *Nat Rev Mol Cell Biol* (2020) 21(11):658–9. doi: 10.1038/s41580-020-00299-6
87. Lin F, Zeng Z, Song Y, Li L, Wu Z, Zhang X, et al. YBX-1 Mediated Sorting of miR-133 Into Hypoxia/Reoxygenation-Induced EPC-derived Exosomes to Increase Fibroblast Angiogenesis and Mendot. *Stem Cell Res Ther* (2019) 10 (1):263. doi: 10.1186/s13287-019-1377-8
88. Li L, Zhu D, Huang L, Zhang J, Bian Z, Chen X, et al. Argonaute 2 Complexes Selectively Protect the Circulating microRNAs in Cell-Secreted Microvesicles. *PloS One* (2012) 7(10):e46957. doi: 10.1371/journal.pone.0046957
89. Arroyo JD, Chevillet JR, Kroh EM, Ruf IK, Pritchard CC, Gibson DF, et al. Argonaute2 Complexes Carry a Population of Circulating microRNAs Independent of Vesicles in Human Plasma. *Proc Natl Acad Sci USA* (2011) 108(12):5003–8. doi: 10.1073/pnas.1019055108
90. Buchet-Poyau K, Courchet J, Le Hir H, Seraphin B, Scoazec JY, Duret L, et al. Identification and Characterization of Human Mex-3 Proteins, a Novel Family of Evolutionarily Conserved RNA-binding Proteins Differentially

Localized to Processing Bodies. *Nucleic Acids Res* (2007) 35(4):1289–300. doi: 10.1093/nar/gkm016
91. Lu P, Li H, Li N, Singh RN, Bishop CE, Chen X, et al. MEX3C Interacts With Adaptor-Related Protein Complex 2 and Involves in miR-451a Exosomal Sorting. *PloS One* (2017) 12(10):e0185992. doi: 10.1371/journal.pone.0185992
92. Cerutti H, Ibrahim F. Turnover of Mature miRNAs and siRNAs in Plants and Algae. *Adv Exp Med Biol* (2011) 700:124–39. doi: 10.1007/978-1-4419-7823-3_11
93. Khan N, Mironov G, Berezovski MV. Direct Detection of Endogenous MicroRNAs and Their Post-Transcriptional Modifications in Cancer Serum by Capillary Electrophoresis-Mass Spectrometry. *Anal Bioanal Chem* (2016) 408(11):2891–9. doi: 10.1007/s00216-015-9277-y
94. Cha DJ, Franklin JL, Dou Y, Liu Q, Higginbotham JN, Demory Beckler M, et al. KRAS-Dependent Sorting of miRNA to Exosomes. *Elife* (2015) 4: e07197. doi: 10.7554/eLife.07197
95. Fatima F, Nawaz M. Long Distance Metabolic Regulation Through Adipose-Derived Circulating Exosomal Mirnas: A Trail for RNA-Based Therapies? *Front Physiol* (2017) 8:545. doi: 10.3389/fphys.2017.00545
96. Fatima F, Nawaz M. Vesiculated Long non-Coding RNAs: Offshore Packages Deciphering Trans-Regulation Between Cells, Cancer Progression and Resistance to Therapies. *Noncoding RNA* (2017) 3(1):10. doi: 10.3390/ncrna3010010
97. Squadrito ML, Baer C, Burdet F, Maderna C, Gilfillan GD, Lyle R, et al. Endogenous RNAs Modulate microRNA Sorting to Exosomes and Transfer to Acceptor Cells. *Cell Rep* (2014) 8(5):1432–46. doi: 10.1016/j.celrep.2014.07.035
98. Li Y, Zheng Q, Bao C, Li S, Guo W, Zhao J, et al. Circular RNA is Enriched and Stable in Exosomes: A Promising Biomarker for Cancer Diagnosis. *Cell Res* (2015) 25(8):981–4. doi: 10.1038/cr.2015.82
99. Kim KM, Abdelmohsen K, Mustapic M, Kapogiannis D, Gorospe M. RNA in Extracellular Vesicles. *Wiley Interdiscip Rev RNA* (2017) 8(4):e1413. doi: 10.1002/wrna.1413
100. Fanale D, Taverna S, Russo A, Bazan V. Circular RNA in Exosomes. *Adv Exp Med Biol* (2018) 1087:109–17. doi: 10.1007/978-981-13-1426-1_9
101. Wei M, Gao X, Liu L, Li Z, Wan Z, Dong Y, et al. Visceral Adipose Tissue Derived Exosomes Exacerbate Colitis Severity Via Pro-inflammatory MiRNAs in High Fat Diet Fed Mice. *ACS Nano* (2020) 14(4):5099–110. doi: 10.1021/acsnano.0c01860
102. Liu XL, Pan Q, Cao HX, Xin FZ, Zhao ZH, Yang RX, et al. Lipotoxic Hepatocyte-Derived Exosomal MicroRNA 192-5p Activates Macrophages Through Rictor/Akt/Forkhead Box Transcription Factor O1 Signaling in Nonalcoholic Fatty Liver Disease. *Hepatology* (2020) 72(2):454–69. doi: 10.1002/hep.31050
103. Real JM, Ferreira LRP, Esteves GH, Koyama FC, Dias MVS, Bezerra-Neto JE, et al. Exosomes From Patients With Septic Shock Convey miRNAs Related to Inflammation and Cell Cycle Regulation: New Signaling Pathways in Sepsis? *Crit Care* (2018) 22(1):68. doi: 10.1186/s13054-018-2003-3
104. Zhou Q, Li M, Wang X, Li Q, Wang T, Zhu Q, et al. Immune-Related microRNAs are Abundant in Breast Milk Exosomes. *Int J Biol Sci* (2012) 8 (1):118–23. doi: 10.7150/ijbs.8.118
105. Yanez-Mo M, Siljander PR, Andreu Z, Zavec AB, Borras FE, Buzas EI, et al. Biological Properties of Extracellular Vesicles and Their Physiological Functions. *J Extracell Vesicles* (2015) 4:27066. doi: 10.3402/jev.v4.27066
106. Xu JF, Yang GH, Pan XH, Zhang SJ, Zhao C, Qiu BS, et al. Altered microRNA Expression Profile in Exosomes During Osteogenic Differentiation of Human Bone Marrow-Derived Mesenchymal Stem Cells. *PloS One* (2014) 9(12):e114627. doi: 10.1371/journal.pone.0114627
107. Morel L, Regan M, Higashimori H, Ng SK, Esau C, Vidensky S, et al. Neuronal Exosomal miRNA-dependent Translational Regulation of Astroglial Glutamate Transporter GLT1. *J Biol Chem* (2013) 288(10):7105–16. doi: 10.1074/jbc.M112.410944
108. Forterre A, Jalabert A, Chikh K, Pesenti S, Euthine V, Granjon A, et al. Myotube-Derived Exosomal miRNAs Downregulate Sirtuin1 in Myoblasts During Muscle Cell Differentiation. *Cell Cycle* (2014) 13(1):78–89. doi: 10.4161/cc.26808
109. Sun Z, Yang S, Zhou Q, Wang G, Song J, Li Z, et al. Emerging Role of Exosome-Derived Long non-Coding RNAs in Tumor Microenvironment. *Mol Cancer* (2018) 17(1):82. doi: 10.1186/s12943-018-0831-z
110. Hannafon BN, Ding WQ. Functional Role of miRNAs in the Progression of Breast Ductal Carcinoma in Situ. *Am J Pathol* (2019) 189(5):966–74. doi: 10.1016/j.ajpath.2018.06.025
111. Zhang N, Nan A, Chen L, Li X, Jia Y, Qiu M, et al. Circular RNA circSATB2 Promotes Progression of non-Small Cell Lung Cancer Cells. *Mol Cancer* (2020) 19(1):101. doi: 10.1186/s12943-020-01221-6
112. Fukayama M, Kunita A, Kaneda A. Gastritis-Infection-Cancer Sequence of Epstein-Barr Virus-Associated Gastric Cancer. *Adv Exp Med Biol* (2018) 1045:437–57. doi: 10.1007/978-981-10-7230-7_20
113. Koppers-Lalic D, Hogenboom MM, Middeldorp JM, Pegtel DM. Virus-Modified Exosomes for Targeted RNA Delivery; a New Approach in Nanomedicine. *Adv Drug Delivery Rev* (2013) 65(3):348–56. doi: 10.1016/j.addr.2012.07.006
114. Feng Z, Hirai-Yuki A, McKnight KL, Lemon SM. Naked Viruses That Aren't Always Naked: Quasi-Enveloped Agents of Acute Hepatitis. *Annu Rev Virol* (2014) 1(1):539–60. doi: 10.1146/annurev-virology-031413-085359
115. Wang L, Liao Y, Yang R, Yu Z, Zhang L, Zhu Z, et al. Sja-miR-71a in Schistosome Egg-Derived Extracellular Vesicles Suppresses Liver Fibrosis Caused by Schistosomiasis Via Targeting Semaphorin 4D. *J Extracell Vesicles* (2020) 9(1):1785738. doi: 10.1080/20013078.2020.1785738
116. Meningher T, Barsheshet Y, Ofir-Birin Y, Gold D, Brant B, Dekel E, et al. Schistosomal Extracellular Vesicle-Enclosed miRNAs Modulate Host T Helper Cell Differentiation. *EMBO Rep* (2020) 21(1):e47882. doi: 10.15252/embr.201947882
117. Hu W, Liu C, Bi ZY, Zhou Q, Zhang H, Li LL, et al. Comprehensive Landscape of Extracellular Vesicle-Derived RNAs in Cancer Initiation, Progression, Metastasis and Cancer Immunology. *Mol Cancer* (2020) 19 (1):102. doi: 10.1186/s12943-020-01199-1
118. Cheng J, Meng J, Zhu L, Peng Y. Exosomal Noncoding RNAs in Glioma: Biological Functions and Potential Clinical Applications. *Mol Cancer* (2020) 19(1):66. doi: 10.1186/s12943-020-01189-3
119. Zeuschner P, Linxweiler J, Junker K. Non-Coding RNAs as Biomarkers in Liquid Biopsies With a Special Emphasis on Extracellular Vesicles in Urological Malignancies. *Expert Rev Mol Diagn* (2020) 20(2):151–67. doi: 10.1080/14737159.2019.1665998
120. Wang J, Ni J, Beretov J, Thompson J, Graham P, Li Y. Exosomal microRNAs as Liquid Biopsy Biomarkers in Prostate Cancer. *Crit Rev Oncol Hematol* (2020) 145:102860. doi: 10.1016/j.critrevonc.2019.102860
121. Visci G, Tolomeo D, Agostini A, Traversa D, Macchia G, Storlazzi CT. CircRNAs and Fusion-circRNAs in Cancer: New Players in an Old Game. *Cell Signal* (2020) 75:109747. doi: 10.1016/j.cellsig.2020.109747
122. Wang Y, Liu J, Ma J, Sun T, Zhou Q, Wang W, et al. Exosomal circRNAs: Biogenesis, Effect and Application in Human Diseases. *Mol Cancer* (2019) 18 (1):116. doi: 10.1186/s12943-019-1041-z
123. Chen Z, Yang Y, Yamaguchi H, Hung MC, Kameoka J. Isolation of Cancer-Derived Extracellular Vesicle Subpopulations by a Size-Selective Microfluidic Platform. *Biomicrofluidics* (2020) 14(3):034113. doi: 10.1063/5.0008438
124. Kang YT, Hadlock T, Jolly S, Nagrath S. Extracellular Vesicles on Demand (EVOD) Chip for Screening and Quantification of Cancer-Associated Extracellular Vesicles. *Biosens Bioelectron* (2020) 168:112535. doi: 10.1016/j.bios.2020.112535
125. Zhou Y, Ma Z, Tayebi M, Ai Y. Submicron Particle Focusing and Exosome Sorting by Wavy Microchannel Structures Within Viscoelastic Fluids. *Anal Chem* (2019) 91(7):4577–84. doi: 10.1021/acs.analchem.8b05749
126. Yang XX, Sun C, Wang L, Guo XL. New Insight Into Isolation, Identification Techniques and Medical Applications of Exosomes. *J Control Release* (2019) 308:119–29. doi: 10.1016/j.jconrel.2019.07.021
127. Li P, Kaslan M, Lee SH, Yao J, Gao Z. Progress in Exosome Isolation Techniques. *Theranostics* (2017) 7(3):789–804. doi: 10.7150/thno.18133
128. Gheinani AH, Vogeli M, Baumgartner U, Vassella E, Draeger A, Burkhard FC, et al. Improved Isolation Strategies to Increase the Yield and Purity of Human Urinary Exosomes for Biomarker Discovery. *Sci Rep* (2018) 8 (1):3945. doi: 10.1038/s41598-018-22142-x
129. Wang LL, Chen WQ, Wang YR, Zeng LP, Chen TT, Chen GY, et al. Numerous Long Single-Stranded DNAs Produced by Dual Amplification Reactions for Electrochemical Detection of Exosomal Micrornas. *Biosens Bioelectron* (2020) 169:112555. doi: 10.1016/j.bios.2020.112555
130. Wu X, Zhao H, Natalia A, Lim CZJ, Ho NRY, Ong CJ, et al. Exosome-Templated Nanoplasmonics for Multiparametric Molecular Profiling. *Sci Adv* (2020) 6(19):eaba2556. doi: 10.1126/sciadv.aba2556

131. Narita M, Nishida H, Asahina R, Nakata K, Yano H, Dickinson PJ, et al. Expression of microRNAs in Plasma and in Extracellular Vesicles Derived From Plasma for Dogs With Glioma and Dogs With Other Brain Diseases. *Am J Vet Res* (2020) 81(4):355–60. doi: 10.2460/ajvr.81.4.355
132. Zheng P, Zhang H, Gao H, Sun J, Li J, Zhang X, et al. Plasma Exosomal Long Noncoding Rna lnc-SLC2A12-10:1 as a Novel Diagnostic Biomarker for Gastric Cancer. *Onco Targets Ther* (2020) 13:4009–18. doi: 10.2147/ott.s253600
133. Lee H, Park H, Noh GJ, Lee ES. pH-responsive Hyaluronate-Anchored Extracellular Vesicles to Promote Tumor-Targeted Drug Delivery. *Carbohydr Polym* (2018) 202:323–33. doi: 10.1016/j.carbpol.2018.08.141
134. Sancho-Albero M, Navascués N, Mendoza G, Sebastián V, Arruebo M, Martín-Duque P, et al. Exosome Origin Determines Cell Targeting and the Transfer of Therapeutic Nanoparticles Towards Target Cells. *J Nanobiotechnol* (2019) 17(1):16. doi: 10.1186/s12951-018-0437-z
135. Perets N, Betzer O, Shapira R, Brenstein S, Angel A, Sadan T, et al. Golden Exosomes Selectively Target Brain Pathologies in Neurodegenerative and Neurodevelopmental Disorders. *Nano Lett* (2019) 19(6):3422–31. doi: 10.1021/acs.nanolett.8b04148
136. Morales-Kastresana A, Musich TA, Welsh JA, Telford W, Demberg T, Wood JCS, et al. High-Fidelity Detection and Sorting of Nanoscale Vesicles in Viral Disease and Cancer. *J Extracell Vesicles* (2019) 8(1):1597603. doi: 10.1080/20013078.2019.1597603
137. Kibria G, Ramos EK, Wan Y, Gius DR, Liu H. Exosomes as a Drug Delivery System in Cancer Therapy: Potential and Challenges. *Mol Pharm* (2018) 15 (9):3625–33. doi: 10.1021/acs.molpharmaceut.8b00277
138. Yang L, Han B, Zhang Z, Wang S, Bai Y, Zhang Y, et al. Extracellular Vesicle-Mediated Delivery of Circular Rna SCMH1 Promotes Functional Recovery in Rodent and Nonhuman Primate Ischemic Stroke Models. *Circulation* (2020) 142(6):556–74. doi: 10.1161/circulationaha.120.045765
139. Upadhya R, Madhu LN, Attaluri S, Gitaí DLG, Pinson MR, Kodali M, et al. Extracellular Vesicles From Human iPSC-derived Neural Stem Cells: miRNA and Protein Signatures, and Anti-Inflammatory and Neurogenic Properties. *J Extracell Vesicles* (2020) 9(1):1809064. doi: 10.1080/20013078.2020.1809064
140. Fang SB, Zhang HY, Wang C, He BX, Liu XQ, Meng XC, et al. Small Extracellular Vesicles Derived From Human Mesenchymal Stromal Cells Prevent Group 2 Innate Lymphoid Cell-Dominant Allergic Airway Inflammation Through Delivery of Mir-146a-5p. *J Extracell Vesicles* (2020) 9(1):1723260. doi: 10.1080/20013078.2020.1723260
141. Dou G, Tian R, Liu X, Yuan P, Ye Q, Liu J, et al. Chimeric Apoptotic Bodies Functionalized With Natural Membrane and Modular Delivery System for Inflammation Modulation. *Sci Adv* (2020) 6(30):eaba2987. doi: 10.1126/sciadv.aba2987
142. Xie M, Tao L, Zhang Z, Wang W. Mesenchymal Stem Cells Mediated Drug Delivery in Tumor-Targeted Therapy. *Curr Drug Delivery* (2020). doi: 10.2174/1567201817999200819140912
143. Lang FM, Hossain A, Gumin J, Momin EN, Shimizu Y, Ledbetter D, et al. Mesenchymal Stem Cells as Natural Biofactories for Exosomes Carrying miR-124a in the Treatment of Gliomas. *Neuro Oncol* (2018) 20(3):380–90. doi: 10.1093/neuonc/nox152
144. Liang G, Kan S, Zhu Y, Feng S, Feng W, Gao S. Engineered Exosome-Mediated Delivery of Functionally Active miR-26a and its Enhanced Suppression Effect in HepG2 Cells. *Int J Nanomed* (2018) 13:585–99. doi: 10.2147/ijn.s154458
145. Zhang H, Freitas D, Kim HS, Fabijanic K, Li Z, Chen H, et al. Identification of Distinct Nanoparticles and Subsets of Extracellular Vesicles by Asymmetric Flow Field-Flow Fractionation. *Nat Cell Biol* (2018) 20 (3):332–43. doi: 10.1038/s41556-018-0040-4
146. Jeppesen DK, Fenix AM, Franklin JL, Higginbotham JN, Zhang Q, Zimmerman LJ, et al. Reassessment of Exosome Composition. *Cell* (2019) 177(2):428–445.e18. doi: 10.1016/j.cell.2019.02.029
147. Zhang Q, Higginbotham JN, Jeppesen DK, Yang YP, Li W, McKinley ET, et al. Transfer of Functional Cargo in Exomeres. *Cell Rep* (2019) 27(3):940–954.e6. doi: 10.1016/j.celrep.2019.01.009
148. Anand S, Samuel M, Mathivanan S. Exomeres: A New Member of Extracellular Vesicles Family. *Subcell Biochem* (2021) 97:89–97. doi: 10.1007/978-3-030-67171-6_5
149. Hoshino A, Kim HS, Bojmar L, Gyan KE, Cioffi M, Hernandez J, et al. Extracellular Vesicle and Particle Biomarkers Define Multiple Human Cancers. *Cell* (2020) 182(4):1044–1061.e18. doi: 10.1016/j.cell.2020.07.009

Conflict of Interest: The authors declare that the research was conducted in the absence of any commercial or financial relationships that could be construed as a potential conflict of interest.

frontiers in Oncology

ORIGINAL RESEARCH
published: 16 June 2021
doi: 10.3389/fonc.2021.687629

A Non-Coding RNA Network Involved in KSHV Tumorigenesis

Julián Naipauer[1,2†], Martín E. García Solá[2,3,4†], Daria Salyakina[1], Santas Rosario[1], Sion Williams[2,5], Omar Coso[2,3,4], Martín C. Abba[2,6], Enrique A. Mesri[1,2] and Ezequiel Lacunza[2,6*]*

[1] Tumor Biology Program, Sylvester Comprehensive Cancer Center and Miami Center for AIDS Research, Department of Microbiology and Immunology, University of Miami Miller School of Medicine, Miami, FL, United States, [2] UM-CFAR/Sylvester CCC Argentina Consortium for Research and Training in Virally Induced AIDS-Malignancies, University of Miami Miller School of Medicine, Miami, FL, United States, [3] Departamento de Fisiología y Biología Molecular, Universidad de Buenos Aires, Facultad de Ciencias Exactas y Naturales, Buenos Aires, Argentina, [4] Instituto de Fisiología, Biología Molecular y Neurociencias (IFIBYNE), CONICET-Universidad de Buenos Aires, Buenos Aires, Argentina, [5] Neurology Basic Science Division, Sylvester Comprehensive Cancer Center, University of Miami Miller School of Medicine, Miami, FL, United States, [6] Centro de Investigaciones Inmunológicas Básicas y Aplicadas, Facultad de Ciencias Médicas, Universidad Nacional de La Plata, La Plata, Argentina

OPEN ACCESS

Edited by:
Hernandes F Carvalho, State University of Campinas, Brazil

Reviewed by:
Flora Guerra, University of Salento, Italy
Joanna Sztuba-Solinska, Auburn University, United States

***Correspondence:**
Enrique A. Mesri
emesri@med.miami.edu
Ezequiel Lacunza
ez.lacunza@gmail.com

†These authors have contributed equally to this work

Specialty section:
This article was submitted to Molecular and Cellular Oncology, a section of the journal Frontiers in Oncology

Received: *30 March 2021*
Accepted: *24 May 2021*
Published: *16 June 2021*

Citation:
Naipauer J, García Solá ME, Salyakina D, Rosario S, Williams S, Coso O, Abba MC, Mesri EA and Lacunza E (2021) A Non-Coding RNA Network Involved in KSHV Tumorigenesis. Front. Oncol. 11:687629. doi: 10.3389/fonc.2021.687629

Regulatory pathways involving non-coding RNAs (ncRNAs), such as microRNAs (miRNAs) and long non-coding RNAs (lncRNA), have gained great relevance due to their role in the control of gene expression modulation. Using RNA sequencing of KSHV Bac36 transfected mouse endothelial cells (mECK36) and tumors, we have analyzed the host and viral transcriptome to uncover the role lncRNA-miRNA-mRNA driven networks in KSHV tumorigenesis. The integration of the differentially expressed ncRNAs, with an exhaustive computational analysis of their experimentally supported targets, led us to dissect complex networks integrated by the cancer-related lncRNAs Malat1, Neat1, H19, Meg3, and their associated miRNA-target pairs. These networks would modulate pathways related to KSHV pathogenesis, such as viral carcinogenesis, p53 signaling, RNA surveillance, and cell cycle control. Finally, the ncRNA-mRNA analysis allowed us to develop signatures that can be used to an appropriate identification of druggable gene or networks defining relevant AIDS-KS therapeutic targets.

Keywords: long non-coding RNAs, microRNAs, KSHV, network pathways, druggable targets

INTRODUCTION

Non-coding RNAs (ncRNAs) are RNA transcripts that do not encode proteins and based on the length can be divided into two classes: small ncRNAs (sncRNAs), with transcripts shorter than 200 nucleotides, and long ncRNAs (lncRNAs), with transcripts longer than 200 nucleotides (1). Regulatory pathways involving ncRNAs, such as microRNAs (miRNAs), belonging to the class of sncRNA, and lncRNAs have gained great relevance due to their role in the control of gene (mRNA) expression. Different modes of interactions between lncRNAs and miRNAs have been reported: miRNA decay of lncRNAs, lncRNAs competing with mRNAs to bind to miRNAs, lncRNAs competing with miRNAs to bind to mRNA, and lncRNAs being shortened to miRNAs (2, 3). All these interactions regulate the expression levels of mRNAs and in turn affect core protein signals, resulting in changes in the physiological functions of cells.

Kaposi's sarcoma (KS) is an AIDS-associated malignancy caused by the KS herpesvirus (KSHV). Despite the reduction of its incidence since the implementation of anti-retroviral therapy (ART), KS continues to be a global, difficult-to-treat health problem, in particular for ART-resistant forms (4, 5). KS is characterized by the proliferation of KSHV-infected spindle cells and profuse angiogenesis (6).

The life cycle of KSHV has two well-defined phases: latent and lytic. In the latent phase, the virus expresses a few genes involved in viral persistence and host immune evasion. During the lytic phase, which is triggered by environmental and/or physiological stimuli, the viral genome replicates and new virions are formed (7). At this stage, KSHV is particularly effective at exploiting host gene expression for its own benefit. In this sense, the coevolution of the virus and its host has developed an intricate association between the virus genome, with its coding genes and non-coding genes, and the host RNA biosynthesis machinery (8). To the point that KSHV can seize control of RNA surveillance pathways, such as DNA damage response (DDR), pre-mRNA control machinery and the Nonsense-mediated mRNA decay (NMD), to fine-tuning the global gene expression environment throughout both phases of infection (7, 9, 10).

A recent study of KSHV-infected TIVE cells using wild-type and miRNA-deleted KSHV in conjunction with microarray technology to profile lncRNA expression found that KSHV can deregulate hundreds of host lncRNAs. These data established that KSHV de-regulates lncRNA in a miRNA-dependent fashion (11).

Using deep RNA sequencing of KSHV Bac36 transfected mouse endothelial cells (mECK36) and tumors (12), we have previously analyzed the host and viral transcriptome to characterize mechanisms of KSHV-dependent and -independent sarcomagenesis, as well as the contribution of host mutations (13). We now decided to study in this model, in a genome-wide fashion, the ncRNAs landscape to better understand the relationship between mRNAs, lncRNAs, and miRNAs in shaping KSHV tumorigenesis mechanisms.

This study allowed us to identify the most relevant host lncRNAs involved in KSHV tumorigenesis through the mouse KS-model (*Malat1, Neat1, H19*, and *Meg3*). In addition to having common target genes, pathway analysis showed that the four lncRNAs also share common related processes, mainly associated with cancer and viral infections, which would contribute with a network of gene-pathways closely associated with KSHV oncogenesis. We also showed evidence of the most frequent viral lncRNAs transcripts expressed in our model.

On the other hand, small RNA-sequencing and miRNA analysis revealed a high proportion of upregulated host miRNAs dependent of KSHV infection, indicating that the presence of KSHV has a significant impact on the metabolism of host miRNAs, whose target genes are mainly associated to angiogenesis, ECM, spliceosome, p53 signaling, viral infections, and cell cycle control. Similarly, functional analysis of KSHV miRNA targets showed enrichment in processes, such as cell cycle, spliceosome, RNA transport, microRNA regulation of DDR, and p53 signaling, suggesting that viral miRNAs might mimic cellular miRNAs.

The integrative analysis of viral and host non-coding and coding RNAs and the related processes showed a landscape of the potential relationships of lncRNA-miRNA-mRNA in a KSHV setting. This network highlights that the upregulated genes are involved in processes previously related to KSHV tumorigenesis while downregulated genes are associated with host cell cycle checkpoints and RNA surveillance pathways: *G1 to S cycle control*, *p53 activity regulation*, *MicroRNA regulation of DDR*, *Spliceosome*, *RNA transport*, *E2F transcription factor network*. Finally, the ncRNA-mRNA analysis in the animal model presented here allowed us to develop signatures that can be used to identify druggable gene or networks defining relevant AIDS-KS therapeutic targets.

METHODS

RNA-Sequencing Analysis

RNA-sequencing raw data used in the present study were obtained as previously described (13). Data are available at https://www.ncbi.nlm.nih.gov/geo/, GSE144101. Briefly, RNA was isolated and purified using the RNeasy mini kit (Qiagen). RNA concentration and integrity were measured on an Agilent 2100 Bioanalyzer (Agilent Technologies). Only RNA samples with RNA integrity values (RIN) over 8.0 were considered for subsequent analysis. mRNA from cell lines and tumor samples were processed for directional mRNA-sequencing library construction using the Preparation Kit according to the manufacturer's protocol. Paired-end sequencing using an Illumina NextSeq500 platform was used, all samples were processed in the same sequencing run of Illumina NextSeq 500 system and analyzed together with the aim to avoid the batches effect. The short sequenced reads were mapped to the mouse reference genome (GRCm38.82) by the splice junction aligner TopHat V2.1.0. Several R/Bioconductor packages to accurately calculate the gene expression abundance at the whole-genome level using the aligned records (BAM files) were used. The number of reads mapped to each gene based on the Mus musculus genome assembly GRCm38 (mm10) were counted, reported and annotated using the featureCounts package. To identify DE genes between cell lines and tumor samples, we utilized the DESeq2 package in R/Bioconductor. DESeq2 performs an internal normalization where geometric mean is calculated for each gene across all samples. The counts for a gene in each sample are then divided by this mean. For ncRNA annotation we employed biomaRt package in R/Bioconductor. We considered the Ensemble transcript ID, the Ensembl gene ID, the Entrezgene ID, the HGNC symbol, the Refseq ncRNA ID and the ReqSeq ncRNA predicted ID. After Deseq2 analysis on all ncRNAs, we filtered out those belonged to the following classes: small nuclear RNA (snRNA), small nucleolar RNA (snRNA), predicted and or pseudogenes, and RIKEN genes; and kept the classes lncRNA and miRNA.

Cell Culture and Tumors

Cells and tumors employed in the present study were the same as previously described (13). mECK36, KSHV (+) cells, were

originated from frozen batches of mECK36 cells previously generated (12). Briefly, mECs were obtained from Balb/C An Ncr-nu mice (NCI, Bethesda, MD) bone marrow. Mice femurs were flushed twice with PBS, and the eluates were incubated in DMEM media plus 30% FBS (Gemini Bioproducts, Calabasas, CA), 0.2 mg/ml Endothelial Growth Factor (EGF) (Sigma, Saint Louis, MO), 0.2 mg/ml Endothelial Cell Growth Factor Supplement (ECGS) (Sigma, Saint Louis, Missouri), 1.2 mg/1 heparin (Sigma, Saint Louis, MO), insulin transferrin selenium (Invitrogen,Carlsbad, CA), 1% penicillin-streptomycin (Invitrogen, Carlsbad, CA), and BME vitamin (VWR Scientific, Rochester, NY). Cells transfected with KSHVBac36, the vector containing the insert with the genome of KSHV in Bacterial Artificial Chromosome (KSHVBac36) was obtained as described previously, were selected with Hyg-B (12). KSHV (+) tumors were obtained as previously shown, 1x106 KSHV (+) cells were injected subcutaneously into the flanks of nude mice and KSHV (+) tumors formed 5 weeks after injection. KSHV (−) cells were used from frozen populations of KSHV null mECK36 previously obtained (12). KSHV (−) tumor cells were obtained from frozen stocks previously generated by explanted mECK36 tumor cells that have lost the Bac36-KSHV episome (12). These KSHV-negative cells were obtained from frozen stocks previously generated (14). KSHV (−) tumors were obtained as previously shown (12), $1x10^6$ KSHV (−) tumor cells were injected subcutaneously into the flanks of nude mice and KSHV (−) tumors formed 3 weeks after injection.

KSHV lncRNA Analysis

Cells and tumors employed in the present study were the same as previously described (13). For lncRNA analysis we included the generated BAM files from eight samples (2 KSHV (+) cells and six KSHV (+) tumors). Based on the KSHV 2.0 reference genome and genome coordinates, we annotated 12 lncRNAs. For measuring gene expression, we applied featureCounts function of the RSubread package in R/Bioconductor. For DEG analysis, we employed DESeq2 package in R/Biocoductor.

Small RNA Sequencing and miRNA Analysis

RNA was isolated and purified using RNeasy Plus Mini Kit (Qiagen, #74134) following the RNeasy MinElute Cleanup Kit (Qiagen, #74204) to separate purification of small RNA (containing miRNA) and larger RNA, the small RNA eluate is enriched in various RNAs of <200 nucleotides. A total of 15 small RNA ranged from cell lines to primary mouse tumors in the presence or absence of KSHV, were processed and sequenced on a HiSeq 2500 System (Illumina, USA). Each sample yielded, on average, 17 million reads, with the exception of one sample (DS016) that was excluded from the analysis for presenting a low number of total reads. Nearly all bases showed scores > Q30 for all reads. Trimmomatic was used to remove adapters and quality control was checked with FastQC. Reads were mapped to a combined mouse and KSHV genome using the bowtie aligner (ver. 1.1.1). To identify novel and known miRNAs we used miRDeep2 package (ver. 2.0.0.7). A hybrid genome of the mouse and the KSHV virus was used for all analyzes in order not to bias the mapping results for or against any of the two separate genomes. The source for all known miRNAs was miRBase (ver. 21). KSHV transcriptome was analyzed using previous resources and KSHV 2.0 reference genome. To identify DE miRNAs across the different comparisons, we utilized the DESeq2 test based on the normalized number of counts mapped to each miRNA. For data integration and visualization of DE transcripts we used R/Bioconductor. Data were submitted to the SRA database, reference PRJNA602753.

Integrative Computational and Bioinformatics Analysis

To identify EVT genes regulated by the selected lncRNAs we employed LncRNA2Targetv2.0 (http://123.59.132.21/lncrna2target) and LncTarD (http://biocc.hrbmu.edu.cn/LncTarD/) databases (15, 16). To identify the common targets among the different lncRNAs we used Venn diagrams. To obtain the experimentally supported targets of the DE host miRNAs identified in this study, we employed DIANA TARBASE v8 (https://carolina.imis.athena-innovation.gr/diana_tools/). For KSHV miRNAs targets we also used DIANA TARBASE v8 resource (17). In both cases, only those targets identified by High-throughput methodologies were considered. To identify relevant pairs of lncRNA-miRNA in our model, we used DIANA-LncBase v3 (18), in which lncRNA/miRNA interactions are defined by low-/high-throughput methodologies; for each of the four lncRNAs we searched for their highly confident experimentally supported viral and host miRNA targets. To identify drug-associated genes or networks we used the drug gene interaction database (DGIdb; https://www.dgidb.org/) and the miRNA Pharmacogenomics Database (Pharmaco miR; http://www.pharmaco-mir.org/) (19, 20). ClinicalTrials.gov database (https://clinicaltrials.gov/) was consulted to search for all recruiting and non-recruiting studies of KS patients.

Functional enrichment analyses were performed using the ClueGo Cytoscape's plug-in (http://www.cytoscape.org/) and the Enrichr resource (https://maayanlab.cloud/Enrichr/) based on the lists of EVT that were in turn deregulated transcripts across the different comparisons of our model. For pathways terms and annotation, we used those provided by KEGG and BioPlanet (http://tripod.nih.gov/bioplanet/; https://www.genome.jp/kegg/pathway.html). Significant pathways were based on the Bonferroni Adjusted p value <0.05. To combine and integrate expression data with the results of the functional analysis we used the GOplot package. For the construction of the networks, we used Sankey plots.

All statistical analyses and data visualization plots were done with R/Bioconductor packages.

RESULTS

Genome-Wide Analysis of Non-Coding RNAs in a Cell and Animal Model of Kaposi's Sarcoma

To analyze the ncRNA expression profile in a cell and animal model of Kaposi's sarcoma, we performed deep RNA-seq

analysis of all the stages of this model. **Figure 1A** shows a schematic representation of the model: tumors formed by KSHV Bac36 transfected mouse endothelial cells, KSHV (+) cells, are all episomally infected with KSHV Bac36, and when KSHV (+) cells prior to form tumors lose the KSHV episome *in vitro* by withdrawal of antibiotic selection, KSHV (−) cells, they completely lose tumorigenicity (12, 13). In contrast to KSHV (−) cells, cells explanted from KSHV (+) BAC36 tumors and grown in the absence of antibiotic selection lose the KSHV episome, KSHV (−) tumor cells, are tumorigenic and are able to form KSHV (−) tumors (12–14).

Unsupervised clustering (**Figure 1B**) and Multidimensional plot (**Figure 1C**) of the host ncRNAs shows how KSHV status and tissue type cluster with each other. As was previously reported based on mRNA proliles, *in vitro* and *in vivo* models clustered separately (13).

To identify changes in host lncRNAs expression profile, we analyzed the number of differentially expressed (DE; FC>1.5, p value <0.05) lncRNAs in key biological comparisons that were detected by RNA-sequencing analysis of: two KSHV (+) cells, two KSHV (−) cells, six KSHV (+) tumors, two KSHV (−) tumor cells and three KSHV (−) tumors (**Supplementary Table 1**). This mouse model allows for unique experimental comparisons in the same cell and KS-like mouse tumor types: 1) KSHV (−) cells *versus* KSHV (+) cells can be used to study KSHV mediated effects *in vitro*, 2) KSHV (−) tumors *versus* KSHV (+) tumors can be used to dissect the role of ncRNAs in tumorigenesis by comparing tumors driven by KSHV *versus* tumors driven by host mutations, 3) KSHV (+) cells grown *in vitro* and in tumors can be used to study *in vitro versus in vivo* variations induced by micro-environmental cues, and 4) KSHV (−) tumor cells *versus* KSHV (−) tumors can be used to study *in vitro versus in vivo* variations in the absence of KSHV (13). We first analyzed lncRNAs expression in these comparisons and found that the highest number of DE lncRNAs was observed in KSHV (+) tumors in both comparisons *versus* KSHV (−) tumors and *versus* KSHV (+) cells (**Figure 1D** and **Supplementary Table 1**).

Identification of Relevant lncRNAs in KSHV (+) Tumors

We performed heat map representations of all or top-50 DE lncRNAs -according to each comparison- for all the four biological relevant comparisons mentioned previously (**Figure 2A**). To select and further evaluate relevant KSHV-associated lncRNAs we searched for the common up-modulated lncRNAs in KSHV (+) tumors *versus* the different comparisons (**Figure 2B**). Of the 10 lncRNAs up-modulated in KSHV (+) cells compared to KSHV (−) cells, 3 lncRNAs (*Malat1*, *Neat1* and *Kcnq1ot1*) were also up modulated in the comparison of KSHV (+) tumors *versus* KSHV (−) tumors (**Figure 2B**, top panel). In addition, of the 40 up-modulated lncRNAs in KSHV (+) tumors *versus* KSHV (+) cells, 18 were common to the 25 up-modulated lncRNAs in the comparison between KSHV (+) tumors and KSHV (−) tumors (**Figure 2B**, bottom panel). These 18 genes included lncRNAs such as *Malat1*, *H19*, *Meg3*, *Neat1*, *Dio3os*, *Miat*, *Mirg*, and *Rian*, but also the miRNA genes *Mir140*, *Mir142*,

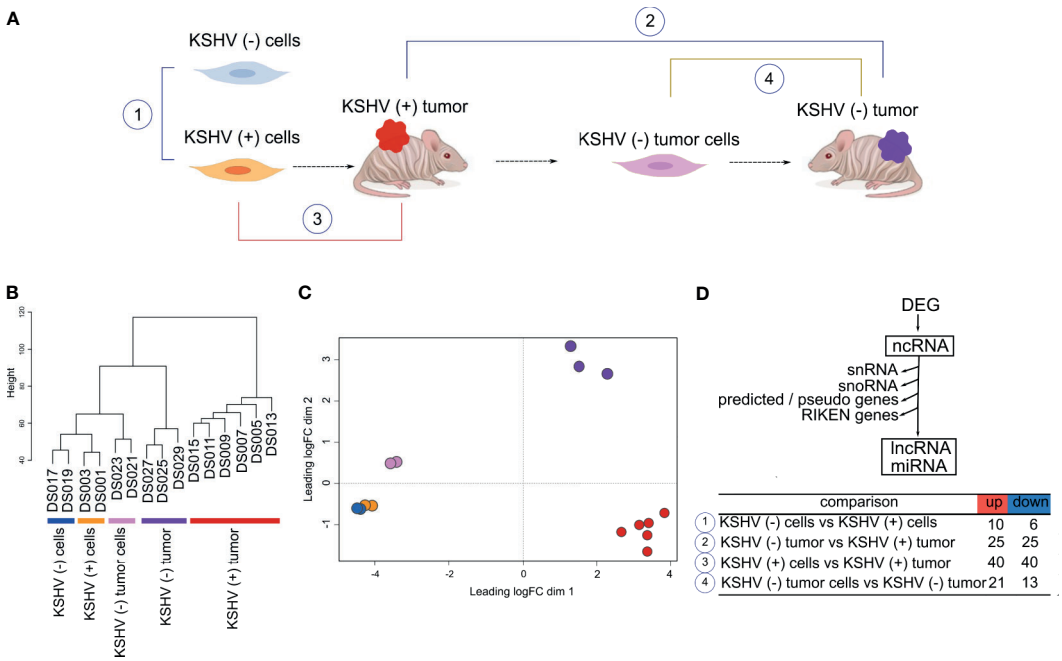

FIGURE 1 | Genome-wide analysis of Non-coding RNAs in a cell and animal model of Kaposi's Sarcoma. **(A)** Schematic representation of the mouse-KS cell and tumor model. **(B)** Unsupervised clustering of the host ncRNA transcriptome. **(C)** Multidimensional scaling plot of the host ncRNAs showing the distance of each sample from each other determined by their leading log Fold Change (FC). **(D)** Workflow analysis and number of DE lncRNAs in key biological comparisons that were detected by RNA-sequencing analysis of: two KSHV (+) cells, two KSHV (−) cells, six KSHV (+) tumors, two KSHV (−) tumor cells and three KSHV (−) tumors.

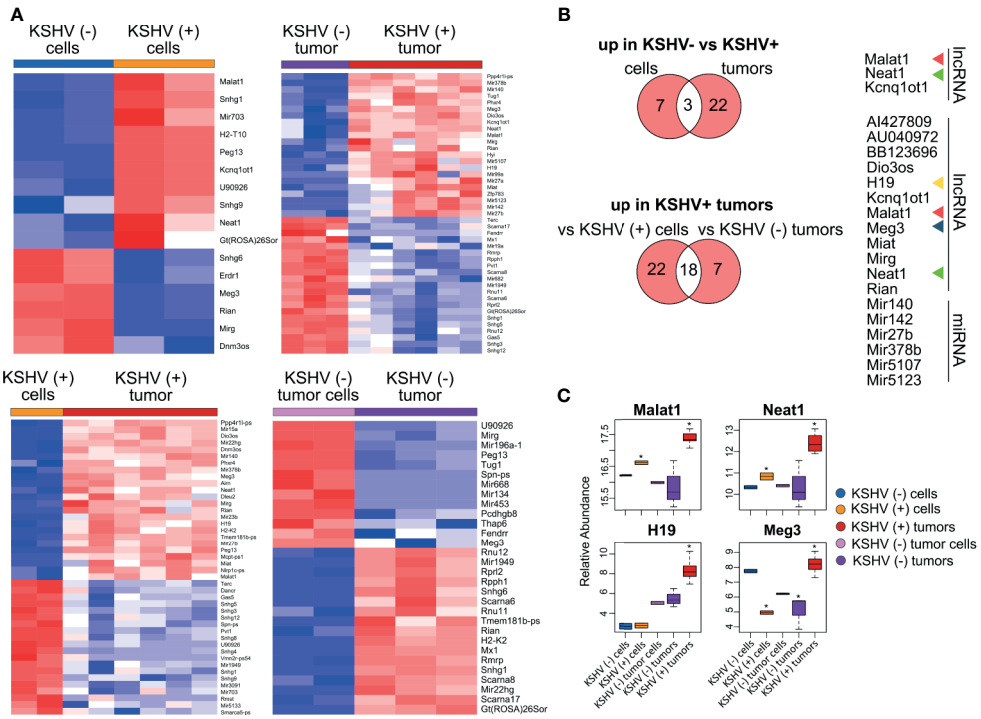

FIGURE 2 | Host lncRNAs expression. **(A)** Heat maps for fold change expression of host lncRNAs based on analysis of RNA sequencing data, all or the top 25 upregulated (red) and top 25 downregulated (blue) DE lncRNAs are shown in each comparison. **(B)** Venn diagrams showing upregulated host lncRNAs common in KSHV (+) cells and tumors *versus* KSHV (–) cells and tumors (top), and upregulated host lncRNAs common in KSHV (+) tumors *versus* KSHV (+) cells and KSHV (+) tumors *versus* KSHV (–) tumors (bottom). **(C)** Relative abundance of selected lncRNA RNAs across the different steps of the mouse-KS cell and tumor model. The asterisk refers to the level of statistical significance, established at p value <0.01.

Mir27b, and *Mir378b*, among others (**Figure 2B**). Eventually, the analysis allowed us to select four lncRNAs with a very interesting pattern of expression through the different biological relevant comparisons (*Malat1, Neat1, H19* and *Meg3*). *Malat1* and *Neat1* are upregulated in KSHV (+) cells and KSHV (+) tumors when compare with their KSHV (–) counterparts, suggesting a KSHV-dependent upregulation of these lncRNAs (**Figure 2C**). *H19* and *Meg3* are upregulated during the transition *in vitro* to *in vivo* in the presence of KSHV (KSHV (+) tumors *versus* KSHV (+) cells), but in this same transition in the absence of KSHV these lncRNAs are not upregulated (KSHV (–) tumors *versus* KSHV (–) tumor cells). This pattern of expression indicates a KSHV-dependent regulation of these lncRNAs during this transition induced by environmental cues (**Figure 2C**).

Pathway Analysis of the lncRNAs, Reveals KSHV Closely Related Bioprocesses

To contextualize the selected lncRNAs into functional processes, we employed LncRNA2Target v2.0 and LncTarD databases (15, 16) as resources of lncRNA-target relationships. Since the four selected lncRNAs have been studied more extensively in humans than in mice we searched for their experimentally validated targets (EVT) (**Supplementary Table 2**). Functional enrichment analysis (KEGG) of the resulting lists of genes revealed several related pathways common to the four lncRNAs, mainly cancer-related pathways and bioprocesses associated with viral diseases (**Supplementary Figure 1** and **Supplementary Table 2**). Interestingly, *KSHV infection* and *MicroRNAs in cancer* were the common signature of the 4 lncRNAs (**Supplementary Figure 1**).

Next, we established a list of the total human target genes contributed by the 4 lncRNAs and looked for their homologues among the DE host genes previously obtained across the different comparisons of our model (**Figure 3A** and **Supplementary Table 3**). **Figures 3B–D**, shows the chord plots illustrating the biological process terms and the target genes of the four lncRNAs contributing to that enrichment arranged in order of their expression level in the corresponding comparisons (**Supplementary Table 3**). Processes such as *Integrins in Angiogenesis* (with the genes *Spp1, Vegfa, Fn1, Kdr, Igf1r*), *Signaling by PDGF* (*Vegfa, Kdr, Cdkn1a, Igf1r*), *HIF-1 signaling* (*Vegfa, Hif1A, Stat3, Il6, Cdkn1a, Pik3r1, Igf1r*), *MicroRNAs in cancer* (*Dicer1, Zeb1, Zeb2, etc.*) and *KSHV infection* (*Fgf2, Hif1a, Stat3, Il6, Pik3r1, Jak2, Rb1, Jun*) were overrepresented by upregulated target genes in KSHV (+) tumors compared with KSHV (–) tumors. *Apoptosis* (*Mdm2, Bax, Myc, Casp3*) and *p53 activity regulation (Mdm2, Bax, Casp3, Pcna)* were instead associated with downregulated genes in the KSHV-bearing tumors (**Figure 3B** and **Supplementary Table 3**). Similar findings were observed in the comparison KSHV (+) cells

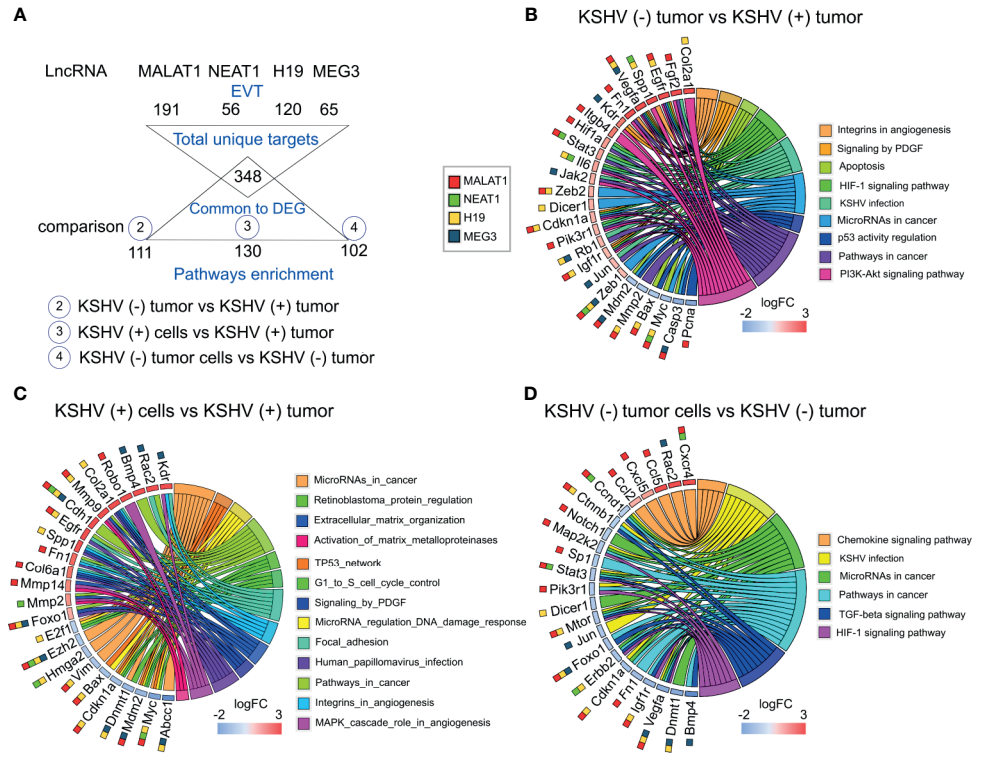

FIGURE 3 | Pathway analysis of selected DE lncRNAs and their EVT genes. **(A)** Schematic representation of the EVT genes of Malat1, Neat1, H19 and Meg3 that were correlated with gene expression in the RNA-sequencing analysis. **(B–D)** Chord plot illustrating the GO biological process terms and the target genes contributing to that enrichment arranged in order of their expression level in KSHV (–) tumors *versus* KSHV (+) tumors **(B)**, KSHV (+) cells *versus* KSHV (+) tumors **(C)** and KSHV (–) tumor cells *versus* KSHV (–) tumors **(D)**. The corresponding lncRNAs are indicated with color boxes besides each target gene.

versus KSHV (+) tumors (*in vitro* to *in vivo* transition), with the particular contribution of upregulated target genes associated with *Extracellular Matrix Organization* and *Activation of Matrix Metalloproteinases (MMP)*, represented by *Mmp2, Mmp9, Mmp13*, and *Mmp14* (**Figure 3C** and **Supplementary Table 3**). Also, pathways of DNA integrity control and cell cycle checkpoints, such as *Tp53 network*, *MicroRNA regulation of DDR* and *G1 to S cell cycle control* were revealed in this comparison, represented by the downregulated genes *E2f1*, *Bax*, *Dnmt1*, *Cdkn1a*, *Myc*, or *Mdm2*. Interestingly, in the transition *in vitro* to *in vivo* but in the absence of KSHV we found processes related to the terms *KSHV infection* (*Ccnd1*, *Ctnnb1*, *Map2k2*, *Stat3*, *Pik3r1*, *Jun*, *Erbb2*, *Igf1r*) and *MicroRNAs in cancer* (*Dicer1*, *Ccnd1*, *Ctnnb1*, *Sp1*, etc.) associated with down-modulated genes in KSHV (–) tumors (**Figure 3D** and **Supplementary Table 3**), in contrast to that observed in the KSHV-dependent transition (**Figure 3C**).

Taking together, the integrative in-silico analysis of the lncRNAs-EVT and their associated pathways, with the host transcriptome derived from our model, reveals that the upregulation of *Malat1*, *Neat1, H19*, and *Meg3* in KSHV (+) tumors would contribute with a network of gene-pathways closely related with KSHV oncogenesis.

KSHV-Dependent *In Vitro* to *In Vivo* Transition Is Defined by a Significant Up-Regulation of Host miRNAs

LncRNAs have been demonstrated to regulate gene expression by various mechanisms, including epigenetic modifications, lncRNA-miRNA specific interactions, and lncRNAs as miRNA precursors. Our previous approach showed clear relationship among the four selected lncRNAs and miRNAs in cancer. Therefore, we performed small-RNA sequencing on the samples obtained from our model to identify host DE miRNAs. Next, we conducted an integrated bioinformatics workflow to elucidate relevant networks of lncRNA-miRNA-mRNA during KSHV tumorigenesis.

Unsupervised analysis of 14 samples based on miRNAs expression profiles shows how they cluster together in an unsupervised way according to their predefined features (**Figure 4A**). Interestingly, the samples cluster in the same pattern as when the analysis was made for lncRNAs (**Figure 1B**) and also for all host genes in our previous study (13). The distance among groups is reflexed in the number of DE miRNAs (**Figure 4B** and **Supplementary Table 4**). Remarkably, the higher proportion of upregulated miRNAs was observed in KSHV (+) tumors (95% of DE miRNAs) compared with KSHV

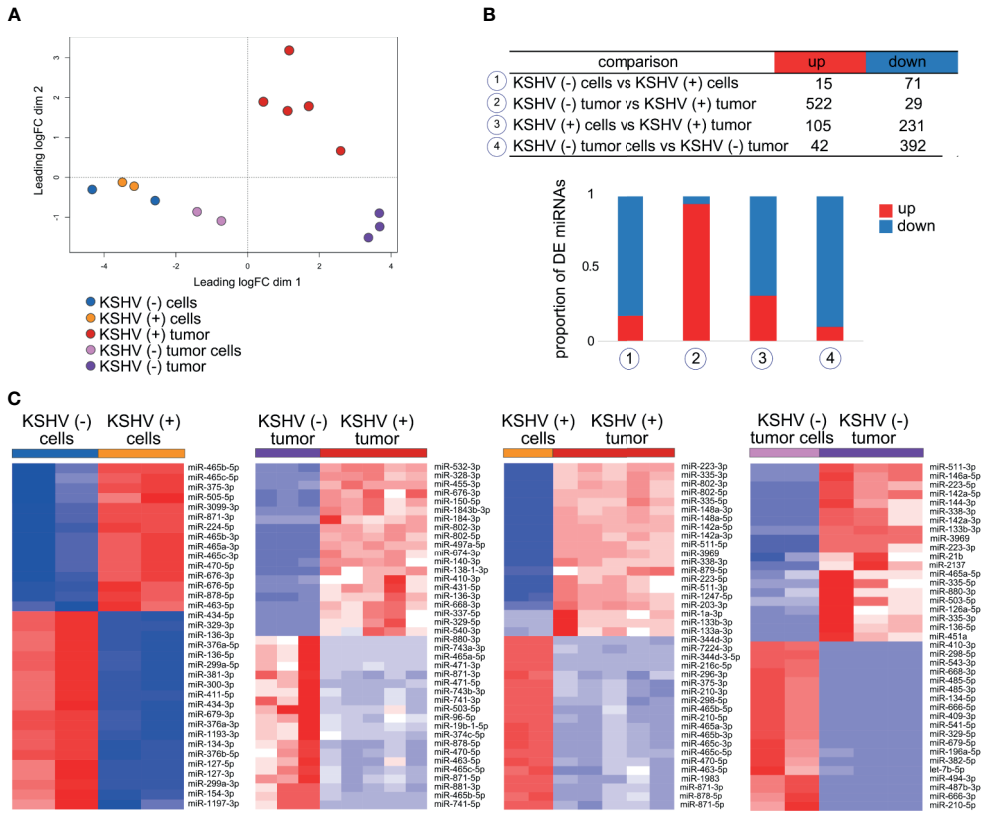

FIGURE 4 | Host miRNAs expression. **(A)** Multidimensional scaling plot of the host miRNAs showing the distance of each sample from each other determined by their leading logFC. **(B)** Number of DE miRNAs in key biological comparisons that were detected by small RNA-sequencing analysis of: two KSHV (+) cells, two KSHV (–) cells, six KSHV (+) tumors, two KSHV (–) tumor cells and three KSHV (–) tumors. **(C)** Heat maps for fold change expression of host miRNAs based on analysis of small RNA sequencing data, only top 20 upregulated and top 20 downregulated DE host miRNAs are shown in each comparison.

(–) tumors, while downregulated miRNAs were more prevalent in KSHV (–) tumors (90% of DE miRNAs) compared with KSHV (–) tumor cells (**Figure 4B** and **Supplementary Table 4**). This result is consistent with that previously described in which the term *MicroRNAs in cancer* was associated with upregulated genes in KSHV (+) tumors and down-regulated genes in KSHV (–) tumors (**Figures 2B, C**). Such difference could be partly explained by *Dicer1*, a master regulator of miRNA biosynthesis, which is in turn linked to the lncRNA H19 (**Figures 3B, D**). We performed heat map representations of all or top-50 DE microRNAs -according to each comparison- for all the 4 biological relevant comparisons mentioned previously (**Figure 4C**).

Differentially Expressed miRNAs Regulate Gene Targets Related to KSHV Affected Biological Processes

Mature miRNAs regulate gene expression at the posttranscriptional level *via* partial base-pairing with their target mRNAs. Such interaction leads to mRNA degradation and/or translational inhibition, causing the downregulation of proteins encoded by the miRNA-targeted mRNAs, a biological phenomenon termed RNA interference (RNAi) (21). *In silico*-based functional analysis of miRNAs usually consists of miRNA target prediction and functional enrichment analysis of miRNA targets.

To identify the experimentally supported targets from our previous published work (13) for the DE miRNAs identified in this study, we employed DIANA TARBASE v8 (17). Next, we selected those targets whose expression antagonizes with that of its miRNA in the corresponding comparison (**Figure 5A** and **Supplementary Table 5**). As we mentioned before, most of DE miRNAs in the KSHV (–) tumors *versus* KSHV (+) tumors were upregulated in KSHV (+) tumors, thus their corresponding targets were downregulated in the same group. Pathways analysis of these downregulated genes indicated enrichment in: *P53 signaling pathway (Bax, Gorab, Ccng1*, Rrrm2, etc.), *Spliceosome (Tra2a*, *Tra2b*, *Srsf10*, *Snrpb*, *Snrpb2*, etc.), *E2F transcription factor (E2f6, E2f7, Rrm1, Rbl1, etc.)* and *Cell cycle (Xpo1, Nedd1, Zwint, Psma1, Psma3, etc.)*, among others (**Figure 5B** and **Supplementary Table 5**).

In the *in vitro* to *in vivo* transition, with a more proportional distribution of DE miRNAs, upregulated and downregulated target genes were consequently identified, which provided greater enrichment of bioprocesses closely related to the obtained with the lncRNA targets in the same comparison. As can be seen in the chord plot of **Figure 5C**, upregulated target

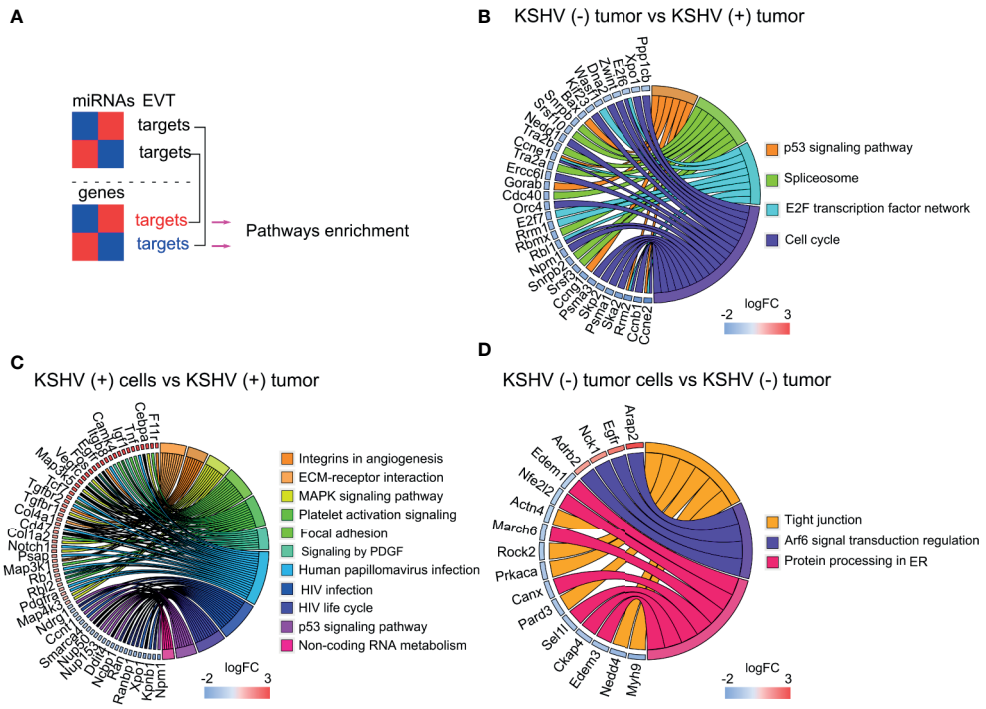

FIGURE 5 | Pathway analysis of DE miRNAs and their experimentally validated target (EVT) genes. **(A)** Schematic representation of the miRNA–mRNA pairs with significant ($p < 0.05$) antagonistic expression. **(B–D)** Chord plot illustrating the GO biological process terms and the target genes contributing to that enrichment arranged in order of their expression level in KSHV (–) tumors *versus* KSHV (+) tumors **(B)**, KSHV (+) cells *versus* KSHV (+) tumors; for a better visualization only a fraction of the genes corresponding to the plot is shown. The full list is available in **Supplementary Table 5 (C)** and KSHV (–) tumor cells *versus* KSHV (–) tumors **(D)**.

genes, in the upper half of the circle, are significantly associated with processes such as *Integrins in Angiogenesis* (*Col1a12, Col4a1, Col6a2, Itgb3*, etc.), *ECM-receptor interaction* (*Itga4, Itgb3, Itgb8, Sdc1, Col1a2, etc.)*, *MAPK signaling pathway* (*Rps6ka3, Cebpa, Map3k1, Map314*, etc.), *Platelet activation signaling* (*Vav3, App, Fga, Col1a2, Tgfb3*, etc.) and *Signaling by PDGF* (*Pdgfra, Col4a1, Col4a2, Col6a2, Camk4, Foxo1*, etc.). Meanwhile, in the lower half of the plot, the viral infections related processes *HPV* (*Tcf7, Fzd4, Itga4, Tcf7, Tnf*, etc.) and *HIV* (*Xpo1, Npm1, Nup50, Nup153, Nup160, Nup205*, etc.), and the *p53 signaling* (*Dusp5, Ddit4, Ccng1*, etc.) are over-represented by downregulated genes (**Figure 5C** and **Supplementary Table 5**). Within the latter, it is worth highlighting the presence of numerous genes related to the nuclear export machinery (*Ranbp1, Ran, Xpo1, Nup50, Nup153, Kpnb1, Ncbp1*). Lastly, in the *in vitro* to *in vivo* transition in the absence of KSHV, fewer terms were significantly over-represented by the miRNAs target genes. Among them highlights *Tight junctions*, linked to down-regulated genes, and *Arf6 signal transduction* over-represented by the up-regulated ones (**Figure 5D** and **Supplementary Table 5**).

Collectively, these results indicate that the presence of KSHV has a significant impact on the metabolism of host miRNAs, which contribute to the regulation of host genes linked to processes of angiogenesis, ECM, transcriptional metabolism, viral infections and cell cycle control, mainly.

KSHV miRNAs and lncRNAs Expression in Mouse KSHV (+) Tumors

To study the relevance of KSHV miRNA expression in KSHV tumorigenesis we used the small-RNA sequencing data of read counts to analyze the relative expression between miRNAs in KSHV (+) tumors (**Figure 6A**). The ten most frequent microRNAs in KSHV (+) tumors were K12-4-3p, K12-3-5p, K12-8-3p, K12-10a-3p, K12-2-5p, K12-7-3p, K12-4-5p, K12-1-5p, K12-11-3p, K12-3-3p representing 97% of the counts detected for viral microRNAs in KSHV (+) tumors (**Supplementary Table 6**).

Following the same criteria used for host ncRNAs, we searched for KSHV miRNA targets. To do this, we considered the top 10 most frequent KSHV miRNAs (**Figure 6A**). We used *Tarbase V8* database (17), and obtained a list of 2168 human experimentally supported gene targets (**Supplementary Table 6**). Next, we looked for their homologues in mice, which were downregulated in KSHV (+) tumors in comparisons 2 and 3 (**Figure 1A**). A total of 220 genes were obtained for which functional enrichment was performed (**Supplementary Table 6**). Interestingly, once again, processes closely related to those previously found for host ncRNAs were obtained (**Figure 6B**): *Cell cycle* (*Ccne2, Cdkn1a, Hdac2, Mdm2, Pcna*, etc.); *Spliceosome* (*Hnrnpc, Hnrnpk, Hnrnpu, Magohb, Prpf40a, Sf3a1, Snrpb2, Srsf1*, etc.); *miRNA regulation of DDR* (*Casp3, Ccne2, Ccng1, Cdkn1a, Mdm2, Tnfrsf10b*); *Viral carcinogenesis*

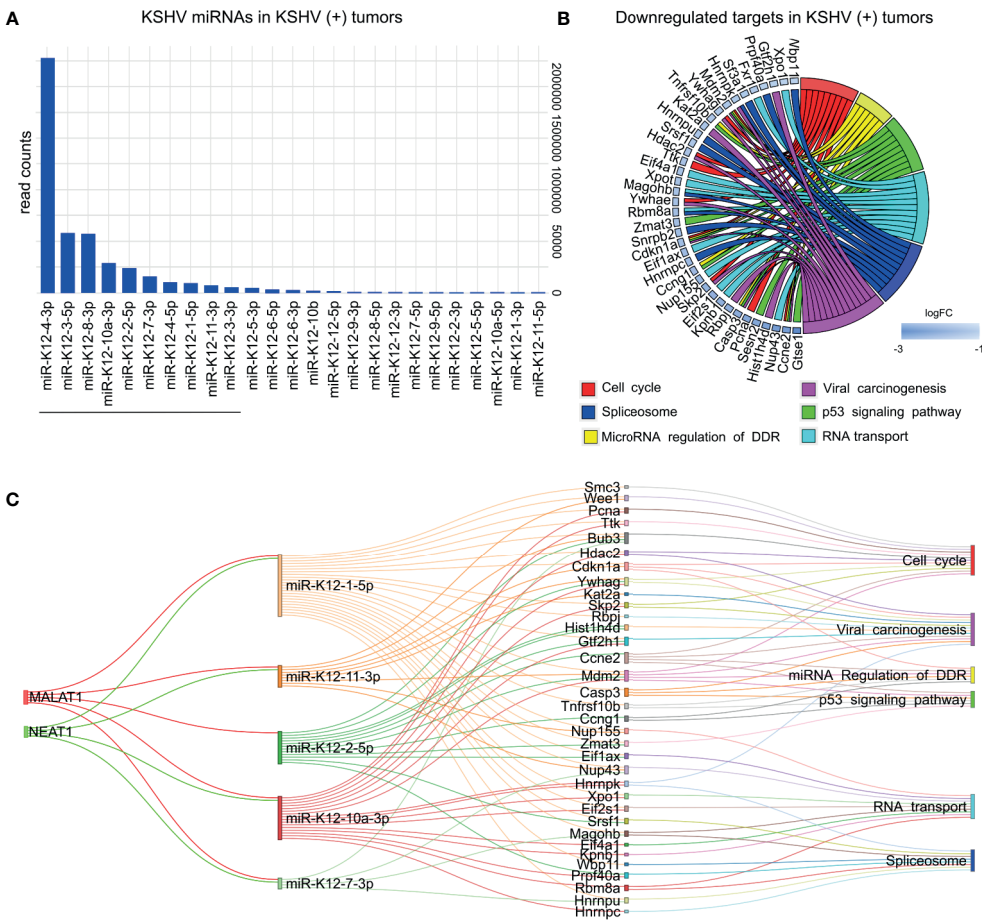

FIGURE 6 | KSHV miRNAs expression analysis in KSHV (+) tumors. **(A)** Bar plot of KSHV miRNAs relative abundance by showing counts in KSHV (+) tumors. Underlined are shown the top ten most frequent miRNAs **(B)** Pathway analysis showing host downregulated target genes of the ten KSHV miRNAs most abundant in KSHV (+) tumors. **(C)** Network relationship among lncRNAs, KSHV microRNAs, mRNAs and their enriched pathways.

(*Casp3, Ccne2, Cdkn1, Gtf2h1, Hdac2, Hist1h4d, Kat2a, Mdm2*, etc.), *p53 signaling* (*Casp3, Ccne2, Ccng1, Cdkn1a, Gtse1, Mdm2, Sesn2, Tnfrsf10b*, etc.) or *RNA transport* (*Eif1ax, Eif2s1, Eif4a1, Fxr1, Kpnb1, Magohb, Nup155, Nup43, Xpo1, Xpot*).

Among other non-coding RNAs KSHV encodes a number of lncRNAs (7). We inquired into the RNA-seq data and identified seven out of twelve annotated lncRNAs, with detectable levels of expression in KSHV (+) cells and tumors. As-ORF7, as-K5/K6, as-ORF65/69, and ALT were the most abundant transcripts (**Supplementary Table 6**). DEG analysis between KSHV (+) cells and KSHV (+) tumors identified as-ORF7 and as-K5/6 upregulated in the transition *in vitro to in vivo* (**Supplementary Figure 2** and **Supplementary Table 6**), further indicating a possible role of these KSHV lncRNAs in tumorigenesis.

Identification of a lncRNA-miRNA-mRNA Interaction Network Involved With KSHV Tumorigenesis

LncRNAs can also serve as regulatory elements of the RNAi pathway (22). Indeed, host lncRNA transcripts are involved not only with the maturation of miRNA transcripts but also they may interfere with miRNA induced translation inhibition, thus acting as competing endogenous RNAs (ceRNAs), or "sponge RNAs" (22). Such lncRNA-miRNA associations allow for a fine tuning of gene expression regulation. Therefore, dysregulation of the lncRNA-miRNA balance could contribute to the onset of KSHV pathogenesis.

To identify relevant pairs of lncRNA-miRNA in our model, we used DIANA-LncBase v3 (18). For each of the four lncRNAs we searched for their highly confident experimentally supported viral and host miRNA targets, derived from high-throughput methodologies, which were in turn DE in the corresponding comparison.

Within the ten most abundant KSHV miRNAs, we found that five of them have been associated with the human lncRNAs *MALAT1* and *NEAT1*. When analyzing the targets (downregulated in KSHV + tumors) of these five miRNAs, we observed that they share most of the genes obtained with the ten miRNAs, which is therefore reflected in the same enriched pathways (**Figure 6C** and **Supplementary Table 7**).

Using the same approach, we proceeded with the analyses for the lncRNA-host miRNAs associations. For the *in vitro* to *in vivo* transition dependent of KSHV, 31 miRNAs accomplished the criteria, of which 23 were upregulated and 8 were downregulated in KSHV (+) tumors (**Figure 7** and **Supplementary Table 7**). The highest contribution was made by *Malat1* (29 miRNAs) and *Neat1* (21 miRNAs), followed by *Meg3* (11 miRNAs) and *H19* (8 miRNAs). Among the downregulated miRNAs highlights the members of the miR17-92 family: miR-17-5p, miR-19a-3p, miR-20a-5p, and miR-92a-3p. Their respective targets are represented by genes such as *Egfr, Foxo1, Pdgfra, Rb1, Igf1, Map3k1*, etc. all upregulated in KSHV (+) tumors (**Figure 7**). Other relevant downregulated miRNAs were miR-128-3p and miR-155-5p, which target multiple common genes. On the other hand, up-modulated miRNAs were linked mostly to *Malat1* and *Neat1*. Remarkably, among them are miR27-b-3p, miR-140-3p, miR-142-3p, and miR-142-5p, whose gene precursors were also found up-modulated in KSHV (+) tumors (**Figure 2B**). As can be seen in **Figure 7**, the functional analysis that arose from the lncRNA-miRNA-mRNA triad shows that the pathways are arranged in an unsupervised way in three main clusters. The *MAPK signaling* together with *Pathways in cancer* would make up the 1st group, over-represented by the upregulated target genes contributed mainly by miR-671-5p, miR-128a-3p, miR-155-5p, and let 7e-5p, as well as the miRNAs of the miR17-92 cluster. A second group is integrated by processes related to *Viral infection* (HPV infection), *Matrix organization* and *Angiogenesis*, represented by genes contributed by the miRNAs of the miR17-92 cluster, let-7d-5p and miR-124-3p, along with others (**Figure 7**). A third group would be made up of the pathways *HIV life cycle* and *p53 signaling*, over-represented by negatively regulated genes, targets of the miRNAs miR-27b-3p, miR-101a-3p, miR-140-3p, and miR-142, among others (**Figure 7**).

For the comparison KSHV (−) tumors *versus* KSHV (+) tumors, we obtained a network of the four lncRNAs targeting 26 miRNAs all upregulated in KSHV (+) tumors with their corresponding downregulated target genes (**Figure 8** and **Supplementary Table 7**). It is evident a shift in the expression of specific miRNAs, such as let-7e-5p, let-7d-5p, miR-123-3p, and miR-31-5p, compared to that observed in the KSHV-dependent transition. Other relevant miRNAs that appear are miR-26b-5p, miR-181 (with its variants a, b and c), miR-378-3p, and miR-381-3p. Here again, the presence of miR-140-3p and miR-378-3p correlates with their respective immature precursors that had been identified previously as upregulated along with the lncRNAs (**Figure 3B**). By analyzing the mRNA targets of the miRNA signature, previously identified as downregulated in KSHV (+) tumors, we obtained a relatively small group of genes that function in two major related processes: the regulation of cell cycle control (*G1 to S cycle control*, *p53 activity regulation, MicroRNA regulation of DDR*) and the transcription machinery, with the pre-mRNA splicing machinery (*Spliceosome)* and the *E2F transcription factor network* (**Figure 8**). Remarkably, this functional pattern resembles that observed with the KSHV miRNAs (**Figure 6**).

Collectively, our analysis revealed a functional network of lncRNA-miRNA-mRNA in a KSHV animal model.

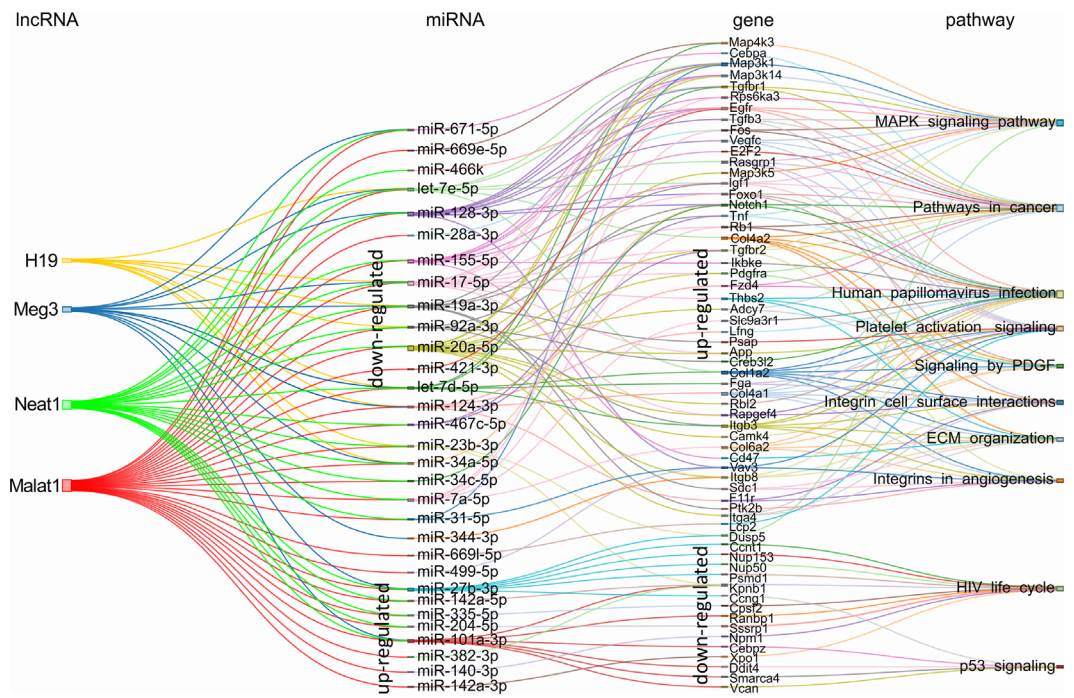

FIGURE 7 | Schematic representation of the experimentally supported triad lncRNA-miRNA-mRNA and the pathways in which the later are involved for the KSHV-dependent *in vitro* to *in vivo* transition. The expression status in KSHV (+) tumors is indicated for miRNAs and their respective targets.

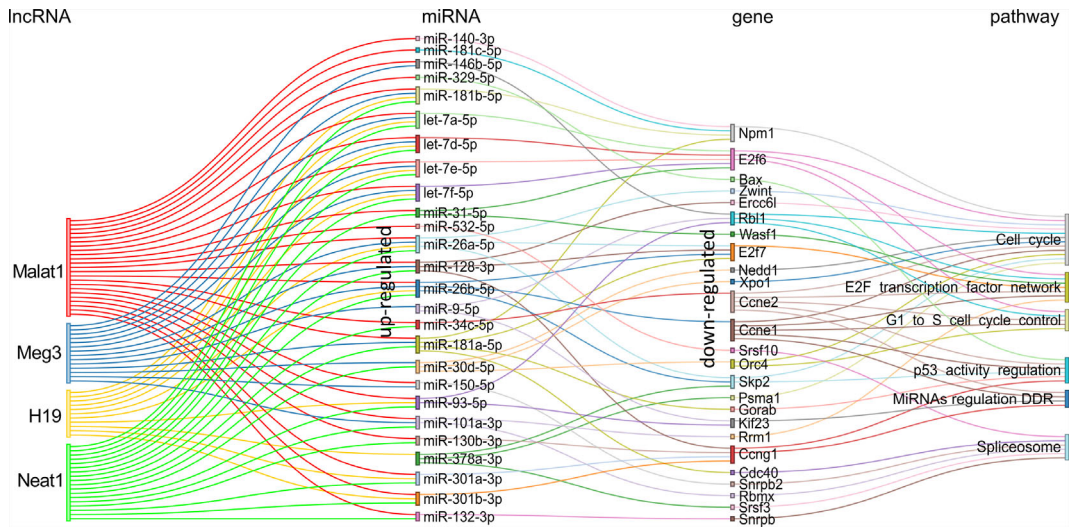

FIGURE 8 | Schematic representation of the experimentally supported triad lncRNA-miRNA-gene and the pathways in which the later are involved for the comparison KSHV (–) tumor vs KSHV (+) tumor. Pairs lncRNA-miRNA were identified only for the up-modulated miRNAs.

Gene Signatures Used to Identify Drug-Associated Genes or Networks

KS remains potentially life threatening for patients with advanced or ART-resistant disease, where systemic therapy is indicated and three FDA-approved agents that include liposomal anthracyclines are available (4, 23, 24). Despite the effectiveness of these agents, most patients progress within six to seven months of treatment and require additional therapy (25). Therefore, there is a need to develop alternative strategies. Identifying drugs or clinical candidates that synergize with the current KS frontline therapeutic approaches has immediate translational potential that would be realized in a clinical trial if identified drug combinations show sustained efficacy in animal models. Our animal model allowed us to develop signatures that can be used to identify druggable gene or networks defining relevant AIDS-KS therapeutic targets.

For this end we used two approaches: 1) druggable miRNAs-gene pairs, and 2) the complete signature of the lncRNA-miRNA-mRNA network for upregulated genes.

Since miRNAs can affect the expression of druggable genes eventually affecting drug efficacy, we searched for drugs for the miRNAs-down/genes-up pairs. We employed the Pharmaco-Mir Database (19), which identifies associations of miRNAs, genes they regulate, and the drugs dependent on these genes. **Supplementary Table 8** summarizes the list of drugs identified for each miRNA-gene pair. Among the drugs identified in our analysis there were some used against targets in experimental KSHV models or in clinical practice: Abacavir (mir19a-TNF), Bevacizumab (miR19a-IGF1), Celecoxib (miR17-RB1), Imatinib (miR17-PDGFRA), Oxaliplatin (miR19a-IGF1), Sirolimus (miR19a-IGF1; miR20a-MAP3K5), Sunitinib (miR-128-VEGFC; miR17-PDGFRA; miR-19a-TNF; miR-20a-PDGFRA), and Thalidomide (miR19a-TNF) (**Table 1**, upper half of the table).

As a second approach, we used the signature of the lncRNA-miRNA-mRNA network from **Figure 7** to search for drugs for the upregulated genes in the drug gene interaction database dgidb (20). We found, among others, chemotherapeutics agents such as Cisplatin (targeting SMARCA4, MAP3K1, RB1, EGFR, RRM1, and BAX) and Bortezomib (targeting PSMD1, RB1, NOTCH1, PSMA1, and BAX) and HDAC inhibitors, such as Vorinostat (targeting NPM1 and RB1) (**Table 1**, bottom half of the table). Moreover, we found kinase inhibitors such as Palbociclib (SMARCA4, RB1, RPS6KA3, and CCNE1), Midostaurin (PDGFRA), and ENMD-2076 (PDGFRA). Finally, Daunorubicin (APP) that is currently used to treat Kaposi's sarcoma (26).

Importantly, some of the aforementioned drugs (abacavir, doxorubicin, bevacizumab, bortezomib, imatinib, sirolimus, and thalidamide) have been evaluated alone or in combination with other drugs in different KS clinical trials. The description of such studies is found in **Supplementary Table 8**. The fact that our analyses pointed to drugs that target KS oncogenic pathways identified in the laboratory or drugs that are currently in use of being tested in AIDS-KS, reinforces the possibility of involvement of the KSHV regulated ncRNA network in viral sarcomagenesis.

DISCUSSION

Virus-host interactions trigger a set of mechanisms that eventually affect the expression of host genes involved in the regulation of the viral replicative cycle as well as the pathogenesis of the disease (27). Whereas dysregulation of host protein-coding genes caused by KSHV infection is well explored, host ncRNAs and KSHV dependency remains poorly characterized. Currently, miRNAs and lncRNAs are by far two of the most commonly studied ncRNA biotypes (28, 29).

TABLE 1 | Drug-associated to miRNA-gene pairs (upper half of the table) or genes (bottom half of the table) obtained from the lncRNA-miRNA-mRNA network.

Drug	miRNA-gene targets	Source	Drug Tested in Clinical Trials (ID)
ABACAVIR	mir19a-TNF	Pharmaco-Mir	NCT00834457
BEVACIZUMAB	miR19a-IGF1	Pharmaco-Mir	NCT00055237, NCT01296815, NCT00923936
CELECOXIB	miR17-RB1	Pharmaco-Mir	–
IMATINIB	miR17-PDGFRA	Pharmaco-Mir	NCT00090987
OXALIPLATIN	miR19a-IGF1	Pharmaco-Mir	–
SIROLIMUS	miR19a-IGF1; miR20a-MAP3K5	Pharmaco-Mir	NCT00450320
SUNITINIB	miR-128-VEGFC; miR17-PDGFRA; miR-19a-TNF; miR-20a-PDGFRA	Pharmaco-Mir	–
THALIDOMIDE	miR19a-TNF	Pharmaco-Mir	NCT00049296, NCT00019123
BORTEZOMIB	PSMD1, RB1, NOTCH	Pharmaco-Mir	NCT01016730
Drug	**gene targets**	**Source**	**Drug Tested in Clinical Trials (ID)**
CHEMBL3397300	EGFR	DGIdb	–
CISPLATIN	SMARCA4, RB1, MAP3K1, EGFR	DGIdb	–
DAUNORUBICIN	APP	DGIdb	NCT00002093, NCT00002985, NCT00427414
ENMD-2076	PDGFR	DGIdb	–
ISONIAZID	TNF	DGIdb	–
LORLATINIB	RB1	DGIdb	–
MIDOSTAURIN	PDGFRA	DGIdb	–
PALBOCICLIB	SMARCA4, RB1, RPS6KA3	DGIdb	–
VORINSTAT	RB1	DGIdb	–

We have previously developed and characterized a unique multistep KSHV tumorigenesis model in which cells explanted from a KSHV (+) tumor that lose the episome can form KSHV (−) tumors driven by host mutations such as the PDGFRA-D842V (12, 30). Using NGS on this model, we interrogated the transcriptional, genetic and epigenetic (CpG island methylation) landscape upon KSHV tumor formation and upon KSHV-loss in cells and tumors (13). In such study, we focused on the host and virus coding genes. Therefore, taking advantage of the model and the RNA-sequencing technology, we decided—for this study—to explore the transcriptional consequences of KSHV tumorigenesis on the ncRNAs setting, with the aim of identifying a functional interplay between lncRNAs and miRNAs dependent of KSHV.

Here we identified four relevant lncRNAs upregulated in KSHV (+) tumors: Malat1, Neat1, H19 and Meg3. Accumulating evidence has shown that lncRNA exert its functions by regulating the expression of target genes. As a first approach, using databases that collects all lncRNA–target relationships confirmed by binding experimental technologies, we searched for the target genes for the human homologues of each of the selected lncRNAs. In addition to having common target genes, pathway analysis showed that the four lncRNAs also share common related processes, mainly associated with cancer and viral infections. Interestingly, *KSHV infection* and *MicroRNAs in cancer* were among the common over-represented terms.

Next, we interrogated the transcriptome of our model to identify the 4-lncRNAs common targets into the DEG. The integrated analysis allowed us to define a reduced group of host lncRNAs-target genes that significantly would contribute with KSHV tumorigenesis and related processes. The integration of the in silico approach of the lncRNAs-EVT and their associated pathways, with the host transcriptome derived from our model, reveals a network of gene-pathways closely related with KSHV oncogenesis: *Integrins in angiogenesis*, *KSHV infection*, *signaling by PDGF*, *HIF1-signaling pathway* or *MicroRNAs in cancer* were represented by upregulated genes such as *Egfr; Vegfa, Hif1a, Dicer1, Zeb1, Zeb2, Rb1, or Il6.*

In addition, one of the distinctive pathways of the *in vitro* to *in vivo* transition dependent of KSHV, provided by the lncRNA targets, was *Extracellular Matrix Organization* and *Activation of Matrix Metalloproteinases*, overrepresented by the MMPs *Mmp2*, *Mmp9*, *Mmp13*, and *Mmmp14*. MMPs are associated with KS and may contribute to the mechanism of KS tumor growth. They are usually synthesized by the tumor stromal cells, including fibroblasts, myofibroblasts, inflammatory cells and endothelial cells. These components can also integrate a tumor derived from cells *in vitro*. Although the mechanism by which Malat1, Neat1, or H19 regulate the expression of MMPs is not yet clear, different studies have shown that the silencing or overexpression of these lncRNAs positively correlate with the expression of MMPs, such as MMP9 or MMP2 (31–33).

MALAT1 is perhaps the most studied lncRNA and consequently the one with the most targets. It has been shown to regulate EGFR expression promoting carcinogenesis (34); it has been shown to regulate endothelial cell function and vessel growth (35); it has been defined as a hypoxia-induced lncRNA (36); it modulates *ZEB1* and *ZEB2* by sponging miRNAs (37, 38). Remarkably, *MALAT1* expression is induced by the platelet-derived growth factor BB (PDGF-BB) (39). In a recent study, we have shown that the KSHV-ligand mediated activation of the PDGF signaling pathway is critical for KS development (30). Later, we found that two PDGFs, Pdgfa and Pdgfb, and their receptor Pdgfra were both hypo-methylated and up-regulated in KSHV (+) tumors (13). Overall, the evidence clearly shows that *Malat1* is a key regulator of several target genes involved in KSHV-dependent signaling pathways. It remains to be determined whether Malat1 is a driver or simply a passenger of KSHV tumorigenesis.

NEAT1, is closely related to *MALAT1* (aka NEAT2), and both have been shown to bind multiple genomic loci on active genes, but display distinct binding patterns, suggesting independent but

complementary functions (40). As *MALAT1*, *NEAT1* is retained in the nucleus where it forms the core structural component of the paraspeckle sub-organelles. The formation of paraspeckle increases in response to viral infection or proinflammatory stimuli (41). Furthermore, Viollet et al. (42) demonstrated that *NEAT1* is upregulated in KSHV infected cells *versus* non-infected cells under hypoxic conditions. Our results show that *Neat1* is upregulated in KSHV- cells *versus* KSHV+ cells and indeed is upregulated in KHSV (+) tumors, during the *in vitro* to *in vivo* transition. On the other hand, the lncRNA target analysis showed that *Neat1* positively associates with the upregulated targets *Il6*, *Stat3* and *Spp1* in the KSHV (+) tumors. In this regard, *NEAT1* has been shown to strengthen IL-6/STAT3 signaling and promote tumor growth and proliferation through nuclear trapping of mRNAs and proteins which acts as inhibitors of the IL-6/STAT3 signaling pathway (43). Previously, it had been demonstrated that STAT3 is activated by KSHV infection and correlates with IL6 release in dendritic cells (44). In summary, these data taking together reveal a host network in which upregulation of Neat1 would favor the activation of IL6/STAT3 signaling contributing directly or indirectly to KSHV tumorigenesis.

MEG3 is generally considered as a tumor suppressor lncRNA. In this study we found a downregulation of *Meg3* in KSHV (−) cells *versus* KSHV (+) cells. However, a significant increase of the lncRNA was evidenced in the *in vitro* to *in vivo* transition. Sethuraman et al. (11) showed that KSHV employs its miRNAs to target *MEG3* promoting its downmodulation to potentially contribute to sarcomagenesis. Therefore, it is possible to speculate on a downmodulation of *Meg3* by the expressed KSHV miRNAs as an early event in the viral cycle followed by an upmodulation of *Meg3* as a response of the host cell to the already triggered tumor growth.

KSHV drives latently infected cells towards proliferation by a variety of mechanisms such as interfering with *MEG3* or the p53 pathway through miRNAs or the protein LANA, respectively (11, 45). In this study, we identified that p53 network would be regulated in a KSHV-dependent manner by the modulation of key genes targeted by the lncRNAs, such as *Casp3*, *Bax*, *Mdm2*, *Cdkn1a*, or *Pcna*. Interestingly, these genes along with *E2f1* are linked to other related processes such as *G1 to S phase regulation* and *MicroRNA DDR*. KSHV needs to face various cellular defense mechanisms designed to eradicate the viral infection. One such response can include DDR response factors, which can promote an arrest in cell growth (G1-S regulation) and trigger cell death (p53 network, Apoptosis). Our findings indicate that those processes would be repressed through the downmodulation of the mention lncRNA targets in KSHV (−) tumors *versus* KSHV (+) tumors, as well as in the KSHV *in vitro to in vivo* transition. Remarkably, several studies have shown that viruses including KSHV have developed suppressive strategies against DDR (9, 46). In this sense, KSHV miRNAs are relevant for protecting cells from DDR (47, 48). In addition, cellular *lncRNAs* are important gene regulators of DDR in a process which involve essential players of miRNA biosynthesis such as DICER1 and DROSHA (22, 48). In fact, *Dicer1* was one of the significantly upregulated target genes linked to H19 in the comparison KSHV (−) tumors *versus* KSHV (+) tumors. In summary, there is a complex network between KSHV and host ncRNAs that would regulate DDR factors in order to bypass cell cycle checkpoints.

miRNA analysis revealed a high proportion of upregulated host miRNAs dependent of KSHV infection. This finding led us to interrogate the functional processes associated to the miRNAs targets. Enriched terms were linked to *p53 signaling*, *Spliceosome* and *Cell cycle*. When evaluating the *in vitro* to *in vivo* transition which involved both up and downregulated miRNAs, processes such as *Integrins in Angiogenesis, Platelet activation*, or *signaling by PDGF* were associated to the upregulated targets, whereas *viral infection (HPV, HIV) or p53 signaling* were linked to the downregulated targets.

Furthermore, we evaluated the relevance of viral lncRNAs and miRNAs expression in KSHV tumorigenesis. KSHV encodes at least 16 potential lncRNAs (49). In our analysis, we were able to annotate 12 lncRNAs of which 7 showed detectable levels of expression in KSHV (+) cells and tumors. PAN RNA (polyadenylated nuclear RNA), the most abundant and characterized KSHV lncRNA linked to KSHV lytic gene expression (49), is expressed in KSHV (+) tumors (**Supplementary Figure 2**) correlating with the *in vivo* up-regulation of KSHV lytic gene expression (13). In addition, we identified as-ORF7 and as-K5/6 upregulated in KHSV (+) tumors compared to KSHV (+) cells. Although their functions are still not reported, our results indicate that these transcripts would have a potential role in KSHV tumorigenesis. Regarding miRNAs, we identified a group of ten relevant members which constituted the most frequent in mouse KSHV (+) tumors. Among them highlights K12-4-3p, K12-3-5p, K12-8-3p, previously identified as highly expressed in human KS lesions (50). Moreover, K12-4-3p, which represented 50% of the KSHV miRNAs detected in this analysis in mouse KSHV (+) tumors, was shown to be able to restore the transforming phenotype of a mutant KSHV containing a deletion of all KSHV microRNAs (51), indicating its association with cellular transformation and tumor induction. Similarly, K12-3-5p was shown to promotes cell migration and invasion of endothelial cells (52). The functional analysis of their targets—downregulated in mouse KSHV (+) tumors—showed enrichment in processes such as *Cell cycle*, *Spliceosome*, *RNA transport*, *MicroRNA Regulation of DDR*, and *p53 signaling*, coinciding with what was observed with the host miRNAs, which suggests that viral miRNAs might mimic cellular miRNAs. It is possible that the same targets are also relevant to the infection of human cells by KSHV (KSHV miRNA) and to KSHV pathogenesis (host miRNA) (53, 54).

Since the similarity with the one found with respect to the lncRNA targets, we decided to carry out an integration network dependent of KSHV between the 4-lncRNAs, the DE miRNAs (from virus and host) related to those lncRNAs, their validated targets, and the related processes.

The integration showed a more concise landscape of the potential relationships of lncRNA-miRNA-mRNA in a KSHV setting, in which, once more, highlights that the upregulated genes are involved in processes, such as pathways in cancer and those previously closely related to KSHV tumorigenesis, including *Angiogenesis, PDGF signaling, MAPK signaling or*

ECM organization. Similarly, down-modulated genes linked preferentially to *p53 signaling, Spliceosome, miRNA regulation of DDR, or RNA transport*, among others. In the latter Proteasome subunit protein *PSMD1*, nucleoporins *NUP50*, *NUP153*, nucleolar protein NPM1, or exportin 1 XPO1 have been shown to modulate HIV infection or other viral cycles (55–58). In addition, in a preprint article it was postulated an extensive destruction of the nuclear and nucleolar architecture during lytic reactivation of KSHV, with redistribution or degradation of proteins such as NPM1 (59). More interestingly NPM1 (aka NPM) is a critical regulator of KSHV latency *via* functional interactions with v-cyclin and LANA. Strikingly, depletion of NPM in PEL cells has led to viral reactivation, and production of new infectious virus particles (60). On the other hand, using a model of oncogenic virus KSHV-driven cellular transformation of primary cells, Gruffaz et al. (61) illustrate that XPO1 is a vulnerable target of cancer cells and reveal a novel mechanism for blocking cancer cell proliferation by XPO1 inhibition.

Spliceosome has been other of the relevant terms yielded by our network analysis. In the presence of KSHV, positively regulated miRNAs linked to a group of down-modulated targets closely related to the splicing machinery (*Snrpb*, *Snrpb2*, *Rbmx*, *Srsf3*, *Srsf10*). *NEAT1* and *MALAT1* were the first lncRNAs to be identified as having a relevant role in mRNA splicing in both human and mouse cells. The mechanisms by which both lncRNAs modulate splicing is extensively reviewed in Romero-Barrios et al. (62). Remarkably, it has been postulated that *MALAT1* modulates the phosphorylation status of a pool of Serine/arginine-rich (SR) proteins (proteins involved in splicing), resulting in the mislocalization of speckle components and changes in alternative splicing of pre-mRNAs, impacting in other SR-dependent post-transcriptional regulatory mechanisms, including RNA export, NMD and translation (63). In addition, cells depleted for *MALAT1* show an increased cytoplasmic pool of poly(A)+ RNA, suggesting that *MALAT1* contribute with the retention of nuclear mRNAs. Before RNAs can interact with nuclear export machinery, they must undergo processes that regulate the number of transcripts that is exported to the cytoplasm or nuclear decay pathways. KSHV manipulation of nuclear RNA regulation is one of the strategies acquired by the virus to influence the host RNAs during viral infection (8). In fact, it was very recently demonstrated that NMD pathway targets KSHV RNAs to restrict the virus (10). In summary, our network reveals another intricate relationship between lncRNA-miRNA-targets that can function in modulating spliceosome pathway and RNA transport during virus-host interaction.

Other relevant miRNAs that emerged from our network were members of the cluster 17-92 and the let-7 family whose multiple targets regulate different pathways associated with cancer. Moreover, miR 140-3p or miR378b also stand out, of which, like miR143-3p, their precursors were found upregulated in KSHV (+) tumors.

It has been demonstrated that miR140 in the nucleus can interact with *NEAT1*, leading to the increased *NEAT1* expression (64). Remarkably, there is another interesting link with *NEAT1*, which is p53 signaling, a frequent pathway represented in our networks. It has been shown that silencing *Neat1* in mice prevents paraspeckle formation, which sensitizes preneoplastic cells to DDR activating cell death and impairing skin tumorigenesis (65). Moreover, activation of p53 stimulates the formation of NEAT1 paraspeckles, establishing a direct functional link between p53 and paraspeckle biology (65). P53 regulates NEAT1 expression to stimulate paraspeckle formation and NEAT1 paraspeckles, in turn, dampen replication-associated DNA damage and p53 activation in a negative regulatory feedback (65). These data indicate that upregulation of Neat1 in KSHV (+) tumors could attenuate p53 signaling network, and infected cells may benefit from this situation evading the p53 checkpoint in response to DNA damage.

As mentioned before, we have used this same mECK36 tumor model to analyze the consequences of KSHV loss by comparing the mutational and methylation landscape of KSHV (+) and KSHV (−) tumors. We found that KSHV loss led to irreversible oncogenic alterations including oncogenic mutations and irreversible epigenetic alterations that were essential in driving oncogenesis in the absence of KSHV (13). In contrast to these irreversible effects of KSHV tumorigenesis, the ncRNA network we describe in the present study display a high degree of plasticity and reversibility upon KSHV loss further supporting the idea that these oncogenic networks are driving tumorigenesis and are more strictly dependent on the presence of KSHV.

Along the study, we integrate mice genes and their homologues in humans to understand the ncRNA biology in KSHV tumorigenesis and to develop signatures that can be used to identify druggable gene or networks defining relevant AIDS-KS therapeutic targets.

Interestingly, we identified drugs usually used against targets in experimental KSHV models or in clinical trials: Abacavir, Bevacizumab, Bortezomib, Celecoxib, Doxorubicin, Imatinib, Oxaliplatin, Sirolimus, Sunitinib, Thalidomide and Vorinostat. Interestingly, we have previously shown a combinatory effect between Bortezomib and Vorinostat for the treatment for primary effusion lymphoma (66). The fact that our analyses pointed to drugs that target KS oncogenic pathways identified in the laboratory or drugs that are currently in use of being tested in AIDS-KS further validate the bioinformatic analysis in our KSHV mouse tumorigenic model and reinforces the idea of the involvement of the KSHV regulated ncRNA network in viral sarcomagenesis.

In summary, in the present study the integration of the transcriptional analysis of ncRNAs in a KSHV model in cells and mouse tumors, with an exhaustive computational analysis of their experimentally supported targets, has allowed us to dissect a complex network that defines the main pathways involved in KSHV pathogenesis and host response. Understanding the relationships between these different RNA species will allow a better understanding of the biology of KSHV and can aid in the identification of relevant AIDS-KS druggable targets.

DATA AVAILABILITY STATEMENT

The data sets presented in this study can be found in online repositories. The names of the repository/repositories and accession number(s) can be found in the article/**Supplementary Material**.

AUTHOR CONTRIBUTIONS

JN: conceptualization, investigation, methodology, resources, supervision, writing—original draft, writing—review and editing. MS: formal analysis, methodology, writing—original draft. DS: methodology. SR: methodology. SW: methodology. OC: funding acquisition, writing—review and editing. MA: funding acquisition writing—review and editing. EM: funding acquisition, resources, supervision, writing—review and editing. EL: conceptualization, formal analysis, funding acquisition, investigation, resources, supervision, writing—original draft, Writing—review and editing. All authors contributed to the article and approved the submitted version.

FUNDING

This work was supported by the NIH grants CA136387 (to EM) and CA221208 (to EM and OC); by the Florida Biomedical Foundation, Bankhead Coley Foundation grant 3BB05 (to EM), by Ubacyt Grant 20020150100200BA (to OC), NCI/OHAM supplements from the Miami CFAR grant 5P30AI07396 (to EM and DS), by National Agency of Scientific and Technological Promotion: PICT 2015-3436 (to OC), PICT-2018-01403 (to MA), PICT 2017-0418 (to EL), and by CONICET: PIP0159 (to EL).

ACKNOWLEDGMENTS

We would like to thank the Oncogenomics Core Facility at the Sylvester Comprehensive Cancer Center from the University of Miami and the Laboratory Core of the Miami CFAR for performing high-throughput sequencing.

SUPPLEMENTARY MATERIAL

The Supplementary Material for this article can be found online at: https://www.frontiersin.org/articles/10.3389/fonc.2021.687629/full#supplementary-material

Supplementary Table 1 | DE lncRNAs in key biological comparisons detected by RNA-sequencing. Results were obtained after DeSeq2 analysis of: two KSHV (+) cells, two KSHV (–) cells, six KSHV (+) tumors, two KSHV (–) tumor cells and three KSHV (–) tumors.

Supplementary Table 2 | Pathway analysis of the lncRNAs EVT.

Supplementary Table 3 | Pathway analysis of the selected lncRNAs and their EVT genes DE in the corresponding comparisons.

Supplementary Table 4 | DE miRNAs in key biological comparisons detected by small RNA-sequencing.

Supplementary Table 5 | Pathway analysis of DE miRNAs and their EVT genes DE in the corresponding comparisons.

Supplementary Table 6 | KSHV miRNAs analysis in KSHV (+) tumors and pathway analysis of their EVT.

Supplementary Table 7 | lncRNA-miRNA-mRNA-Pathway networks.

Supplementary Table 8 | Drugs associated with miRNA-gene pairs obtained from network analysis.

REFERENCES

1. Ponting CP, Oliver PL, Reik W. Evolution and Functions of Long Noncoding RNAS. *Cell* (2009) 136:629–41. doi: 10.1016/j.cell.2009.02.006
2. Hu G, Niu F, Humburg BA, Liao K, Bendi S, Callen S, et al. Molecular Mechanisms of Long Noncoding RNAs and Their Role in Disease Pathogenesis. *Oncotarget* (2018) 9:18648–63. doi: 10.18632/oncotarget.24307
3. Li T, Mo X, Fu L, Xiao B, Guo J. Molecular Mechanisms of Long Noncoding RNAs on Gastric Cancer. *Oncotarget* (2016) 7:8601–12. doi: 10.18632/oncotarget.6926
4. Cesarman E, Damania B, Krown SE, Martin J, Bower M, Whitby D. Kaposi Sarcoma. *Nat Rev Dis Primers* (2019) 5:9. doi: 10.1038/s41572-019-0060-9
5. Dittmer DP, Krown SE. Targeted Therapy for Kaposi's Sarcoma and Kaposi's Sarcoma-Associated Herpesvirus. *Curr Opin Oncol* (2007) 19:452–7. doi: 10.1097/CCO.0b013e3281eb8ea7
6. Mesri EA, Cesarman E, Boshoff C. Kaposi's Sarcoma and Its Associated Herpesvirus. *Nat Rev Cancer* (2010) 10:707–19. doi: 10.1038/nrc2888
7. Yan L, Majerciak V, Zheng ZM, Lan K. Towards Better Understanding of KSHV Life Cycle: From Transcription and Posttranscriptional Regulations to Pathogenesis. *Virol Sin* (2019) 34:135–61. doi: 10.1007/s12250-019-00114-3
8. Macveigh-Fierro D, Rodriguez W, Miles J, Muller M. Stealing the Show: Kshv Hijacks Host RNA Regulatory Pathways to Promote Infection. *Viruses* (2020) 12:1024. doi: 10.3390/v12091024
9. Ohsaki E, Ueda K. Interplay Between KSHV and the Host DNA Damage Response. *Front Cell Infect Microbiol* (2020) 10:604351. doi: 10.3389/fcimb.2020.604351
10. Zhao Y, Ye X, Shehata M, Dunker W, Xie Z, Karijolich J. The RNA Quality Control Pathway Nonsense-Mediated mRNA Decay Targets Cellular and Viral RNAs to Restrict KSHV. *Nat Commun* (2020) 11:3345. doi: 10.1038/s41467-020-17151-2
11. Sethuraman S, Gay LA, Jain V, Haecker I, Renne R. microRNA Dependent and Independent Deregulation of Long Non-Coding RNAs by an Oncogenic Herpesvirus. *PloS Pathog* (2017) 13(7):e1006508. doi: 10.1371/journal.ppat.1006508
12. Mutlu AD, Cavallin LE, Vincent L, Chiozzini C, Eroles P, Duran EM, et al. *In Vivo*-Restricted and Reversible Malignancy Induced by Human Herpesvirus-8 KSHV: A Cell and Animal Model of Virally Induced Kaposi's Sarcoma. *Cancer Cell* (2007) 11:245–58. doi: 10.1016/j.ccr.2007.01.015
13. Naipauer J, Salyakina D, Journo G, Rosario S, Williams S, Abba M, et al. High-Throughput Sequencing Analysis of a "Hit and Run" Cell and Animal Model of KSHV Tumorigenesis. *PLoS Pathog* (2020) 16:e1008589. doi: 10.1371/journal.ppat.1008589
14. Ma Q, Cavallin LE, Leung HJ, Chiozzini C, Goldschmidt-Clermont PJ, Mesri EA. A Role for Virally Induced Reactive Oxygen Species in Kaposi's Sarcoma Herpesvirus Tumorigenesis. *Antioxid Redox Signal* (2013) 18:80–90. doi: 10.1089/ars.2012.4584
15. Cheng L, Wang P, Tian R, Wang S, Guo Q, Luo M, et al. LncRNA2Target v2.0: A Comprehensive Database for Target Genes of lncRNAs in Human and Mouse. *Nucleic Acids Res* (2019) 47:D140–4. doi: 10.1093/nar/gky1051
16. Zhao H, Shi J, Zhang Y, Xie A, Yu L, Zhang C, et al. LncTarD: A Manually-Curated Database of Experimentally-Supported Functional lncRNA-target Regulations in Human Diseases. *Nucleic Acids Res* (2020) 48(D1):D118–26. doi: 10.1093/nar/gkz985
17. Karagkouni D, Paraskevopoulou MD, Chatzopoulos S, Vlachos IS, Tastsoglou S, Kanellos I, et al. Diana-TarBase v8: A Decade-Long Collection of

Experimentally Supported miRNA-gene Interactions. *Nucleic Acids Res* (2018) 46:D239–45. doi: 10.1093/nar/gkx1141
18. Karagkouni D, Paraskevopoulou MD, Tastsoglou S, Skoufos G, Karavangeli A, Pierros V, et al. Diana-LncBase v3: Indexing Experimentally Supported miRNA Targets on Non-Coding Transcripts. *Nucleic Acids Res* (2020) 8;48: D101–10. doi: 10.1093/nar/gkz1036
19. Rukov JL, Wilentzik R, Jaffe I, Vinther J, Shomron N. Pharmaco-miR: Linking microRNAs and Drug Effects. *Brief Bioinform* (2014) 15:648–59. doi: 10.1093/bib/bbs082
20. Cotto KC, Wagner AH, Feng YY, Kiwala S, Coffman AC, Spies G, et al. Dgidb 3.0: A Redesign and Expansion of the Drug-Gene Interaction Database. *Nucleic Acids Res* (2018) 46:D1068–73. doi: 10.1093/nar/gkx1143
21. Valencia-Sanchez MA, Liu J, Hannon GJ, Parker R. Control of Translation and mRNA Degradation by miRNAs and Sirnas. *Genes Dev* (2006) 20:515–24. doi: 10.1101/gad.1399806
22. Statello L, Guo CJ, Chen LL, Huarte M. Gene Regulation by Long non-Coding RNAs and Its Biological Functions. *Nat Rev Mol Cell Biol* (2020) 22:1–23. doi: 10.1038/s41580-020-00315-9
23. Casper C. The Increasing Burden of HIV-Associated Malignancies in Resource-Limited Regions. *Annu Rev Med* (2011) 62:157–70. doi: 10.1146/annurev-med-050409-103711
24. Sullivan RJ, Pantanowitz L, Casper C, Stebbing J, Dezube BJ. HIV/AIDS: Epidemiology, Pathophysiology, and Treatment of Kaposi Sarcoma-Associated Herpesvirus Disease: Kaposi Sarcoma, Primary Effusion Lymphoma, and Multicentric Castleman Disease. *Clin Infect Dis* (2008) 47:1209–15. doi: 10.1086/592298
25. Nguyen HQ, Magaret AS, Kitahata MM, Van Rompaey SE, Wald A, Casper C. Persistent Kaposi Sarcoma in the Era of Highly Active Antiretroviral Therapy: Characterizing the Predictors of Clinical Response. *AIDS* (2008) 22:937–45. doi: 10.1097/QAD.0b013e3282ff6275
26. Petre CE, Dittmer DP. Liposomal Daunorubicin as Treatment for Kaposi's Sarcoma. *Int J Nanomed* (2007) 2:277–88.
27. Jones JE, Le Sage V, Lakdawala SS. Viral and Host Heterogeneity and Their Effects on the Viral Life Cycle. *Nat Rev Microbiol* (2020) 6:1–11. doi: 10.1038/s41579-020-00449-9
28. Cech TR, Steitz JA. The Noncoding RNA Revolution-Trashing Old Rules to Forge New Ones. *Cell* (2014) 157:77–94. doi: 10.1016/j.cell.2014.03.008
29. Slack FJ, Chinnaiyan AM. The Role of Non-Coding RNAS in Oncology. *Cell* (2019) 179:1033–55. doi: 10.1016/j.cell.2019.10.017
30. Cavallin LE, Ma Q, Naipauer J, Gupta S, Kurian M, Locatelli P, et al. KSHV-Induced Ligand Mediated Activation of PDGF Receptor-Alpha Drives Kaposi's Sarcomagenesis. *PLoS Pathog* (2018) 14(7):e1007175. doi: 10.1371/journal.ppat.1007175
31. Zhou X, Liu S, Cai G, Kong L, Zhang T, Ren Y, et al. Long Non Coding RNA Malat1 Promotes Tumor Growth and Metastasis by Inducing Epithelial-Mesenchymal Transition in Oral Squamous Cell Carcinoma. *Sci Rep* (2015) 5:15972. doi: 10.1038/srep15972
32. Liu X, Shang W, Zheng F. Long Non-Coding RNA NEAT1 Promotes Migration and Invasion of Oral Squamous Cell Carcinoma Cells by Sponging Microrna-365. *Exp Ther Med* (2018) 16:2243–50. doi: 10.3892/etm.2018.6493
33. Zhu X, Li W, Meng Q. Lncrna H19 Promotes Proliferation and Invasion in A375 Human Melanoma Cell Line. *Int J Clin Exp Pathol* (2018) 11:1063–73.
34. Zhang Y, Gao L, Ma S, Ma J, Wang Y, Li S, et al. Malat1-KTN1-EGFR Regulatory Axis Promotes the Development of Cutaneous Squamous Cell Carcinoma. *Cell Death Differ* (2019) 26:2061–73. doi: 10.1038/s41418-019-0288-7
35. Michalik KM, You X, Manavski Y, Doddaballapur A, Zörnig M, Braun T, et al. Long Noncoding RNA MALAT1 Regulates Endothelial Cell Function and Vessel Growth. *Circ Res* (2014) 114:1389–97. doi: 10.1161/CIRCRESAHA.114.303265
36. Kölling M, Genschel C, Kaucsar T, Hübner A, Rong S, Schmitt R, et al. Hypoxia-Induced Long Non-Coding RNA Malat1 Is Dispensable for Renal Ischemia/Reperfusion-Injury. *Sci Rep* (2018) 8:3438. doi: 10.1038/s41598-018-21720-3
37. Xiao H, Tang K, Liu P, Chen K, Hu J, Zeng J, et al. Lncrna MALAT1 Functions as a Competing Endogenous RNA to Regulate ZEB2 Expression by Sponging miR-200s in Clear Cell Kidney Carcinoma. *Oncotarget* (2015) 6:38005–15. doi: 10.18632/oncotarget.5357
38. Chen L, Yao H, Wang K, Liu X. Long Non-Coding Rna MALAT1 Regulates ZEB1 Expression by Sponging miR-143-3p and Promotes Hepatocellular Carcinoma Progression. *J Cell Biochem* (2017) 2017118:4836–43. doi: 10.1002/jcb.26158
39. Lin L, Li Q, Hao W, Zhang Y, Zhao L, Han W. Upregulation of LncRNA Malat1 Induced Proliferation and Migration of Airway Smooth Muscle Cells Via miR-150-eIF4E/Akt Signaling. *Front Physiol* (2019) 10:1337. doi: 10.3389/fphys.2019.01337
40. West JA, Davis CP, Sunwoo H, Simon MD, Sadreyev RI, Wang PI, et al. The Long Noncoding RNAs NEAT1 and MALAT1 Bind Active Chromatin Sites. *Mol Cell* (2014) 55:791–802. doi: 10.1016/j.molcel.2014.07.012
41. Morchikh M, Cribier A, Raffel R, Amraoui S, Cau J, Severac D, et al. HEXM1 and NEAT1 Long Non-Coding RNA Form a Muti-Subunit Complex That Regulates DNA-Mediated Innate Immune Response. *Mol Cell* (2017) 67:387–99. doi: 10.1016/j.molcel.2017.06.020
42. Viollet C, Davis DA, Tekeste SS, Reczko M, Ziegelbauer JM, Pezzella F, et al. RNA Sequencing Reveals That Kaposi Sarcoma-Associated Herpesvirus Infection Mimics Hypoxia Gene Expression Signature. *PLoS Pathog* (2017) 13:e1006143. doi: 10.1371/journal.ppat.1006143
43. Wang S, Zhang Q, Wang Q, Shen Q, Chen X, Li Z, et al. NEAT1 Paraspeckle Promotes Human Hepatocellular Carcinoma Progression by Strengthening IL-6/STAT3 Signaling. *Oncoimmunology* (2018) 7(11):e1503913. doi: 10.1080/2162402X.2018.1503913
44. Santarelli R, Gonnella R, Di Giovenale G, Cuomo L, Capobianchi A, Granato M, et al. STAT3 Activation by KSHV Correlates With IL-10, IL-6 and IL-23 Release and an Autophagic Block in Dendritic Cells. *Sci Rep* (2014) 4:4241. doi: 10.1038/srep04241
45. Schulz TF, Cesarman E. Kaposi Sarcoma-associated Herpesvirus: Mechanisms of Oncogenesis. *Curr Opin Virol* (2015) 14:116–28. doi: 10.1016/j.coviro.2015.08.016
46. Weitzman MD, Fradet-Turcotte A. Virus DNA Replication and the Host DNA Damage Response. *Annu Rev Virol* (2018) 5:141–64. doi: 10.1146/annurev-virology-092917-043534
47. Liu X, Happel C, Ziegelbauer JM. Kaposi's Sarcoma-Associated Herpesvirus MicroRNAs Target GADD45B to Protect Infected Cells From Cell Cycle Arrest and Apoptosis. *J Virol* (2017) 91(3):e02045–16. doi: 10.1128/JVI.02045-16
48. Michelini F, Pitchiaya S, Vitelli V, Sharma S, Gioia U, Pessina F, et al. Damage-Induced lncRNAs Control the DNA Damage Response Through Interaction With DDRNAs At Individual Double-Strand Breaks. *Nat Cell Biol* (2017) 19:1400–11. doi: 10.1038/ncb3643
49. Schifano JM, Corcoran K, Kelkar H, Dittmer DP. Expression of the Antisense-to-Latency Transcript Long Noncoding RNA in Kaposi's Sarcoma-Associated Herpesvirus. *J Virol* (2017) 91(4):e01698–16. doi: 10.1128/JVI.01698-16
50. Wu XJ, Pu XM, Zhao ZF, Zhao YN, Kang XJ, Wu WD, et al. The Expression Profiles of microRNAs in Kaposi's Sarcoma. *Tumour Biol* (2015) 36:437–46. doi: 10.1007/s13277-014-2626-1
51. Moody R, Zhu Y, Huang Y, Cui X, Jones T, Bedolla R, et al. Kshv microRNAs Mediate Cellular Transformation and Tumorigenesis by Redundantly Targeting Cell Growth and Survival Pathways. *PLoS Pathog* (2013) 9(12): e1003857. doi: 10.1371/journal.ppat.1003857
52. Hu M, Wang C, Li W, Lu W, Bai Z, Qin D, et al. A KSHV Microrna Directly Targets G Protein-Coupled Receptor Kinase 2 to Promote the Migration and Invasion of Endothelial Cells by Inducing CXCR2 and Activating Akt Signaling. *PLoS Pathog* (2015) 11(9):e1005171. doi: 10.1371/journal.ppat.1005171
53. Forte E, Raja AN, Shamulailatpam P, Manzano M, Schipma MJ, Casey JL, et al. MicroRNA-mediated Transformation by the Kaposi's Sarcoma-Associated Herpesvirus Kaposin Locus. *J Virol* (2015) 89(4):2333–41. doi: 10.1128/JVI.03317-14
54. Hussein HAM, Alfhili MA, Pakala P, Simon S, Hussain J, McCubrey JA, et al. miRNAs and Their Roles in KSHV Pathogenesis. *Virus Res* (2019) 266:15–24. doi: 10.1016/j.virusres.2019.03.024
55. Gadad SS, Rajan RE, Senapati P, Chatterjee S, Shandilya J, Dash PK, et al. HIV-1 Infection Induces Acetylation of NPM1 That Facilitates Tat Localization and Enhances Viral Transactivation. *J Mol Biol* (2011) 410:997–1007. doi: 10.1016/j.jmb.2011.04.009
56. Behrens RT, Aligeti M, Pocock GM, Higgins CA, Sherer NM. Nuclear Export Signal Masking Regulates HIV-1 Rev Trafficking and Viral RNA Nuclear Export. *J Virol* (2017) 91(3):e02107–16. doi: 10.1128/JVI.02107-16
57. Kane M, Rebensburg SV, Takata MA, Zang TM, Yamashita M, Kvaratskhelia M, et al. Nuclear Pore Heterogeneity Influences HIV-1 Infection and the Antiviral Activity of MX2. *Elife* (2018) 7:e35738. doi: 10.7554/eLife.35738

58. Rathore A, Iketani S, Wang P, Jia M, Sahi V, Ho DD. CRISPR-Based Gene Knockout Screens Reveal Deubiquitinases Involved in HIV-1 Latency in Two Jurkat Cell Models. *Sci Rep* (2020) 10(1):5350. doi: 10.1038/s41598-020-62375-3
59. Atari N, Rajan S, Chikne V, Cohen-Chalamish S, Orbaum O, Jacob A, et al. Lytic Reactivation of the Kaposi's Sarcoma-Associated Herpesvirus (KSHV) Is Accompanied by Major Nucleolar Alterations. *bioRxiv preprint* (2020). doi: 10.1101/2020.05.15.097808
60. Sarek G, Järviluoma A, Moore HM, Tojkander S, Vartia S, Biberfeld P, et al. Nucleophosmin Phosphorylation by v-Cyclin-CDK6 Controls KSHV Latency. *PLoS Pathog* (2010) 6(3):e1000818. doi: 10.1371/journal.ppat.1000818
61. Gruffaz M, Yuan H, Meng W, Liu H, Bae S, Kim JS, et al. Crispr-Cas9 Screening of Kaposi's Sarcoma-Associated Herpesvirus-Transformed Cells Identifies XPO1 as a Vulnerable Target of Cancer Cells. *mBio* (2019) 10(3): e00866–19. doi: 10.1128/mBio.00866-19
62. Romero-Barrios N, Legascue MF, Benhamed M, Ariel F, Crespi M. Splicing Regulation by Long Noncoding RNAs. *Nucleic Acids Res* (2018) 46(5):2169–84. doi: 10.1093/nar/gky095
63. Tripathi V, Ellis JD, Shen Z, Song DY, Pan Q, Watt AT, et al. The Nuclear-Retained Noncoding RNA MALAT1 Regulates Alternative Splicing by Modulating SR Splicing Factor Phosphorylation. *Mol Cell* (2010) 39:925–38. doi: 10.1016/j.molcel.2010.08.011
64. Gernapudi R, Wolfson B, Zhang Y, Yao Y, Yang P, Asahara H, et al. MicroRNA 140 Promotes Expression of Long Noncoding RNA NEAT1 in Adipogenesis. *Mol Cell Biol* (2015) 36:30–8. doi: 10.1128/MCB.00702-15
65. Adriaens C, Standaert L, Barra J, Latil M, Verfaillie A, Kalev P, et al. p53 Induces Formation of NEAT1 lncRNA-Containing Paraspeckles That Modulate Replication Stress Response and Chemosensitivity. *Nat Med* (2016) 22:861–8. doi: 10.1038/nm.4135
66. Bhatt S, Ashlock BM, Toomey NL, Diaz LA, Mesri EA, Lossos IS, et al. Efficacious Proteasome/HDAC Inhibitor Combination Therapy for Primary Effusion Lymphoma. *J Clin Invest* (2013) 123(6):2616–28. doi: 10.1172/JCI64503

Conflict of Interest: The authors declare that the research was conducted in the absence of any commercial or financial relationships that could be construed as a potential conflict of interest.

frontiers in Oncology

ORIGINAL RESEARCH
published: 20 January 2022
doi: 10.3389/fonc.2021.795090

Enhancer RNA LINC00242-Induced Expression of PHF10 Drives a Better Prognosis in Pancreatic Adenocarcinoma

*Wen Tong[1], Liuyang Zhu[1], Yi Bai[2], Long Yang[2], Zirong Liu[2] and Yamin Zhang[2]**

[1] Tianjin First Central Hospital Clinic Institute, Tianjin Medical University, Tianjin, China, [2] Department of Hepatobiliary Surgery, Tianjin First Central Hospital, School of Medicine, Nankai University, Tianjin, China

OPEN ACCESS

Edited by:
Hernandes F. Carvalho, State University of Campinas, Brazil

Reviewed by:
Qian Yang, Cedars Sinai Medical Center, United States
Shaolong Cao, University of Texas MD Anderson Cancer Center, United States

***Correspondence:**
Yamin Zhang
13802122219@163.com

Specialty section:
This article was submitted to Molecular and Cellular Oncology, a section of the journal Frontiers in Oncology

Received: *14 October 2021*
Accepted: *27 December 2021*
Published: *20 January 2022*

Citation:
Tong W, Zhu L, Bai Y, Yang L, Liu Z and Zhang Y (2022) Enhancer RNA LINC00242-Induced Expression of PHF10 Drives a Better Prognosis in Pancreatic Adenocarcinoma. Front. Oncol. 11:795090. doi: 10.3389/fonc.2021.795090

Enhancer RNA is a kind of non-coding RNA, which is transcribed from the enhancer region of gene and plays an important role in gene transcription regulation. However, the role of eRNA in pancreatic adenocarcinoma (PAAD) is still unclear. In this study, we identified the key eRNA and its target gene in PAAD. The transcriptome data and clinical information of pancreatic cancer were downloaded from the UCSC Xena platform. A total of 2,695 eRNAs and its target gene predicted by the PreSTIGE method were selected as candidate eRNA–target pairs. After survival analysis, we found that LINC00242 was the eRNA most related to patients' survival, and correlation analysis further indicated that LINC00242 and its target gene PHF10 had a significant co-expression relationship. Downregulation of LINC00242 was significantly associated with unfavorable clinicopathological features. Based on pan-cancer analysis, we found that LINC00242 was associated with the survival of multiple cancers, and LINC00242 was co-expressed with its target genes in multiple cancer types. External experiments further demonstrated that PHF10 was the downstream target gene of LINC00242. After ssGSEA analysis, PAAD patients were classified as high, medium, and low immune cell infiltration clusters. Compared with the low and medium immune infiltration clusters, the expression level of PHF10 was significantly upregulated in the high immune infiltration clusters. After performing the CIBERSORT algorithm, we found that there was a significant difference in the abundance of immune infiltrating cells between the PHF10 high- and low-expression groups. Additionally, the web tool TIMER was used to detect the distribution and expression of PHF10 in pan-cancer.

Keywords: enhancer RNA, LINC00242, PHF10, pancreatic cancer, biomarker

INTRODUCTION

According to reports, pancreatic adenocarcinoma ranks fourth in cancer-related deaths, with a 5-year survival rate of approximately 9% (1). Up to now, surgical resection is still the only effective treatment in theory. However, pancreatic adenocarcinoma tends to be asymptomatic in its early stages, and most patients with PAAD are not suitable for surgical treatment when they are diagnosed in the late stage (2). In recent years, studies have confirmed that several treatment methods including immunotherapy (3, 4) and targeted therapy (5, 6) can improve the survival rate of PAAD patients, but the effect is still limited. This may be related to the different sensitivity caused by the complexity and heterogeneity of tumor tissue. Therefore, there is an urgent need to find biomarkers related to the prognosis of PAAD and to predict the sensitivity of immunotherapy and targeted therapy.

Previous studies have shown that active enhancers are transcribed and produce a series of non-coding RNAs called enhancer RNA (eRNA) (7–9). Some research suggests that eRNAs interact with RNA polymerase to promote the formation of the promoter–enhancer loop and act as a significant role in the regulation of gene expression (10, 11). The production of eRNA is a widespread phenomenon, which is related to the regulation of gene expression in a variety of cells. It has been confirmed that the transcriptional regulation process involved in eRNAs was associated with tumorigenesis and progression (12, 13). Elodie Bal reported that mutations in enhancer RNA elements may weaken the activity of enhancers and lead to abnormal activation of Hedgehog signaling pathways, thus promoting tumor development (14). In addition, Pan found that the abnormal expression of eRNA in prostate cancer was associated with cancer progression (15).

In this study, we found that eRNA LINC00242 transcribed from the enhancer region of PHF10 was significantly correlated with patients' survival. The downregulation of LINC00242 expression was related with poor clinicopathological features. Then, we further analyzed the expression of PHF10 in pancreatic cancer and its prognostic value. Additionally, the web tool Tumor Immune Estimation Resource (TIMER) was used to study the expression level of PHF10 in pan-cancer. In addition, we also explored the relationship between the expression of PHF10 and immune infiltration. By running the single-sample gene set enrichment analysis (ssGSEA) algorithm, we divided PAAD patients into high, medium, and low immune clusters. Then, we investigate the relationship between PHF10 and three immune clusters. In order to evaluate the effect of PHF10 on the tumor microenvironment, we analyzed the tumor-infiltrating immune cells (TIICs) associated with PHF10 expression by CIBERSORT on the basis of TCGA cohort.

Abbreviations: PAAD, pancreatic adenocarcinoma; eRNA, enhancer RNA; OS, overall survival; TCGA, The Cancer Genome Atlas; PresSTIGE, Predicting Specific Tissue Interactions of Genes and Enhancers; GO, Gene Ontology; KEGG, Kyoto Encyclopedia of Genes and Genomes; AJCC, American Joint Committee on Cancer.

MATERIALS AND METHODS

Data Acquisition and Identification of eRNAs Related to the Prognosis of PAAD

The transcriptome data and clinical information about PAAD and 32 other cancer types were downloaded from the UCSC website (https://xena.ucsc.edu/). The PAAD data set from UCSC was selected as the training set. We select ICGC-PAAD (N= 182) and GSE15471 (N = 36) as the validation set. ICGC-PAAD (N = 182) included 182 pancreatic cancer samples from different patients. GSE15471 (N = 36) included 36 pairs of pancreatic cancer and normal tissue samples. The full clinical information about these two cohorts is shown in **Supplementary Table 4**.

Based on previous studies, we obtained a list of eRNAs and its target genes predicted by the PresSTIGE method (16, 17). In the training set, the patients' eRNA transcriptional data and clinical data were matched together. We used R software package "survival" and "survminer" to investigate the relationship between eRNAs and OS in PAAD patients. The correlation level of eRNAs and its target gene was evaluated through co-expression analysis methods. The most significant survival-associated eRNA and its target gene were selected for further analysis.

Comprehensive Analysis of LINC00242 and PHF10

Based on the website Human Protein Atlas (HPA, http://www.proteinatlas.org/) (18, 19), we explored the mRNA and protein levels of PHF10 in various cancer tissues and normal tissues. Meanwhile, we downloaded the immunohistochemical images of PHF10 protein in pancreatic cancer from this website. The differential mRNA expression level of LINC00242 and PHF10 between PAAD tissues and normal tissues were analyzed *via* the Gene Expression Profiling Interactive Analysis (GEPIA) web tool (http://gepia.cancer-pku.cn/) (20). GSE15471 was selected to verify the difference in the expression of LINC00242 and PHF10 between PAAD tissues and normal tissues. Through univariate and multivariate Cox regression analyses, we determined the independent prognostic value of LINC00242. The correlation between LINC00242 expression level and clinicopathological was explored. ICGC-PAAD was selected to verify the relationship between LINC00242 expression and clinical parameter. Besides, we selected the differentially expressed genes in tumor compared with normal tissues and co-expressed genes to do the GO and KEGG analyses. Next, the prognostic value of LINC00242 and its co-expression relationship with PHF10 were verified in TCGA (32 other types of cancer) pan-cancer data.

Cell Lines and Transfection

The human pancreatic cancer cell line (PANC-1) was purchased from the Cell Bank of the Chinese Academy of Sciences (Shanghai, China). We use DMEM medium supplemented with 10% fetal bovine serum (Thermo Fisher Scientific, USA) and 1% penicillin–streptomycin to culture the cells at 37°C, 5% CO2 atmosphere. LINC00242 siRNAs were synthesized by GeneChem (Shanghai, China), and Lipofectamine 2000

(Invitrogen, California, USA) was employed to achieve the cell transfection.

The Relationship Between LINC00242 and PHF10 Was Verified by qPCR

Differently treated PAAD cell lines were collected in the logarithmic growth phase and mixed with 1 ml TRIzol. Chloroform was added and kept at room temperature for 15 min, then isopropanol was added to the solution and centrifuged to obtain RNA precipitate. qRT-PCR analyses of LINC00242 and PHF10 were performed as described previously. The transcription level was calculated by the $2^{-\Delta\Delta Ct}$ method. GAPDH was used as an internal reference gene. The primer sequences of LINC00242 were 5'-GCGGGAAGATTTCA GGCGCTTT-3' (forward) and 5'-CAGGTGGTGAAGTGAGG AACAG-3' (reverse). The primer sequences of PHF10 were 5'-GCACTCTAGGCTTAACAGCATT (forward) and 5'-AGCATGTTTGGCTGGATATTCTT-3' (reverse). The primer sequences of GAPDH were 5'-GTCTCCTCTGACTTCA ACAGCG-3' (forward) and 5'-ACCACCCTGTTGCTGTA GCCAA-3' (reverse).

Analysis of Immune Cell Patterns in the Microenvironment

The abundance of 22 immune cells in UCSC-PAAD and ICGC-PAAD was estimated *via* the CIBERSOFT website (https://cibersort.stanford.edu/index.php) (21). Monte Carlo sampling was used to calculate the p value. Only samples with CIBERSORT $p < 0.05$ were included in the further study. Based on the median value of PHF10 expression, we divided PAAD patients into a high-expression group (PHF10-H) and a low-expression group (PHF10-L). We used violin diagrams to show the difference in the content of 22 immune cells between PHF10-H and PHF10-L groups. From the previous studies, we obtained the immune-related gene set with 29 immune cell types and immune-related functions (22). Then, we used the ssGSEA algorithm to obtain the enrichment score with the "GSVA" package in R (23). PAAD samples from UCSC-PAAD and ICGC-PAAD were divided into three immune subgroups by the unsupervised clustering method based on ssGSEA scores. In order to further explore the difference of the immune microenvironment between three immune subgroups, the "estimate" package in R (24) was used to calculate the immune score, stromal score, and ESTIMATE score. Next, we use the "pheatmap" package in R to visualize the results. Additionally, the expression levels of PHF10 and the human leukocyte antigen (HLA) gene family were compared between three immune subgroups.

Intergrated Analysis of PHF10 Expression and Immune Cell Infiltration and Immune Subtype in Pan-Cancer

The Tumor Immune Estimation Resource (TIMER, https://cistrome.shinyapps.io/timer/) website (25) was used to evaluate the relationship between the expression level of PHF10 and immune cell infiltration. TIMER applies a statistical method called deconvolution to infer the abundance of TIICs according to RNA sequencing data. The relationship between immune subtype and mRNA level of PHF10 was explored *via* tumor–immune system interactions and DrugBank (TISIDB, http://cis.hku.hk/TISIDB/index.php) (26) database by the Subtype module.

Statistical Analysis

All statistical analyses were operated *via* R software (version 4.0.3), GraphPad Prism (version 8.0), and IBM SPSS Statistics (version 25.0). The correlations between PHF10 and clinicopathological features were analyzed by the $\chi 2$ test. Univariate and multivariate analyses were used to determine prognostic factors. Spearman rank correlation analysis was used to estimate the correlation strength. Kaplan–Meier analysis was used to compare the survival rate among different groups. Unless noted otherwise, $p < 0.05$ was considered statistically significant.

RESULTS

Prognostic Value of eRNAs in PAAD

After removing samples with missing values, a total of 177 patients were included in the study. The clinicopathological characteristics of the patients are shown in **Supplementary Table 1**. We obtained 2,695 eRNA transcripts and 2,303 predicted target genes from previous studies. Next, the 2,695 eRNA transcript IDs were mapped to their corresponding 1,559 genes based on the Ensembl Gene ID from the Ensembl database (http://asia.ensembl.org/info/data/ftp/index.html). According to gene expression profile and clinical information from 177 PAAD patients, we identified 15 of the 1,559 candidate eRNAs, which were significantly correlated with patients' OS (Kaplan–Meier, $p < 0.01$; **Supplementary Table 2**). Then, we found that all 15 eRNAs were significantly correlated with their target genes ($R > 0.4$, $p < 0.01$; **Supplementary Table 2**). The relationship between top 10 eRNAs associated with survival and its target gene is shown in **Figure 1A**.

LINC00242 Is a Key eRNA in PAAD

LINC00242 is the most survival related eRNA, and it is significantly positively correlated with the predicted target PHF10 (**Figure 1A** and **Supplementary Table 2**). Then, LINC00242 and its target PHF10 were selected for further analysis. According to the gene expression data of 179 PAAD tissues and 171 normal pancreatic tissues from the TCGA and GTEx databases, the mRNA level of LINC00242 was significantly upregulated in PAAD samples (**Figure 1B**, $p < 0.05$). However, there was no significant difference in LINC00242 expression between pancreatic carcinoma and normal tissues in our validation set (**Supplementary Figure 3C**). The expression level of LINC00242 was significantly correlated with some clinical features of PAAD, including cancer status ($p = 0.005$), race ($p = 0.02$), and history of chronic pancreatitis ($p = 0.004$) (**Supplementary Table 1**). Compared with G1, the expression level of LINC00242 of G2 was lower (**Figure 1C**, $p < 0.05$).

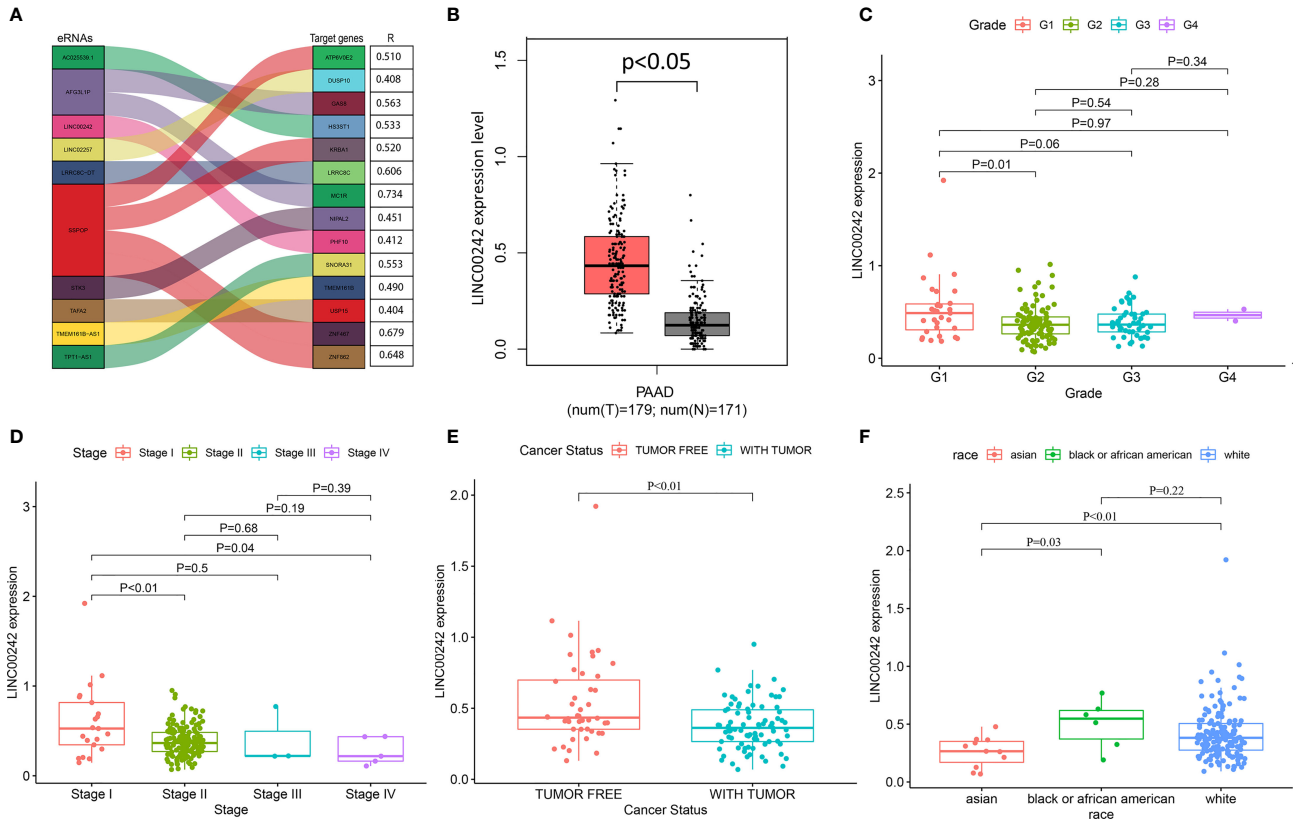

FIGURE 1 | The correlation analysis between LINC00242 and the clinicopathological characteristics of PAAD. **(A)** Top 10 eRNAs and their target genes most relevant to survival. **(B)** LINC00242 expression was significantly upregulated in PAAD samples compared with normal samples. **(C, D)** LINC00242 expression was negatively correlated with histological grade **(C)** and AJCC stage **(D)**. **(E)** Tumor status had a low expression level of LINC00242 compared with tumor-free status. **(F)** The expression level of LINC00242 in Asian patients was significantly lower than that in the other two races.

In addition, patients with advanced tumor stage were also correlated with low expression level of LINC00242 (**Figure 1D**, $p < 0.05$). Furthermore, cancer status also associated with LINC00242 expression level. Tumor free status had higher gene expression level when compared with tumor status (**Figure 1E**, $p < 0.05$). Interestingly, we found that patients of Asian descent had lower gene expression than patients of the other two races, including black or African American and white (**Figure 1F**, $p < 0.05$).

Based on the median expression level of LINC00242, we divided 177 patients into high- and low-expression groups. High-expression LINC00242 was significantly correlated with better OS (Kaplan–Meier, $p < 0.01$, **Figure 2A**). Unfortunately, we did not find a significant relationship between LINC00242 expression and prognosis as well as clinical parameters (TNM stage, grade, data not displayed) in ICGC-PAAD ($N = 182$), which may be related to the low abundance of non-coding RNA and the different sequencing methods (**Supplementary Figure 3A**). High PHF10 expression was also associated with better OS ($p < 0.01$, **Figure 2B**). The analysis based on ICGC-PAAD showed that high expression of PHF10 was closely related to the better prognosis of the patients (**Supplementary Figure 3B**). What is more, the prognostic value of LINC00242 was explored in other cancer types from the TCGA database. LINC00242 also plays a prognostic role in KIRC and ACC. A high expression level of LINC00242 was significantly associated with poor OS in KIRC and ACC ($p < 0.01$, **Figures 2C, D** and **Supplementary Table 3**).

In addition, we found a significant co-expression correlation between LINC00242 and its target gene PHF10 in multiple cancer types, including PAAD, KIRC, ACC, TGCT, UVM, LIHC, and UCS ($p < 0.01$, **Figures 3A–E** and **Supplementary Table 3**). To further verify the regulatory relationship between LINC00242 and PHF10, we knocked down the expression of LINC00242 with transfection of LINC00242 siRNA. We used qRT-PCR to examine the efficiency of knockdown. As depicted in **Figure 3F**, the expression of LINC00242 was significantly downregulated after si-LINC00242 transfection ($p < 0.05$, **Figure 3F**). Of note, compared with the si-control group, the expression of PHF10 was significantly downregulated in si-LINC00242 group ($p < 0.05$, **Figure 3G**).

Independent Prognostic Value of LINC00242 in PAAD

The univariate and multivariate Cox analyses were used to estimate the prognostic value of LINC00242 in PAAD.

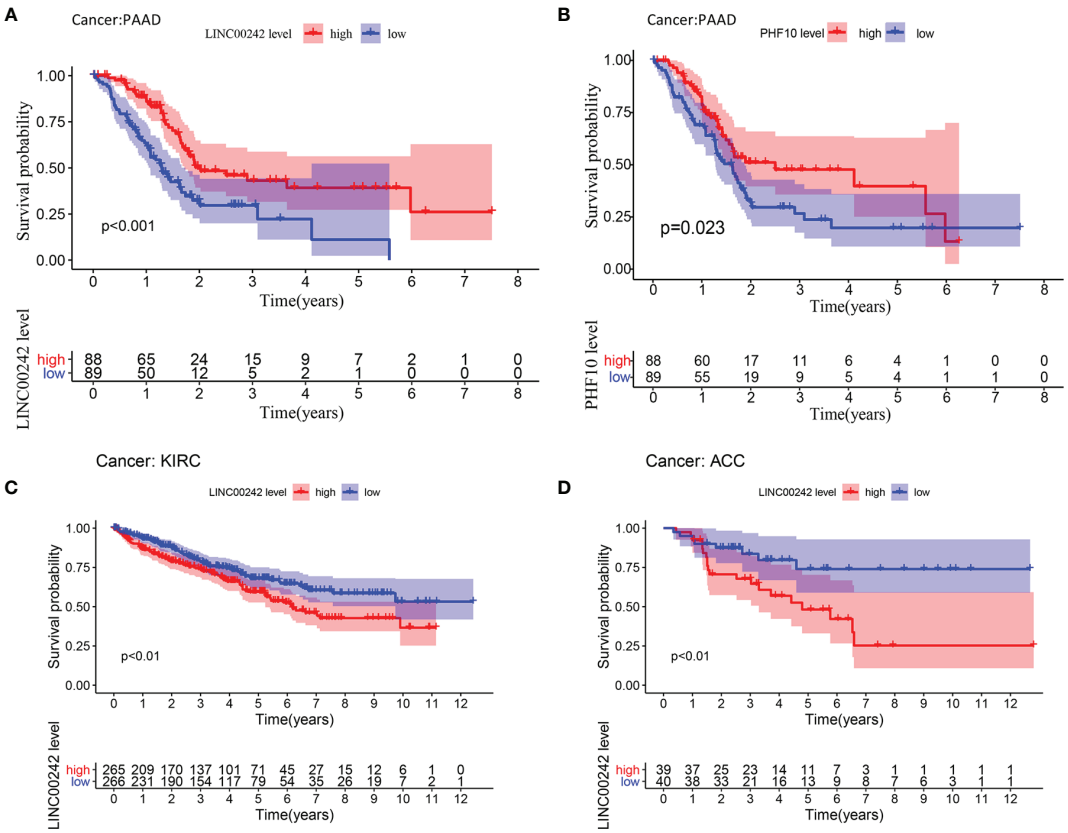

FIGURE 2 | Survival analysis of LINC00242 and its target gene PHF10. **(A)** LINC00242 upregulation was significantly correlated with better OS in PAAD. **(B)** PHF10 upregulation was significantly correlated with better OS in PAAD. **(C)** LINC00242 upregulation was significantly correlated with worse OS in KIRC. **(D)** LINC00242 upregulation was significantly correlated with worse OS in ACC. PAAD, pancreatic adenocarcinoma; KIRC, kidney renal clear cell carcinoma; ACC, adrenocortical carcinoma.

The univariate analysis showed that age ($p < 0.05$), grade ($p < 0.05$), PHF10 ($p < 0.01$), and LINC00242 ($p < 0.01$) were significantly associated with OS (**Figure 4A**). In the multivariate analysis, LINC00242 ($p < 0.01$) was still an independent prognostic factor of OS (**Figure 4B**).

Functional Enrichment Analysis

Through the intersection of differentially expressed genes and co-expressed genes, we identified a total of 103 genes. GO and KEGG enrichment analyses showed that these genes were involved in many kinds of immune-related pathways and signaling pathways, such as T cell activation and lymphocyte differentiation (**Figures 4C, D**).

mRNA and Protein Expression Profile of PHF10

The HPA website was used to analyze the expression level of PHF10 in different tissues. The RNA expression of PHF10 in normal pancreatic tissue was relatively low (**Figure 5A**), but the protein level of PHF10 was relatively high among 43 normal human tissue types (**Figure 5B**). Additionally, the PHF10 mRNA level in PAAD samples was relatively low among 17 cancer types (**Figure 5C**); However, the expression of PHF10 was significantly upregulated in PAAD compared with normal tissues (**Figure 5D**). Based on GSE15471 analysis, the expression of PHF10 in pancreatic cancer tissues was significantly higher than that in normal tissues (**Supplementary Figure 3D**). In terms of the expression level of PHF10 protein, pancreatic cancer showed a low positive rate, ranking seventh from the bottom among 43 common cancer types (**Figure 5E**). The representative IHC images with different PHF10 expression levels, including low, medium, and high, are shown in **Figure 5F**. Based on web tool TIMER, we further examined PHF10 expression in multiple human cancers with RNA-seq data from the TCGA database. Interestingly, the PHF10 expression level varied significantly among different cancer types. PHF10 expression was significantly upregulated in CHOL, COAD, LIHC, and STAD and significantly downregulated in BLCA, BRCA, KICH, KIRC, KIRP, LUAD, THCA, and UCEC, than in normal tissues (**Supplementary Figure 1**).

Integrated Analysis of PHF10 Expression and Immune Infiltration in PAAD

After performing the CIBERSORT algorithm, 134 tumor samples with $p< 0.05$ in the TCGA cohort were enrolled in this study. The

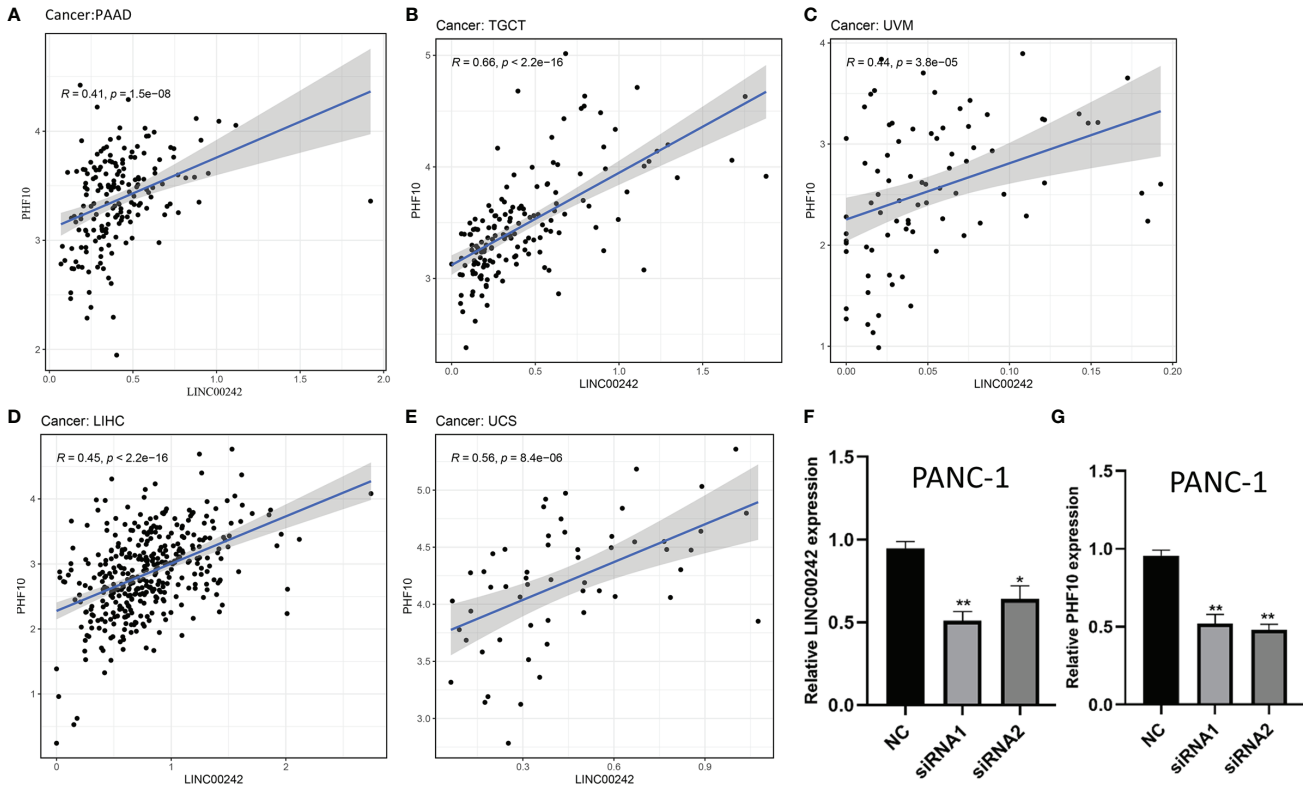

FIGURE 3 | The correlation analysis between LINC00242 and its target PHF10 in pan-cancer. **(A–E)** A significant co-expression relationship between LINC00242 and PHF10 was observed in PAAD, TCGT, UVM, LIHC, and UCS. **(F)** The expression level of LINC00242 were significantly downregulated after being transfected with LINC00242 siRNA. **(G)** The expression level of PHF10 was significantly downregulated after transfected with LINC00242 siRNA. TCGT, testicular germ cell tumors; UVM, uveal melanoma; LIHC, liver hepatocellular carcinoma; UCS, uterine carcinosarcoma (*p < 0.05, **p < 0.01).

landscape of immune infiltrations consisted by 22 immune cells is shown in **Figure 6A**. There was a significant positive correlation between activated $CD4^+$ memory T cells and $CD8^+$ T cells, and a significant negative correlation between $CD8^+$ T cells and M0 macrophage (**Figure 6B**). To further investigate the effect of PHF10 on TIICs, all PAAD samples were assigned into high-expression (PHF10-H) and low-expression (PHF10-L) groups based on the median expression level of PHF10. Obviously, there was a significant difference in the proportion of TIICs between the two groups (**Figure 6C**). Compared with the PHF10-H group, the PHF10-L group contained a higher proportion of activated NK cells and M0 macrophages, but the proportion of naive B cells and resting $CD4^+$ memory T cells was relatively lower (all $p < 0.05$, **Figure 6C**).

We used the ssGSEA algorithm to obtain the enrichment score. Using an unsupervised clustering algorithm, PAAD samples were assigned into three immune infiltration clusters, including high immune cell infiltration cluster (Immunity-H, n = 97), medium immune cell infiltration cluster (Immunity-M, n = 28), and low immune cell infiltration cluster (Immunity-L, n = 53). Then, we calculated the Immune score, Stromal score, and ESTIMATE score based on the normalized gene expression data. The Immune score, Stromal score, and ESTIMATE score of the Immunity-H cluster are higher than the other two clusters (**Figure 7A**). The box plot also showed that with the increase in PHF10 expression, the expression levels of several HLA related genes were upregulated (**Figure 7B**). Additionally, the expression level of PHF10 in the Immunity-H cluster was significantly upregulated compared with the Immunity-M and Immunity-L clusters (all $p < 0.05$, **Figure 7C**). Based on ssGESA analysis, pancreatic cancer patients in the ICGC-PAAD cohort can be divided into three categories, which was consistent with the results of the training set (**Supplementary Figure 4A**). In addition, there was infiltration of more B cell-naive and fewer M0 macrophages in the PHF10 high-expression group, which was consistent with the training set (**Supplementary Figure 4B**). At the same time, the expression of PHF10 in the Immunity-H group was significantly higher than that in the Immunity-M group (**Supplementary Figure 4C**).

Concomitantly, we further investigate the relationships between PHF10 expression and immune checkpoint genes (PD-L1 and CTLA-4) in PAAD *via* GEPIA. The results demonstrated that PHF10 was positively correlated with the expression of PD-L1 ($R = 0.32$, $p < 0.01$, **Figure 7D**) and CTLA4 ($R = 0.35$, $p < 0.01$, **Figure 7E**).

Pan-Cancer Analysis of the Association of PHF10 With Immune Subtypes and Immune Cell Infiltration

Then, we use the TISIDB database to explore whether PHF10 was correlated with the immune subtype of PAAD. All tumor

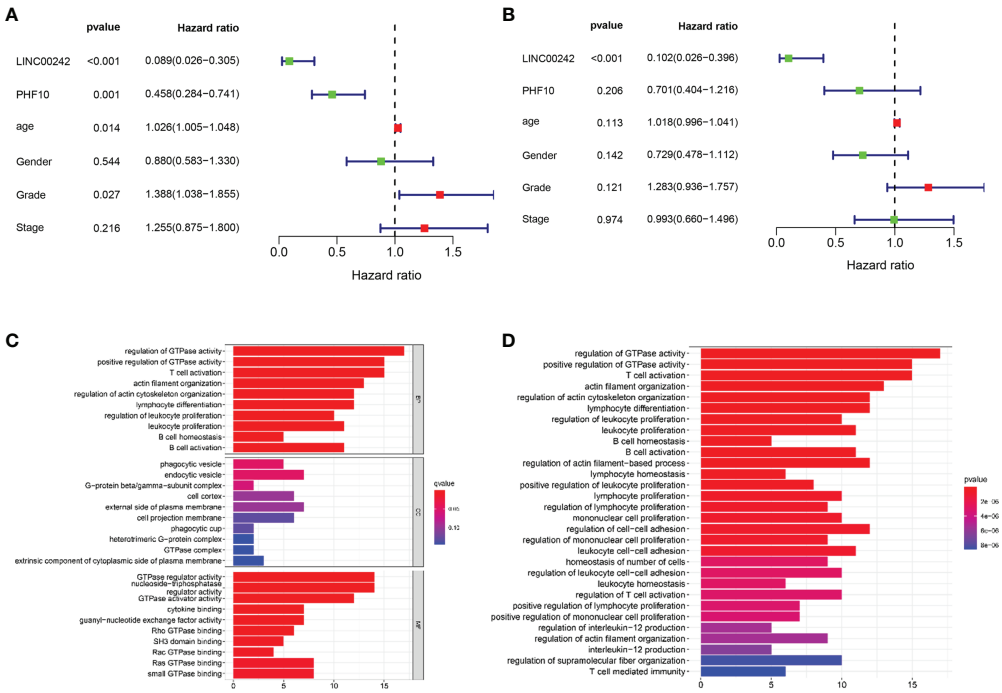

FIGURE 4 | Forest plot of Cox regression analysis and functional enrichment analysis in PAAD. **(A)** Univariate Cox regression analysis. **(B)** Multivariate Cox regression analysis. **(C, D)** The biological processes of Gene Ontology (GO) analysis **(C)** and enrichment pathway of Kyoto Encyclopedia of Genes and Genomes (KEGG) analysis **(D)**.

samples in the TISIDB database were divided into six immune subtypes, including C1: wound healing, C2: IFN-gamma dominant, C3: inflammatory, C4: lymphocyte depleted, C5: immunologically quiet, and C6: TGF-b dominant). We found that the expression level of PHF10 varied significantly among the five immune subtypes ($p < 0.01$, **Figure 8A**). Next, we investigated the correlations between PHF10 expression and immune subtypes in human pan-cancer. Specifically, PHF10 expression was significantly correlated with immune subtypes in BLCA, STAD, LGG, BRCA, COAD, and KIRC (all $p < 0.01$, **Figures 8B–G**). The relationship between PHF10 and immune infiltration in PAAD and human pan-cancer was explored *via* the TIMER database. PHF10 expression was significantly associated with the content of immune cells in PAAD, including CD4+ T cells ($R = 0.47$), CD8+ T cells ($R = 0.52$), B cells ($R = 0.35$), neutrophils ($R = 0.46$), macrophages ($R = 0.54$), and dendritic cells ($R = 0.48$) (all $p < 0.001$, **Figures 9A–F**). Moreover, we further investigated the relationship between PHF10 and immune infiltration in human pan-cancer. The results showed that PHF10 mRNA level was associated with the immune infiltration in various types of cancer, including KICH, KIRC, SKCM, and THCA (all $p < 0.05$, $R > 0.3$, **Supplementary Figures 2A-L**). Overall, these findings strongly suggest that PHF10 plays an important role in tumor immunity.

DISCUSSION

Pancreatic cancer has a high morbidity and mortality across the world, and the treatment of PAAD still remains a challenge for human beings. Therefore, there is an urgent need to find new prognostic and therapeutic indicators to improve the survival of patients with PAAD. Recently, with the rapid development of bioinformatics, more and more novel biomarkers have been found, and eRNAs are one of them. eRNAs are a special subtype of non-coding RNAs, which are transcribed from the gene enhancer region and could regulate the expression of corresponding genes (6). Many studies demonstrated that the dysregulation of eRNA expression was associated with the occurrence of various human tumors (27, 28). Based on previous studies, we obtained a total of 1,559 eRNAs and its predicted targets. First, we identified a subset of eRNAs that significantly correlated with overall survival. Then, we further select the eRNAs that co-expressed with the target gene. The most survival-related eRNAs and its target genes were selected for further analysis. We found that LINC00242 was the most survival-related eRNAs and highly correlated with the predicted target PHF10.

In this study, we found that LINC00242 and its target gene PHF10 were significantly upregulated in PAAD tissues compared with that in normal tissues. Downregulation of LINC00242 showed a significant correlation with poor clinicopathological features, including higher histological grade, tumor recurrence, and advanced AJCC stage. Furthermore, we found that downregulated LINC00242 was significantly correlated with poor OS. All results indicated that LINC00242 had a tumor-suppressive effect in PAAD. Additionally, univariate and multivariate Cox analyses revealed

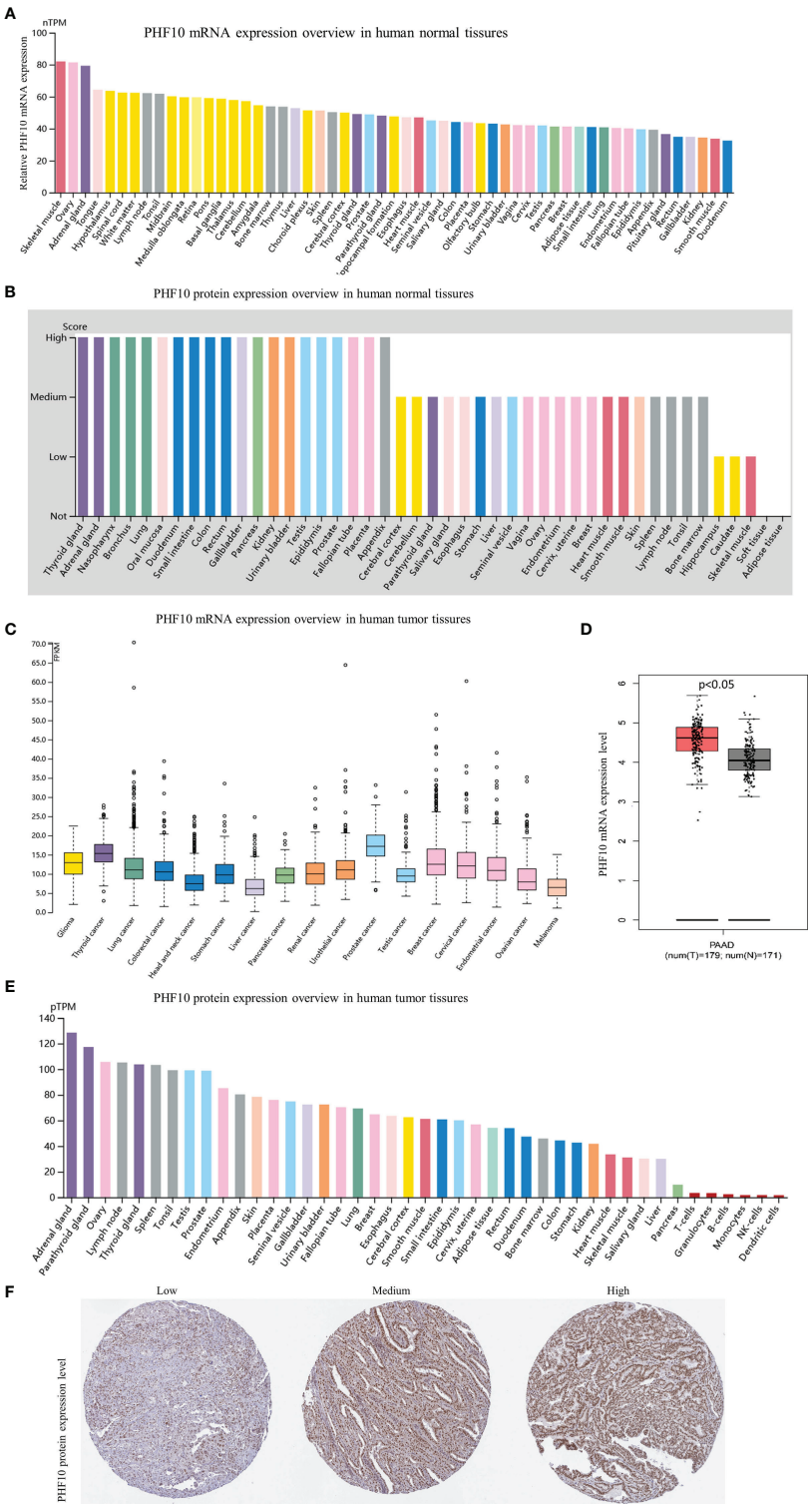

FIGURE 5 | Gene and protein expression profiles of PHF10 in tumor tissues and normal tissues. **(A)** PHF10 mRNA expression overview in human normal tissues. **(B)** PHF10 protein expression overview in human normal tissues. **(C)** PHF10 mRNA expression overview in human tumor tissues. **(D)** Comparison of PHF10 mRNA expression between pancreatic cancer tissues and normal tissues. **(E)** PHF10 protein expression overview in human tumor tissues. **(F)** Representative immunohistochemistry (IHC) images pictures with PHF10 antibody (1:50, Cat#HPA055649, Sigma-Aldrich). All data were obtained from the HPA database (https://www.proteinatlas.org/).

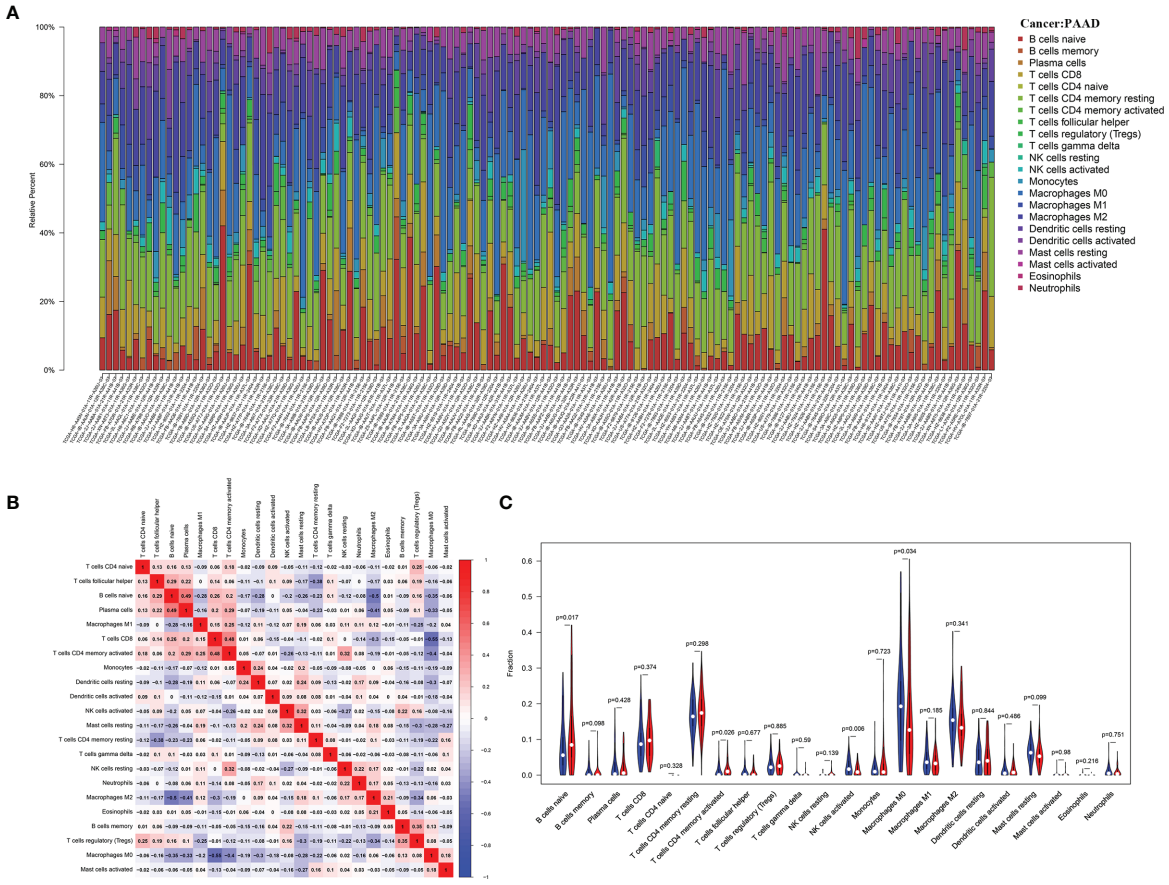

FIGURE 6 | Correlation's analysis of PHF10 expression with immune infiltration calculated by the CIBERSORT algorithm in the TCGA cohort. **(A)** The landscape of immune infiltration in 133 pancreatic cancer tissues. **(B)** Correlation analysis of different types of immune cell infiltration. **(C)** Analysis of the difference of immune cell abundance between the low and high PHF10 expression group.

that LINC00242 and PHF10 were associated with patients' OS in PAAD, but only LINC00242 had an independent prognostic effect. Furthermore, we used external experiments to further study the regulatory relationship between LINC00242 and PHF10 in pancreatic cancer cell lines. LINC00242 was knocked down by transfection with siRNA. We found that PHF10 expression was significantly downregulated in the si-LINC00242 group compared with the si-control group. This suggests that PHF10 is a downstream target gene of LINC00242.

Pan-cancer analysis can find the similarity and difference of tumor, which is helpful in cancer prevention and treatment. Recently, many pan-cancer analyses demonstrated that gene mutation and RNA alterations were associated with the occurrence and development of cancer (29, 30). However, the function of LINC00242 and PHF10 in human pan-cancer is not clear. In the current study, pan-cancer analysis demonstrated that LINC00242 and PHF10 co-expressed in many types of cancer. This result suggested that there was a regulatory relationship between LINC00242 and PHF10. Interestingly, a high expression of LINC00242 was closely related to poor prognosis in KIRC and ACC, which was contrary to PAAD.

Since the function of LINC00242 is not yet clear, we tried to clarify its role by identifying its co-expressed genes. Then, a total of 1,640 genes were found to be significantly correlated with LINC00242. The enrichment analysis of GO and KEGG shows that LINC00242 was related to the immune-related processes. Based on these results, novel therapies that increase the expression of LINC00242 may help induce protective immunity to effectively treat PAAD.

The tumor microenvironment (TME) plays a key role in tumor immunotherapy and has attracted more and more attention from researchers in recent years. On the one hand, immune cells in the tumor microenvironment play an antitumor role by recognizing and killing cancer cells. On the other hand, tumor cells can avoid being killed by immune cells in a number of ways. CD4+ and CD8+T cells are an important part of the tumor microenvironment and kill tumor cells by exerting specific immune responses (31). M1 tumor-associated macrophages play an antitumor role, while M2 tumor-associated macrophages can promote tumor growth and metastasis (32). These results demonstrate that the immune microenvironment plays a critical role in tumor progression. Up to now, there are few studies on PHF10 and immune infiltration. We found that the

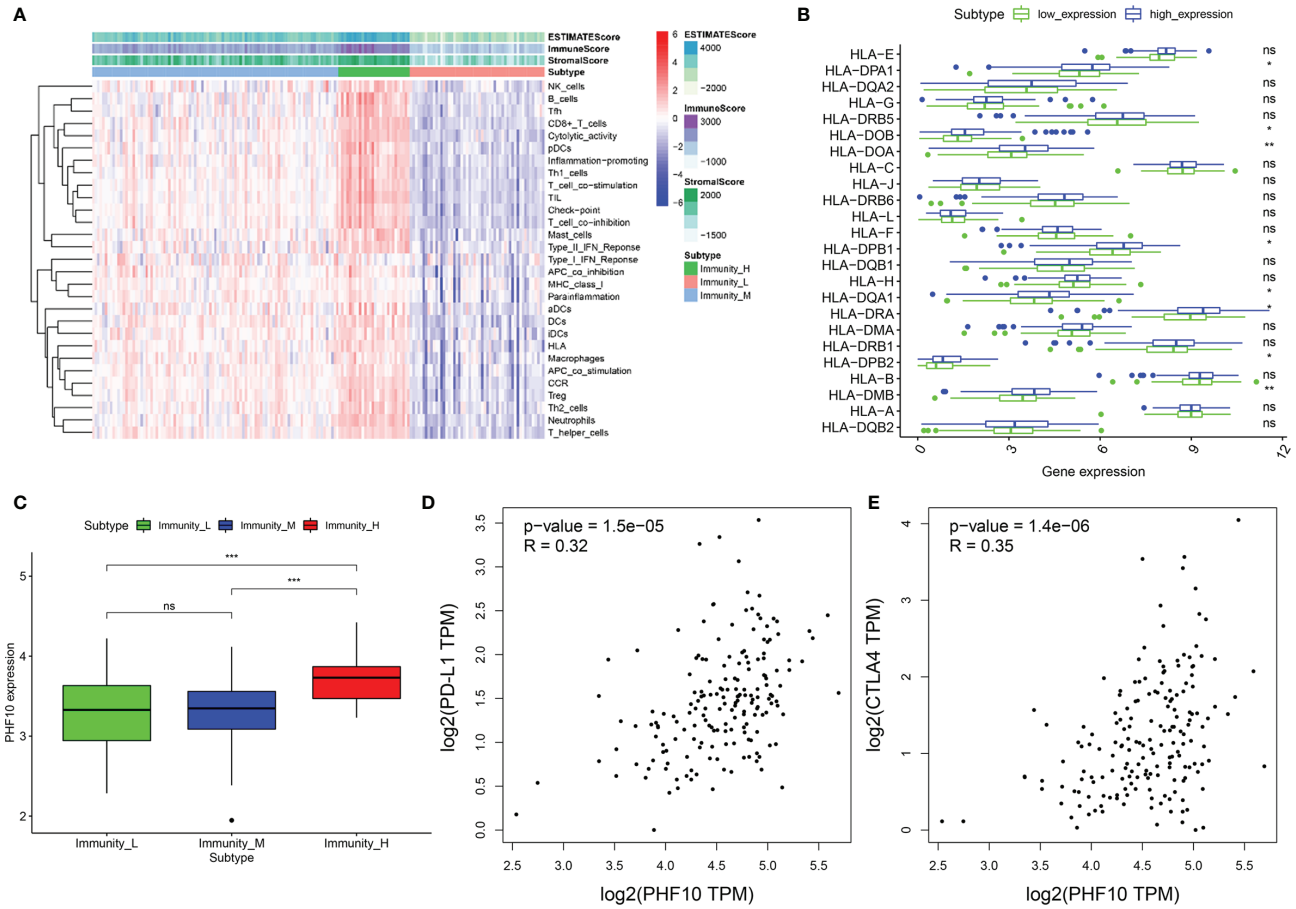

FIGURE 7 | The integrated analysis of PHF10 with immune infiltration. **(A)** The enrichment levels of 29 immune-related gene sets were calculated *via* the ssGSEA method. **(B)** The expression of the HLA gene family in the PHF10 high-expression group was significantly different with that of the PHF10 low-expression group. **(C)** The expression of PHF10 varied significantly among the three clusters, which were obtained by the unsupervised clustering method based on ssGSEA results. **(D, E)** Co-expression analysis of PHF10 and immune checkpoint genes PD-L1 and CTLA4. (*p < 0.05, **p < 0.01, ***p < 0.001. ns, no statistically significant).

mRNA level of PHF10 was significantly associated with the immune infiltration in various types of cancer. After further analysis by the CIBERSORT algorithm, we found that the levels of immune cell infiltration were significantly different between the PHF10-H and PHF10-L groups. These new findings have made substantial progress in determining the significant role of PHF10 in immune infiltration.

In this study, we use the unsupervised hierarchical clustering algorithm to divide the samples into three categories based on 29 immune cell types. Compared with the Immunity-M and Immunity-L groups, the expression of PHF10 was higher in the Immunity-H group, suggesting that elevated PHF10 level could recruit more immune cells. Additionally, PHF10 has a significant co-expression relationship with immune checkpoint genes CTLA-4 and PD-L1. It seems that high expression of PHF10 may be a candidate predictor of the efficacy of anti-PDL-1/CTLA4 therapy, and combination of PHF10 blockade and anti-PD-L1/CTLA4 mAb may be a potentially effective treatment for PAAD. As there are great differences in the sensitivity of different immune subtypes to immunotherapy, it is very important to correctly distinguish different immune subtypes for cancer immunotherapy. In this study, the expression of PHF10 varied significantly among the five immune subtypes in pancreatic cancer. The pan-cancer results further confirmed that there was a significant correlation between PHF10 and immunophenotype, indicating that PHF10 may have potential value in immunotherapy.

There are some limitations to this study. Firstly, further experiments are needed to verify the regulatory relationship between LINC00242 and its target genes PHF10. Second, the sample size and the clinical information were limited. Third, the prognostic efficacy of LINC00242 and PHF10 and their regulatory relationship should be verified in more pancreatic cancer datasets.

In conclusion, this study demonstrated that LINC00242 is a key survival-associated eRNA in PAAD. Downregulation of LINC00242 showed a significant correlation with poor clinicopathological features. Pan-cancer analysis further confirmed the prognostic value of LINC00242. PHF10 is a target gene of LINC00242 and has been shown to co-express with LINC00242 in a variety of cancers. External experiments further demonstrated that PHF10 is the downstream target gene of LINC00242. PHF10 expression was found to be significantly

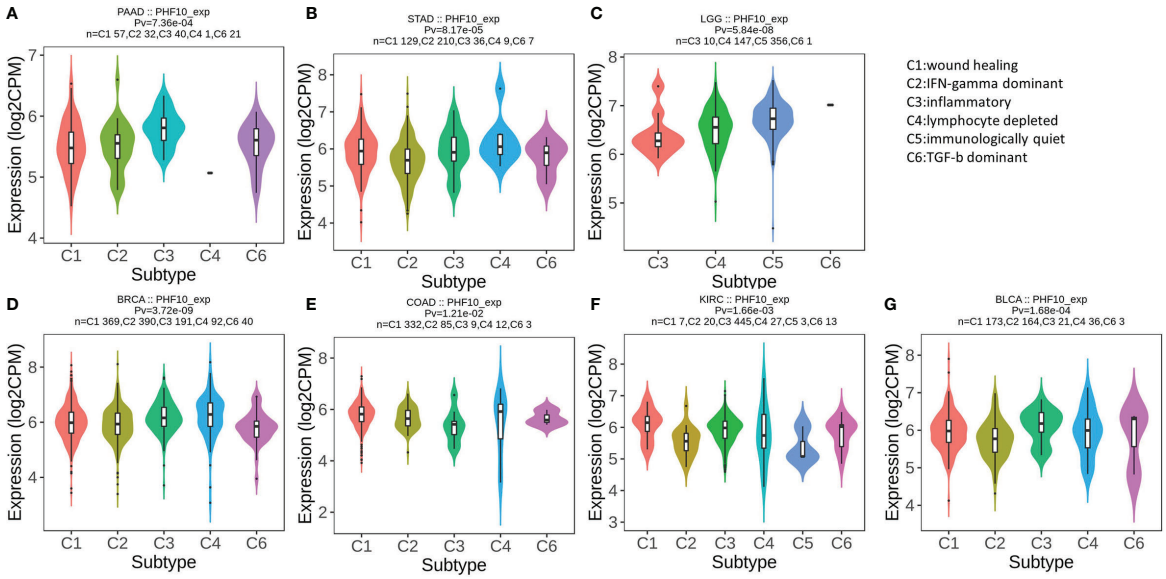

FIGURE 8 | Correlation analysis of PHF10 expression with immune subtype in pan-cancer. **(A–G)** Correlation of PHF10 expression and immune subtypes in PAAD, STAD, LGG, BRCA, COAD, KIRC, and BLCA. STAD, stomach adenocarcinoma; LGG, brain lower grade glioma; BRCA, breast invasive carcinoma; COAD, colon adenocarcinoma; BLCA, bladder urothelial carcinoma.

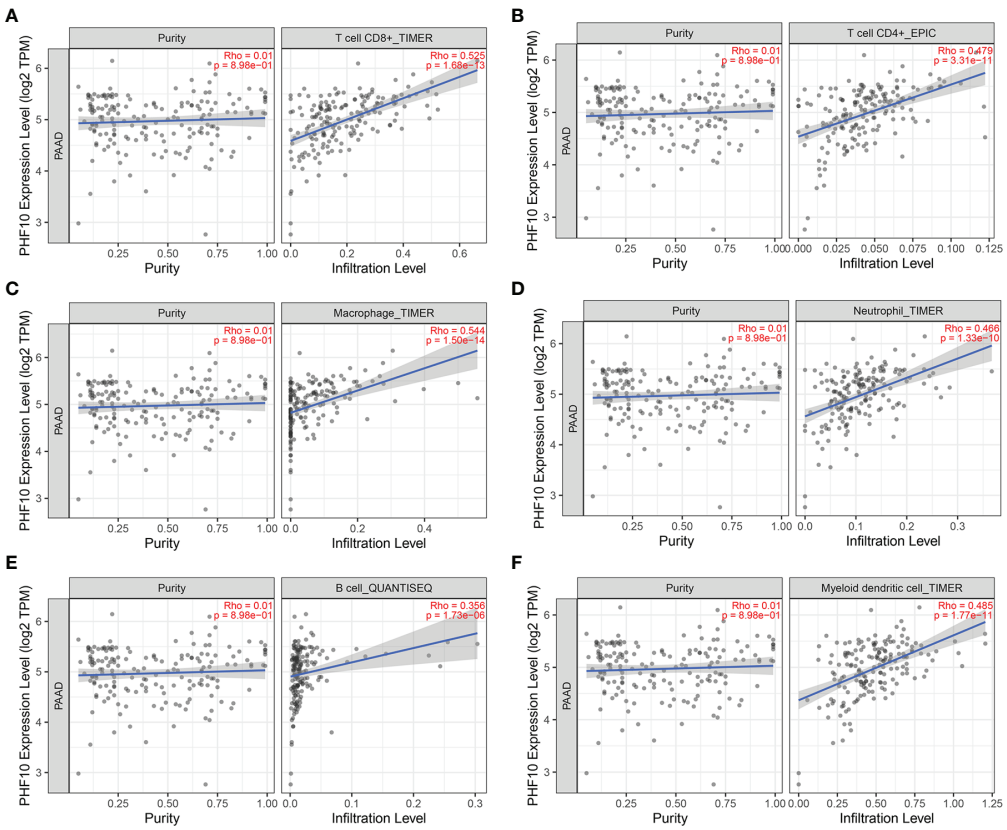

FIGURE 9 | Correlation analysis between PHF10 expression and immune cell infiltration in PAAD. **(A–F)** The expression of PHF10 was positively correlated with the infiltration of immune cells.

correlated with the immune cell infiltration and immune subtype across many cancer types. The results of this study provide a means for predicting the prognosis of patients with PAAD and a promising target for immunotherapy.

DATA AVAILABILITY STATEMENT

The original contributions presented in the study are included in the article/**Supplementary Material**. Further inquiries can be directed to the corresponding author.

AUTHOR CONTRIBUTIONS

WT conceived and designed the study. WT and LZ performed the experiments. WT and LZ wrote the manuscript. LZ, ZL, and LY revised the manuscript. YZ supervised the study. All authors contributed to the article and approved the submitted version.

FUNDING

This work was supported by the Tianjin Natural Science Foundation (20JCYBJC01310), Tianjin Science and Technology Project (19ZXDBSY00010), Tianjin Health Science and Technology Project (ZC20218), and Tianjin Health Science and Technology Project (ZC20064).

ACKNOWLEDGMENTS

We are grateful to the TCGA and GEO working group.

SUPPLEMENTARY MATERIAL

The Supplementary Material for this article can be found online at: https://www.frontiersin.org/articles/10.3389/fonc.2021.795090/full#supplementary-material

Supplementary Figure 1 | PHF10 mRNA expression overview in pan-cancer from TIMER database (https://cistrome.shinyapps.io/timer/).

Supplementary Figure 2 | Correlation analysis between PHF10 expression and immune cell infiltration in pan-cancer. **(A-L)** The expression of PHF10 was positively correlated with the infiltration of immune cells in pan-cancer.

Supplementary Figure 3 | Survival analysis of LINC00242 and its target gene PHF10 in ICGC-PAAD cohort. **(A, B)** Correlation analysis of LINC00242 expression **(A)** as well as PHF10 expression **(B)** and patient survival in PAAD. **(C, D)** Comparison of LINC00242 expression **(C)** as well as PHF10 expression **(D)** between pancreatic cancer tissues and normal tissues.

Supplementary Figure 4 | The integrated analysis of PHF10 with immune infiltration in ICGC-PAAD cohort. **(A)** The enrichment levels of 29 immune-related gene sets were calculated *via* the ssGSEA method. **(B)** Analysis of the difference of immune cell abundance between the low and high PHF10 expression group. **(C)** The expression of PHF10 varied significantly among the three clusters.

REFERENCES

1. Siegel RL, Miller KD, Jemal A. Cancer Statistics, 2020. *CA: Cancer J Clin* (2020) 70(1):30–7. doi: 10.3322/caac.21590
2. Kamisawa T, Wood LD, Itoi T, Takaori K. Pancreatic Cancer. *Lancet (London England)* (2016) 388(10039):73–85. doi: 10.1016/S0140-6736(16)00141-0
3. Xu J-W, Wang L, Cheng Y-G, Zhang G-Y, Hu S-Y, Zhou B, et al. Immunotherapy for Pancreatic Cancer: A Long and Hopeful Journey. *Cancer Lett* (2018) 425:143–51. doi: 10.1016/j.canlet.2018.03.040
4. Pu N, Zhao G, Yin H, Li J-A, Nuerxiati A, Wang D, et al. CD25 and TGF-β Blockade Based on Predictive Integrated Immune Ratio Inhibits Tumor Growth in Pancreatic Cancer. *J Transl Med* (2018) 16(1):294. doi: 10.1186/s12967-018-1673-6
5. Lai E, Puzzoni M, Ziranu P, Pretta A, Impera V, Mariani S, et al. New Therapeutic Targets in Pancreatic Cancer. *Cancer Treat Rev* (2019) 81:101926. doi: 10.1016/j.ctrv.2019.101926
6. Zhang Z, Lee J-H, Ruan H, Ye Y, Krakowiak J, Hu Q, et al. Transcriptional Landscape and Clinical Utility of Enhancer RNAs for eRNA-Targeted Therapy in Cancer. *Nat Commun* (2019) 10(1):4562. doi: 10.1038/s41467-019-12543-5
7. Liu F. Enhancer-Derived RNA: A Primer. *Genomics Proteomics Bioinf* (2017) 15(3):196–200. doi: 10.1016/j.gpb.2016.12.006
8. Rothschild G, Basu U. Lingering Questions About Enhancer RNA and Enhancer Transcription-Coupled Genomic Instability. *Trends Genet* (2017) 33(2):143–54. doi: 10.1016/j.tig.2016.12.002
9. Mao R, Wu Y, Ming Y, Xu Y, Wang S, Chen X, et al. Enhancer RNAs: A Missing Regulatory Layer in Gene Transcription. *Sci China Life Sci* (2019) 62(7):905–12. doi: 10.1007/s11427-017-9370-9
10. Arnold PR, Wells AD, Li XC. Diversity and Emerging Roles of Enhancer RNA in Regulation of Gene Expression and Cell Fate. *Front Cell Dev Biol* (2019) 7:377. doi: 10.3389/fcell.2019.00377
11. Lam MTY, Li W, Rosenfeld MG, Glass CK. Enhancer RNAs and Regulated Transcriptional Programs. *Trends Biochem Sci* (2014) 39(4):170–82. doi: 10.1016/j.tibs.2014.02.007
12. Ding M, Liu Y, Li J, Yao L, Liao X, Xie H, et al. Oestrogen Promotes Tumorigenesis of Bladder Cancer by Inducing the Enhancer RNA-Egreb1. *J Cell Mol Med* (2018) 22(12):5919–27. doi: 10.1111/jcmm.13861
13. Zhu C, Li L, Zhang Z, Bi M, Wang H, Su W, et al. A Non-Canonical Role of YAP/TEAD Is Required for Activation of Estrogen-Regulated Enhancers in Breast Cancer. *Mol Cell* (2019) 75(4):806–791.e8. doi: 10.1016/j.molcel.2019.06.010
14. Bal E, Park H-S, Belaid-Choucair Z, Kayserili H, Naville M, Madrange M, et al. Mutations in ACTRT1 and its Enhancer RNA Elements Lead to Aberrant Activation of Hedgehog Signaling in Inherited and Sporadic Basal Cell Carcinomas. *Nat Med* (2017) 23(10):1226–33. doi: 10.1038/nm.4368
15. Pan C-W, Wen S, Chen L, Wei Y, Niu Y, Zhao Y. Functional Roles of Antisense Enhancer RNA for Promoting Prostate Cancer Progression. *Theranostics* (2021) 11(4):1780–94. doi: 10.7150/thno.51931
16. Vučićević D, Corradin O, Ntini E, Scacheri PC, Ørom UA. Long ncRNA Expression Associates With Tissue-Specific Enhancers. *Cell Cycle* (2015) 14(2):253–60. doi: 10.4161/15384101.2014.977641
17. Corradin O, Saiakhova A, Akhtar-Zaidi B, Myeroff L, Willis J, Cowper-Sal lari R, et al. Combinatorial Effects of Multiple Enhancer Variants in Linkage Disequilibrium Dictate Levels of Gene Expression to Confer Susceptibility to Common Traits. *Genome Res* (2014) 24(1):13–1. doi: 10.1101/gr.164079.113
18. Uhlen M, Oksvold P, Fagerberg L, Lundberg E, Jonasson K, Forsberg M, et al. Towards a Knowledge-Based Human Protein Atlas. *Nat Biotechnol* (2010) 28(12):1248–50. doi: 10.1038/nbt1210-1248
19. Uhlén M, Fagerberg L, Hallström BM, Lindskog C, Oksvold P, Mardinoglu A, et al. Proteomics. Tissue-Based Map of the Human Proteome. *Science* (2015) 347(6220):1260419. doi: 10.1126/science.1260419
20. Tang Z, Li C, Kang B, Gao G, Li C, Zhang Z. GEPIA: A Web Server for Cancer and Normal Gene Expression Profiling and Interactive Analyses. *Nucleic Acids Res* (2017) 45(W1):W102–98. doi: 10.1093/nar/gkx247

21. Newman AM, Liu CL, Green MR, Gentles AJ, Feng W, Xu Y, et al. Robust Enumeration of Cell Subsets From Tissue Expression Profiles. *Nat Methods* (2015) 12(5):453–7. doi: 10.1038/nmeth.3337
22. Ye L, Zhang T, Kang Z, Guo G, Sun Y, Lin K, et al. Tumor-Infiltrating Immune Cells Act as a Marker for Prognosis in Colorectal Cancer. *Front Immunol* (2019) 10:2368. doi: 10.3389/fimmu.2019.02368
23. Hänzelmann S, Castelo R, Guinney J. GSVA: Gene Set Variation Analysis for Microarray and RNA-Seq Data. *BMC Bioinf* (2013) 14:7. doi: 10.1186/1471-2105-14-7
24. Yoshihara K, Shahmoradgoli M, Martínez E, Vegesna R, Kim H, Torres-Garcia W, et al. Inferring Tumour Purity and Stromal and Immune Cell Admixture From Expression Data. *Nat Commun* (2013) 4:2612. doi: 10.1038/ncomms3612
25. Li T, Fan J, Wang B, Traugh N, Chen Q, Liu JS, et al. TIMER: A Web Server for Comprehensive Analysis of Tumor-Infiltrating Immune Cells. *Cancer Res* (2017) 77(21):e108–e10. doi: 10.1158/0008-5472.CAN-17-0307
26. Ru B, Wong CN, Tong Y, Zhong JY, Zhong SSW, Wu WC, et al. TISIDB: An Integrated Repository Portal for Tumor-Immune System Interactions. *Bioinf (Oxford England)* (2019) 35(20):4200–2. doi: 10.1093/bioinformatics/btz210
27. Sartorelli V, Lauberth SM. Enhancer RNAs are an Important Regulatory Layer of the Epigenome. *Nat Struct Mol Biol* (2020) 27(6):521–8. doi: 10.1038/s41594-020-0446-0
28. Lee J-H, Xiong F, Li W. Enhancer RNAs in Cancer: Regulation, Mechanisms and Therapeutic Potential. *RNA Biol* (2020) 17(11):1550–9. doi: 10.1080/15476286.2020.1712895
29. Cui X, Zhang X, Liu M, Zhao C, Zhang N, Ren Y, et al. A Pan-Cancer Analysis of the Oncogenic Role of Staphylococcal Nuclease Domain-Containing Protein 1 (SND1) in Human Tumors. *Genomics* (2020) 112(6):3958–67. doi: 10.1016/j.ygeno.2020.06.044
30. Robichaux JP, Elamin YY, Vijayan RSK, Nilsson MB, Hu L, He J, et al. Pan-Cancer Landscape and Analysis of ERBB2 Mutations Identifies Poziotinib as a Clinically Active Inhibitor and Enhancer of T-DM1 Activity. *Cancer Cell* (2019) 36(4):457–44.e7. doi: 10.1016/j.ccell.2019.09.001
31. Farhood B, Najafi M, Mortezaee K. CD8 Cytotoxic T Lymphocytes in Cancer Immunotherapy: A Review. *J Cell Physiol* (2019) 234(6):8509–21. doi: 10.1002/jcp.27782
32. Komohara Y, Fujiwara Y, Ohnishi K, Takeya M. Tumor-Associated Macrophages: Potential Therapeutic Targets for Anti-Cancer Therapy. *Adv Drug Delivery Rev* (2016) 99(Pt B):180–5. doi: 10.1016/j.addr.2015.11.009

Conflict of Interest: The authors declare that the research was conducted in the absence of any commercial or financial relationships that could be construed as a potential conflict of interest.

Publisher's Note: All claims expressed in this article are solely those of the authors and do not necessarily represent those of their affiliated organizations, or those of the publisher, the editors and the reviewers. Any product that may be evaluated in this article, or claim that may be made by its manufacturer, is not guaranteed or endorsed by the publisher.

frontiers in Cell and Developmental Biology

ORIGINAL RESEARCH
published: 24 January 2022
doi: 10.3389/fcell.2022.795084

LncPep: A Resource of Translational Evidences for lncRNAs

*Teng Liu[1†], Jingni Wu[1†], Yangjun Wu[2†], Wei Hu[1], Zhixiao Fang[1], Zishan Wang[3], Chunjie Jiang[4] and Shengli Li[1]**

[1]Precision Research Center for Refractory Diseases, Institute for Clinical Research, Shanghai General Hospital, Shanghai Jiao Tong University School of Medicine, Shanghai, China, [2]Department of Gynecological Oncology, Fudan University Shanghai Cancer Center, Shanghai, China, [3]Department of Genetics and Genomic Sciences, Center for Transformative Disease Modeling, Tisch Cancer Institute, Icahn Institute for Data Science and Genomic Technology, Icahn School of Medicine at Mount Sinai, New York, NY, United States, [4]Institute for Diabetes Obesity, and Metabolism, Perelman School of Medicine at the University of Pennsylvania, Philadelphia, PA, United States*

Long noncoding RNAs (lncRNAs) are a type of transcript that is >200 nucleotides long with no protein-coding capacity. Accumulating studies have suggested that lncRNAs contain open reading frames (ORFs) that encode peptides. Although several noncoding RNA-encoded peptide-related databases have been developed, most of them display only a small number of experimentally validated peptides, and resources focused on lncRNA-encoded peptides are still lacking. We used six types of evidence, coding potential assessment tool (CPAT), coding potential calculator v2.0 (CPC2), N6-methyladenosine modification of RNA sites (m6A), Pfam, ribosome profiling (Ribo-seq), and translation initiation sites (TISs), to evaluate the coding potential of 883,804 lncRNAs across 39 species. We constructed a comprehensive database of lncRNA-encoded peptides, LncPep (http://www.shenglilabs.com/LncPep/). LncPep provides three major functional modules: 1) user-friendly searching/browsing interface, 2) prediction and BLAST modules for exploring novel lncRNAs and peptides, and 3) annotations for lncRNAs, peptides and supporting evidence. Taken together, LncPep is a user-friendly and convenient platform for discovering and investigating peptides encoded by lncRNAs.

Keywords: lncRNA, peptide, translation, cancer, m6A, ribo-seq

OPEN ACCESS

Edited by:
Hernandes F. Carvalho, State University of Campinas, Brazil

Reviewed by:
Max Shokhirev, Salk Institute for Biological Studies, United States
Xavier Roucou, Université de Sherbrooke, Canada

****Correspondence:***
Shengli Li
shengli.li@shsmu.edu.cn

[†]These authors have contributed equally to this work

Specialty section:
This article was submitted to Molecular and Cellular Oncology, a section of the journal Frontiers in Cell and Developmental Biology

Received: *14 October 2021*
Accepted: *05 January 2022*
Published: *24 January 2022*

Citation:
Liu T, Wu J, Wu Y, Hu W, Fang Z, Wang Z, Jiang C and Li S (2022) LncPep: A Resource of Translational Evidences for lncRNAs. Front. Cell Dev. Biol. 10:795084. doi: 10.3389/fcell.2022.795084

INTRODUCTION

Long noncoding RNAs (lncRNAs) are defined as RNAs longer than 200 nucleotides (nt) and have been shown to be extensively expressed and exert powerful regulatory functions (Marchese et al., 2017). Mechanistically, lncRNAs can regulate protein-protein and protein-DNA interactions by serving as scaffolds or guides, binding to proteins as decoys and modulating mRNA expression as microRNA (miRNA) sponges. Evidence accumulated over the past decade demonstrates that lncRNA regulation plays key roles in diverse biological and pathological contexts, such as the immune response (Chen et al., 2017), cell proliferation (Li et al., 2018), neuronal disorders (Salta and De Strooper, 2017), and tumour biology (Liu et al., 2021). LncRNAs have been regarded as "junk RNAs" and have no potential to encode functional proteins. Recently, a growing amount of evidence has demonstrated that lncRNAs are able to encode functional peptides that play vital roles in physiological processes (Anderson et al., 2015; Matsumoto et al., 2017; Anastasia et al., 2019; Niu et al., 2020; Cai et al., 2021; Zhang et al., 2021). For example, the translated peptides from lncRNA *Aw112010* are essential for the orchestration of mucosal immunity during bacterial infection and

colitis (Jackson et al., 2018). Matsumoto *et al.* identified and functionally characterized a novel polypeptide encoded by the lncRNA LINC00961(Matsumoto et al., 2017). A LINC00961-encoded peptide was found to negatively regulate mTORC1 activation by interacting with lysosomal v-ATPase and stimulating amino acids, which further promoted muscle regeneration. The lncRNA HOXB-AS3 was discovered to encode a conserved 53 amino acid (aa) peptide that suppresses colon cancer growth by competitively binding to the arginine residues in the RGG motif of hnRNP A1 (Huang et al., 2017). These studies expand our understanding of lncRNAs and the coding potential of the genome. With increasing numbers of experimentally validated lncRNA-encoded peptides, a comprehensive identification and annotation of peptides translated from lncRNAs is urgently needed.

Various computational algorithms and biotechnologies have been developed to directly or indirectly capture translational evidence of RNAs. The coding potential assessment tool (CPAT) (Wang et al., 2013) and coding potential calculator v2.0 (CPC2) (Kang et al., 2017) are the most commonly used algorithms to assess RNA coding ability. Ribosome profiling (Ribo-seq) is a common method to identify translated RNAs (Ingolia et al., 2009), as well as the N6-methyladenosine modification of RNA (m6A) that promotes RNA translation initiation (Meyer et al., 2015), and the translation initiation site (TIS) detected by global translation initiation sequencing is important evidence for encoding proteins or peptides (Lee et al., 2012). Ribo-seq, m6A sites, and TIS provide indirect proof of lncRNA-encoded peptides. Although there is other indirect evidence supporting lncRNA-encoded peptides, none of these lines of evidence offers dependable predictions by themselves.

Several databases have annotated a few lncRNAs (Ma et al., 2019; Volders et al., 2019; Zhao et al., 2021), but a comprehensive database for translatable lncRNA annotation is still lacking. Some existing databases, for example Funcpep (Dragomir et al., 2020), ncEP (Liu et al., 2020), cncRNAdb (Huang et al., 2021), OpenProt (Brunet et al., 2021), and SmProt (Hao et al., 2018), include a fraction of lncRNA encoded information. However, Funcpep, ncEP, and cncRNAdb only collected experimentally validated peptides for a very limited number of lncRNAs; OpenProt predicts and annotates ORFs with MS, Ribo-seq, and conservation information, but only includes 10 species; SmProt did not provide related Ribo-seq, m6A, and TIS evidence for peptides and focused on peptides shorter than 100 amino acids. Some lncRNA encoded functional peptides are longer than 100 aa (Lun et al., 2020; Meng et al., 2020; Cai et al., 2021); for example, one 153 aa peptide encoded by LOC90024 promotes "cancerous" RNA splicing and tumorigenesis (Meng et al., 2020).

To identify the peptides encoded by lncRNAs, we built a comprehensive database, LncPep, that contains 10, 580, 228 peptides that were predicted to be translated from 883,804 lncRNAs across 39 species. Direct and indirect evidence is integrated to evaluate the peptide-encoding potential of lncRNAs. This database provides a convenient data search and browse engine, detailed information on each lncRNA and its translated peptide, and supporting evidence. Moreover, prediction and BLAST searches for novel lncRNAs and peptides are available for users. LncPep is expected to serve as an important resource to discover and investigate biologically functional peptides hidden in lncRNAs. All the information and data are freely accessible at http://www.shenglilabs.com/LncPep/.

RESULTS

Data Source and Summary

The current version of LncPep contains 883,804 lncRNAs across 39 species together with six different peptide-encoding lines of evidence to evaluate their translation potential (**Figure 1**). This evidence provides direct or indirect support for lncRNA translation. For convenience, we normalized a score for each line of evidence ranging from 0 to 1 and combined these scores for a comprehensive translation potential evaluation (see Materials and Methods).

The numbers of lncRNAs, predicted peptides, and supported lines of evidence in each species are summarized in **Table 1**. Detailed information on lncRNAs was retrieved from NONCODE, LncBook, and LNCipedia (**Figure 1**). Both ATG and non-ATG were considered start codons in all the predicted ORFs. The ORF length was set to ≥10 aa, and the longest ORF was selected when multiple ORFs overlapped in the same lncRNAs. Five different pieces of evidence to support translation are included in LncPep (**Figure 1**), including CPAT, CPC2, Ribo-seq, TISs, and m6A sites. Only humans and mice have five pieces of evidence, while other species have three or fewer pieces of evidence (**Figure 1**). The CPAT and CPC2 algorithms are the most commonly used tools for RNA coding potential evaluation, and these two tools provided the coding probability scores that were used in LncPep as evidence (Wang et al., 2013; Kang et al., 2017). Since ribosomes and TISs are necessary for RNA translation, we used Ribo-seq and validated TISs as two pieces of evidence to support lncRNA translation (Ramakrishnan, 2002; Wan and Qian, 2014; Wang et al., 2019). m6A modification was reported to promote RNA translation, and the detected m6A sites were also used as evidence (Liu et al., 2019; Meyer, 2019). "Natural" peptides are more likely to be functional, and we used the Pfam domain to assess lncRNA-translated peptides as one evidence of functionality (Mistry et al., 2021).

LncRNA Translating Features

Peptides were predicted from extracted lncRNA sequences based on ORF searching, and translating evidence scores were calculated for predicted peptides. We defined high-confidence peptides (HCPs) as peptides with Ribo-seq evidence in human and mouse, with no less than 4 pieces of evidence in *Arabidopsis thaliana*, *Caenorhabditis elegans*, fruit fly, rat, yeast, and zebrafish, and with no less than 3 pieces of evidence in the other species. On average, less than one HCP was encoded per lncRNA in all species (**Figure 2A**). Although the numbers of HCPs per lncRNA in humans and mice were 0.016 and 0.01, humans and mice have a large number of lncRNAs, which makes HCPs occupy a considerable part of the human and mouse proteome. Most of the lncRNA-encoded peptides were less

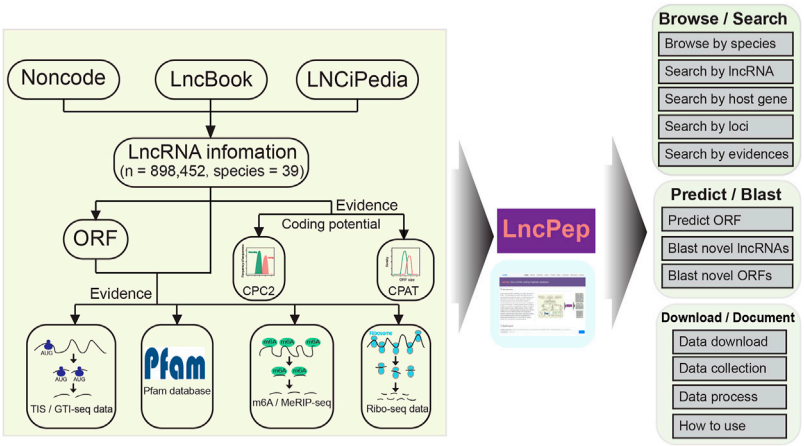

FIGURE 1 | Data curation and construction pipeline of the LncPep database. LncPep collects lncRNA information from NONCODE, LncBook, and LNCipedia, including 898,452 lncRNAs across 39 different species. The peptide-translating potential of all lncRNAs was evaluated by five different tools/resources, including CPC2, CPAT, m6A, Ribo-seq, and TIS. The major functions of LncPep include Browse, Search, Predict, Blast, Download, and Document.

than 100 aa in length (**Figure 2B**). For evidence, the vast majority of peptides are supported by more than two pieces of evidence (**Figure 2C**). In humans, approximately 5% of peptides are supported by more than 2 types of evidence. We compared predicted peptides in LncPep with those in sORFs and Microproteins. Only 153 peptides were shared by all databases, and about 95% of LncPep peptides were unique in these three databases.

Data Access and Download

LncPep provides convenient and flexible routes to mine the data. In the "Browse" module, users can select the species they are interested in, and a brief summary of the peptides will be provided, including the host lncRNA, peptide sequence and length, the evidence and the scores (**Figure 3A**). Users can further browse summarized details of host lncRNAs by clicking the lncRNA ID. A popup window of peptide sequences will appear by clicking the arrow in the "Pep_seq" column. Detailed evidence supporting peptides of interest will be shown after clicking the arrow in the "Evd" column. The summary table can be flexibly browsed by ranking peptide length, CPAT scores, CPC2 scores, m6A numbers, Pfam numbers, Ribo-seq numbers, TIS numbers, or integrated peptide-encoding scores. In addition, users can filter the summary table by selecting single or multiple pieces of evidence.

LncPep allows users to search the entire database by lncRNA ID, host gene, genomic location, and evidence on the search page (**Figure 3B**). The results table will contain peptide numbers, query names, species, lncRNA IDs, ORF genomic loci, peptide lengths, peptide sequences, ORF start sites, ORF end sites, translation scores, and supporting evidence. Search results can be ranked by peptide length, ORF start sites, and integrated peptide-encoding scores by clicking the corresponding table header names. On the lncRNA or peptide page, detailed information on the lncRNAs, peptides, and evidence is provided (**Figure 4**). All the data are free to download on the "Download" page (http://www.shenglilabs.com/LncPep/#!/download) (**Figure 3C**).

As a growing number of lncRNA-encoded peptides have been reported, we also curated experimentally validated lncRNA-encoded peptides. Through literature research and integration, we collected experimentally validated peptides from 27 articles and applied detailed information for the host lncRNAs, peptides, and articles (**Figure 3D**). Most of the studies were based on human lncRNAs, and another small group was based on mice. This module will continue to be updated.

Predict and BLAST

With the development of high-throughput sequencing technology, a large number of lncRNAs and peptides have been or will be discovered. Prediction and BLAST modules will be useful for users to identify their own functional lncRNAs and peptides. Thus, we developed the "Predict" (**Figure 3E**) and "Blast" modules (**Figure 3F**) in the LncPep database, wherein users can input their own lncRNA sequences in *Fasta* format. The results table contains peptide numbers, lncRNA IDs, species, ORF numbers, ORF sequences, and options for BLAST. Users can view the ORF sequences and lengths in a popup window by clicking the arrow in the "ORF sequence" column. Users are also allowed to BLAST interested ORFs by clicking "Blast ORF" in the "Blast" column. Furthermore, users can BLAST specific lncRNA or ORF sequences based on datasets deposited in LncPep. LncRNA or ORF sequences in *Fasta* format are required for input. Before clicking the "Blast" button, users are also required to indicate whether inputting sequences are peptides or lncRNAs. The species and threshold E values are available for the user to select. Currently, up to 1,000 sequences are allowed to be uploaded and analysed at the same time, and results should be obtained within a few minutes.

TABLE 1 | Summary of lncRNAs, peptides, and evidences across 39 species.

Species	lncRNAs	Peptides	CPAT	CPC2	m6A	Pfam	Ribos	TIS
A. thaliana	3,858	21,247	3,334	3,858	2,613	214	57	240
Apple	1779	16,926	1,614	1779	N/A	261	N/A	N/A
B. napus	8,123	82,712	7,489	8,123	N/A	1740	N/A	N/A
B. rapa	6,206	67,935	5,615	6,206	N/A	1,157	N/A	N/A
Banana	1791	45,255	1,688	1791	N/A	744	N/A	N/A
C. Elegans	2,963	12,088	2,335	2,963	N/A	954	3,248	N/A
C. reinhardtii	771	3,876	638	771	N/A	15	N/A	N/A
Cacao	3,458	33,875	3,239	3,458	N/A	41	N/A	N/A
Cassava	5,502	233,129	5,135	5,502	N/A	4,596	N/A	N/A
Chicken	12,617	84,258	11,250	12,617	N/A	358	4,562	N/A
Chimpanzee	17,619	134,692	14,335	17,619	177	1758	N/A	N/A
Cow	21,978	97,526	17,500	21,978	N/A	201	N/A	N/A
Cucumber	2,466	19,019	2,225	2,466	N/A	112	N/A	N/A
Fruitfly	41,279	534,143	34,694	41,279	3,169	6,632	N/A	N/A
G. raimondii	1,154	5,578	948	1,154	N/A	40	N/A	N/A
Gorilla	17,886	111,120	15,451	17,886	N/A	824	N/A	N/A
Grape	3,314	173,447	3,138	3,314	N/A	4,153	N/A	N/A
Human	339,490	4,984,213	317,169	339,490	6,625	30,081	98,051	10,686
M. *truncatula*	2,177	18,751	1990	2,177	N/A	125	N/A	N/A
Maize	4,567	28,712	4,014	4,567	N/A	113	N/A	N/A
Mouse	218,223	2,571,605	122,199	218,223	5,769	11,453	24,838	5,735
O. rufipogon	7,383	104,241	6,658	7,383	N/A	1,374	N/A	N/A
O. sativa	1,118	6,702	967	1,118	N/A	33	N/A	N/A
Opossum	26,623	158,615	23,155	26,623	N/A	976	N/A	N/A
Orangutan	14,833	87,856	12,878	14,833	N/A	779	N/A	N/A
P. patens	458	3,408	421	458	N/A	38	N/A	N/A
P. trichocarpa	2,207	15,322	1978	2,207	N/A	94	N/A	N/A
Pig	29,252	261,535	26,342	29,252	N/A	390	N/A	N/A
Platypus	10,979	52,770	9,055	10,979	N/A	223	N/A	N/A
Potate	2,964	24,356	2,585	2,964	N/A	156	N/A	N/A
Quinoa	9,675	155,336	8,867	9,675	N/A	1,596	N/A	N/A
Rat	24,793	142,444	22,787	24,793	4,125	4,212	5,500	N/A
Rhesus	9,059	62,026	8,229	9,059	N/A	474	N/A	N/A
Soybean	2,209	29,999	2033	2,209	N/A	626	N/A	N/A
Tomato	3,742	89,879	3,497	3,742	N/A	1,286	N/A	N/A
Trefoil	4,969	26,120	4,223	4,969	N/A	297	N/A	N/A
Wheat	11,534	51,776	9,590	11,534	N/A	238	N/A	N/A
Yeast	50	233	37	50	76	6	N/A	N/A
Zebrafish	4,735	27,503	4,239	4,735	1,415	283	10,526	N/A

Notes: CPAT: coding-potential assessment tool, CPC2: coding potential calculator v2.0, m6A: N6-methyladenosine modification of RNA, Pfam: Protein families database, Ribos: ribosome profiling, and TIS: translation initiation site.

Example Application

Users can investigate potential translated peptides of lncRNAs of interest. For example, HSALNT0229539 is a 1646 nt-long human lncRNA annotated in the LncBook database (https://ngdc.cncb.ac.cn/lncbook/transcript?transid=HSALNT0229539), which is located at chr16:29679186-29698684 (+) (**Figure 4A**). The CPAT and CPC2 scores of HSALNT0229539 were 0.286 and 0.209, respectively (**Figure 4A**). ORFs are covered by more than one line of evidence (Ribo-seq, and TIS) on average (**Figure 4B**). Only HSALNT0229539 ORF-1 is supported by Pfam evidence (**Figure 4B**). Detailed sequence information of lncRNA HSALNT0229539 is shown in a popup window after clicking the hyperlink on the "Sequence" arrow (**Figure 4C**). In total, 5 ORFs were discovered in lncRNA HSALNT0229539, and detailed information is summarized in the following "ORF and peptide information" table (**Figure 4B**). LncRNA HSALNT0229539 is much more highly expressed in fallopian tube than in other normal human tissues (**Figure 4D**). Furthermore, HSALNT0229539 is extensively expressed in multiple cancer cell lines, indicating that HSALNT0229539 is a cancer-universally expressed lncRNA (**Figure 4E**). HSALNT0229539 ORF-1 is located at 19–372 of lncRNA HSALNT0229539, which is predicted to translate as the following peptide: MKQAVRAARQAADFTLK VEVECSSLQEAVQAAEAGADLVLLDNFKPEELHPTATVLK AQFPSVAVEASGGITLDNLPQFCGPHIDVISMGMLTQAAP ALDFSLKLFAKEVAPVPKIH (**Figure 4F**). HSALNT0229539 ORF-1 is predicted with coding potential scores of 0.286 and 0.209 for CPAT and CPC2, respectively. In the Pfam database, QRPTase_C is matched the ORF-1 sequence. In the RPFdb database, 154 Ribo-seq signals were mapped to the ORF-1 region. In addition, two pieces of TIS evidence was found in the HSALNT0229539 ORF-1 region. Evidence from outside public databases can be accessed by clicking the corresponding hyperlinks in the "Database" column.

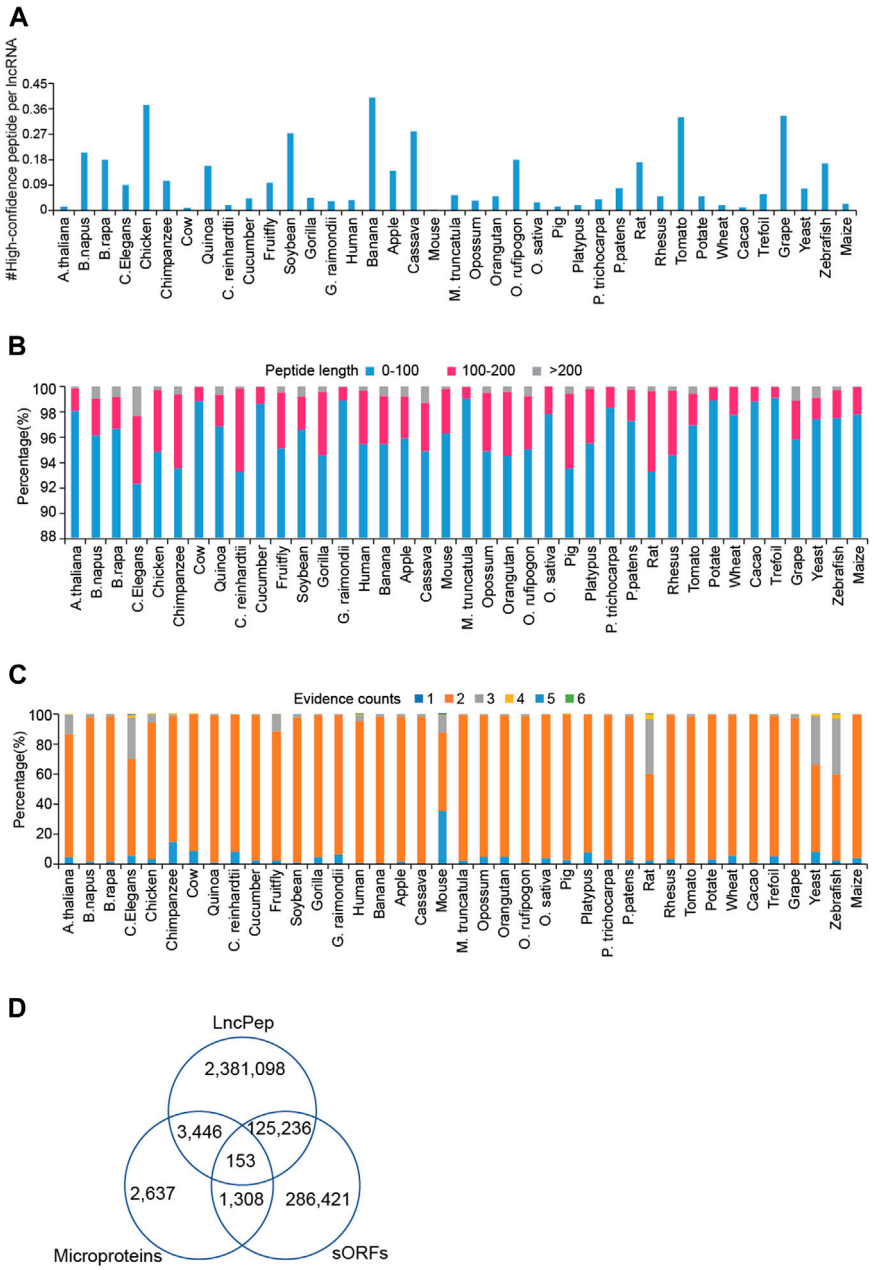

FIGURE 2 | Characterization of lncRNA-encoded peptides across different species. **(A)** The distribution of high-confidence ORFs per lncRNA across 39 species. **(B)** Bar plots show the length distribution of lncRNA-encoded peptides in each species. **(C)** The distribution of supporting evidence of lncRNA-encoded peptides across different species. **(D)** The comparison of peptides among LncPep, sORFs, and Microproteins.

DISCUSSION

The rapid development of high-throughput RNA sequencing technologies largely facilitates the discovery and deep investigation of lncRNAs (Atkinson et al., 2012; Brar and Weissman, 2015; Stark and Grzelak, 2019). These RNAs transcribed from typically non-protein-coding regions of genomes have recently been demonstrated to encode functional peptides in various biological contexts. The LncPep database provides an online resource for peptide-encoded lncRNAs and contains 883,804 lncRNAs across 39 species with translational evidence. LncPep offers various ways to browse and search lncRNA-encoding peptide resources and supports users in predicting and blasting customized lncRNA/peptide sequences for exploratory research on novel lncRNA transcripts or peptides. Furthermore, users can download the full datasets deposited in LncPep, which will empower researchers to explore the "coding realm" of lncRNAs. A

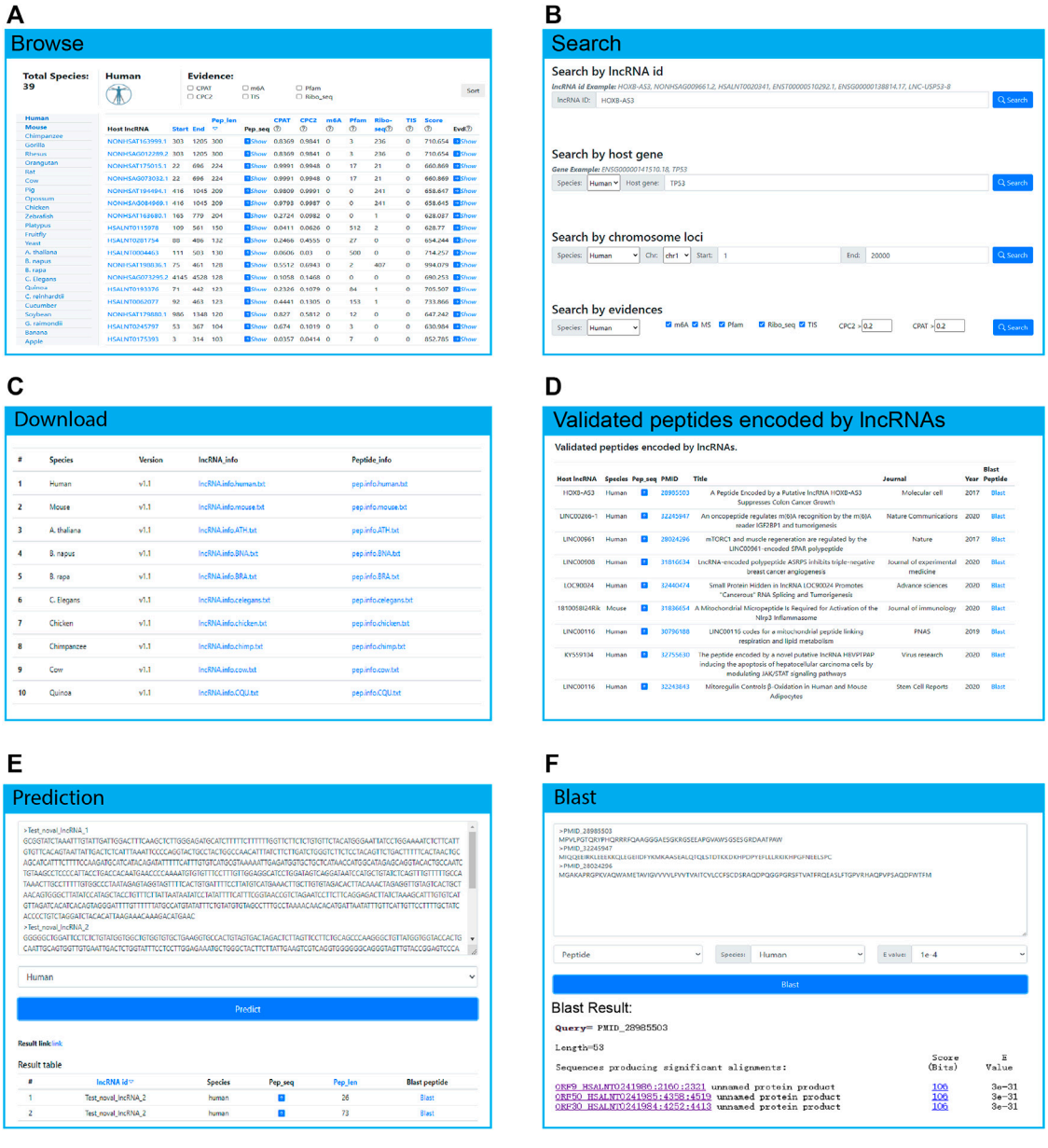

FIGURE 3 | The functional modules of the LncPep database. **(A)** Users can browse the whole database by species. **(B)** The search page provides a search of lncRNA IDs, host genes, chromosome loci, and evidence. **(C)** All datasets deposited in LncPep are free to download. **(D)** The experimentally validated peptides were collected and browsed. **(E,F)** A prediction and BLAST search service was provided to explore novel lncRNAs and peptides. Species and e-values are set as parameters to choose.

"document" page is offered for users to understand and use this database quickly.

To date, FuncPEP (Dragomir et al., 2020), ncEP (Liu et al., 2020), cncRNAdb (Huang et al., 2021), and SmProt (Hao et al., 2018) have been developed for noncoding RNA peptides. FuncPEP, ncEP, and cncRNAdb curated experimentally validated peptides encoded by noncoding RNAs, including lncRNAs, circRNAs, and miRNAs. SmProt collected peptides shorter than 100 mino acids (aa) identified from ribosome profiling data, literature, or MS, but no peptides longer than 100 aa encoded by lncRNAs were included (Lun et al., 2020; Meng et al., 2020; Cai et al., 2021). Compared to these existing databases of noncoding RNA-encoded peptides, LncPep is focused on lncRNAs and has four advantages: 1) both validated and predicted lncRNA-encoded peptides are included in LncPep; 2) abundant evidence and detailed annotations are supplied to support peptides and lncRNAs; 3) LncPep does not have a length limitation for peptides, and peptides longer than 100 aa are also important, which has been reported by multiple studies; and 4) the "Predict" and

FIGURE 4 | HSALNT0275775 as an example application of the LncPep database. **(A)** Basic information of lncRNA HSALNT0275775, including lncRNA ID, alias, species, genome reference, genomic locus, and length. **(B)** The summarized table of ORF and peptide information of lncRNA HSALNT0275775. **(C)** The RNA sequence and length of lncRNA HSALNT0275775 shown in the popup window by clicking the "sequence" arrow in **(A)**. **(D)** The expression levels of lncRNA HSALNT0275775 across 32 different normal human tissues. **(E)** The expression levels of lncRNA HSALNT0275775 across 44 different human cancer cell lines. **(F)** Detailed evidence of the selected peptide of lncRNA HSALNT0275775.

"Blast" modules will help users to explore novel lncRNAs and peptides.

Some limitations still need improvement. Internal ribosome entry sites (IRESs) (Hellen and Sarnow, 2001; Bonnal et al., 2003) are functional cis-acting RNA elements that can direct 40S ribosomes to an internal position on the RNA for translation initiation; thus, IRESs are also an important support for lncRNA translation. RNA structure (Mao et al., 2014; Mauger et al., 2019) also affects its translation; thus, lncRNA structure needs to be taken into account. We did not include these lines of evidence due to the limited available datasets. In the future, we will continue to update the database and add IRES, lncRNA structure, and more Ribo-seq data to support lncRNA translation; we will also further improve the web interface of the database.

MATERIALS AND METHODS

Data Collection

Basic information on lncRNAs was retrieved from LncBook (Ma et al., 2019), NONCODE (Zhao et al., 2021), and LNCipedia (Volders et al., 2019), and 898,452 lncRNA transcripts across 39 species were included. The lncRNA transcript expression profiles in different normal human tissues and multiple types of cancer cell lines were retrieved from LncExpDB (Li et al., 2021) and were previously collected from the Human Protein Atlas (HPA) (Uhlen et al., 2017) and the Cancer Cell Line Encyclopedia (CCLE) (Ghandi et al., 2019), respectively. In particular, the lncRNA expression of normal human tissues included 122 samples in 32 different tissue types, and the expression of cancer cell lines was from 659 cancer cell lines in 44 primary sites.

Analysis of Evidence for lncRNA-Translated Peptides

The CPAT algorithm and CPC2 were employed to evaluate RNA encoding potential. The CPAT algorithm is based on a logistic regression model built with sequence features from known coding RNA candidates (Wang et al., 2013). We calculated the CPAT scores of lncRNAs for all species, and the CPAT scores were used as one of the criteria to assess the reliability of lncRNA encoding potential. CPC2 is a fast and accurate coding potential calculator based on intrinsic sequence features and is a species-neutral tool (Kang et al., 2017). Thus, the CPC2 scores were calculated for all lncRNA transcripts of 39 species as one line of evidence for encoding potential.

Ribosomes are key modules in polysomes with actively translated RNAs (Ramakrishnan, 2002). Therefore, the association with ribosomes/polysomes detected by ribosome profiling (Ribo-seq) can serve as strong evidence for peptide-translated lncRNAs. RPFdb (Wang et al., 2019) is a public resource for ribosome profiling containing Ribo-seq data from 3,603 samples. We downloaded the Ribo-seq data for humans, mice, *C. elegans*, chicken, rat, zebrafish, and *Arabidopsis thaliana* and then mapped them to ORFs of lncRNA transcripts with coverage >90% by using bedtools. The mapped Ribo-seq signals are evidence of lncRNA translation.

Translation initiation sites (TISs) are important for protein/peptide production from transcripts. Global translation initiation sequencing technology (Wan and Qian, 2014) was used to identify genome-wide TISs. TISdb (Wan and Qian, 2014) is a database that curates human and mouse TISs characterized by global translation initiation sequencing. We downloaded these validated TISs from TISdb and mapped them to ORFs of lncRNA transcripts, and the mapped TISs were used as evidence for lncRNA translation.

The N6-methyladenosine modification of RNA (m6A) is the most abundant internal modification on RNA transcripts in eukaryotic cells. m6A located in 3′ UTRs can promote the translation of capped RNAs (Helm and Motorin, 2017). The RNA EPItranscriptome Collection (REPIC) database (Liu et al., 2019) and m6A-Atlas database (Tang et al., 2021) are two commonly used m6A modification resources. We downloaded and merged the m6A profiles for humans, mice, Arabidopsis, chimpanzees, fruit flies, rats, yeast, and zebrafish from these two databases and mapped them to the 3′ UTRs of lncRNAs. Mapped m6A modification sites are used to support lncRNA translation.

The Pfam database (Mistry et al., 2021) is a large collection of existing protein families and is the most famous database to analyse novel genomes and proteins. Thus, we downloaded the Pfam datasets and applied hmmsearch to search all the predicted lncRNA peptides, and an e-value < 0.0001 was used as the cut-off.

Peptide Sequence Prediction

The potential peptide sequences translated from candidate lncRNAs were predicted by using Open Reading Frame (ORF) Finder, which searches for ORFs in the DNA sequences of lncRNAs of interest (Wheeler et al., 2003). If peptides overlapped, then we used the longer one. In particular, ORF Finder performs a six-frame translation of DNA sequences of interest and returns candidate ORF sequences. Both ATG and non-ATG parameters were applied in ORF prediction, as non-ATG sequences have been shown to be an important group of translation initiation sites (Ingolia et al., 2011; Lee et al., 2012).

Calculation of Peptide-Encoding Scores of lncRNA

We defined a peptide-encoding score to quantitatively assess the lncRNA translation potential, which is a summation of the CPAT, CPC2, m6A, Pfam, Ribo-seq, and TIS scores as follows:

$$Score = \sum\left(S_{(CPAT)}, S_{(CPC)}, S_{(m6A)}, S_{(Pfam)}, S_{(Ribo-seq)}, S_{(TIS)}\right)$$

For m6A, Pfam, Ribo_seq, and TIS, if one sample or sequence mapped to the related peptides, we defined the related score as 1; if no sequence mapped, the score was 0. Scores of these 5 pieces of evidence were calculated as follows:

Score of m6A:

$$S_{(m6A)} = \frac{Hits(m6A)}{Median(m6A)}$$

Score of Pfam:

$$S_{(Pfam)} = \frac{Hits(Pfam)}{Median(Pfam)}$$

Score of Ribo-seq:

$$S_{(Ribo-seq)} = 5 \times \frac{Hits(Ribo-seq)}{Median(Ribo-seq)}$$

Score of TIS:

$$S_{(TIS)} = \frac{Hits(TIS)}{Median(TIS)}$$

For the CPAT and CPC2, the scores were based on the coding probability that these two algorithms provided. In addition, the scores of CPAT and CPC2 were as follows:

Score of CPAT:

$$S_{(CPTA)} = CPAT_{(coding\_probability)}$$

Score of CPC2

$$S_{(CPC2)} = CPC2_{(coding\_probability)}$$

Database Implementation

LncPep was built with Python FLASK_REST API (https://flask-restful.readthedocs.io/) as the backend web framework. MongoDB (https://www.mongodb.com/) was adopted for data deposition and management in the LncPep database. Angular

(https://angular.io/) was utilized to develop web interfaces. Bootstrapping (https://getbootstrap.com/) was employed as the frontend framework, and Echarts (https://echarts.apache.org/) was applied for data visualization. The LncPep database is freely available to all users at http://www.shenglilabs.com/LncPep. The LncPep website is tested and supported in popular web browsers, such as Google Chrome, Microsoft Edge, Firefox, and Safari.

DATA AVAILABILITY STATEMENT

The original contributions presented in the study are included in the article/Supplementary Material, further inquiries can be directed to the corresponding author.

AUTHOR CONTRIBUTIONS

SL and TL conceived and designed the study. TL, JW, and YW collected data and literature. TL performed data analysis and database construction. WH, ZF, ZW, and CJ interpreted results. SL and TL wrote the manuscript with comments from all other authors. All authors reviewed the manuscript and consented for publication.

FUNDING

This study was supported by National Natural Science Foundation of China (32100517) and Shanghai General Hospital Startup Funding (02.06.01.20.06 and 02.06.02.21.01).

REFERENCES

Anastasia, C., Elizaveta, L., Pavel, M., Aleksandra, M., Tsimafei, N., Dmitry, B., et al. (2019). LINC00116 Codes for a Mitochondrial Peptide Linking Respiration and Lipid Metabolism. *Proc. Natl. Acad. Sci. U. S. A.* 116, 4940–4945. doi:10.1073/PNAS.1809105116

Anderson, D. M., Anderson, K. M., Chang, C.-L., Makarewich, C. A., Nelson, B. R., McAnally, J. R., et al. (2015). A Micropeptide Encoded by a Putative Long Noncoding RNA Regulates Muscle Performance. *Cell* 160, 595–606. doi:10.1016/j.cell.2015.01.009

Atkinson, S. R., Marguerat, S., and Bähler, J. (2012). Exploring Long Non-coding RNAs through Sequencing. *Semin. Cel Develop. Biol.* 23, 200–205. doi:10.1016/j.semcdb.2011.12.003

Bonnal, S., Boutonnet, C., Prado-Lourenço, L., and Vagner, S. (2003). IRESdb: the Internal Ribosome Entry Site Database. *Nucleic Acids Res.* 31, 427–428. doi:10.1093/NAR/GKG003

Brar, G. A., and Weissman, J. S. (2015). Ribosome Profiling Reveals the what, when, where and How of Protein Synthesis. *Nat. Rev. Mol. Cel Biol.* 16, 651–664. doi:10.1038/nrm4069

Brunet, M. A., Lucier, J.-F., Levesque, M., Leblanc, S., Jacques, J.-F., Al-Saedi, H. R. H., et al. (2021). OpenProt 2021: Deeper Functional Annotation of the Coding Potential of Eukaryotic Genomes. *Nucleic Acids Res.* 49, D380–D388. doi:10.1093/nar/gkaa1036

Cai, T., Zhang, Q., Wu, B., Wang, J., Li, N., Zhang, T., et al. (2021). LncRNA-encoded Microproteins: A New Form of Cargo in Cell Culture-derived and Circulating Extracellular Vesicles. *J. Extracellular Vesicles* 10, e12123. doi:10.1002/JEV2.12123

Chen, Y. G., Satpathy, A. T., and Chang, H. Y. (2017). Gene Regulation in the Immune System by Long Noncoding RNAs. *Nat. Immunol.* 18, 962–972. doi:10.1038/ni.3771

Dragomir, M. P., Manyam, G. C., Ott, L. F., Berland, L., Knutsen, E., Ivan, C., et al. (2020). Funcpep: A Database of Functional Peptides Encoded by Non-coding Rnas. *ncRNA* 6, 41–18. doi:10.3390/ncrna6040041

Ghandi, M., Huang, F. W., Jané-Valbuena, J., Kryukov, G. V., Lo, C. C., McDonald, E. R., et al. (2019). Next-generation Characterization of the Cancer Cell Line Encyclopedia. *Nature* 569, 503–508. doi:10.1038/s41586-019-1186-3

Hao, Y., Zhang, L., Niu, Y., Cai, T., Luo, J., He, S., et al. (2018). SmProt: a Database of Small Proteins Encoded by Annotated Coding and Non-coding RNA Loci. *Brief Bioinform* 19, bbx005–643. doi:10.1093/bib/bbx005

Hellen, C. U. T., and Sarnow, P. (2001). Internal Ribosome Entry Sites in Eukaryotic mRNA Molecules. *Genes Dev.* 15, 1593–1612. doi:10.1101/GAD.891101

Helm, M., and Motorin, Y. (2017). Detecting RNA Modifications in the Epitranscriptome: Predict and Validate. *Nat. Rev. Genet.* 18, 275–291. doi:10.1038/nrg.2016.169

Huang, J.-Z., Chen, M., Chen, D., Gao, X.-C., Zhu, S., Huang, H., et al. (2017). A Peptide Encoded by a Putative lncRNA HOXB-AS3 Suppresses Colon Cancer Growth. *Mol. Cel* 68, 171–184. e6. doi:10.1016/j.molcel.2017.09.015

Huang, Y., Wang, J., Zhao, Y., Wang, H., Liu, T., Li, Y., et al. (2021). cncRNAdb: a Manually Curated Resource of Experimentally Supported RNAs with Both Protein-Coding and Noncoding Function. *Nucleic Acids Res.* 49, D65–D70. doi:10.1093/nar/gkaa791

Ingolia, N. T., Ghaemmaghami, S., Newman, J. R. S., and Weissman, J. S. (2009). Genome-Wide Analysis *In Vivo* of Translation with Nucleotide Resolution Using Ribosome Profiling. *Science* 324, 218–223. doi:10.1126/SCIENCE.1168978

Ingolia, N. T., Lareau, L. F., and Weissman, J. S. (2011). Ribosome Profiling of Mouse Embryonic Stem Cells Reveals the Complexity and Dynamics of Mammalian Proteomes. *Cell* 147, 789–802. doi:10.1016/j.cell.2011.10.002

Jackson, R., Kroehling, L., Khitun, A., Bailis, W., Jarret, A., York, A. G., et al. (2018). The Translation of Non-canonical Open reading Frames Controls Mucosal Immunity. *Nature* 564, 434–438. doi:10.1038/s41586-018-0794-7

Kang, Y.-J., Yang, D.-C., Kong, L., Hou, M., Meng, Y.-Q., Wei, L., et al. (2017). CPC2: A Fast and Accurate Coding Potential Calculator Based on Sequence Intrinsic Features. *Nucleic Acids Res.* 45, W12–W16. doi:10.1093/nar/gkx428

Lee, S., Liu, B., Lee, S., Huang, S.-X., Shen, B., and Qian, S.-B. (2012). Global Mapping of Translation Initiation Sites in Mammalian Cells at Single-Nucleotide Resolution. *Proc. Natl. Acad. Sci.* 109, E2424–E2432. doi:10.1073/pnas.1207846109

Li, Z., Zhang, J., Liu, X., Li, S., Wang, Q., Di Chen, T., et al. (2018). The LINC01138 Drives Malignancies via Activating Arginine Methyltransferase 5 in Hepatocellular Carcinoma. *Nat. Commun.* 9, 1572. doi:10.1038/s41467-018-04006-0

Li, Z., Liu, L., Jiang, S., Li, Q., Feng, C., Du, Q., et al. (2021). LncExpDB: An Expression Database of Human Long Non-coding RNAs. *Nucleic Acids Res.* 49, D962–D968. doi:10.1093/nar/gkaa850

Liu, H., Zhou, X., Yuan, M., Zhou, S., Huang, Y.-e., Hou, F., et al. (2020). ncEP: A Manually Curated Database for Experimentally Validated ncRNA-Encoded Proteins or Peptides. *J. Mol. Biol.* 432, 3364–3368. doi:10.1016/j.jmb.2020.02.022

Liu, S., He, C., and Chen, M. (2019). REPIC: A Database for Exploring N6-Methyladenosine Methylome. *Genome Biol.* 21 (1), 100. doi:10.1101/2019.12.11.873299

Liu, S. J., Dang, H. X., Lim, D. A., Feng, F. Y., and Maher, C. A. (2021). Long Noncoding RNAs in Cancer Metastasis. *Nat. Rev. Cancer* 21, 446–460. doi:10.1038/s41568-021-00353-1

Lun, Y.-Z., Pan, Z.-P., Liu, S.-A., Sun, J., Ming, H., Liu, B., et al. (2020). The Peptide Encoded by a Novel Putative lncRNA HBVPTPAP Inducing the Apoptosis of Hepatocellular Carcinoma Cells by Modulating JAK/STAT Signaling Pathways. *Virus. Res.* 287, 198104. doi:10.1016/J.VIRUSRES.2020.198104

Ma, L., Cao, J., Liu, L., Du, Q., Li, Z., Zou, D., et al. (2019). Lncbook: A Curated Knowledgebase of Human Long Non-coding Rnas. *Nucleic Acids Res.* 47, D128–D134. doi:10.1093/nar/gky960

Mao, Y., Liu, H., Liu, Y., and Tao, S. (2014). Deciphering the Rules by Which Dynamics of mRNA Secondary Structure Affect Translation Efficiency in *Saccharomyces cerevisiae*. *Nucleic Acids Res.* 42, 4813–4822. doi:10.1093/NAR/GKU159

Marchese, F. P., Raimondi, I., and Huarte, M. (2017). The Multidimensional Mechanisms of Long Noncoding RNA Function. *Genome Biol.* 18, 206–672. doi:10.1186/s13059-017-1348-2

Matsumoto, A., Pasut, A., Matsumoto, M., Yamashita, R., Fung, J., Monteleone, E., et al. (2017). MTORC1 and Muscle Regeneration Are Regulated by the LINC00961-Encoded SPAR Polypeptide. *Nature* 541, 228–232. doi:10.1038/nature21034

Mauger, D. M., Cabral, B. J., Presnyak, V., Su, S. V., Reid, D. W., Goodman, B., et al. (2019). mRNA Structure Regulates Protein Expression through Changes in Functional Half-Life. *Proc. Natl. Acad. Sci. USA* 116, 24075–24083. doi:10.1073/PNAS.1908052116

Meng, N., Chin, M., Chen, X. H., Wang, J. Z., Zhu, S., He, Y. T., et al. (2020). Small Protein Hidden in lncRNA LOC90024 Promotes "Cancerous" RNA Splicing and Tumorigenesis. *Adv. Sci.* 7, 1903233. doi:10.1002/ADVS.201903233

Meyer, K. D. (2019). m6A-Mediated Translation Regulation. *Biochim. Biophys. Acta (Bba) - Gene Regul. Mech.* 1862, 301–309. doi:10.1016/J.BBAGRM.2018.10.006

Meyer, K. D., Patil, D. P., Zhou, J., Zinoviev, A., Skabkin, M. A., Elemento, O., et al. (2015). 5′ UTR m6A Promotes Cap-independent Translation. *Cell* 163, 999–1010. doi:10.1016/J.CELL.2015.10.012

Mistry, J., Chuguransky, S., Williams, L., Qureshi, M., Salazar, G. A., Sonnhammer, E. L. L., et al. (2021). Pfam: The Protein Families Database in 2021. *Nucleic Acids Res.* 49, D412–D419. doi:10.1093/nar/gkaa913

Niu, L., Lou, F., Sun, Y., Sun, L., Cai, X., Liu, Z., et al. (2020). A Micropeptide Encoded by lncRNA MIR155HG Suppresses Autoimmune Inflammation via Modulating Antigen Presentation. *Sci. Adv.* 6, eaaz2059. doi:10.1126/sciadv.aaz2059

Ramakrishnan, V. (2002). Ribosome Structure and the Mechanism of Translation. *Cell* 108, 557–572. doi:10.1016/S0092-8674(02)00619-0

Salta, E., and De Strooper, B. (2017). Noncoding RNAs in Neurodegeneration. *Nat. Rev. Neurosci.* 18, 627–640. doi:10.1038/nrn.2017.90

Stark, R., Grzelak, M., and Hadfield, J. (2019). RNA Sequencing: the Teenage Years. *Nat. Rev. Genet.* 20, 631–656. doi:10.1038/s41576-019-0150-2

Tang, Y., Chen, K., Song, B., Ma, J., Wu, X., Xu, Q., et al. (2021). M6A-Atlas: A Comprehensive Knowledgebase for Unraveling the N6-Methyladenosine (m6A) Epitranscriptome. *Nucleic Acids Res.* 49, D134–D143. doi:10.1093/nar/gkaa692

Uhlen, M., Zhang, C., Lee, S., Sjöstedt, E., Fagerberg, L., Bidkhori, G., et al. (2017). A Pathology Atlas of the Human Cancer Transcriptome. *Science* 357, 357. doi:10.1126/science.aan2507

Volders, P.-J., Anckaert, J., Verheggen, K., Nuytens, J., Martens, L., Mestdagh, P., et al. (2019). Lncipedia 5: Towards a Reference Set of Human Long Non-coding Rnas. *Nucleic Acids Res.* 47, D135–D139. doi:10.1093/nar/gky1031

Wan, J., and Qian, S.-B. (2014). TISdb: A Database for Alternative Translation Initiation in Mammalian Cells. *Nucl. Acids Res.* 42, D845–D850. doi:10.1093/nar/gkt1085

Wang, H., Yang, L., Wang, Y., Chen, L., Li, H., and Xie, Z. (2019). RPFdb v2.0: An Updated Database for Genome-wide Information of Translated mRNA Generated from Ribosome Profiling. *Nucleic Acids Res.* 47, D230–D234. doi:10.1093/nar/gky978

Wang, L., Park, H. J., Dasari, S., Wang, S., Kocher, J.-P., and Li, W. (2013). CPAT: Coding-Potential Assessment Tool Using an Alignment-free Logistic Regression Model. *Nucleic Acids Res.* 41, e74. doi:10.1093/nar/gkt006

Wheeler, D. L., Church, D. M., Federhen, S., Lash, A. E., Madden, T. L., Pontius, J. U., et al. (2003). Database Resources of the National center for Biotechnology. *Nucleic Acids Res.* 31, 28–33. doi:10.1093/nar/gkg033

Zhang, Q., Wu, E., Tang, Y., Cai, T., Zhang, L., Wang, J., et al. (2021). Deeply Mining a Universe of Peptides Encoded by Long Noncoding RNAs. *Mol. Cell Proteomics* 20, 100109. doi:10.1016/j.mcpro.2021.100109

Zhao, L., Wang, J., Li, Y., Song, T., Wu, Y., Fang, S., et al. (2021). NONCODEV6: An Updated Database Dedicated to Long Non-coding RNA Annotation in Both Animals and Plants. *Nucleic Acids Res.* 49, D165–D171. doi:10.1093/nar/gkaa1046

Conflict of Interest: The authors declare that the research was conducted in the absence of any commercial or financial relationships that could be construed as a potential conflict of interest.

Publisher's Note: All claims expressed in this article are solely those of the authors and do not necessarily represent those of their affiliated organizations, or those of the publisher, the editors, and the reviewers. Any product that may be evaluated in this article, or claim that may be made by its manufacturer, is not guaranteed or endorsed by the publisher.

frontiers in Cell and Developmental Biology

REVIEW
published: 02 February 2022
doi: 10.3389/fcell.2021.806181

An Update on the Roles of circRNA-ZFR in Human Malignant Tumors

Lang Liu†, Haicun Wang†, Shaobo Yu†, Xin Gao, Guanglin Liu, Dongsheng Sun and Xingming Jiang**

Department of General Surgery, The 2nd Affiliated Hospital of Harbin Medical University, Harbin, China

CircRNAs (circular RNAs) are single-stranded RNAs that form covalently closed loops and function as important regulatory elements of the genome through multiple mechanisms. Increasing evidence had indicated that circRNAs, which might serve as either oncogenes or tumor suppressors, played vital roles in the pathophysiology of human diseases, especially in tumorigenesis and progression. CircRNA-ZFR (circular RNA zinc finger RNA binding protein) is a circular RNA that had attracted much attention in recent years. It has been found that circRNA-ZFR was abnormally expressed in a variety of malignant tumors, and its dysregulated expression was closely related to tumor stage, cancer metastasis and patients' prognosis. Recent studies had shown that aberrantly expressed circRNA-ZFR could regulate the malignant biological behaviors of tumors through various mechanisms; further exploration of circRNA-ZFR expression in tumors and its regulation on malignant biological behaviors such as tumor proliferation, invasion and drug resistance will provide new ideas for clinical tumors diagnosis and treatment.

Keywords: circular RNA, circRNA-ZFR, malignant tumors, expression, mechanism

OPEN ACCESS

Edited by:
Valeria Poli,
University of Turin, Italy

Reviewed by:
Isaia Barbieri,
University of Cambridge, United Kingdom
Francesca Orso,
University of Turin, Italy

****Correspondence:***
Xingming Jiang
xmjiang@hrbmu.edu.cn
Dongsheng Sun
sundongsheng@hrbmu.edu.cn

†These authors have contributed equally to this work and share first authorship

Specialty section:
This article was submitted to Molecular and Cellular Oncology, a section of the journal Frontiers in Cell and Developmental Biology

Received: *31 October 2021*
Accepted: *16 December 2021*
Published: *02 February 2022*

Citation:
Liu L, Wang H, Yu S, Gao X, Liu G, Sun D and Jiang X (2022) An Update on the Roles of circRNA-ZFR in Human Malignant Tumors. Front. Cell Dev. Biol. 9:806181. doi: 10.3389/fcell.2021.806181

INTRODUCTION

The genome-wide studies showed that greater than 70% of the human genome is transcribed into RNAs, while only approximately 2% of the sequences have the capacity to encode proteins. The non-coding RNAs (ncRNAs), which were long assumed to be transcriptional noise, comprise the most proportion of the transcripts Covalently closed circRNAs (circular RNAs) were originally identified in plant viroids, yeast mitochondrial RNAs, and hepatitis virus (Kristensen et al., 2019; Xu et al., 2020). CircRNAs are a large class of endogenously expressed non-coding RNAs characterized by covalently closed loop structures with neither 5′ to 3′ polarity nor polyadenylated tail. Compared with linear RNAs, circRNAs with closed loop structure are very stable and resistant to RNase, and also highly specific in human tissues and cell samples (Patop et al., 2019; Yu et al., 2019; Chen et al., 2019). With deepening research, more and more circRNAs have been found to show abnormal expression in a variety of malignant tumors, and affected the tumor occurrence and development by targeting key genes (Huang et al., 2020; Lei et al., 2020; Zhou C. et al., 2020). CircRNAs dysregulation could promote proliferation, invasion and metastasis of tumor cells and inhibit cellular senescence and apoptosis by multiple mechanisms, including working as miRNA sponges, protein scaffolds, regulatory signals or transcript decoys. Additionally, circRNAs might serve as potential therapeutic targets and biomarkers for patients' diagnosis or prognosis due to elevated stability, high efficiency and tissue specificity (Han et al., 2018; Zhang et al., 2018; Li et al., 2019).

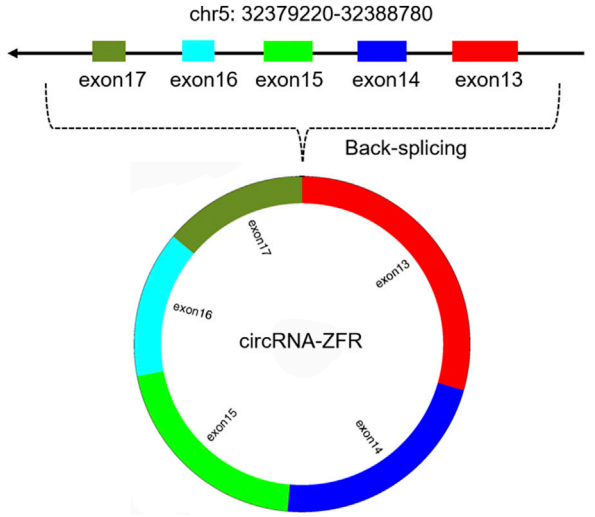

FIGURE 1 | The chromosomic location and biogenesis of circRNA-ZFR.

CircRNA-ZFR (zinc finger RNA binding protein) is a new circRNA (circBase ID: hsa_circ_0072088), which had been confirmed to be located on human chromosome 5p13.3 (Shown in **Figure 1**). As a member of the circular RNA family, circRNA-ZFR had been shown to be abnormally expressed in human malignant tumors such as hepatocellular carcinoma, breast cancer and thyroid carcinoma, and several researches also proved that circRNA-ZFR could impact the tumors development through affecting the glycolysis of tumor cells, regulating the tumor microenvironment and cell cycle (Li et al., 2020; Zhang et al., 2020). The clinical data analysis indicated that circRNA-ZFR expression was closely related to tumor TNM stage and patients' prognosis. Current studies had shown that circRNA ZFR played roles as a tumor suppressor or oncogene in many tumors (Shown in **Table 1**); the regulatory mechanisms included acting as molecular sponges to competitively adsorb miRNA and then regulate the expression of target genes, or interacting with target RNA binding protein through specific RNA binding domain to form RNA protein complex, so as to affect the process of human malignant tumors (Shown in **Figure 2**).

TABLE 1 | The expressions and regulation mechanisms of circRNA-ZFR on malignant tumors.

Cancer types	Expression	Related genes and pathways	Biological significance *in vitro*	Biological significance *in vivo*
Breast cancer	Upregulated	miR-758/HIF1A	Proliferation ↑, migration ↑, invasion ↑, glycolysis ↑, apoptosis ↓	Promote tumor growth
Thyroid carcinoma	Upregulated	miR-1261/C8orf4	Proliferation ↑, migration ↑ and invasion ↑	/
		miR-16/MAPK1	Proliferation ↑, migration ↑, invasion ↑, apoptosis ↓	/
Renal cell cancer	Upregulated	miR-206/Met	Proliferation ↑, migration ↑, invasion ↑, apoptosis ↓	/
Bladder cancer	Upregulated	miR-1270/miR-545/WNT5A	Proliferation ↑, migration ↑ and invasion ↑	Promote tumor growth
		miR-377/ZEB2	Proliferation ↑, migration ↑, invasion ↑, apoptosis ↓	/
Cervical cancer	Upregulated	Rb-E2F1	Proliferation ↑, migration ↑, invasion ↑	Promote tumor growth
Esophageal squamous cell carcinoma	Upregulated	miR-377/VEGF	Proliferation ↑, migration ↑, invasion ↑	Promote tumor growth
Hepatocellular carcinoma	Upregulated	miR-375/HMGA2	Proliferation ↑, migration ↑, invasion ↑, glycolysis ↑, apoptosis ↓	Promote tumor growth
		miR-3619-5p/CTNNB1	Proliferation ↑	/
		miR-511/AKT1	Proliferation ↑, migration ↑, invasion ↑ and apoptosis ↓	Promote tumor growth
		MAP2K1	Proliferation ↑	/
Non-small cell lung carcinoma	Upregulated	miR-377-5p/NOVA2	Proliferation ↑, migration ↑, invasion ↑ and apoptosis ↓	Promote tumor growth
		miR-101-3p/CUL4B	Proliferation ↑, migration ↑ and invasion ↑	/
		miR-195-5p/KPNA4	Proliferation ↑, migration ↑, invasion ↑, apoptosis ↓ and chemoresistance ↑	Promote tumor growth
		miR-545-3p/CBLL1	Proliferation ↑, migration ↑, invasion ↑, apoptosis ↓ and chemoresistance ↑	Promote tumor growth
Gastric cancer	Downregulated	miR-130a/miR-107/PTEN	Proliferation ↓ and apoptosis ↑	Curb tumor growth
Colorectal cancer	Downregulated	miR-532-3p/FOXO4	Proliferation ↓, migration ↓ and invasion ↓	/

HIF1A, hypoxia-inducible factor 1α; C8orf4, transcriptional and immune response regulator; MAPK1, mitogen-activated protein kinase 1; Met, met proto-oncogene; WNT5A, Wnt family member 5A; ZEB2, zinc finger E-box binding homeobox 2; E2F1, E2F transcription factor 1; VEGF, vascular endothelial growth factor; HMGA2, high mobility group AT-hook 2; CTNNB1, catenin beta 1; AKT1, AKT, serine/threonine kinase 1; MAP2K1, mitogen-activated protein kinase kinase 1; NOVA2, NOVA, alternative splicing regulator 2; CUL4B, cullin 4B; KPNA4, karyopherin subunit alpha 4; CBLL1, Cbl proto-oncogene like 1; PTEN, phosphatase and tensin homolog; FOXO4, forkhead box O4.

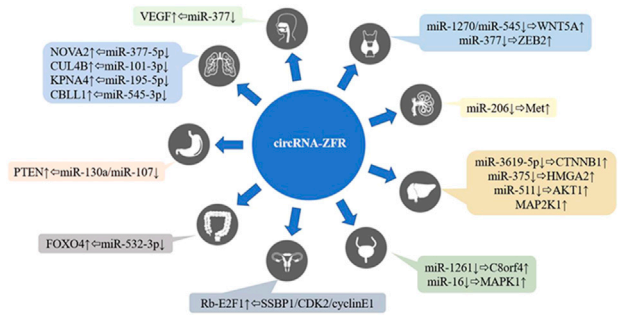

FIGURE 2 | The regulatory network of circRNA-ZFR on human malignant tumors. HIF1A, hypoxia-inducible factor 1α; C8orf4, transcriptional and immune response regulator; MAPK1, mitogen-activated protein kinase 1; Met, met proto-oncogene; WNT5A, Wnt family member 5A; ZEB2, zinc finger E-box binding homeobox 2; E2F1, E2F transcription factor 1; VEGF, vascular endothelial growth factor; HMGA2, high mobility group AT-hook 2; CTNNB1, catenin beta 1; AKT1, AKT serine/threonine kinase 1; MAP2K1, mitogen-activated protein kinase kinase 1; NOVA2, NOVA alternative splicing regulator 2; CUL4B, cullin 4B; KPNA4, karyopherin subunit alpha 4; CBLL1, Cbl proto-oncogene like 1; PTEN, phosphatase and tensin homolog; FOXO4, forkhead box O4.

CIRCULAR RNA ZINC FINGER RNA BINDING PROTEIN IN MALIGNANT TUMORS

Circular RNA Zinc Finger RNA Binding Protein in Breast Cancer

Breast cancer (BC) is one of the most common gynecological cancers. The deteriorating environment and lifestyle flaws are raising the frequency of this cancer (Ellis and Ma 2019; Liang et al., 2019). The current view is that breast cancer is a stem cell disease characterized by the existence of cancer cells with stem-like features and tumor-initiating potential. Existing therapies were not universally-effective to this stem cell disease, and usually caused side effects, relapses, and high mortality rate (Dittmer 2018; Rossi et al., 2019). Therefore, it is necessary to seek ideal plans for the palliative treatment of advanced BC.

Chen et al. (2020) initially demonstrated that circRNA-ZFR expression was significantly increased in 70 BC tissues and tumor cells compared to the corresponding tissues. Moreover, circRNA-ZFR overexpression was remarkably correlated with tumor size, depth of invasion and TNM stage; Kaplan-Meier survival curves showed that the patients with low circRNA-ZFR expression had longer survival time. Functionally, downregulation of circRNA-ZFR significantly inhibited cell viability, migration and invasion and strongly promoted apoptosis; circRNA-ZFR silencing resulted in decreased glucose uptake, lactate product and ATP level. In xenograft model assays, tumor growth was remarkably stunted after transfecting low circRNA-ZFR expressed tumor cells. To further understand the roles of circRNA-ZFR in BC development, researchers performed detailed analysis for its targeted miRNAs and the results verified that circRNA-ZFR directly interacted with miR-578. In BC tissues and cell lines, miR-578 expression was significantly decreased and it was inversely correlated with circRNA-ZFR expression; and the miR-578 expression decreasing partially reversed the promoting effect of circRNA-ZFR on the tumor cells malignant biological behaviors. Furthermore, the researchers identified HIF1A (hypoxia-inducible factor 1α) as a functional target of miR-578 in regulating BC cell viability, migration, invasion, glycolysis and anti-apoptosis. In BC tissues and cell lines, HIF1A mRNA expression was positively correlated with circRNA-ZFR expression and negatively correlated with miR-578 expression. The results of luciferase report assay and RNA pull-down indicated that circRNA-ZFR modulated HIF1A expression via acting as a sponge of miR-578. These findings suggested that the aberrant expression of circRNA-ZFR in breast cancer promoted the tumor proliferation, invasion, migration and inhibited cell apoptosis by regulating miR-578/HIF1A axis.

CIRCULAR RNA ZINC FINGER RNA BINDING PROTEIN IN THYROID CARCINOMA

By analyzing the Gene Expression Omnibus (GEO) dataset, Xiong et al. (2021) confirmed that circRNA-ZFR expression in TC (thyroid carcinoma) tissues was significantly upregulated compared with that in adjacent normal tissues; exogenously downregulated circRNA-ZFR expression suppressed the malignant behaviors of TC tumor cells. Mechanically, there was a complementary sequence in circRNA-ZFR for miR-16, and miR-16 could target the 3′-untranslated region of MAPK1 (mitogen-activated protein kinase 1); as a member of the MAPK family, MAPK1 is well known as an oncogene that is activated or highly expressed in various types of human cancer (Jiang et al., 2019; Deng et al., 2020; Janardhan et al., 2020). The western blot analysis results further demonstrated that augmented levels of circRNA-ZFR promoted MAPK1 expression in TPC-1 cells, while miR-16 augmentation partially counteracted the increased MAPK1 expression induced by circRNA-ZFR overexpression. In addition, the inhibition of cell viability, invasion and apoptosis induced by circRNA-ZFR knockdown were partially reversed in TPC-1 and IHH-4 cells after miR-16 depletion or MAPK1 promotion. All these data provided the evidence that circRNA-ZFR/miR-16/MAPK1 axis might serve as promotion effect for TC progression.

Wei et al. (2018) analyzed circRNA-ZFR expression in 41 pairs of PTC (papillary thyroid carcinoma) tissues and adjacent normal tissues. The results confirmed that circRNA-ZFR was remarkably overexpressed in PTC tissue specimens compared with that in paired non-neoplastic specimens, and increased circRNA-ZFR was significantly associated with tumor volume, depth of tumor invasion, lymph node metastasis, haematogenous metastasis, and patients' poorer outcomes. Moreover, Kaplan-Meier curve analysis data indicated higher circRNA-ZFR expression in PTC patients was associated with worse prognosis. Functional experiments results illustrated that circRNA-ZFR knockdown significantly inhibited the proliferation, migration and invasion potential in TPC-1 and SW579 cells. By bioinformatics prediction and luciferase analysis, the researchers found that circRNA-ZFR

could directly interact with miR-1261, and miR-1261 could target downstream oncogene C8orf4 (transcriptional and immune response regulator); Western blot and qRT-PCR results also verified that circRNA-ZFR knockdown and miR-1261 overexpression both significantly downregulated C8orf4 expression, while circRNA-ZFR overexpression abrogated the inhibition effect of miR-1261 mimics on C8orf4 expression. The rescue experiment results showed C8orf4 overexpression also attenuated the proliferation, migration and invasion-promoting effects of circRNA-ZFR silencing on PTC cells. Taken together, circRNA-ZFR exerted oncogenic roles via regulating miR-1261/C8orf4 axis in papillary thyroid carcinoma, which suggested circRNA-ZFR might be a potential therapeutic target.

CIRCULAR RNA ZINC FINGER RNA BINDING PROTEIN IN RENAL CELL CANCER

The qRT-PCR detection results showed that circRNA-ZFR expression was remarkably escalated in RCC (renal cell cancer) tissues as compared with para-carcinoma tissues, and circRNA-ZFR expression was also notably raised in CAKI-1, ACHN, A498 and KTCTL-26 cells. Wang et al. (2019) demonstrated that knocking-down circRNA-ZFR inhibited cell proliferation, migration, invasion and induced apoptosis of CAKI-1 and ACHN cells; bioinformatics analysis data also showed that miR-206 was the candidate circRNA-ZFR target. In RCC cell lines, reduction of circRNA-ZFR significantly increased miR-206 expression; luciferase reporter assay results also verified circRNA-ZFR could directly sponge miR-206, and the decline of cell proliferation, migration and invasion capacity was alleviated by downregulating miR-206. As showed in this study, Met (met proto-oncogene) expression was markedly raised by reducing miR-206; previous studies had reported that Wnt/β-catenin and PI3K/AKT pathways were the downstream effectors of Met; both signaling pathways were in manage of multiple biological processes and frequently aberrantly activated in human cancers (Shorning et al., 2020; Zhang and Wang 2020). To determine the potential mechanism of circRNA-ZFR in RCC, western blot was carried out to detect the associated proteins expression. When circRNA-ZFR was silenced, the expression of Met, Wnt3a, β-catenin, PI3K and AKT was significantly reduced. Conversely, the expression of Met, Wnt3a, β-catenin, PI3K and AKT was significantly increased in CAKI-1 cells by decreasing miR-206. The above data suggested that circRNA-ZFR can promote RCC development by targeting the miR-206/Met axis to activate the Wnt/β-catenin and PI3K/AKT pathways.

CIRCULAR RNA ZINC FINGER RNA BINDING PROTEIN IN BLADDER CANCER

Luo et al. (2021) found that the expression of circRNA-ZFR was significantly higher in the tumor group than in the control group by analyzing the expression of circRNA-ZFR in 60 pairs of bladder cancer (BC) tissues and para-cancerous tissues, and circRNA-ZFR expression levels were positively correlated with tumor volume, TNM stage, and the proportion of metastatic lymph nodes. Immediately, circRNA-ZFR was shown to promote BC cell proliferation, migration and invasion both *in vivo* and *in vitro*; and as shown in the bioinformatics analysis, circRNA-ZFR was predicted to possess binding sites for miR-1270 and miR-545. The western blot and qRT-PCR detection results indicated that miR-1270 and miR-545 expression was significantly elevated in both T24 and J82 cells when circRNA-ZFR was attenuated. The results from RNA pull-down and dual-luciferase reporter assay also proved that circRNA-ZFR could directly interact with miR-545 and miR-1270. Otherwise, the probability of WNT5A (Wnt family member 5A) binding with miR-545 and miR-1270 was predicted by starBase, and these targeting relationships were verified by luciferase reporter assay. Previous studies had found that Wnt family genes played a vital part in human organogenesis and tumor genesis through regulating WNT/β-catenin signaling stimulate (Zhan et al., 2017; Krishnamurthy and Kurzrock 2018; Steinhart and Angers 2018). In addition, the expression of significant signaling components of the Wnt/β-Catenin pathway (PCNA, Ki-67, MMP-9 and N-catenin proteins) was significantly reduced by the attenuation of circRNA-ZFR, which was partially rescued by the application of miR-1270/545 inhibitors or WNT5A overexpression. Interestingly, Zhang H.,et al. (2019) found circRNA-ZFR was remarkably upregulated in tumor tissues and cell lines and related with poor prognosis of tumor patients. They also provided comprehensive evidences that knocking-down of circRNA-ZFR could effectively inhibit cell proliferation and migration by targeting the miR-377/ZEB2 axis, suggesting a potential therapeutic target for circRNA-ZFR in BC treatment.

CIRCULAR RNA ZINC FINGER RNA BINDING PROTEIN IN CERVICAL CANCER

CC (cervical cancer) is one of the most common gynecological cancers in women all over the world. In the early stages, HPV-associated CC development is asymptomatic and its high invasiveness and mortality threaten the health of more and more women (Crosbie et al., 2013; Gaffney et al., 2018; Olusola et al., 2019). In the process looking for new biomarkers and intervention targets for the treatment of cervical cancer, Zhou et al. (2021) found that circRNA-ZFR high expression consistently could be identified as the biomarker for patients' poor prognosis in cervical cancer. Especially, circRNA-ZFR overexpressed cells (HeLa and SiHa cells) were significantly exhibit a more malignant phenotype than control cells; cell cycle detection analysis revealed that the proportion of cells in S phase was significantly decreased after inhibiting the circRNA-ZFR expression, and a large number of cells were blocked in G0/G1 phase. By using Co-IP assay, it was found that circRNA-ZFR overexpression promoted the formation of CDK2/Rb, CDK2/Cyclin E1, and CDK2/SSBP1 complexes; conversely, attenuating circRNA-ZFR inhibited the

formation of the same complexes. Subsequently, these complexes were proved to activate Rb/E2F1 pathway by inducting p-Rb S807 and S608 phosphorylation and activating E2F1 signaling. Interestingly, the Rb/E2F1 pathway activating could promote cervical cancer progression by allowing the transcription of genes required for the G1-S phase transition and DNA replication. In conclusion, circRNA-ZFR can act as a molecular scaffold by directly interacting with Rb to recruit CDK2, further promote the formation of related protein complexes and thus activate the Rb/E2F1 pathway. CircRNA-ZFR, a novel positive regulator of E2F1 signaling, could be a potential biomarker for cervical cancer detection.

CIRCULAR RNA ZINC FINGER RNA BINDING PROTEIN IN NON-SMALL CELL LUNG CANCER

By comparing the circRNA-ZFR expression between NSCLC (non-small cell lung cancer) tumor tissues and matching nontumor tissues of 45 patients, Tan et al. (2020) proved that there was a significant upregulation in the expression of circRNA-ZFR in NSCLC. And the analysis about the relationship between the relative circRNA-ZFR expression and clinical characteristics in patients with NSCLC indicated that circRNA-ZFR expression was an independent risk factor for cancer recurrence and poor prognosis in non-small-cell lung cancer. The cellular experiment results showed that circRNA-ZFR was also abnormally highly expressed in tumor cells; after exogenous silencing the circRNA-ZFR expression in tumor cells, the ability of cell proliferation, invasion and migration were decreased significantly. Due to the circRNA-ZFR downregulation, the percentage of NSCLC cells in G1 phase was significantly increased, indicating that more cells were blocked in the transition phase of G1/S phase. The bioinformatics tools prediction data suggested that miR-377-5p was a downstream target of circRNA-ZFR and NOVA2 (NOVA alternative splicing regulator 2) could also bind to miR-377-5p in NSCLC cells. Furthermore, the dual-luciferase reporter and RIP assays results were consistent with the concept that circRNA-ZFR could regulate NOVA2 expression by sponging miR-377-5p. The flow cytometry, wound healing and transwell invasion assay results demonstrated that circRNA-ZFR acted as an oncogenic molecule through sponging miR-377-5p in NSCLC cells. While, NOVA2 overexpression partially overturned miR-377-5p-mediated inhibition on the malignant potential of NSCLC cells. Collectively, circRNA-ZFR accelerated the proliferation, migration and invasion of NSCLC cells through miR-377-5p/NOVA2 axis.

Besides, the study of Zhang S. et al. (2019) showed that circRNA-ZFR was upregulated in NSCLC tissues and cell lines. CircRNA-ZFR knocking-down in NSCLC cells significantly inhibited cell proliferation, migration and invasion. According to the predicted results from bioinformatics tools, circRNA-ZFR might regulate CUL4B (cullin 4B) expression by directly targeting miR-101-3p; then luciferase reporter and RIP assays results validated these predictions. The miR-101-3p inhibitor transfection partially abrogated the inhibitory effect of circRNA-ZFR on NSCLC cells, and the CUL4B overexpression diminished the tumor suppressive effect of miR-101-3p on NSCLC cells. These results proved that circRNA-ZFR exhibited a carcinogenic role by sponging miR-101-3p to regulate CUL4B expression in NSCLC.

Currently, the treatment strategies for NSCLC include surgery, radiotherapy, chemotherapy and immunotherapy. Drug resistance in patients with NSCLC in the context of chemotherapy remains a major barrier to the treatment of NSCLC (Jonna and Subramaniam 2019; Proto et al., 2019). CircRNA-ZFR was found to be highly expressed in PTX-resistant NSCLC tissues and cell lines by Li et al. (2021). After exogenous restraint of circRNA-ZFR expression, the PTX-resistant NSCLC cells' proliferation, migration and invasion abilities were significantly decreased; and flow cytometry data results exhibited circRNA-ZFR knockdown promoted cell cycle arrest and induced apoptosis in PTX-resistant tumor cells. As shown in starBase, miR-195-5p possessed the binding sites of circRNA-ZFR; and the inhibition of miR-195-5p ameliorated the effects of circRNA-ZFR knockdown on PTX sensitivity and cell progression in PTX-resistant NSCLC cells. In addition, KPNA4 (karyopherin subunit alpha 4) was found to be a target gene of miR-195-5p, dual-luciferase reporter assay and western blot results confirmed that miR-195-5p negatively modulated KPNA4 expression by direct interaction. The flow cytometry and transwell analysis results showed that miR-195-5p overexpression promoted apoptosis and inhibited cell migration and invasion in A549/PTX and H460/PTX cells, and this effect was preserved by increasing KPNA4. Subsequently, circRNA-ZFR silencing was found to significantly reduce KPNA4 mRNA and protein levels in A549/PTX and H460/PTX cells, while miR-195-5p inhibition effectively restored these effects. In conclusion, these results suggest that circRNA-ZFR promotes cell cycle progression, proliferation, migration and invasion, inhibits apoptosis and enhances patient's PTX resistance in NSCLC by regulating miR-195-5p/KPNA4 axis. Similar to the above studies' results, Li et al. (2020) revealed the involvement of circRNA ZFR as a molecular sponge in the regulatory mechanism of cisplatin resistance in NSCLC tumor cells by competitively sponging miR-545-3p and then inhibiting the binding of miR-545-3p to the downstream target gene CBLL1 (Cbl proto-oncogene like 1). CircRNA-ZFR participated in the negative regulation of miR-545-3p, which induced the isochronous expression with CBLL1 thereby achieving enhancing cisplatin resistance of NSCLC tumor cells *in vivo* and *in vitro*.

CIRCULAR RNA ZINC FINGER RNA BINDING PROTEIN IN ESOPHAGEAL SQUAMOUS CELL CARCINOMA

Fang et al. (2020) confirmed circRNA ZFR expression was significantly higher in esophageal squamous cell carcinoma (ESCC) tumor tissue than in paraneoplastic tissue; qRT-PCR detection results also revealed that the significantly elevated

circRNA-ZFR expression in different ESCC cell lines compared to the normal esophageal epithelial cells. The analysis results of the correlation between circRNA-ZFR expression and patients' clinicopathological characteristics demonstrated that circRNA-ZFR overexpression was associated with the ESCC malignant phenotypes. In addition, circRNA-ZFR knocking-down inhibited the malignant biological behavior of ESCC cells, including proliferation, colony formation, migration, and invasion. The dual-luciferase reporter, RIP and qRT-PCR assay results suggested circRNA-ZFR could act as a sponge to absorb miR-377 in ESCC cells. VEGF (vascular endothelial growth factor), the most important regulatory factor in angiogenesis, had been proved to promote tumor growth and metastasis (Itatani et al., 2018; Apte et al., 2019; Peng et al., 2019). The prediction data suggested that VEGF is one of the potential binding targets of miR-377. Western blot and qRT-PCR results demonstrated that the miR-377 downregulation in ECA109 cells could significantly increase VEGF mRNA and protein expression levels; and the miR-377 overexpression could relatively reverse the up-regulated effects of circRNA-ZFR on VEGF protein. Taken together, circRNA-ZFR could regulate the VEGF expression to promote proliferation, migration, and invasion of ESCC by acting as a sponge for miR-377.

CIRCULAR RNA ZINC FINGER RNA BINDING PROTEIN IN HEPATOCELLULAR CARCINOMA

Xu et al. (2021) found that circRNA-ZFR level was obviously higher in HCC (hepatocellular carcinoma) tissues than that in normal tissues by qRT-PCR detection. Next, the relationship between the of circRNA-ZFR relative expression and clinical characteristics in patients with HCC was analyzed; the data results proved that high circRNA-ZFR expression was significantly associated with tumor node metastasis stage, tumor size and hepatitis B virus (HBV) infection, but not with patients' age and gender. The functional experiments results indicated that the circRNA-ZFR down-regulation significantly decreased glucose uptake, lactate production and intracellular ATP content of Huh7 cells. Moreover, cell proliferation, migration and invasion were remarkably weakened due to the circRNA-ZFR down-regulation. The results of dual-luciferase reporter and RIP assays verified that circRNA-ZFR could directly target to miR-375; the silence of circRNA-ZFR inhibited the HCC cells progression by upregulating miR-375. As an important regulatory molecule of glucose metabolism (Zhang W. Y. et al., 2019; Unachukwu et al., 2020; Wu et al., 2020), HMGA2 (high mobility group AT-hook 2) was proved to be a downstream target gene of miR-375 involved in the regulation of HCC progression. The miR-375 overexpression or circRNA-ZFR reducing suppressed the HCC progression by downregulating HMGA2. The rescue experiments results showed that the inhibitory effects of silencing circRNA-ZFR and transfecting miR-375 mimics on glucose uptake and lactate production of Huh7 cells could be partially reversed by HMGA2 overexpression. In conclusion, this research demonstrated that circRNA-ZFR restraint suppressed glycolysis and proliferation of HCC cells via miR-375/HMGA2 axis.

As an important component of MAP kinase signal transduction pathway, MAP2K1 (mitogen-activated protein kinase kinase 1) has been proved to be involved in the regulation of cell proliferation, differentiation and gene transcription (Smits et al., 2020; Zhou W. Y. et al., 2020; Bu et al., 2021). Cedric' study (2020) demonstrated that circRNA-ZFR was highly expressed in HCC tumor tissues and cells, correlated with the poor prognosis of HCC patients, and circRNA-ZFR was also proved to promote tumor cells' proliferative capacity by targeting MAP2K1. Furthermore, Tan et al. (2019) and Yang et al. (2019) respectively revealed that abnormally high expression of circRNA-ZFR was closely associated with poor prognosis in patients with HCC. In the study of Tan, circRNA-ZFR was confirmed to accelerate HCC progression through regulating miR-3619-5p/CTNNB1 axis and activating Wnt/β-catenin pathway. Whereas, Yang et al. (2019) emphasized AKT1 (serine/threonine kinase 1) is a crucial receptor for activation of highly oncogenic Wnt/β-catenin signal pathway, which is closely linked to HCC cell proliferation and migration. The results of Yang's research implied that circRNA-ZFR and AKT1 expressions were up-regulated and miR-511 expression was down-regulated in hepatocellular carcinoma. What's more, circRNA-ZFR silencing or miR-511 overexpression suppressed cell proliferation, migration and invasion, and induced apoptosis of HCC cells. Mechanistically, circRNA-ZFR acted as a miR-511 sponge to up-regulate its target gene AKT1, and activated cascades of proliferation-related proteins (c-Myczd, cyclin D1, Survivin and Bcl-2). These data indicated that circRNA-ZFR might promote cell proliferation and migration by regulating miR-511/AKT1 axis in hepatocellular carcinoma.

CIRCULAR RNA ZINC FINGER RNA BINDING PROTEIN EXCEPTIONAL LOW EXPRESSION

The qRT-PCR detection results showed that circ-ZFR was drastically downregulated in gastric cancer tissues and cells. As confirmed by CCK-8 assay, overexpression of circ-ZFR observably suppressed GC (gastric cancer) cell proliferation; flow cytometry analysis disclosed that the apoptosis rate of GC cells was significantly increased after circRNA-ZFR overexpression, and the proportion of cells staying in G1/G0 phase significantly increased. Through starBase, a bioinformatics prediction website, Liu et al. (2018) found that there was a binding site between miR-107/miR-130a with circRNA-ZFR; and then, they crossed the targeting gene regulated by both p53 pathway and miR-130a/miR-107 *via* venn diagram, and the intersection was PTEN (phosphatase and tensin homolog). Moreover, The RIP and dual-luciferase reporter assay results indicated that circRNA-ZFR could target miR-107/miR-130a and PTEN was the downstream target gene of miR-107/miR-130a. The CCK-8 assay and flow cytometry analysis results displayed

that circ-ZFR influenced GC cell propagation, cell cycle and apoptosis resistance by miR-107/miR-130a/PTEN axis. Interestingly, the rescue experiment results showed PTEN overexpression also attenuated the effects of circRNA-ZFR silence in GC cells, and the xenograft mice model experiment results showed that circRNA-ZFR curbed GC tumor growth and affected p53 protein expression *in vivo*. In general, circRNA-ZFR inhibited cell proliferation and promoted apoptosis in GC by miR-130a/miR-107/PTEN axis. By analyzing the circRNA-ZFR expression in 30 colorectal cancer tissues and matched non-tumor normal tissue specimens, Bian et al. (2018) confirmed that circRNA-ZFR expression was dysregulated in CRC tissues. In addition, they analyzed the effect of circRNA-ZFR on cell migration using wound healing and transwell migration assays, CCK8 and clone formation assays were also conducted to analyze cell proliferation; these results suggested that circRNA-ZFR restraint could promote the proliferation and migration of colorectal cancer cells. Bioinformatic techniques suggested that circRNA-ZFR and FOXO4 (forkhead box O4) share a common site of action on miR-532-3p; declining miR-532-3p by using siRNAs could increase the expression of circRNA-ZFR and FOXO4 in SW620 cells. Moreover, knocking-down miR-532-3p also promoted cell proliferation and migration. The western blot results showed reducing miR-532-3p could promote FOXO4 expression and mitigating circRNA-ZFR could reverse this phenomenon. All these results indicated that the circRNA-ZFR expression was down-regulated in gastric cancer and colorectal cancer, and circRNA-ZFR might play as a tumor suppressor in these cancers through the endogenous competitive mechanism.

CONCLUSION AND PERSPECTIVE

With the research development, the aberrant expression of circRNAs has been gradually recognized as a hallmark feature in cancer. Investigating these molecules as biomarkers or therapeutic targets will be a promising field for cancer treatment (Liu et al., 2019; Pandey et al., 2020; Di Timoteo et al., 2020). Numerous studies have confirmed that circRNA-ZFR played very important roles in the occurrence and development of various tumors. CircRNA-ZFR was abnormally highly expressed in most malignant tumors such as bladder cancer and hepatocellular carcinoma, and promoted the malignant biological behaviors through numerous complex regulatory pathways; it could also act as a tumor suppressor in gastric cancer and colorectal cancer, and has a certain inhibitory effect on tumor proliferation, invasion and migration. Moreover, in non-small cell lung cancer, the abnormal expression of circRNA ZFR has a certain impact on patients' chemotherapy sensitivity. Mechanistically, circRNA-ZFR could act as a competitive endogenous RNA in most tumors, exerting corresponding oncogenic effects by adsorbing miRNAs and thus regulating the expression of downstream target genes. The downstream miRNAs of circRNA-ZFR mainly include the miR-377 family (adsorbing miR-377 in bladder and esophageal squamous cell carcinoma and targeting miR-377-5p in non-small cell lung cancer), the miR-545 family (adsorbing miR-545 in bladder cancer and targeting miR-545-3p in non-small cell lung cancer) and other miRNAs. Furthermore, in cervical cancer, circRNA-ZFR could also act as scaffolding RNA to promote the formation of protein complexes by targeting CDK2 with RB and further regulating downstream signaling pathways. And the latter finding proved that there might be two or even more mechanisms of action of circRNA-ZFR in tumors, which might be related to the heterogeneity among tumors or the characteristics of tumors themselves, providing us with new ideas for the subsequent study of circRNA-ZFR. It is believed that with the deepening of research, the regulatory mechanisms of circRNA-ZFR in human malignant tumors will be more clearly displayed, which will provide new ideas and targets for tumor diagnosis and clinical treatment.

AUTHOR CONTRIBUTIONS

LL, WH, and YS wrote the manuscript and prepared the tables. GX and LG collected relevant data. SD and JX are in charge of project administration and funding acquisition. All authors contributed to the article and approved the submitted version.

FUNDING

This work was supported by the National Natural Science Foundation of Heilongjiang Province (LH 2020H058), Chen Xiaoping Foundation for the Development of Science and Technology of Hubei Province (CXPJJH12000002-2020015).

REFERENCES

Apte, R. S., Chen, D. S., and Ferrara, N. (2019). VEGF in Signaling and Disease: Beyond Discovery and Development. *Cell* 176, 1248–1264. doi:10.1016/j.cell.2019.01.021

Bian, L., Zhi, X., Ma, L., Zhang, J., Chen, P., Sun, S., et al. (2018). Hsa_circRNA_103809 Regulated the Cell Proliferation and Migration in Colorectal Cancer via miR-532-3p/FOXO4 axis. *Biochem. Biophysical Res. Commun.* 505, 346–352. doi:10.1016/j.bbrc.2018.09.073

Bu, R., Siraj, A. K., Masoodi, T., Parvathareddy, S. K., Iqbal, K., Al-Rasheed, M., et al. (2021). Recurrent Somatic MAP2K1 Mutations in Papillary Thyroid Cancer and Colorectal Cancer. *Front. Oncol.* 11, 670423. doi:10.3389/fonc.2021.670423

Chen, L.-L. (2020). The Expanding Regulatory Mechanisms and Cellular Functions of Circular RNAs. *Nat. Rev. Mol. Cel Biol* 21, 475–490. doi:10.1038/s41580-020-0243-y

Chen, X., Yang, T., Wang, W., Xi, W., Zhang, T., Li, Q., et al. (2019). Circular RNAs in Immune Responses and Immune Diseases. *Theranostics* 9, 588–607. doi:10.7150/thno.29678

Chen, Z., Wang, F., Xiong, Y., Wang, N., Gu, Y., and Qiu, X. (2020). CircZFR Functions as a Sponge of miR-578 to Promote Breast Cancer Progression by Regulating HIF1A Expression. *Cancer Cel Int* 20, 400. doi:10.1186/s12935-020-01492-5

Crosbie, E. J., Einstein, M. H., Franceschi, S., and Kitchener, H. C. (2013). Human Papillomavirus and Cervical Cancer. *The Lancet* 382, 889–899. doi:10.1016/S0140-6736(13)60022-7

Deng, R., Zhang, H.-L., Huang, J.-H., Cai, R.-Z., Wang, Y., Chen, Y.-H., et al. (2020). MAPK1/3 Kinase-dependent ULK1 Degradation Attenuates Mitophagy and Promotes Breast Cancer Bone Metastasis. *Autophagy* 17, 3011–3029. doi:10.1080/15548627.2020.1850609

Di Timoteo, G., Rossi, F., and Bozzoni, I. (2020). Circular RNAs in Cell Differentiation and Development. *Development* 147, dev182725. doi:10.1242/dev.182725

Dittmer, J. (2018). Breast Cancer Stem Cells: Features, Key Drivers and Treatment Options. *Semin. Cancer Biol.* 53, 59–74. doi:10.1016/j.semcancer.2018.07.007

Ellis, H., and Ma, C. X. (2019). PI3K Inhibitors in Breast Cancer Therapy. *Curr. Oncol. Rep.* 21, 110. doi:10.1007/s11912-019-0846-7

Fang, N., Shi, Y., Fan, Y., Long, T., Shu, Y., Zhou, J., et al. (2020). Circ_0072088 Promotes Proliferation, Migration, and Invasion of Esophageal Squamous Cell Cancer by Absorbing miR-377. *J. Oncol.* 2020, 1–14. doi:10.1155/2020/8967126

Gaffney, D. K., Hashibe, M., Kepka, D., Maurer, K. A., and Werner, T. L. (2018). Too many Women Are Dying from Cervix Cancer: Problems and Solutions. *Gynecol. Oncol.* 151, 547–554. doi:10.1016/j.ygyno.2018.10.004

Han, B., Chao, J., and Yao, H. (2018). Circular RNA and its Mechanisms in Disease: From the Bench to the Clinic. *Pharmacol. Ther.* 187, 31–44. doi:10.1016/j.pharmthera.2018.01.010

Huang, A., Zheng, H., Wu, Z., Chen, M., and Huang, Y. (2020). Circular RNA-Protein Interactions: Functions, Mechanisms, and Identification. *Theranostics* 10, 3503–3517. doi:10.7150/thno.42174

Itatani, Y., Kawada, K., Yamamoto, T., and Sakai, Y. (2018). Resistance to Anti-angiogenic Therapy in Cancer-Alterations to Anti-VEGF Pathway. *Ijms* 19, 1232. doi:10.3390/ijms19041232

Janardhan, H. P., Meng, X., Dresser, K., Hutchinson, L., and Trivedi, C. M. (2020). KRAS or BRAF Mutations Cause Hepatic Vascular Cavernomas Treatable with MAP2K-MAPK1 Inhibition. *J. Exp. Med.* 217, e20192205. doi:10.1084/jem.20192205

Jiang, H., Liang, M., Jiang, Y., Zhang, T., Mo, K., Su, S., et al. (2019). The lncRNA TDRG1 Promotes Cell Proliferation, Migration and Invasion by Targeting miR-326 to Regulate MAPK1 Expression in Cervical Cancer. *Cancer Cel Int* 19, 152. doi:10.1186/s12935-019-0872-4

Jonna, S., and Subramaniam, D. S. (2019). Molecular Diagnostics and Targeted Therapies in Non-small Cell Lung Cancer (NSCLC): an Update. *Discov. Med.* 27, 167–170.

Krishnamurthy, N., and Kurzrock, R. (2018). Targeting the Wnt/beta-Catenin Pathway in Cancer: Update on Effectors and Inhibitors. *Cancer Treat. Rev.* 62, 50–60. doi:10.1016/j.ctrv.2017.11.002

Kristensen, L. S., Andersen, M. S., Stagsted, L. V. W., Ebbesen, K. K., Hansen, T. B., and Kjems, J. (2019). The Biogenesis, Biology and Characterization of Circular RNAs. *Nat. Rev. Genet.* 20, 675–691. doi:10.1038/s41576-019-0158-7

Lei, M., Zheng, G., Ning, Q., Zheng, J., and Dong, D. (2020). Translation and Functional Roles of Circular RNAs in Human Cancer. *Mol. Cancer* 19, 30. doi:10.1186/s12943-020-1135-7

Li, H., Liu, F., and Qin, W. (2020). Circ_0072083 Interference Enhances Growth-Inhibiting Effects of Cisplatin in Non-small-cell Lung Cancer Cells via miR-545-3p/CBLL1 axis. *Cancer Cel Int* 20, 78. doi:10.1186/s12935-020-1162-x

Li, J., Fan, R., and Xiao, H. (2021). Circ_ZFR Contributes to the Paclitaxel Resistance and Progression of Non-small Cell Lung Cancer by Upregulating KPNA4 through Sponging miR-195-5p. *Cancer Cel Int* 21, 15. doi:10.1186/s12935-020-01702-0

Li, J., Sun, D., Pu, W., Wang, J., and Peng, Y. (2020). Circular RNAs in Cancer: Biogenesis, Function, and Clinical Significance. *Trends Cancer* 6, 319–336. doi:10.1016/j.trecan.2020.01.012

Li, Z., Ruan, Y., Zhang, H., Shen, Y., Li, T., and Xiao, B. (2019). Tumor-suppressive Circular RNAs: Mechanisms Underlying Their Suppression of Tumor Occurrence and Use as Therapeutic Targets. *Cancer Sci.* 110, 3630–3638. doi:10.1111/cas.14211

Liang, Y., Zhang, H., Song, X., and Yang, Q. (2020). Metastatic Heterogeneity of Breast Cancer: Molecular Mechanism and Potential Therapeutic Targets. *Semin. Cancer Biol.* 60, 14–27. doi:10.1016/j.semcancer.2019.08.012

Liu, J., Li, D., Luo, H., and Zhu, X. (2019). Circular RNAs: The star Molecules in Cancer. *Mol. Aspects Med.* 70, 141–152. doi:10.1016/j.mam.2019.10.006

Liu, T., Liu, S., Xu, Y., Shu, R., Wang, F., Chen, C., et al. (2018). Circular RNA-ZFR Inhibited Cell Proliferation and Promoted Apoptosis in Gastric Cancer by Sponging miR-130a/miR-107 and Modulating PTEN. *Cancer Res. Treat.* 50, 1396–1417. doi:10.4143/crt.2017.537

Luo, L., Miao, P., Ming, Y., Tao, J., and Shen, H. (2021). Circ-ZFR Promotes Progression of Bladder Cancer by Upregulating WNT5A via Sponging miR-545 and miR-1270. *Front. Oncol.* 10, 596623. doi:10.3389/fonc.2020.596623

Olusola, P., Banerjee, H. N., Philley, J. V., and Dasgupta, S. (2019). Human Papilloma Virus-Associated Cervical Cancer and Health Disparities. *Cells* 8, 622. doi:10.3390/cells8060622

Pandey, P. R., Munk, R., Kundu, G., De, S., Abdelmohsen, K., and Gorospe, M. (2020). Methods for Analysis of Circular RNAs. *WIREs RNA* 11, e1566. doi:10.1002/wrna.1566

Patop, I. L., Wüst, S., and Kadener, S. (2019). Past, Present, and Future of Circ RNA S. *EMBO J.* 38, 16. doi:10.15252/embj.2018100836

Peng, K., Bai, Y., Zhu, Q., Hu, B., and Xu, Y. (2019). Targeting VEGF-Neuropilin Interactions: a Promising Antitumor Strategy. *Drug Discov. Today* 24, 656–664. doi:10.1016/j.drudis.2018.10.004

Proto, C., Ferrara, R., Signorelli, D., Lo Russo, G., Galli, G., Imbimbo, M., et al. (2019). Choosing Wisely First Line Immunotherapy in Non-small Cell Lung Cancer (NSCLC): what to Add and what to Leave Out. *Cancer Treat. Rev.* 75, 39–51. doi:10.1016/j.ctrv.2019.03.004

Rossi, L., Mazzara, C., and Pagani, O. (2019). Diagnosis and Treatment of Breast Cancer in Young Women. *Curr. Treat. Options. Oncol.* 20, 86. doi:10.1007/s11864-019-0685-7

Shorning, B. Y., Dass, M. S., Smalley, M. J., and Pearson, H. B. (2020). The PI3K-AKT-mTOR Pathway and Prostate Cancer: At the Crossroads of AR, MAPK, and WNT Signaling. *Ijms* 21, 4507. doi:10.3390/ijms21124507

Smits, P. J., Konczyk, D. J., Sudduth, C. L., Goss, J. A., and Greene, A. K. (2020). Endothelial MAP2K1 Mutations in Arteriovenous Malformation Activate the RAS/MAPK Pathway. *Biochem. Biophysical Res. Commun.* 529, 450–454. doi:10.1016/j.bbrc.2020.06.022

Steinhart, Z., and Angers, S. (2018). Wnt Signaling in Development and Tissue Homeostasis. *Development* 145, dev146589. doi:10.1242/dev.146589

Tan, A., Li, Q., and Chen, L. (2019). CircZFR Promotes Hepatocellular Carcinoma Progression through Regulating miR-3619-5p/CTNNB1 axis and Activating Wnt/β-Catenin Pathway. *Arch. Biochem. Biophys.* 661, 196–202. doi:10.1016/j.abb.2018.11.020

Tan, Z., Cao, F., Jia, B., and Xia, L. (2020). Circ_0072088 Promotes the Development of Non-small Cell Lung Cancer via the miR -377-5p/NOVA2 axis. *Thorac. Cancer* 11, 2224–2236. doi:10.1111/1759-7714.13529

Unachukwu, U., Chada, K., and D'Armiento, J. (2020). High Mobility Group AT-Hook 2 (HMGA2) Oncogenicity in Mesenchymal and Epithelial Neoplasia. *Ijms* 21, 3151. doi:10.3390/ijms21093151

Wang, M., Gao, Y., and Liu, J. (2019). Silencing circZFR Inhibits the Proliferation, Migration and Invasion of Human Renal Carcinoma Cells by Regulating miR-206. *Ott* Vol. 12, 7537–7550. doi:10.2147/OTT.S215012

Wei, H., Pan, L., Tao, D., and Li, R. (2018). Circular RNA circZFR Contributes to Papillary Thyroid Cancer Cell Proliferation and Invasion by Sponging miR-1261 and Facilitating C8orf4 Expression. *Biochem. Biophysical Res. Commun.* 503, 56–61. doi:10.1016/j.bbrc.2018.05.174

Wu, Y., Wang, X., Xu, F., Zhang, L., Wang, T., Fu, X., et al. (2020). The Regulation of Acetylation and Stability of HMGA2 via the HBXIP-Activated Akt-PCAF Pathway in Promotion of Esophageal Squamous Cell Carcinoma Growth. *Nucleic Acids Res.* 48, 4858–4876. doi:10.1093/nar/gkaa232

Xiong, H., Yu, H., Jia, G., Yu, J., Su, Y., Zhang, J., et al. (2021). circZFR Regulates Thyroid Cancer Progression by the miR -16/MAPK1 axis. *Environ. Toxicol.* 36, 2236–2244. doi:10.1002/tox.23337

Xu, R., Yin, S., Zheng, M., Pei, X., and Ji, X. (2021). Circular RNA circZFR Promotes Hepatocellular Carcinoma Progression by Regulating miR-375/HMGA2 Axis. *Dig. Dis. Sci.* 66, 4361–4373. doi:10.1007/s10620-020-06805-2

Xu, X., Zhang, J., Tian, Y., Gao, Y., Dong, X., Chen, W., et al. (2020). CircRNA Inhibits DNA Damage Repair by Interacting with Host Gene. *Mol. Cancer* 19, 128. doi:10.1186/s12943-020-01246-x

Yang, X., Liu, L., Zou, H., Zheng, Y.-W., and Wang, K. P. (2019). circZFR Promotes Cell Proliferation and Migration by Regulating miR-511/AKT1 axis in Hepatocellular Carcinoma. *Dig. Liver Dis.* 51, 1446–1455. doi:10.1016/j.dld.2019.04.012

Yu, T., Wang, Y., Fan, Y., Fang, N., Wang, T., Xu, T., et al. (2019). CircRNAs in Cancer Metabolism: a Review. *J. Hematol. Oncol.* 12, 90. doi:10.1186/s13045-019-0776-8

Zhan, T., Rindtorff, N., and Boutros, M. (2017). Wnt Signaling in Cancer. *Oncogene* 36, 1461–1473. doi:10.1038/onc.2016.304

Zhang, H., Wang, X., Hu, B., Zhang, F., Wei, H., and Li, L. (2019). Circular RNA ZFR Accelerates Non-small Cell Lung Cancer Progression by Acting as a miR-101-3p Sponge to Enhance CUL4B Expression. *Artif. Cell Nanomedicine, Biotechnol.* 47, 3410–3416. doi:10.1080/21691401.2019.1652623

Zhang, Q., Wang, W., Zhou, Q., Chen, C., Yuan, W., Liu, J., et al. (2020). Roles of circRNAs in the Tumour Microenvironment. *Mol. Cancer* 19, 14. doi:10.1186/s12943-019-1125-9

Zhang, S., Mo, Q., and Wang, X. (2019). Oncological Role of HMGA2 (Review). *Int. J. Oncol.* 55, 775–788. doi:10.3892/ijo.2019.4856

Zhang, W.-Y., Liu, Q.-H., Wang, T.-J., Zhao, J., Cheng, X.-H., and Wang, J.-S. (2019). CircZFR Serves as a Prognostic Marker to Promote Bladder Cancer Progression by Regulating miR-377/ZEB2 Signaling. *Biosci. Rep.* 39, BSR20192779. doi:10.1042/BSR20192779

Zhang, Y., and Wang, X. (2020). Targeting the Wnt/β-Catenin Signaling Pathway in Cancer. *J. Hematol. Oncol.* 13, 165. doi:10.1186/s13045-020-00990-3

Zhang, Z., Yang, T., and Xiao, J. (2018). Circular RNAs: Promising Biomarkers for Human Diseases. *EBioMedicine* 34, 267–274. doi:10.1016/j.ebiom.2018.07.036

Zhou, C., Wang, P., Tu, M., Huang, Y., Xiong, F., and Wu, Y. (2020). Long Non-coding RNA PART1 Promotes Proliferation, Migration and Invasion of Hepatocellular Carcinoma Cells via miR-149-5p/MAP2K1 Axis. *Cmar* Vol. 12, 3771–3782. doi:10.2147/CMAR.S246311

Zhou, M., Yang, Z., Wang, D., Chen, P., and Zhang, Y. (2021). The Circular RNA circZFR Phosphorylates Rb Promoting Cervical Cancer Progression by Regulating the SSBP1/CDK2/cyclin E1 Complex. *J. Exp. Clin. Cancer Res.* 40, 48. doi:10.1186/s13046-021-01849-2

Zhou, W.-Y., Cai, Z.-R., Liu, J., Wang, D.-S., Ju, H.-Q., and Xu, R.-H. (2020). Circular RNA: Metabolism, Functions and Interactions with Proteins. *Mol. Cancer* 19, 172. doi:10.1186/s12943-020-01286-3

Conflict of Interest: The authors declare that the research was conducted in the absence of any commercial or financial relationships that could be construed as a potential conflict of interest.

Publisher's Note: All claims expressed in this article are solely those of the authors and do not necessarily represent those of their affiliated organizations, or those of the publisher, the editors and the reviewers. Any product that may be evaluated in this article, or claim that may be made by its manufacturer, is not guaranteed or endorsed by the publisher.

frontiers in Cell and Developmental Biology

REVIEW
published: 18 February 2022
doi: 10.3389/fcell.2022.809132

miR-1269a and miR-1269b: Emerging Carcinogenic Genes of the miR-1269 Family

Zijun Xie[1,2†], *Chenming Zhong*[1,2†] *and Shiwei Duan*[1,3*]

[1]School of Medicine, Zhejiang University City College, Hangzhou, China, [2]Medical Genetics Center, School of Medicine, Ningbo University, Ningbo, China, [3]Department of Clinical Medicine, Zhejiang University City College School of Medicine, Hangzhou, China

miRNAs play an important role in the occurrence and development of human cancer. Among them, hsa-mir-1269a and hsa-mir-1269b are located on human chromosomes 4 and 17, respectively, and their mature miRNAs (miR-1269a and miR-1269b) have the same sequence. miR-1269a is overexpressed in 9 cancers. The high expression of miR-1269a not only has diagnostic significance in hepatocellular carcinoma and non-small cell lung cancer but also is related to the poor prognosis of cancer patients such as esophageal cancer, hepatocellular carcinoma, and glioma. miR-1269a can target 8 downstream genes (CXCL9, SOX6, FOXO1, ATRX, RASSF9, SMAD7, HOXD10, and VASH1). The expression of miR-1269a is regulated by three non-coding RNAs (RP11-1094M14.8, LINC00261, and circASS1). miR-1269a participates in the regulation of the TGF-β signaling pathway, PI3K/AKT signaling pathway, p53 signaling pathway, and caspase-9-mediated apoptotic pathway, thereby affecting the occurrence and development of cancer. There are fewer studies on miR-1269b compared to miR-1269a. miR-1269b is highly expressed in hepatocellular carcinoma, non-small cell lung cancer, oral squamous cell carcinoma, and pharyngeal squamous cell carcinoma, but miR-1269b is low expressed in gastric cancer. miR-1269b can target downstream genes (METTL3, CDC40, SVEP1, and PTEN) and regulate the PI3K/AKT signaling pathway. In addition, sequence mutations on miR-1269a and miR-1269b can affect their regulation of cancer. The current studies have shown that miR-1269a and miR-1269b have the potential to be diagnostic and prognostic markers for cancer. Future research on miR-1269a and miR-1269b can focus on elucidating more of their upstream and downstream genes and exploring the clinical application value of miR-1269a and miR-1269b.At present, there is no systematic summary of the research on miR-1269a and miR-1269b. This paper aims to comprehensively analyze the abnormal expression, diagnostic and prognostic value, and molecular regulatory pathways of miR-1269a and miR-1269b in multiple cancers. The overview in our work can provide useful clues and directions for future related research.

Keywords: miR-1269a, miR-1269b, target gene, non-coding RNAs, prognosis

OPEN ACCESS

Edited by:
Hernandes F. Carvalho, State University of Campinas, Brazil

Reviewed by:
Sabrina Battista, Consiglio Nazionale Delle Ricerche (CNR), Italy
Bashdar Mahmud Hussen, Hawler Medical University, Iraq

***Correspondence:**
Shiwei Duan
duansw@zucc.edu.cn

†*These authors share first authorship*

Specialty section:
This article was submitted to Molecular and Cellular Oncology, a section of the journal Frontiers in Cell and Developmental Biology

Received: *04 November 2021*
Accepted: *20 January 2022*
Published: *18 February 2022*

Citation:
Xie Z, Zhong C and Duan S (2022) miR-1269a and miR-1269b: Emerging Carcinogenic Genes of the miR-1269 Family. Front. Cell Dev. Biol. 10:809132. doi: 10.3389/fcell.2022.809132

INTRODUCTION

MicroRNA (miRNA) is an endogenous non-coding RNA with a length of 20–22 nucleotides, which can usually bind to the 3′-untranslated region of its target gene to silence gene expression (Ambros, 2004). hsa-mir-1269a at chromosome 4 and hsa-mir-1269b at chromosome 17 are members of the miR-1269 family. They can produce mature miRNAs (miR-1269a and miR-1269b) (Kong et al., 2016) with the same sequence.

At present, there are many bioinformatics studies on miRNA. Tens of miRNA research tools are integrated on the tools4mirs website (https://tools4mirs.org/) (Lukasik et al., 2016). miRNA target gene prediction tools mainly used in the miR-1269 related studies include TargetScan (http://www.targetscan.org/) (McGeary et al., 2019), miRDB (http://www.mirdb.org/miRDB/) (Chen and Wang, 2020), and mirwalk (http://mirwalk.umm.uni-heidelberg.de/) (Sticht et al., 2018).

miR-1269a is abnormally highly expressed in 9 cancers, used for the diagnosis of 6 cancers, and is also related to the prognosis of 6 cancers. miR-1269a is also involved in the occurrence and progression of diseases other than cancer. For example, the high expression of miR-1269a may be a risk factor for ectopic pregnancy (Zhang et al., 2018). miR-1269a can regulate the expression of 8 downstream genes and is related to the regulation of three signaling pathways. As to miR-1269b, it is abnormally expressed in 4 kinds of cancers (3 kinds of high expression, one kind of low expression), and is related to the prognosis of two kinds of cancers. miR-1269b can regulate 4 downstream genes and participate in two signaling pathways. In addition, the genetic variants of both miR-1269a and miR-1269b can affect the function of their wild types.

Although there are many reports on miR-1269a and miR-1269b, there is no systematic summary of the two miRNAs. Because miR-1269a and miR-1269b have the same sequence and similar names, researchers may confuse these two miRNAs. Therefore, this article summarizes the abnormal expression of miR-1269a and miR-1269b in various cancers and their diagnostic and prognostic value in cancer. In addition, this article comprehensively analyzes the molecular regulation pathways related to miR-1269a and miR-1269b, which is expected to provide guidance for future related research.

ONCOLOGICAL ROLE OF MIR-1269A AND MIR-1269B IN CANCER

miR-1269a is highly expressed in 9 cancers, including hepatocellular carcinoma (Wojcicka et al., 2014; Yang et al., 2014; Gan et al., 2015; Elemeery et al., 2017; Wang et al., 2019; Cho et al., 2020), lung cancer (Bao et al., 2018; Jin et al., 2018; Guo et al., 2020; Wang et al., 2020; Du et al., 2021; Le and Le, 2021), gastric cancer (Liu et al., 2019; Zhang K. et al., 2020), colon cancer (Bu et al., 2015; Xiong et al., 2021), esophageal cancer (Bai et al., 2021; Yu and Ren, 2021; Zhao et al., 2021), clear cell renal cell carcinoma (Qin et al., 2019; Zhan et al., 2021), head and neck squamous cell carcinoma (Nunez Lopez et al., 2018), glioma (Zhang Y. et al., 2020), and acute myeloid leukemia (Li and Ge, 2021). Highly expressed miR-1269a can promote cancer cell proliferation, migration, invasion, epithelial-mesenchymal transition, and inhibit cancer cell apoptosis (**Table 1**). It is worth noting that in hepatocellular carcinoma (Xiong et al., 2015; Min et al., 2017) and gastric cancer (Li et al., 2017), there are highly expressed miR-1269a mutant and low expressed miR-1269a wild type. Interestingly, the miR-1269a mutant can inhibit the cancer-promoting effect of wild-type miR-1269a, which provides very valuable evidence for targeted cancer therapy.

Similarly, miR-1269b is also highly expressed in hepatocellular carcinoma (Kong et al., 2016; Chen et al., 2020; Ma et al., 2020), lung cancer (Yang et al., 2020), and oral and pharyngeal squamous cell carcinoma (Chen et al., 2016). Overexpression of miR-1269b can down-regulate METTL3, thereby inhibiting the proliferation, migration, and invasion of gastric cancer cells (Kang et al., 2021). It is worth noting that miR-1269b is low expressed in gastric cancer (**Table 1**).

Changes in miRNA expression are a fundamental component of cancer progression. The current study shows that the aberrant expression of miR-1269a or miR-1269b is present in a variety of cancers. Overall, abnormal expression of miR-1269a and miR-1269b can promote or interfere with the occurrence and development of cancer by regulating biological processes such as cancer cell proliferation, migration, invasion, apoptosis, and epithelial-mesenchymal transition. The abnormal expression of miR-1269a and miR-1269b may reflect the regulation of ceRNAs or other upstream genes in different tumors. We also observed that different detection methods of miR-1269a/b were used in these studies. As shown in **Supplementary Table S1**, qRT-PCR is commonly used to detect the expression of miR-1269a (Yang et al., 2014; Bu et al., 2015; Gan et al., 2015; Scaravilli et al., 2015; Kong et al., 2016; Li et al., 2017; Min et al., 2017; Jin et al., 2018; Liu et al., 2019; Zhang K. et al., 2020; Zhang Y. et al., 2020; Chen et al., 2020; Cho et al., 2020; Guo et al., 2020; Bai et al., 2021; Kang et al., 2021; Li and Ge, 2021; Xiong et al., 2021). Some studies have also applied RT-PCR technology to detect miR-1269 expression for hepatocellular carcinoma (Xiong et al., 2015; Elemeery et al., 2017), lung cancer (Elemeery et al., 2017; Wang et al., 2020), and oropharyngeal squamous cell carcinoma (Chen et al., 2016). In addition, studies in hepatocellular carcinoma and acute myeloid leukemia used next-generation sequencing technology (Wojcicka et al., 2014; Chen et al., 2020; Cho et al., 2020) and transcriptome high-throughput sequencing (Li and Ge, 2021) to detect miR-1269. Most of the studies provided the primer sequences used in the experiments, but some studies directly used the data in the database without providing the corresponding primer sequences (Wojcicka et al., 2014; Yang et al., 2014; Bu et al., 2015; Scaravilli et al., 2015; Xiong et al., 2015; Chen et al., 2016; Elemeery et al., 2017; Min et al., 2017; Bao et al., 2018; Yang et al., 2020; Bai et al., 2021; Le and Le, 2021; Li and Ge, 2021). Furthermore, we notice that there is a microarray platform (Illumina HumanHT-12 V4.0 expression beadchip) that can detect miR-1269a, but not

TABLE 1 | The role of miR-1269a and miR-1269b in different human cancers.

miR-1269a/b	Tumor type	Expression pattern	Number of clinical samples	Assessed cell lines	Effect *in vitro*	Effect *in vivo*	Regulatory mechanism	Ref
miR-1269a								
	HCC	Up-regulated	723 cases and 698 controls	HepG2 and SMMC-7721	Proliferation↑, Apoptosis ↓	—	miR-1269a/ SPATS2L and LRP6 axis	Min et al. (2017)
	HCC	Up-regulated	590 cases and 549 controls	HepG2 and Huh7	Proliferation↑	—	miR-1269a/ SOX6 axis	Xiong et al. (2015)
	HCC	Up-regulated	23 paired tissues	HepG2, Huh7, Hep3B, THLE3, BEL-7402, BEL-7404, SNU-398, SNU-449, and QGY-7703	Proliferation↑, Tumorigenicity↑, Cell cycle↑	—	miR-1269a/ FOXO1 axis	Yang et al. (2014)
	HCC	Up-regulated	24 paired tissues	—	—	—	—	Wojcicka et al. (2014)
	HCC	Up-regulated	375 cases and 50 controls	—	—	—	—	Wang et al. (2019)
	HCC	Up-regulated	108 tissues and 720 serums	—	—	—	—	Cho et al. (2020)
	HCC	Up-regulated	95 paired tissues	—	—	—	—	Gan et al. (2015)
	HCC	Up-regulated	474 cases and 84 controls	—	—	—	—	Elemeery et al. (2017)
	GC	Up-regulated	373 paired tissues and 402 controls	MGC803 and HGC27	Proliferation↑, Apoptosis↓	—	miR-1269a/ ZNF70 axis	Li et al. (2017)
	GC	Up-regulated	—	AGS, MKN45, NCI-N87, MGC803, and GES-1	—	Tumor growth↑	RP11-1094M14.8/miR-1269a/CXCL9 axis	Zhang K. et al. (2020)
	GC	Up-regulated	73 paired tissues	AGS, MKN45, BGC-823, SGC7901, and GES-1	Proliferation↑, Cell cycle↑, Apoptosis↓	—	miR-1269a/ RASSF9 axis	Liu et al. (2019)
	NSCLC	Up-regulated	147 peripheral blood samples and 149 controls	A549 and H1975	Proliferation↑, Migration and Invasion↑, EMT↑	—	miR-1269a/ FOXO1 axis	Wang et al. (2020)
	NSCLC	Up-regulated	49 paired tissues	A549, SPC-A1, PC-9, H1299, H1975, H460, and BEAS-2B	Proliferation↑, Colony formation↑, Cell cycle↑	—	miR-1269a/ SOX6 axis	Jin et al. (2018)
	NSCLC	Up-regulated	134 cases and 50 controls	—	—	—	—	Le and Le, (2021)
	LC	Up-regulated	78 paired tissues	A549, SPC-A1, CBP60577, NCI-H1299, NCI-H23, L78, and BEAS-2B	Proliferation↑, Migration and Invasion↑, Cell cycle↑, Apoptosis↓	Tumor growth↑	LINC00261/miR-1269a/FOXO1 axis	Guo et al. (2020)
	LC	Up-regulated	52 paired tissues	A549	Proliferation↑, Apoptosis↓	—	miR-1269a/TP53 and CASP9 axis	Bao et al. (2018)
	CRC	Up-regulated	100 cases	HCT116, LoVo, HT29, SW480, SW620, DLD1, and LS174T	Migration and Invasion↑, EMT↑	Tumor growth and metastasis↑	TGF-β positive feedback pathway	Bu et al. (2015)
	CRC	Up-regulated	10 paired tissues	HCT116, LoVo, HT29, SW480, Caco2, and HIEC 6	Proliferation↑, Migration and Invasion↑, Apoptosis↓	—	circASS1/miR-1269a/VASH1 axis	Xiong et al. (2021)
	ESCC	Up-regulated	107 paired tissues	Eca-109, TE-1, KYSE-150, TE-10, and Het-1A	Proliferation↑, Migration and Invasion↑	—	miR-1269a/ SOX6 axis	Bai et al. (2021)
	ccRCC	Up-regulated	480 cases and 68 controls	—	—	—	—	Qin et al. (2019)
	Glioma	Up-regulated	107 paired tissues; 84 cases and 10 controls	U251, SNB19, SHG44, A172, and HEB	Progression↑, Migration and Invasion↑, Apoptosis ↓	Tumor growth↑	miR-1269a/ATRX axis	Zhang Y. et al. (2020)
	PC	Up-regulated	135 cases	PC3, DU145, LNCaP, 22Rv1, VCaP, and HT-1080	—	—	—	Scaravilli et al. (2015)
	AML	Up-regulated		—	—	—	—	

(Continued on following page)

TABLE 1 | (*Continued*) The role of miR-1269a and miR-1269b in different human cancers.

miR-1269a/b	Tumor type	Expression pattern	Number of clinical samples	Assessed cell lines	Effect *in vitro*	Effect *in vivo*	Regulatory mechanism	Ref
			47 cases and 32 controls					Li and Ge, (2021)
miR-1269b								
	HCC	Up-regulated	—	HepG2, SMMC-7721, and HepG2.2.15	Proliferation↑, Migration↑, Cell cycle↑	—	HBx/NF-κB/miR-1269b/CDC40 axis	Kong et al. (2016)
	HCC	Up-regulated	220 cases	Huh7, Hep3B, PLC, HLE, MHCCLM3, MHCC97H, and MHCC97L	Proliferation↑, Migration and Invasion↑, Chemotaxis↑	Tumor growth and metastasis↑	miR-1269b/SVEP1; PI3K/AKT pathways	Chen et al. (2020)
	HCC	Up-regulated	415 cases and 334 controls	—	—	—	—	Ma et al. (2020)
	GC	Down-regulated	143 paired tissues	AGS, NCI-N87, HGC27, SNU-16, and GES-1	Proliferation↓, Migration and Invasion↓	—	miR-1269b/METTL3 axis	Kang et al. (2021)
	NSCLC	Up-regulated	32 paired tissues	A549, A549/DDP, SPC-A1, PC-9, H1299, H358, and 16HBE	Proliferation↑, Apoptosis↓, Drug resistance↑	Tumor growth↑	miR-1269b/PTEN; PI3K/AKT pathways	Yang et al. (2020)
	OPSCC	Up-regulated	1087 cases and 865 controls	—	—	—	—	Chen et al. (2016)

HCC, hepatocellular carcinoma; GC, gastric cancer; NSCLC, Non-small cell lung cancer; LC, lung cancer; CRC, colorectal cancer; ESCC, esophageal squamous cell carcinoma; ccRCC, clear cell renal cell carcinoma; PC, prostate cancer; AML, acute myeloid leukemia; OPSCC, oropharyngeal squamous cell carcinoma; ↑, Promotion; ↓, Inhibition.

TABLE 2 | The prognostic value of miR-1269a and miR-1269b in cancers.

miR-1269a/b	Tumor type	Sample size	Expression pattern	Prognostic/Diagnostic value	Ref
miR-1269a					
	HCC	254 patients	Up-regulated	Prognostic factor of OS and DFS	Cho et al. (2020)
	HCC	95 patients	Up-regulated	Positively associated with vaso-invasion, multiple tumor nodes and TNM stage; AUC = 0.640	Gan et al. (2015)
	HCC	224 patients	Up-regulated	Positively associated with late fibrosis; AUC = 0.691, sensitivity = 0.786, specificity = 0.598	Elemeery et al. (2017)
	ESCC	322 patients	Up-regulated	Positively associated with TNM stage; prognostic factor of OS and RFS	Jang et al. (2017)
	ESCC	107 patients	Up-regulated	Positively associated with lymph node metastasis and TNM stage; Prognostic factor of OS	Bai et al. (2021)
	ESCC	125 patients	Up-regulated	Positively associated with low differentiation, lymph node metastasis, TNM stage and AJCC stage; Prognostic factor of OS (AUC = 0.716) and CSS (AUC = 0.764)	Yu and Ren, (2021)
	NSCLC	147 patients	Up-regulated	AUC = 0.793	Wang et al. (2020)
	NSCLC	84 patients	Up-regulated	Positively associated with lymph node metastasis and TNM stage; AUC = 0.906, sensitivity = 0.86, specificity = 0.833	Le and Le, (2021)
	LC	78 patients	Up-regulated	Positively associated with lymph node metastasis and TNM stage; Prognostic factor of OS	Guo et al. (2020)
	ccRCC	480 patients	Up-regulated	Prognostic factor of OS	Qin et al. (2019)
	ccRCC	512 patients	Up-regulated	Prognostic factor of OS	Zhan et al. (2021)
	Glioma	99 patients	Up-regulated	Prognostic factor of OS	Zhang Y. et al. (2020)
miR-1269b					
	HCC	—	Up-regulated	Prognostic factor of OS	Ma et al. (2020)
	NSCLC	32 patients	Up-regulated	Prognostic factor of OS	Yang et al. (2020)

HCC, hepatocellular carcinoma; ESCC, esophageal squamous cell carcinomas; NSCLC, Non-small cell lung cancer; LC, lung cancer; ccRCC, clear cell renal cell carcinoma; OS, overall survival; DFS, Disease-free survival; TNM, Tumour-node-metastasis; AUC, area under the curve; RFS, Recurrence-free survival; AJCC, american joint committee on cancer; CSS, Cancer-specific survival.

miR-1269b. Therefore, the current few studies of miR-1269b may be related to relatively few detection methods.

THE DIAGNOSTIC AND PROGNOSTIC VALUE OF MIR-1269

As shown in **Table 2**, the high expression of miR-1269a is closely related to the clinicopathological characteristics of cancer patients. In hepatocellular carcinoma, high expression of miR-1269a is significantly positively correlated with vascular invasion and TNM staging (Gan et al., 2015). In lung cancer, highly expressed miR-1269a is significantly associated with lymph node metastasis and advanced TNM staging (Guo et al., 2020; Wang et al., 2020; Le and Le, 2021). In addition, in esophageal squamous cell carcinoma, highly expressed miR-1269a is significantly associated with poor tumor differentiation, lymph node metastasis, and TNM staging (Jang et al., 2017; Bai et al., 2021; Yu and Ren, 2021).

ROC analysis showed that the AUC of miR-1269a expression was 0.640, indicating that the level of miR-1269a has a certain diagnostic value for hepatocellular carcinoma (Gan et al., 2015). In addition, the sensitivity, specificity, and AUC for miR-1269a were 0.598, 0.786, and 0.691 in the classification between liver fibrosis patients and hepatocellular carcinoma patients, indicating that miR-1269a can be used as a biomarker to track the progression of liver fibrosis to hepatocellular carcinoma (Elemeery et al., 2017). ROC curve analysis showed that the sensitivity, specificity, and AUC for miR-1269a in the diagnosis of lung cancer were 0.833, 0.86, and 0.906 (Le and Le, 2021). In addition, miR-1269a in serum exosomes might be used to diagnose tumors. The current study showed that serum exosomal miR-1269a can be used as a diagnostic marker for hepatocellular carcinoma (Cho et al., 2020) and non-small cell lung cancer (Wang et al., 2020).

The expression levels of miR-1269a and miR-1269b are significantly related to the prognosis of cancer patients (**Table 2**). The high expression of miR-1269a is significantly associated with the lower overall survival (OS) of 6 kinds of cancer patients, including hepatocellular carcinoma (Cho et al., 2020), esophageal squamous cell carcinoma (Jang et al., 2017; Bai et al., 2021; Yu and Ren, 2021), lung cancer (Guo et al., 2020), clear cell renal cell carcinoma (Qin et al., 2019; Zhan et al., 2021), glioma (Zhang Y. et al., 2020) and acute myeloid leukemia (Li and Ge, 2021). In hepatocellular carcinoma, high expression of miR-1269a is significantly associated with shorter disease-free survival (DFS) in patients with hepatocellular carcinoma (Cho et al., 2020) and lower cancer-specific survival (CSS) in patients with esophageal squamous cell carcinoma (Yu and Ren, 2021). These results suggest that miR-1269a is expected to be a biomarker for predicting poor prognosis in cancer patients. Similarly, high expression of miR-1269b was significantly associated with lower overall survival in patients with hepatocellular carcinoma (Ma et al., 2020) and non-small cell lung cancer (Yang et al., 2020). Highly expressed miR-1269b is also associated with cisplatin resistance in patients with non-small cell lung cancer (Yang et al., 2020).

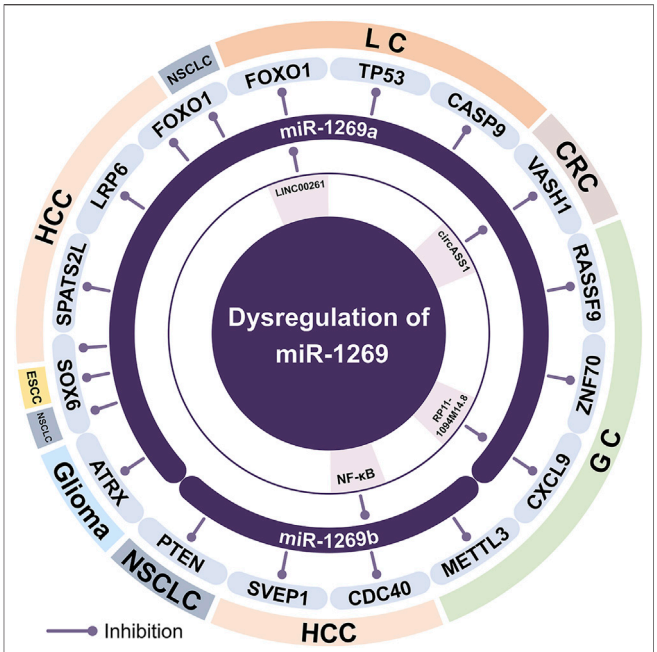

FIGURE 1 | The dysregulation of miR-1269a and miR-1269b in different cancers. miR-1269a can be regulated by three upstream ncRNAs. miR-1269a and miR-1269b can regulate the occurrence and development of cancer by targeting downstream genes. HCC, Hepatocellular carcinoma; GC, Gastric cancer; CRC, Colorectal cancer; NSCLC, Non-small cell lung cancer; ESCC, Esophageal squamous cell carcinomas; LC, Lung cancer.

MOLECULAR MECHANISM OF MIR-1269A IN TUMOR

miR-1269a and its ceRNA Network

Competitive endogenous RNA (ceRNA) can link the function of protein-coding mRNA with the function of non-coding RNA (such as microRNA, long non-coding RNA, and circular RNA) (Qi et al., 2015). The ceRNAs of miR-1269a includes lncRNA RP11-1094M14.8, LINC00261, and circASS1, which can form the RP11-1094M14.8/miR-1269a/CXCL9 axis, LINC00261/miR-1269a/FOXO1 axis and circASS1/miR-1269a/VASH1 axis.

CXCL9 plays an important regulatory role in immune infiltration, and its expression level is significantly positively correlated with the infiltration of various immune cells such as NK cells, B cells, and dendritic cells (DCs) (Zhang K. et al., 2020). There is a lncRNA RP11-1094M14.8/miR-1269a/CXCL9 axis in gastric cancer. In gastric cancer specimens of immunotherapy patients, lncRNA RP11-1094M14.8 up-regulated the expression of CXCL9 by inhibiting miR-1269a, thereby promoting CXCL9-mediated lymphocyte infiltration into the lesion and inhibiting tumor growth (Zhang K. et al., 2020) (**Figure 1**).

FOXO1 is a key regulatory factor in the development of multiple organs or tissue cells. The absence of FOXO1 is more likely to promote the occurrence and development of tumors (Guo et al., 2020). The expression of LINC00261 is down-regulated in lung cancer, and the overexpression of LINC00261 inhibits the growth

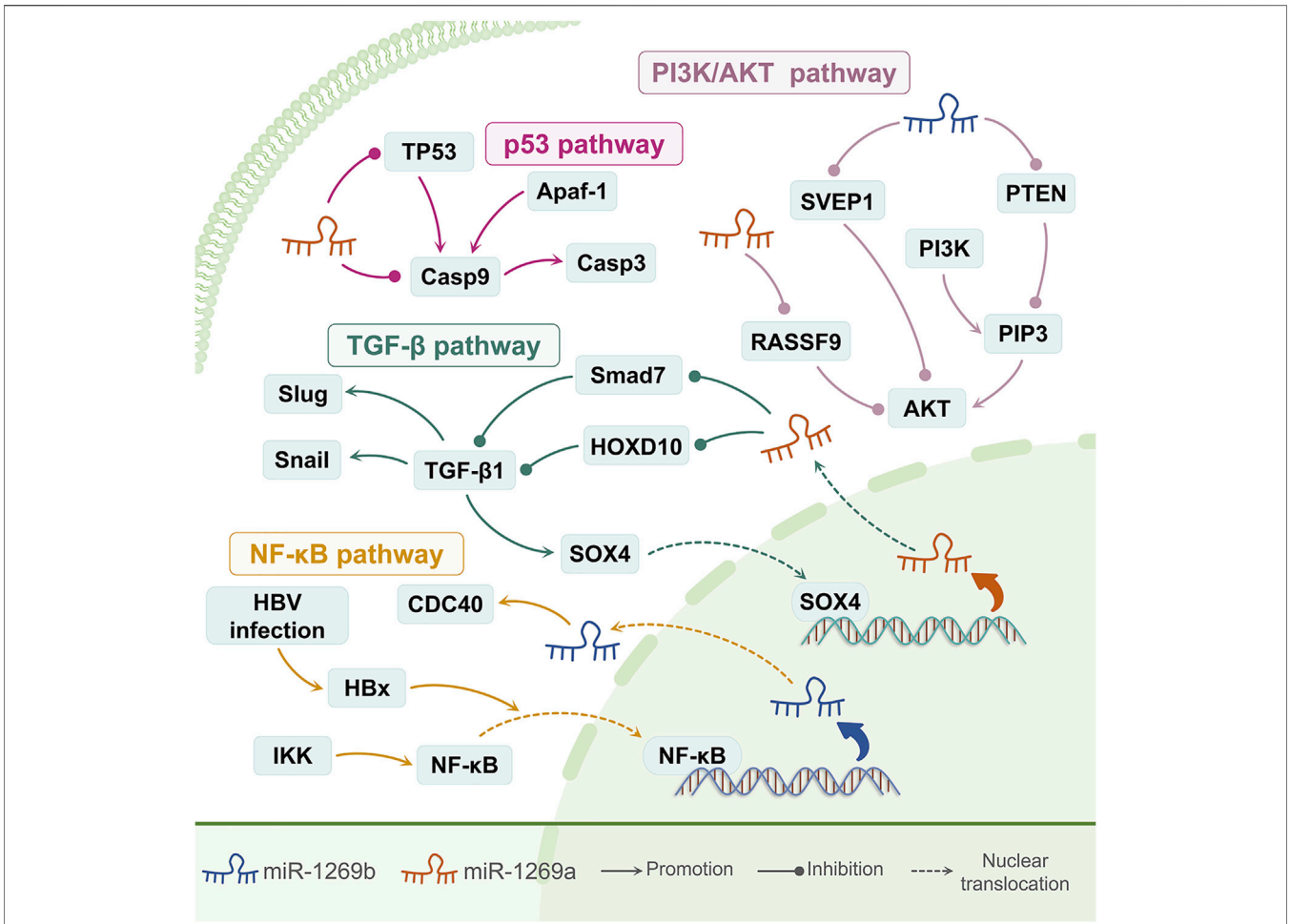

FIGURE 2 | The signaling pathways involved with miR-1269a and miR-1269b. A schematic illustration of the roles of miR-1269a and miR-1269b in multiple signaling pathways. miR-1269a can inhibit apoptosis by inhibiting TP53, the core of the p53 signaling pathway, and Casp9, the initiation factor of apoptosis. miR-1269a up-regulates TGF-β signaling by suppressing its antagonists Smad7 and HOXD10. TGF-β, in turn, up-regulates miR-1269a *via* SOX4 to form a positive feedback loop in the TGF-β signaling pathway. miR-1269a also activates the PI3K/AKT signaling pathway by inhibiting RASSF9. miR-1269b participates in the activation of the PI3K/AKT signaling pathway by inhibiting SVEP1 and PTEN, and HBx promotes tumor progression by inducing miR-1269b to up-regulate CDC40 in an NF-κB dependent manner.

and metastasis of lung cancer by regulating the miR-1269a/FOXO1 axis (Guo et al., 2020) (**Figure 1**).

VASH1 is an endogenous angiogenesis inhibitor induced by VEGF and FGF-2 (Sato, 2013). VASH1 overexpression promotes cancer cell apoptosis and senescence and inhibits tumor occurrence and metastasis (Xiong et al., 2021). In colon cancer cells, the expression of circASS1 and VASH1 is reduced, and the high expression of circASS1 can down-regulate miR-1269a, thereby up-regulating VASH1 to inhibit the growth and metastasis of colon cancer (Xiong et al., 2021) (**Figure 1**).

Downstream Genes of miR-1269a and Their Functions

miR-1269a can directly target SOX6, FOXO1, and ATRX to affect the occurrence and development of tumors (**Figure 1**). SOX6 is a member of the SOX transcription factor family, which is low expressed in a variety of tumors (Jin et al., 2018). SOX6 reduces tumor cell proliferation by promoting the expression of P21 and inhibiting CyClin D1 (Jin et al., 2018). In non-small cell lung cancer, miR-1269a can down-regulate SOX6 to promote tumor growth (Jin et al., 2018). In addition, in hepatocyte carcinoma (Xiong et al., 2015) and esophageal squamous cell carcinoma (Bai et al., 2021), the miR-1269a/SOX6 axis promotes cell proliferation, migration, and invasion, thereby promoting the development of tumors. FOXO1 is a transcriptional activation factor, which can regulate the expression of cell cycle blocking, apoptosis, DNA repair, and hypoxia reaction (Yang et al., 2014). In non-small cell lung cancer, miR-1269a can inhibit FOXO1 to promote cell proliferation, migration, and invasion (Wang et al., 2020). In hepatocellular carcinoma, miR-1269a/FOXO1 can up-regulate Cyclin D1, thereby promoting tumor cell proliferation (Yang et al., 2014). ATRX plays a vital role in chromatin remodeling and maintaining genome and telomere stability. It is one of the

key molecular biomarkers for the classification and diagnosis of glioma (Zhang Y. et al., 2020). In glioma cells, the significantly increased expression of miR-1269a can promote the proliferation and invasion of glioma cells and inhibit apoptosis. miR-1269a can significantly down-regulate the expression of ATRX *in vivo* and *in vitro*, and the overexpression of ATRX can also reverse the tumor-promoting effect induced by miR-1269a (Zhang Y. et al., 2020).

The Positive Feedback Regulation Between miR-1269a and TGF-β

Transforming growth factor-β (TGF-β) family members play a vital role in cellular processes such as immunosuppression, growth inhibition, EMT, and cell invasion (Xie et al., 2018). In the late stages of cancer progression, the TGF-β signaling pathway can increase the expression of mesenchymal markers and reduce the expression of epithelial markers to promote EMT (Xie et al., 2018). In colorectal cancer, TGF-β can activate miR-1269a by promoting Sox4, inhibit SMAD7 and HOXD10, thereby enhancing TGF-β signaling and forming a positive feedback loop, promoting the EMT and metastasis of tumor cells (Bu et al., 2015) (**Figure 2**).

miR-1269a and the p53 Signaling Pathway

p53 is an important tumor suppressor gene, and abnormalities of the p53 signaling pathway usually occur in tumors with higher malignancy (Bao et al., 2018). Caspase-9 is the initiation factor of cell apoptosis, and p53 can activate the caspase-9-mediated apoptotic pathway (Kim et al., 2015). In lung cancer, miR-1269a promotes lung cancer cell proliferation and inhibits apoptosis through targeted inhibition of p53 and caspase-9 (Bao et al., 2018) (**Figure 1**).

miR-1269a and the PI3K/AKT Signaling Pathway

The PI3K/AKT signaling pathway can regulate the cell cycle by directly phosphorylating target proteins or indirectly controlling protein expression (Liu et al., 2019). As an N-terminal gene of the RASSF family, RASSF9 is involved in cell growth, survival, and apoptosis. By down-regulating the expression of *p*-AKT and other related proteins, RASSF9 can restrict the AKT signaling pathway (Liu et al., 2019). In gastric cancer, the overexpression of miR-1269a can inhibit RASSF9 to activate the AKT signaling pathway, and up-regulate the transcription factors CDK2 and Cyclin D1, thereby inducing the transition of the cell cycle from the G1 phase to the S phase, promoting cell proliferation. The regulation of the PI3K/AKT signaling pathway by miR-1269a can maintain the balance between the pro-apoptotic factor Bax and the anti-apoptotic factor Bcl-2, and prevent tumor cell apoptosis (Liu et al., 2019) (**Figure 1**).

THE MOLECULAR MECHANISMS OF MIR-1269B IN TUMORS

Downstream Genes of miR-1269a and Their Functions

m6A is a ubiquitous mRNA epigenetic modification in eukaryotes. METTL3 contains two domains that bind to S-adenosylmethionine (SAM) and has the activity of independently catalyzing the modification of RNA m6A. METTL3 is an important regulator of malignant tumors, which can promote the malignant biological behavior of tumor cells (Kang et al., 2021). miR-1269b is low expressed in gastric cancer, while overexpression of miR-1269b can inhibit the proliferation, migration, and invasion of tumors by targeting METTL3 (Kang et al., 2021) (**Figure 1**).

The HBx/NF-κB/miR-1269b/CDC40 Axis

HBx is the smallest protein (17 kDa) encoded by the hepatitis B virus (HBV). HBx does not bind to DNA but can directly inhibit or activate transcription factors to regulate downstream genes (Kong et al., 2016). HBx can activate the transcription factor NF-κB (Yang et al., 2020). CDC40 is a splicing factor involved in cell cycle control, which can remove E-cadherin and enhance vimentin, thereby promoting tumor cell migration (Kong et al., 2016). In hepatocellular carcinoma, HBx protein can promote the introduction of NF-κB from the cytoplasm into the nucleus, thereby activating miR-1269b, up-regulating CDC40, and promoting the growth and migration of liver cancer cells (Kong et al., 2016) (**Figure 2**).

miR-1269b and the PI3K/AKT Signaling Pathway

SVEP1 is one of the most important cell adhesion molecules, and it is often highly expressed in normal tissues. In liver cancer cells, down-regulation of SVEP1 expression can significantly enhance the Akt phosphorylation at Thr308, thereby promoting the proliferation and metastasis of liver cancer cells (Chen et al., 2020). miR-1269b can activate the PI3K/Akt signaling pathway by inhibiting SVEP1 in liver cancer cells, thereby promoting tumor recurrence and metastasis (Chen et al., 2020). PTEN is a known prognostic marker and tumor suppressor for non-small cell lung cancer. Its inactivation can enhance the PI3K/AKT signaling pathway, thereby promoting the development of cisplatin resistance (Yang et al., 2020) (**Figure 1**). miR-1269b can inhibit the PTEN/PI3K/AKT signaling pathway, thereby driving cisplatin resistance in non-small cell lung cancer.

THE MECHANISM OF MIR-1269 VARIANTS IN TUMOR

rs73239138 is a single nucleotide polymorphism located in the sequence of miR-1269a. miR-1269a rs73239138 is also associated with a reduced risk of breast cancer among women in southeastern Iran (Sarabandi et al., 2021). In gastric cancer and liver cancer cells, overexpressed miR-1269a can inhibit the apoptosis of gastric cancer cells. In contrast, the miR-1269a variant (rs73239138) can promote the apoptosis of gastric cancer cells by up-regulating the apoptotic proteins Bik, Bim, and Bak, thereby inhibiting the tumor-promoting effect of wild-type miR-1269a (Li et al., 2017). In addition, miR-1269a can inhibit the expression of tumor suppressor gene ZNF70, while miR-1269a rs73239138 can up-regulate ZNF70, thereby reducing the susceptibility to gastric cancer (Li et al., 2017). In liver cancer, miR-1269a rs73239138 can prevent miR-1269a from binding to the 3′-

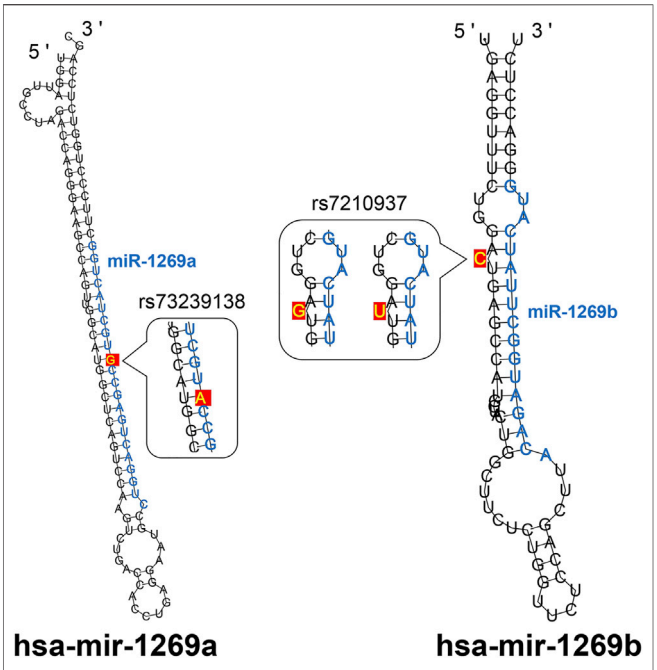

FIGURE 3 | The stem-loop structures of hsa-mir-1269a and hsa-mir-1269b. The schematic diagram mainly shows the obvious differences in the stem-loop structure of hsa-mir-1269a and hsa-mir-1269b. The blue letters in the figure are the sequences of mir-1269a and mir-1269b. It is worth noting that they have the same mature sequence. In addition, the sites marked with yellow letters are known SNP site.

UTR of SOX6, thereby inhibiting the development of cancer (Xiong et al., 2015). At the same time, miR-1269a rs73239138 can disrupt the regulation of miR-1269a in the expression of NME1, SHMT1, SLC29A1, TP53, and UCK1, resulting in a poor prognosis for patients with advanced colon cancer receiving capecitabine chemotherapy (Mao et al., 2017).

However, another study of hepatocellular carcinoma showed that miR-1269a rs73239138 can promote tumor progression (Min et al., 2017). SPATS2L is ubiquitously expressed in a variety of tissues (Wang et al., 2021). SPATS2L is involved in ribosome biogenesis and translational control of oxidative stress response (Zhu et al., 2008). LRP6 is a transmembrane Wnt co-receptor necessary for the Wnt/β-catenin signaling pathway, and excessive activation of the Wnt/β-catenin signaling pathway is thought to be a key step in tumorigenesis (Dong et al., 2019). miR-1269a can down-regulate the expression of SPATS2L and LRP6, thereby inhibiting the proliferation of liver cancer cells; while miR-1269a rs73239138 can inhibit the down-regulation of SPATS2L and LRP6 by miR-1269a to promote the occurrence and development of cancer (Min et al., 2017). In the future, the role of miR-1269a rs73239138 in hepatocellular carcinoma needs further research.

There is also a common genetic variant (rs7210937) of miR-1269b (**Figure 3**). miR-1269b rs7210937 is associated with a reduced risk of oral precancerous lesions and pharyngeal squamous cell carcinoma associated with habitual chewing of betel quid, indicating that miR-1269b rs7210937 has potential protection of cancer (Chen et al., 2016).

DISCUSSION

As miRNAs have been confirmed to be involved in the progression of cancer from the initial stage to metastasis, research on miRNAs has become popular (Alwani and Baj-Krzyworzeka, 2021). Numerous studies have identified miRNAs as tumor diagnostic markers and potential targets for modern cancer therapy (Alwani and Baj-Krzyworzeka, 2021). In recent years, miR-1269a and miR-1269b are involved in a variety of cancers. miR-1269a is highly expressed in 9 cancers. Growing evidence suggests that miRNAs are frequently deregulated in cancer cells, thereby affecting tumor growth, migration, invasion, apoptosis, and drug resistance (Arghiani and Shah, 2021). miR-1269a is of great significance in the diagnosis of hepatocellular carcinoma and lung cancer. In addition, the abnormal expression of miR-1269a is associated with the poor prognosis of 6 cancers. miR-1269a can regulate the occurrence and development of cancer by targeting downstream genes (CXCL9, SOX6, FOXO1, ATRX, RASSF9, SMAD7, HOXD10, and VASH1). At the same time, miR-1269a can interact with RP11-1094M14.8, LINC00261, and circASS1 in gastric cancer, lung cancer, and colon cancer, respectively. In colorectal cancer, a positive feedback loop is formed between miR-1269a and TGF-β pathway to amplify the signal of cancer metastasis, which suggests that miR-1269a is expected to become a potential therapeutic target to prevent tumor metastasis. In lung cancer and gastric cancer, miR-1269a can also promote tumor cell proliferation and cell cycle progression and inhibit tumor cell apoptosis by activating the PI3K/AKT signaling pathway and inhibiting the caspase-9-mediated apoptotic pathway, respectively.

miR-1269b is highly expressed in three types of cancer, and lowly expressed in one type of cancer. miRNA is a key regulator involved in cell carcinoma proliferation, apoptosis, invasion, metastasis, EMT, angiogenesis, drug resistance, and autophagy (Xu et al., 2018). In addition, research has shown that miRNA (such as miR-21) has an important role in promoting cell proliferation and invasion, angiogenesis, and chemical and radioresistance in non-small cell lung cancer (Cecilia et al., 2018). Our work shows that the high expression of miR-1269b is associated with the lower overall survival of patients with hepatocellular carcinoma (Ma et al., 2020) and non-small cell lung cancer (Yang et al., 2020). In non-small cell lung cancer, the high expression of miR-1269b can also promote the occurrence of cisplatin resistance (Yang et al., 2020). Accordingly, miR-1269b can affect the progression of cancer by targeting downstream genes (METTL3, CDC40, SVEP1, and PTEN). In addition, miR-1269b can also affect the progress of cancer through a series of regulatory methods, such as directly targeting the downstream gene METTL3 or by targeting SVEP1 and PTEN to drive the PI3K/AKT signaling pathway, thereby mediating tumor recurrence and metastasis. miR-1269b can also be induced by HBx to up-regulate CDC40 in an NF-κB-dependent manner to promote tumor cell growth and migration.

In hepatocellular carcinoma and gastric cancer, miR-1269a variant can reduce tumor susceptibility and inhibit tumor progression by inhibiting the effect of miR-1269a, which

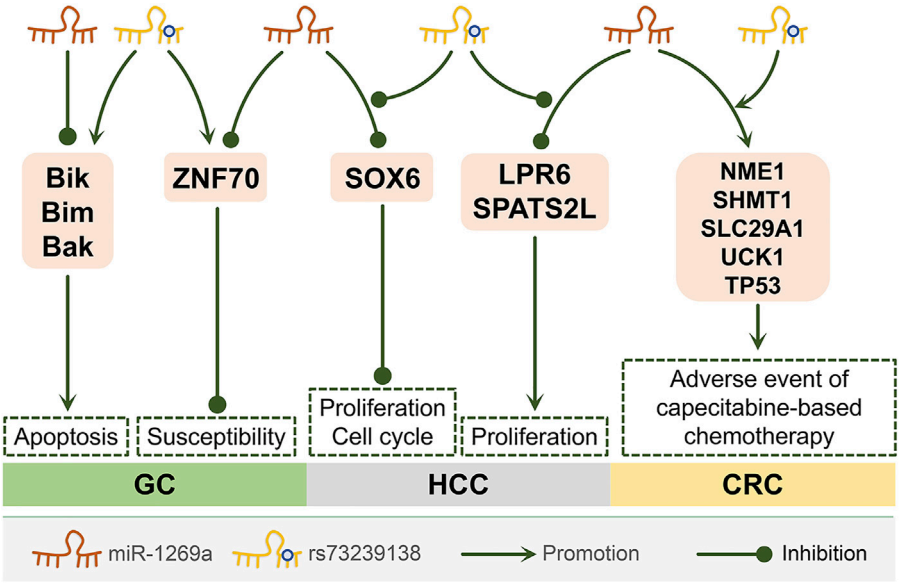

FIGURE 4 | The molecular mechanism of miR-1269a rs73239138 in different cancers. miR-1269a rs73239138 can affect three cancers through five molecular mechanisms. GC, Gastric cancer; HCC, Hepatocellular carcinoma; CRC, Colorectal cancer. (Li et al., 2017; Xiong et al., 2015; Mao et al., 2017; Min et al., 2017; Wang et al., 2021; Zhu et al., 2008; Dong et al., 2019).

provides new ideas for future targeted cancer treatments. In oral cancer, the miR-1269b variant has also been proven to have potential cancer protection.

At present, most of the researches use PCR-based technology, microarray, or next-generation sequencing technology to identify miR-1269a/b. The primer sequences they used to detect miR-1269a/b are shown in Supplementary Table. They differentiated the roles of the miR-1269a and miR-1269b by detecting hsa-mir-1269a and hsa-mir-1269b. Our work shows different molecular mechanisms between miR-1269a and miR-1269b, which may be caused by the different focus of the research content. We also checked the research of miR-1269 in the NCBI GEO database and found that hsa-mir-1269a can be detected by Illumina HumanHT-12 V4.0 expression beadchip (GPL10558), however, there is no probeset to detect hsa-mir-1269b. We believe that the current paucity of miR-1269b research may be related to the lack of detection methods for hsa-mir-1269b. Therefore, more methods need to be explored in the future for the effective detection of hsa-mir-1269b to distinguish whether there is a functional difference between miR-1269a and miR-1269b.

At present, our understanding of miR-1269a and miR-1269b is still very limited, and we have not conducted a comprehensive exploration of these two oncogenic miRNAs in cancer. Studies on miR-1269a or miR-1269b are often combined with other miRNAs, and there are relatively few independent studies on miR-1269a or miR-1269b. There is still some controversy as to whether the miR-1269a variant promotes or suppresses cancer. In addition, miR-1269b has been confirmed to be highly expressed in hepatocellular carcinoma, lung cancer, and oral and pharyngeal squamous cell carcinoma. However, miR-1269b is low expressed in gastric cancer, which may be caused by some unknown regulatory mechanisms in gastric cancer, and this needs to be further studied.

In summary, miR-1269a and miR-1269b are both promising miRNAs. In the future, it is necessary to further explore the mechanism of miR-1269a and miR-1269b in a variety of cancers, to establish a richer miR-1269a and miR-1269b regulatory network. At the same time, the variants of miR-1269a and miR-1269b also have great research value, which can provide support for cancer diagnosis, targeted therapy, and prognosis prediction.

AUTHOR CONTRIBUTIONS

ZX, CZ, and SD contributed to the conception, design and final approval of the submitted version. ZX and CZ collected and analyzed literature. ZX, CZ, and SD contributed to manuscript writing. All the authors conceived and gave the approval of the final manuscript.

FUNDING

The research was supported by Qiantang Scholar Fund in Zhejiang University City College.

SUPPLEMENTARY MATERIAL

The Supplementary Material for this article can be found online at: https://www.frontiersin.org/articles/10.3389/fcell.2022.809132/full#supplementary-material

Supplementary Table S1 | The detection of miR-1269a/b in different studies.

REFERENCES

Alwani, A., and Baj-Krzyworzeka, M. (2021). mikroRNA Jako Cel Terapeutyczny W Chorobach Nowotworowych. *Postepy Biochem.* 67, 259–267. Print 2021 Sep 30. doi:10.18388/pb.2021_390

Ambros, V. (2004). The Functions of Animal microRNAs. *Nature* 431, 350–355. doi:10.1038/nature02871

Arghiani, N., and Shah, K. (2021). Modulating microRNAs in Cancer: Next-Generation Therapies. *Cancer Biol. Med.* 18, 2095–3941. doi:10.20892/j.issn.2095-3941.2021.0294

Bai, X., Wang, Q., Rui, X., Li, X., and Wang, X. (2021). Upregulation of miR-1269 Contributes to the Progression of Esophageal Squamous Cell Cancer Cells and Is Associated with Poor Prognosis. *Technol. Cancer Res. Treat.* 20, 153303382098585. doi:10.1177/1533033820985858

Bao, M., Song, Y., Xia, J., Li, P., Liu, Q., and Wan, Z. (2018). miR-1269 Promotes Cell Survival and Proliferation by Targeting Tp53 and Caspase-9 in Lung Cancer. *Ott* Vol. 11, 1721–1732. doi:10.2147/OTT.S157715

Bu, P., Wang, L., Chen, K.-Y., Rakhilin, N., Sun, J., Closa, A., et al. (2015). miR-1269 Promotes Metastasis and Forms a Positive Feedback Loop with TGF-β. *Nat. Commun.* 6, 6879. doi:10.1038/ncomms7879

Cecilia, B. P., Roxana, C. P., Magdo, L., Raduly, L., Gulei, D., and Berindan-Neagoe, I. (2018). Overview upon miR-21 in Lung Cancer: Focus on NSCLC. *Cell. Mol. Life Sci.* 75, 3539–3551. doi:10.1007/S00018-018-2877-x

Chen, H.-C., Tseng, Y.-K., Chi, C.-C., Chen, Y.-H., Yang, C.-M., Huang, S.-J., et al. (2016). Genetic Variants in microRNA-146a (C > G) and microRNA-1269b (G > C) Are Associated with the Decreased Risk of Oral Premalignant Lesions, Oral Cancer, and Pharyngeal Cancer. *Arch. Oral Biol.* 72, 21–32. doi:10.1016/j.archoralbio.2016.08.010

Chen, L., Liu, D., Yi, X., Qi, L., Tian, X., Sun, B., et al. (2020). The Novel miR-1269b-Regulated Protein SVEP1 Induces Hepatocellular Carcinoma Proliferation and Metastasis Likely through the PI3K/Akt Pathway. *Cell Death Dis* 11, 320. doi:10.1038/s41419-020-2535-8

Chen, Y., and Wang, X. (2020). miRDB: an Online Database for Prediction of Functional microRNA Targets. *Nucleic Acids Res.* 48, D127–D131. doi:10.1093/nar/gkz757

Cho, H. J., Baek, G. O., Seo, C. W., Ahn, H. R., Sung, S., Son, J. A., et al. (2020). Exosomal microRNA-4661-5p-Based Serum Panel as a Potential Diagnostic Biomarker for Early-stage Hepatocellular Carcinoma. *Cancer Med.* 9, 5459–5472. doi:10.1002/cam4.3230

Dong, Y., Zhang, Y., Kang, W., Wang, G., Chen, H., Higashimori, A., et al. (2019). VSTM2A Suppresses Colorectal Cancer and Antagonizes Wnt Signaling Receptor LRP6. *Theranostics* 9, 6517–6531. doi:10.7150/thno.34989

Du, Y., Yuan, S., Zhuang, X., Zhang, Q., and Qiao, T. (2021). Multiomics Differences in Lung Squamous Cell Carcinoma Patients with High Radiosensitivity Index Compared with Those with Low Radiosensitivity Index. *Dis. Markers* 2021, 1–11. doi:10.1155/2021/3766659

Elemeery, M. N., Badr, A. N., Mohamed, M. A., and Ghareeb, D. A. (2017). Validation of a Serum microRNA Panel as Biomarkers for Early Diagnosis of Hepatocellular Carcinoma post-hepatitis C Infection in Egyptian Patients. *Wjg* 23, 3864–3875. doi:10.3748/wjg.v23.i21.3864

Gan, T. Q., Tang, R. X., He, R. Q., Dang, Y. W., Xie, Y., and Chen, G. (2015). Upregulated MiR-1269 in Hepatocellular Carcinoma and its Clinical Significance. *Int. J. Clin. Exp. Med.* 8, 714–721.

Guo, C., Shi, H., Shang, Y., Zhang, Y., Cui, J., and Yu, H. (2020). LncRNA LINC00261 Overexpression Suppresses the Growth and Metastasis of Lung Cancer via Regulating miR-1269a/FOXO1 axis. *Cancer Cel Int* 20, 275. doi:10.1186/s12935-020-01332-6

Jang, H.-J., Lee, H.-S., Burt, B. M., Lee, G. K., Yoon, K.-A., Park, Y.-Y., et al. (2017). Integrated Genomic Analysis of Recurrence-Associated Small Non-coding RNAs in Oesophageal Cancer. *Gut* 66, 215–225. doi:10.1136/gutjnl-2015-311238

Jin, R. H., Yu, D. J., and Zhong, M. (2018). MiR-1269a Acts as an Onco-miRNA in Non-small Cell Lung Cancer via Down-Regulating SOX6. *Eur. Rev. Med. Pharmacol. Sci.* 22, 4888–4897. doi:10.26355/eurrev_201808_15625

Kang, J., Huang, X., Dong, W., Zhu, X., Li, M., and Cui, N. (2021). MicroRNA-1269b Inhibits Gastric Cancer Development through Regulating Methyltransferase-like 3 (METTL3). *Bioengineered* 12, 1150–1160. doi:10.1080/21655979.2021.1909951

Kim, B., Srivastava, S. K., and Kim, S.-H. (2015). Caspase-9 as a Therapeutic Target for Treating Cancer. *Expert Opin. Ther. Targets* 19, 113–127. doi:10.1517/14728222.2014.961425

Kong, X.-x., Lv, Y.-r., Shao, L.-p., Nong, X.-y., Zhang, G.-l., Zhang, Y., et al. (2016). HBx-Induced MiR-1269b in NF-κB Dependent Manner Upregulates Cell Division Cycle 40 Homolog (CDC40) to Promote Proliferation and Migration in Hepatoma Cells. *J. Transl. Med.* 14, 189. doi:10.1186/s12967-016-0949-y

Le, J., and Le, X. (2021). The Clinical Application Value of miR-1269 as an Unfavorable Prognostic Indicator of Lung Cancer. *Am. J. Transl. Res.* 13, 3270–3277.

Li, J., and Ge, Z. (2021). High HSPA8 Expression Predicts Adverse Outcomes of Acute Myeloid Leukemia. *BMC Cancer* 21, 475. doi:10.1186/s12885-021-08193-w

Li, W., Zhang, H., Min, P., Zhu, J., Xu, D., Jiang, W., et al. (2017). Downregulated miRNA-1269a V-ariant (R-s73239138) D-ecreases the S-usceptibility to G-astric C-ancer via T-argeting ZNF70. *Oncol. Lett.* 14, 6345–6354. doi:10.3892/ol.2017.7091

Liu, W.-L., Wang, H.-x., Shi, C.-x., Shi, F.-y., Zhao, L.-y., Zhao, W., et al. (2019). MicroRNA-1269 Promotes Cell Proliferation via the AKT Signaling Pathway by Targeting RASSF9 in Human Gastric Cancer. *Cancer Cel Int* 19, 308. doi:10.1186/s12935-019-1026-4

Lukasik, A., Wójcikowski, M., and Zielenkiewicz, P. (2016). Tools4miRs - One Place to Gather All the Tools for miRNA Analysis. *Bioinformatics* 32, 2722–2724. doi:10.1093/bioinformatics/btw189

Ma, X., Zhou, L., and Zheng, S. (2020). Transcriptome Analysis Revealed Key Prognostic Genes and microRNAs in Hepatocellular Carcinoma. *PeerJ* 8, e8930. doi:10.7717/peerj.8930

Mao, Y., Zou, C., Meng, F., Kong, J., Wang, W., and Hua, D. (2017). The SNPs in Pre-miRNA Are Related to the Response of Capecitabine-Based Therapy in Advanced colon Cancer Patients. *Oncotarget* 9, 6793–6799. doi:10.18632/oncotarget.23190

McGeary, S. E., Lin, K. S., Shi, C. Y., Pham, T. M., Bisaria, N., Kelley, G. M., et al. (2019). The Biochemical Basis of microRNA Targeting Efficacy. *Science* 366, 6472. doi:10.1126/science.aav1741

Min, P., Li, W., Zeng, D., Ma, Y., Xu, D., Zheng, W., et al. (2017). A Single Nucleotide Variant in microRNA-1269a Promotes the Occurrence and Process of Hepatocellular Carcinoma by Targeting to Oncogenes SPATS2L and LRP6. *Bull. du Cancer* 104, 311–320. doi:10.1016/j.bulcan.2016.11.021

Nunez Lopez, Y. O., Victoria, B., Golusinski, P., Golusinski, W., and Masternak, M. M. (2018). Characteristic miRNA Expression Signature and Random forest Survival Analysis Identify Potential Cancer-Driving miRNAs in a Broad Range of Head and Neck Squamous Cell Carcinoma Subtypes. *Rep. Pract. Oncol. Radiother.* 23, 6–20. doi:10.1016/j.rpor.2017.10.003

Qi, X., Zhang, D.-H., Wu, N., Xiao, J.-H., Wang, X., and Ma, W. (2015). ceRNA in Cancer: Possible Functions and Clinical Implications. *J. Med. Genet.* 52, 710–718. doi:10.1136/jmedgenet-2015-103334

Qin, S., Shi, X., Wang, C., Jin, P., and Ma, F. (2019). Transcription Factor and miRNA Interplays Can Manifest the Survival of ccRCC Patients. *Cancers* 11, 1668. doi:10.3390/cancers11111668

Sarabandi, S., Sattarifard, H., Kiumarsi, M., Karami, S., Taheri, M., Hashemi, M., et al. (2021). Association between Genetic Polymorphisms of miR-1307, miR-1269, miR-3117 and Breast Cancer Risk in a Sample of South East Iranian Women. *Asian Pac. J. Cancer Prev.* 22, 201–208. doi:10.31557/APJCP.2021.22.1.201

Sato, Y. (2013). The Vasohibin Family: a Novel Family for Angiogenesis Regulation. *J. Biochem.* 153, 5–11. doi:10.1093/jb/mvs128

Scaravilli, M., Porkka, K. P., Brofeldt, A., Annala, M., Tammela, T. L., Jenster, G. W., et al. (2015). MiR-1247-5p Is Overexpressed in Castration Resistant Prostate Cancer and Targets MYCBP2. *Prostate* 75, 798–805. doi:10.1002/pros.22961

Sticht, C., De La Torre, C., Parveen, A., and Gretz, N. (2018). miRWalk: An Online Resource for Prediction of microRNA Binding Sites. *PLoS One* 13, e0206239. doi:10.1371/journal.pone.0206239

Wang, H., Wang, X., Xu, L., Zhang, J., and Cao, H. (2021). Analysis of the EGFR Amplification and CDKN2A Deletion Regulated Transcriptomic Signatures

Reveals the Prognostic Significance of SPATS2L in Patients with Glioma. *Front. Oncol.* 11, 551160. doi:10.3389/fonc.2021.551160

Wang, X., Gao, J., Zhou, B., Xie, J., Zhou, G., and Chen, Y. (2019). Identification of Prognostic Markers for Hepatocellular Carcinoma Based on miRNA Expression Profiles. *Life Sci.* 232, 116596. doi:10.1016/j.lfs.2019.116596

Wang, X., Jiang, X., Li, J., Wang, J., Binang, H., Shi, S., et al. (2020). Serum Exosomal miR -1269a Serves as a Diagnostic Marker and Plays an Oncogenic Role in Non-small Cell Lung Cancer. *Thorac. Cancer* 11, 3436–3447. doi:10.1111/1759-7714.13644

Wojcicka, A., Swierniak, M., Kornasiewicz, O., Gierlikowski, W., Maciag, M., Kolanowska, M., et al. (2014). Next Generation Sequencing Reveals microRNA Isoforms in Liver Cirrhosis and Hepatocellular Carcinoma. *Int. J. Biochem. Cel Biol.* 53, 208–217. doi:10.1016/j.biocel.2014.05.020

Xie, F., Ling, L., van Dam, H., Zhou, F., and Zhang, L. (2018). TGF-β Signaling in Cancer Metastasis. *Acta Biochim. Biophys. Sin.* 50, 121–132. doi:10.1093/abbs/gmx123

Xiong, G., Wang, Y., Ding, Q., and Yang, L. (2015). Hsa-mir-1269 Genetic Variant Contributes to Hepatocellular Carcinoma Susceptibility through Affecting SOX6. *Am. J. Transl. Res.* 7, 2091–2098.

Xiong, H.-L., Zhong, X.-H., Guo, X.-H., Liao, H.-J., and Yuan, X. (2021). circASS1 Overexpression Inhibits the Proliferation, Invasion and Migration of Colorectal Cancer Cells by Regulating the miR-1269a/VASH1 axis. *Exp. Ther. Med.* 22, 1155. doi:10.3892/etm.2021.10589

Xu, X., Tao, Y., Shan, L., Chen, R., Jiang, H., Qian, Z., et al. (2018). The Role of MicroRNAs in Hepatocellular Carcinoma. *J. Cancer* 9, 3557–3569. doi:10.7150/jca.26350

Yang, W., Xiao, W., Cai, Z., Jin, S., and Li, T. (2020). miR-1269b Drives Cisplatin Resistance of Human Non-small Cell Lung Cancer via Modulating the PTEN/PI3K/AKT Signaling Pathway. *Ott* Vol. 13, 109–118. doi:10.2147/OTT.S225010

Yang, X.-W., Shen, G.-Z., Cao, L.-Q., Jiang, X.-F., Peng, H.-P., Shen, G., et al. (2014). MicroRNA-1269 Promotes Proliferation in Human Hepatocellular Carcinoma via Downregulation of FOXO1. *BMC Cancer* 14, 909. doi:10.1186/1471-2407-14-909

Yu, Y., and Ren, K.-M. (2021). Development of a Prognostic Prediction Model Based on microRNA-1269a in Esophageal Cancer. *Wjgo* 13, 943–958. doi:10.4251/wjgo.v13.i8.943

Zhan, Y., Zhang, R., Li, C., Xu, X., Zhu, K., Yang, Z., et al. (2021). A microRNA-clinical Prognosis Model to Predict the Overall Survival for Kidney Renal clear Cell Carcinoma. *Cancer Med.* 10, 6128–6139. doi:10.1002/cam4.4148

Zhang, K., Zhang, L., Mi, Y., Tang, Y., Ren, F., Liu, B., et al. (2020). A ceRNA Network and a Potential Regulatory axis in Gastric Cancer with Different Degrees of Immune Cell Infiltration. *Cancer Sci.* 111, 4041–4050. doi:10.1111/cas.14634

Zhang, S., Sun, Q., Jiang, X., and Gao, F. (2018). Clinical Significance of Expression of Hsa-Mir-1247 and Hsa-Mir-1269a in Ectopic Pregnancy Due to Salpingitis. *Exp. Ther. Med.* 15, 4901–4905. doi:10.3892/etm.2018.5998

Zhang, Y., Wang, Q., Luo, N., Liu, J., Ren, H., Shao, X., et al. (2020). MicroRNA-1269a Promotes Proliferation and Arrest of Apoptosis of Glioma Cells by Directly Targeting ATRX. *Front. Oncol.* 10, 563901. doi:10.3389/fonc.2020.563901

Zhao, Y., Xu, L., Wang, X., Niu, S., Chen, H., and Li, C. (2021). A Novel Prognostic mRNA/miRNA Signature for Esophageal Cancer and its Immune Landscape in Cancer Progression. *Mol. Oncol.* 15, 1088–1109. doi:10.1002/1878-0261.12902

Zhu, C.-H., Kim, J., Shay, J. W., and Wright, W. E. (2008). SGNP: an Essential Stress Granule/Nucleolar Protein Potentially Involved in 5.8s rRNA Processing/transport. *PLoS. One* 3, e3716. doi:10.1371/journal.pone.0003716

Conflict of Interest: The authors declare that the research was conducted in the absence of any commercial or financial relationships that could be construed as a potential conflict of interest.

Publisher's Note: All claims expressed in this article are solely those of the authors and do not necessarily represent those of their affiliated organizations, or those of the publisher, the editors and the reviewers. Any product that may be evaluated in this article, or claim that may be made by its manufacturer, is not guaranteed or endorsed by the publisher.

frontiers in Oncology

REVIEW
published: 21 February 2022
doi: 10.3389/fonc.2022.847745

LncRNA PCGEM1 in Human Cancers: Functions, Mechanisms and Promising Clinical Utility

Yuanshuai Su†, Xinyu Gu†, Qiuxian Zheng†, Lingxiao Zhu, Juan Lu and Lanjuan Li**

State Key Laboratory for Diagnosis and Treatment of Infectious Diseases, National Clinical Research Center for Infectious Diseases, Collaborative Innovation Center for Diagnosis and Treatment of Infectious Diseases, The First Affiliated Hospital, College of Medicine, Zhejiang University, Hangzhou, China

As novel members of the noncoding RNA family, long noncoding RNAs (lncRNAs) have been widely reported to function as powerful regulators in gene expression processes, including chromosome remodeling, transcription interference and posttranscriptional modification. With the rapid development of metagenomic sequencing, numerous studies have indicated that the dysregulation of lncRNAs is closely associated with diverse human diseases, especially cancers. Prostate Gene Expression Marker 1 (PCGEM1), a recently identified lncRNA, has been reported to play a crucial role in the initiation and progression of multiple tumors by interacting with pivotal regulators of tumor-related signaling pathways. In this review, we will retrospectively review the recent studies of the expression of lncRNA PCGEM1 in human cancers and comprehensively describe the underlying regulatory mechanism by which PCGEM1 functions in tumors. More importantly, based on the relationship between PCGEM1 and cancers, the potential application of PCGEM1 in clinical diagnosis, prognosis and therapeutic treatment will also be highlighted.

Keywords: lncRNA, PCGEM1, cancer, mechanism, biomarker

OPEN ACCESS

Edited by:
Valeria Poli,
University of Turin, Italy

Reviewed by:
Fatemeh Mirzadeh Azad,
Tarbiat Modares University, Iran
Mara Maldotti,
University of Turin, Italy

****Correspondence:***
Lanjuan Li
ljli@zju.edu.cn
Juan Lu
lujuanzju@zju.edu.cn

†These authors have contributed equally to this work

Specialty section:
This article was submitted to Molecular and Cellular Oncology, a section of the journal Frontiers in Oncology

Received: *03 January 2022*
Accepted: *31 January 2022*
Published: *21 February 2022*

Citation:
Su Y, Gu X, Zheng Q, Zhu L, Lu J and Li L (2022) LncRNA PCGEM1 in Human Cancers: Functions, Mechanisms and Promising Clinical Utility. Front. Oncol. 12:847745. doi: 10.3389/fonc.2022.847745

1 INTRODUCTION

Cancer is a complex human disease with multiple risk factors that involves biological processes such as genetic mutations, chromosomal remodeling and epigenetic alterations (1). To a certain extent, early diagnosis and timely treatment are the greatest challenges in the field of oncology. As research on the roles of genomic alternations and the immune system further develops, many new biomarkers or therapeutic strategies targeted to specific molecular changes or other biological

Abbreviations: PCGEM1, prostate gene expression marker 1; lncRNAs, long noncoding RNAs; EC, endometrial cancer; HCC, hepatocellular carcinoma; PC, prostate cancer; GC, gastric cancer; TNM, tumor-node-metastasis; LC, lung cancer; NSCLC, non-small-cell lung cancer; CC, cervical cancer; FIGO, International Federation of Gynecology and Obstetrics; CRPC, castration-resistant prostate cancer; DIM, diindolylmethane; ceRNA, competing endogenous RNA; FGF2, fibroblast growth factor 2; WTAP, WT1-associated protein; SOX11, SRY-box transcription factor 11; FBXW11, F-box and WD repeat domain containing 11; AR, androgen receptor; DOT1L, DOT1-like histone H3K79 methyltransferase; PYGO2, pygopus family PHD finger 2; H3K4me, H3 lysine 3 trimethylation; MEF2, myocyte enhancer factor 2; P4HA2, prolyl 4-hydroxylase subunit alpha 2; ETV1, ETS variant 1; EMT, epithelial-mesenchymal transition; TCA, tricarboxylic acid; PSA, prostate-specific antigen.

characteristics have emerged such as specific molecular agonist that enables T cells to mediate tumor killing and generating immune memory more efficiently (2–4). Despite the rapid development of cancer research, the death rate of diverse malignancies remains high due to the lack of efficient interventions. Therefore, new potential molecular biomarkers and therapeutic targets with high sensitivity and specificity need to be investigated.

Long noncoding RNAs (lncRNAs), which are over 200 nucleotides in length, are a class of endogenous and non-protein-coding RNAs (5, 6). The majority of lncRNAs are expressed in particular tissues at specific times and are broadly involved in the transcriptional or posttranscriptional regulation of the expression of coding genes, including key regulators of multiple pathways (7, 8). In recent years, a variety of cancer studies have uncovered that lncRNAs can fulfil oncogenic or tumor-suppressive functions in cancer biology (9), impacting cancer cell biological characteristics such as multiplication capacity, invasiveness and motility through diverse mechanisms (10). Hence, lncRNAs have a powerful effect on the occurrence and development of human cancers. Classified from function, there are four types of lincRNAs: signaling, guide, decoy, and scaffold lncRNAs (1, 11). Signaling lncRNAs are correlated with particular signaling pathways and their expression is often accompanied by active signaling events (9). Guide lncRNAs combine with and direct regulatory protein complexes to specific loci and then regulate downstream biological events. Decoy lncRNAs bind to the target gene promoters and interact with transcription factors or suppressor (9). Scaffold lncRNAs function as a central platform for various protein complexes to connect and target to specific location and then regulate genomic activities. Intriguingly, accumulating evidence has revealed mechanism of action between lncRNAs and another type of noncoding RNA—miRNAs (12). For example, lncRNA CDC6 accelerates breast cancer progression by directly sponging miR-215, which further regulates the expression of CDC6 (13). Thoroughly investigating the features of lncRNAs will greatly expand our current knowledge of cancer biology and provide novel perspectives for oncotherapy.

As one of the earliest oncogenic lncRNAs discovered in prostate cancer (14), PCGEM1 has received increasing attention in recent years. The PCGEM1 gene is located at chromosome 2q32.3, without protein-coding capacity (14) and lncRNA PCGEM1 was found to distribute uniformly in cell nucleus and cytoplasm (15). In the past two decades, many studies have suggested crucial functions of PCGEM1 in the initiation and progression of various cancers, such as renal carcinoma and endometrial cancer (EC) (16, 17). Through diverse functional mechanisms, PCGEM1 has a large effect on downstream genes and then regulates cancer cell proliferation, invasion and apoptosis. PCGEM1 was also reported to modulate oxaliplatin resistance in hepatocellular carcinoma (HCC) (18). PCGEM1 can influence other diseases, such as osteoarthritis and asthma (19–21). More importantly, preclinical experiments and *in vitro* studies have shown the tremendous clinical potential of PCGEM1.

Herein, we summarized the recent progress regarding the dysregulation and cancer-related functions of PCGEM1 in cell lines and clinical samples of different types of cancer. Furthermore, the comprehensive specific molecular mode of action and potential clinical implications of PCGEM1 will also be discussed.

2 ASSOCIATION BETWEEN PCGEM1 AND CLINICOPATHOLOGICAL FEATURES IN CANCERS

In the past few years, PCGEM1 has been widely reported to be aberrantly expressed in various human cancers, such as glioma, oral carcinoma and EC. Associations between the dysregulation of PCGEM1 and clinical characteristics have also been observed in patients. In this section, we will discuss the aberrant expression of PCGEM1 in clinical samples from cancer patients with an emphasis on the correlated clinical features and cancer growth traits in tumor xenograft models (**Table 1**).

2.1 Clinical Samples and Cell Lines

2.1.1 Prostate Cancer

According to global cancer statistics, with approximately 1.4 million new cases and 375,000 related deaths around the world (39), prostate cancer (PC) was the second most common cancer and the fifth leading cause of cancer-related death in 2020. Initially, PCGEM1 was uncovered as an emerging noncoding RNA in prostate cancer and was found to be overexpressed in a significant proportion of tumor tissues (14). Consistently, in subsequent studies, the expression level of PCGEM1 was observed to be higher in PC tissue samples than in matched normal tissues from patients, and the same result was overserved in PC cell line experiments *in vitro* (15, 23, 26), especially in black patients and high-risk patients with a family history of PC (25). Moreover, the overexpression of PCGEM1 is positively correlated with PC initiation, progression and chemotherapy resistance, which indicates the potential tumor-related functions of PCGEM1. Notably, Parolia et al. (15) revealed that PCEGM1 was upregulated in primary PC in early stages but not in metastasized PC (15). And genes positively associated with PCGEM1 expression were significantly downregulated in higher grade PC patients from multiple independent studies. Thus, the clinical expression profile of PCGEM1 warrants further research in different tumor stages.

2.1.2 Gastric Cancer

Gastric cancer (GC) ranks fourth in mortality and fifth in incidence globally (40), accounting for over 1 million new cases and approximately 769,000 deaths in 2020. On account of the lack of distinct clinical symptoms or credible biomarkers in the early stage and the poor prognosis, GC remains a major clinical challenge worldwide (41, 42). Reports from the last few years have indicated that aberrantly expressed lncRNA PCGEM1 may influence the occurrence and metastasis of GC. The expression level of PCGEM1 in GC tissues is higher than that in adjacent normal tissues (28, 29). Furthermore, the expression level of PCGEM1 is significantly correlated with tumor-node-metastasis (TNM) stage and tumor differentiation in GC (29). *In vitro* experiments also verified PCGEM1 overexpression in GC cell lines (30, 43).

TABLE 1 | Expression files of PCGEM1 and relevant clinicopathological features in various cancers.

Cancer type	Expression	Samples	Animal experiment	Clinicopathological features	Refs
PC	upregulated	/	tumor xenograft volume, tumor growth rate, tumor weight	/	(22)
PC	upregulated	60 PC tissues and adjacent normal tissues from patients	/	/	(23)
PC	upregulated	Matched PC and adjacent normal tissues from patients	/	/	(14)
PC	upregulated	/	tumor xenograft volume, tumor growth rate	/	(24)
PC	upregulated	131 primary PC tissues, 19 metastasized PC tissues and 29 normal tissues from patients	AR regulates expression of PCGEM1 in vivo	tumor stage	(15)
PC	upregulated	90 PC tissues and adjacent normal tissues from patients	/	family history of CaP	(25)
PC	upregulated	Matched PC and adjacent normal tissues from patients	tumor xenograft volume, tumor growth rate	/	(26)
PC	upregulated	Non-DRE urine from 271 PC patients	/	biopsy grade	(27)
GC	upregulated	40 GC tissues and adjacent normal tissues from patients	/	/	(28)
GC	upregulated	cancer and normal tissues from 317 GC patients and 100 healthy individuals	/	tumor differentiation, TNM stage	(29)
GC	upregulated	/	/	/	(30)
NSCLC	upregulated	NSCLC and adjacent normal tissues from 50 patients	/	/	(31)
NSCLC	upregulated	40 NSCLC tissues and adjacent normal tissues from patients	/	/	(32)
NSCLC	upregulated	NSCLC and adjacent normal tissues from 48 patients	/	lymph node metastasis, TNM stage	(33)
Cervical carcer	upregulated	/	/	/	(34)
Cervical carcer	upregulated	68 GC tissues and adjacent normal tissues from patients	/	FIGO stage, lymph node, distant metastasis and prognosis	(35)
EC	upregulated	95 EC tissues and 27 normal tissues from patients	tumor xenograft volume, tumor growth rate	tumor stage	(17)
Ovarian Carcinoma	upregulated	50 epithelial ovarian cancer tissues and 14 normal tisseus from patients	tumor xenograft volume, tumor growth rate	tumor differentiation	(36)
HCC	upregulated	/	/		(18)
Oral carcinoma	upregulated	60 GC tissues and adjacent normal tissues from patients	/	tumor differentiation, TNM stage, lymph node metastasis	(37)
Glioma	upregulated	43 glioma tissues and adjacent normal tissues from patients	tumor xenograft volume, tumor growth rate	WHO grades, prognosis, overall survival rate	(38)
Renal carcinoma	upregulated	renal carcinoma cancer and normal tissues from 47 patients	/	Prognose, TNM stage, tumor size and metastasis	(16)

2.1.3 Non-Small-Cell Lung Cancer

With approximately 2.2 million new cases and 1.8 million deaths in 2020 globally, lung cancer (LC) is the major cause of cancer-related mortality (18.0% of the total cancer-related deaths) (44). Non-small-cell lung cancer (NSCLC) currently accounts for the majority of LC cases (more than 85%) (45), and the 5-year overall survival rate is below 15.9% (46). In recent years, accumulating studies have uncovered that PCGEM1 is abnormally expressed and functions as a powerful tumor regulator in NSCLC. The expression levels of PCGEM1 in NSCLC tissues are significantly higher than those in adjacent normal tissues. PCGEM1 expression have also been quantified in NSCLC cell lines and is notably upregulated compared to that in normal control cells (31–33). Moreover, PCGEM1 expression is closely associated with TNM stage (P=0.020) and lymph node metastasis (P=0.034) (33).

2.1.4 Female Reproductive System Cancers

Cervical cancer (CC) and EC are two commonly diagnosed female cancers worldwide and accounted for approximately 342,000 cases and 97,000 deaths in 2020 (39). The *in situ* recurrence rate is more than 17% in CC patients, and the 5-year survival rate is less than 20% (47, 48). The 5-year survival rate of patients with stage IV EC is merely 5–15% (49). Recently, several studies have demonstrated that PCGEM1 expression is markedly upregulated in both CC and EC tissues versus normal tissues (17, 34, 35). Moreover, the overexpression of PCGEM1 is significantly associated with advanced International Federation of Gynecology and Obstetrics (FIGO) stage, lymph node and distant metastasis and a poor prognosis (35). Similarly, the PCGEM1 expression level in EC was positively correlated with the tumor stage (17). In ovarian cancer, another legal gynecological malignancy, PCEGM1 was also observed to be highly expressed in ovarian cancer tissues and PCGEM1 was higher in poor differentiation group than in well differentiation group (36).

2.1.5 Other Tumors

Consistent with the above results, PCEGM1 is reported to be aberrantly upregulated in other tumors. In glioma, the most common primary malignant cancer of the central nervous system (50), the expression of PCGEM1 was significantly elevated in higher WHO grade and the lower overall survival rate of patients (38). Additionally, PCGEM1 overexpression is

positively correlated with tumor differentiation, TNM stage and lymph node metastasis in both renal carcinoma and oral carcinoma (16, 37). Broadly speaking, these findings indicate the aberrant expression profiles of PCGEM1 in the different types of cancer and the crucial relation of PCGEM1 and clinicopathological characteristics of cancer, which indicates that PCGEM1 probably plays an important role in the initiation and progression of various cancers.

2.2 Tumor Xenograft Model

To reveal the roles of PCGEM1 in diverse cancers, an *in vivo* tumor xenograft model was established by researchers, and the effects of PCGEM1 on tumor growth (tumor volume, tumor weight and tumor growth rate, **Table 1**) were evaluated. An article published in *Nature* suggested that shRNA-mediated inhibition of PCGEM1 strongly suppressed tumor growth in a CWR22Rv1-induced PC xenograft mouse model, indicating a significant regulatory effect of PCGEM1 on the growth of castration-resistant prostate cancer (CRPC) (26). Ho et al. (22) found that 3,3'-diindolylmethane (DIM) could inhibit PC tumor growth by suppressing PCGEM1 expression in a xenograft mouse model (22). Furthermore, siRNA PCGEM1 had a potent diminishing effect on PC tumor volume, whereas PCGEM1 overexpression had an adverse effect (24). Further studies in other tumors reported that the tumor growth of the PCGEM1 groups was greater than that of the control groups in *in vivo* experiments of OC, EC and glioma (17, 36, 38).

3 FUNCTIONS OF PCGEM1 AND UNDERLYING MECHANISMS

Apart from the association between dysregulated expression profiles and clinicopathological characteristics of PCGEM1 in multiple cancers, related biological effects and diverse underlying mechanisms were also explored through *in vitro* and *in vivo* experiments. Generally, PCGEM1 facilitates oncogenic pathophysiologic processes such as cancer cell proliferation and invasion through multiple axes or key modulators. In the next section, we will review the biological roles of PCGEM1 in tumors and the underlying mechanisms of PCGEM1 functions, highlighting the upstream regulators and downstream effectors in the network model. Additionally, the comprehensive functions of PCGEM1 and pivotal molecules in various tumors are listed in **Table 2**.

3.1 Cell Growth and Apoptosis

3.1.1 CeRNA Activity

Human cancers share common characteristics descried as hallmarks, among which excessive proliferation and hypoactive apoptosis are the most prominent (57). With the progress regarding molecular biology techniques such as RNA immunoprecipitation, RNA pull-down and luciferase reporter assays, the competing endogenous RNA (ceRNA) (lncRNA-miRNA-mRNA) network has been universally acknowledged to exert a crucial impact on physiological and pathological processes that PCGEM1 mediates in cancers (**Figure 1**) (58). Some lncRNAs contain sequence motifs which could interact with the complementary regions of targeted miRNAs which regulate genes by suppressing protein translation or degrading target mRNAs through binding to targeted mRNAs (59, 60). Hence, these lncRNAs compete with targeted mRNAs and release the negative regulatory effect of miRNA on mRNA. Cai et al. (16) found that PCGEM1 in renal carcinoma cell lines could interact with miR-433-3p as a ceRNA and then upregulate fibroblast growth factor 2 (FGF2), leading to enhanced cell proliferation (16). Moreover, promoted cell apoptosis with PCGEM1 silencing was observed by Caspase-3 activity assay (16). In NSCLC cell lines, PCGEM1 was capable of modulating the expression of WT1-associated protein (WTAP) and SRY-box transcription factor 11 (SOX11) by sponging miR-433-3p and miR-590-3p (32, 61), respectively, to strongly promote cell growth. Huang et al. (33) argued that miR-152-3p might be another PCGEM1 target in NSCLC. In CC cell lines, PCGEM1 was also shown to function as a promotor of cell proliferation and cell cycle progression *via* the miR-642a-5p/LGMN axis (34). In addition, PCGEM1 is capable of modulating the NF-kB and β-catenin/TCF pathways, which play a crucial role in oncogenesis and PCGEM1 regulates these two signaling pathways *via* miR-182/F-box and WD repeat domain containing 11 (FBXW11) axis (35). Zhang et al. used a dual luciferase reporter system and revealed these two pathways were enhanced by overexpressed PCGEM1. Moreover, genes regulated by NF-κB and β-catenin/TCF were significantly upregulated by PCGEM1 which was weakened by FBXW11 silencing (35). Other researchers demonstrated that PCGEM1 facilitates cell proliferation and colony formation through the miR-148a/TGFβ2/Smad2, miR-539-5p/CDK6 and miR-129-5p/STAT3 axes in OC, glioma and EC (17, 37, 38), respectively. Moreover, PCGEM1 negatively regulates the expression of miR-145 and miR-148a and then upregulates PC cell proliferation and downregulates cell apoptosis (23, 24), but the downstream target genes of this axis remain to be explored. In general, interactions with diverse miRNAs are of paramount importance in the oncogenic functions of PCGEM1 (**Figure 1**).

3.1.2 Scaffolding Activity

Endonuclear functions of PCGEM1, e.g. interacting with transcription factors, chromatin looping and hindering DNA repair are also key aspects of diverse cellular processes. Androgen receptor (AR) is an essential transcription factor for many central genes regulating prostate cell growth, and the AR signaling pathway plays a crucial role in the occurrence and development of PC (62). Hence, AR pathway inhibitors have achieved favorable results in most cases and are the long-standing first-line treatment for PC (63). However, the AR transduction pathway can function in a ligand-independent manner when PC became castration-resistant after initial androgen-deprivation treatment (26). Some studies demonstrated a close association between PCGEM1 and AR signaling. Functional assays in PC cell lines revealed the oncogenic roles of PCGEM1, indicated by the enhancement of proliferation and colony formation and the inhibition of

TABLE 2 | Functions and upstream/downstream regulators of PCGEM1 in various cancer cell lines.

Cancer type	Cell lines	Upstream regulators	Target	Downstream molecules/pathways	Function	Biological effect	Refs
Renal carcinoma	HK-2, OSRC-2, ACHN, A498, 786O	/	miR-433-3p	FGF2	oncogenic	cell proliferation, migration, apoptosis	(16)
PC	LNCaP	/	/	/	oncogenic	drug susceptibility, autophagy	(51)
PC	LNCaP, LNCap95, CWR22Rv1	DIM/p54/nrb	/	AR3	oncogenic	cell apoptosis	(22)
PC	LNCaP, DU145, PC-3, PrEC	MEF2	miR-148a	/	oncogenic	cell proliferation, apoptosis	(23)
PC	RWPE-1, HEK293T, LNCaP	/	miR-145	/	oncogenic	cell proliferation, invasion and migration, apoptosis	(24)
PC	/	androgen in vivo	/	/	oncogenic	/	(15)
PC	PCGEM1, NIH3T3, LNCaP	/	/	Rb (Ser807/811)	oncogenic	cell cycle, cell proliferation, colony formation	(25)
PC	LNCaP, PC3, HEK293T	/	AR+c-Myc	Metabolic genes	oncogenic	cell growth, cell cycle progression/proliferation, apoptosis; carbohydrate metabolism, lipid synthesis, glutamine metabolism, and TCA cycle	(52)
PC	LNCaP	/	/	p53/p21	oncogenic	apoptosis	(53)
PC	LNPCaP, RWPE, WPE, LNCaP-cds1, LNCaP-cds2, CWR22Rv1	/	AR	AR target genes	oncogenic	/	(26)
PC	PC-3, DU145	cholesterol and phytosterols	/	/	oncogenic	cell proliferation, mitosis, apoptosis	(54)
PC	LNCaP, LNCaP-AR+, VCaP	PCA3	/	/	oncogenic	cell proliferation	(55)
PC	PC3, DU145, LNCaP	γ-oryzanol	/	/	oncogenic		(56)
GC	BGC-823, SGC-7901, GES-1	/	miR-129-5p	P4HA2	oncogenic	cell invasion and metastasis	(43)
GC	GSE-1, SGC-7901, BGC-823	hypoxia-responsive		SNAI1	oncogenic	cell invasion and metastasis; EMT	(28)
GC	/	/	/	/	oncogenic	/	(29)
GC	AGS, MKN45	/		SNAI1	oncogenic	cell invasion and migration; EMT	(30)
NSCLC	BEAS-2B, A549, NCI-H1299, NCI-H1650, PC-9	/	miR-433-3p	WTAP	oncogenic	cell proliferation, migration and invasion, apoptosis	(31)
NSCLC	A549, H1299, H460, H1975, BEAS-2B, HEK293T	/	miR-590-3p	SOX11	oncogenic	cell viability, proliferation, invasion and migration	(32)
NSCLC	SK-MES-1, A549, H460, H522, NHBE	/	miR-152-3p	/	oncogenic	cell proliferation, invasion and migration	(33)
HCC	Hep3B/OXA	/	miR-129-5p	ETV1	oncogenic	cell invasion and migration, cell viabililty, oxaliplatin resistance	(18)
Cervical carcer	HeLa, SiHa, Caski, H8	/	miR-642a-5p	LGMN	oncogenic	cell cycle, cell proliferation, invasion and migration	(34)
Cervical cancer	Ect1/E6E7, C33A, HeLa, SiHa, CaSki	/	miR-182	FBXW11/NF-κb+β-catenin/TCF	oncogenic	cell cycle, cell proliferation, invasion and migration, EMT	(35)
Ovarian Carcinoma	A2780, OVCAR3	/		RhoA/YAP, MMP2, Bcl-xL, P70S6K	oncogenic	cell proliferation, invasion and migration, cell apoptosis	(36)
Oral carcinoma	OMEC, KB, BcaCD885, SCC-4, CAL27, SCC-15	/	miR-148a	TGFβ2/Smad2	oncogenic	cell proliferation, invasion and migaration	(37)
Glioma	U251, U-87, LN-229, NHA	/	miR-539-5p	CDK6	oncogenic	cell growth, proliferation, colony formation, invasion and migration	(38)
EC	RPMI-1640, DMEM, Ishikawa, HEC-1B	/	miR-129-5p	STAT3	oncogenic	cell proliferation, invasion and migration, apoptosis	(17)

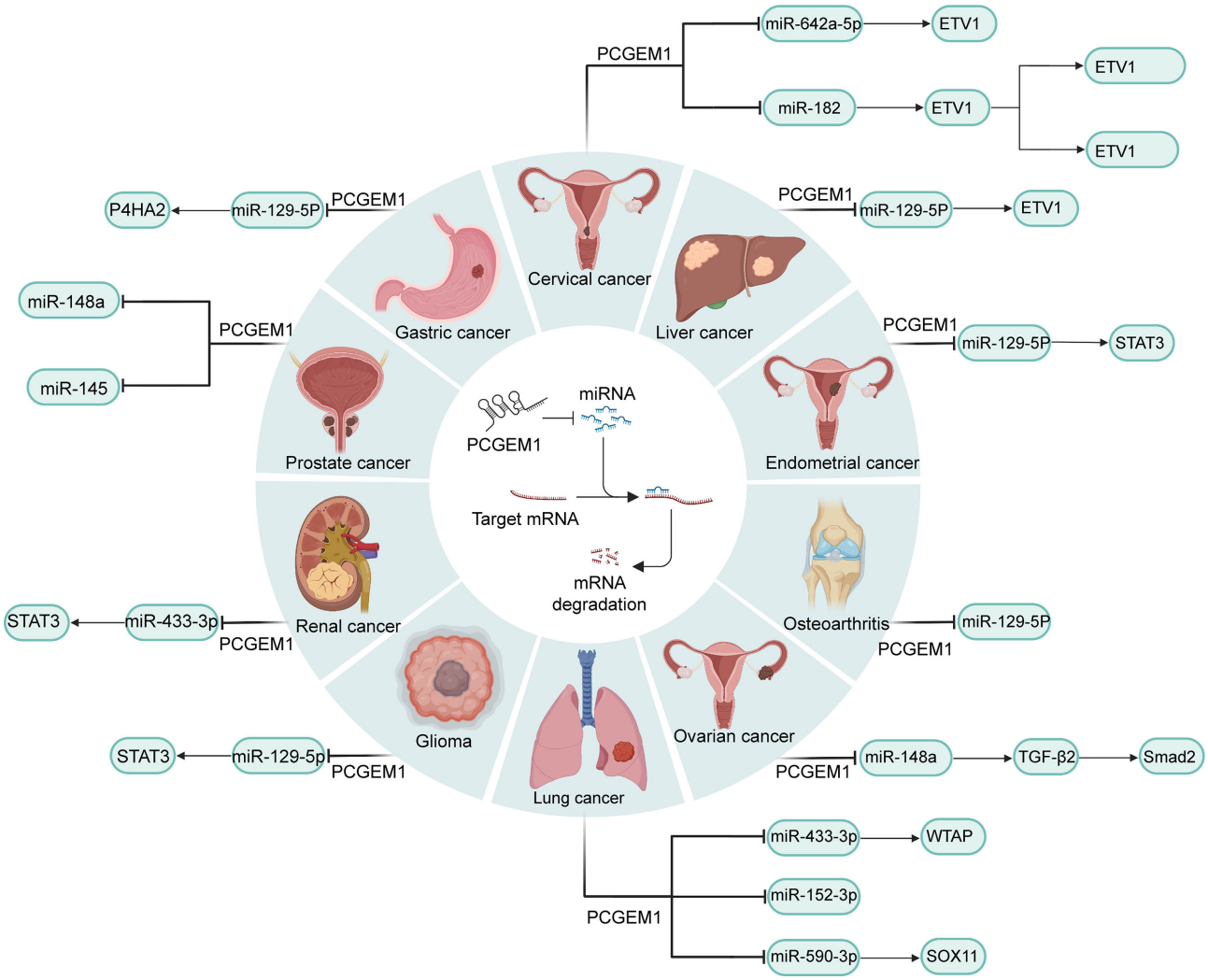

FIGURE 1 | PCGEM1-miRNA-mRNA networks in various cancers. By combining with diverse miRNAs that degrade mRNAs or repress translation at a posttranscriptional level, PCGEM1 modulates the expression of key factors in tumor-related pathways, such as STAT3, Smad2 and NF-kB.

apoptosis (22, 25, 53, 64). In terms of the mechanism (**Figure 2**), Yang et al. (26) demonstrated that PCGEM1 cooperates with another lncRNA, PRNCR1, in AR-targeted gene transcription. Further studies revealed that PRNCR1 combines with the acetylated C-terminus of AR enhancers and then recruits DOT1-like histone H3K79 methyltransferase (DOT1L), which subsequently methylates AR at K349 in the N-terminus and links PCGEM1 to AR. PCGEM1 also enhances the recruitment of pygopus family PHD finger 2 (PYGO2) to the enhancer-promoter loop, were it can interact with a typical histone promoter mark—H3 lysine 3 trimethylation (H3K4me), leading to the transcription of AR target genes (26). Nevertheless, a subsequent study indicated that PCGEM1 neither associated with CRPC nor combined with AR (65). Regardless of this, the crucial roles of PCGEM1 have been studied extensively in PC cells.

Intriguingly, PCGEM1 transcription could be upregulated by myocyte enhancer factor 2 (MEF2) and p54/nrb which enhance the activity of the PCGEM1 promoter (22, 23) (**Figure 3**). Moreover, Parolia et al. (15) observed that PCGEM1 was significantly downregulated after castration and upregulated upon AR activation *in vivo*; no such phenomenon was observed *in vitro*, indicating different transcriptional procedures *in vivo* and *in vitro* (15). Another functional study demonstrated that PCGEM1 expression could be upregulated by cholesterols even in androgen-insensitive PC cell lines; this promoted cell growth and motility, which could be reversed by phytosterols (54).

3.2 Cell Motility

Metastasis is the dominant cause of advanced tumor stage (66), and enhanced cell invasion and migration and PCGEM1 overexpression have been observed in diverse cancer cell lines. Zhang et al. (43)

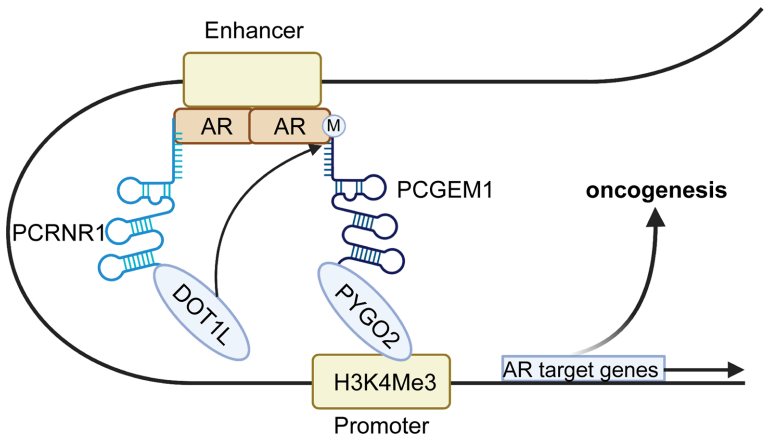

FIGURE 2 | Mechanism by which PCGEM1 mediates AR target gene transcription. First, PRNCR1 combines with the acetylated AR on the enhancer and subsequently recruits DOT1-like histone H3K79 methyltransferase (DOT1L), which induces AR methylation at K349. Later, PCGEM1 is recruited to the AR and enhances PYGO2 to recognize a canonical promoter histone mark (H3K4me), thereby stabilizing enhancer-promoter looping to contribute to AR gene transcription and oncogenesis.

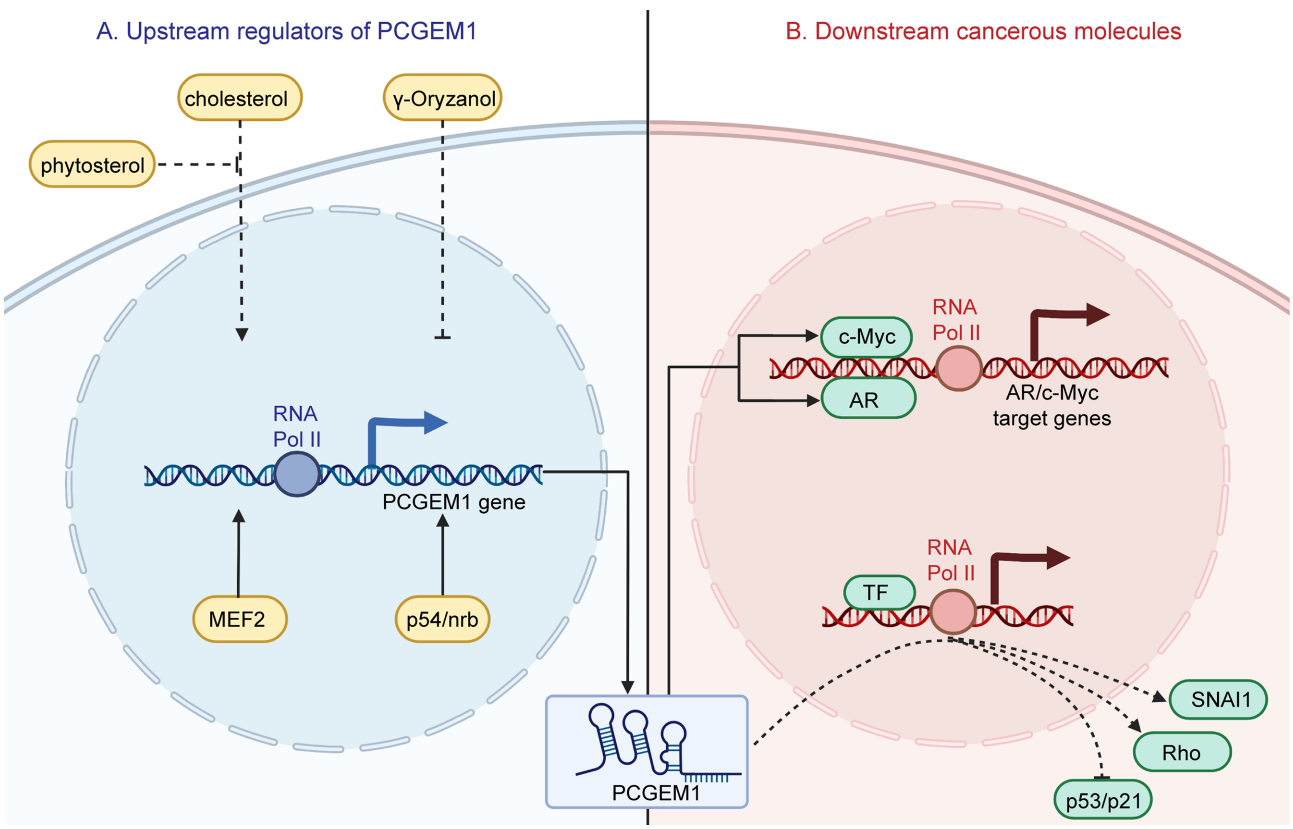

FIGURE 3 | Upstream regulators of PCGEM1 and their effects on downstream cancerous molecules. **(A)** Cholesterol upregulates PCGEM1 expression, which could be reversed by phytosterol. In addition, γ-oryzanol downregulates PCGEM1. MEF2 and p54/nrb could promote PCGEM1 expression at the transcriptional level. **(B)** Regarding downstream effects, PCGEM1 could interact with AR and c-Myc to promote target gene expression. Moreover, overexpressing PCGEM1 promotes the expression of SNAI1 and Rho and delays the induction of p53/p21.

revealed that PCGEM1 facilitates GC cell invasion and metastasis *via* the miR-129-5p/prolyl 4-hydroxylase subunit alpha 2 (P4HA2) axis (43). In HCC, PCGEM1 silencing significantly suppressed the motility of Hep3B/OXA cells. Mechanistically, PCGEM1 acts as a molecular sponge of miR-129-5p to upregulate ETS variant 1 (ETV1) expression (18). Epithelial-mesenchymal transition (EMT), an essential trigger of cell invasion and migration, is closely associated with cancer progression (67, 68). Further functional assays in GC cells demonstrated that PCGEM1 promoted invasion and motility of GC cells through regulating SNAI1 (28, 30), a transcription factor that modulates the E-cadherin/N-cadherin ratio and induces EMT (69) (**Figure 3**). Piao et al. (30) found that mRNA levels of SNAI1 were not altered by the PCGEM1, but protein levels of SNAI1 were elevated as PCGEM1 was overexpressed. And then they found that the stability of SNAI1 protein significantly increased in GC cells co-cultured with exosomes that were rich in PCGEM1.

3.3 Metabolism

For the most part, dysregulated metabolism is interwoven with the fundamental hallmarks of cancers, either as a cause or as a consequence (70). For example, the resistance of cancer cell mitochondria to apoptosis-related permeabilization is closely associated with the variant contribution of these organelles to cancer cell metabolism (71). Cancer-cellular activities require more energy and biosynthetic activity to generate multiple macromolecular complexes throughout the cell cycle (72). Hence, it is not surprising that the metabolic activities of cancer cells and normal cells are completely disparate. Hung et al. (52) indicated that PCGEM1 regulates multiple metabolic genes and subsequently affects diverse metabolic pathways, including carbohydrate metabolism, lipid synthesis, glutamine metabolism and the tricarboxylic acid (TCA) cycle. In terms of mechanism, PCGEM1 combines with the promoters of metabolic genes and enhances the recruitment of c-Myc (73, 74), which is implicated in modulating cellular metabolism as a significant transcription factor, inducing alterations of metabolic processes at the transcriptional level (52) (**Figure 3**).

4 CLINICAL PROSPECTS OF PCGEM1

Biomarkers are defined as biological molecules existing in serum, other body fluids or human tissues that could be measured and assessed to indicate biological processes and disease features. Biomarkers are principally used for disease diagnosis and prognosis evaluation, prediction of the disease tendency, and evaluation of the response to treatment, facilitating the improvement of intervention measures for patients (75, 76). The search for effective biomarkers for PC has been ongoing for a few decades, and it has come a long way owing to advanced genomic technologies and tools (77, 78). However, the discovered specific biomarkers may be invalidated by tumor heterogeneity because these molecular mediators are closely correlated with cancer etiopathogenesis (79). Prostate-specific antigen (PSA) has been extensively used for PC screening and monitoring for a long time, but its sensitivity and specificity are inherently limited by the cancer concealment and nonsignificant increases in expression (80, 81). Considering these limitations, the thorough investigation of up/downstream molecules and the relation of biomarkers with tumor etiology is indispensable.

Above, we discussed the expression profiles and oncogenic roles of PCGEM1 in various tumors. As a novel noncoding RNA, it was confirmed to be overexpressed in PC, especially in African-American patients (14), and was found to be significantly associated with CRPC. The close relationship between PCGEM1 and clinical features, including tumor stage, metastasis and overall survival rate, has also been well demonstrated. Notably, PCGEM1 is highly expressed in noncancer prostate tissues of PC patients with a family history of PC (25). Xue and colleagues revealed that polymorphisms of PCGEM1 may make contribution to PCa risk in Chinese men (82). All of the above findings indicate its potential for early prevention, diagnosis and prognosis evaluation as a favorable biomarker. More encouragingly, the interaction between PCGEM1 and AR in PC has been brilliantly described (26), which provides new ideas for early detection and a novel therapeutic target for PC. From previous studies in multiple separate laboratories, there seems to be no consensus on the interaction of PCGEM1 and AR, although these controversial findings were preliminarily interpreted through *in vivo* and *in vitro* experiments (15, 26, 52, 65). The expression of PCGEM1 in peripheral blood was also measured in a study enrolling 144 patients with PC, and PCGEM1 expression was significantly higher in metastatic group than localized group. Moreover, the expression level in patients with poor prognosis was critically upregulated (83). Another study carried out in a multiracial population demonstrated that a 2-gene (PC3 and PCEGM1) expression panel in urine exosomes could differentiate aggressive PC from nonaggressive PC (27). Thus, the promising application of PCGEM1 needs more evaluation. Because of the important roles by which PCGEM1 facilitates PC progression in an AR-dependent or AR-independent manner, PCGEM1-targeted treatment is also an attractive area of study. For example, PCGEM1 silencing could increase the sensitivity of PC cells to baicalein and enzalutamide (51, 55), laying the groundwork for PC combination therapy. Further clinical trials are needed to design and assess the therapeutic effects of targeting PCGEM1. PCGEM1 is also regarded as a potential target in other tumors. For example, it could modulate oxaliplatin resistance *via* the miR-129-5p/ETV1 axis in HCC, indicating a promising strategy for combating HCC chemotherapy resistance (18). Currently, endoscopy and biopsy are the standard diagnostic approaches for GC, and their utility is confined to the invasiveness of the disease and limited medical resources (84). Jiang et al. (29) assessed PCGEM1 expression in GC patient serum and found that it could reflect the pathophysiological state of GC (29), demonstrating that this molecule might be a favorable indicator for GC diagnosis and prognosis.

5 CONCLUSION

As an important member of the lncRNA family located on chromosome 2q32, PCGEM1 has been confirmed to function as a

tumor promotor in diverse tumors. In this review, we presented retrospective evidence of its upregulated expression based on data from multiple cancer cell lines and matched tumor/nontumor tissues. Additionally, tumor xenograft growth in a mouse model and clinical features in patients, such as tumor stage and metastasis, were found to be significantly associated with PCGEM1 dysregulation. Functional analysis also revealed that multiple biological effects, including proliferation, invasion and migration, apoptosis, drug resistance and metabolism of cancer cells, could be potently modulated by PCGEM1 overexpression. Thus, this oncogenic lncRNA plays a critical role in the initiation and progression of cancers. In terms of the underlying mechanisms, diverse modes of PCGEM1 action in various cancers with different regulatory factors and downstream signaling pathways or molecules have been investigated in various cancer types. Even in a given cancer type, such as PC, PCGEM1 functions in various ways, including the lncRNA-miRNA-mRNA network and interaction with transcription factors. Our comprehensive interpretation of the underlying molecular mechanism of PCGEM1 seems feasible, but some questions and challenges still exist. For example, what accounts for the differences in the PCGEM1 transcriptional process *in vivo* and *in vitro*? Are there other tumor-related factors co-acting with PCGEM1?

Overall, the exploration of PCGEM1 in the oncology field is undoubtedly in the initial stage. To comprehensively understand its biological roles at multiple tumor stages, we must perform additional studies. From the standpoint of etiology, clarification of the comprehensive signaling network of PCGEM1 will provide us with more challenges and opportunities to exploit novel strategies for early prevention, specific diagnosis, accurate treatment to improve the prognosis by targeting PCGEM1.

AUTHOR CONTRIBUTIONS

LL and JL designed and guided the study. YS, XG, and QZ wrote and edited the manuscript. LZ helped with reference collection. All authors read and approved the final manuscript.

FUNDING

This work was funded by the National Key Research and Development Program of China (2021YFC2301800), and the National Nature Science Foundation of China (U20A20343).

REFERENCES

1. Bhan A, Soleimani M, Mandal SS. Long Noncoding RNA and Cancer: A New Paradigm. *Cancer Res* (2017) 77:3965–81. doi: 10.1158/0008-5472.Can-16-2634
2. Tsimberidou AM, Fountzilas E, Nikanjam M, Kurzrock R. Review of Precision Cancer Medicine: Evolution of the Treatment Paradigm. *Cancer Treat Rev* (2020) 86:102019. doi: 10.1016/j.ctrv.2020.102019
3. Vonderheide RH, Glennie MJ. Agonistic CD40 Antibodies and Cancer Therapy. *Clin Cancer Res* (2013) 19:1035–43. doi: 10.1158/1078-0432.Ccr-12-2064
4. Byrne KT, Vonderheide RH. CD40 Stimulation Obviates Innate Sensors and Drives T Cell Immunity in Cancer. *Cell Rep* (2016) 15:2719–32. doi: 10.1016/j.celrep.2016.05.058
5. Nair L, Chung H, Basu U. Regulation of Long Non-Coding RNAs and Genome Dynamics by the RNA Surveillance Machinery. *Nat Rev Mol Cell Biol* (2020) 21:123–36. doi: 10.1038/s41580-019-0209-0
6. Kopp F, Mendell JT. Functional Classification and Experimental Dissection of Long Noncoding RNAs. *Cell* (2018) 172:393–407. doi: 10.1016/j.cell.2018.01.011
7. Rinn JL, Chang HY. Genome Regulation by Long Noncoding RNAs. *Annu Rev Biochem* (2012) 81:145–66. doi: 10.1146/annurev-biochem-051410-092902
8. Chen LL. Linking Long Noncoding RNA Localization and Function. *Trends Biochem Sci* (2016) 41:761–72. doi: 10.1016/j.tibs.2016.07.003
9. Wapinski O, Chang HY. Long Noncoding RNAs and Human Disease. *Trends Cell Biol* (2011) 21:354–61. doi: 10.1016/j.tcb.2011.04.001
10. Martens-Uzunova ES, Böttcher R, Croce CM, Jenster G, Visakorpi T, Calin GA. Long Noncoding RNA in Prostate, Bladder, and Kidney Cancer. *Eur Urol* (2014) 65:1140–51. doi: 10.1016/j.eururo.2013.12.003
11. Wang KC, Chang HY. Molecular Mechanisms of Long Noncoding RNAs. *Mol Cell* (2011) 43:904–14. doi: 10.1016/j.molcel.2011.08.018
12. Salmena L, Poliseno L, Tay Y, Kats L. Pandolfi PP. A ceRNA Hypothesis: The Rosetta Stone of a Hidden RNA Language? *Cell* (2011) 146:353–8. doi: 10.1016/j.cell.2011.07.014
13. Kong X, Duan Y, Sang Y, Li Y, Zhang H, Liang Y, et al. LncRNA-CDC6 Promotes Breast Cancer Progression and Function as ceRNA to Target CDC6 by Sponging microRNA-215. *J Cell Physiol* (2019) 234:9105–17. doi: 10.1002/jcp.27587
14. Srikantan V, Zou Z, Petrovics G, Xu L, Augustus M, Davis L, et al. PCGEM1, a Prostate-Specific Gene, Is Overexpressed in Prostate Cancer. *Proc Natl Acad Sci USA* (2000) 97:12216–21. doi: 10.1073/pnas.97.22.12216
15. Parolia A, Crea F, Xue H, Wang Y, Mo F, Ramnarine VR, et al. The Long Non-Coding RNA PCGEM1 Is Regulated by Androgen Receptor Activity *In Vivo*. *Mol Cancer* (2015) 14:46. doi: 10.1186/s12943-015-0314-4
16. Cai X, Zhang X, Mo L, Zhu J, Yu H. LncRNA PCGEM1 Promotes Renal Carcinoma Progression by Targeting miR-433-3p to Regulate FGF2 Expression. *Cancer biomark* (2020) 27:493–504. doi: 10.3233/cbm-190669
17. Li Q, Shen F, Zhao L. The Relationship Between lncRNA PCGEM1 and STAT3 During the Occurrence and Development of Endometrial Carcinoma. *BioMed Pharmacother* (2018) 107:918–28. doi: 10.1016/j.biopha.2018.08.091
18. Chen J, Yuan D, Hao Q, Zhu D, Chen Z. LncRNA PCGEM1 Mediates Oxaliplatin Resistance in Hepatocellular Carcinoma *via* miR-129-5p/ETV1 Axis *In Vitro*. *Adv Clin Exp Med* (2021) 30:831–8. doi: 10.17219/acem/135533
19. Zhao Y, Xu J. Synovial Fluid-Derived Exosomal lncRNA PCGEM1 as Biomarker for the Different Stages of Osteoarthritis. *Int Orthop* (2018) 42:2865–72. doi: 10.1007/s00264-018-4093-6
20. Kang Y, Song J, Kim D, Ahn C, Park S, Chun CH, et al. PCGEM1 Stimulates Proliferation of Osteoarthritic Synoviocytes by Acting as a Sponge for miR-770. *J Orthop Res* (2016) 34:412–8. doi: 10.1002/jor.23046
21. Xu Z, Meng L, Xie Y, Guo W. lncRNA PCGEM1 Strengthens Anti-Inflammatory and Lung Protective Effects of Montelukast Sodium in Children With Cough-Variant Asthma. *Braz J Med Biol Res* (2020) 53:e9271. doi: 10.1590/1414-431x20209271
22. Ho TT, Huang J, Zhou N, Zhang Z, Koirala P, Zhou X, et al. Regulation of PCGEM1 by P54/Nrb in Prostate Cancer. *Sci Rep* (2016) 6:34529. doi: 10.1038/srep34529
23. Zhang S, Li Z, Zhang L, Xu Z. MEF2–Activated Long Non–Coding RNA PCGEM1 Promotes Cell Proliferation in Hormone–Refractory Prostate Cancer Through Downregulation of Mir–148a. *Mol Med Rep* (2018) 18:202–8. doi: 10.3892/mmr.2018.8977
24. He JH, Zhang JZ, Han ZP, Wang L, Lv YB, Li YG. Reciprocal Regulation of PCGEM1 and miR-145 Promote Proliferation of LNCaP Prostate Cancer Cells. *J Exp Clin Cancer Res* (2014) 33:72. doi: 10.1186/s13046-014-0072-y

25. Petrovics G, Zhang W, Makarem M, Street JP, Connelly R, Sun L, et al. Elevated Expression of PCGEM1, a Prostate-Specific Gene With Cell Growth-Promoting Function, Is Associated With High-Risk Prostate Cancer Patients. *Oncogene* (2004) 23:605–11. doi: 10.1038/sj.onc.1207069
26. Yang L, Lin C, Jin C, Yang JC, Tanasa B, Li W, et al. lncRNA-Dependent Mechanisms of Androgen-Receptor-Regulated Gene Activation Programs. *Nature* (2013) 500:598–602. doi: 10.1038/nature12451
27. Kohaar I, Chen Y, Banerjee S, Borbiev T, Kuo HC, Ali A, et al. A Urine Exosome Gene Expression Panel Distinguishes Between Indolent and Aggressive Prostate Cancers at Biopsy. *J Urol* (2021) 205:420–5. doi: 10.1097/ju.0000000000001374
28. Zhang J, Jin HY, Wu Y, Zheng ZC, Guo S, Wang Y, et al. Hypoxia-Induced LncRNA PCGEM1 Promotes Invasion and Metastasis of Gastric Cancer Through Regulating SNAI1. *Clin Transl Oncol* (2019) 21:1142–51. doi: 10.1007/s12094-019-02035-9
29. Jiang H, Guo S, Zhao Y, Wang Y, Piao HY, Wu Y, et al. Circulating Long Non-Coding RNA PCGEM1 as a Novel Biomarker for Gastric Cancer Diagnosis. *Pathol Res Pract* (2019) 215:152569. doi: 10.1016/j.prp.2019.152569
30. Piao HY, Guo S, Wang Y, Zhang J. Exosome-Transmitted lncRNA PCGEM1 Promotes Invasive and Metastasis in Gastric Cancer by Maintaining the Stability of SNAI1. *Clin Transl Oncol* (2021) 23:246–56. doi: 10.1007/s12094-020-02412-9
31. Weng L, Qiu K, Gao W, Shi C, Shu F. LncRNA PCGEM1 Accelerates Non-Small Cell Lung Cancer Progression *via* Sponging miR-433-3p to Upregulate WTAP. *BMC Pulm Med* (2020) 20:213. doi: 10.1186/s12890-020-01240-5
32. Wen H, Feng H, Ma Q, Liang C. LncRNA PCGEM1 Induces Proliferation and Migration in Non-Small Cell Lung Cancer Cells Through Modulating the miR-590-3p/SOX11 Axis. *BMC Pulm Med* (2021) 21:234. doi: 10.1186/s12890-021-01600-9
33. Huang J, Lou J, Liu X, Xie Y. LncRNA PCGsEM1 Contributes to the Proliferation, Migration and Invasion of Non-Small Cell Lung Cancer Cells *via* Acting as a Sponge for miR-152-3p. *Curr Pharm Des* (2021) 27:4663–70. doi: 10.2174/1381612827666210827104828
34. Liu Y, Wang Y, Shen X, Chen C, Ni H, Sheng N, et al. Down-Regulation of lncRNA PCGEM1 Inhibits Cervical Carcinoma by Modulating the miR-642a-5p/LGMN Axis. *Exp Mol Pathol* (2020) 117:104561. doi: 10.1016/j.yexmp.2020.104561
35. Zhang Q, Zheng J, Liu L. The Long Noncoding RNA PCGEM1 Promotes Cell Proliferation, Migration and Invasion *via* Targeting the miR-182/FBXW11 Axis in Cervical Cancer. *Cancer Cell Int* (2019) 19:304. doi: 10.1186/s12935-019-1030-8
36. Chen S, Wang LL, Sun KX, Liu Y, Guan X, Zong ZH, et al. LncRNA PCGEM1 Induces Ovarian Carcinoma Tumorigenesis and Progression Through RhoA Pathway. *Cell Physiol Biochem* (2018) 47:1578–88. doi: 10.1159/000490931
37. Weng X, Li JS, Fan S. Mechanism of Long-Chain Noncoding RNA PCGEM1 in the Regulation of the Invasion and Metastasis of Oral Squamous Carcinoma Cells *via* Transforming Growth Factor β2/Smad2 Signaling Pathway. *Hua Xi Kou Qiang Yi Xue Za Zhi* (2020) 38:550–7. doi: 10.7518/hxkq.2020.05.014
38. Liu SL, Chen MH, Wang XB, You RK, An XW, Zhao Q, et al. LncRNA PCGEM1 Contributes to Malignant Behaviors of Glioma by Regulating miR-539-5p/CDK6 Axis. *Aging (Albany NY)* (2021) 13:5475–84. doi: 10.18632/aging.202476
39. Siegel RL, Miller KD, Jemal A. Cancer Statistics, 2020. *CA Cancer J Clin* (2020) 70:7–30. doi: 10.3322/caac.21590
40. Torre LA, Bray F, Siegel RL, Ferlay J, Lortet-Tieulent J, Jemal A. Global Cancer Statistics, 2012. *CA Cancer J Clin* (2015) 65:87–108. doi: 10.3322/caac.21262
41. Thrift AP, El-Serag HB. Burden of Gastric Cancer. *Clin Gastroenterol Hepatol* (2020) 18:534–42. doi: 10.1016/j.cgh.2019.07.045
42. Zhang J, Wu Y, Jin HY, Guo S, Dong Z, Zheng ZC, et al. Prognostic Value of Sorting Nexin 10 Weak Expression in Stomach Adenocarcinoma Revealed by Weighted Gene Co-Expression Network Analysis. *World J Gastroenterol* (2018) 24:4906–19. doi: 10.3748/wjg.v24.i43.4906
43. Zhang T, Piao HY, Guo S, Zhao Y, Wang Y, Zheng ZC, et al. LncRNA PCGEM1 Enhances Metastasis and Gastric Cancer Invasion Through Targeting of miR-129-5p to Regulate P4HA2 Expression. *Exp Mol Pathol* (2020) 116:104487. doi: 10.1016/j.yexmp.2020.104487
44. Sung H, Ferlay J, Siegel RL, Laversanne M, Soerjomataram I, Jemal A, et al. Global Cancer Statistics 2020: GLOBOCAN Estimates of Incidence and Mortality Worldwide for 36 Cancers in 185 Countries. *CA Cancer J Clin* (2021) 71:209–49. doi: 10.3322/caac.21660
45. Black RC, Khurshid H. NSCLC: An Update of Driver Mutations, Their Role in Pathogenesis and Clinical Significance. *R I Med J* (2013) 2015) 98:25–8.
46. Chen Z, Fillmore CM, Hammerman PS, Kim CF, Wong KK. Non-Small-Cell Lung Cancers: A Heterogeneous Set of Diseases. *Nat Rev Cancer* (2014) 14:535–46. doi: 10.1038/nrc3775
47. Amkreutz LCM, Pijnenborg JMA, Joosten DWL, Mertens H, Van Kuijk SMJ, Engelen MJA, et al. Contribution of Cervical Cytology in the Diagnostic Work-Up of Patients With Endometrial Cancer. *Cytopathology* (2018) 29:63–70. doi: 10.1111/cyt.12511
48. Lucia F, Visvikis D, Desseroit MC, Miranda O, Malhaire JP, Robin P, et al. Prediction of Outcome Using Pretreatment (18)F-FDG PET/CT and MRI Radiomics in Locally Advanced Cervical Cancer Treated With Chemoradiotherapy. *Eur J Nucl Med Mol Imaging* (2018) 45:768–86. doi: 10.1007/s00259-017-3898-7
49. Jemal A, Siegel R, Ward E, Hao Y, Xu J, Thun MJ. Cancer Statistics, 2009. *CA Cancer J Clin* (2009) 59:225–49. doi: 10.3322/caac.20006
50. Siegel RL, Miller KD, Fuchs HE, Jemal A. Cancer Statistics, 2021. *CA Cancer J Clin* (2021) 71:7–33. doi: 10.3322/caac.21654
51. Han Z, He J, Zou M, Chen W, Lv Y, Li Y. Small Interfering RNA Target for Long Noncoding RNA PCGEM1 Increases the Sensitivity of LNCaP Cells to Baicalein. *Anat Rec (Hoboken)* (2020) 303:2077–85. doi: 10.1002/ar.24454
52. Hung CL, Wang LY, Yu YL, Chen HW, Srivastava S, Petrovics G, et al. A Long Noncoding RNA Connects C-Myc to Tumor Metabolism. *Proc Natl Acad Sci USA* (2014) 111:18697–702. doi: 10.1073/pnas.1415669112
53. Fu X, Ravindranath L, Tran N, Petrovics G, Srivastava S. Regulation of Apoptosis by a Prostate-Specific and Prostate Cancer-Associated Noncoding Gene, PCGEM1. *DNA Cell Biol* (2006) 25:135–41. doi: 10.1089/dna.2006.25.135
54. Ifere GO, Barr E, Equan A, Gordon K, Singh UP, Chaudhary J, et al. Differential Effects of Cholesterol and Phytosterols on Cell Proliferation, Apoptosis and Expression of a Prostate Specific Gene in Prostate Cancer Cell Lines. *Cancer Detect Prev* (2009) 32:319–28. doi: 10.1016/j.cdp.2008.12.002
55. Özgür E, Celik AI, Darendeliler E, Gezer U. PCA3 Silencing Sensitizes Prostate Cancer Cells to Enzalutamide-Mediated Androgen Receptor Blockade. *Anticancer Res* (2017) 37:3631–7. doi: 10.21873/anticanres.11733
56. Hirsch GE, Parisi MM, Martins LA, Andrade CM, Barbé-Tuana FM, Guma FT. γ-Oryzanol Reduces Caveolin-1 and PCGEM1 Expression, Markers of Aggressiveness in Prostate Cancer Cell Lines. *Prostate* (2015) 75:783–97. doi: 10.1002/pros.22960
57. Macheret M, Halazonetis TD. DNA Replication Stress as a Hallmark of Cancer. *Annu Rev Pathol* (2015) 10:425–48. doi: 10.1146/annurev-pathol-012414-040424
58. Karreth FA, Pandolfi PP. ceRNA Cross-Talk in Cancer: When Ce-Bling Rivalries Go Awry. *Cancer Discovery* (2013) 3:1113–21. doi: 10.1158/2159-8290.Cd-13-0202
59. Kozomara A, Birgaoanu M, Griffiths-Jones S. Mirbase: From microRNA Sequences to Function. *Nucleic Acids Res* (2019) 47:D155–d62. doi: 10.1093/nar/gky1141
60. Bartel DP, Chen CZ. Micromanagers of Gene Expression: The Potentially Widespread Influence of Metazoan microRNAs. *Nat Rev Genet* (2004) 5:396–400. doi: 10.1038/nrg1328
61. Hancocks S. An Ever Present Adversary. *Br Dent J* (2013) 214:603. doi: 10.1038/sj.bdj.2013.584.23787827
62. Mostaghel EA, Plymate SR, Montgomery B. Molecular Pathways: Targeting Resistance in the Androgen Receptor for Therapeutic Benefit. *Clin Cancer Res* (2014) 20:791–8. doi: 10.1158/1078-0432.Ccr-12-3601
63. Sandhu S, Moore CM, Chiong E, Beltran H, Bristow RG, Williams SG. Prostate Cancer. *Lancet* (2021) 398:1075–90. doi: 10.1016/s0140-6736(21)00950-8
64. Lenoski DSWB. Yeats and Celtic Spiritual Power. *Can J Irish Stud* (1979) 5:26–51. doi: 10.2307/25512450
65. Prensner JR, Sahu A, Iyer MK, Malik R, Chandler B, Asangani IA, et al. The lncRNAs PCGEM1 and PRNCR1 Are Not Implicated in Castration Resistant Prostate Cancer. *Oncotarget* (2014) 5:1434–8. doi: 10.18632/oncotarget.1846
66. Fadul J, Zulueta-Coarasa T, Slattum GM, Redd NM, Jin MF, Redd MJ, et al. KRas-Transformed Epithelia Cells Invade and Partially Dedifferentiate by Basal Cell Extrusion. *Nat Commun* (2021) 12:7180. doi: 10.1038/s41467-021-27513-z

67. O'Brien SJ, Bishop C, Hallion J, Fiechter C, Scheurlen K, Paas M, et al. Long Non-Coding RNA (lncRNA) and Epithelial-Mesenchymal Transition (EMT) in Colorectal Cancer: A Systematic Review. *Cancer Biol Ther* (2020) 21:769–81. doi: 10.1080/15384047.2020.1794239
68. Takahashi K, Taniue K, Ono Y, Fujiya M, Mizukami Y, Okumura T. Long Non-Coding RNAs in Epithelial-Mesenchymal Transition of Pancreatic Cancer. *Front Mol Biosci* (2021) 8:717890. doi: 10.3389/fmolb.2021.717890
69. Nieto MA, Cano A. The Epithelial-Mesenchymal Transition Under Control: Global Programs to Regulate Epithelial Plasticity. *Semin Cancer Biol* (2012) 22:361–8. doi: 10.1016/j.semcancer.2012.05.003
70. Kroemer G, Pouyssegur J. Tumor Cell Metabolism: Cancer's Achilles' Heel. *Cancer Cell* (2008) 13:472–82. doi: 10.1016/j.ccr.2008.05.005
71. Berthenet K, Castillo Ferrer C, Fanfone D, Popgeorgiev N, Neves D, Bertolino P, et al. Failed Apoptosis Enhances Melanoma Cancer Cell Aggressiveness. *Cell Rep* (2020) 31:107731. doi: 10.1016/j.celrep.2020.107731
72. Cai L, Ying M, Wu H. Microenvironmental Factors Modulating Tumor Lipid Metabolism: Paving the Way to Better Antitumoral Therapy. *Front Oncol* (2021) 11:777273. doi: 10.3389/fonc.2021.777273
73. Cairns RA, Harris IS, Mak TW. Regulation of Cancer Cell Metabolism. *Nat Rev Cancer* (2011) 11:85–95. doi: 10.1038/nrc2981
74. Ward PS, Thompson CB. Metabolic Reprogramming: A Cancer Hallmark Even Warburg did Not Anticipate. *Cancer Cell* (2012) 21:297–308. doi: 10.1016/j.ccr.2012.02.014
75. Ilyin SE, Belkowski SM, Plata-Salamán CR. Biomarker Discovery and Validation: Technologies and Integrative Approaches. *Trends Biotechnol* (2004) 22:411–6. doi: 10.1016/j.tibtech.2004.06.005
76. Prensner JR, Rubin MA, Wei JT, Chinnaiyan AM. Beyond PSA: The Next Generation of Prostate Cancer Biomarkers. *Sci Transl Med* (2012) 4:127rv3. doi: 10.1126/scitranslmed.3003180
77. Cucchiara V, Cooperberg MR, Dall'Era M, Lin DW, Montorsi F, Schalken JA, et al. Genomic Markers in Prostate Cancer Decision Making. *Eur Urol* (2018) 73:572–82. doi: 10.1016/j.eururo.2017.10.036
78. Coplan B, Fleming S. The Need for Greater Diversity in the PA Profession. *JAAPA* (2019) 32:54–8. doi: 10.1097/01.JAA.0000554743.08935.d0
79. Ifere GO, Ananaba GA. Prostate Cancer Gene Expression Marker 1 (PCGEM1): A Patented Prostate- Specific Non-Coding Gene and Regulator of Prostate Cancer Progression. *Recent Pat DNA Gene Seq* (2009) 3:151–63. doi: 10.2174/187221509789318360
80. Saini S. PSA. And Beyond: Alternative Prostate Cancer Biomarkers. *Cell Oncol (Dordr)* (2016) 39:97–106. doi: 10.1007/s13402-016-0268-6
81. Stenman UH, Leinonen J, Zhang WM, Finne P. Prostate-Specific Antigen. *Semin Cancer Biol* (1999) 9:83–93. doi: 10.1006/scbi.1998.0086
82. Xue Y, Wang M, Kang M, Wang Q, Wu B, Chu H, et al. Association Between Lncrna PCGEM1 Polymorphisms and Prostate Cancer Risk. *Prostate Cancer Prostatic Dis* (2013) 16:139–44, s1. doi: 10.1038/pcan.2013.6
83. Yang W, He FW, Li Y, Zhai YK, Tan B, Wu HX. Long Non-Coding RNA PCGEM1 as a Biomarker for Prostate Cancer. *ScienceAsia* (2016) 42:201–6. doi: 10.2306/scienceasia1513-1874.2016.42.201
84. Chen J, Wu L, Sun Y, Luo C, Chen X, Wu L, et al. Diagnostic Value and Clinical Significance of Circulating miR-650 and CA211 in Detecting of Gastric Carcinoma. *Oncol Lett* (2020) 20:254. doi: 10.3892/ol.2020.12117

Conflict of Interest: The authors declare that the research was conducted in the absence of any commercial or financial relationships that could be construed as a potential conflict of interest.

frontiers in Cell and Developmental Biology

ORIGINAL RESEARCH
published: 14 March 2022
doi: 10.3389/fcell.2022.817028

circSSU72 Promotes Cell Proliferation, Migration and Invasion of Papillary Thyroid Carcinoma Cells by Targeting miR-451a/S1PR2 Axis

*Zeyu Zhang, Fada Xia, Lei Yao, Bo Jiang and Xinying Li**

Department of Thyroid Surgery, Xiangya Hospital, Central South University, Changsha, China

Introduction: Thyroid cancer is the most common endocrine malignancy with Papillary Thyroid Carcinoma (PTC) as the most common pathological type. Due to low mortality but a high incidence, PTC still causes a relatively heavy burden on financial costs, human health, and quality of life. Emerging researches have indicated that circular RNAs (circRNAs) play a significant regulatory role in various cancers, including PTC. However, the functions and mechanisms of circRNAs derived from SSU72 remain unknown.

Method: The expression level of circRNAs derived from the exons of SSU72, miR-361–3p, miR-451a, and S1PR2 was evaluated by qRT-PCR assay or western blot assay. The interactions between circSSU72 (hsa_circ_0009294), miR-451a, and S1PR2 were verified by dual-luciferase reporter assay. Effects of circSSU72, miR-451a, and S1PR2 on cell proliferation, migration, and invasion were confirmed by colony formation assay, cell counting kit-8 (CCK-8), wound healing assay, and Transwell assays *in vitro*.

Results: circSSU72 was upregulated in PTC; circSSU72 knockdown inhibited PTC cell proliferation, migration, and invasion. In addition, circSSU72 could negatively regulate miR-451a by functioning as a sponge. circSSU72 promoted PTC cell proliferation, migration, and invasion by targeting miR-451a *in vitro*. We further found that miR-451a inhibited PTC cell proliferation, migration, and invasion by regulating S1PR2. Overall, the circSSU72/miR-451a/S1PR2 axis might influence PTC cell proliferation, migration, and invasion.

Conclusions: Overall, circSSU72 (hsa_circ_0009294)/miR-451a/S1PR2 axis may promote cell proliferation, migration, and invasion in PTC. Thus, circSSU72 may serve as a potential biomarker and therapeutic target for PTC.

Keywords: thyroid cancer, papillary thyroid carcinoma, circRNAs, cell proliferation, migration, invasion

OPEN ACCESS

Edited by:
Valeria Poli,
University of Turin, Italy

Reviewed by:
Vittorio Colantuoni,
University of Sannio, Italy
Francesca Orso,
University of Turin, Italy

****Correspondence:***
Xinying Li
lixinyingcn@protonmail.com
lixinyingcn@126.com

Specialty section:
This article was submitted to Molecular and Cellular Oncology, a section of the journal Frontiers in Cell and Developmental Biology

Received: *17 November 2021*
Accepted: *31 January 2022*
Published: *14 March 2022*

Citation:
Zhang Z, Xia F, Yao L, Jiang B and Li X (2022) circSSU72 Promotes Cell Proliferation, Migration and Invasion of Papillary Thyroid Carcinoma Cells by Targeting miR-451a/S1PR2 Axis. Front. Cell Dev. Biol. 10:817028. doi: 10.3389/fcell.2022.817028

Abbreviations: ANOVA, One-way analysis of variance; circRNAs, circular RNAs; ceRNAs, competitive endogenous RNAs; CCK8, cell counting kit-8; DMEM, Dulbecco's modifed Eagle's medium; EdU, 5-Ethynyl-20-deoxyuridine; FBS, fetal bovine serum; miRNAs, micro RNAs; PTC, papillary thyroid carcinoma; TC, thyroid cancer.

INTRODUCTION

Thyroid cancer (TC) is the most common endocrine malignancy with papillary thyroid carcinoma (PTC) as the most common pathological type of TC. Although accounting for over 80% TC, PTC usually carries a very good patient prognosis with surgical treatments. (Kim et al., 2020) However, 10–15% of advanced PTC patients suffer from recurrence, and 5–25% from distant metastasis, with radioactive iodine ablation, thyroid-stimulating hormone suppression, and available targeted therapies. (DeGroot et al., 1990; Sebastian et al., 2000; Laha et al., 2020) Due to the low mortality but the high incidence, PTC still causes a relatively heavy burden on financial costs, human health, and quality of life. Thus, studies on oncogenesis and the development of PTC are still needed for more promising therapeutic targets.

Circular RNAs (circRNAs), as a large class of non-coding RNAs, contain a unique covalent loop structure without 5′-cap and 3′-poly (A) structures, resulting in their resistance to exonuclease degradation. circRNAs usually function as competitive endogenous RNAs (ceRNAs) by sponging micro RNAs (miRNAs), therefore influencing mRNAs expression and further oncogenesis and development of diseases. (Xia et al., 2021) Due to their conservation, circRNAs are expected to be valuable biomarkers and therapeutic targets in various cancer types.

SSU72 (SSU72 Homolog, RNA Polymerase II CTD Phosphatase) is a novel phosphatase with dual specificity that can dephosphorylate both phosphoserine/threonine and phosphotyrosine, which is also essential for RNA polymerase II. (Rodríguez-Torres et al., 2013) SSU72 intervenes at different stages of the transcription process by interacting with RNAPII subunits including Rpb2, TFIIB, and other mediators. SSU72 has a unique active site with specific structural characteristics at the C-terminus. It consists of a central 5-stranded β-sheet (β1–β5) enclosed by helices on both sides. SSU72 not only physiologically functions as a cohesin-binding phosphatase, but is also involved in various diseases, including nonalcoholic steatohepatitis, hepatocellular carcinoma, and autoimmune diseases. (Hwang et al., 2021) Moreover, SSU72 shows the highest expression in the thyroid among all the normal tissues. (Fagerberg et al., 2014) Thus, we consider that the SSU72-derived circRNAs may participate in the oncogenesis and development of PTC.

In this study, for the first time, we comprehensively uncovered the biological roles of SSU72-derived circRNAs in oncogenesis and development of PTC, which might provide a potential biomarker and a therapeutic target of PTC.

METHODS

Patient Samples

30 pairs of PTC tissues and adjacent normal tissues were obtained from PTC patients in the Xiangya Hospital, Central South University from January to June 2020. This study was approved by the Ethics Committee of the Xiangya Hospital and written consent was obtained from all subjects.

Cell Culture

Human thyroid normal epithelial cell line (Nthy-ori 3-1), and human PTC cell lines (B-CPAP, KTC-1, K1, IHH-4, TPC-1) were purchased from the Shanghai Academy of Sciences. Nthy-ori 3-1 was cultured in Dulbecco's modified Eagle's medium (DMEM), while B-CPAP, KTC-1, K1, IHH-4, and TPC-1 in RPMI-1640 medium (Gibco, USA), supplemented with penicillin (100 U/mL), streptomycin (100 μg/ml), and 10% fetal bovine serum (FBS, S Hyclone). All the cell lines were maintained at 37°C with 5% CO2.

RNA Extraction and Quantitative Real-Time PCR Assay

Total RNAs of thyroid cancer tissues and cells were extracted by using RNAEX reagent (Accurate Biotechnology, Hunan) with instructions of the manufacturer. RNase R (Epicenter Technologies) was used for 15 min at 37°C when RNase R treatment was necessary. The first strand of cDNA was synthesized with Evo M-MLV Mix Kit (Accurate Biotechnology, Hunan). Particularly, the first strand of cDNA of miR-361–3p and miR-451a was synthesized using the stem-loop method, while the first strand of cDNA of U6 was synthesized with a gene-specific primer. SYBR Green Premix Pro Taq HS qPCR Kit (Accurate Biotechnology, Hunan) was used for subsequent qRT-PCR assay on QuantStudio 5 system (ThermoFisher Scientific, USA). The relative expression levels were analyzed using the $2^{-\Delta\Delta Ct}$ method and normalized by beta-actin or U6. The sequences of primers involved in this study were shown in **Table 1**.

Fluorescence *In Situ* Hybridization Assay

In situ hybridization was carried out using probes specific to the circSSU72 sequence. The Nthy-ori 3-1 cell was cultured in a 24-well plate. RNA localization was determined using a FISH kit from RiboBio according to the manufacturer's protocol. The nucleus was stained using the 4′,6-diamidino-2-phenylindole (DAPI) and the signals were measured by fluorescence microscopy.

Oligonucleotide Transfection

The hsa_circ_0009294 siRNAs, miR-451a inhibitors, and mimics, as well as negative control (NC), were obtained from Sangon (Shanghai, China). Transfection was performed by Lipofectamine™ RNAi MAX (Invitrogen) according to the instructions of the manufacturer.

Stable Transfection

Human lentivirus-S1PR2 and lentivirus-hsa_circ_0009294 were purchased from Genechem (Shanghai, China) and transfected into cells using HitransG P (Genechem). Puromycin (Gibco, USA) was used for the selection of cells and green fluorescent protein (GFP) was used to exam the transfection efficiency. The 3' UTR was contained in the expression vectors for further investigations.

Dual-Luciferase Activity Assay

The interactions between circSSU72, miR-451a, and S1PR2 were measured by dual-luciferase activity assay in Nthy-ori 3-1 cell. The original sequence of circSSU72 and S1PR2 was constructed into Luc-circSSU72-WT and Luc-S1PR2-WT plasmid, while we

TABLE 1 | The sequence of primers involved in this study.

Gene		Sequence (5′-3′)
SSU72	Forward	CGACAAGCCCAATGTTTATGAT
	Reverse	ATCAAACAGGTCTTTGCAGTTC
circ_0009293	Forward	CAGATGCTGCTGTCAATCCA
	Reverse	TGGGCTCAGTAGAAGCAGAC
circ_0009294	Forward	GTGTGCACTTCCCGACATAC
	Reverse	GGAATTCAGATTGACAGCAGCA
circ_0009295	Forward	GTGTGCACTTCCCGACATAC
	Reverse	TGTGTATAGTGACAGCAGCATC
circ_0009296	Forward	GTGTGCACTTCCCGACATAC
	Reverse	GAATCCCCGTTTGTGACAGC
circ_0009297	Forward	GTGTGCACTTCCCGACATAC
	Reverse	AGACCCGCACTCCACAAG
miR-361–3p	Forward	GCTCCCCCAGGTGTGATTC
	Reverse	GTGCAGGGTCCGAGGT
	RT	GTCGTATCCAGTGCAGGGTCCGAGGTATTCGCACTGGATACGACAAATCA
miR-451a	Forward	GCGCAAACCGTTACCATTAC
	Reverse	GTGCAGGGTCCGAGGT
	RT	GTCGTATCCAGTGCAGGGTCCGAGGTATTCGCACTGGATACGACAACTCA
S1PR2	Forward	CATCCTCCTTCTGGACTATGC
	Reverse	GTGTAGATGACGGGGTTGAG
MIF	Forward	GAACAACTCCACCTTCGCCTAAGAG
	Reverse	TCTAAACCGTTTATTTCTCCCCACCAG
PSMB8	Forward	CTTTAGATGACACGACCCTACC
	Reverse	CAATCTGAACGTTCCTTTCTCC
CAB39	Forward	TGAGGCCTTTCACGTTTTTAAG
	Reverse	GGTTCTTGAGGAGGATGTCTAG
beta-actin	Forward	CCTGGCACCCAGCACAAT
	Reverse	GGGCCGGACTCGTCATAC
U6	Forward	CTCGCTTCGGCAGCACA
	Reverse	AACGCTTCACGAATTTGCGT

RT, reverse transcription.

mutated the predicted binding site of miR-451a on circSSU72 and S1PR2 in Luc-circSSU72-MUT and Luc-S1PR2-MUT plasmid. Nthy-ori 3-1 cell was cultured in 24-well plates. Plasmids were transfected using X-tremegene HP (ROCHE), while miR-451a mimics and NC mimics were transfected using Lipofectamine™ RNAi MAX (Invitrogen). After incubation of 48 h, relative luciferase activity was detected by a Dual-Luciferase® Reporter Assay System (Promega, Madison, WI) with the renilla luciferase activity as an internal reference.

Target Prediction of circSSU72 and miR-451a

Three bioinformatics databases were used for target prediction of circSSU72 (hsa_circ_0009294), including Circbank (http://www.circbank.cn/), (Liu et al., 2019) starBase (http://starbase.sysu.edu.cn/), (Li et al., 2014) and CircInteractome (https://circinteractome.irp.nia.nih.gov/). (Dudekula et al., 2016) Meanwhile, TargetScan (http://www.targetscan.org/) (Agarwal et al., 2015) and miRDB (http://mirdb.org/) (Chen and Wang, 2020) were used for target prediction of miR-451a.

Western Blot Assay

Proteins were extracted using RIPA buffer (Beyotime, Shanghai, China), and the concentration was determined by a BCA kit (ThermoFisher Scientific). An equivalent amount of proteins was isolated by SDS-PAGE, and transferred to polyvinyl fluoride membrane (Merck KGaA). After incubation with primary antibodies overnight at 4°C, and incubation with horseradish peroxidase-conjugated secondary antibodies (FDM007 and FDR007, Fudebio, Hangzhou, China) for 2 h. The membranes were treated with the enhanced chemiluminescent reagents (MILLIPORE, WBKLS0500). The signals were examined by ChemiDox (bio-rad, USA) with the treatment of an enhanced chemiluminescence kit (FD8030, Fudebio, Hangzhou, China). The primary antibodies involved in the present study were GAPDH (1:1000, Abcam), anti-S1PR2 (1:500, Proteintech), anti-AKT (1:1000, Wanleibio), anti-p-AKT (Ser473) (1:1000, Wanleibio).

Cell Counting Kit-8 Assay

Cell Counting Kit-8 (Beyotime, Shanghai, China) was used to detect cell proliferation ability. An equivalent amount of cells was plated on 96-well plates and CCK8 solution (10 ul/well) was added at pointed time. The absorbance at 450 nm was measured subsequently after 2 h incubation at 37°C.

5-Ethynyl-20-Deoxyuridine Incorporation Assay

The EdU assay was performed using a BeyoClick™ EdU Cell Proliferation Kit with Alexa Fluor 555 (Beyotime, Shanghai, China) according to the instructions of the manufacturer.

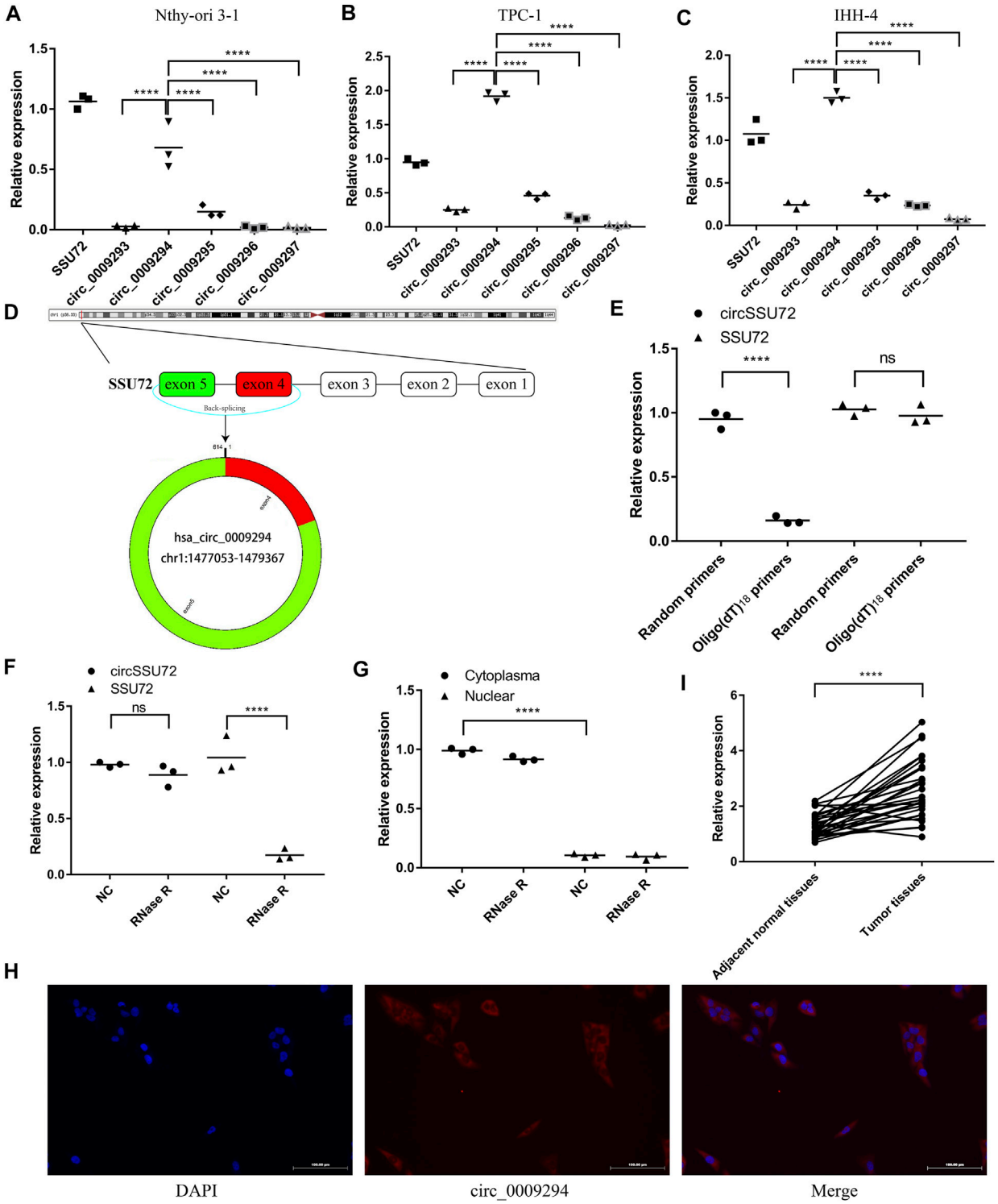

FIGURE 1 | circSSU72 was upregulated in PTC **(A)** The expression of SSU72-related circRNAs in the Nthy-ori 3-1 cells (n = 3). **(B)** The expression of SSU72-related circRNAs in the TPC-1 cells (n = 3). **(C)** The expression of SSU72-related circRNAs in the IHH-4 cells (n = 3). **(D)** The diagram exhibiting the formation of circSSU72 (hsa_circ_0009294). **(E)** qRT-PCR detected the levels of circSSU72 and SSU72 mRNA after reverse transcribed with random primers and oligo $(dT)_{18}$ primers (n = 3). **(F)** The relative expression of circSSU72 and SSU72 mRNA after treatment of RNase R (n = 3). **(G)** circSSU72 was separately detected in nuclear and cytoplasm (n = 3). **(H)** The expression level of circSSU72 (hsa_circ_0009294) was evaluated by FISH assay in Nthy-ori 3-1 cells. circSSU72 was stained red and nuclei were stained blue using 4′,6-diamidino-2-phenylindole (DAPI). Scale bars = 100 μm. **(I)** The expression of circSSU72 was assessed by qRT-PCR assay in PTC tissues and adjacent normal tissues (n = 30). $^{*}p < 0.05$; $^{**}p < 0.01$; $^{***}p < 0.001$; $^{****}p < 0.0001$.

Colony Formation Assay

An equivalent amount of TPC-1 and IHH-4 cells were planted into the 6-well plates and incubated for 14 days at 37°C. After being fixed and stained with 0.1% crystal violet, the colony was counted for comparisons.

Wound Healing Assay

Cells were cultured in 6-well plates at 37°C. Scratch wounds were created by using the fine end of 100-μL pipette tips. Images of migrated cells were captured under phase-contrast microscopy at different times.

Transwell Assay

Transwell assays were used to detect cell migration and invasion and conducted as previously described. (Xia et al., 2020)

Tumor Formation Assay *In Vivo*

The 6-week old male BALB/c nude mice were purchased from the Department of Laboratory Animal Science, Central South University for the *in vivo* tumor formation assay. TPC-1 cells (1×10^6) that were stably transfected with circSSU72 overexpression vectors or NC vectors were subcutaneously injected into the left armpit of nude mice. Tumor growth was detected at 0, 1, 2, 3, and 4 weeks after injection, and the volume of tumors was recorded as the length×width (DeGroot et al., 1990)×0.5. Four weeks after injection, the mice were euthanized with CO2, and the tumors were collected.

Statistical Analyses

R 3.3.0 and Statistical Package for Social Sciences 23.0 for Windows (SPSS Inc., Chicago, IL, United States) were used to perform statistical analyses, while GraphPad Prism v7.0 software (GraphPad Software, La Jolla, CA, USA) was used for generating illustrations. One-way analysis of variance (ANOVA) was used for homogeneous variance, while Welch's ANOVA was applied when the variance was heterogeneous.

RESULTS

circSSU72 (hsa_circ_0009294) was Upregulated in PTC

circRNAs derived from SSU72 were investigated in the CircBank Database, and 8 circRNAs were found. After excluding 3 circRNAs containing introns, 5 circRNAs derived from extrons were finally included in this study (hsa_circ_0009293, hsa_circ_0009294, hsa_circ_0009295, hsa_circ_0009296, hsa_circ_0009297). We subsequently confirmed the expression pattern of these SSU72-related circRNAs in Nthy-ori 3-1, TPC-1, IHH-4 cells by qRT-PCR assay with divergent primers (**Figures 1A–C**) Results showed that hsa_circ_0009294 dominated the SSU72-related circRNAs. Thus, we named hsa_circ_0009294 as circSSU72 and the following researches were focused on circSSU72 (**Figure 1D**).

As shown in **Figure 1E**, oligo $(dT)_{18}$ primers were not able to achieve reverse transcription, indicating circSSU72 was a closed-loop structure. To confirm the cyclization and stability of circSSU72, an RNase R treatment was applied. The liner SSU72 mRNA decreased significantly, while the circSSU72 showed insensitivity to RNase R (**Figure 1F**). Meanwhile, nuclear and cytoplasmic RNA was extracted respectively, and qRT-PCR showed circSSU72 was mainly localized in the cytoplasm with insensitivity to RNase R (**Figure 1G**). The FISH assay also demonstrated that circSSU72 (hsa_circ_0009294) was expressed in the cytoplasm of Nthy-ori 3-1 cell (**Figure 1H**).

To determine the role of circSSU72 in PTC, the expression of circSSU72 was examined by qRT-PCR in 30 PTC patients. And the results showed circSSU72 was significantly upregulated in PTC tissues than adjacent normal tissues (**Figure 1I**). Patients were subsequently divided into the circSSU72-low group and the circSSU72-high group, and the patient and tumor characteristics were shown in **Table 2**. The higher level of circSSU72 was significantly associated with bigger lesions, capsule invasion, and lymph node metastasis.

TABLE 2 | Patient and tumor characteristics.

Characteristics	circSSU72-low group (*n* = 15)	circSSU72-high group (*n* = 15)	*P*
Age (years)	41.13 ± 8.52	36.80 ± 8.21	0.167
Gender			1.000
Female	10 (66.7)	11 (73.3)	
Male	5 (33.3)	4 (26.7)	
Bilateral lesion			0.080
Yes	1 (6.7)	6 (40.0)	
No	14 (93.3)	9 (60.0)	
Largest tumor size (cm)	0.63 ± 0.81	1.26 ± 0.59	0.021
Number of lesion			0.064
Single	12 (80.0)	7 (46.7)	
Multiple	3 (20.0)	8 (53.3)	
Capsule invasion			0.042
Yes	0 (0.0)	5 (33.3)	
No	15 (100.0)	10 (66.7)	
Lymph node metastasis			0.008
Yes	2 (13.3)	10 (66.7)	
No	13 (86.7)	5 (33.3)	

Data are expressed as mean ± standard deviation or n (%).

The Silence of circSSU72 Inhibited PTC Cell Proliferation, Migration, and Invasion

The expression of circSSU72 was subsequently investigated in multiple cell lines. Among five PTC cell lines (B-CPAP, KTC-1, K1, IHH-4, TPC-1), TPC-1 and IHH-4 showed the highest level of circSSU72 expression (**Figure 2A**). To explore whether circSSU72 could affect the progression of PTC, TPC-1 and IHH-4 cells were transfected with circSSU72 siRNAs. As shown in **Figure 2B**, two siRNAs both decreased the expression of circSSU72 in TPC-1 cells, however there was no significant difference between the NC group and si-circ_0009294-2 in IHH-4 cells. Thus, si-circ_0009294-1 was chosen for further experiments. The clone formation (**Figure 2C**), CCK-8 assay (**Figures 2D,E**), and EdU assay (**Figures 2F,G**) revealed that the proliferation of PTC cells was inhibited in the si-circSSU72 group compared with the NC group. Meanwhile, wound healing assay

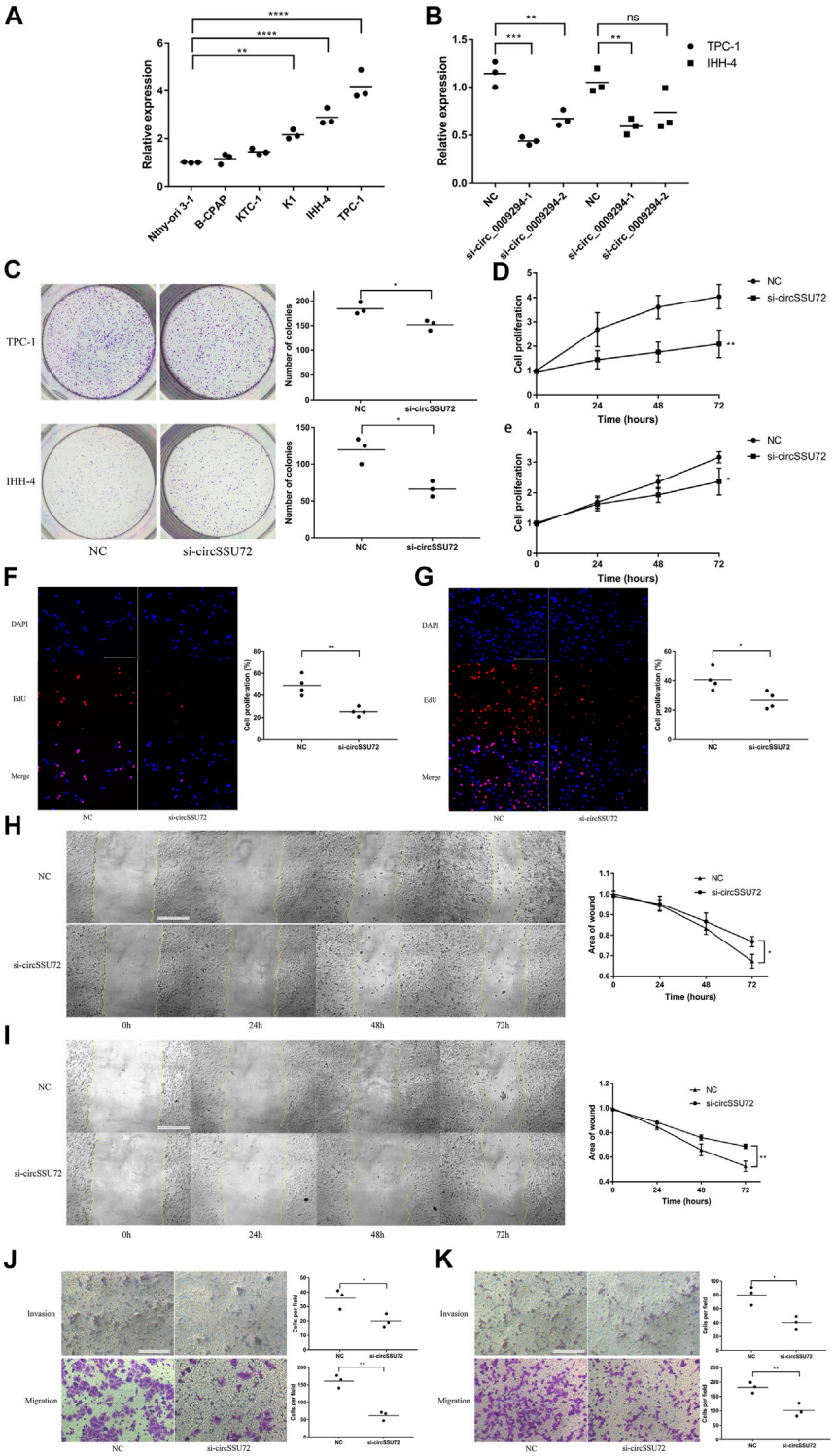

FIGURE 2 | The silence of circSSU72 inhibited PTC cell proliferation, migration, and invasion. **(A)** The expression of circSSU72 was investigated in five PTC cell lines ($n = 3$). **(B)** TPC-1 and IHH-4 cells were transfected with siRNAs of circSSU72, and the expression level of circSSU72 was analyzed by qRT-PCR assay ($n = 3$). **(C)** Colony formation assay of the cell proliferation ability in TPC-1 and IHH-4 cells transfected with si-circSSU72 ($n = 3$). **(D)** CCK8 assay to assess the influence of circSSU72 on TPC-1 cell ($n = 3$). **(E)** CCK8 assay to assess the influence of circSSU72 on IHH-4 cell ($n = 3$). **(F)** EdU assay of the cell proliferation ability in TPC-1 cell transfected with si-circSSU72 (scale bar = 100 um, $n = 4$). **(G)** EdU assay of the cell proliferation ability in IHH-4 cell transfected with si-circSSU72 (scale bar = 100 um, $n = 4$). **(H)** Scratch wound healing assays in transfected TPC-1 cell (scale bar = 200 um, $n = 3$). **(I)** Scratch wound healing assays in transfected IHH-4 cell (scale bar = 200 um, $n = 3$). **(J)** Transwell invasion and migration assay in transfected TPC-1 cell (scale bar = 100 um, $n = 3$). **(K)** Transwell invasion and migration assay in transfected IHH-4 cell (scale bar = 100 um, $n = 3$). $p < 0.05$; $^{**}p < 0.01$; $^{***}p < 0.001$; $^{****}p < 0.0001$.

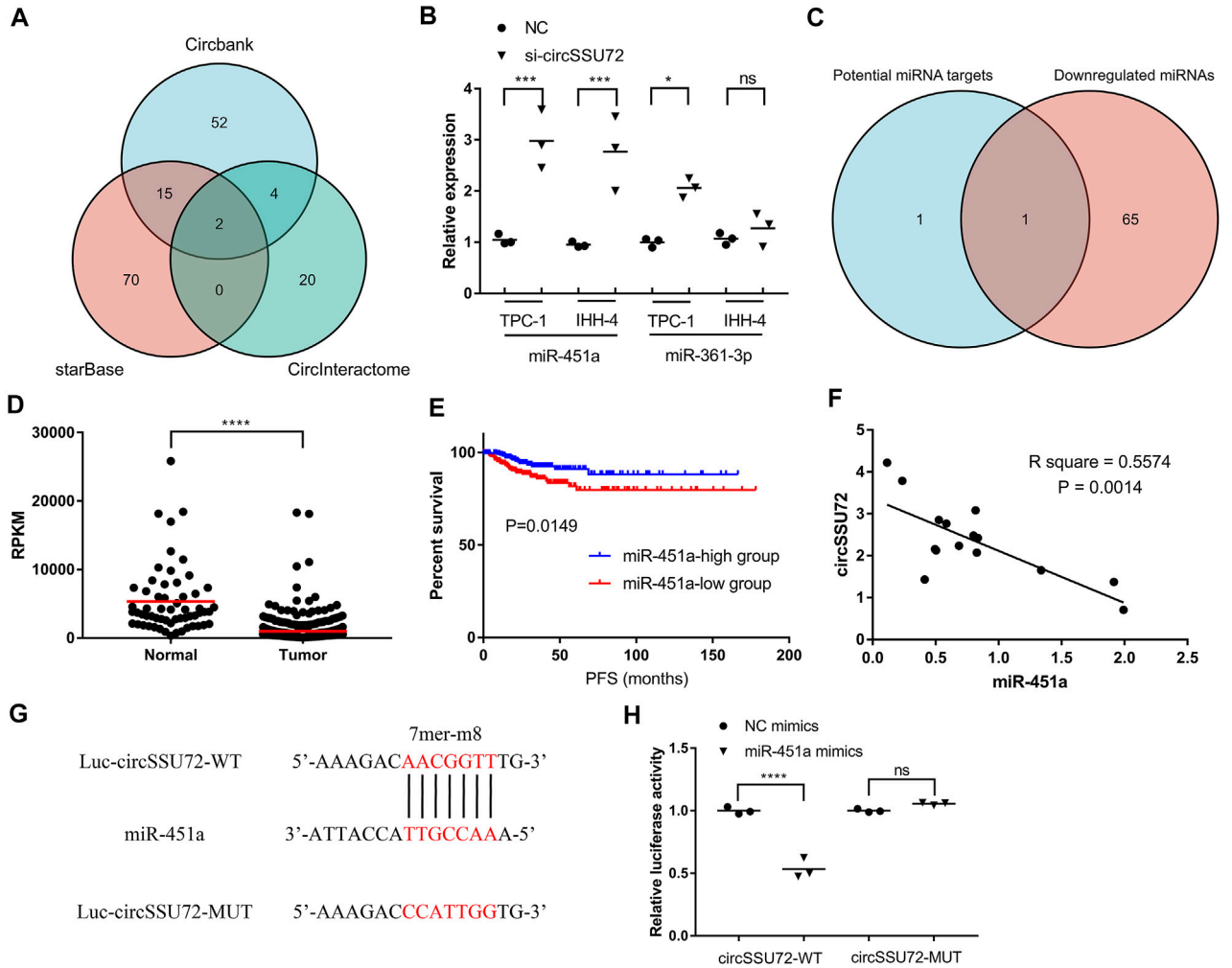

FIGURE 3 | circSSU72 functioned as a sponge for miR-451a. **(A)** Venn plot of three databases, including Circbank, starBase, and CircInteractome, to predict the targets of circSSU72. **(B)** The expression of miR-361–3p and miR-451a in TPC-1 and IHH-4 cells with or without si-circSSU72 by qRT-PCR (n = 3). **(C)** Venn plot of potential target miRNAs and downregulated miRNAs in TCGA-THCA. **(D)** The expression of miR-451a in TCGA-THCA. **(E)** The Kaplan-Miere curve of miR-451a concerning the progression-free survival of TCGA-THCA. **(F)** Correlation between circSSU72 and miR-451a expression in 15 pairs PTC tissues (n = 15). **(G,H)** A putative interaction site with miR-451a in circSSU72 was predicted and verified by dual-luciferase reporter assay in TPC-1 cell (n = 3). $^{*}p < 0.05$; $^{**}p < 0.01$; $^{***}p < 0.001$; $^{****}p < 0.0001$.

(**Figures 2H,I**) and Transwell invasion and migration assay (**Figures 2J,K**) revealed the ability of invasion and migration of PTC cells was also inhibited by interfering circSSU72.

Meantime, circSSU72 overexpressing cell lines were also constructed by circSSU72 overexpression vectors using consistent cell lines (**Supplementary Figure S1**). CCK-8 assay, EdU assay, and Transwell invasion and migration assay confirmed that circSSU72 overexpressing promoted cell proliferation, invasion, migration in these two PTC cell lines (**Supplementary Figure S1**). Tumor growth was assayed *in vivo* to further investigate the roles of circSSU72. The volume and weight of tumors from circSSU72 overexpressing TPC-1 cells were significantly higher compared with tumors from NC TPC-1 cells (**Supplementary Figure S1**).

circSSU72 Functioned as a Sponge for miR-451a

Multiple studies have proven that circRNAs could function by sponging miRNAs. Therefore, we subsequently explored the potential miRNAs associated with circSSU72. Three databases, including Circbank, starBase, and CircInteractome, were used for the selection of circSSU72-associated miRNAs. The Venn plot showed two miRNAs (miR-361–3p, miR-451a) were potential targets of circSSU72 (**Figure 3A**). We further examined the expression of these two miRNAs with or without si-circSSU72 by qRT-PCR. miR-451a was significantly upregulated when inhibiting circSSU72 in both TPC-1 and IHH-4 cells, while the expression of miR-361–3p did not change significantly in IHH-4 cells (**Figure 3B**). Meanwhile, we also investigated miRSeq data of

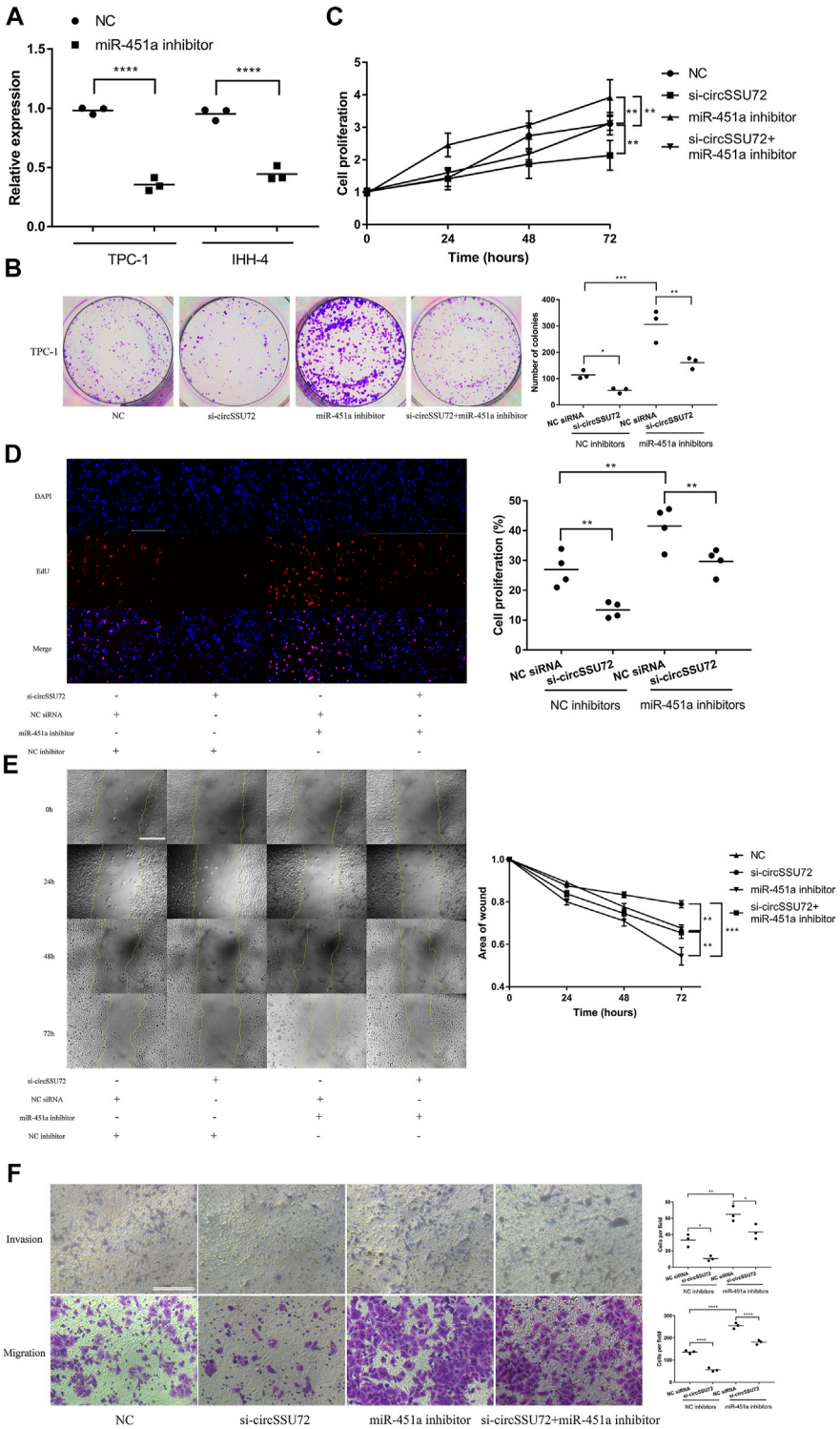

FIGURE 4 | The silence of circSSU72 inhibited PTC cell proliferation, migration, and invasion by targeting miR-451a. **(A)** The expression of miR-451a in TPC-1 and IHH-4 cells with the transfection of miR-451a inhibitor ($n = 3$). **(B)** Colony formation assay of the cell proliferation ability in TPC-1 cell transfected with si-circSSU72 and miR-451a inhibitor ($n = 3$). **(C)** CCK8 assay to assess the influence of circSSU72 and miR-451a on TPC-1 cell ($n = 3$). **(D)** EdU assay of the cell proliferation ability in TPC-1 cell transfected with si-circSSU72 and miR-451a inhibitor (scale bar = 100 um, $n = 4$). **(E)** Scratch wound healing assays in transfected TPC-1 cell (scale bar = 200 um, $n = 3$). **(F)** Transwell invasion and migration assay in transfected TPC-1 cell (scale bar = 100 um, $n = 3$). $^{*}p < 0.05$; $^{**}p < 0.01$; $^{***}p < 0.001$; $^{****}p < 0.0001$.

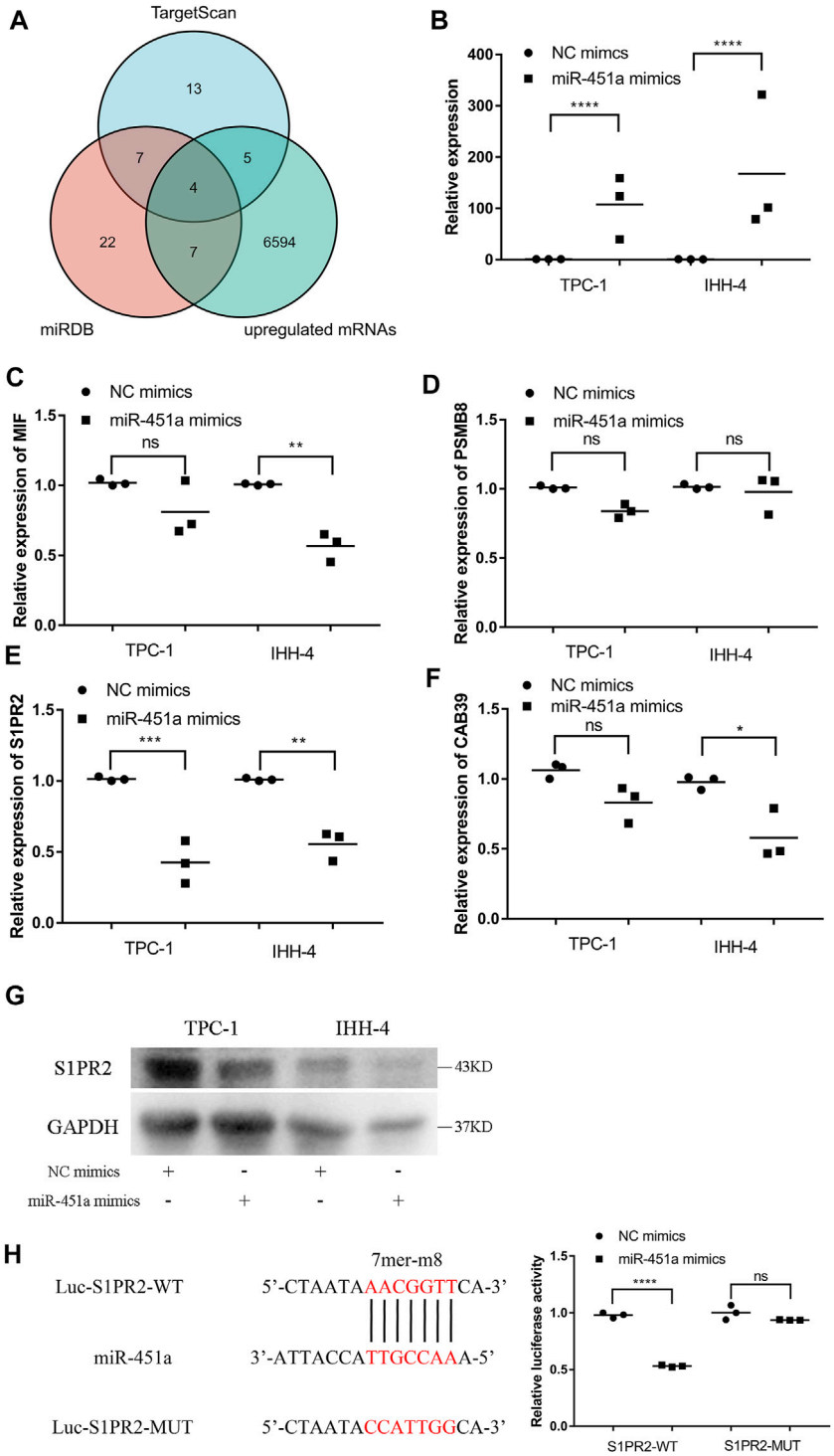

FIGURE 5 | miR-451a targeted S1PR2 in PTC cells. **(A)** Venn plot of three databases, including TargetScan, miRDB, and upregulated mRNAs in TCGA-THCA. **(B)** The expression of miR-451a in TPC-1 and IHH-4 cells with the transfection of miR-451a mimics (n = 3). **(C)** The expression of MIF in TPC-1 and IHH-4 cells with or without miR-451a mimics by qRT-PCR (n = 3). **(D)** The expression of PSMB8 in TPC-1 and IHH-4 cells with or without miR-451a mimics by qRT-PCR (n = 3). **(E)** The expression of S1PR2 in TPC-1 and IHH-4 cells with or without miR-451a mimics by qRT-PCR (n = 3). **(F)** The expression of CAB39 in TPC-1 and IHH-4 cells with or without miR-451a mimics by qRT-PCR (n = 3). **(G)** The expression of S1PR2 protein in TPC-1 and IHH-4 cells with or without miR-451a mimics by western blot assay. **(H)** A putative interaction site with miR-451a in S1PR2 was predicted and verified by dual-luciferase reporter assay in TPC-1 cell (n = 3). $^{*}p < 0.05$; $^{**}p < 0.01$; $^{***}p < 0.001$; $^{****}p < 0.0001$.

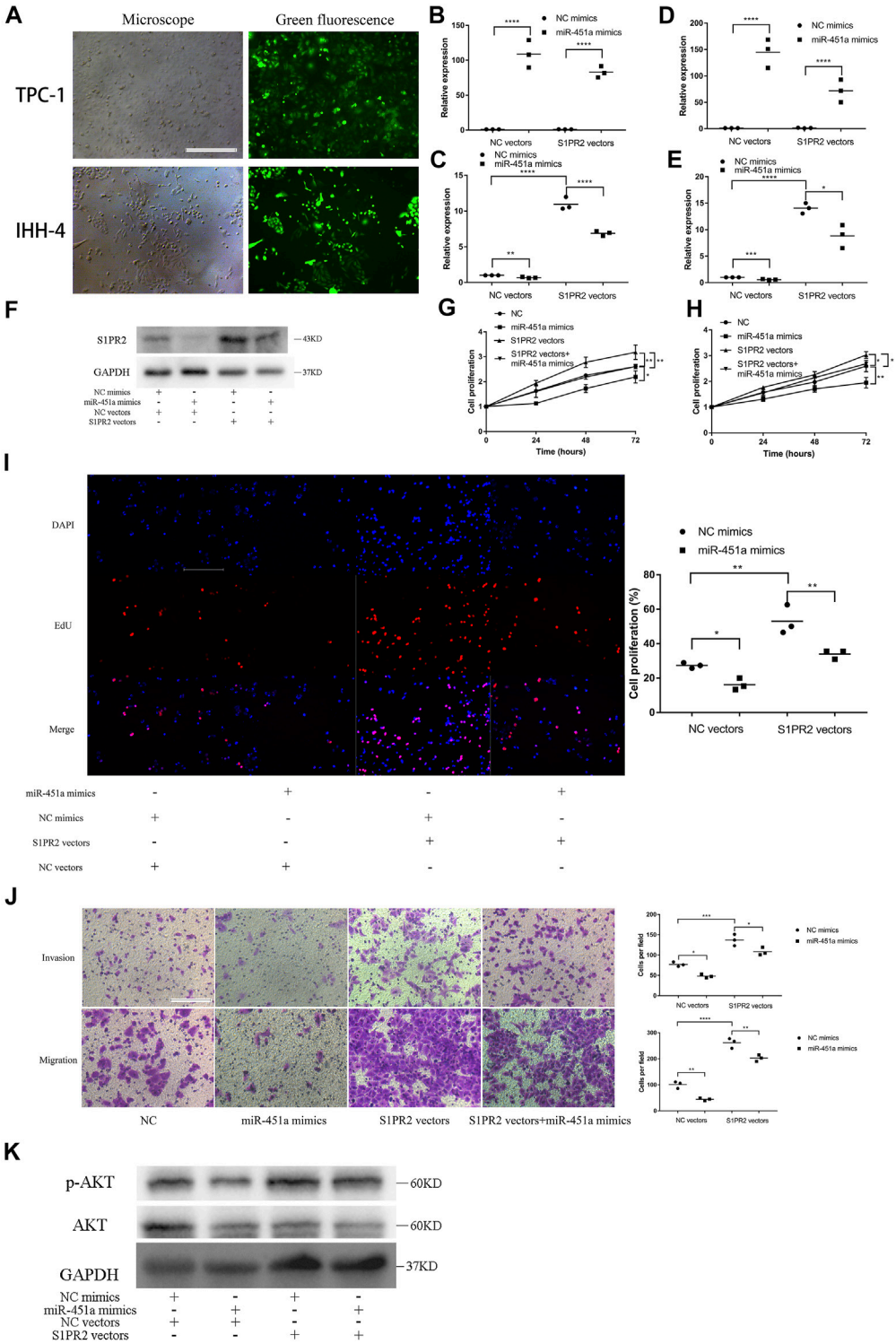

FIGURE 6 | miR-451a inhibited the proliferation, migration, and invasion of PTC cells by targeting S1PR2. **(A)** Green fluorescent showing the successful transfection of S1PR2 overexpression vectors in TPC-1 and IHH-4 cells (scale bar = 200 um). **(B)** The efficacy of miR-451a mimics was reconfirmed in TPC-1 cell with the transfection of S1PR2 vectors and NC vectors ($n = 3$). **(C)** The expression of S1PR2 in TPC-1 cell with the transfection of S1PR2 vectors miR-451a mimics ($n = 3$). **(D)** The efficacy of miR-451a mimics was reconfirmed in IHH-4 cell with the transfection of S1PR2 vectors and NC vectors ($n = 3$). **(E)** The expression of S1PR2 in IHH-4 cell with the transfection of S1PR2 vectors miR-451a mimics ($n = 3$). **(F)** The expression of S1PR2 protein in transfected TPC-1 cell by western blot assay. **(G)** CCK8 assay to assess the influence of miR-451a and S1PR2 on TPC-1 cell ($n = 3$). **(H)** CCK8 assay to assess the influence of miR-451a and S1PR2 on IHH-4 cell ($n = 3$). **(I)** EdU assay of the cell proliferation ability in TPC-1 cell transfected with miR-451a mimics and S1PR2 vectors (scale bar = 100 um, $n = 3$). **(J)** Transwell invasion and migration assay in transfected TPC-1 cell (scale bar = 100 um, $n = 3$). **(K)** The expression of AKT, p-AKT proteins in transfected TPC-1 cell by western blot assay.*$p < 0.05$; **$p < 0.01$; ***$p < 0.001$; ****$p < 0.0001$.

THCA patients in the TCGA database, and the intersection between potential miRNA targets and downregulated miRNAs with $\log_2$ (fold change) ≤-1 included only miR-451a (**Figure 3C**). The expression data of miR-451a in TCGA-THCA were shown in **Figure 3D**, and the Kaplan-Meier plot also showed that miR-451a was associated with better progression-free survival (**Figure 3E**), which was consistent with being a target of circSSU72. Furthermore, the circSSU72 expression was negatively associated with the miR-451a expression in PTC tissues (**Figure 3F**). Dual-luciferase reporters assay also validated the direct interaction between circSSU72 and miR-451a (**Figures 3G,H**).

The Silence of circSSU72 Inhibited PTC Cell Proliferation, Migration, and Invasion by Targeting miR-451a

miR-451a inhibitors were proven to be effective in both two PTC cells (**Figure 4A**), and further assays were performed to confirm the function of the circSSU72/miR-451a axis. The clone formation, CCK-8 assay, and EdU assay revealed that the proliferation of PTC cells was inhibited by si-circSSU72 and miR-451a inhibitor reversed the suppressive effects in TPC-1 (**Figures 4B–D**) and IHH-4 cells (**Supplementary Figure S2**). Meanwhile, wound healing assay and Transwell invasion and migration assay revealed the suppressive effects of si-circSSU72 on the ability of invasion and migration of TPC-1 (**Figures 4E,F**) and IHH-4 cells (**Supplementary Figure S2**) could also be reversed by miR-451a inhibiting. These results indicated that circSSU72 affected the proliferation, migration, and invasion of PTC cells by targeting miR-451a.

miR-451a Targeted S1PR2 in PTC Cells

To explore the potential target of miR-451a, TargetScan, miRDB, and transcriptome data from TCGA-THCA were used for predicting potential targets. As shown in **Figure 5A 4** genes, including MIF (Macrophage Migration Inhibitory Factor), PSMB8 (Proteasome 20S Subunit Beta 8), S1PR2 (Sphingosine-1-Phosphate Receptor 2), and CAB39 (Calcium Binding Protein 39), were candidates for the target of miR-451a. miR-451a mimics were successfully transfected into PTC cells (**Figure 5B**), and qRT-PCR showed that only S1PR2 was significantly regulated after the transfection of miR-451a mimics in both TPC-1 and IHH-4 cells (**Figures 5C–F**). Subsequently, a western blot assay was performed to confirm the downregulation of S1PR2 by miR-451a mimics (**Figure 5G**). Dual-luciferase reporters assay also validated the direct interaction between miR-451a and S1PR2 (**Figure 5H**).

miR-451a Inhibited the Proliferation, Migration, and Invasion of PTC Cells by Targeting S1PR2

TPC-1 and IHH-4 cells were transfected with S1PR2 overexpression vectors or NC vectors. Green fluorescence showed that the transfections were successful (**Figure 6A**). The efficacy of miR-451a mimics and the expression of S1PR2 were also validated in TPC-1 (**Figures 6B,C**) and IHH-4 cells (**Figures 6D,E**). Subsequently, western blot assay was performed to confirm the overexpression of S1PR2 and the downregulation of S1PR2 by miR-451a mimics in TPC-1 cells (**Figure 6F**). CCK-8, EdU, Transwell invasion and migration assay indicated that S1PR2 reversed the inhibition effects of miR-451a on cell proliferation, migration, and invasion in TPC-1 (**Figures 6G,I,J**) and IHH-4 (**Figure 6H**; **Supplementary Figure S3**) cells, indicating that the effects of miR-451a on thyroid cancer cell proliferation, migration, and invasion depended on S1PR2 suppression.

To explore the potential pathway that circSSU72/miR451a/S1PR2 axis is involved in, the phosphorylation level of AKT was further investigated by western blot assay. And the results showed that the AKT pathway was activated by circSSU72/miR451a/S1PR2 axis (**Figure 6K**).

DISCUSSION

In this study, we comprehensively investigated the role of circRNAs derived from SSU72 in PTC, and further explored the mechanisms of circSSU72. We firstly found that circSSU72 (hsa_circ_0009294)/miR-451a/S1PR2 axis could regulate cell proliferation, migration, and invasion of PTC cells by the AKT pathway, which could serve as a novel therapeutic target in PTC.

The majority of circRNAs derive from the exons of protein-coding genes through back-splicing, while some circRNAs contain introns. (Starke et al., 2015) When spliceosomes or canonical pre-mRNA processing events are dysregulated, circRNAs may be the preferred output gene type. (Liang et al., 2017) Many studies have indicated that circRNAs are involved in the initiation and progression of multiple systematic diseases, cancers, etc., including thyroid cancer. (Xia et al., 2021) Since 2018, many circRNAs were found to be associated with the proliferation, migration, and invasion of thyroid cancer cells. (Chen et al., 2018; Cai et al., 2019) Recently, circTP53 was found to promote thyroid cancer cell proliferation by targeting miR-1233–3p/MDM2 axis. (Ma et al., 2021) Meanwhile, circRNA_102002 was found to facilitate metastasis of papillary thyroid cancer through regulating the miR-488–3p/HAS2 axis. To our knowledge, this was the first study reporting the role of circSSU72 (hsa_circ_0009294) in the development of thyroid cancer.

miRNAs are well-studied rich ncRNAs without coding protein. miR-451a was found to be a tumor suppressor in lung cancer, (Shen et al., 2018) colorectal cancer, (Xu et al., 2019) and prostate cancer. (Liu et al., 2020) In thyroid cancer, it has also been reported that miR-451a inhibited cell proliferation, migration, and invasion. Fan et al. reported that miR-451a could inhibit proliferation, epithelial-mesenchymal transition, and induce apoptosis in PTC cells. (Fan and Zhao, 2019) Moreover, Wang et al. also reported that miR-451a restrained the growth and metastatic phenotypes of PTC cells through targeting ZEB1. (Wang et al., 2020) In this study, we confirmed the tumor-suppressive role of miR-451a in PTC cell

proliferation, migration, and invasion. Moreover, we also found that miR-451 might function through regulating S1PR2.

S1PRs are G protein-coupled receptors, which regulate various functions, including cell survival and growth, migration, and cytoskeleton organization. (Aarthi et al., 2011) S1PR2 is located on the plasma membrane and in the cytoplasm of mammalian cells, and couples to members of the G_i, G_q, and $G_{12/13}$ families. (Yu, 2021) Furthermore, S1PR2 was reported to be associated with various cancers. Yin et al. reported that S1PR2 was involved in the growth of hepatocellular carcinoma cells, (Yin et al., 2018) while Pang et al. demonstrated that the knockdown of S1PR2 might contribute to the initial extramedullary translocation by promoting myeloma cell migration and invasion through NF-κB pathway activation. (Pang et al., 2020) More recently, S1PR2 was reported to contribute to the growth of hepatocellular carcinoma through the AKT pathway. (Yin et al., 2018) In the present study, we firstly found that over-expressing S1PR2 might promote the abilities of proliferation, migration, and invasion of PTC cells.

Different behaviors were shown in the mechanism mediated by miR-451a between IHH-4 cells and TPC-1 cells. Although the miR-451a/S1PR2 axis was universal in these PTC cell lines, the BRAF gene mutation may cause the different behaviors since the IHH-4 involves BRAF gene mutation while the TPC-1 do not. Future studies should focus on the associations between the mechanisms mediated by miR-451a and BRAF gene mutation.

This was a pre-clinical study with certainly some limitations. A large cohort of thyroid cancer patients is needed to validate the expression pattern of circSSU72. Meanwhile, the relationships between the circSSU72 and its parental mRNA SSU72 should be comprehensively investigated in future studies. Lastly, *in vivo* studies will be performed in the near future to prompt the translation from experimental discoveries to clinical practices of circSSU72-related therapies.

CONCLUSION

The expression of circSSU72 (hsa_circ_0009294) increases in PTC. The inhibition of circSSU72 is shown to suppress cell proliferation, migration, and invasion of PTC cells by regulating the miR-451a/S1PR2 axis. The circSSU72/miR-451a/S1PR2 axis may regulate cell proliferation, migration, and invasion of PTC.

DATA AVAILABILITY STATEMENT

The original contributions presented in the study are included in the article/**Supplementary Material**, further inquiries can be directed to the corresponding author.

ETHICS STATEMENT

The studies involving human participants were reviewed and approved by Institutional Ethics Committee of Xiangya Hospital, Central South University. The patients/participants provided their written informed consent to participate in this study. The animal study was reviewed and approved by Institutional Ethics Committee of Xiangya Hospital, Central South University.

AUTHOR CONTRIBUTIONS

Conceptualization, XL; Data curation, ZZ; Formal analysis, LY; Funding acquisition, XL; Investigation, FX; Methodology, ZZ, FX, and LY; Project administration, ZZ; Software, FX; Supervision, XL; Validation, BJ and XL; Visualization, BJ; Writing—original draft, ZZ and FX; Writing—review and editing, LY, BJ, and XL.

FUNDING

This work was supported by the National Natural Science Foundation of China (grant No. 82073262) and the Hunan Province Natural Science Foundation (grant number 2019JJ40475).

SUPPLEMENTARY MATERIAL

The Supplementary Material for this article can be found online at: https://www.frontiersin.org/articles/10.3389/fcell.2022.817028/full#supplementary-material

Supplementary Figure S1 | The overexpression of circSSU72 promoted PTC cell proliferation, migration, and invasion. (a) TPC-1 and IHH-4 cells were transfected with circSSU72 overexpressing vectors or NC vectors, and the expression level of circSSU72 was analyzed by qRT-PCR assay (n=3). (b) CCK8 assay to assess the influence of circSSU72 on TPC-1 cell (n=3). (c) CCK8 assay to assess the influence of circSSU72 on IHH-4 cell (n=3). (d) EdU assay of the cell proliferation ability in TPC-1 cell transfected with oe-circSSU72 (n=3). (e) EdU assay of the cell proliferation ability in IHH-4 cell transfected with oe-circSSU72 (n=3). (f) Transwell invasion and migration assay in transfected TPC-1 cell (n=3). (g) Transwell invasion and migration assay in transfected IHH-4 cell (n=3). (h) Tumors after 4 weeks post-injection. (i) Tumor volume. (j) Tumor weight.*P<0.05; **P<0.01;***P<0.001;****P<0.0001.

Supplementary Figure S2 | The silence of circSSU72 inhibited PTC cell proliferation, migration, and invasion by targeting miR-451a. (a) Colony formation assay of the cell proliferation ability in IHH-4 cell transfected with si-circSSU72 and miR-451a inhibitor (n=3). (b) CCK8 assay to assess the influence of circSSU72 and miR-451a on IHH-4 cell (n=3). (c) EdU assay of the cell proliferation ability in IHH-4 cell transfected with si-circSSU72 and miR-451a inhibitor (scale bar=100um, n=4). (d) Scratch wound healing assays in transfected IHH-4 cell (scale bar=200um, n=3). (e) Transwell invasion and migration assay in transfected IHH-4 cell (scale bar=100um, n=3).*P<0.05; **P<0.01;***P<0.001;****P<0.0001.

Supplementary Figure S3 | miR-451a inhibited the proliferation, migration, and invasion of PTC cells by targeting S1PR2. (a) EdU assay of the cell proliferation ability in IHH-4 cell transfected with miR-451a mimics and S1PR2 vectors (scale bar=100um, n=3). (b) Transwell invasion and migration assay in transfected IHH-4 cell (scale bar=100um, n=3).*P<0.05; **P<0.01;***P<0.001;****P<0.0001.

REFERENCES

Aarthi, J. J., Darendeliler, M. A., and Pushparaj, P. N. (2011). Dissecting the Role of the S1P/S1PR axis in Health and Disease. *J. Dent. Res.* 90 (7), 841–854. doi:10.1177/0022034510389178

Agarwal, V., Bell, G. W., Nam, J. W., and Bartel, D. P. (2015). Predicting Effective microRNA Target Sites in Mammalian mRNAs. *Elife* 4, e05005. doi:10.7554/eLife.05005

Cai, X., Zhao, Z., Dong, J., Lv, Q., Yun, B., Liu, J., et al. (2019). Circular RNA circBACH2 Plays a Role in Papillary Thyroid Carcinoma by Sponging miR-139-5p and Regulating LMO4 Expression. *Cell Death Dis.* 10 (3), 184. doi:10.1038/s41419-019-1439-y

Chen, F., Feng, Z., Zhu, J., Liu, P., Yang, C., Huang, R., et al. (2018). Emerging Roles of circRNA_NEK6 Targeting miR-370-3p in the Proliferation and Invasion of Thyroid Cancer via Wnt Signaling Pathway. *Cancer Biol. Ther.* 19 (12), 1139–1152. doi:10.1080/15384047.2018.1480888

Chen, Y., and Wang, X. (2020). miRDB: an Online Database for Prediction of Functional microRNA Targets. *Nucleic Acids Res.* 48 (D1), D127–D131. doi:10.1093/nar/gkz757

DeGroot, L. J., Kaplan, E. L., McCormick, M., and Straus, F. H. (1990). Natural History, Treatment, and Course of Papillary Thyroid Carcinoma*. *J. Clin. Endocrinol. Metab.* 71 (2), 414–424. doi:10.1210/jcem-71-2-414

Dudekula, D. B., Panda, A. C., Grammatikakis, I., De, S., Abdelmohsen, K., and Gorospe, M. (2016). CircInteractome: A Web Tool for Exploring Circular RNAs and Their Interacting Proteins and microRNAs. *RNA Biol.* 13 (1), 34–42. doi:10.1080/15476286.2015.1128065

Fagerberg, L., Hallström, B. M., Oksvold, P., Kampf, C., Djureinovic, D., Odeberg, J., et al. (2014). Analysis of the Human Tissue-specific Expression by Genome-wide Integration of Transcriptomics and Antibody-Based Proteomics. *Mol. Cell Proteomics* 13 (2), 397–406. doi:10.1074/mcp.m113.035600

Fan, X., and Zhao, Y. (2019). miR-451a Inhibits Cancer Growth, Epithelial-mesenchymal Transition and Induces Apoptosis in Papillary Thyroid Cancer by Targeting PSMB8. *J. Cel. Mol. Med.* 23 (12), 8067–8075. doi:10.1111/jcmm.14673

Hwang, S., Kim, M., and Lee, C. (2021). Ssu72 Dual-specific Protein Phosphatase: From Gene to Diseases. *Int. J. Mol. Sci.* 22 (7), 3791. doi:10.3390/ijms22073791

Kim, J., Gosnell, J. E., and Roman, S. A. (2020). Geographic Influences in the Global Rise of Thyroid Cancer. *Nat. Rev. Endocrinol.* 16 (1), 17–29. doi:10.1038/s41574-019-0263-x

Laha, D., Nilubol, N., and Boufraqech, M. (2020). New Therapies for Advanced Thyroid Cancer. *Front. Endocrinol.* 11, 82. doi:10.3389/fendo.2020.00082

Li, J. H., Liu, S., Zhou, H., Qu, L. H., and Yang, J. H. (2014). starBase v2.0: Decoding miRNA-ceRNA, miRNA-ncRNA and Protein-RNA Interaction Networks from Large-Scale CLIP-Seq Data. *Nucleic Acids Res.* 42 (Database issue), D92–D97. doi:10.1093/nar/gkt1248

Liang, D., Tatomer, D. C., Luo, Z., Wu, H., Yang, L., Chen, L. L., et al. (2017). The Output of Protein-Coding Genes Shifts to Circular RNAs when the Pre-mRNA Processing Machinery Is Limiting. *Mol. Cel.* 68 (5), 940–e3. doi:10.1016/j.molcel.2017.10.034

Liu, M., Wang, Q., Shen, J., Yang, B. B., and Ding, X. (2019). Circbank: a Comprehensive Database for circRNA with Standard Nomenclature. *RNA Biol.* 16 (7), 899–905. doi:10.1080/15476286.2019.1600395

Liu, Y., Yang, H. Z., Jiang, Y. J., and Xu, L. Q. (2020). miR-451a Is Downregulated and Targets PSMB8 in Prostate Cancer. *Kaohsiung J. Med. Sci.* 36 (7), 494–500. doi:10.1002/kjm2.12196

Ma, W., Zhao, P., Zang, L., Zhang, K., Liao, H., and Hu, Z. (2021). CircTP53 Promotes the Proliferation of Thyroid Cancer via Targeting miR-1233-3p/MDM2 axis. *J. Endocrinol. Invest.* 44 (2), 353–362. doi:10.1007/s40618-020-01317-2

Pang, M., Li, C., Zheng, D., Wang, Y., Wang, J., Zhang, W., et al. (2020). S1PR2 Knockdown Promotes Migration and Invasion in Multiple Myeloma Cells via NF-Kb Activation. *Cmar* Vol. 12, 7857–7865. doi:10.2147/cmar.s237330

Rodríguez-Torres, A. M., Lamas-Maceiras, M., García-Díaz, R., and Freire-Picos, M. A. (2013). Structurally Conserved and Functionally Divergent Yeast Ssu72 Phosphatases. *Febs Lett.* 587 (16), 2617–2622. doi:10.1016/j.febslet.2013.06.044

Sebastian, S. O., Gonzalez, J. M., Paricio, P. P., Perez, J. S., Flores, D. P., Madrona, A. P., et al. (2000). Papillary Thyroid Carcinoma: Prognostic index for Survival Including the Histological Variety. *Arch. Surg.* 135 (3), 272–277. doi:10.1001/archsurg.135.3.272

Shen, Y. Y., Cui, J. Y., Yuan, J., and Wang, X. (2018). MiR-451a Suppressed Cell Migration and Invasion in Non-small Cell Lung Cancer through Targeting ATF2. *Eur. Rev. Med. Pharmacol. Sci.* 22 (17), 5554–5561. doi:10.26355/eurrev_201809_15818

Starke, S., Jost, I., Rossbach, O., Schneider, T., Schreiner, S., Hung, L.-H., et al. (2015). Exon Circularization Requires Canonical Splice Signals. *Cel. Rep.* 10 (1), 103–111. doi:10.1016/j.celrep.2014.12.002

Wang, Q., Shang, J., Zhang, Y., Zhou, Y., and Tang, L. (2020). MiR-451a Restrains the Growth and Metastatic Phenotypes of Papillary Thyroid Carcinoma Cells via Inhibiting ZEB1. *Biomed. Pharmacother.* 127, 109901. doi:10.1016/j.biopha.2020.109901

Xia, F., Chen, Y., Jiang, B., Bai, N., and Li, X. (2020). Hsa_circ_0011385 Accelerates the Progression of Thyroid Cancer by Targeting miR-361-3p. *Cancer Cel. Int.* 20, 49. doi:10.1186/s12935-020-1120-7

Xia, F., Zhang, Z., and Li, X. (2021). Emerging Roles of Circular RNAs in Thyroid Cancer. *Front. Cel. Dev. Biol.* 9, 636838. doi:10.3389/fcell.2021.636838

Xu, K., Han, B., Bai, Y., Ma, X.-Y., Ji, Z.-N., Xiong, Y., et al. (2019). MiR-451a Suppressing BAP31 Can Inhibit Proliferation and Increase Apoptosis through Inducing ER Stress in Colorectal Cancer. *Cel. Death Dis.* 10 (3), 152. doi:10.1038/s41419-019-1403-x

Yin, Y., Xu, M., Gao, J., and Li, M. (2018). Alkaline Ceramidase 3 Promotes Growth of Hepatocellular Carcinoma Cells via Regulating S1P/S1PR2/PI3K/AKT Signaling. *Pathol. - Res. Pract.* 214 (9), 1381–1387. doi:10.1016/j.prp.2018.07.029

Yu, H. (2021). Targeting S1PRs as a Therapeutic Strategy for Inflammatory Bone Loss Diseases-Beyond Regulating S1P Signaling. *Ijms* 22 (9), 4411. doi:10.3390/ijms22094411

Conflict of Interest: The authors declare that the research was conducted in the absence of any commercial or financial relationships that could be construed as a potential conflict of interest.

frontiers in Oncology

ORIGINAL RESEARCH
published: 29 March 2022
doi: 10.3389/fonc.2022.852515

BAP1-Related ceRNA (NEAT1/miR-10a-5p/SERPINE1) Promotes Proliferation and Migration of Kidney Cancer Cells

Rui-ji Liu[1,2‡], Zhi-Peng Xu[1,2‡], Shu-Ying Li[3], Jun-Jie Yu[1,2], Ning-han Feng[4], Bin Xu[1,2*] and Ming Chen[1,2,5*†]*

[1] Department of Urology, Affiliated Zhongda Hospital of Southeast University, Nanjing, China, [2] Surgical Research Center, Institute of Urology, Southeast University Medical School, Nanjing, China, [3] Sichuan Cancer Hospital & Institute, Sichuan Cancer Center, Cancer Hospital affiliate to School of Medicine, UESTC, Chengdu, China, [4] Department of Urology, Wuxi No.2 People's Hospital of Nanjing Medical University, Wuxi, China, [5] Nanjing Lishui District People's Hospital, Zhongda Hospital Lishui Branch, Southeast University, Nanjing, China

Background: *BAP1* is an important tumor suppressor involved in various biological processes and is commonly lost or inactivated in clear-cell renal cell carcinoma (ccRCC). However, the role of the BAP1-deficient tumor competing endogenous RNA (ceRNA) network involved in ccRCC remains unclear. Thus, this study aims to investigate the prognostic BAP1-related ceRNA in ccRCC.

Methods: Raw data was obtained from the TCGA and the differentially expressed genes were screened to establish a BAP1-related ceRNA network. Subsequently, the role of the ceRNA axis was validated using phenotypic experiments. Dual-luciferase reporter assays and fluorescence *in situ* hybridization (FISH) assays were used to confirm the ceRNA network.

Results: Nuclear enriched abundant transcript 1 (NEAT1) expression was significantly increased in kidney cancer cell lines. NEAT1 knockdown significantly inhibited cell proliferation and migration, which could be reversed by miR-10a-5p inhibitor. Dual-luciferase reporter assay confirmed miR-10a-5p as a common target of NEAT1 and Serine protease inhibitor family E member 1 (SERPINE1). FISH assays revealed the co-localization of NEAT1 and miR-10a-5p in the cytoplasm. Additionally, the methylation level of SERPINE1 in ccRCC was significantly lower than that in normal tissues. Furthermore, SERPINE1 expression was positively correlated with multiple immune cell infiltration levels.

Conclusions: In BAP1-deficient ccRCC, NEAT1 competitively binds to miR-10a-5p, indirectly upregulating SERPINE1 expression to promote kidney cancer cell proliferation. Furthermore, NEAT1/miR-10a-5p/SERPINE1 were found to be independent prognostic factors of ccRCC.

Keywords: ceRNA, DNA methylation, immune microenvironment, clear-cell renal cell carcinoma, prognosis

OPEN ACCESS

Edited by:
Hernandes F. Carvalho, State University of Campinas, Brazil

Reviewed by:
Shan Gao, Suzhou Institute of Biomedical Engineering and Technology (CAS), China
Ting Li, University of Pennsylvania, United States

****Correspondence:***
Ning-han Feng
n.feng@njmu.edu.cn
Bin Xu
njxb1982@126.com
Ming Chen
mingchenseu@126.com

†ORCID:
Ming Chen
orcid.org/0000-0002-3572-6886

‡These authors have contributed equally to this work

Specialty section:
This article was submitted to Molecular and Cellular Oncology, a section of the journal Frontiers in Oncology

Received: *11 January 2022*
Accepted: *25 February 2022*
Published: *29 March 2022*

Citation:
Liu R-j, Xu Z-P, Li S-Y, Yu J-J, Feng N-h, Xu B and Chen M (2022) BAP1-Related ceRNA (NEAT1/miR-10a-5p/SERPINE1) Promotes Proliferation and Migration of Kidney Cancer Cells. Front. Oncol. 12:852515. doi: 10.3389/fonc.2022.852515

INTRODUCTION

Kidney cancer is a common malignancy, with approximately 430,000 new global cases in 2020 and approximately 170,000 kidney cancer-related deaths (1). The pathology of clear-cell renal cell carcinoma (ccRCC) is characterized by a 'clear cytoplasm', owing to its ability to accumulate glycogen and lipids in the cytoplasm. It accounts for up to 80% of all renal cell carcinomas (RCC) and is also considered the most aggressive subtype. Loss or inactivation of tumor suppressors is crucial in tumorigenesis. The role of the classic *VHL* gene and its pathway in ccRCC have been extensively studied (2). Moreover, drugs targeting the VHL–HIF–VEGF pathway, such as sunitinib, sorafenib and axitinib, have been shown to benefit patients with ccRCC, becoming the standard treatment for patients in the advanced stages of ccRCC (3). Unlike other epithelial tumors, mutations in the classic tumor suppressors, such as *BRAF*, *TP53*, *PTEN*, *RB1*, and *EGFR*, are rare in ccRCC (4, 5). In addition to *VHL* inactivation, a recurrent loss of chromosome 3p fragments in ccRCC has been reported (6, 7). Furthermore, BRCA1-Associated Protein 1 (BAP1) on chromosome 3p was identified as a novel tumor-driver gene in ccRCC using extensive parallel sequencing techniques (8, 9).

BAP1 is a novel ubiquitin carboxy-terminal hydrolase and a subfamily member of deubiquitinating enzymes (10, 11). BAP1 is located in the nucleus and binds to *BRCA1* to enhance its tumor suppressor activity (12). Additionally, BAP1 is involved in many biological processes, such as DNA damage repair, cell differentiation and cell proliferation, *via* its deubiquitinating activity (12). Various studies have reported that BAP1 is commonly lost or inactivated in numerous human malignancies, especially in ccRCC, hepatocellular carcinoma and mesothelioma (13). The majority of chromosomes have a 3p deletion, which is an initial marker for nonhereditary ccRCC (14). The mutated frequency of BAP1 was also reported to be as high as 20% in ccRCC (15, 16), with RCC accounting for 9% of BAP1 tumor predisposition syndrome (BAP1-TPDS) (17). Compared with sporadic tumors, BAP1-TPDS RCC has earlier onset, more aggressive tumors and poorer patient survival (17, 18). Due to the poor treatment response, a standard treatment for BAP1 mutated tumors is yet to be identified (19). Recently, several studies have reported the direct targeting of differentially expressed genes in BAP1-deficient tumors (20, 21). For example, histone deacetylase and enhancer of Zeste 2 Polycomb repressive complex 2 are upregulated in BAP1-deficient tumors; therefore, targeting these genes could improve BAP1-deficient tumor sensitivity to treatment (22, 23). Therefore, understanding differentially expressed genes in BAP1-deficient tumors could provide a novel perspective for targeted therapy.

Long noncoding RNAs (lncRNA), longer than 200 nucleotides (nt), are non-protein-coding RNAs that are involved in various tumor developments, including ccRCC, and specific lncRNAs are associated with tumor migration, invasion and poor prognosis (24, 25). MicroRNA (miRNA) is a single-stranded non-coding RNA of approximately 19–25 nt, which can bind to the 3' untranslated mRNA region and regulate target gene expression (26). Non-coding RNAs (namely, lncRNAs and circular RNAs) could serve as competitive endogenous RNAs (ceRNA) that competitively bind to miRNAs (a post-transcriptional regulator) for cell–cell communication and gene expression co-regulation (27–30).

METHODS AND MATERIALS

Data Collection and Processing

RNAseq (lncRNA, mRNA and miRNA) and relevant clinical data for kidney renal clear cell carcinoma (KIRC) were obtained from the TCGA database (https://portal.gdc.cancer.gov/).

Identification of Differentially Expressed lncRNAs, miRNAs and mRNAs

Based on the median expression of BAP1, patients were divided into the $BAP1^{high}$ and the $BAP1^{low}$ groups. For differential expression analysis, the cutoff value of DElncRNA was set at $|\log_2 FC| > 0.5$ and *P*. adj <0.05; DEmiRNA with cutoff value of $|\log_2 FC| > 0.7$ and *P*. adj <0.05; DEmRNA with cutoff value of $|\log_2 FC| > 0.5$ and *P*. adj <0.05.

Construction of ceRNA Networks

Highly conserved microRNA family files were downloaded from the miRcode database (http://mircode.org/). Subsequently, the obtained DElncRNAs were used to find potential miRNAs targeting these DElncRNAs. Then, the selected miRNAs were inputted into the miRBD database (http://mirdb.org/) (31) and the Targetscan database (http://www.targetscan.org/vert_72/) (32) to explore target mRNAs. Finally, the screened DElncRNAs, DEmiRNAs, and DEmRNAs were put into Cytoscape (version 3.6.1) for ceRNA network construction, using the plug-in 'cytoHubba' for hub genes network construction (33, 34).

Functional Annotation

To investigate the functional annotation implicated with DEmRNAs, the Gene Ontology annotation and the Kyoto Encyclopedia of Genes and Genomes pathway analysis were performed using the Metascape website (https://metascape.org/) (35).

Expression of Hub Genes and Survival Analysis

The expression of the hub genes in tumor and normal tissues based on the ccRCC dataset were compared using the Wilcoxon rank-sum test ($P < 0.05$). Overall survival (OS) analysis for the expression of the hub genes between the high- and low-expression groups was performed, with $P < 0.05$ indicating statistical significance.

Clinical Relevance of the Nuclear Enriched Abundant Transcript 1 (NEAT1)/miR-10a-5p/SERPINE1 Axis in Patients With ccRCC

To explore the clinical relevance of the ceRNA axis, the expression levels of NEAT1, miR-10a-5p, and SERPINE1 with different clinical characteristics were evaluated, and the Bonferroni method was used to correct the results of multiple

hypothesis testing (Dunn's test, *P*. adj <0.05). Moreover, univariate and multivariate Cox regression analyses were conducted to investigate the prognostic significance of clinical features.

Cell Culture

The ACHN and 786-O cell lines were obtained from the American Type Culture Collection (Manassas, VA, USA). Both cell lines were cultured in Dulbecco's modified Eagle's medium (Gibco) containing 10% fetal bovine serum (Gibco) and 1% penicillin/streptomycin and incubated at 37°C in a humidified 5% CO_2 atmosphere.

Cell Transfection

Cells were seeded into six-well plates and cultured until the cell density reached approximately 60%. The cells were then transfected with small-interfering RNA (siRNA-NEAT1#1, #2) or miR-10a-5p mimic/inhibitor, using jetPRIME® transfection reagent (NY, USA) following the protocol of the manufacturer. Additionally, a relevant negative control (NC) was used. These siRNAs, miR-10a-5p mimic/inhibitor and relevant NC were designed by GenePharma (Shanghai, China).

RT-qPCR (Quantitative Reverse Transcription-Polymerase Chain Reaction) and Western Blotting

Total RNA was extracted using RNAeasy™ (Beyotime; Shanghai, China), following the instructions of the manufacturer. HiScript® II reverse transcriptase (Vazyme; Nanjing, China) was used to convert RNA to cDNA. RT-qPCR was performed in a LineGene 9600 Plus system (Bioer Technology, Hangzhou, China), using 2 × SYBR Green qPCR Master Mix (High ROX; Servicebio; Wuhan, China), following the protocol of the manufacturer. The expression of miR-10a-5p was normalized to control U6, while that of the others were normalized to GAPDH, and relative expression was calculated using the $2^{-\Delta\Delta Ct}$ method. Western blotting was performed as previously described (36), and anti-SERPINE1 (Rabbit Polyclonal Antibody, AF7965, Beyotime), anti-GAPDH (Mouse Monoclonal Antibody, AF5009, Beyotime) antibodies were used for further experimentation.

Cell Viability

After 48 h of transfection, 100 μl cell suspension containing 1 × 10^3 cells were seeded into 96-well plates and cultured. After 24, 48, 72, and 96 h, 10 μl of CCK-8 (Beyotime; Shanghai, China) was added to each well and incubated at 37°C for another 2 h. The absorbance was detected using a microplate reader at 450 nm.

Colony Formation Assay

After transfection for 48 h, the cell suspension was added to six-well plates with approximately 1 × 10^3 cells per well and incubated at 37°C in a humidified 5% CO_2 atmosphere for 2 weeks. After culturing, the cells were washed twice with PBS, fixed with 4% paraformaldehyde for 15 min, stained with 0.1% crystal violet for 15 min, washed thrice with PBS again. The number of cell colonies with a diameter of >0.1 mm was further observed under the microscope.

Wound Healing Assay

The treated cells were seeded into six-well plates. When the cell density was close to 90%, a linear scratch was made using a 200 μl plastic pipette tip. The wound-healing time in different treatment groups were observed under a microscope and photographed at 0 and 12 h. The wound closure rate was measured thrice and averaged.

Luciferase Reporter Assays

The dual-luciferase reporter gene plasmids containing wild-type and mutant sequences were synthesized using Promega (Madison, WI, USA). The wild-type or mutant (NEAT1, SERPINE1) reporter plasmid and miR-10a-5p mimic or mimic-NC were co-transfected into 293T cells. Luciferase activity was measured 48 h after transfection.

Fluorescence *In Situ* Hybridization (FISH)

FISH analysis on the ACHN cells was performed to determine the subcellular localization of *NEAT1* and miR-10a-5p. The RNA probes were designed and synthesized *via* Servicebio (Wuhan, China). Briefly, the cells were fixed with 4% paraformaldehyde for 20 min and washed with PBS. Then, proteinase K (20 ug/ml) was digested for 8 min, followed by PBS washes. Subsequently, a pre-hybridization solution was added for 1 h at 37°C and then discarded. RNA probes containing a hybridization solution was added to the cells and hybridized overnight at 37°C. Next, DAPI staining solution was added after the washes and incubated for 8 min, followed by rinsing and the addition of an anti-fluorescence quenching blocker dropwise to seal the slice. Finally, the slices were visualized under a Nikon fluorescence microscope.

DNA Methylation Analysis of SERPINE1

To investigate the DNA methylation level of SERPINE1, co-expression analysis of SEPRINE1 was conducted using three DNA methyltransferases (DNMT1, DNMT3A, DNMT3B). Following this, methylation analysis of SERPINE1 was performed between tumor and normal tissues using the online database DiseaseMeth version 2.0 (http://bio-bigdata.hrbmu.edu.cn/diseasemeth/). MEXPRESS (https://mexpress.be/) was used to further determine the relationship between *SERPINE1* expression and DNA methylation status (37).

Correlation Between Immune Infiltration and Expression of SERPINE1 in KIRC

TIMER (https://cistrome.shinyapps.io/timer/) was used for the comprehensive analysis of the relationship between SERPINE1 expression and tumor-infiltrating immune cell levels, namely, neutrophils, macrophages, dendritic cells, B cells, $CD4^+$ T cells, and $CD8^+$ T cells (38).

Software and Versions

R software (x64, version 4.0.3) was used for the statistical analyses (https://www.r-project.org/).

RESULTS

BAP1 Acts as a Tumor Suppressor in ccRCC

Figure 1 presents a flow diagram of ceRNA construction and analysis. A pan-cancer analysis was performed to evaluate the RNA and protein expression level of BAP1 using data from the UCSC XENA (https://xenabrowser.net/datapages/) and the Human Protein Atlas (HPA) databases (https://www.proteinatlas.org/), respectively. BAP1 RNA expression was found to be significantly downregulated in ccRCC (**Figure 2A**), while BAP1 protein level was the lowest in renal cancer (**Figure S1**). Furthermore, immunohistochemistry staining data obtained from the HPA validated BAP1 downregulation in tumor tissue (**Figure 2B** and **Table S1**). Additionally, Kaplan–Meier survival curves indicated that the low expression of BAP1 was associated with poor OS in ccRCC (**Figure 2C**).

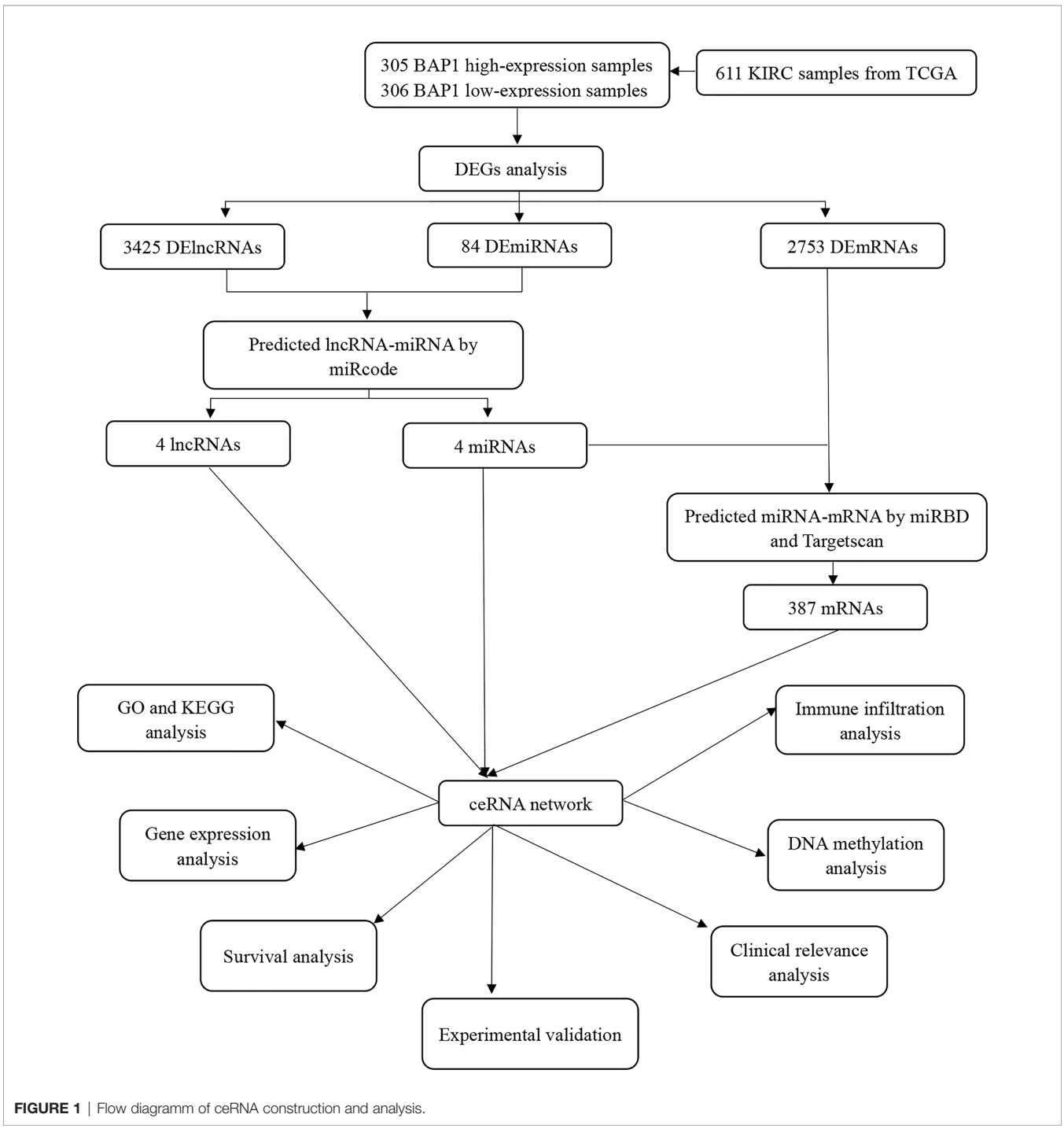

FIGURE 1 | Flow diagramm of ceRNA construction and analysis.

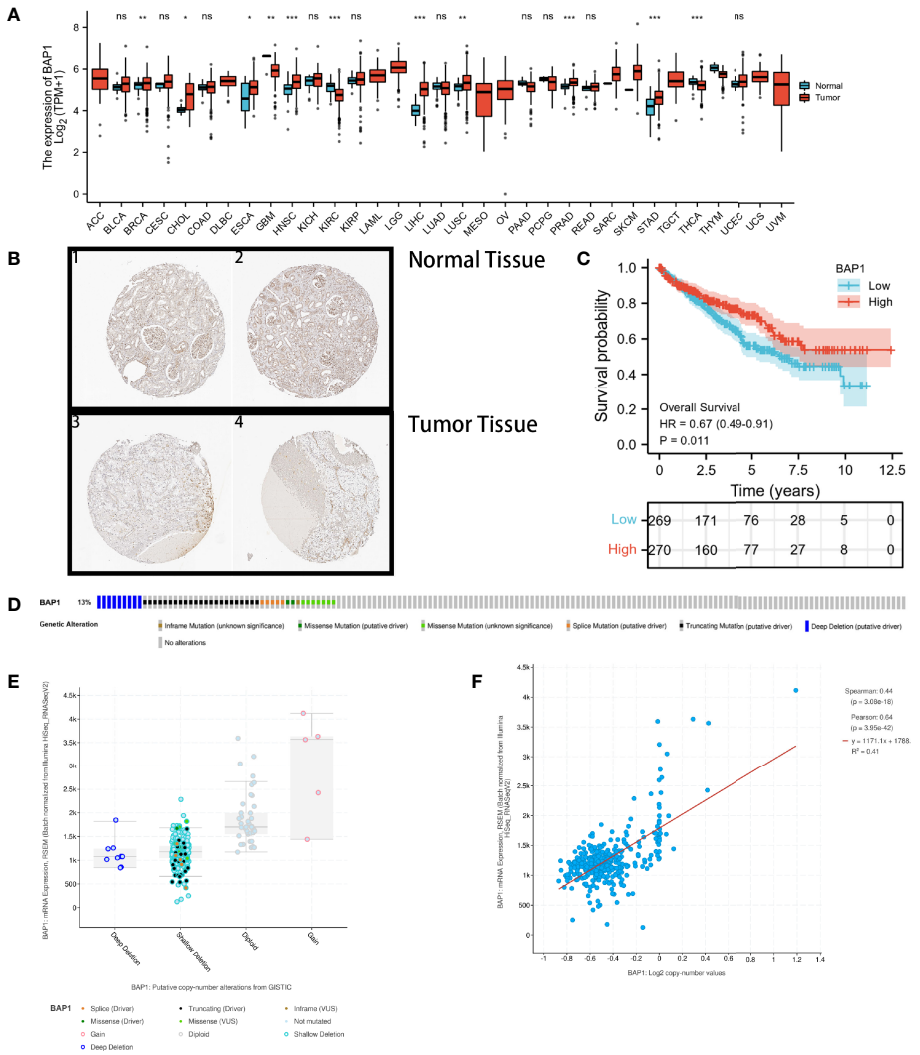

FIGURE 2 | BAP1 acts as a tumor suppressor in kidney renal clear cell carcinoma (KIRC). **(A)** Pan-cancer analysis of BAP1; **(B)** Immunohistochemical analysis of BAP1 in renal tumor and normal tissues; **(C)** Survival analysis comparing high- and low expression of BAP1; **(D)** Distribution of BAP1 genomic alterations inTCGA KIRC; **(E, F)** Relationship between copy number alterations and BAP1 expression: scatter plot **(E)**, correlation plot **(F)**. ns, not significant, $p \geq 0.05$; *$p < 0.05$; **$p < 0.01$; ***$p < 0.001$.

Moreover, the cBioPortal (http://www.cbioportal.org/) was used to explore the potential mechanisms underlying the abnormally low expression of BAP1 in ccRCC (39). **Figure 2D** shows that the genetic alteration rate of BAP1 was found to be 13%, with gene deletions (deep deletion and shallow deletion) accounting for more than half of the copy number alterations in ccRCC samples (**Figure 2E**). Additionally, the mRNA expression level of BAP1 was found to be positively correlated with the copy number value (**Figure 2F**).

Identification of DERNAs and lncRNA–miRNA–mRNA Networks

DERNAs were screened according to the cut-off value (**Figure 3**) and intersected with the predicted RNAs. The shortlisted genes were inputted into Cytoscape for hub genes network construction (**Figure 4A**). Finally, lncRNAs (NEAT1, HELLPAR, PURPL), miRNAs (miR-10a-5p, miR-508-3p, miR-135a-5p) and mRNAs (IRS1, SERPINE1, KCAN1, TRIM2, RORB, SIX4) were identified (**Figure 4B**). A functional enrichment analysis of DEmRNAs demonstrated their involvement in mesenchyme development, transmembrane receptor protein tyrosine kinase signaling pathway and cell adhesion regulation (**Figure 4C**).

Construction of Prognostic-Related ceRNA in ccRCC

Expression and survival analyses of hub genes are shown in **Figures 5**, **6**. In total, two DElncRNAs (NEAT1, HELLPAR), one DEmiRNA (miR-10a-5p) and four DEmRNAs (SERPINE1,

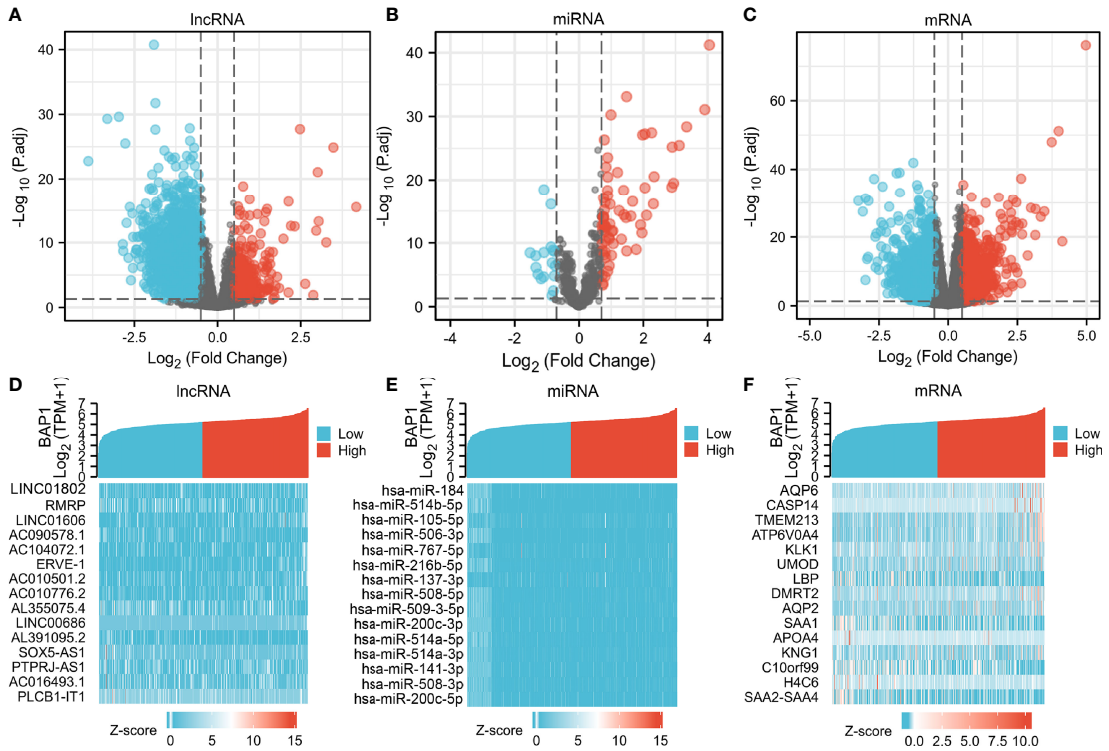

FIGURE 3 | Volcano plots and heatmap plots of DElncRNAs, DEmiRNAs, and DEmRNAs between the expression of BAP1high and BAP1low in KIRC samples. Red color represents up-regulated genes, blue represents down-regulated genes. **(A)** 3425 DElncRNAs (|log2 FC| > 0.5 and P. adj < 0.05); **(B)** 84 DEmiRNAs (|log2 FC| > 0.7 and P. adj < 0.05); **(C)** 2753 DEmRNAs with cutoff value of |log2 FC| > 0.5 and P. adj < 0.05; **(D–F)** Heatmaps of the top 15 significant DElncRNAs, miRNAs and mRNAs.

TRIM2, RORB, SIX4) were found to be prognostic-related genes. Moreover, the lncLocator (www.csbio.sjtu.edu.cn/bioinf/lncLocator/) showed that NEAT1 was mainly distributed in the cytoplasm (**Figure S2**), indicating its role as a ceRNA in enhancing SERPINE1 expression by sponging miR-10a-5p. Finally, a prognostic-related NEAT1/miR-10a-5p/SERPINE1 ceRNA network was constructed (**Figure 7A**).

Clinical Relevance of the NEAT1/miR-10a-5p/SERPINE1 Axis in Patients With ccRCC

In this study, NEAT1 was correlated with gender (P <0.05, **Figure S3A**). The lower expression level of miR-10a-5p was associated with higher T stage, M stage, pTNM stage, tumor grade and gender (P <0.05, **Figure S3B**). Moreover, SERPINE1 was strongly correlated with T stage, N stage, pTNM stage, tumor grade and gender (P <0.05, **Figure S3C**). The multivariate Cox regression analysis showed that NEAT1 (hazard ratio (HR) = 1.488, P = 0.011), SERPINE1 (HR = 1.456, P = 0.015) and miR-10a-5p (HR = 0.681, P = 0.014) were independent prognostic factors in ccRCC (**Tables S2–4**). The AUC (area under the curve) of the receiver operating characteristics (ROC) analysis (**Figure S4**) indicated a good prognostic performance of SERPINE1 (AUC = 0.789) and miR-10a-5p (AUC = 0.892). Additionally, the pan-cancer analysis showed that SERPINE1 mRNA was highly expressed in kidney cancer (**Figure S5A**). Furthermore, immunohistochemical analysis revealed that SERPINE1 was located in the cytoplasmic/membranous area (**Figure S5B**).

lncRNA NEAT1 Regulates Tumor Proliferation and Migration in Kidney Cancer Cell Lines

RT-qPCR analysis showed that NEAT1 was highly expressed in kidney cancer cell lines compared to that in HK-2, with more significant differences in 786-O and ACHN cell lines (**Figure 7B**). The knockdown efficiency of the two siRNAs was verified using RT-qPCR (**Figure 7C**). CCK-8 and colony formation assays showed that 786-O and ACHN cell proliferation was significantly suppressed after NEAT1 knockdown (**Figures 7D, E**). Wound healing assays showed that the migration ability of the cells was inhibited after transfection with siNEAT1 (**Figure 7F**).

NEAT1 Serves as a Sponge for miR-10a-5p and Upregulates SERPINE1 to Regulate the Proliferation of Kidney Cancer Cells

The target site of NEAT1 to miR-10a-5p was predicted using the starBase (https://starbase.sysu.edu.cn/), and the wild-type and mutant sequences are shown in **Figure 8A**. A dual fluorescein

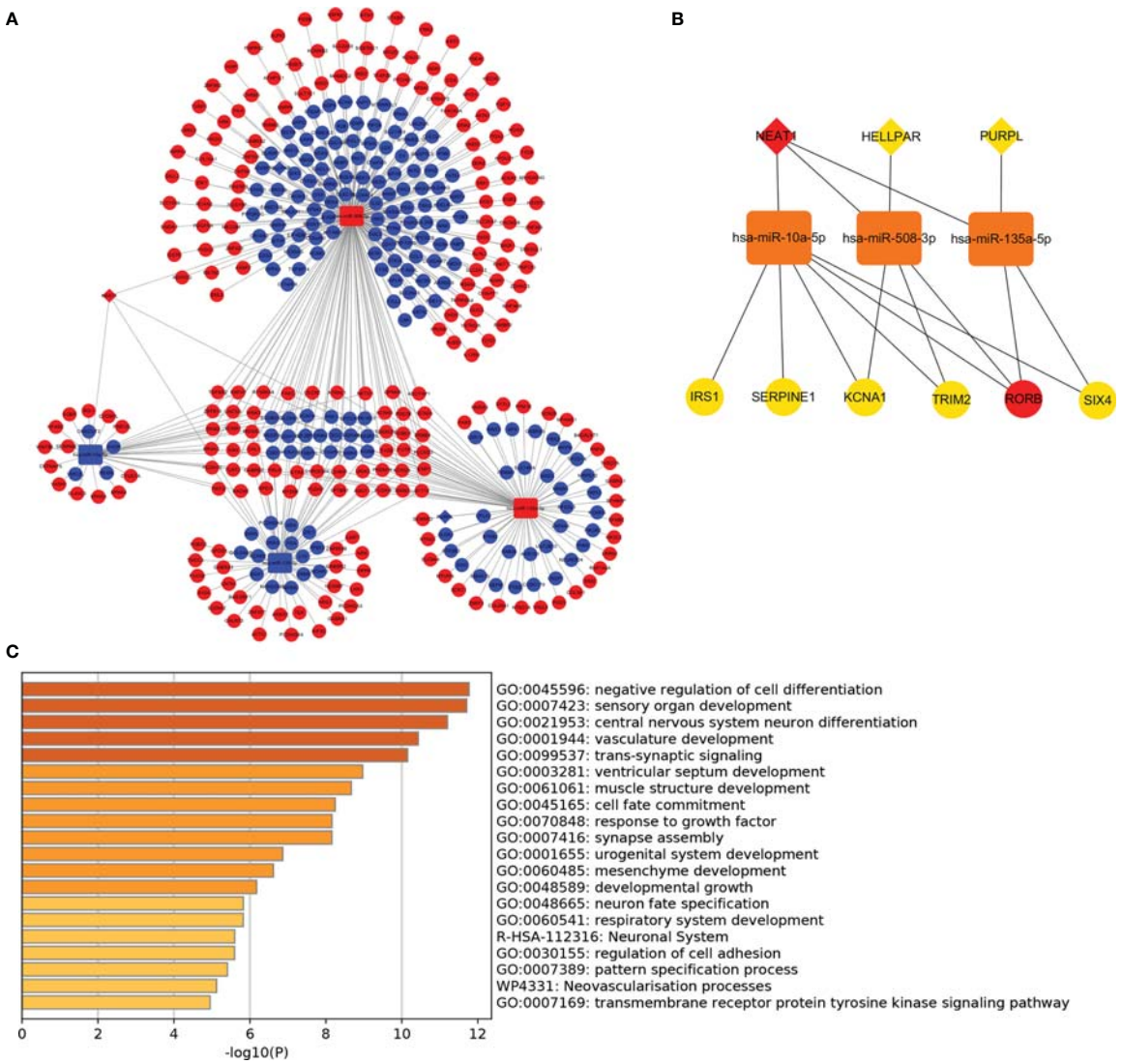

FIGURE 4 | Construction of ceRNA networks and functional annotation. **(A)** A triple regulatory network based on 4 lncRNAs, 4 miRNAs, and 387 mRNAs; **(B)** Hub genes network was constructed using plug-in "cytoHubba"; **(C)** Functional enrichment analysis of DEmRNAs.

reporter gene plasmid (NEAT1-WT/NEAT1-MUT) was constructed and co-transfected into 293T cells with miR-10a-5p mimic and miR-NC. Overexpression of miR-10a-5p significantly reduced luciferase activity in the NEAT1-WT group but not in the NEAT1-MUT group (**Figure 8B**), confirming that miR-10a-5p binds directly to NEAT1. Moreover, FISH assays revealed that miR-10a-5p co-localized with NEAT1 in the cytoplasm of ACHN cells (**Figure 8C**). Therefore, NEAT1 serves as a sponge for miR-10a-5p and inhibit its function in kidney cancer cells.

Next, the efficiency of the miR-10a-5p mimic and inhibitor on miR-10a-p expression was verified using RT-qPCR (**Figure 8D**). On transfection with siNEAT1 in ACHN and 786-O cells, miR-10a-5p expression was significantly enhanced (**Figure 8E**). Therefore, co-transfection siRNA and miR-inhibitor (siNC + inhibitor NC; siNC + inhibitor; siNEAT1 + inhibitor NC; siNEAT1 + inhibitor) in ACHN and 786-O cells, CCK-8 and colony formation assays suggested that the knockdown of NEAT1 on the suppression of cell proliferation and colony formation in ACHN and 786-O cells could be reversed by a miR-10a-5p inhibitor (**Figures 8F, G**).

To confirm that miR-10a-5p regulates the expression of SERPINE1 by binding directly to the target sequence, a luciferase reporter gene plasmid was constructed for SERPINE1-WT/MUT (**Figure 9A**). The results showed that miR-10a-5p mimic significantly reduced the luciferase activity of SERPINE1-WT; however, no significant changes were observed for SERPINE1-MUT (**Figure 9B**). siNEAT1 was co-transfected with miR-10a-5p inhibitor into ACHN and 786-O cells and evaluated using RT-qPCR and western blot to verify the

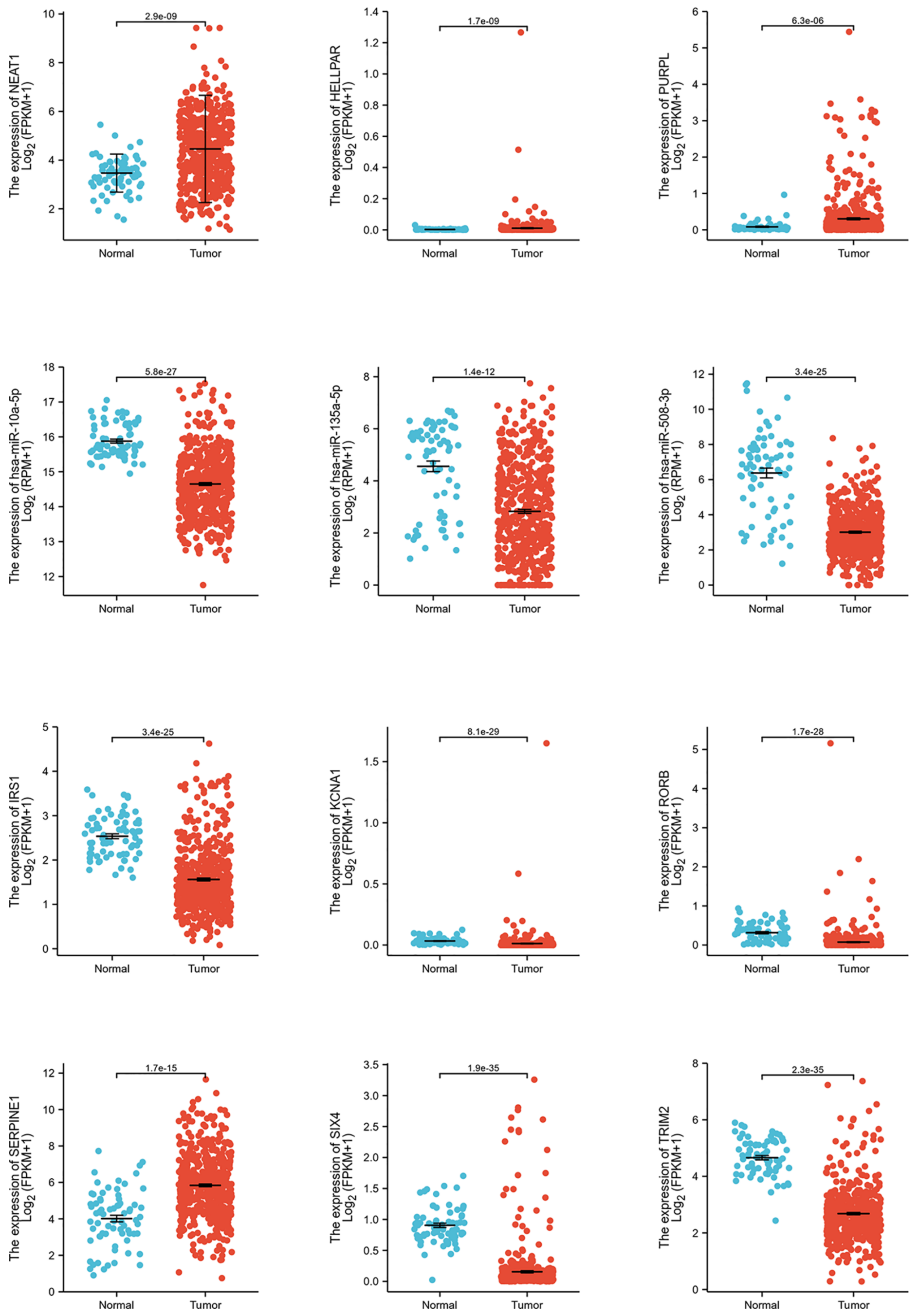

FIGURE 5 | Hub genes expression analysis. Expression analysis of 12 hub genes (3 lncRNAs, 3 miRNAs, 6 mRNAs) comparing tumor and normal tissues.

regulation of SERPINE1 expression. The results demonstrated that the knockdown of NEAT1 significantly downregulated the expression of SERPINE1; however, this effect could be reversed by a miR-10a-5p inhibitor (**Figures 9C, D**).

DNA Methylation Analysis of SERPINE1

To elucidate the mechanism of the abnormally high expression of SERPINE1 in ccRCC, a series of methylation analyses of SERPINE1 was performed. Co-expression analysis suggested that SERPINE1 expression was positively correlated with DNMT1, DNMT3A, and DNMT3B expression levels (P <0.05, **Figure 10A**). Additionally, the methylation level of SERPINE1 in normal tissues was much higher than ccRCC tissue samples (P <0.001, **Figure 10B**). Moreover, 12 DNA methylation sites that were negatively correlated with SERPINE1 expression were identified (**Figure 10C**).

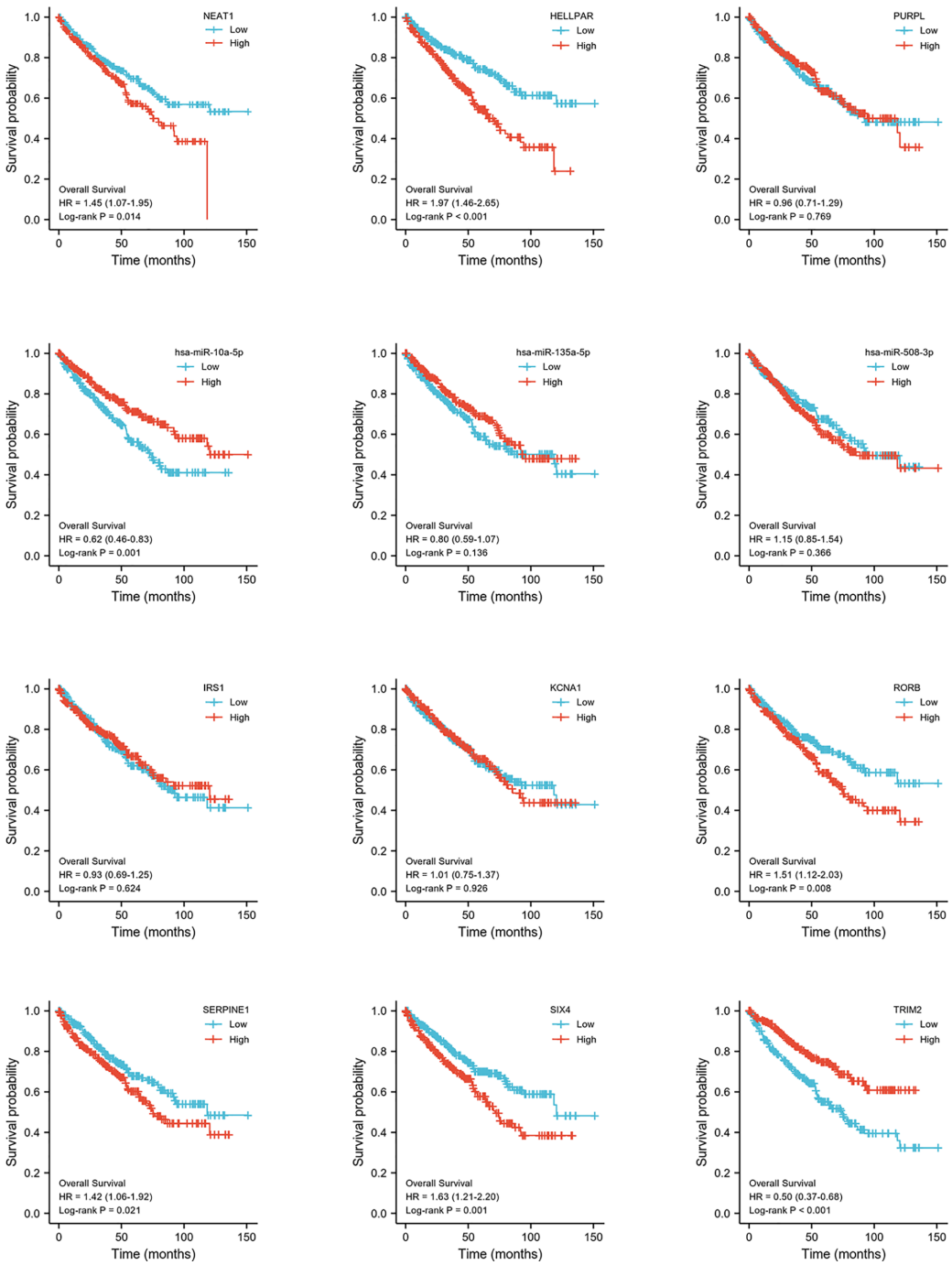

FIGURE 6 | Hub genes survival analysis. Survival analysis of 12 hub genes (3 lncRNAs, 3 miRNAs, 6 mRNAs) comparing high- and low expression group.

Immune Infiltration Analysis of SERPINE1 in KIRC

To further investigate the relationship between SERPINE1 expression and the immune microenvironment in ccRCC, an immune infiltration analysis was performed using TIMER. 'SCNA' module analysis indicated that the immune infiltration level of CD 4^+ T cell was associated with the altered copy numbers of SERPINE1 (**Figure 11A**). Moreover, 'Gene' module analysis showed that the expression of SERPINE1 was positively related to the immune infiltration level of $CD4^+$ T cell, $CD8^+$ T cell, macrophages, dendritic cells and neutrophils (**Figure 11B**).

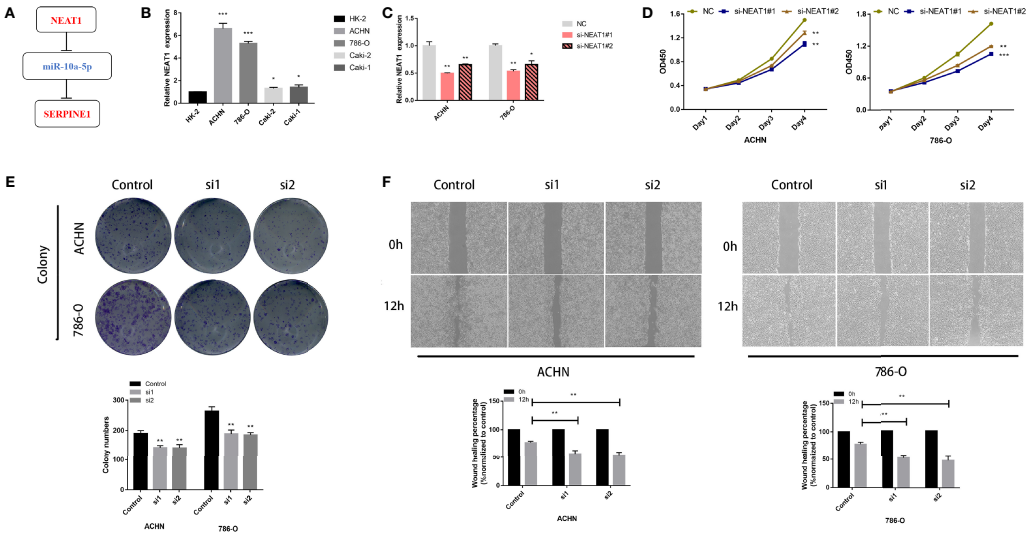

FIGURE 7 | LncRNA NEAT1 promotes proliferation and migration in kidney cancer cell lines. **(A)** Construction of a ceRNA axis; **(B)** NEAT1 is upregulated in kidney cancer cell lines; **(C)** Validation of knockdown efficiency of siNEAT1 by RT-qPCR; Knockdown of NEAT1 inhibits proliferation **(D)**, colony formation **(E)** and migration **(F)** of kidney cancer cells. p≥0.05; *p < 0.05; **p < 0.01; ***p < 0.001.

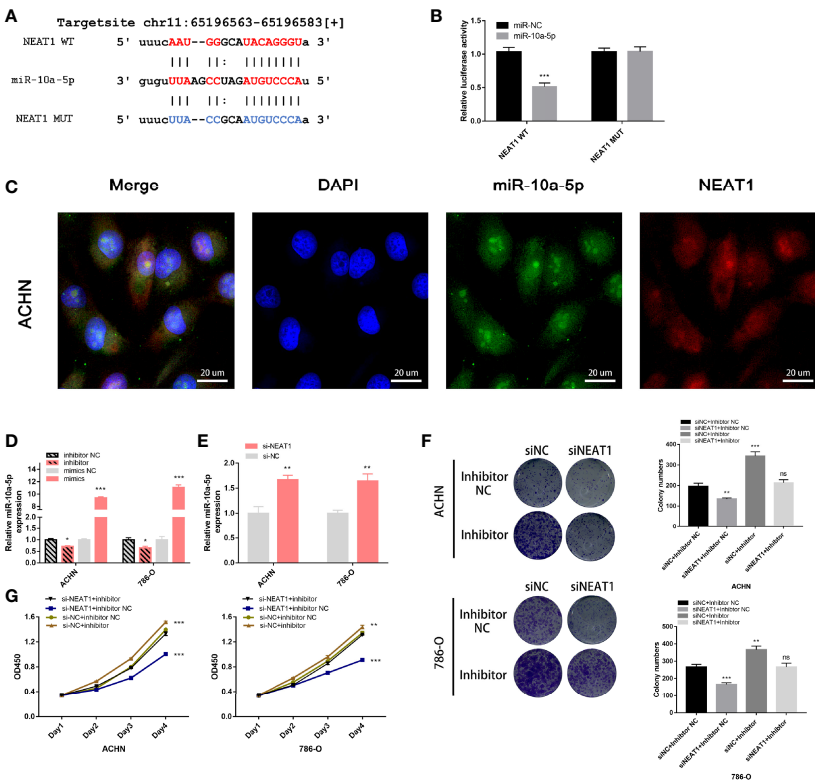

FIGURE 8 | NEAT1 serves as sponge for miR-10a-5p in kidney cancer cells. **(A)** Prediction the target sequence of NEAT1 bonding to miR-10a-5p by starBase; **(B)** Dual luciferase reporter gene assays verify the direct binding of miR-10a-5p to NEAT1 target sequence; **(C)** FISH assays confirm that NEAT1 co-localizes with miR-10a-5p in the cytoplasm of kidney cancer cells; **(D)** Validation the efficiency of miR-10a-5p mimic and inhibitor by RT-qPCR; **(E)** Knockdown of NEAT1 enhances the expression of miR-10a-5p; **(F, G)** miR-10a-5p inhibitor reverses the inhibition of cell proliferation caused by siNEAT1. ns, not significant, p ≥ 0.05; *p < 0.05; **p < 0.01; ***p < 0.001.

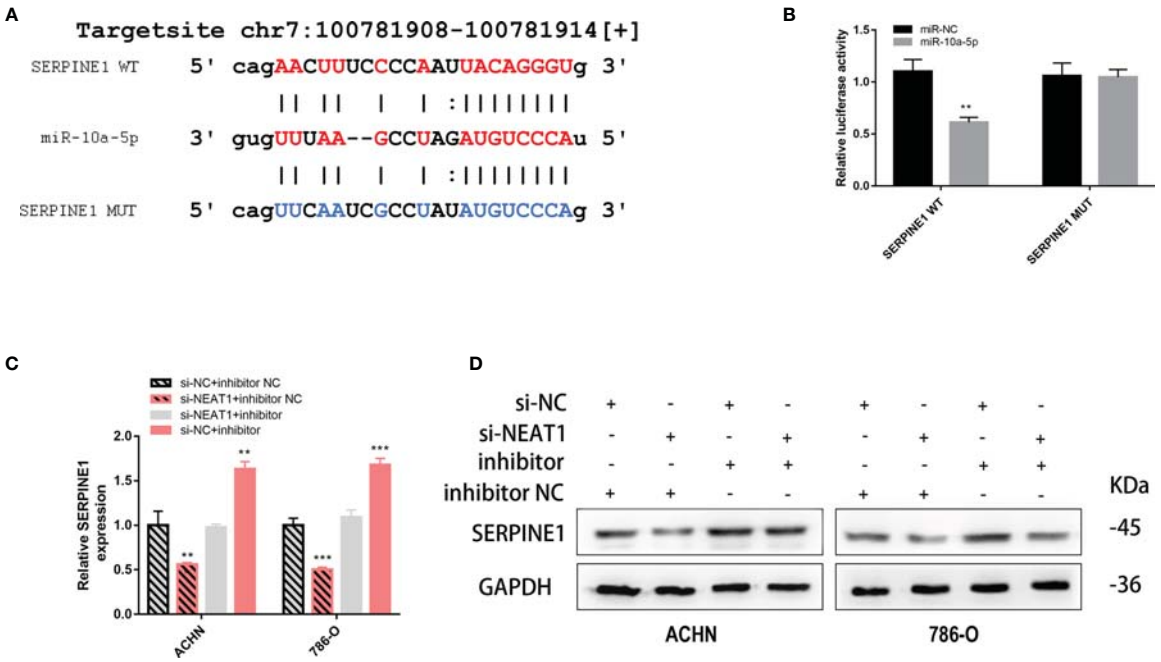

FIGURE 9 | NEAT1 sponging miR-10a-5p to regulate SERPINE1. **(A)** Prediction the target sequence of SERPINE1 bonding to miR-10a-5p by starBase; **(B)** Dual luciferase reporter gene assays verify the direct binding of miR-10a-5p to SERPINE1 target sequence; **(C, D)** Knockdown of NEAT1 can downregulate the expression of SERPINE1 but can be reversed by miR-10a-5p inhibitor. **p < 0.01; ***p < 0.001.

DISCUSSION

Numerous studies have shown that transcription occurs in approximately 80% of the human genome, with protein-coding genes accounting for only 2% of the human genome. This suggests that the majority of RNAs are non-coding genes (40). Cancer is often associated with abnormal transcriptomes; moreover, increasing evidence indicates that the non-coding transcriptome is often dysregulated in cancer and plays an important role in determining its pathogenesis (41, 42). Therefore, on analyzing the differentially expressed non-coding RNAs in BAP1-deficient ccRCC, this study identified NEAT1/miR-10a-5p/SERPINE1 as a BAP1-related prognostic ceRNA.

NEAT1, which is located in the nuclear paraspeckles, has been reported to be involved in various biological processes, such as tumorigenesis, infection, neuropathy, and immunity (43–46). Previous studies have shown that NEAT1 plays a key role in carcinogenesis by mediating gene expression. For example, NEAT1 induces transcription factors to relocate from the promoters of downstream genes to the paraspeckles, altering gene transcription (44). NEAT1 also acts as a scaffold to bind multiple proteins located in the paraspeckles together or as a bridge for protein complexes (47, 48). Recently, NEAT1 has been reported to act as a ceRNA to regulate the expression of downstream genes by sponging miRNAs in malignant tumors (49–51). Previous studies have demonstrated that BRCA1 as a transcription factor can directly bind 1.4 kb upstream of the TSS region of NEAT1 and negatively regulate its expression (52). In the nucleus, BAP1 binds to BRCA1 and enhances its tumor suppressive activity. Thereby, the loss of BAP1 was hypothesized to indirectly affect the tumor suppressor activity of BRCA1, resulting in an abnormally high expression of NEAT1.

SERPINE1, encoding plasminogen activator inhibitor 1 (PAI-1), is an essential inhibitor of tissue plasminogen activator and urokinase (uPA). Previous studies have focused on the effect of SERPINE1 on human thrombosis, cardiac fibrosis, inflammatory injury, ageing and metabolism (53–57). However, current studies report on the importance of SERPINE1 in promoting tumor malignant progression, distant metastasis and chemotherapy resistance through multiple pathways. Moreover, high SERPINE1 expression is significantly associated with poor prognosis (58, 59). The underlying mechanism has been speculated to be the migratory effect of uPA–uPAR–PAI-1 systems on endothelial cells, with fibrin deposition playing an important role in tumor angiogenesis (60); SERPINE1 also functions as an extracellular matrix (ECM) component to stabilize tumor cell adhesion in migration (61). ECM is composed of proteins and proteoglycans that are secreted by keratinocytes, fibroblasts and immune cells (62). In the complex tumor microenvironment (TME), dynamic cell–cell and cell–ECM interactions play a crucial role in tumor initiation and immune cell regulation (63). The tumor immune microenvironment determines the biological behaviour of tumour cells, with immune cell infiltration levels correlating with tumor

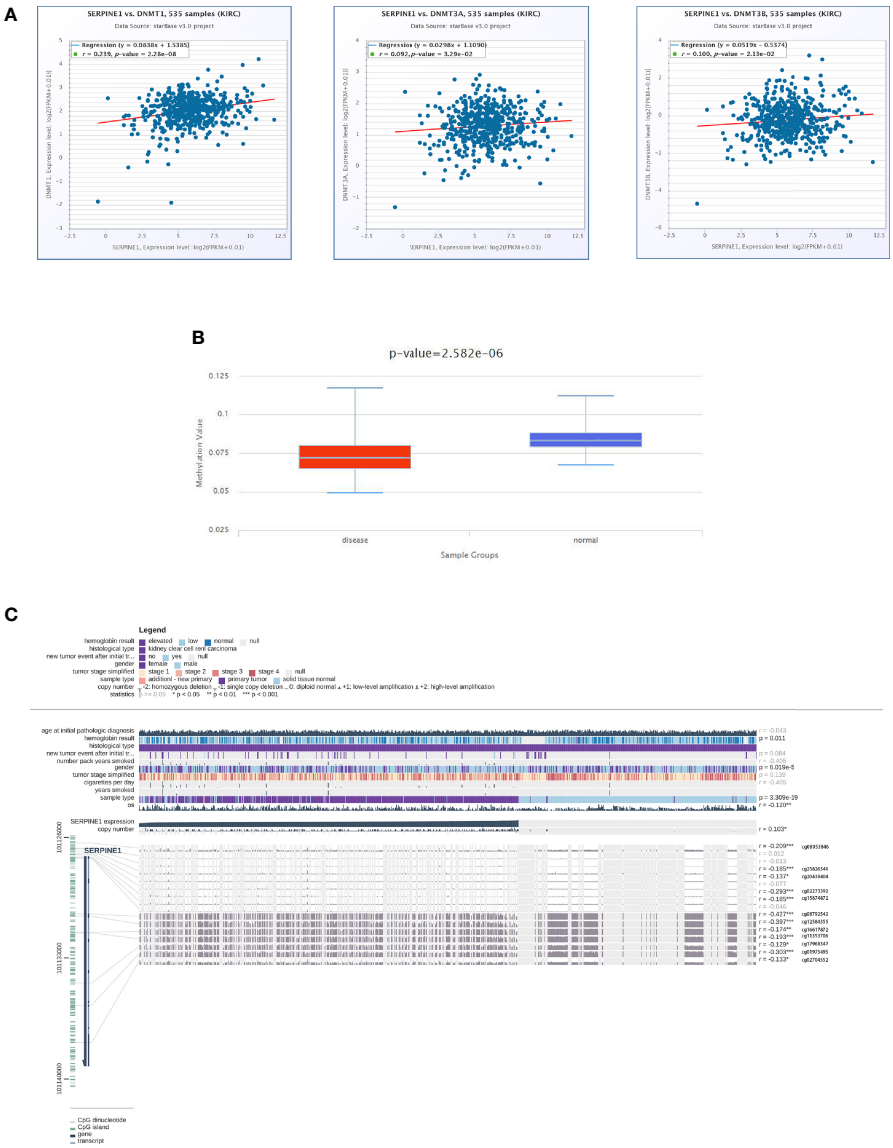

FIGURE 10 | DNA methylation analysis of SERPINE1. **(A)** Co-expression analysis of SERPINE1 with three DNMTS (DNMT1, DNMT3A and DNMT3B); **(B)** Methylation level of SERPINE1 comparing KIRC and normal samples; **(C)** Relationship between SERPINE1 expression and genome-wide methylation by MEXPRESS.

prognosis (64–66). In this study, the copy number of SERPINE1 was found to be associated with the immune infiltration of $CD4^+$ T cells, and the expression of SERPINE1 was related to the level of immune infiltration of $CD4^+$ T cells, $CD8^+$ T cells, macrophages, dendritic cells and neutrophils. Roelofs et al. demonstrated that SERPINE1 regulated neutrophil influx during renal fibrosis, suggesting that SERPINE1 acts as a chemokine to mediate immune cell infiltration (67). Moreover, in oral squamous cell carcinoma, PAI-1 has been shown to induce $CD14^+$ monocytes to differentiate into $CD206^+$ tumor-associated macrophages (TAMs), producing epidermal growth factors to mediate tumor cell migration (68). In the TME, cancer-associated fibroblasts induce the M2-polarization of macrophages and produce chemokine ligand 12 to promote the secretion of PAI-1 in TAMs, leading to the malignant process of hepatocellular carcinoma (69).

Current anti-cancer drug research uses a two-dimensional model of cytotoxicity *in vitro* (63), which does not accurately represent the three-dimensional TME. Moreover, the individual differences and intra-tumor cell heterogeneity are not sufficiently considered, resulting in many clinically ineffective anti-cancer drugs (70). Therefore, targeting the abnormally elevated functional proteins of ECMs in the TME could be a new direction for the development of anti-tumor drugs. In this study, the loss of BAP1 resulted in an abnormal upregulation of SERPINE1 (PAI-1) and hence, SERPINE1 could be a new target for the treatment of BAP1-deficient ccRCC.

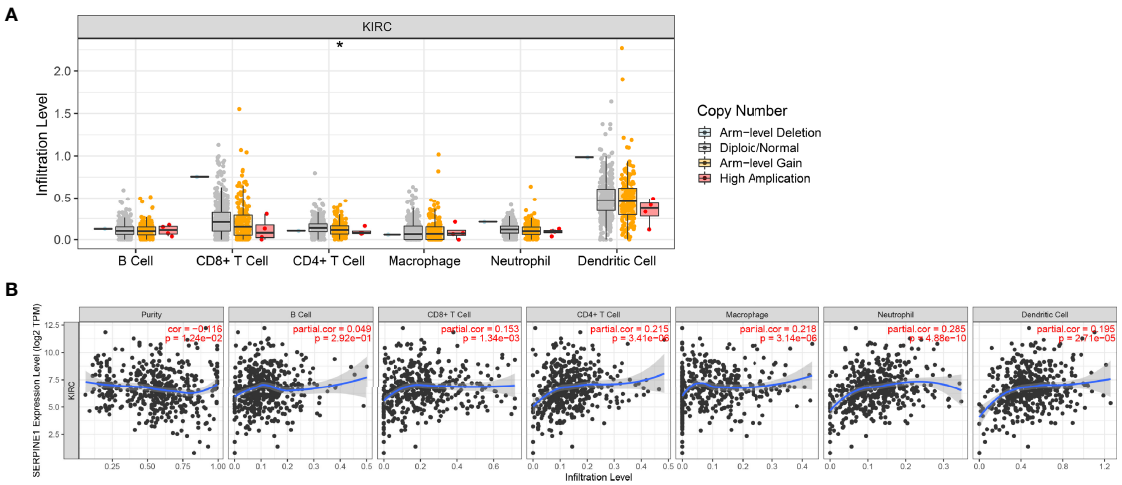

FIGURE 11 | Immune infiltration analysis of SERPINE1 in KIRC. **(A)** Relationship between the level of immune cell infiltration and the copy number of SERPINE1 in KIRC. **(B)** Correlation of SERPINE1 expression and immune cell infiltration in KIRC. *p < 0.05.

CONCLUSIONS

A ceRNA (NEAT1/miR-10a-5p/SERPINE1) network was constructed that could be used as a prognostic biomarker of BAP1-deficient ccRCC. Furthermore, miR-10a-5p/SERPINE1 was significantly associated with clinical features, indicating their role as independent prognostic factors of ccRCC.

DATA AVAILABILITY STATEMENT

The original contributions presented in the study are included in the article/**Supplementary Material**. Further inquiries can be directed to the corresponding authors.

AUTHOR CONTRIBUTIONS

RJL designed the study and conducted data extraction, analysis and experimentation. RJL, ZPX, SYL, JJY, and BX wrote the manuscript. RJL, ZPX, NHF, BX, and MC reviewed and revised the manuscript. All authors listed have made a substantial, direct, and intellectual contribution to the work and approved it for publication.

FUNDING

This study was funded by The National Natural Science Foundation of China (Nos. 81872089, 81370849, 81672551, 81300472, 81070592, 81202268, 81202034); the Six Talent Peaks Project in Jiangsu Province, Jiangsu Provincial Medical Innovation Team (CXTDA2017025); the Natural Science Foundation of Jiangsu Province (BK20161434, BL2013032, BK20150642, and BK2012336); the Major Project of Jiangsu Commission of Health: (No: ZD2021002); the Wuxi 'Taihu Talents Program' Medical Expert Team Project (Nos. THRCJH20200901, THRCJH20200902).

ACKNOWLEDGMENTS

We thank all authors for their support in this study.

SUPPLEMENTARY MATERIAL

The Supplementary Material for this article can be found online at: https://www.frontiersin.org/articles/10.3389/fonc.2022.852515/full#supplementary-material

REFERENCES

1. Sung HA-O, Ferlay J, Siegel RL, Laversanne M, Soerjomataram I, Jemal A, et al. Global Cancer Statistics 2020: GLOBOCAN Estimates of Incidence and Mortality Worldwide for 36 Cancers in 185 Countries. *CA Cancer J Clin* (2021) 71(3):209–49. doi: 10.3322/caac.21660
2. Gossage L, Eisen T, Maher ER. VHL, the Story of a Tumour Suppressor Gene. *Nat Rev Cancer* (2015) 15(1):55–64. doi: 10.1038/nrc3844
3. Escudier B, Szczylik C, Porta C, Gore M. Treatment Selection in Metastatic Renal Cell Carcinoma: Expert Consensus. *Nat Rev Clin Oncol* (2012) 9 (6):327–37. doi: 10.1038/nrclinonc.2012.59
4. Dalgliesh GL, Furge K, Greenman C, Chen L, Bignell G, Butler A, et al. Systematic Sequencing of Renal Carcinoma Reveals Inactivation of Histone Modifying Genes. *Nature* (2010) 463(7279):360–3. doi: 10.1038/nature08672
5. Tate JG, Bamford S, Jubb H, Sondka Z, Beare D, Bindal N, et al. *COSMIC: The Catalogue Of Somatic Mutations In Cancer. Nucleic Acids Res* (2019) 47(D1): D941–7. doi: 10.1093/nar/gky1015
6. van den Berg A, Dijkhuizen T, Draaijers T, Hulsbeek M, Maher E, Berg E, et al. Analysis of Multiple Renal Cell Adenomas and Carcinomas Suggests Allelic Loss at 3p21 to be a Prerequisite for Malignant Development. *Genes Chromosomes Cancer* (1997) 19(4):228–32. doi: 10.1002/(SICI)1098-2264 (199708)19:4<228::AID-GCC4>3.0.CO;2-Z

7. Clifford SC, Prowse AH, Affara NA, Buys CH, Maher ER. Inactivation of the Von Hippel-Lindau (VHL) Tumour Suppressor Gene and Allelic Losses at Chromosome Arm 3p in Primary Renal Cell Carcinoma: Evidence for a VHL-Independent Pathway in Clear Cell Renal Tumourigenesis. *Genes Chromosomes Cancer* (1998) 22(3):200–9. doi: 10.1002/(SICI)1098-2264(199807)22:3<200::AID-GCC5>3.0.CO;2-#
8. Guo G, Gui YT, Gao SJ, Tang AF, Hu XD, Huang Y, et al. Frequent Mutations of Genes Encoding Ubiquitin-Mediated Proteolysis Pathway Components in Clear Cell Renal Cell Carcinoma. *Nat Genet* (2011) 44(1):17–9. doi: 10.1038/ng.1014
9. Creighton CJ. Comprehensive Molecular Characterization of Clear Cell Renal Cell Carcinoma. *Nature* (2013) 499:43–9. doi: 10.1038/nature12222
10. Carbone M, Harbour JW, Brugarolas J, Bononi A, Pagano I, Dey A, et al. Biological Mechanisms and Clinical Significance of BAP1 Mutations in Human Cancer. *Cancer Discovery* (2020) 10(8):1103–20. doi: 10.1158/2159-8290.CD-19-1220
11. Carbone M, Yang HN, Pass H, Krausz T, Testa JR, Gaudino M. BAP1 and Cancer. *Nat Rev Cancer* (2013) 13(3):153–9. doi: 10.1038/nrc3459
12. Wang A, Papneja A, Hyrcza M, Al-Habeeb A, Ghazarian D. Gene of the Month: BAP1. *J Clin Pathol* (2016) 69(9):750–3. doi: 10.1136/jclinpath-2016-203866
13. Masclef L, Ahmed O, Estavoyer B, Larrivée B, Labrecque N, Nijnik A, et al. Roles and Mechanisms of BAP1 Deubiquitinase in Tumor Suppression. *Cell Death Differ* (2021) 28(2):606–25. doi: 10.1038/s41418-020-00709-4
14. Jonasch EA-O, Walker CL, Rathmell WA-O. Clear Cell Renal Cell Carcinoma Ontogeny and Mechanisms of Lethality. *Nat Rev Nephrol* (2021) 17(4):245–61. doi: 10.1038/s41581-020-00359-2
15. Kapur P, Peña-Llopis S, Christie A, Zhrebker L, Pavía-Jiménez A, Rathmell WK, et al. Effects on Survival of BAP1 and PBRM1 Mutations in Sporadic Clear-Cell Renal-Cell Carcinoma: A Retrospective Analysis With Independent Validation. *Lancet Oncol* (2013) 14(2):159–67. doi: 10.1016/S1470-2045(12)70584-3
16. Peña-Llopis S, Vega-Rubín-de-Celis S, Liao A, Leng N, Pavía-Jiménez A, Wang S, et al. BAP1 Loss Defines a New Class of Renal Cell Carcinoma. *Nat Genet* (2012) 44(7):751–9. doi: 10.1038/ng.2323
17. Haugh AM, Njauw CN, Bubley JA, Verzì AE, Zhang B, Kudalkar E, et al. Genotypic and Phenotypic Features of BAP1 Cancer Syndrome: A Report of 8 New Families and Review of Cases in the Literature. *JAMA Dermatol* (2017) 153(10):999–1006. doi: 10.1001/jamadermatol.2017.2330
18. Rai K, Pilarski R, Cebulla CM, Abdel-Rahman MH. Comprehensive Review of BAP1 Tumor Predisposition Syndrome With Report of Two New Cases. *Clin Genet* (2016) 89(3):285–94. doi: 10.1111/cge.12630
19. Louie BH, Kurzrock R. BAP1: Not Just a BRCA1-Associated Protein. *Cancer Treat Rev* (2020) 90:102091. doi: 10.1016/j.ctrv.2020.102091
20. Landreville S, Agapova OA, Matatall KA, Kneass ZT, Onken MD, Lee RS, et al. Histone Deacetylase Inhibitors Induce Growth Arrest and Differentiation in Uveal Melanoma. *Clin Cancer Res* (2012) 18(2):408–16. doi: 10.1158/1078-0432.CCR-11-0946
21. LaFave LM, Béguelin W, Koche R, Teater M, Spitzer B, Chramiec A, et al. Loss of BAP1 Function Leads to EZH2-Dependent Transformation. *Nat Med* (2015) 21(11):1344–9. doi: 10.1038/nm.3947
22. Sacco JJ, Kenyani J, Butt Z, Carter R, Chew HY, Cheesemanet LP, et al. Loss of the Deubiquitylase BAP1 Alters Class I Histone Deacetylase Expression and Sensitivity of Mesothelioma Cells to HDAC Inhibitors. *Oncotarget* (2015) 6(15):13757–71. doi: 10.18632/oncotarget.3765
23. Sun C, Zhao CC, Li SG, Wang JQ, Zhou QD, Sun JL, et al. EZH2 Expression is Increased in BAP1-Mutant Renal Clear Cell Carcinoma and is Related to Poor Prognosis. *J Cancer* (2018) 9(20):3787–96. doi: 10.7150/jca.26275
24. Hu G, Ma J, Zhang J, Chen Y, Liu H, Huang Y, et al. LncRNA HOTAIR Regulates HIF-1a/AXL Signaling Through Inhibition of miR-217 in Renal Cell Carcinoma. *Mol Ther* (2021) S1525-0016(21):00302–6. doi: 10.1016/j.ymthe.2021.05.020.
25. Hong Q, Li O, Zheng W, Xiao WZ, Zhang L, Wu D, et al. LncRNA HOTAIR Regulates HIF-1α/AXL Signaling Through Inhibition of miR-217 in Renal Cell Carcinoma. *Cell Death Dis* (2017) 8(5):e2772. doi: 10.1038/cddis.2017.181
26. Fabian MR, Sonenberg N. The Mechanics of miRNA-Mediated Gene Silencing: A Look Under the Hood of miRISC. *Nat Struct Mol Biol* (2012) 9(6):1586–93. doi: 10.1038/nsmb.2296
27. Cazalla D, Yario T Fau - Steitz JA, Steitz JA. Down-Regulation of a Host microRNA by a Herpesvirus Saimiri Noncoding RNA. *Science* (2010) 328(5985):1563–6. doi: 10.1126/science.1187197
28. Franco-Zorrilla JM, Valli A, Todesco M, Mateos I, Puga MI, Rubio-Somoza I, et al. Target Mimicry Provides a New Mechanism for Regulation of microRNA Activity. *Nat Genet* (2007) 39(8):1033–7. doi: 10.1038/ng2079
29. Poliseno L, Salmena L, Zhang J, Carver B, Haveman WJ, Pandolfi PP. A Coding-Independent Function of Gene and Pseudogene mRNAs Regulates Tumour Biology. *Nature* (2010) 465(7301):1033–8. doi: 10.1038/nature09144
30. Mao W, Wang K, Xu B, Zhang H, Sun S, Hu Q, et al. ciRS-7 is a Prognostic Biomarker and Potential Gene Therapy Target for Renal Cell Carcinoma. *Mol Cancer* (2021) 20(1):142. doi: 10.1186/s12943-021-01443-2
31. Chen Y, Wang X. miRDB: An Online Database for Prediction of Functional microRNA Targets. *Nucleic Acids Res* (2020) 48(D1):127–31. doi: 10.1093/nar/gkz757
32. Agarwal V, Bell GW, Nam JW, Bartel DP. *Predicting Effective microRNA Target Sites in Mammalian mRNAs. Elife* (2015) 4:e05005. doi: 10.7554/eLife.05005.028
33. Chin C-H, Chen S-H, Wu H-H, Ho C-W, Ko MT, Lin C-Y. *Cytohubba: Identifying Hub Objects and Sub-Networks From Complex Interactome. BMC Syst Biol* (2014) Suppl 4:S11. doi: 10.1186/1752-0509-8-S4-S11
34. Shannon P, Markiel A, Ozier O, Baliga NS, Wang JT, Ramage D, et al. Cytoscape: A Software Environment for Integrated Models of Biomolecular Interaction Networks. *Genome Res* (2003) 13(11):2498–504. doi: 10.1101/gr.1239303
35. Zhou Y, Zhou B, Pache L, Chang M, Khodabakhshi AH, Tanaseichuk O, et al. Metascape Provides a Biologist-Oriented Resource for the Analysis of Systems-Level Datasets. *Nat Commun* (2019) 10(1):1523. doi: 10.1038/s41467-019-09234-6
36. Mao W, Wang K, Sun S, Wu J, Chen M, Geng J. ID2 Inhibits Bladder Cancer Progression and Metastasis via PI3K/AKT Signaling Pathway. *Front Cell Dev Biol* (2021) 9:738364. doi: 10.3389/fcell.2021.738364
37. Koch A, Jeschke J, Van Criekinge W, van Engeland M, De Meyer T. *MEXPRESS Update 2019. Nucleic Acids Res* (2019) 47(W1):W561–5. doi: 10.1093/nar/gkz445
38. Li T, Fan J, Wang B, Traugh N, Chen Q, Liu JS, et al. TIMER: A Web Server for Comprehensive Analysis of Tumor-Infiltrating Immune Cells. *Cancer Res* (2017) 77(21):e108-e110. doi: 10.1158/0008-5472.CAN-17-0307
39. Cerami E, Gao JJ, Dogrusoz U, Gross EB, Sumer SO, Aksoy BA, et al. The Cbio Cancer Genomics Portal: An Open Platform for Exploring Multidimensional Cancer Genomics Data. *Cancer Discovery* (2012) 2(5):401–4. doi: 10.1158/2159-8290.CD-12-0095
40. Tay Y, Rinn J, Pandolfi PP. The Multilayered Complexity of ceRNA Crosstalk and Competition. *Nature* (2014) 505(7483):344–52. doi: 10.1038/nature12986
41. Mattick JS. Non-Coding RNAs: The Architects of Eukaryotic Complexity. *EMBO Rep* (2001) 2(11):986–91. doi: 10.1093/embo-reports/kve230
42. Mattick JS, Gagen MJ. The Evolution of Controlled Multitasked Gene Networks: The Role of Introns and Other Noncoding RNAs in the Development of Complex Organisms. *Mol Biol Evol* (2001) 18(9):1611–30. doi: 10.1093/oxfordjournals.molbev.a003951
43. Zhang P, Cao L, Zhou R, Yang X, Wu M. The lncRNA Neat1 Promotes Activation of Inflammasomes in Macrophages. *Nat Commun* (2019) 10(1):1495. doi: 10.1038/s41467-019-09482-6
44. Imamura K, Imamachi N, Akizuki G, Kumakura M, Kawaguchi A, Nagata K, et al. Long Noncoding RNA NEAT1-Dependent SFPQ Relocation From Promoter Region to Paraspeckle Mediates IL8 Expression Upon Immune Stimuli. *Mol Cell* (2014) 53(3):393–406. doi: 10.1016/j.molcel.2014.01.009
45. Li Y, Cheng C. Long Noncoding RNA NEAT1 Promotes the Metastasis of Osteosarcoma via Interaction With the G9a-DNMT1-Snail Complex. *Am J Cancer Res* (2018) 8(1):81–90.
46. Boros FA, Vécsei L, Klivényi P. NEAT1 on the Field of Parkinson's Disease: Offense, Defense, or a Player on the Bench? *J Parkinsons Dis* (2021) 11(1):123–38. doi: 10.3233/JPD-202374
47. Zhang M, Weng W, Zhang Q, Wu Y, Ni S, Tan C, et al. The lncRNA NEAT1 Activates Wnt/β-Catenin Signaling and Promotes Colorectal Cancer Progression via Interacting With DDX5. *J Hematol Oncol* (2018) 11(1):113. doi: 10.1186/s13045-018-0656-7
48. Guttman M, Rinn JL. Modular Regulatory Principles of Large non-Coding RNAs. *Nature* (2012) 482(7385):339–46. doi: 10.1038/nature10887

49. Wang C, Chen Y, Wang Y, Liu X, Liu Y, Li Y, et al. Inhibition of COX-2, mPGES-1 and CYP4A by Isoliquiritigenin Blocks the Angiogenic Akt Signaling in Glioma Through ceRNA Effect of miR-194-5p and lncRNA Neat1. *J Exp Clin Cancer Res* (2019) 22:371. doi: 10.1186/s13046-019-1361-2
50. Yu H, Xu A, Wu B, Wang M, Chen Z. Long Noncoding RNA NEAT1 Promotes Progression of Glioma as a ceRNA by Sponging miR-185-5p to Stimulate DNMT1/mTOR Signaling. *J Cell Physiol* (2021) 236(1):121–30. doi: 10.1002/jcp.29644
51. Luo Y, Chen J, Lv Q, Qin J, Huang Y, Yu M, et al. Long non-Coding RNA NEAT1 Promotes Colorectal Cancer Progression by Competitively Binding miR-34a With SIRT1 and Enhancing the Wnt/β-Catenin Signaling Pathway. *Cancer Lett* (2019) 440-441:11–22. doi: 10.1016/j.canlet.2018.10.002
52. Lo PK, Zhang YS, Wolfson B, Gernapudi R, Yao Y, Duru N, et al. Dysregulation of the BRCA1/long non-Coding RNA NEAT1 Signaling Axis Contributes to Breast Tumorigenesis. *Oncotarget* (2016) 7(40):65067–89. doi: 10.18632/oncotarget.11364
53. Khan SS, Shah SJ, Strande JL, Baldridge AS, Flevaris P, Puckelwartz MJ, et al. Identification of Cardiac Fibrosis in Young Adults With a Homozygous Frameshift Variant in SERPINE1. *JAMA Cardiol* (2021) 6(7):841–6. doi: 10.1001/jamacardio.2020.6909
54. Li S, Wei X, He J, Tian X, Yuan S, Sun L. Plasminogen Activator Inhibitor-1 in Cancer Research. *BioMed Pharmacother* (2018) 105:83–94. doi: 10.1016/j.biopha.2018.05.119
55. Wang T, Lu H, Li D, Huang TWG. TGF-β1-Mediated Activation of SERPINE1 is Involved in Hemin-Induced Apoptotic and Inflammatory Injury in HT22 Cells. *Neuropsychiatr Dis Treat* (2021) 17:423–33. doi: 10.2147/NDT.S293772
56. Khan SA-O, Shah SJ, Klyachko E, Baldridge AS, Eren M, Place AT, et al. A Null Mutation in SERPINE1 Protects Against Biological Aging in Humans. *Sci Adv* (2017) 3(11):1617. doi: 10.1126/sciadv.aao1617
57. Xu Y, Chen W, Liang J, Zeng X, Ji K, Zhou J, et al. The miR-1185-2-3p-GOLPH3L Pathway Promotes Glucose Metabolism in Breast Cancer by Stabilizing P53-Induced SERPINE1. *J Exp Clin Cancer Res* (2021) 40(1):47. doi: 10.1186/s13046-020-01767-9
58. Chen S, Li Y, Zhu Y, Fei J, Song L, Sun G, et al. SERPINE1 Overexpression Promotes Malignant Progression and Poor Prognosis of Gastric Cancer. *J Oncol* (2022) 2022:2647825. doi: 10.1155/2022/2647825
59. Zhang Q, Lei L, Jing D. Knockdown of SERPINE1 Reverses Resistance of Triple−Negative Breast Cancer to Paclitaxel via Suppression of VEGFA. *Oncol Rep* (2020) 44(5):1875–84. doi: 10.3892/or.2020.7770
60. Binder BR, Mihaly J Fau - Prager GW, Prager GW. uPAR-uPA-PAI-1 Interactions and Signaling: A Vascular Biologist's View. *Thromb Haemost* (2007) 97(3):336–42. doi: 10.1160/TH06-11-0669
61. Boccaccio C, Comoglio PM. A Functional Role for Hemostasis in Early Cancer Development. *Cancer Res* (2005) 65(19):8579–82. doi: 10.1158/0008-5472.CAN-05-2277
62. Bhattacharjee O, Ayyangar U, Kurbet A, Ashok D, Raghavan S. Unraveling the ECM-Immune Cell Crosstalk in Skin Diseases. *Front Cell Dev Biol* (2019) 7:68. doi: 10.3389/fcell.2019.00068
63. Bahcecioglu G, Basara G, Ellis BW, Ren X, Zorlutuna P. Breast Cancer Models: Engineering the Tumor Microenvironment. *Acta Biomater* (2020) 106:1–21. doi: 10.1016/j.actbio.2020.02.006
64. Pagès F, Berger A, Camus M, Sanchez-Cabo F, Costes A, Molidor R, et al. Effector Memory T Cells, Early Metastasis, and Survival in Colorectal Cancer. *N Engl J Med* (2005) 353(25):2654–66. doi: 10.1056/NEJMoa051424
65. Galon J, Costes A, Sanchez-Cabo F, Kirilovsky A, Mlecnik B, Lagorce-Pagès C, et al. Type, Density, and Location of Immune Cells Within Human Colorectal Tumors Predict Clinical Outcome. *Science* (2006) 313(5795):960–4. doi: 10.1126/science.1129139
66. Mlecnik B, Tosolini M, Kirilovsky A, Berger A, Bindea G, Meatchi T, et al. Histopathologic-Based Prognostic Factors of Colorectal Cancers are Associated With the State of the Local Immune Reaction. *J Clin Oncol* (2011) 29(6):610–8. doi: 10.1200/JCO.2010.30.5425
67. Roelofs JJ, Teske GJ, Bonta PI, Vries CJ, Meijers JC, Weening JJ, et al. Plasminogen Activator Inhibitor-1 Regulates Neutrophil Influx During Acute Pyelonephritis. *Kidney Int* (2009) 75(1):52–9. doi: 10.1038/ki.2008.454
68. Kai K, Moriyama M, Haque A, Hattori T, Chinju A, Hu C, et al. Oral Squamous Cell Carcinoma Contributes to Differentiation of Monocyte-Derived Tumor-Associated Macrophages via PAI-1 and IL-8 Production. *Int J Mol Sci* (2021) 22(17):9475. doi: 10.3390/ijms22179475
69. Chen S, Morine Y, Tokuda K, Yamada S, Saito Y, Nishi M, et al. Cancer−associated Fibroblast−Induced M2−polarized Macrophages Promote Hepatocellular Carcinoma Progression via the Plasminogen Activator Inhibitor−1 Pathway. *Int J Onco* (2021) 59(2):59. doi: 10.3892/ijo.2021.5239
70. Unger C, Kramer N, Walzl A, Scherzer M, Hengstschläger M, Dolznig H, et al. Modeling Human Carcinomas: Physiologically Relevant 3D Models to Improve Anti-Cancer Drug Development. *Adv Drug Delivery Rev* (2014) 79–80:50–67. doi: 10.1016/j.addr.2014.10.015

Conflict of Interest: The authors declare that the research was conducted in the absence of any commercial or financial relationships that could be construed as a potential conflict of interest.

Publisher's Note: All claims expressed in this article are solely those of the authors and do not necessarily represent those of their affiliated organizations, or those of the publisher, the editors and the reviewers. Any product that may be evaluated in this article, or claim that may be made by its manufacturer, is not guaranteed or endorsed by the publisher.

frontiers | Frontiers in Oncology

ORIGINAL RESEARCH
published: 04 April 2022
doi: 10.3389/fonc.2022.852952

In Vivo miRNA Decoy Screen Reveals miR-124a as a Suppressor of Melanoma Metastasis

*Rana S. Moubarak[1,2,3], Lisa Koetz-Ploch[1,2], Gavriel Mullokandov[4], Avital Gaziel[1,2], Ana de Pablos-Aragoneses[1,2], Diana Argibay[1,2], Kevin Kleffman[1,2], Elena Sokolova[1,2], Marianne Berwick[5], Nancy E. Thomas[6], Iman Osman[2,3,7], Brian D. Brown[4] and Eva Hernando[1,2,3]**

[1] Department of Pathology, New York University (NYU) School of Medicine, New York, NY, United States, [2] Interdisciplinary Melanoma Cooperative Group (IMCG), New York University (NYU) Cancer Institute, New York, NY, United States, [3] Laura and Isaac Perlmutter Cancer Center, New York University (NYU) Langone Health, New York, NY, United States, [4] Department of Genetics and Genomic Sciences, Icahn School of Medicine at Mount Sinai, New York, NY, United States, [5] Division of Epidemiology, Biostatistics and Preventive Medicine, Department of Internal Medicine, University of New Mexico, Albuquerque, NM, United States, [6] Department of Dermatology, University of North Carolina, Chapel Hill, NC, United States, [7] Ronald O. Perelman Department of Dermatology, New York University (NYU) School of Medicine, New York, NY, United States

OPEN ACCESS

Edited by:
Jawed Akhtar Siddiqui, University of Nebraska Medical Center, United States

Reviewed by:
Vadim Kumeiko, Far Eastern Federal University, Russia
Andrzej T. Slominski, University of Alabama at Birmingham, United States

***Correspondence:**
Eva Hernando
eva.hernando-monge@nyulangone.org

Specialty section:
This article was submitted to Molecular and Cellular Oncology, a section of the journal Frontiers in Oncology

Received: *11 January 2022*
Accepted: *24 February 2022*
Published: *04 April 2022*

Citation:
Moubarak RS, Koetz-Ploch L, Mullokandov G, Gaziel A, de Pablos-Aragoneses A, Argibay D, Kleffman K, Sokolova E, Berwick M, Thomas NE, Osman I, Brown BD and Hernando E (2022) In Vivo miRNA Decoy Screen Reveals miR-124a as a Suppressor of Melanoma Metastasis. Front. Oncol. 12:852952. doi: 10.3389/fonc.2022.852952

Melanoma is a highly prevalent cancer with an increasing incidence worldwide and high metastatic potential. Brain metastasis is a major complication of the disease, as more than 50% of metastatic melanoma patients eventually develop intracranial disease. MicroRNAs (miRNAs) have been found to play an important role in the tumorigenicity of different cancers and have potential as markers of disease outcome. Identification of relevant miRNAs has generally stemmed from miRNA profiling studies of cells or tissues, but these approaches may have missed miRNAs with relevant functions that are expressed in subfractions of cancer cells. We performed an unbiased *in vivo* screen to identify miRNAs with potential functions as metastasis suppressors using a lentiviral library of miRNA decoys. Notably, we found that a significant fraction of melanomas that metastasized to the brain carried a decoy for miR-124a, a miRNA that is highly expressed in the brain/neurons. Additional loss- and gain-of-function *in vivo* validation studies confirmed miR-124a as a suppressor of melanoma metastasis and particularly of brain metastasis. miR-124a overexpression did not inhibit tumor growth *in vivo*, underscoring that miR-124a specifically controls processes required for melanoma metastatic growth, such as seeding and growth post-extravasation. Finally, we provide proof of principle of this miRNA as a promising therapeutic agent by showing its ability to impair metastatic growth of melanoma cells seeded in distal organs. Our efforts shed light on miR-124a as an antimetastatic agent, which could be leveraged therapeutically to impair metastatic growth and improve patient survival.

Keywords: Melanoma, metastasis, microRNA, brain metastasis, tumor suppressor

INTRODUCTION

Melanoma, together with lung and breast cancer, has a high potential to metastasize to the brain. Up to 50% of patients with stage IV melanoma have been reported to develop brain metastases at the time of their diagnosis or during the course of their illness (1). The prognosis of brain metastasis patients is poor, with a median overall survival of 17–22 weeks (2, 3), since their progression can lead to rapid neurodegeneration and a fast decline in quality of life. Despite therapeutic advances in melanoma with targeted and immune therapies (4) and the recent inclusion of brain metastasis patients in clinical trials, their prognosis remains poor. Symptomatic brain metastasis patients show a modest response to immunotherapy, while targeted therapy shows less durable intracranial activity (5, 6). A full understanding of the mechanisms controlling brain metastasis formation remains an unmet need for these patients.

Genetic alterations seem insufficient to explain melanoma metastatic behavior; thus, tumors with the same mutation profile at diagnosis can have disparate outcomes. As such, we hypothesize that non-genetic programs [i.e., epigenetic, non-coding RNA (ncRNA)] can mediate metastasis by driving a pro-metastatic transcriptional output downstream of a certain genetic makeup. Because mutations and expression profiling alone may not identify events occurring in rare cells, such as those involved in transition to metastatic phenotype, unbiased *in vivo* functional screens can help reveal alternative mechanisms.

MicroRNAs (miRNAs) are a class of 18–23-nucleotide ncRNAs, with demonstrated ability to impact multiple genes and pathways simultaneously (7). A strong body of evidence supports an important role for miRNA alterations in the tumorigenicity of multiple cancers (8, 9). miRNAs can play tumor suppressor (10) or oncogenic functions in melanoma (11–13). We and others have defined prognostic miRNA signatures for metastatic (14–16) and brain metastatic melanoma (17), shown the therapeutic potential of anti-miRNA therapies (18), and identified miRNAs that functionally contribute to various aspects of melanoma progression (19–23). Therefore, dysregulated miRNAs could regulate the complex multistep metastatic process. Despite great advances in available screen strategies using miRNA inhibition *via* Clustered Regularly Interspaced Short Palindromic Repeats (CRISPR)/Cas9 *in vitro* (24), this approach has proven challenging for efficient inhibition of miRNA biogenesis and function. In order to determine the functional role of miRNAs in metastasis *in vivo*, we performed a screen using a pooled library of miRNA Decoys (25), which revealed miR-124a as a strong suppressor of metastasis and particularly of brain metastasis. Examination of miRNA expression in human melanoma metastasis found that lower levels of miR-124a were associated with worse prognosis and with increased recurrence and brain metastasis incidence. When miR-124a was overexpressed in melanoma cells, melanoma metastasis in the brain and other organs was dramatically reduced, further demonstrating the role of miR-124a as a tumor suppressor and suggesting the potential for miR-124a mimics as a therapeutic means to control melanoma metastasis.

RESULTS

In Vivo Unbiased miRNA Decoy Screen Identifies miR-124a as a Potential Suppressor of Melanoma Brain Metastasis

We hypothesized that miRNAs could play a critical role in governing molecular mechanisms responsible for the establishment and growth of melanoma metastasis, such as chemotaxis, adhesion, migration, survival, or proliferation in the host microenvironment. First, we performed a loss-of-function *in vivo* screen for metastasis suppressors using a lentiviral library of miRNA decoy vectors targeting and inhibiting 291 conserved mouse and human miRNAs (**Figure 1A**). The efficacy of this decoy library for miRNA knockdown and loss-of-function studies has been previously demonstrated (25). As a melanoma model, we utilized 113/6-4L cells, which have been previously described to display tropism to the liver after subcutaneous injection (26). In our hands, these cells have limited ability to colonize the brain upon ultrasound-guided intracardiac injection, a well-described model of brain metastasis (27, 28). We transduced the 113/6-4L melanoma cells with the miRNA decoy Library or Empty Vector, which encodes Green Fluorescent Protein (GFP) but no miRNA decoy. Cells were transduced at a low multiplicity of infection [(MOI) 0.3] to achieve a single vector copy per cell, and then GFP+ cells were sorted to obtain a pure population of vector-expressing cells. The cells were injected into the left ventricle of athymic/nude mice, and after 2–3 months, when mice showed signs of discomfort or weight loss, they were euthanized and organs were collected for analysis. The number of brain and liver metastases was scored and GFP-positive metastatic foci were dissected, followed by deep sequencing for the detection of enriched decoys in the metastatic lesions (**Figure 1B**). To determine whether any particular miRNA decoys were enriched in the metastases, we extracted DNA from the tissues and performed deep sequencing to determine the frequency of each decoy in the library. Strikingly, out of the 291 vectors in the library, the miR-124a decoy was the dominant decoy in the metastatic lesions found in 3 out of 4 different mouse brains (**Figure 1C**). These findings suggested that inhibition of miR-124a promotes 113/6-4L melanoma metastasis to the brain.

miR-124a Is a Potent Suppressor of Melanoma Metastasis

miR-124a was initially described as a neuron-specific miRNA and is not detected at appreciable levels in cells outside the nervous system (29, 30). It has an important role in neuronal differentiation (31) and was subsequently shown to function as a tumor suppressor gene in the brain and found to be lost in glioblastoma (32). However, a role for miR-124a in melanoma metastasis has not been described, though it was intriguing that its inhibition was associated with brain metastasis. To validate miR-124a's potential function as a metastasis suppressor, we transduced 113/6-4L melanoma cells with lentiviral vectors carrying mCherry-luciferase and a GFP-tagged single decoy against miR-124a (Dc-124a) or a scrambled decoy control (Dc-Scr). We confirmed that

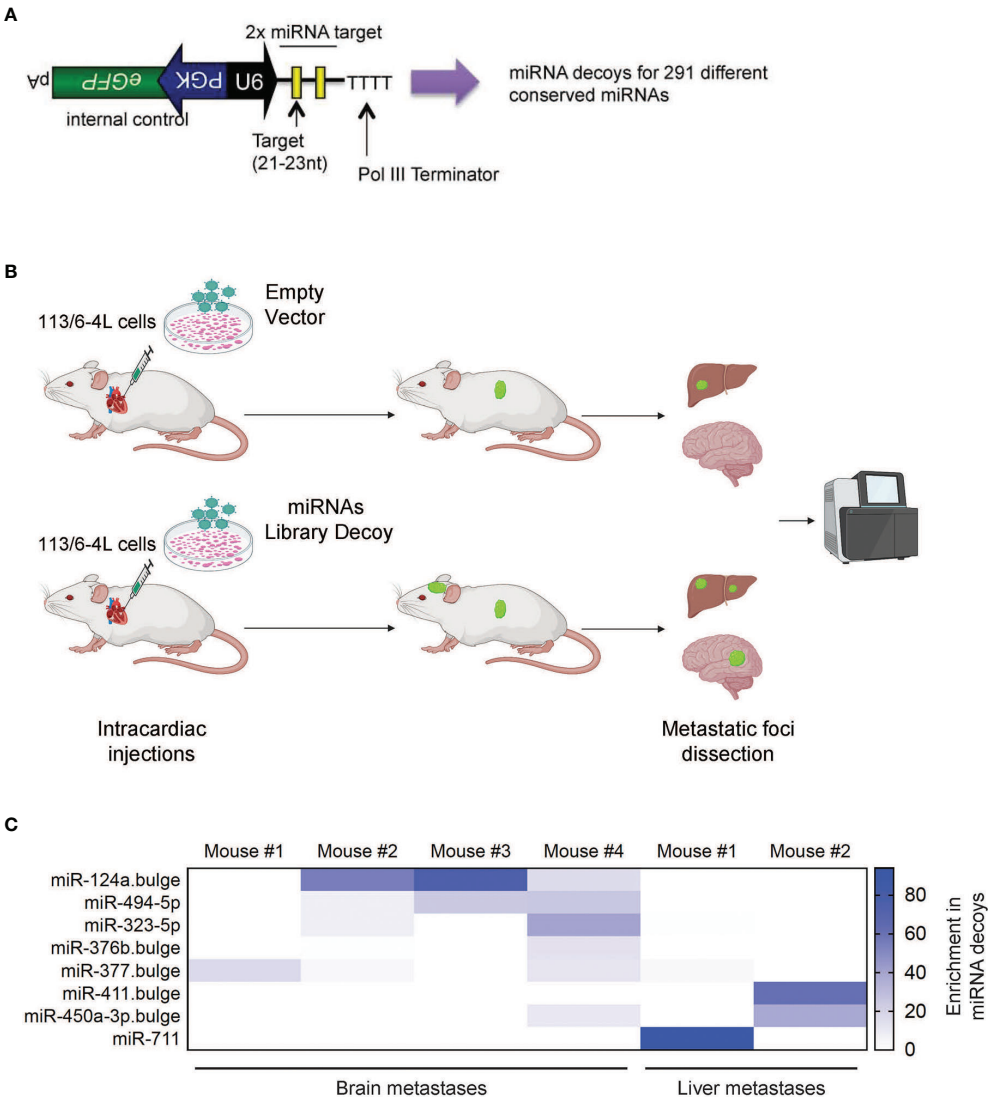

FIGURE 1 | *In vivo* screen of suppressors of melanoma metastasis. **(A)** Schematic of the lentiviral vector-based miRNA decoy vector (25). miRNA decoy target sites were cloned into a lentiviral vector downstream of the U6 promoter. This vector also encodes GFP as a reporter from a separate promoter. **(B)** Schematic representation of the *in vivo* brain metastasis screen: The 113/6-4L melanoma cells transduced with control (Empty Vector) or with a lentiviral library pool of decoys targeting 291 miRNAs (miRNAs Library Decoy) were transplanted by ultrasound-guided intracardiac injection in athymic/nude female mice (Decoy Empty, n = 6; miRNA Decoy Library, n = 12). **(C)** Deep sequencing of accelerated metastatic lesions revealed miR-124a decoy as enriched (% reads for a particular Decoy over total number of reads) in brain metastases from different mice. Scale shows enrichment of specific miRNA decoys in the metastatic lesions sequenced.

the miR-124a decoy efficiently inhibited miR-124, as miR-124a levels were reduced (**Figure 2A**), an indicator of decoy activity (33), and established targets of miR-124a EZH2 (34), MAPK14 (35), and SPRY2 (36) were significantly upregulated (**Figure 2B**). Nude mice were inoculated with Dc-124a- or Dc-Scr-transduced melanoma cells in the left heart ventricle and monitored by luminescence imaging throughout the experiment (**Figure 2C**). The group inoculated with Dc-124a-expressing cells displayed a significantly accelerated brain and extracranial metastasis burden relative to control (**p = 0.0069 and ***p = 0.001, respectively) (**Figures 2D, E**). Accordingly, miR-124a knockdown significantly shortened mouse survival in this model (**p = 0.0055) (**Figure 2F**). These data validate the findings of our positive selection screen, confirming miR-124a as a metastasis suppressor miRNA.

To further validate these findings, we conducted a gain-of-function approach. We transduced 113/6-4L cells with a lentivirus expressing mCherry-luciferase, together with a lentivirus overexpressing miR-124a coupled to GFP (miRH-124a) or its scrambled control (miRH-Scr). MiR-124a upregulation (**Figure 3A**) effectively reduced the expression of its established targets EZH2, MAPK14, and SPRY2 (**Figure 3B**).

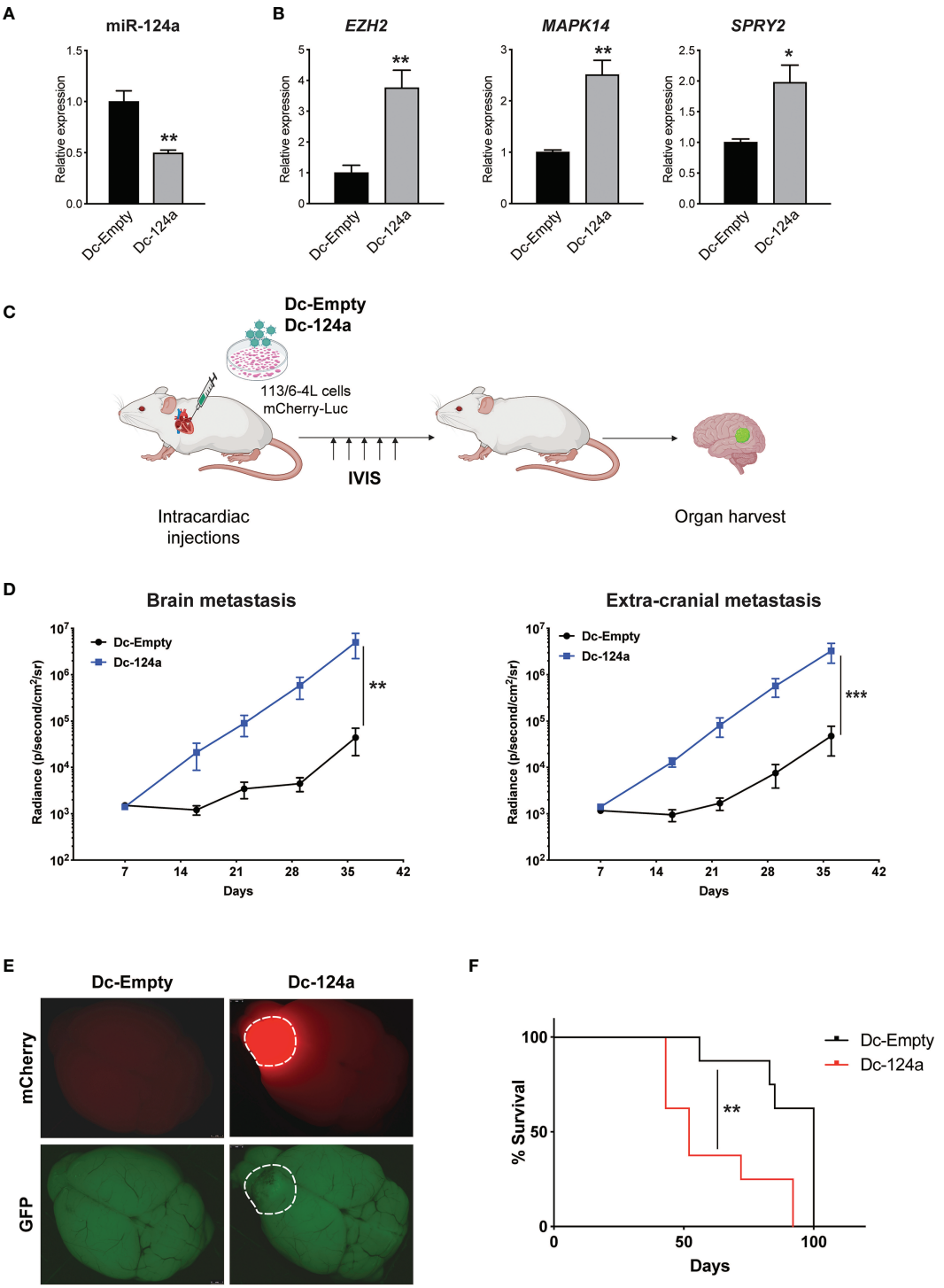

FIGURE 2 | miR-124a silencing enhances melanoma metastasis. **(A)** Relative expression of miR-124a (unpaired t test; **p = 0.003) and **(B)** its targets was measured by quantitative RT-PCR after lentiviral infection of 113/6-4L with mCherry-Luciferase and Dc-Scr or Dc-124a tagged with a GFP reporter (unpaired t test; *EZH2* **p = 0.0019, *MAPK14* **p = 0.0059, and *SPRY2* *p = 0.0189). **(C)** Schematic representation of the *in vivo* metastasis model in athymic/nude female mice (n = 8 per group). **(D)** miR-124a silencing significantly accelerates both brain (**p = 0.0069) and extracranial metastasis (***p = 0.001) burden, as measured by *in vivo* bioluminescence imaging using IVIS (Mann–Whitney test). **(E)** Representative brain images at termination were obtained using a dissecting scope (Leica). **(F)** Overall survival is significantly decreased upon miR-124a silencing. Mice were humanely euthanized once they present symptoms of distress or >20% of weight loss. The experiment was terminated when mice from the Dc-Scr group that remained alive at day 100 were euthanized (Mantel–Cox test; **p = 0.0055).

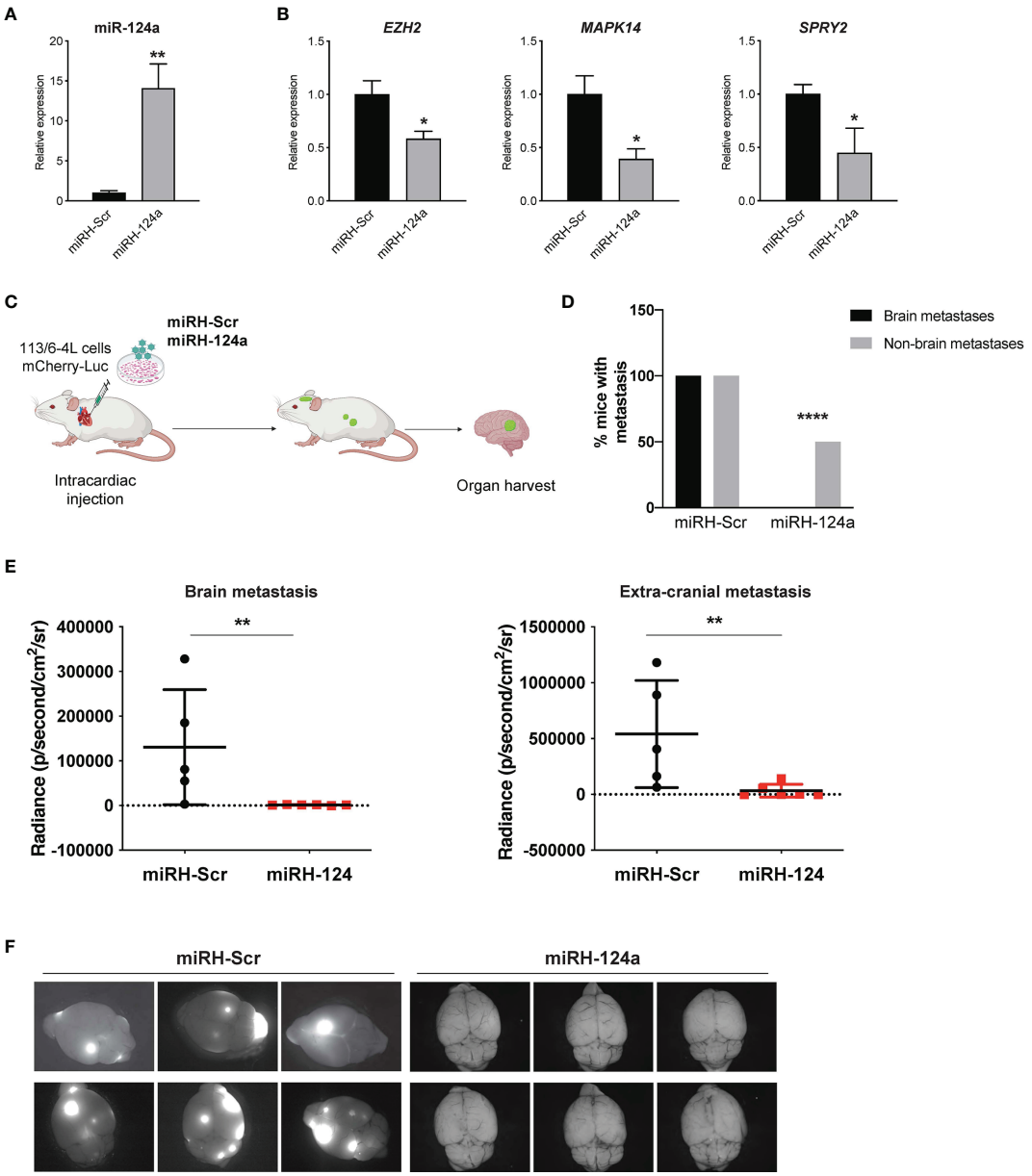

FIGURE 3 | miR-124a constitutive overexpression suppresses metastasis and particularly brain metastasis. The 113/6-4L-mCherry-Luciferase cells were transduced with miRH-Scr or miRH-124a tagged with a GFP reporter. **(A)** Efficient miRNA-124a overexpression (unpaired t test; **p = 0.0083) and **(B)** consequent repression of its targets were measured by quantitative RT-PCR (unpaired t test; *EZH2* *p = 0.05, *MAPK14* *p = 0.02, and *SPRY2* *p = 0.038). **(C)** Schematic representation of the *in vivo* metastasis model using cells generated in **(A)** in nude female mice (n = 6 per group). **(D)** Incidence of brain and extracranial metastases in both groups is shown. Extracranial metastases refer to lung and/or ovary metastases (two-sided chi-square test, ****p < 0.0001). **(E)** miR-124a overexpression significantly inhibits both brain (**p = 0.0043) and extracranial metastasis (**p = 0.0087) burden, as measured by *in vivo* bioluminescence imaging using IVIS at experiment termination (Mann–Whitney test). **(F)** Representative GFP fluorescence pictures of brain metastasis in mice from both groups are shown (Leica).

miRH-124a- or miRH-Scr-transduced cells were inoculated in the left ventricles of nude mice using ultrasound-guided intracardiac injection (**Figure 3C**). Mice were euthanized 5 weeks post-injection when some started to display signs of discomfort. In agreement with its loss-of-function effects, miR-124a overexpression significantly suppressed brain and extracranial metastases to lungs and ovaries (two-sided chi-square test, ****p < 0.0001; **Figure 3D**), as measured by bioluminescence at experiment termination (brain metastasis, **p = 0.0043; extracranial metastasis, **p = 0.0087; **Figure 3E**). Remarkably, while all mice injected with miRH-Scr-transduced cells developed brain metastases, none of the mice injected with miRH-124a-overexpressing cells developed any brain metastasis (**Figures 3D–F**). We conclude that miR-124a overexpression

abolishes brain metastasis formation and significantly inhibits melanoma metastasis to other organs.

To determine if miR-124a was suppressing growth, rather than metastasis specially, we examined the effect of either constitutive or inducible miR-124a overexpression in relevant xenograft models. We subcloned the miR-124a precursor and its Scrambled control (Scr) into the TRIPZ™ inducible lentiviral vector (Dharmacon). This vector is configured for the expression of shRNAs and miRNAs of interest, together with the turboRFP (tRFP) reporter, in the presence of doxycycline (Tet-On configuration). Importantly, in this construct, miRNA expression and tRFP expression are coupled, as both arise from the same promoter, in a doxycycline-dependent manner.

Melanoma cells were transduced with a GFP-luciferase–expressing construct, followed by TRIPZ-Scr/miR-124a lentiviral particles, and were injected subcutaneously in the flanks of immune-compromised NOD/Scid/IL2γRnull (NSG) mice. Cells were treated with doxycycline prior to inoculation, and mice were fed doxycycline-containing food pellets immediately for constitutive miR124a overexpression (**Figure 4A**). Once palpable, tumor growth was regularly measured by caliper. In another set of experiments, mice were fed doxycycline-containing food pellets starting 14 days after inoculation, when tumors became palpable (**Figure 4D**). Comparison of tumor growth found that neither miR-124a constitutive (**Figures 4B, C**) nor inducible overexpression after tumors' engraftment (**Figures 4E, F**) affected tumor growth. This indicates that miR-124a specifically suppresses melanoma metastatic progression without affecting primary tumor growth.

miR-124a Overexpression Impairs the Growth of Seeded Metastases

We postulated that miR-124a overexpression in already seeded metastatic cells might impair further growth. To test this hypothesis, we aimed to conditionally induce miR-124a in melanoma cells after reaching distal organs. Melanoma cells were transduced with GFP-Luciferase followed by TRIPZ-Scr or TRIPZ-miR-124a lentiviral infections. Efficient miRNA-124a overexpression after doxycycline treatment *in vitro* was assessed by qRT-PCR (**Figure 5A**). Subsequently, puromycin-selected cells cultured in tetracycline-free serum were inoculated in the left ventricle of NSG mice. We have found in previous studies that most melanoma cells have already extravasated from the vasculature and colonized the brain microenvironment by day 7 after intracardiac injection in mice (Kleffman et al., Biorxiv). We thus started feeding mice with doxycycline-containing chow at day 8 after cell inoculation, aiming for efficient miR-124a induction 2–3 days later. The experiment was terminated 36 days after inoculation, when some mice showed signs of discomfort (**Figure 5B**). Harvested organs (brain, liver, lung, and kidneys) were imaged using a dissecting scope to detect both GFP+ (which marks all melanoma cells) and RFP+ (which marks miR-Scr- or miR-124a-expressing cells) (**Figure 5B**). In the group injected with miR-Scr-transduced cells, most mice developed brain metastases, and the GFP and RFP signals vastly overlapped (**Figure 5C**, upper brain panels). In the miR-124a-transduced group, however, RFP+ lesions were found absent from all harvested brains, with the exception of a small lesion in one mouse (**Figure 5C**; brain panels, eighth counting from left). In the liver and kidney, we found a similar suppression of RFP+ lesions, further supporting a negative selection of cells carrying miR-124a overexpression. These results strongly suggest that miR-124a expression is deleterious for metastases, and only those cells that escape miR-124a induction, either by insufficient doxycycline levels or by compensatory adaptations, are able to successfully colonize the brain. To prove this, we tested if RFP fluorescence was a faithful reporter of miR-124a overexpression. In contrast to the brain, several liver metastatic lesions were GFP+/RFP+ in the mice injected with miR-124a-transduced cells. We carefully dissected RFP-/GFP+ and RFP+/GFP+ liver metastatic foci from 2 different mice of the miR-124a-overexpressing group and assessed miR-124a expression by qRT-PCR. We found that RFP+/GFP+ lesions have significantly higher miR-124a expression than RFP-/GFP+ lesions from the same mice (**Figure 5D**). While miR-124a-overexpressing lesions were still present in liver and kidneys (**Figure 5C**), metastasis burden and organ size were reduced in mice injected with miR-124a-overexpressing cells than those instilled with miR-Scr-transduced cells (**Figure 5E**). Taken together, our data indicate that miR-124a acts as a potent barrier against metastatic growth, and that cells expressing miR-124a are negatively selected in general and even more so in the brain parenchyma, supporting its value as an anti-metastatic miRNA.

miR-124a Levels in Primary Melanoma Correlate With Recurrence, Brain Metastasis, and Brain Metastasis-Free Survival

miRNA profiling of 92 human primary melanoma specimens (stages I and II, GSE62372) (20) revealed higher expression of miR-124a in non-recurrent (n = 44) vs. recurrent (n = 48) primary melanoma samples ($p = 0.047$; **Figure 6A**). Moreover, primary tumors that eventually metastasized to the brain (n = 26) displayed lower miR-124a levels compared to those that did not (n = 66) ($p = 0.02$; **Figure 6B**). Finally, low miR-124a levels associate with decreased brain metastasis-free survival ($p = 0.05$; **Figure 6C**). These data further support the clinical relevance of miR-124a as a negative regulator of metastasis in general and of brain metastasis in particular.

DISCUSSION

Melanomas are highly metastatic tumors, thus representing a pertinent model to study metastatic progression. However, genetic alterations have been deemed insufficient to explain melanoma metastatic potential. While melanoma cells display a high propensity to translocate from primary to distant metastatic sites, the colonization of a host microenvironment can represent a bottleneck for metastasis (37). Only those cells that undergo molecular and cellular changes befitting their new environment will be able to adapt and survive in distant organs (38–41). Brain metastases grow in part by co-opting existing

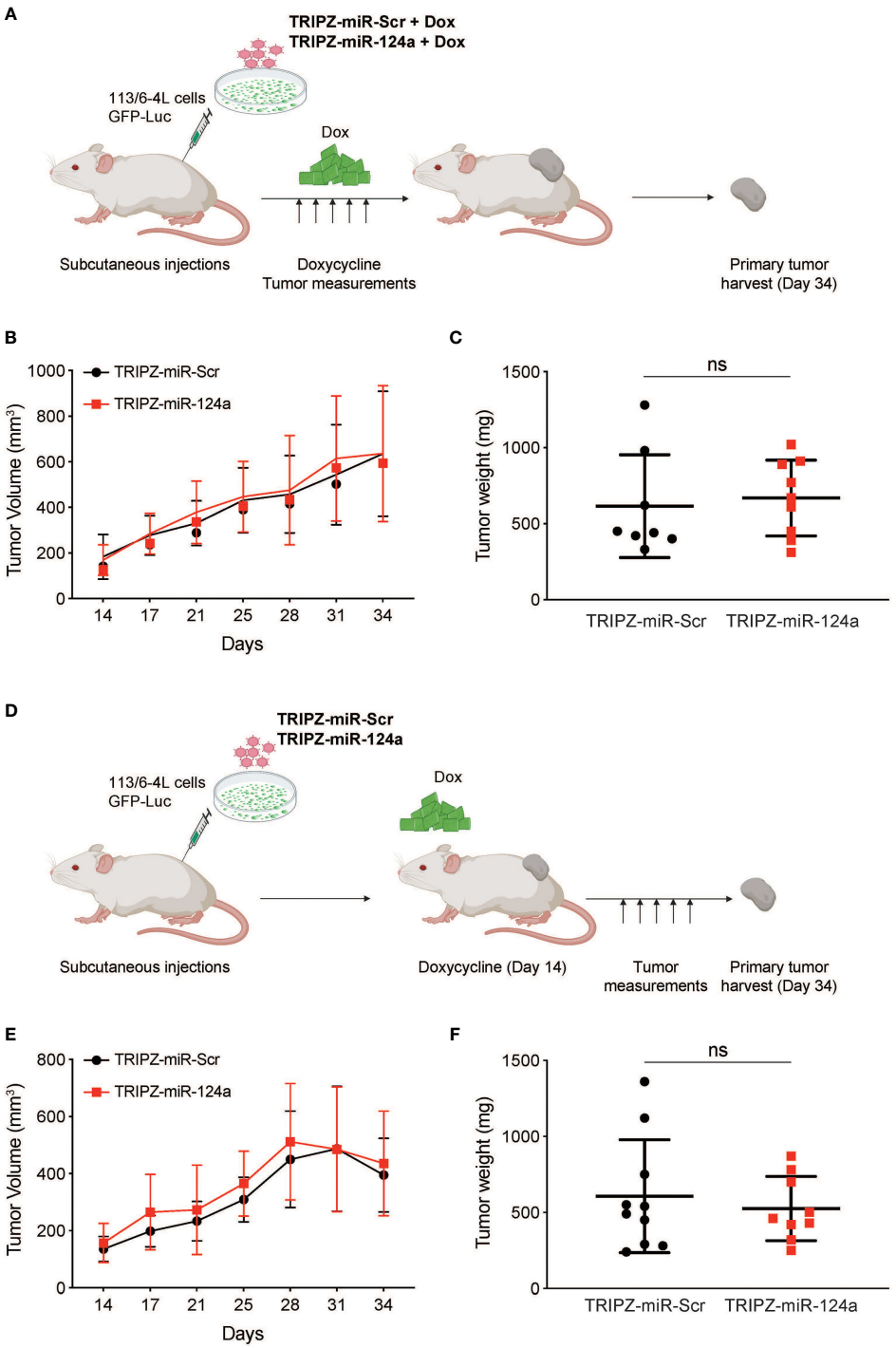

FIGURE 4 | miR-124a overexpression does not inhibit subcutaneous tumor formation nor established tumor growth. **(A)** Schematic representation of *in vivo* tumor growth model: The 113/6-4L -GFP-Luciferase cells were stably transduced with doxycycline-inducible control TRIPZ-miR-Scr or TRIPZ-miR-124a tagged with a tRFP reporter and injected with Matrigel (1:1) into the flank of NSG female mice. Cells were treated with doxycycline (2 μg/ml) prior to injection, and mice were fed doxycycline chow since the intracardiac inoculation. **(B)** Constitutive miR-124a overexpression in 113/6-4L cells did not affect tumor volume **(C)** nor weight at termination of the experiment (Day 34). **(D)** Schematic representation of *in vivo* growth after implantation: The 113/6-4L -GFP-Luciferase cells were stably transduced with doxycycline-inducible control TRIPZ-miR-Scr or TRIPZ-miR-124a tagged with a tRFP reporter and injected with Matrigel (1:1) into the flank of NOG/SCID female mice. Once tumors were palpable (Day 14 post-injection), mice were fed doxycycline chow (200 mg/kg). **(E)** Inducible miR-124a overexpression in established tumors did not affect tumor volume **(F)** nor weight at termination of the experiment (Day 34). ns, non significant.

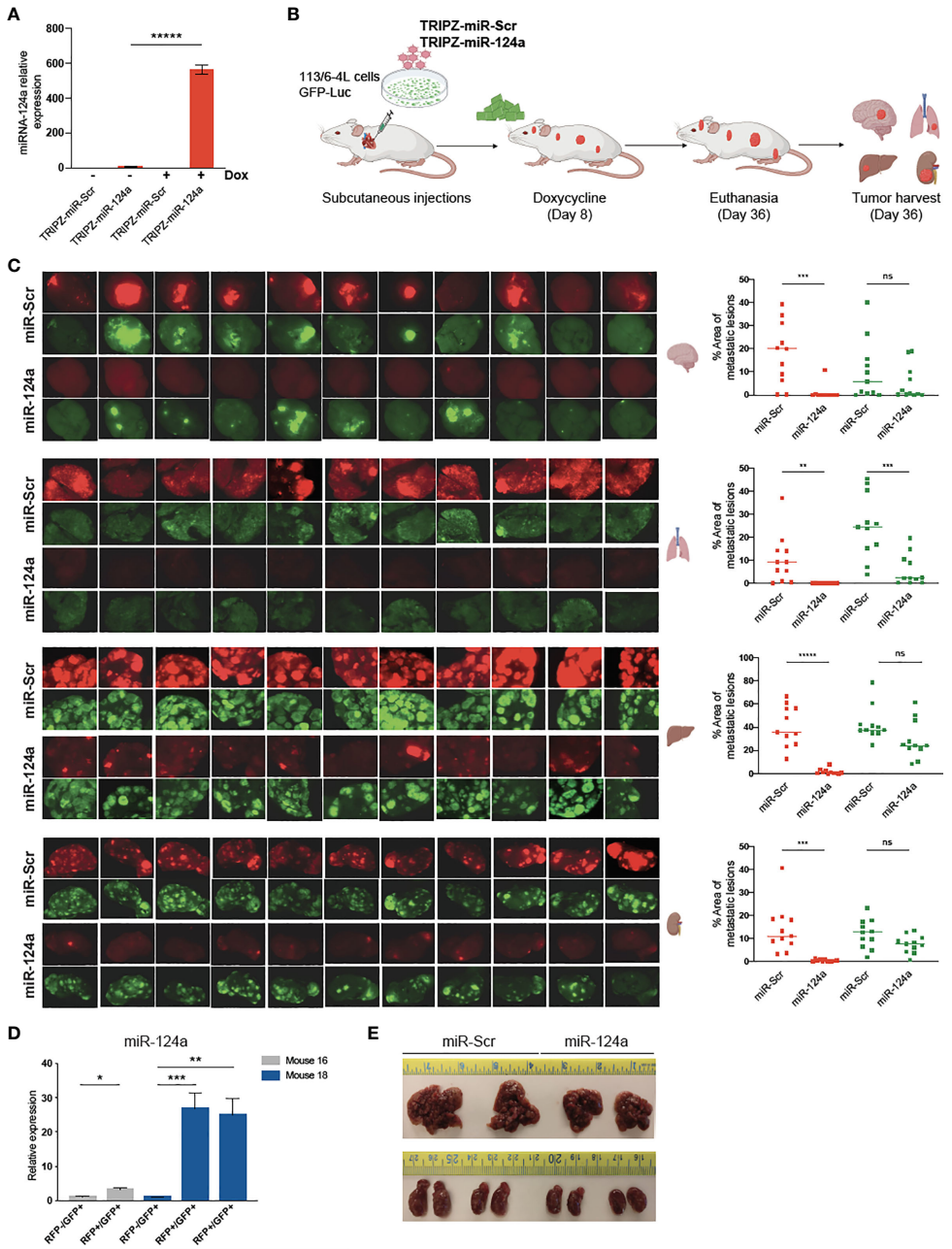

FIGURE 5 | miR-124a overexpression inhibits established metastases. **(A)** The 113/6-4L melanoma cells were transduced with GFP-Luciferase followed by TRIPZ-Scr or TRIPZ-miR-124a lentiviral infections. Efficient miRNA-124 overexpression after doxycycline treatment *in vitro* was assessed by RT-qPCR (unpaired t test; *****p = 0.000005). **(B)** Schematic representation of *in vivo* metastasis assay with inducible overexpression of miR-124a: The 113/6-4L-GFP-Luciferase cells transduced with doxycycline-inducible control (TRIPZ-miR-Scr) or (TRIPZ-miR-124a) tagged with a tRFP reporter were selected with puromycin, and ultrasound-guided intracardiac injection was performed in NSG mice (n = 11 per group). Mice were initiated on doxycycline (200 mg/kg) chow 8 days post-injection. **(C)** RFP and GFP fluorescence images of brain, lung, liver, and kidneys in all mice are shown, and the areas of metastatic lesions were plotted using ImageJ (red dots: RFP+ metastases; green dots: GFP+ metastases). Unpaired t test was used for statistical significance of differences in brain (***p = 0.0006 for RFP+ metastases in miR124a vs. miR-Scr group; ns, p = 0.274 for GFP+ in miR124a vs. miR-Scr group), lung (**p = 0.0041 for RFP+ metastases in miR124a vs. miR-Scr group; ***p = 0.00056 for GFP+ in miR124a vs. miR-Scr group), liver (*****p < 0.000001 for RFP+ metastases in miR124a vs. miR-Scr group; ns, p = 0.056 for GFP+ in miR124a vs. miR-Scr group), and kidney (***p = 0.00033 for RFP+ metastases in miR124a vs. miR-Scr group; ns, p = 0.058 for GFP+ in miR124a vs. miR-Scr group) metastases. **(D)** Expression of miR-124a in RFP-/GFP+ and RFP+/GFP+ liver metastatic foci dissected from two representative mice (#16 and #18) from the miR124a group is measured by quantitative RT-qPCR (unpaired t test; *p = 0.018 for mouse 16 and ***p = 0.0011 and **p = 0.005 for mouse 18). **(E)** Representative images of the liver and kidney sizes of two mice from both groups are shown. ns, non significant.

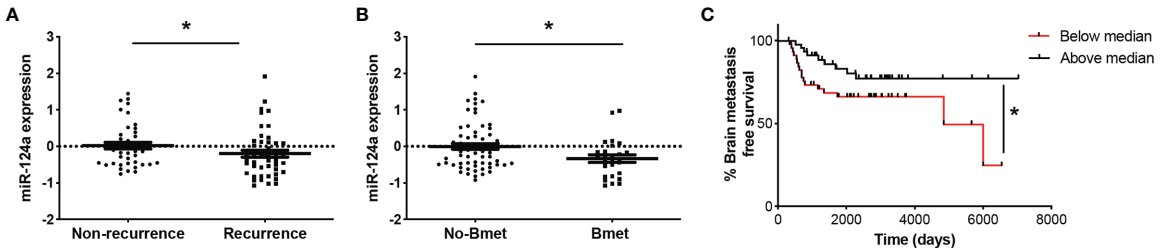

FIGURE 6 | Low miR-124a levels in primary melanoma correlate with recurrence, brain metastasis recurrence, and decreased brain metastasis-free survival. Primary human melanoma samples were collected at the time of surgery from 92 patients enrolled in the NYU Melanoma Program (IMCG) database. miRNA expression profiling of FFPE-extracted RNAs from primary melanomas was performed by Exiqon, Inc., using miRCURY^{TM} LNA arrays (Exiqon, Denmark) (20). **(A)** Relative miRNA-124 expression was compared between primary tumors based on their recurrence status (Mann–Whitney test; *p = 0.047). **(B)** Relative miRNA-124 expression in primary tumors that eventually metastasized to the brain (Bmet) vs. primary tumors that did not metastasize or metastasized to other organs (No-Bmet) (Mann–Whitney test; *p = 0.02). **(C)** Brain metastasis-free survival analysis shows that low miR-124a correlates with increased brain metastasis incidence (Breslow–Wilcoxon test; *p = 0.05). Low and high miR-124a levels are relative to the median expression.

blood vessels and astrocytes (42) and are the most common types of brain tumor leading to high morbidity and mortality. In the United States, approximately 150,000 cases of brain metastases are diagnosed every year (43). A variety of primary tumors such as breast, lung, and melanoma can develop brain metastasis through complex mechanisms during the multiple-step metastatic process (44).

Metastatic cells can harbor aberrant signaling or express dysregulated ncRNAs to promote their motility and survival. We and others have shown that miRNAs and circular RNAs (7, 45–48) play important roles in these processes. miRNAs regulate gene expression in multiple ways, such as translational repression, mRNA cleavage, and mRNA decay. Roles for miR-146a in suppressing (49) and for miR-210 in promoting (50) melanoma brain metastasis have been reported.

In this study, we undertook an unbiased approach to investigate the ability of miRNAs to suppress the metastatic fitness of malignant cells using an *in vivo* screen with positive selection. A decoy of miRNA-124a appeared consistently enriched in multiple brain metastasis lesions, suggesting that this miRNA could be a strong suppressor of melanoma brain metastasis (**Figure 1**). This result was unexpected because miR-124a is a miRNA the expression of which is associated with the brain and not melanoma. We further validated miR-124a as able to impair both brain and extracranial metastases (**Figures 2**, **3**). Future studies should be conducted in additional cell lines to further strengthen the general applicability of our findings to melanomas with various genetic backgrounds. It has been shown that melanin synthesis can affect melanoma behavior (51, 52). We did not observe noticeable changes in pigmentation upon manipulation of miR-124 levels *in vivo* in both primary tumors and metastatic lesions. The role of melanin synthesis in metastatic progression merits further investigation and should be formally examined. An antitumoral role for miR-124a, the most brain-abundant miRNA (53), has been previously reported in glioblastoma (54, 55). It can be packaged in extracellular vesicles, and released miRNA-124a has been found to regulate the glutamate transporter 1 in astrocytes, thus influencing astrocyte-mediated regulation of neurons in a feedback mechanism (56, 57). These observations raise the paradox of a potential crosstalk between metastatic melanoma cells that silence miRNA-124a for adaptation to a miRNA-124a-abundant brain microenvironment. The precise understanding of this crosstalk could reveal pathways that could be targeted to prevent melanoma adaptation in the brain. miRNA-124a has been shown to function as a tumor suppressor by targeting Receptor for Activated Protein C Kinase (RACK1) in cutaneous melanoma (58) and the histone methyltransferase Enhancer of Zest Homolog 2 (EZH2) in uveal melanoma (59). The functional role of EZH2 in promoting melanoma metastasis has been well established (60), suggesting its potential contribution to miRNA-124a metastasis suppressive role reported here.

Our findings suggest that miRNA-124a could serve as a therapeutic target for the treatment of brain and extracranial melanoma metastasis, since its delivery using an inducible system impairs the growth of seeded melanoma cells in the brain (**Figure 5**). This would be particularly impactful against melanoma brain metastasis, given that many patients are non-responsive or develop resistance to checkpoint blockade, the current standard of care for metastatic melanoma. The use of ncRNAs for therapeutic purposes remains an area of active research. A current limitation of miRNA delivery is their tendency to accumulate in the liver with potential toxicity and limited access to other tissues (61). However, new strategies and developments may overcome the biological challenges of miRNA delivery and allow exploiting their therapeutic potential. Recent advances in drug delivery systems using lipid nanoparticles have expedited the preclinical development of mRNA therapeutics (62–64), providing the basis for Food and Drug Administration (FDA)-approved coronavirus disease 2019 (COVID-19) mRNA vaccines (65–67). Additionally, novel chemical modifications for increased mRNA stability utilized for these vaccines could be exploited for improved miRNA stability (68).

Finally, we have shown that miR-124a expression in primary melanomas may be able to predict recurrence and brain metastasis incidence (**Figure 6**). Therefore, miR-124a holds promise as a biomarker for selection of early-diagnosed

patients who would highly benefit from increased surveillance or recently approved adjuvant therapies (69–71).

METHODS

Cell Culture

Cell lines were grown at 37°C in an atmosphere of 5% CO_2. HEK293T cells purchased from American Type Culture Collection (ATCC) were maintained in Dulbecco's Modified Eagle's Medium (DMEM) medium (*Invitro*gen) containing 10% (v/v) FBS and 1% (v/v) penicillin/streptomycin. The 113/6-4L cells (gift of Dr. Robert Kerbel, University of Toronto) were cultured in DMEM (*Invitro*gen) containing 10% (v/v) FBS (Corning) and 1% (v/v) penicillin/streptomycin (*Invitro*gen). The 113/6-4L is a metastatic variant of the WM239A human melanoma cell line (26). Cells were maintained in culture for no more than 20 passages and were routinely tested for mycoplasma contamination (Universal Mycoplasma Detection kit, ATCC).

Viral Production

In this study, 3×10^6 HEK293T cells were seeded per 10-cm tissue culture dish and co-transfected with lentiviral expression constructs (12 μg), viral packaging plasmid (pSPAX2, 8 μg), and viral envelope plasmid (pMD2.G, 4 μg) using Lipofectamine2000 (Invitrogen), following manufacturer's recommendations. Viral supernatant was collected 48 h post-transfection, filtered through 0.45-μm filters, and stored at -80°C for long-term storage.

Viral Transduction

Target cells were seeded, incubated overnight prior to infection, and transduced at 30% of cell confluence. Medium was replaced with 1:4 diluted viral supernatant and 4 μg/ml Polybrene (EMD Millipore) and incubated for 6 h, followed by replacement with growth medium. Cells were checked for fluorescent protein expression, or drug selection agents were added on subsequent days to ensure pure populations of transduced cells. For viral transduction of melanoma cells with the Decoy library, cells were transduced at an MOI of 0.3 to achieve a single vector copy per cell, resulting in transduction of 30% of cells plated in 150-mm^2 dishes. The percentage of GFP-positive transduced cells and their viability were assessed by flow cytometry 3 days after transduction (BD LSR II, BD Biosciences).

RNA Extraction From Cultured Cells and Metastatic Foci

RNA was extracted using the RNeasy mini kit (Qiagen) following manufacturer's recommendations. Eluted RNA was quantified by Nanodrop 2000 or Qubit (Thermo Fisher) following manufacturer's recommendations and stored at -80°C. When indicated, metastatic foci with RFP and/or GFP signal were dissected using a dissecting fluorescent scope (Leica). Samples were immediately frozen in TRIzol buffer prior to RNA extraction.

miRNA Quantification by RT-qPCR

Reverse transcription (RT) was carried out using TaqMan MicroRNA Reverse Transcription Kit in the presence of RNase inhibitor (Applied Biosystems). Briefly, 25 ng of input RNA was reverse transcribed by stem-loop method following manufacturer's recommendations. To determine the levels of mature miRNA-124a, quantitative Real time PCR (qPCR) was performed following cDNA generation. Briefly, 1 μl of cDNA was used as template in a 10-μl qPCR reaction by adding TaqMan Universal Master Mix II, no UNG (Applied Biosystems), and predesigned TaqMan MicroRNA Assays PCR primers and probes (FAM dye-labeled) for target miRNA-124a (ID: 001182). RNU44 small RNA was used as an endogenous reference gene (ID: 001094). All reactions were performed in triplicate using Biorad CFX 384 or ABI StepOne Plus real-time cyclers following manufacturer's recommendations.

mRNA Quantification by RT-qPCR

In this study, 1,000 ng of RNA was reverse transcribed using Applied Biosciences Taqman RT kit (Applied Biosystems, Thermo Fisher) following manufacturer's recommendations. cDNA was diluted with nuclease-free H_2O prior to use in qPCR reactions. Glyceraldehyde 3-phosphate dehydrogenase (GAPDH) was used as endogenous reference gene in RT-qPCR experiments. Biorad CFX 384 or CFX96 real-time cyclers were used with the following 2-step cycling parameters: 10 min at 95°C, 40 cycles of 95°C for 15 s, followed by 60°C for 30 s, followed by melt curve analysis. Technical triplicates of PCR reactions were performed. Primers were purchased from IDT DNA with the following sequences: EZH2_Fw (5'-TGCTTCCTACATCGTAAGTGCAA-3'); EZH2_Rv (5'-GGTGAGAGCAGCAGCAAACT-3'); MAPK14_Fw (5'-GTGGCCACTAGGTGGTACAG-3'); MAPK14_Rv (5'-GGGGTGTTCCTGTCAGACG-3'); SPRY2_Fw (5'-CCGCGATCACGGAGTTCA-3'), and SPRY2_Rv (5'-GACATGTACCTGCTGGGTGAG-3').

Plasmid Preparation

CMV-Luciferase-EF1α-copGFP (GFP-luc) lentiviral plasmid was purchased from BD Biosciences (BLIV511PA-1), and the lentiviral plasmid mCherry-Luc was a kind gift from Dr. Christian Badr (Massachusetts General Hospital). The miRH-Scr and miRH-124a encoding lentiviral vectors were purchased from SBI Biosystems. All plasmid constructs were propagated in Stbl3 (Thermo Fisher Scientific) or XL-1 Blue Ultracompetent bacteria (Agilent Technologies) on LB plates or in LB media with appropriate antibiotics. Plasmids were extracted by mini- or maxi-prep (Qiagen) following manufacturer's recommendations. All cloned constructs were verified by Sanger sequencing prior to use.

Cloning of pTRIPZ-miR-Scr/miR-124a

The tet-inducible tRFP expression vector pTRIPZ vector was purchased from Dharmacon. The human sequence of pre-miR124.3 flanked with its 200 bp of genomic DNA upstream and downstream was custom designed by Gene Art with the synthetic addition of the XhoI/EcoRI restriction sites for subcloning into pTRIPZ vector in the miR30 context. Successful cloning was confirmed by colony PCR and plasmid sequencing (Macrogen). TRIPZ-infected cells were selected using puromycin (2 μg/ml).

miRNA Decoy Library Generation and Sequencing

The miRNA screen decoy library preparation and sequencing of GFP+ melanoma metastases were performed as described previously (25).

Animal Studies

Mice

All experiments were conducted following protocols approved by the NYU Institutional Animal Care Use Committee (IACUC) (protocol number s16-00051). In this study, 6–8-week-old NOD/Shi-scid/IL-2Rgamma null [NOD.Cg-Prkdc^{scid}Il2rg^{tm1Wjl}/SzJ (NSG)] and athymic nude female mice were purchased from Jackson Laboratory (cat # 005557 and 002019, respectively) and maintained under standard pathogen-free conditions. When indicated, doxycycline hyclate (200 mg/kg/day) was administered to mice in food pellets.

Ultrasound-Guided Intracardiac Injection

For each mouse, 1×10^5 cells suspended in 100 µl of PBS were injected by ultrasound guidance (Visualsonics Vevo 770 Ultrasound Imaging System) into the left ventricle of mice anesthetized with isoflurane. For some experiments, mice were monitored for metastatic progression by *in vivo* bioluminescent imaging [*In Vivo* Imaging System (IVIS)]. Upon substantial weight loss and/or signs of distress (neurological signs, abnormal locomotion) in any experimental mouse, experimental endpoint was established. At experimental endpoint, all mice in all experimental groups were euthanized in a CO_2 chamber. Organs harvested were imaged using a fluorescent dissecting scope (Leica), prior to fixation in 10% formalin for 48 h, and embedding in paraffin.

Bioluminescence

Fifteen minutes prior to imaging, D-Luciferin substrate (150 mg/kg body weight; Gold Biotechnologies) was administered to mice by intraperitoneal injection. Mice were anesthetized with isoflurane and imaged by IVIS Illumina instrument (PerkinElmer) for an automatically determined duration (1–120 s). Signal was quantified using Living Image software (Xenogen) by measurement of average luminescent flux (p/s/cm^2/sr) in drawn brain and body regions of interest (ROIs). Data were plotted using GraphPad PRISM, and significance was determined by unpaired t test.

Survival Analyses

Mice were euthanized when their body weight dropped at or under 17 g or developed signs of discomfort or neurological disorders, whichever came first. The experiment was concluded when mice from the Dc-Scr group that remained alive at day 100 were euthanized.

Analysis of miRNA-124a Expression in Clinical Samples

Primary human melanoma samples were collected at the time of surgery from 92 patients. Informed consent was obtained from all patients, and approval was acquired from the institutional review board (IACUC) of NYU School of Medicine (protocol #10362). miRNA expression profiling of FFPE-extracted RNA from primary melanomas was performed by Exiqon, Inc., using dual-color miRCURY^{TM} LNA arrays. The quantified signals were background corrected and normalized using the global Lowess regression algorithm. Data are deposited in GEO (accession: GSE62372) (20).

Statistical Analyses

Statistical analyses were performed with GraphPad Prism (GraphPad Software, Inc.) Data are presented as the mean ± SD. Significance was determined using unpaired Student's t test, chi square test, Mantel–Cox test, or Breslow–Wilcoxon test, where appropriate. The statistical analyses were performed, and p values were indicated in each figure legend. p values are represented as *$p < 0.05$, **$p < 0.01$, ***$p < 0.001$, ****$p < 0.0001$, and *****$p < 0.00001$.

DATA AVAILABILITY STATEMENT

The raw data supporting the conclusions of this article will be made available by the authors without undue reservation.

ETHICS STATEMENT

The animal study was reviewed and approved by IACUC.

AUTHOR CONTRIBUTIONS

All authors listed have made substantial, direct, and intellectual contribution to the work and approved it for publication.

FUNDING

This work was supported by the National Institute of Health/National Cancer Institute (NIH/NCI) grants R01CA202027 (EH), R01CA243446 (EH), P01CA206980 (EH, MB, NET), R33CA182377 (BDB), and NYU Melanoma SPORE 5P50CA225450 (IO).

ACKNOWLEDGMENTS

The authors thank all members of the Hernando lab for advice and critical reading of the article, as well as the Experimental Pathology Research laboratory at NYU Langone Health, supported by the Cancer Center Support Grant P30CA016087 at the Laura and Isaac Perlmutter Cancer Center. The 113/6-4L melanoma cells were kindly gifted by Dr. Robert S Kerbel (University of Toronto). The lentiviral plasmid encoding mCherry-Luciferase was a kind gift from Dr. Christian Badr (Massachusetts General Hospital).

REFERENCES

1. Jakob JA, Bassett RLJr., Ng CS, Curry JL, Joseph RW, Alvarado GC, et al. NRAS Mutation Status Is an Independent Prognostic Factor in Metastatic Melanoma. *Cancer* (2012) 118(16):4014–23. doi: 10.1002/cncr.26724
2. Falchook GS, Long GV, Kurzrock R, Kim KB, Arkenau TH, Brown MP, et al. Dabrafenib in Patients With Melanoma, Untreated Brain Metastases, and Other Solid Tumours: A Phase 1 Dose-Escalation Trial. *Lancet* (2012) 379 (9829):1893–901. doi: 10.1016/S0140-6736(12)60398-5
3. Long GV, Trefzer U, Davies MA, Kefford RF, Ascierto PA, Chapman PB, et al. Dabrafenib in Patients With Val600Glu or Val600Lys BRAF-Mutant Melanoma Metastatic to the Brain (BREAK-MB): A Multicentre, Open-Label, Phase 2 Trial. *Lancet Oncol* (2012) 13(11):1087–95. doi: 10.1016/S1470-2045(12)70431-X
4. Curti BD, Faries MB. Recent Advances in the Treatment of Melanoma. *New Engl J Med* (2021) 384(23):2229–40. doi: 10.1056/NEJMra2034861
5. Tawbi HA, Forsyth PA, Hodi FS, Lao CD, Moschos SJ, Hamid O, et al. Safety and Efficacy of the Combination of Nivolumab Plus Ipilimumab in Patients With Melanoma and Asymptomatic or Symptomatic Brain Metastases (CheckMate 204). *Neuro Oncol* (2021) 23(11):1961–73. doi: 10.1093/neuonc/noab094
6. Tawbi HA, Forsyth PA, Hodi FS, Algazi AP, Hamid O, Lao CD, et al. Long-Term Outcomes of Patients With Active Melanoma Brain Metastases Treated With Combination Nivolumab Plus Ipilimumab (CheckMate 204): Final Results of an Open-Label, Multicentre, Phase 2 Study. *Lancet Oncol* (2021) 22(12):1692–704. doi: 10.1016/S1470-2045(21)00545-3
7. Segura MF, Greenwald HS, Hanniford D, Osman I, Hernando E. MicroRNA and Cutaneous Melanoma: From Discovery to Prognosis and Therapy. *Carcinogenesis* (2012) 33(10):1823–32. doi: 10.1093/carcin/bgs205
8. Croce CM, Calin GA. miRNAs, Cancer, and Stem Cell Division. *Cell* (2005) 122(1):6–7. doi: 10.1016/j.cell.2005.06.036
9. Spizzo R, Nicoloso MS, Croce CM, Calin GA. SnapShot: MicroRNAs in Cancer. *Cell* (2009) 137(3):586–e1. doi: 10.1016/j.cell.2009.04.040
10. Vera O, Bok I, Jasani N, Nakamura K, Xu X, Mecozzi N, et al. A MAPK/miR-29 Axis Suppresses Melanoma by Targeting MAFG and MYBL2. *Cancers (Basel)* (2021) 13(6):1408. doi: 10.3390/cancers13061408
11. Dietrich P, Kuphal S, Spruss T, Hellerbrand C, Bosserhoff AK. MicroRNA-622 Is a Novel Mediator of Tumorigenicity in Melanoma by Targeting Kirsten Rat Sarcoma. *Pigment Cell Melanoma Res* (2018) 31(5):614–29. doi: 10.1111/pcmr.12698
12. Linck-Paulus L, Lammerhirt L, Voller D, Meyer K, Engelmann JC, Spang R, et al. Learning From Embryogenesis-A Comparative Expression Analysis in Melanoblast Differentiation and Tumorigenesis Reveals miRNAs Driving Melanoma Development. *J Clin Med* (2021) 10(11):2259>. doi: 10.3390/jcm10112259
13. Stark MS, Tom LN, Boyle GM, Bonazzi VF, Soyer HP, Herington AC, et al. The "Melanoma-Enriched" microRNA miR-4731-5p Acts as a Tumour Suppressor. *Oncotarget* (2016) 7(31):49677–87. doi: 10.18632/oncotarget.10109
14. Tembe V, Schramm SJ, Stark MS, Patrick E, Jayaswal V, Tang YH, et al. MicroRNA and mRNA Expression Profiling in Metastatic Melanoma Reveal Associations With BRAF Mutation and Patient Prognosis. *Pigment Cell Melanoma Res* (2015) 28(3):254–66. doi: 10.1111/pcmr.12343
15. Segura MF, Belitskaya-Levy I, Rose AE, Zakrzewski J, Gaziel A, Hanniford D, et al. Melanoma MicroRNA Signature Predicts Post-Recurrence Survival. *Clin Cancer Res* (2010) 16(5):1577–86. doi: 10.1158/1078-0432.CCR-09-2721
16. Bonazzi VF, Stark MS, Hayward NK. MicroRNA Regulation of Melanoma Progression. *Melanoma Res* (2012) 22(2):101–13. doi: 10.1097/CMR.0b013e32834f6fbb
17. Hanniford D, Zhong J, Koetz L, Gaziel-Sovran A, Lackaye DJ, Shang S, et al. A miRNA-Based Signature Detected in Primary Melanoma Tissue Predicts Development of Brain Metastasis. *Clin Cancer Res* (2015) 21(21):4903–12. doi: 10.1158/1078-0432.CCR-14-2566
18. Huynh C, Segura MF, Gaziel-Sovran A, Menendez S, Darvishian F, Chiriboga L, et al. Efficient *In Vivo* microRNA Targeting of Liver Metastasis. *Oncogene* (2011) 30(12):1481–8. doi: 10.1038/onc.2010.523
19. Gaziel-Sovran A, Segura MF, Di Micco R, Collins MK, Hanniford D, Vega-Saenz de Miera E, et al. miR-30b/30d Regulation of GalNAc Transferases Enhances Invasion and Immunosuppression During Metastasis. *Cancer Cell* (2011) 20(1):104–18. doi: 10.1016/j.ccr.2011.05.027
20. Hanniford D, Segura MF, Zhong J, Philips E, Jirau-Serrano X, Darvishian F, et al. Identification of Metastasis-Suppressive microRNAs in Primary Melanoma. *J Natl Cancer Inst* (2015) 107(3):dju494. doi: 10.1093/jnci/dju494
21. Segura MF, Hanniford D, Menendez S, Reavie L, Zou X, Alvarez-Diaz S, et al. Aberrant miR-182 Expression Promotes Melanoma Metastasis by Repressing FOXO3 and Microphthalmia-Associated Transcription Factor. *Proc Natl Acad Sci USA* (2009) 106(6):1814–9. doi: 10.1073/pnas.0808263106
22. Mueller DW, Rehli M, Bosserhoff AK. miRNA Expression Profiling in Melanocytes and Melanoma Cell Lines Reveals miRNAs Associated With Formation and Progression of Malignant Melanoma. *J Invest Dermatol* (2009) 129(7):1740–51. doi: 10.1038/jid.2008.452
23. Gilot D, Migault M, Bachelot L, Journe F, Rogiers A, Donnou-Fournet E, et al. A Non-Coding Function of TYRP1 mRNA Promotes Melanoma Growth. *Nat Cell Biol* (2017) 19(11):1348–57. doi: 10.1038/ncb3623
24. Kurata JS, Lin RJ. MicroRNA-Focused CRISPR-Cas9 Library Screen Reveals Fitness-Associated miRNAs. *RNA* (2018) 24(7):966–81. doi: 10.1261/rna.066282.118
25. Mullokandov G, Baccarini A, Ruzo A, Jayaprakash AD, Tung N, Israelow B, et al. High-Throughput Assessment of microRNA Activity and Function Using microRNA Sensor and Decoy Libraries. *Nat Methods* (2012) 9(8):840–6. doi: 10.1038/nmeth.2078
26. Cruz-Munoz W, Man S, Xu P, Kerbel RS. Development of a Preclinical Model of Spontaneous Human Melanoma Central Nervous System Metastasis. *Cancer Res* (2008) 68(12):4500–5. doi: 10.1158/0008-5472.CAN-08-0041
27. Valiente M, Van Swearingen AED, Anders CK, Bairoch A, Boire A, Bos PD, et al. Brain Metastasis Cell Lines Panel: A Public Resource of Organotropic Cell Lines. *Cancer Res* (2020) 80(20):4314–23. doi: 10.1158/0008-5472.CAN-20-0291
28. Morsi A, Gaziel-Sovran A, Cruz-Munoz W, Kerbel RS, Golfinos JG, Hernando E, et al. Development and Characterization of a Clinically Relevant Mouse Model of Melanoma Brain Metastasis. *Pigment Cell Melanoma Res* (2013) 26 (5):743–5. doi: 10.1111/pcmr.12114
29. Landgraf P, Rusu M, Sheridan R, Sewer A, Iovino N, Aravin A, et al. A Mammalian microRNA Expression Atlas Based on Small RNA Library Sequencing. *Cell* (2007) 129(7):1401–14. doi: 10.1016/j.cell.2007.04.040
30. Rose SA, Wroblewska A, Dhainaut M, Yoshida H, Shaffer JM, Bektesevic A, et al. A microRNA Expression and Regulatory Element Activity Atlas of the Mouse Immune System. *Nat Immunol* (2021) 22(7):914–27. doi: 10.1038/s41590-021-00944-y
31. Makeyev EV, Zhang J, Carrasco MA, Maniatis T. The MicroRNA miR-124 Promotes Neuronal Differentiation by Triggering Brain-Specific Alternative Pre-mRNA Splicing. *Mol Cell* (2007) 27(3):435–48. doi: 10.1016/j.molcel.2007.07.015
32. Bhaskaran V, Nowicki MO, Idriss M, Jimenez MA, Lugli G, Hayes JL, et al. The Functional Synergism of microRNA Clustering Provides Therapeutically Relevant Epigenetic Interference in Glioblastoma. *Nat Commun* (2019) 10 (1):442. doi: 10.1038/s41467-019-08390-z
33. Baccarini A, Chauhan H, Gardner TJ, Jayaprakash AD, Sachidanandam R, Brown BD. Kinetic Analysis Reveals the Fate of a microRNA Following Target Regulation in Mammalian Cells. *Curr Biol* (2011) 21(5):369–76. doi: 10.1016/j.cub.2011.01.067
34. Zheng F, Liao YJ, Cai MY, Liu YH, Liu TH, Chen SP, et al. The Putative Tumour Suppressor microRNA-124 Modulates Hepatocellular Carcinoma Cell Aggressiveness by Repressing ROCK2 and EZH2. *Gut* (2012) 61(2):278–89. doi: 10.1136/gut.2011.239145
35. Pan W, Wei N, Xu W, Wang G, Gong F, Li N. MicroRNA-124 Alleviates the Lung Injury in Mice With Septic Shock Through Inhibiting the Activation of the MAPK Signaling Pathway by Downregulating MAPK14. *Int Immunopharmacol* (2019) 76:105835. doi: 10.1016/j.intimp.2019.105835
36. Liu Y, Li S, Liu Y, Lv X, Zhou Q. MicroRNA-124 Facilitates Lens Epithelial Cell Apoptosis by Inhibiting SPRY2 and MMP-2. *Mol Med Rep* (2021) 23 (5):381. doi: 10.3892/mmr.2021.12020
37. Massague J, Obenauf AC. Metastatic Colonization by Circulating Tumour Cells. *Nature* (2016) 529(7586):298–306. doi: 10.1038/nature17038
38. Paget S. The Distribution of Secondary Growths in Cancer of the Breast. *1889 Cancer Metastasis Rev* (1989) 8(2):98–101.

39. Luzzi KJ, MacDonald IC, Schmidt EE, Kerkvliet N, Morris VL, Chambers AF, et al. Multistep Nature of Metastatic Inefficiency: Dormancy of Solitary Cells After Successful Extravasation and Limited Survival of Early Micrometastases. *Am J Pathol* (1998) 153(3):865–73. doi: 10.1016/S0002-9440(10)65628-3
40. Kim JW, Wong CW, Goldsmith JD, Song C, Fu W, Allion MB, et al. Rapid Apoptosis in the Pulmonary Vasculature Distinguishes Non-Metastatic From Metastatic Melanoma Cells. *Cancer Lett* (2004) 213(2):203–12. doi: 10.1016/j.canlet.2004.03.042
41. Fidler IJ. The Pathogenesis of Cancer Metastasis: The 'Seed and Soil' Hypothesis Revisited. *Nat Rev Cancer* (2003) 3(6):453–8. doi: 10.1038/nrc1098
42. Eichler AF, Chung E, Kodack DP, Loeffler JS, Fukumura D, Jain RK. The Biology of Brain Metastases-Translation to New Therapies. *Nat Rev Clin Oncol* (2011) 8(6):344–56. doi: 10.1038/nrclinonc.2011.58
43. Nayak L, Lee EQ, Wen PY. Epidemiology of Brain Metastases. *Curr Oncol Rep* (2012) 14(1):48–54. doi: 10.1007/s11912-011-0203-y
44. Obenauf AC, Massague J. Surviving at a Distance: Organ-Specific Metastasis. *Trends Cancer* (2015) 1(1):76–91. doi: 10.1016/j.trecan.2015.07.009
45. Hanniford D, Ulloa-Morales A, Karz A, Berzoti-Coelho MG, Moubarak RS, Sanchez-Sendra B, et al. Epigenetic Silencing of CDR1as Drives IGF2BP3-Mediated Melanoma Invasion and Metastasis. *Cancer Cell* (2020) 37(1):55–70. doi: 10.1016/j.ccell.2019.12.007
46. Pencheva N, Tran H, Buss C, Huh D, Drobnjak M, Busam K, et al. Convergent Multi-miRNA Targeting of ApoE Drives LRP1/LRP8-Dependent Melanoma Metastasis and Angiogenesis. *Cell* (2012) 151(5):1068–82. doi: 10.1016/j.cell.2012.10.028
47. Wang Q, Chen J, Wang A, Sun L, Qian L, Zhou X, et al. Differentially Expressed circRNAs in Melanocytes and Melanoma Cells and Their Effect on Cell Proliferation and Invasion. *Oncol Rep* (2018) 39(4):1813–24. doi: 10.3892/or.2018.6263
48. Qian P, Linbo L, Xiaomei Z, Hui P. Circ_0002770, Acting as a Competitive Endogenous RNA, Promotes Proliferation and Invasion by Targeting miR-331-3p in Melanoma. *Cell Death Dis* (2020) 11(4):264. doi: 10.1038/s41419-020-2444-x
49. Hwang SJ, Seol HJ, Park YM, Kim KH, Gorospe M, Nam DH, et al. MicroRNA-146a Suppresses Metastatic Activity in Brain Metastasis. *Molecules Cells* (2012) 34(3):329–34. doi: 10.1007/s10059-012-0171-6
50. Camacho L, Guerrero P, Marchetti D. MicroRNA and Protein Profiling of Brain Metastasis Competent Cell-Derived Exosomes. *PloS One* (2013) 8(9):e73790. doi: 10.1371/journal.pone.0073790
51. Slominski A, Kim TK, Brozyna AA, Janjetovic Z, Brooks DL, Schwab LP, et al. The Role of Melanogenesis in Regulation of Melanoma Behavior: Melanogenesis Leads to Stimulation of HIF-1alpha Expression and HIF-Dependent Attendant Pathways. *Arch Biochem Biophys* (2014) 563:79–93. doi: 10.1016/j.abb.2014.06.030
52. Slominski A, Tobin DJ, Shibahara S, Wortsman J. Melanin Pigmentation in Mammalian Skin and its Hormonal Regulation. *Physiol Rev* (2004) 84(4):1155–228. doi: 10.1152/physrev.00044.2003
53. Chi SW, Zang JB, Mele A, Darnell RB. Argonaute HITS-CLIP Decodes microRNA-mRNA Interaction Maps. *Nature* (2009) 460(7254):479–86. doi: 10.1038/nature08170
54. Qiao W, Guo B, Zhou H, Xu W, Chen Y, Liang Y, et al. miR-124 Suppresses Glioblastoma Growth and Potentiates Chemosensitivity by Inhibiting AURKA. *Biochem Biophys Res Commun* (2017) 486(1):43–8. doi: 10.1016/j.bbrc.2017.02.120
55. Lv Z, Yang L. MiR-124 Inhibits the Growth of Glioblastoma Through the Downregulation of SOS1. *Mol Med Rep* (2013) 8(2):345–9. doi: 10.3892/mmr.2013.1561
56. Simeoli R, Montague K, Jones HR, Castaldi L, Chambers D, Kelleher JH, et al. Exosomal Cargo Including microRNA Regulates Sensory Neuron to Macrophage Communication After Nerve Trauma. *Nat Commun* (2017) 8(1):1778. doi: 10.1038/s41467-017-01841-5
57. Xu B, Zhang Y, Du XF, Li J, Zi HX, Bu JW, et al. Neurons Secrete miR-132-Containing Exosomes to Regulate Brain Vascular Integrity. *Cell Res* (2017) 27(7):882–97. doi: 10.1038/cr.2017.62
58. Shen C, Hua H, Gu L, Cao S, Cai H, Yao X, et al. miR-124 Functions As A Melanoma Tumor Suppressor By Targeting Rack1. *Onco Targets Ther* (2019) 12:9975–86. doi: 10.2147/OTT.S225120
59. Chen X, He D, Dong XD, Dong F, Wang J, Wang L, et al. MicroRNA-124a Is Epigenetically Regulated and Acts as a Tumor Suppressor by Controlling Multiple Targets in Uveal Melanoma. *Invest Ophthalmol Vis Sci* (2013) 54(3):2248–56. doi: 10.1167/iovs.12-10977
60. Zingg D, Debbache J, Schaefer SM, Tuncer E, Frommel SC, Cheng P, et al. The Epigenetic Modifier EZH2 Controls Melanoma Growth and Metastasis Through Silencing of Distinct Tumour Suppressors. *Nat Commun* (2015) 6:6051. doi: 10.1038/ncomms7051
61. Chen Y, Gao DY, Huang L. *In Vivo* Delivery of miRNAs for Cancer Therapy: Challenges and Strategies. *Adv Drug Deliv Rev* (2015) 81:128–41. doi: 10.1016/j.addr.2014.05.009
62. Weng Y, Li C, Yang T, Hu B, Zhang M, Guo S, et al. The Challenge and Prospect of mRNA Therapeutics Landscape. *Biotechnol Adv* (2020) 40:107534. doi: 10.1016/j.biotechadv.2020.107534
63. Kim J, Eygeris Y, Gupta M, Sahay G. Self-Assembled mRNA Vaccines. *Adv Drug Deliv Rev* (2021) 170:83–112. doi: 10.1016/j.addr.2020.12.014
64. Gebre MS, Brito LA, Tostanoski LH, Edwards DK, Carfi A, Barouch DH. Novel Approaches for Vaccine Development. *Cell* (2021) 184(6):1589–603. doi: 10.1016/j.cell.2021.02.030
65. Anderson EJ, Rouphael NG, Widge AT, Jackson LA, Roberts PC, Makhene M, et al. Safety and Immunogenicity of SARS-CoV-2 mRNA-1273 Vaccine in Older Adults. *N Engl J Med* (2020) 383(25):2427–38. doi: 10.1056/NEJMoa2028436
66. Baden LR, El Sahly HM, Essink B, Kotloff K, Frey S, Novak R, et al. Efficacy and Safety of the mRNA-1273 SARS-CoV-2 Vaccine. *N Engl J Med* (2021) 384(5):403–16. doi: 10.1056/NEJMoa2035389
67. Polack FP, Thomas SJ, Kitchin N, Absalon J, Gurtman A, Lockhart S, et al. Safety and Efficacy of the BNT162b2 mRNA Covid-19 Vaccine. *N Engl J Med* (2020) 383(27):2603–15. doi: 10.1056/NEJMoa2034577
68. Schoenmaker L, Witzigmann D, Kulkarni JA, Verbeke R, Kersten G, Jiskoot W, et al. mRNA-Lipid Nanoparticle COVID-19 Vaccines: Structure and Stability. *Int J Pharm* (2021) 601:120586. doi: 10.1016/j.ijpharm.2021.120586
69. Luke JJ, Ascierto PA, Carlino MS, Gershenwald JE, Grob JJ, Hauschild A, et al. KEYNOTE-716: Phase III Study of Adjuvant Pembrolizumab Versus Placebo in Resected High-Risk Stage II Melanoma. *Future Oncol* (2020) 16(3):4429–38. doi: 10.2217/fon-2019-0666
70. Eggermont AMM, Blank CU, Mandala M, Long GV, Atkinson V, Dalle S, et al. Adjuvant Pembrolizumab Versus Placebo in Resected Stage III Melanoma. *N Engl J Med* (2018) 378(19):1789–801. doi: 10.1056/NEJMoa1802357
71. Weber J, Mandala M, Del Vecchio M, Gogas HJ, Arance AM, Cowey CL, et al. Adjuvant Nivolumab Versus Ipilimumab in Resected Stage III or IV Melanoma. *N Engl J Med* (2017) 377(19):1824–35. doi: 10.1056/NEJMoa1709030

Conflict of Interest: The authors declare that the research was conducted in the absence of any commercial or financial relationships that could be construed as a potential conflict of interest.

frontiers | Frontiers in Oncology

MINI REVIEW
published: 14 April 2022
doi: 10.3389/fonc.2022.858892

The Role and Mechanism of microRNA-1224 in Human Cancer

Mingwei Ma[1,2†], *Jie Li*[1,2†], *Zimu Zhang*[1,2], *Juan Sun*[1,2], *Zhen Liu*[1,2], *Ziyang Zeng*[1,2], *Siwen Ouyang*[1,2] *and Weiming Kang*[1,2*]

[1] Chinese Academy of Medical Sciences and Peking Union Medical College, Beijing, China, [2] Department of General Surgery, Peking Union Medical College Hospital, Beijing, China

microRNAs (miRNAs) are a type of small endogenous non-coding RNAs composed of 20-22 nucleotides, which can regulate the expression of a gene by targeting 3' untranslated region (3'-UTR) of mRNA. Many studies have reported that miRNAs are involved in the occurrence and progression of human diseases, including malignant tumors. miR-1224 plays significant roles in different tumors, including tumor proliferation, metastasis, invasion, angiogenesis, biological metabolism, and drug resistance. Mostly, it serves as a tumor suppressor. With accumulating proofs of miR-1224, it can act as a potential bio-indicator in the diagnosis and prognosis of patients with cancer. In this article, we review the characteristics and research progress of miR-1224 and emphasize the regulation and function of miR-1224 in different cancer. Furthermore, we conclude the clinical implications of miR-1224. This review may provide new horizons for deeply understanding the role of miR-1224 as biomarkers and therapeutic targets in human cancer.

Keywords: miR-1224, cancer, tumor suppressor, function, clinical implication

OPEN ACCESS

Edited by:
Valeria Poli,
University of Turin, Italy

Reviewed by:
Hou-Qun Ying,
Second Affiliated Hospital of Nanchang University, China

****Correspondence:***
Weiming Kang
kangweiming@163.com

†These authors have contributed equally to this work

Specialty section:
This article was submitted to Molecular and Cellular Oncology, a section of the journal Frontiers in Oncology

Received: *20 January 2022*
Accepted: *22 March 2022*
Published: *14 April 2022*

Citation:
Ma M, Li J, Zhang Z, Sun J, Liu Z, Zeng Z, Ouyang S and Kang W (2022) The Role and Mechanism of microRNA-1224 in Human Cancer. Front. Oncol. 12:858892. doi: 10.3389/fonc.2022.858892

INTRODUCTION

microRNAs (miRNAs) are endogenous non-coding small RNAs that are composed of 20-22 nucleotides and are widely present in eukaryotic cells (1). miRNAs regulate the cellular protein expression through binding to the 3' untranslated region (3'-UTR) of the targeted mRNA, resulting in decreased or degraded expression of the target genes (2). Complete or incomplete binding of 6-8 nucleotide seed sequences of each miRNA can bind up to 100 mRNAs, leading to degradation or translation inhibition, respectively. Therefore, each miRNA can bind and regulate multiple mRNAs, and one mRNA can also be regulated by diverse miRNAs.

miRNAs are generated by endogenous transcribed primary transcripts, which are further cleaved by Drosha (RNase III) in the nucleus to produce stem-loop precursors miRNAs (pre-miRNAs) of approximately 70 nucleotides (3). Pre-miRNAs are transported by Exportin 5 from the nucleus to the cytoplasm and further processed by Dicer (RNase III) for the production of mature miRNAs (4, 5).

To date, more than 1600 miRNAs have been found and identified, most of which are highly conserved in mammalian species. The functions of miRNAs have been validated in developmental

Abbreviation: TNBC, Triple-negative breast cancers; TSCC, Tongue squamous cell carcinoma; RCC, Renal cell carcinoma; HCC, Hepatocellular carcinoma; LGG, Low-grade glioma; BC, Breast cancer; OSCC, Oral squamous cell carcinoma; CRC, Colorectal cancer; OS, Osteosarcoma; GC, Gastric cancer; LAUD, Lung adenocarcinoma; BCa, Bladder cancer; LP, Laryngeal papilloma; GBM, Glioblastoma; OC, Ovarian cancer; RC, Rectal cancer; ESCC, Esophageal squamous cell carcinoma; PC, Pancreatic cancer; ESCA, Esophageal cancer; LC, Lung cancer; EMT, Epithelial-to-mesenchymal transition; NEAT1, Nuclear paraspeckle assembly transcript 1; CGGA, Chinese Glioma Genome Atlas.

timing, cell proliferation, cell differentiation, cell apoptosis, and tumorigenesis additionally (6–10). Considerable research revealed that miRNAs are dysregulated in different tumor types, which act as tumor inhibitors or tumor promotors and actively participate in the oncogenic process (11). In addition, miRNAs also play critical roles in predicting tumor classification, treatment response, and prognosis of patients (12).

miR-1224, located at chromosome 3q27.1, is a class of mammalian mirtron encompassed in the last intron of the VWA5B2 gene (von Willebrand factor A domain containing 5B2) and is discovered that acts vital roles in some diseases, such as acute liver failure, Parkinson's disease, and cerebral ischemia (13–15). miR-1224 has two mature sequences, miR-1224-5p and miR-1224-3p, which perform different functions, respectively. Although some research has reported that miR-1224 expressed abnormally in several tumors, its biological function and specific mechanism in different cancers are still inconsistent (16–18). Moreover, the expression profile and its potential clinical significance of miR-1224 have not been investigated. Therefore, we systematically review the role and the detailed mechanism of miR-1224 in cancer, to gain a better comprehension of its potential role as biomarkers and therapeutic targets in cancer.

MIR-1224 EXPRESSION IN HUMAN CANCER

miR-1224 was expressed variously and mostly downregulated in human cancers (**Table 1**). The expression of miR-1224 in different kinds of tumors was showed followingly.

In the respiratory system, especially in lung cancer, miR-1224 was usually downregulated. miR-1224 was lower level detected by quantitative reverse transcription PCR (qRT-PCR) in lung cancer tissues than normal lung tissues (19). Zuo et al. found that miR-1224-3p was decreased in lung adenocarcinoma (LAUD) tissues compared to that in normal tissues *via* qRT-PCR method. Transcriptional profiling studies also showed that miR-1224-3p was remarkably reduced in LAUD cell lines (21). In the tissues of laryngeal papillomas (LP), further research proved that miR-1224-5p was greatly decreased by using qPCR. In addition, miR-1224-5p was downregulated in LP cell lines when compared to normal cells (20).

In the nervous system, miR-1224 was mostly downregulated in nervous system neoplasms (18, 23, 24). miR-1224-3p was reduced in glioma by using miRNA assay and real time PCR (23, 24), which was also observed in low-grade glioma (LGG)

TABLE 1 | Expression profiles of miR-1224 in human cancers.

Systems	RNAs	Cancer type	Role	Expression	Sources	References
Respiratory system	miR-1224	LC	tumor suppressor	downregulation	tissue and cell	(19)
	miR-1224-5p	LP	tumor suppressor	downregulation	tissue and cell	(20)
	miR-1224-3p	LAUD	tumor suppressor	downregulation	tissue and cell	(21)
Nerve system	miR-1224-3p	LGG	tumor suppressor	downregulation	tissue	(22)
	miR-1224-3p	Glioma	tumor suppressor	downregulation	cell	(23)
	miR-1224-3p	Glioma	tumor suppressor	downregulation	tissue and cell	(24)
	miR-1224-5p	Glioma	tumor suppressor	downregulation	tissue and cell	(18)
	miR-1224-5p	GBM	tumor suppressor	downregulation	tissue and cell	(25)
	miR-1224-5p	GBM	tumor suppressor	downregulation	GEO database	(26)
Muscular and skeletal systems	miR-1224-5p	OS	tumor suppressor	downregulation	tissue and cell	(27)
	miR-1224-5p	OS	tumor suppressor	downregulation	tissue and cell	(28)
Genitourinary system	miR-1224-5p	BCa	tumor suppressor	downregulation	tissue and cell	(29)
	miR-1224-3p	BCa	tumor suppressor	downregulation	tissue	(30)
	miR-1224-5p	BCa	tumor suppressor	upregulation	tissue and cell	(31)
	miR-1224-3p	BC	tumor promotor	upregulation	cell	(32)
Digestive system	miR-1224-5p	TSCC	tumor suppressor	downregulation	cell	(33)
	miR-1224-5p	OSCC	tumor suppressor	downregulation	tissue and cell	(34)
	miR-1224	GC	tumor suppressor	downregulation	tissue and cell	(35)
	miR-1224-5p	GC	tumor suppressor	downregulation	tissue and cell	(36)
	miR-1224	intestinal-type GC	tumor suppressor	downregulation	tissue and cell	(37)
	miR-1224-5p	CRC	tumor suppressor	downregulation	tissue and cell	(38)
	miR-1224-5p	CRC	tumor suppressor	downregulation	tissue and cell	(39)
	miR-1224-5p	CRC	tumor suppressor	downregulation	tissue	(17)
	miR-1224-5p	ESCC	tumor suppressor	downregulation	tissue and cell	(40)
	miR-1224-5p	ESCA	tumor suppressor	downregulation	tissue and cell	(41)
	miR-1224	HCC	tumor suppressor	downregulation	tissue and cell	(42)
	miR-1224	HCC	tumor suppressor	downregulation	tissue and cell	(43)
	miR-1224-5p	HCC	tumor suppressor	downregulation	cell	(44)
	miR-1224-5p	PC	tumor suppressor	downregulation	tissue and cell	(45)
	miR-1224-5p	PC	tumor suppressor	downregulation	tissue and cell	(46)
Skin	miR-1224-5p	Melanoma	tumor suppressor	downregulation	tissue and cell	(47)
	miR-1224-5p	keloids	tumor suppressor	downregulation	tissue and cell	(48)

from GEO and TCGA database (22). Qian et al. also confirmed that miR-1224-5p was downregulated in glioma by *in situ* hybridization of tissue samples (18). In glioblastoma (GBM), Xu et al. and Xiong et al. reported that miR-1224-5p acted as a tumor suppressor and a significant reduction of miR-1224-5p was detected in GBM tissues and cell lines *via* qRT-PCR and GEO database, respectively (25, 26).

Reduced miR-1224 was common in the muscular and skeletal system. For instance, miR-1224-5p was decreased in osteosarcoma (OS) tissues and cell lines by qRT-PCR (27, 28).

Similarly, miR-1224 was reduced in the digestive system. miR-1224-5p was downregulated in the cells of tongue squamous cell carcinoma (TSCC) and oral squamous cell carcinoma (OSCC) by RT-qPCR analysis (33, 34). In gastric cancer (GC), miR-1224 was reduced in GC tissues and cell lines through RT-PCR analysis (35–37). In colorectal cancer (CRC), miR-1224-5p also acted as a tumor suppressor and a significant reduction of miR-1224-5p was detected in CRC tissues and cell lines according to qRT-PCR, western blot, and immunohistochemistry (17, 38, 39). In hepatocellular carcinoma (HCC) and pancreatic cancer (PC), miR-1224 showed a descending trend, especially the miR-1224-5p according to bioinformatics analysis (GEO datasets), RNA sequencing and qRT-PCR validation (42–46). Not only that, but miR-1224-5p also declined in esophageal squamous cell carcinoma (ESCC) and esophageal cancer (ESCA) tissues compared to normal tissues by qRT-PCR (40, 41).

miR-1224 was somewhat controversial in the genitourinary system. Through qRT-PCR experiments, miR-1224 was found downregulated in bladder cancer (BCa) (29, 30). However, Ding et al. reported that miR-1224-5p was elevated in the BCa tissues and cell lines using TCGA database (31). Similarly, Ran et al. found that miR-1224-3p was increased in breast cancer (BC) cells by using RT-qPCR methods (32).

In skin system, miR-1224-5p was significantly downregulated in melanoma tissues and cell lines by using qRT-PCR (47). miR-1224-5p was also downregulated in keloids from miRNA microarray and qRT-PCR (48).

Those data proved that there was wide diversity for miR-1224 expression in different cancers, sometimes even in same cancer.

THE REGULATION OF MIR-1224 IN HUMAN CANCER

Generated by non-coding mRNA splicing, miR-1224 was regulated by multiple signaling molecules such as CREB1, SND1, and β-catenin (**Table 2**). LncRNAs mainly performed as ceRNA to sponge miRNAs and thus to regulate miRNA expression. In LC, miR-1224 was repressed by long-chain non-coding RNA (lncRNA) NEAT1, thereby upregulating KLF3 expression (19). LncRNA NEAT1 also regulated miR-1224-5p in GC by sponging miR-1224-5p, thus regulating RSF1 expression and in turn, altering the evolution of GC (36). Additionally, Linc00460 regulated miR-1224-5p in OS and ESCA, respectively (28, 41). Linc00460 functioned as a molecular sponge to absorb miR-1224-5p, thereby promoting metastasis and epithelial-to-mesenchymal transition (EMT) of ESCA and OS progression (28, 41). There were other lncRNAs to regulate miR-1224 besides LncRNA NEAT1 and Linc00460. Linc00665 was the sponge for miR-1224-5p, which elevated the SND1 in PC cells (46). Zhao et al. discovered that LncRNA IGFL2-AS1 played an oncogenic role in TSCC (33). It interacted with miR-1224-5p to regulate SATB1, which activated the transcriptional activity of Wnt/β-catenin in TSCC cells (33). LncRNA ZEB1-AS1 was generated from the promoters of ZEB1, which played a vital role in tumorigenesis. Experimental data indicated that ZEB1-AS1 directly regulated miR-1224-5p, thus controlling the processes of development and progression in melanoma (47). To sum up, several articles have confirmed that multiple lncRNA molecules are involved in the regulation of miRNA, mainly acting as sponges to inhibit miRNA expression.

Circular RNAs (circRNAs) are identified as a type of endogenous non-coding RNAs and exist conserved miRNA target sites, and therefore circRNAs could act as miRNA sponges to modulate its expression. Circ-CASC15 was highly expressed in BCa, which directly bind to miR-1224-5p. Consequently, CREB1, the target of miR-1224-5p, was increased in BCa (29). Recent studies have shown that circ-EGLN3 was involved in RCC tumorigenesis through downregulating miR-1224-3p, which targeted HMGXB3, thus regulating proliferation, invasion, and migration (49). CircRNAs also played an important role in the progression of digestive system neoplasms, such as circ-RASGRF2 and circ-RNF121 (38, 43). Circ-RASGRF2 was originated from RASGRF2 and identified to be remarkably upregulated in HCC. Further data confirmed that circRASGRF2 facilitated the expression of FAK by sponging miR-1224. The knockdown of circ-RASGRF2 inhibited the proliferation and migration of HCC cells. (43). Circ-RNF121 was remarkably upregulated in CRC. Similarly, circ-RNF121 functioned as a sponge of miR-1224-5p to regulate cell growth, migration, and invasion in CRC (38). Zuo et al. found that circ-ZNF609 sponged miR-1224-3p to downregulate its expression in LAUD. As a result, the molecular target of miR-1224-3p, ETV1, was upregulated in LAUD. Recently, ETV1 has been identified to play an oncogenic role (21). In nerve system, Circ-ZNF609 functioned as a miR-1224-3p sponge and mediated cell behaviors in glioma. It promoted cell proliferation and metastasis by promoting PLK1 *via* binding to miR-1224-3p competitively (24). Other regulatory factors modulated miR-1224-3p expression in gliomas, such as EZH2 and MIR44435-2HG (lncRNA MIR4435-2 Host Gene) (23, 25). EZH2, a core component of PRC2, acted as a histone methyltransferase that trimethylated histone 3 at lysine 27 (H3K27me3), silencing the gene. In gliomas, miR-1224-3p was inhibited by EZH2, which in turn regulated β-catenin expression through binding to its 3′ UTR, thus controlling proliferation, invasion, and glucose metabolism of cells (23). MIR44435-2HG belonged to long non-coding RNAs and was involved in the regulation of brain tumor progression. Knockdown of MIR4435-2HG contributed to the inhibition of cell proliferation and invasion of GBM. MIR4435-2HG suppressed miR-1224-5p expression through similar mechanism (25).

TABLE 2 | Upstream regulations and biological functions of miR-1224 involved in different cancers.

Systems	Cancer type	RNAs	Upstream gene	Biological functions	References
Respiratory system	LC	miR-1224	NEAT1	Inhibit proliferation and invasion, promote apoptosis	(19)
	LAUD	miR-1224-3p	Circ-ZNF609	Inhibit proliferation and cell cycle	(21)
Nerve system	Glioma	miR-1224-3p	Circ-ZNF609	Inhibit proliferation, migration and invasion	(24)
		miR-1224-3p	EZH2	Inhibit proliferation, invasion and glucose metabolism	(23)
	GBM	miR-1224-5p	MIR44435-2HG	Inhibit proliferation and invasion, promote apoptosis	(25)
Muscular and skeletal systems	OS	miR-1224-5p	linc00460	Inhibit proliferation, invasion and migration	(28)
		miR-1224-5p	\	Inhibit proliferation, invasion and EMT, promote apoptosis, autophagy	(27)
Genitourinary system	Bca	miR-1224-5p	circCASC15	Inhibit proliferation	(29)
		miR-1224-5p	FOXI1	Inhibit viability, migration and invasion	(31)
	RCC	miR-1224-3p	circ-EGNL3	Inhibit proliferation, invasion, and migration	(49)
	BC	miR-1224-3p	\	Inhibit apoptosis, promote EMT, migration and metastasis	(50)
		miR-1224-3p	\	Promote cell growth and metastasis	(32)
Digestive system	TSCC	miR-1224-5p	IGFL2-AS1	Inhibit proliferation, migration, invasion and EMT	(33)
	OSCC	miR-1224-5p	APCDD1L-AS1	Inhibit proliferation and promote apoptosis	(34)
	GC	miR-1224-5p	NEAT1	Inhibit proliferation, invasion, and migration	(36)
		miR-1224	\	Inhibit proliferation, migration, invasion, and EMT	(35)
	HCC	miR-1224	CREB	Inhibit proliferation and cell cycle	(42)
		miR-1224	circRASGRF2	Inhibit proliferation, cell cycle, invasion, migration and EMT, promote apoptosis, autophagy	(43)
		miR-1224-5p	/	Inhibit proliferation, migration and invasion, promote apoptosis	(44)
	CRC	miR-1224-5p	Circ-RNF121	Inhibit proliferation, migration, invasion and glycolysis, promote apoptosis	(38)
		miR-1224-5p	/	Inhibit migration, invasion and EMT	(39)
	ESCA	miR-1224-5p	Linc00460	Inhibit migration, invasion and EMT	(41)
	PC	miR-1224-5p	Linc00665	Inhibit proliferation, migration and invasion	(46)
		miR-1224-5p	/	Inhibit proliferation, migration, invasion and EMT	(45)
Skin	Melanoma	miR-1224-5p	ZEB1-AS1	Inhibit proliferation, migration and invasion	(47)
	Keloids	miR-1224-5p	/	Inhibit proliferation, migration and invasion, promote apoptosis	(48)

THE FUNCTION OF MIR-1224 IN HUMAN CANCER

As a tumor suppressor, miR-1224 significantly inhibited the proliferation, migration, and invasion and induced apoptosis of cancer cells (33). Additionally, miR-1224 participated in the process of the cell cycle, apoptosis, autophagy, and EMT to repress development of tumor (40). Also, miR-1224 influenced metabolic behavior such as glucose metabolism to inhibit the cell growth of cancer (1). Interestingly, miR-1224 promoted the migratory ability of cells and induced EMT in BCa and triple-negative breast cancer (TNBC) (32, 50). In the following part, we systematically proposed the functions of miR-1224, including oncogenic factors and tumor suppressors (**Figure 1**).

INHIBITION OF THE CANCEROGENIC PROCESS

Proto-oncogenes normally promoted cell division and proliferation, playing a vital role in the early stages of growth and development. When proto-oncogenes mutated, such as

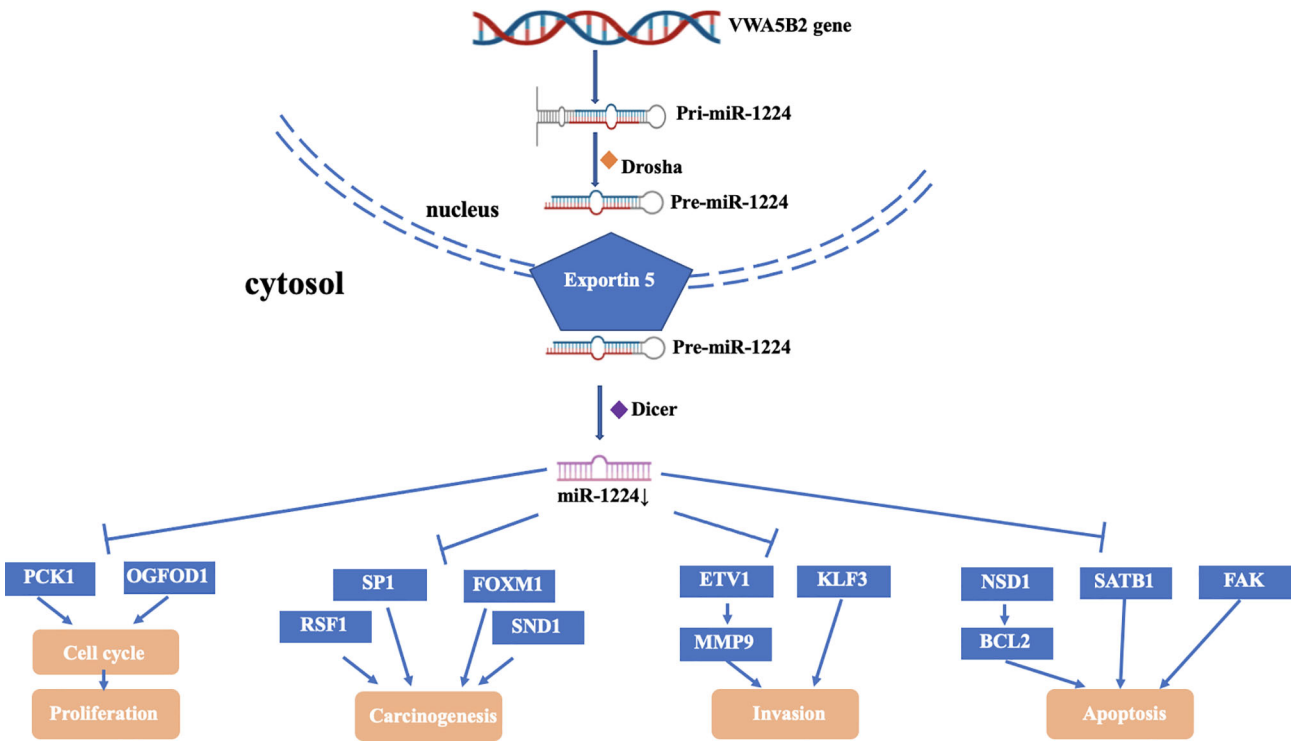

FIGURE 1 | Mechanism and function of miR-1224 downregulation in cancer.

point mutation, gene amplification, chromosomal translocation, promoter insertion, the proto-oncogenes were over-activated and transformed to oncogenes, resulting in excessive cell growth, eventually leading to the initiation and progression of tumors. Abundant studies have found that FOXM1, as an oncogene, was generally highly expressed in tumors. Furthermore, it was implicated in all key features of the cancers described by Hanahan and Weinberg. FOXM1 induced oncogenic WNT and TGFβ signaling pathways by interacting with other proteins such as β-catenin or SMAD3 (51). Jiang et al. revealed that miR-1224 can bind to FOXM1 in CRC cells and inhibited its function, thus blocking the occurrence of cancer (38). Similarly, the oncogenic effects of other oncogenes, such as SP1, RSF1, and SND1, were attenuated when miR-1224 was co-present with them (36, 39, 52).

PROMOTION OF CELL APOPTOSIS AND AUTOPHAGY

Currently, many anti-cancer therapies were targeting molecules involved in cell apoptosis regulation (53–55). BCL2 and BAD belonged to the BCL2 family, which controlled the internal apoptosis pathway. On the whole, BCL2 played a part in anti-apoptotic, while BAD played a part in pro-apoptotic. Recent studies have indicated that NSD2 deficiency repressed the expression of BCL2 but upregulated the expression of BAD (55). However, NSD2 appeared to play an antiapoptotic role in OSCC cells, and its elevated expression was associated with the poor prognosis of OSCC patients. However, miR-1224 reversed the antiapoptotic effects of NSD2 and promoted cell apoptosis by binding to NSD2 (34). SATB1 and FAK played an active function in the apoptotic cleavage of cellular proteins, similarly, miR-1224 accelerated the cell apoptosis *via* targeting SATB1 and FAK in cancer (33, 43). Autophagy was a conserved catabolic biological process widely existing in eukaryotes and lysosomes that participated in digestion and degradation of their macro molecules or damaged organelles to finish their biological functions (56). Autophagy was a double-edged sword in tumor progression (57). It can not only inhibit the formation of tumors but also assist cells to fight against hypoxic condition, lack of nutritional factors, and other adverse growth environments, thus boosting the initiation and progression of tumors. Zhao et al. discovered that FADS1 regulated the process of autophagy in laryngeal squamous cell carcinoma through activating AKT/mTOR signaling (58). A recent study found that miR-1224 restrained the expression of FADS1 in OS (28). Therefore, miR-1224 played a role in promoting autophagy through binding to different targets. Not only that, but miR-1224-5p also inhibited OS autophagy by targeting the PLK1-mediated PI3K/AKT/mTOR pathway. It was well known that autophagy-related molecules such as LC3-II/I, P62, and Beclin-1 can regulate autophagy activity during the autophagy process. Jin et al. have found that miR-1224-5p significantly facilitated the

expression of LC3II/I and Beclin-1 which were autophagy-related in OS by targeting PLK1 (27).

SUPPRESSION OF CELL INVASION

The invasion of a malignant tumor referred to the invasion and diffusion of cells to the surrounding environment. The direct diffusion of cells to the surrounding area without separating from the main body of the tumor was called direct diffusion without metastasis. Cells invaded blood vessels, lymphatics, and body cavities, then were removed from the main body of the tumor and continued to grow in distant organs, forming new tumors of the same type, which was called metastasis. The highly invasive characteristics of tumors were associated with a poor prognosis. Upregulated MMPs were involved in cell migration and invasion (59). Oh et al. disclosed that MMPs were regulated by ETVs, and emphasized that ETV1 was the most important one (60). Recent studies demonstrated that miR-1224 bound to the 3'-UTR of ETV1 to reduce its expression, and overexpressed miR-1224 suppressed ETV1 and MMPs, which significantly inhibited the invasion of cells (21). miR-1224 blocked the translation of KLF3 by binding to the mRNA, and inhibition of miR-1224 led to an increase of KLF3, thus enhancing the aggressiveness of cells (19). These results suggested that miR-1224 played a critical role in the regulation of cell migration and invasion through directly interacting with ETV1 and regulating MMPs, known targets of ETV1.

INDUCTION OF CELL CYCLE ARREST

Mitosis is one of the most important steps in the cell cycle (57). Du et al. reported that miR-1224 was frequently downregulated in glioma, the miR-1224-3p inhibitor significantly reduced the expression of miR-1224-3p and remarkably accelerated the cell proliferation. Another study discovered that miR-1224-3p was bound to PLK1, which was involved in mitosis and the cell cycle. The abovementioned data revealed that miR-1224-3p inhibited tumor growth by directly binding to PLK1 (24). OGFPD1, a stress granule protein, was linked closely to cell cycle G1/2 and G1/M. Recent studies found a significantly increased expression of OGFOD1 in LP tissues and cells, which was associated with the promotion of cell viability and proliferation in LP. Overexpressed miR-1224-5p significantly inhibited OGFOD1-induced cell proliferation and activity by targeted OGFOD1 (20).

ROLE IN EMT

Multiple studies showed that reduced miR-1224 enhanced the invasion and metastasis of a variety of tumors. Oh et al. discovered that miR-1224 was downregulated in the process of EMT (60). In addition, miR-1224 indirectly affected differentiation and EMT by inhibiting metastasis through a network of pre-metastasis stimulators that targeted VEGF, COX2, and MMP9, which were involved in angiogenesis, collagen remodeling, and proteolysis (21).

TUMOR-ONCOGENIC ROLE IN SOME TUMORS

miR-1224 not only acted as a tumor suppressor but sometimes as an oncogene that promoted tumor genesis and development (**Figure 2**). As we all known, one of the signature features of cancer cells was metabolic reprogramming of aerobic glycolysis. PGM5 (A member of the phosphoglucomutase (PGM) group superfamily) catalyzed the bidirectional interconversion metabolism of glucose-1-phosphate (G1P) and glucose-6-phosphate (G6P). A recent study found that miR-1224-3p promoted cell proliferation and migration *via* PGM5-mediated aerobic glycolysis in BC (32). Another study revealed that the high expression of miR-1224-3p was an independent prognostic indicator of poor overall survival of TNBC patients. miR-1224-3p bound to TUSC7, which inhibited cell growth, proliferation, and metastasis both *in vitro* and *in vivo* in BC (50).

CLINICAL IMPLICATION

The occurrence of the tumor was caused by many factors, and its progression was directly related to the therapeutic effects of patients (61). Therefore, early diagnosis and individual treatment were critical for the patients to prolong their survival. Tumor markers were widely used in the screening of many tumors, but the low sensitivity of tumor markers made the results inaccurate and conflicting (62). The differential expression of miRNAs in tumor tissues became the focus of research, which can be combined with the detection of tumor markers to facilitate the screening and prognosis of tumors.

Many research indicated that miR-1224 can be used as a prognostic biomarker in clinical practice (**Table 3**). When miR-1224 acted as tumor-suppressors, reduced miR-1224 indicated a short overall survival for patients with malignant tumors. Zhao et al. compared the expression of miR-1224-5p in TSCC cells with that in normal cells and found that miR-1224-5p was decreased in TSCC cells, suggesting miR-1224 may aid as a new biomarker contributing to TSCC treatments (33). Patients who developed with III+IV stage had a higher miR-1224 expression, suggesting that it can act as a brand-new biomarker for GC patients (35). Wang et al. reported that miR-1224-5p was negatively correlated with lymph node metastasis and FIGO stage in OC, indicating miR-1224-5p was associated with survival of patients with OC (52). Shi et al. found that decreased miR-1224-5p was associated with a high TNM stage thus are an unfavorable prognostic factor for ESCC patients (40). Patients with decreased miR-1224-5p had a poor survival probability (P=0.006) in PC (45). Most Studies demonstrated that miR-1224 served as a blood-based biological indicator for early diagnosis and potential prognostic biomarker in BCa, melanoma, keloid (29, 47, 48). In contrast, Zheng et al. found

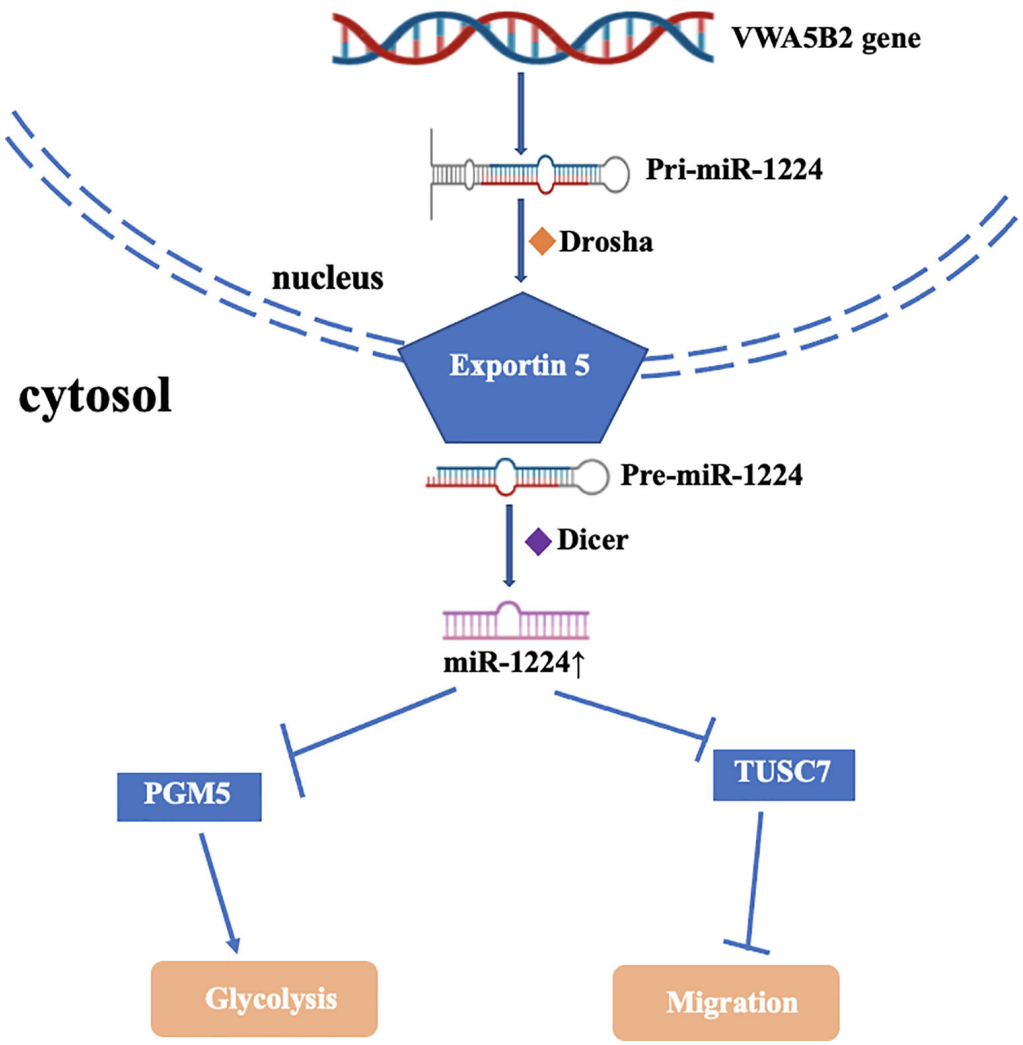

FIGURE 2 | Mechanism and function of miR-1224 upregulation in cancer.

that high miR-1224-3p expression was an independent clinical blood-based factor of poor OS for TNBS patients (50).

Additionally, miR-1224 can act as therapeutic targets in cancer treatment through understanding its mechanism and function (**Table 3**). Zhang et al. demonstrated that the miR-1224-3p/HMGXB3 axis can be used as a target for the treatment of RCC (49). Yang et al. identified a miR-1224/CREB feedback loop, suggesting that blocking this circuit can be a potential molecular treatment for HCC patients (42). Similarly, miR-1224-3p/PGM5 axis played a vital role in cell proliferation, metastasis, and migration, and may be a potential target for therapy of BC (32). Li et al. demonstrated that miR-1224-5p/NSD2 axis participated in the resistance to chemotherapy of 5-FU in OSCC, providing a novel target (34). MiR-1224 can be used as a therapeutic target for CRC, GC, and LAUD in given that abundant research (17, 21, 35, 39).

CONCLUSIONS AND PROSPECTS

At present, diverse tumors with high morbidity and mortality brought heavy burdens for patients and their families. Many studies contributed to revealing the etiology of tumor occurrence and exploring effective therapeutic methods. However, the mechanism of tumor genesis, metastasis, and drug resistance is still not clear. Researchers found that miR-1224 expression in many tumor tissues and cells was significantly different from those in normal tissues and cells. miR-1224 mostly acted as a tumor suppressor in tumor initiation and development, including proliferation, metastasis, blood formation, invasion, and drug resistance. Studies have shown that miR-1224 can be used as a tumor biomarker for early diagnosis and prognosis prediction in the future.

In conclusion, with further research on miR-1224, the mechanism of miR-1224 in the occurrence and development of

TABLE 3 | Clinical implication of miR-1224 in human cancers.

Systems	Cancer type	Aggressive phenotype of low miR-1224	OS of low miR-1224	Therapeutic target	Drug resistance	References
Respiratory system	LC	Yes	Poor	Yes	/	(19)
	LP	/	/	Yes	/	(20)
	LAUD	/	Poor	Yes	/	(21)
Nerve system	LGG	/	Poor	Yes	/	(22)
	Glioma	High grade	Poor	Yes	/	(24)
	GBM	/	Poor	Yes	PDGF receptor resistance	(25)
Muscular and skeletal systems	OS	/	Poor	Yes	/	(27)
Genitourinary system	BCa	High TNM stage	Poor	Yes	/	(29)
	BC	/	Good	Yes	/	(32)
Digestive system	TSCC	/	Poor	/	/	(33)
	OSCC	/	Poor	/	5-FU resistance	(34)
	GC	/	Poor	Yes	/	(35)
	CRC	Yes	Poor	Yes	/	(39)
	ESCC	High grade	Poor	Yes	EGFR resistance	(40)
	HCC	High TNM stage	Poor	Yes	/	(42)
	PC	High TNM stage	Poor	Yes	/	(45)
Skin	Melanoma	High TNM stage	Poor	Yes	/	(47)
	keloids	/	Poor	Yes	/	(48)

tumors will be gradually revealed. miR-1224 can not only serve as an indicator of tumor diagnosis and prognosis but also become an effective target for tumor therapy, providing a new direction for targeted precision therapy.

AUTHOR CONTRIBUTIONS

MM, JL, and WK generated this conception. MM and JL wrote this manuscript and were co-first authors. JS and ZMZ searched and collected the relative articles. ZL, ZYZ, and SO collected the data and produced the tables and figures. WK supervised and revised the manuscript. All authors contributed to the article and approved the submitted version.

FUNDING

This study was funded by the CSCO-ROCHE Research Fund (No. Y-2019 Roche-015), Beijing Xisike Clinical Oncology Research Foundation (Y-HS2019-43), Wu Jieping Medical Foundation (No. 320. 6750.19020, No. 320.6750.2020-08-32), and CAMS Innovation Fund for Medical Sciences (2020-I2M-C&T-B-027).

REFERENCES

1. Lagos-Quintana M, Rauhut R, Lendeckel W, Tuschl T. Identification of Novel Genes Coding for Small Expressed RNAs. *Science* (2001) 294:853–8. doi: 10.1126/science.1064921
2. Bhaskaran M, Mohan M. MicroRNAs: History, Biogenesis, and Their Evolving Role in Animal Development and Disease. *Vet Pathol* (2014) 51:759–74. doi: 10.1177/0300985813502820
3. Lee Y, Ahn C, Han J, Choi H, Kim J, Yim J, et al. The Nuclear RNase III Drosha Initiates microRNA Processing. *Nature* (2003) 425:415–9. doi: 10.1038/nature01957
4. Yi R, Qin Y, Macara IG, Cullen BR. Exportin-5 Mediates the Nuclear Export of Pre-microRNAs and Short Hairpin RNAs. *Genes Dev* (2003) 17:3011–6. doi: 10.1101/gad.1158803
5. Chendrimada TP, Gregory RI, Kumaraswamy E, Norman J, Cooch N, Nishikura K, et al. TRBP Recruits the Dicer Complex to Ago2 for microRNA Processing and Gene Silencing. *Nature* (2005) 436:740–4. doi: 10.1038/nature03868
6. Tsuchiya S, Okuno Y, Tsujimoto G. MicroRNA: Biogenetic and Functional Mechanisms and Involvements in Cell Differentiation and Cancer. *J Pharmacol Sci* (2006) 101:267–70. doi: 10.1254/jphs.CPJ06013X
7. Cho WC. OncomiRs: The Discovery and Progress of microRNAs in Cancers. *Mol Cancer* (2007) 6:60. doi: 10.1186/1476-4598-6-60
8. Liu J. Control of Protein Synthesis and mRNA Degradation by microRNAs. *Curr Opin Cell Biol* (2008) 20:214–21. doi: 10.1016/j.ceb.2008.01.006
9. Drakaki A, Iliopoulos D. MicroRNA Gene Networks in Oncogenesis. *Curr Genomics* (2009) 10:35–41. doi: 10.2174/138920209787581299
10. Tzur G, Israel A, Levy A, Benjamin H, Meiri E, Shufaro Y, et al. Comprehensive Gene and microRNA Expression Profiling Reveals a Role for microRNAs in Human Liver Development. *PloS One* (2009) 4:e7511. doi: 10.1371/journal.pone.0007511
11. Macfarlane LA, Murphy PR. MicroRNA: Biogenesis, Function and Role in Cancer. *Curr Genomics* (2010) 11:537–61. doi: 10.2174/138920210793175895
12. Calin GA, Croce CM. MicroRNA Signatures in Human Cancers. *Nat Rev Cancer* (2006) 6:857–66. doi: 10.1038/nrc1997
13. Hunsberger JG, Fessler EB, Wang Z, Elkahloun AG, Chuang DM. Post-Insult Valproic Acid-Regulated microRNAs: Potential Targets for Cerebral Ischemia. *Am J Transl Res* (2012) 4 (3): 316–32. www.ajtr.org /ISSN:1943-8141/AJTR1207001
14. Sibley CR, Seow Y, Curtis H, Weinberg MS, Wood MJ. Silencing of Parkinson's Disease-Associated Genes With Artificial Mirtron Mimics of miR-1224. *Nucleic Acids Res* (2012) 40:9863–75. doi: 10.1093/nar/gks712
15. Roy S, Bantel H, Wandrer F, Schneider AT, Gautheron J, Vucur M, et al. miR-1224 Inhibits Cell Proliferation in Acute Liver Failure by Targeting the Antiapoptotic Gene Nfib. *J Hepatol* (2017) 67:966–78. doi: 10.1016/j.jhep.2017.06.007

16. Nymark P, Guled M, Borze I, Faisal A, Lahti L, Salmenkivi K, et al. Integrative Analysis of microRNA, mRNA and aCGH Data Reveals Asbestos- and Histology-Related Changes in Lung Cancer. *Genes Chromosomes Cancer* (2011) 50:585–97. doi: 10.1002/gcc.20880
17. Mosakhani N, Lahti L, Borze I, Karjalainen-Lindsberg ML, Sundstrom J, Ristamaki R, et al. MicroRNA Profiling Predicts Survival in Anti-EGFR Treated Chemorefractory Metastatic Colorectal Cancer Patients With Wild-Type KRAS and BRAF. *Cancer Genet* (2012) 205:545–51. doi: 10.1016/j.cancergen.2012.08.003
18. Qian J, Li R, Wang YY, Shi Y, Luan WK, Tao T, et al. MiR-1224-5p Acts as a Tumor Suppressor by Targeting CREB1 in Malignant Gliomas. *Mol Cell Biochem* (2015) 403:33–41. doi: 10.1007/s11010-015-2334-1
19. Yu PF, Wang Y, Lv W, Kou D, Hu HL, Guo SS, et al. LncRNA NEAT1/miR-1224/KLF3 Contributes to Cell Proliferation, Apoptosis and Invasion in Lung Cancer. *Eur Rev Med Pharmacol Sci* (2019) 23:8403–10. doi: 10.26355/eurrev_201910_19151
20. Yin D, Wang Q, Wang S, Zhu G, Tang Q, Liu J. OGFOD1 Negatively Regulated by miR-1224-5p Promotes Proliferation in Human Papillomavirus-Infected Laryngeal Papillomas. *Mol Genet Genomics* (2020) 295:675–84. doi: 10.1007/s00438-020-01649-x
21. Zuo Y, Shen W, Wang C, Niu N, Pu J. Circular RNA Circ-ZNF609 Promotes Lung Adenocarcinoma Proliferation by Modulating miR-1224-3p/ETV1 Signaling. *Cancer Manag Res* (2020) 12:2471–9. doi: 10.2147/CMAR.S232260
22. Wang M, Cui Y, Cai Y, Jiang Y, Peng Y. Comprehensive Bioinformatics Analysis of mRNA Expression Profiles and Identification of a miRNA-mRNA Network Associated With the Pathogenesis of Low-Grade Gliomas. *Cancer Manag Res* (2021) 13:5135–47. doi: 10.2147/CMAR.S314011
23. Wang Y, Wang M, Wei W, Han D, Chen X, Hu Q, et al. Disruption of the EZH2/miRNA/β-Catenin Signaling Suppresses Aerobic Glycolysis in Glioma. *Oncotarget* (2016) 7:49450–8. doi: 10.18632/oncotarget.10370
24. Du S, Li H, Lu F, Zhang S, Tang J. Circular RNA ZNF609 Promotes the Malignant Progression of Glioma by Regulating miR-1224-3p/PLK1 Signaling. *J Cancer* (2021) 12:3354–66. doi: 10.7150/jca.54934
25. Xu H, Zhang B, Yang Y, Li Z, Zhao P, Wu W, et al. LncRNA MIR4435-2HG Potentiates the Proliferation and Invasion of Glioblastoma Cells *via* Modulating miR-1224-5p/TGFBR2 Axis. *J Cell Mol Med* (2020) 24:6362–72. doi: 10.1111/jcmm.15280
26. Xiong DD, Xu WQ, He RQ, Dang YW, Chen G, Luo DZ. In Silico Analysis Identified miRNA–Based Therapeutic Agents Against Glioblastoma Multiforme. *Oncol Rep* (2019) 41:2194–208. doi: 10.3892/or.2019.7022
27. Jin B, Jin D, Zhuo Z, Zhang B, Chen K. MiR-1224-5p Activates Autophagy, Cell Invasion and Inhibits Epithelial-To-Mesenchymal Transition in Osteosarcoma Cells by Directly Targeting PLK1 Through PI3K/AKT/mTOR Signaling Pathway. *Onco Targets Ther* (2020) 13:11807–18. doi: 10.2147/OTT.S274451
28. Lian H, Xie P, Yin N, Zhang J, Zhang X, Li J, et al. Linc00460 Promotes Osteosarcoma Progression *via* miR-1224-5p/FADS1 Axis. *Life Sci* (2019) 233:116757. doi: 10.1016/j.lfs.2019.116757
29. Zhuang C, Huang X, Yu J, Gui Y. Circular RNA Hsa_Circ_0075828 Promotes Bladder Cancer Cell Proliferation Through Activation of CREB1. *BMB Rep* (2020) 53:82–7. doi: 10.5483/BMBRep.2020.53.2.059
30. Miah S, Dudziec E, Drayton RM, Zlotta AR, Morgan SL, Rosario DJ, et al. An Evaluation of Urinary microRNA Reveals a High Sensitivity for Bladder Cancer. *Br J Cancer* (2012) 107:123–8. doi: 10.1038/bjc.2012.221
31. Ding B, Yan L, Zhang Y, Wang Z, Zhang Y, Xia D, et al. Analysis of the Role of Mutations in the KMT2D Histone Lysine Methyltransferase in Bladder Cancer. *FEBS Open Bio* (2019) 9:693–706. doi: 10.1002/2211-5463.12600
32. Ran F, Zhang Y, Shi Y, Liu J, Li H, Ding L, et al. miR-1224-3p Promotes Breast Cancer Cell Proliferation and Migration Through PGM5-Mediated Aerobic Glycolysis. *J Oncol* (2021) 2021:5529770. doi: 10.1155/2021/5529770
33. Zhao R, Wang S, Tan L, Li H, Liu J, Zhang S. IGFL2-AS1 Facilitates Tongue Squamous Cell Carcinoma Progression *via* Wnt/beta-Catenin Signaling Pathway. *Oral Dis* (2021). doi: 10.1111/odi.13935
34. Li S, Shi Z, Fu S, Li Q, Li B, Sang L, et al. Exosomal-Mediated Transfer of APCDD1L-AS1 Induces 5-Fluorouracil Resistance in Oral Squamous Cell Carcinoma *via* miR-1224-5p/Nuclear Receptor Binding SET Domain Protein 2 (NSD2) Axis. *Bioengineered* (2021) 12:7188–204. doi: 10.1080/21655979.2021.1979442
35. Han GD, Sun Y, Hui HX, Tao MY, Liu YQ, Zhu J. MiR-1224 Acts as a Prognostic Biomarker and Inhibits the Progression of Gastric Cancer by Targeting Satb1. *Front Oncol* (2021) 11:748896. doi: 10.3389/fonc.2021.748896
36. Yang L, Wang M, He P. LncRNA NEAT1 Promotes the Progression of Gastric Cancer Through Modifying the miR-1224-5p/RSF1 Signaling Axis. *Cancer Manag Res* (2020) 12:11845–55. doi: 10.2147/CMAR.S267666
37. Wang J, Wen T, Li Z, Che X, Gong L, Yang X, et al. MicroRNA-1224 Inhibits Tumor Metastasis in Intestinal-Type Gastric Cancer by Directly Targeting FAK. *Front Oncol* (2019) 9:222. doi: 10.3389/fonc.2019.00222
38. Jiang Z, Hu H, Hu W, Hou Z, Liu W, Yu Z, et al. Circ-RNF121 Regulates Tumor Progression and Glucose Metabolism by miR-1224-5p/FOXM1 Axis in Colorectal Cancer. *Cancer Cell Int* (2021) 21:596. doi: 10.1186/s12935-021-02290-3
39. Li J, Peng W, Yang P, Chen R, Gu Q, Qian W, et al. MicroRNA-1224-5p Inhibits Metastasis and Epithelial-Mesenchymal Transition in Colorectal Cancer by Targeting SP1-Mediated NF-kappaB Signaling Pathways. *Front Oncol* (2020) 10:294. doi: 10.3389/fonc.2020.00294
40. Shi ZZ, Wang WJ, Chen YX, Fan ZW, Xie XF, Yang LY, et al. The miR-1224-5p/TNS4/EGFR Axis Inhibits Tumour Progression in Oesophageal Squamous Cell Carcinoma. *Cell Death Dis* (2020) 11:597. doi: 10.1038/s41419-020-02801-6
41. Cui Y, Zhang C, Lian H, Xie L, Xue J, Yin N, et al. LncRNA Linc00460 Sponges miR-1224-5p to Promote Esophageal Cancer Metastatic Potential and Epithelial-Mesenchymal Transition. *Pathol Res Pract* (2020) 216:153026. doi: 10.1016/j.prp.2020.153026
42. Yang S, Jiang W, Yang W, Yang C, Yang X, Chen K, et al. Epigenetically Modulated miR-1224 Suppresses the Proliferation of HCC Through CREB-Mediated Activation of YAP Signaling Pathway. *Mol Ther Nucleic Acids* (2021) 23:944–58. doi: 10.1016/j.omtn.2021.01.008
43. Wu D, Xia A, Fan T, Li G. Circrasgrf2 Functions as an Oncogenic Gene in Hepatocellular Carcinoma by Acting as a miR-1224 Sponge. *Mol Ther Nucleic Acids* (2021) 23:13–26. doi: 10.1016/j.omtn.2020.10.035
44. Hu C, Cheng X, Mingyu Q, Wang XB, Shen SQ. The Effects of microRNA-1224-5p on Hepatocellular Carcinoma Tumor Endothelial Cells. *J Cancer Res Ther* (2019) 15:329–35.doi: 10.4103/jcrt.JCRT_40_18
45. Kong L, Liu P, Zheng M, Wang Z, Gao Y, Liang K, et al. The miR-1224-5p/ELF3 Axis Regulates Malignant Behaviors of Pancreatic Cancer *via* PI3K/AKT/Notch Signaling Pathways. *Onco Targets Ther* (2020) 13:3449–66. doi: 10.2147/OTT.S248507
46. Chen W, Yu Z, Huang W, Yang Y, Wang F, Huang H. LncRNA LINC00665 Promotes Prostate Cancer Progression *via* miR-1224-5p/SND1 Axis. *Onco Targets Ther* (2020) 13:2527–35. doi: 10.2147/OTT.S241578
47. Wang Q, Zhang R, Liu D. Long Non-Coding RNA ZEB1-AS1 Indicates Poor Prognosis and Promotes Melanoma Progression Through Targeting miR-1224-5p. *Exp Ther Med* (2019) 17:857–62. doi: 10.3892/etm.2018.7005
48. Yao X, Cui X, Wu X, Xu P, Zhu W, Chen X, et al. Tumor Suppressive Role of miR-1224-5p in Keloid Proliferation, Apoptosis and Invasion *via* the TGF-Beta1/Smad3 Signaling Pathway. *Biochem Biophys Res Commun* (2018) 495:713–20. doi: 10.1016/j.bbrc.2017.10.070
49. Zhang G, Wang J, Tan W, Han X, Han B, Wang H, et al. Circular RNA EGLN3 Silencing Represses Renal Cell Carcinoma Progression Through the miR-1224-3p/HMGXB3 Axis. *Acta Histochem* (2021) 123:151752. doi: 10.1016/j.acthis.2021.151752
50. Zheng BH, He ZX, Zhang J, Ma JJ, Zhang HW, Zhu W, et al. The Biological Function of TUSC7/miR-1224-3p Axis in Triple-Negative Breast Cancer. *Cancer Manag Res* (2021) 13:5763–74. doi: 10.2147/CMAR.S305865
51. Gartel AL. FOXM1 in Cancer: Interactions and Vulnerabilities. *Cancer Res* (2017) 77:3135–9. doi: 10.1158/0008-5472.CAN-16-3566
52. Wang J, Hu Y, Ye C, Liu J. miR-1224-5p Inhibits the Proliferation and Invasion of Ovarian Cancer *via* Targeting SND1. *Hum Cell* (2020) 33:780–9. doi: 10.1007/s13577-020-00364-4
53. Sun ZP, Zhang J, Shi LH, Zhang XR, Duan Y, Xu WF, et al. Aminopeptidase N Inhibitor 4cc Synergizes Antitumor Effects of 5-Fluorouracil on Human Liver Cancer Cells Through ROS-Dependent CD13 Inhibition. *BioMed Pharmacother* (2015) 76:65–72. doi: 10.1016/j.biopha.2015.10.023
54. Velez C, Soto J, Rios K, Silva L, Hernandez W, Rivera LA, et al. Toxicity and Apoptosis Related Effects of Benzimidazo [3,2-Alpha] Quinolinium Salts

Upon Human Lymphoma Cells. *Open Med Chem J* (2017) 11:54–65. doi: 10.2174/1874104501711010054
55. He C, Liu C, Wang L, Sun Y, Jiang Y, Hao Y. Histone Methyltransferase NSD2 Regulates Apoptosis and Chemosensitivity in Osteosarcoma. *Cell Death Dis* (2019) 10:65. doi: 10.1038/s41419-019-1347-1
56. Kim KH, Lee MS. Autophagy–a Key Player in Cellular and Body Metabolism. *Nat Rev Endocrinol* (2014) 10:322–37. doi: 10.1038/nrendo.2014.35
57. Henriques AC, Ribeiro D, Pedrosa J, Sarmento B, Silva PMA, Bousbaa H. Mitosis Inhibitors in Anticancer Therapy: When Blocking the Exit Becomes a Solution. *Cancer Lett* (2019) 440-441:64–81. doi: 10.1016/j.canlet.2018.10.005
58. Zhao R, Tian L, Zhao B, Sun Y, Cao J, Chen K, et al. FADS1 Promotes the Progression of Laryngeal Squamous Cell Carcinoma Through Activating AKT/mTOR Signaling. *Cell Death Dis* (2020) 11:272. doi: 10.1038/s41419-020-2457-5
59. Brinckerhoff CE, Matrisian LM. Matrix Metalloproteinases: A Tail of a Frog That Became a Prince. *Nat Rev Mol Cell Biol* (2002) 3:207–14. doi: 10.1038/nrm763
60. Oh S, Shin S, Janknecht R. ETV1, 4 and 5: An Oncogenic Subfamily of ETS Transcription Factors. *Biochim Biophys Acta* (2012) 1826:1–12. doi: 10.1016/j.bbcan.2012.02.002
61. Ferlay J, Colombet M, Soerjomataram I, Parkin DM, Pineros M, Znaor A, et al. Cancer Statistics for the Year 2020: An Overview. *Int J Cancer* (2021) 149. 778–89. doi: 10.1002/ijc.33588
62. Sauerbrei W, Taube SE, Mcshane LM, Cavenagh MM, Altman DG. Reporting Recommendations for Tumor Marker Prognostic Studies (REMARK): An Abridged Explanation and Elaboration. *J Natl Cancer Inst* (2018) 110:803–11. doi: 10.1093/jnci/djy088

Conflict of Interest: The authors declare that the research was conducted in the absence of any commercial or financial relationships that could be construed as a potential conflict of interest.

Publisher's Note: All claims expressed in this article are solely those of the authors and do not necessarily represent those of their affiliated organizations, or those of the publisher, the editors and the reviewers. Any product that may be evaluated in this article, or claim that may be made by its manufacturer, is not guaranteed or endorsed by the publisher.

frontiers | Frontiers in Oncology

ORIGINAL RESEARCH
published: 25 July 2022
doi: 10.3389/fonc.2022.809847

Comprehensive Analysis of SLC17A9 and Its Prognostic Value in Hepatocellular Carcinoma

Xue-Yan Kui[1†], Yan Gao[2†], Xu-Sheng Liu[2†], Jing Zeng[3], Jian-Wei Yang[4], Lu-Meng Zhou[5], Xiao-Yu Liu[2], Yu Zhang[2], Yao-Hua Zhang[2] and Zhi-Jun Pei[1,2,6]*

[1] Postgraduate Training Basement of Jinzhou Medical University, Taihe Hospital, Hubei University of Medicine, Shiyan, China, [2] Department of Nuclear Medicine and Institute of Anesthesiology and Pain, Taihe Hospital, Hubei University of Medicine, Shiyan, China, [3] Department of Infection Control, Taihe Hospital, Hubei University of Medicine, Shiyan, China, [4] Department of Nuclear Medicine, Xiangyang Cenral Hospital, Affiliated Hospital of Hubei University of Arts and Science, Xiangyang, China, [5] Department of Nuclear Medicine, Huanggang Central Hospital, Huanggang, China, [6] Hubei Key Laboratory of Embryonic Stem Cell Research, Shiyan, China

OPEN ACCESS

Edited by:
Giovanni Blandino, Hospital Physiotherapy Institutes (IRCCS), Italy

Reviewed by:
Jaroslav Truksa, Institute of Biotechnology (ASCR), Czechia
Yanhong Cui, The University of Chicago, United States

***Correspondence:**
Zhi-Jun Pei
pzjzml1980@taihehospital.com

[†]These authors have contributed equally to this work

Specialty section:
This article was submitted to Molecular and Cellular Oncology, a section of the journal Frontiers in Oncology

Received: *05 November 2021*
Accepted: *21 June 2022*
Published: *25 July 2022*

Citation:
Kui X-Y, Gao Y, Liu X-S, Zeng J, Yang J-W, Zhou L-M, Liu X-Y, Zhang Y, Zhang Y-H and Pei Z-J (2022) Comprehensive Analysis of SLC17A9 and Its Prognostic Value in Hepatocellular Carcinoma. Front. Oncol. 12:809847. doi: 10.3389/fonc.2022.809847

Background: Solute carrier family 17 member 9 (SLC17A9) encodes a member of a family of transmembrane proteins that are involved in the transport of small molecules. SLC17A9 is involved in the occurrence and development of various cancers, but its biological role in liver hepatocellular carcinoma (LIHC) is unclear.

Methods: The expression level of SLC17A9 was assessed using The Cancer Genome Atlas (TCGA) database and immunohistochemistry of tumor tissues and adjacent normal liver tissues. The receiver operating characteristic (ROC) and R software package performed diagnosis and prognosis. Gene Ontology/Kyoto Encyclopedia of Genes and Genomes functional enrichment and co-expression of SLC17A9, gene–gene interaction (GGI), and protein–protein interaction (PPI) networks were performed using R, GeneMANIA, and STRING. Western blot, real-time quantitative PCR (RT-qPCR), immunofluorescence, colony formation, wound scratch assay, ATP production assays, and high connotation were applied to determine the effect of SLC17A9 knockdown on HEPG2 (hepatocellular liver carcinoma) cells. TIMER, GEPIA, and TCGA analyzed the relationship between SLC17A9 expression and immune cells, m6A modification, and ferroptosis.

Results: SLC17A9 expression in LIHC tissues was higher than in normal liver tissues ($p < 0.001$), and SLC17A9 was related to sex, DSS (disease-specific survival), and PFI (progression-free interval) ($p = 0.015$, 0.006, and 0.023). SLC17A9 expression has diagnostic (AUC: 0.812; CI: 0.770–0.854) and prognostic potential ($p = 0.015$) in LIHC. Gene Ontology/Kyoto Encyclopedia of Genes and Genomes (GO/KEGG) functional enrichment analysis showed that SLC17A9 was closely related to neuronal cell body, presynapse, axonogenesis, PI3K/Akt signaling pathway. GGI showed that SLC17A9 was closely related to MYO5A. PPI showed that SLC17A9 was closely related to SLC18A3. SLC17A9 silencing inhibited HepG2 cells proliferation, migration, colony formation, and reduced their ATP level. SLC17A9 expression level was related to immune cells: B cells ($r = 0.094$, $P = 8.06E-02$), $CD4^+$ T cells ($r = 0.184$, $P = 5.95E-04$), and macrophages ($r = 0.137$,

P = 1.15E-02); m6A modification: HNRNPC (r = 0.220, p < 0.001), METTL3 (r = 0.180, p < 0.001), and WTAP (r = 0.130, p = 0.009); and ferroptosis: HSPA5 (r = 0.240, p < 0.001), SLC7A11 (r = 0.180, p < 0.001), and FANCD2 (r = 0.280, p < 0.001).

Conclusion: Our data show that SLC17A9 may influence LIHC progression. SLC17A9 expression correlates with tumor immune infiltration, m6A modification, and ferroptosis in LIHC and may have diagnostic and prognostic value in LIHC.

Keywords: SLC17A9, hepatocellular carcinoma, immune infiltration, m6A modification, TCGA, ferroptosis

INTRODUCTION

Liver hepatocellular carcinoma (LIHC) is one of the most common malignant tumors in the world the most commonly diagnosed cancer in 13 countries and the leading cause of cancer death in 20 countries (1). Patients with advanced liver cancer often suffer liver failure. Liver cancer is mainly treated surgically, but it has high recurrence and metastasis. Its prognosis is very poor and its mortality rate is 8.2% (2). China has the heaviest burden of hepatitis and accounts for one in three global cases of chronic HBV infection and about 7% of HCV infections (3). Thus, effective liver cancer treatments are urgently needed.

SLC17A9 (solute carrier family 17 member 9), a vesicular nucleotide transporter (VUNT), is most abundantly expressed in the stomach, intestines, skeletal muscles, and liver (4). SLC17A9 is involved in ATP vesicular storage and exocytosis. SLC17A9 and its function were first described in bile duct cells (5). SLC17A9 is also highly enriched on lysosomes in various several cell types, including C2C12, COS-1, and HEK-293T cells, and actively transports ATP across lysosomal membranes (6). It is reported that ATP accumulates in lysosomes of astrocytes and microglia (7, 8). Once SLC17A9 is damaged, it will decrease in the accumulation of ATP in lysosomes, which results in cell death. SLC17A9 is expressed in biliary epithelial cells (9), osteoblasts (10), AR42J cells, and pancreatic acinar cells (11), but its specific role in LIHC has not been explored. Immunotherapy is a targeted method for the treatment of cancer. It is a common anti-tumor method to use the body's immune system to fight tumor cells to promote the response to cancer cells (12, 13). Currently, m6A modification is widely used for the treatment of various cancers (14, 15). However, there are no studies on the role of SLC17A9 in LIHC, especially in the context of LIHC immunotherapy and m6A modification. Iron-dependent cell death has recently emerged as a novel form of cell death that occurs mainly due to an abnormal increase in intracellular iron-dependent lipid oxygen free radicals and an imbalance in redox homeostasis (16–18). However, little is known about the relationship between SLC17A9 and genes associated with iron-dependent cell death in LIHC. Here, we sought to characterize SLC17A9 expression in LIHC, its clinical significance, and its diagnostic and prognostic potential. We also examined the effect of SLC17A9 on the proliferation, migration, and colony formation capacity of LIHC cells and evaluated its biological function with the help of the database.

MATERIALS AND METHODS

Database Analysis

Datasets on SLC17A9 expression in pan-cancer, LIHC, and normal liver tissues were downloaded from The Cancer Genome Atlas (TCGA) (https://portal.gdc.cancer.gov/) (19). Correlation between SLC17A9 expression in LIHC and clinicopathological features was analyzed using TCGA LIHC data. Receiver operating characteristic (ROC) curve analysis was done on R to detect the sensitivity and specificity of SLC17A9 expression in LIHC. Analysis of correlation between SLC17A9 expression and LIHC prognosis was done on R. LinkedOmics database (www.linkedomics.org/login.php) (20) was used to identify genes that are co-expressed with SLC17A9 in the TCGA LIHC dataset. Pearson's correlation coefficient was used for statistical analysis. Volcano plots and heatmaps were used to visualize analysis results. An R package was used for GO and KEGG pathway enrichment analysis of SLC17A9 in LIHC. GeneMANIA (www.genemania.org) and STRING (www.string-db.org) were used to construct gene–gene interaction (GGI) and protein–protein interaction (PPI) networks (21, 22), respectively. TIMER (https://cistrome.shinyapps.io/timer) (23) was used to assess correlation between SLC17A9 gene expression and immune cell infiltration. TIMER's SCNA module was used to associate SLC17A9's genetic copy number variation (CNV) with the relative abundance of tumor-infiltrating cells. The proportion of immune cells in LIHC samples expressing high and low SLC17A9 levels was identified on R using the CiberSort plug-in. GEPIA (gepia.cancer-pku.cn) (24) was used to assess the relationship between SLC17A9 and immune cell markers in LIHC. Immune cell markers were obtained from the website of R&D Systems (www.rndsystems.com/cn/resources/cell-markers/immune-cells). Correlation between SLC17A9 and m6A and ferroptosis was analyzed using TCGA LIHC datasets.

Liver Cancer Tissues Specimens

We recruited 28 patients with liver cancer who underwent surgery in Taihe Hospital, Shiyan City, Hubei province. Ethical approval for this study was granted by Taihe Hospital's medical ethics committee. The study adhered to the Helsinki Declaration and its subsequent amendments.

Cell Transfection

HepG2 cells were seeded on six-well plates at 6×10^5 cells per well and cultured for 24 h. Transfection was done using Lipofectamine

8000 reagent (Beyotime) following the manufacturer's guides. For each transfected well, 125 μl of serum-free OptiMEM, 2.5μg of plasmid DNA, and 4 μl of Lipo8000™ transfection reagent were mixed in a sterile centrifuge tube. The transfection mixture was applied to the cells. The oligonucleotide sequences of the small interfering RNA (siRNA) were displayed as follows: SLC17A9: (forward: 5′-CTTGCTCCAAGGGGTTTACTTC-3′, reverse: 5′-CCGGAGAAATAGAAGATGCTCT-3′); and GAPDH: (forward: 5′-CGCTGAGTACGTCGTGGAGTC-3′, reverse: 5′ GCTGATGATCTTGAGGCTGTTGTC-3′).

Western Blot Analysis

At 48 h after transfection, cells were homogenized in RIPA lysis buffer (Promega, Madison, USA) on ice for 30 min, and then, protein was measured by the Bicinchoninic Acid (BCA) assay (Beyotime, Beijing, China). Protein was separated on 10% sodium dodecyl sulfate–polyacrylamide gels and transferred onto a polyvinylidene difluoride membrane using a semiwet method; next, we blocked the membrane with 5% dried skimmed milk for 1 h and incubated overnight with a SLC17A9 rabbit anti-human monoclonal antibody (1:200, Abcam, USA) in a 4°C refrigerator. Next day, horseradish peroxidase (HRP)–conjugated secondary antibodies (1:1,000; ProteinTech Group) for 1 h at room temperature. Images were obtained using a gel imaging system.

RNA Isolation and Real-Time Quantitative PCR Analysis

Total RNA was extracted from cells 48 h after transfection using Trizol reagent (Invitrogen). Trizol Reagen (600 μl) was added, and the samples were placed on ice for 20 min to lyse the cells. Subsequently, the cell lysate in Tirol was phase separated by addition of 120 μl of chloroform, and the RNA was precipitated by addition of 300 μl of isopropanol, and then, cDNA was synthesized by utilizing the TaqMan Reverse Transcription Reagents kit (TaKaRa). Real-time quantitative PCR (RT-qPCR) analysis was performed with different primer sequences using the SYBR Green Master Mix (TaKaRa). The primers used for RT-PCR were in **Table 1**.

Immunofluorescence Experiment

Cells were fixed with 4% formaldehyde for 1 h and permeabilized with 0.5% Triton X-100 at room temperature. They were then blocked with 1% Bovine Serum Albumin (BSA) for 2 h then incubated with primary antibody at 4°C, overnight. Next, they were incubated with secondary antibody 2 h and nuclei counterstained 2-(4-Amidinophenyl)-6-indolecarbamidine dihydrochloride (DAPI). They were then examined and imaged fluorescent confocal microscopy.

TABLE 1 | Primer sequence (5′-3′).

Primer	Primer sequence (5′- 3′)
HNRNPC	Forward: CGTGTACCTCCTCCTCCTCCTATTG
	Reverse: CCCGCTGTCCACTCTTAGAATTGAAG
WTAP	Forward: CTGACAAACGGACCAAGTAATG
	Reverse: AAAGTCATCTTCGGTTGTGTTG
METTL3	Forward: CCAGCACAGCTTCAGCAGTTCC
	Reverse: GCGTGGAGATGGCAAGACAGATG
ACSL4	Forward: ACCAGGGAAATCCTAAGTGAAG
	Reverse: GGTGTTCTTTGGTTTTAGTCCC
CISD1	Forward: AACCTTCACATCCAGAAAGACAACCC
	Reverse: GACCTCCAACAACGGCAGTACAC
ATP5MC3	Forward: GGCTGGTTCTGGTGCTGGTATTG
	Reverse: AGCTTCAGACAAGGCAAATC

Colony Formation Experiment

The cells were seeded onto 12-well plates at 100 cells per well and cultured for 2 weeks. They were then fixed with 4% Paraformaldehyde (PFA) for 10 min and rinsed with Phosphate Buffered Saline (PBS) before staining with crystal violet. They were then examined by microscopy and imaged.

Wound Scratch Assay

HepG2 cells (1×10^6 per well) were seeded onto 12-well plates and cultured until confluent. A white gun was used to make vertical scratch along the ruler to ensure uniform scratches in each well. The image was taken at 0, 12, 24, and 48 h.

ATP Detection Assay

Control and siSLC17A9 groups cells were cultured for 72 h, and their culture media and cells were collected. Cellular ATP levels were then measured using an ATP bioluminescent assay kit (Beyotime, China).

High Connotation Cell Imaging Analysis

Control and siSLC17A9 groups were suspended at 1×10^4/ml and seeded onto 96-well plates in six replicate wells. After 24 h of culture, the 96-well plates were moved into a high-connotation instrument. High-connotation cell images were then taken using a 10× objective. Multiple visual fields were selected per well for monitoring and cell growth recording.

Statistical Analysis

Gene expression analysis was done using Pearson correlation analysis. Other experimental results were analyzed using two-tailed t-test. Data were expressed as mean ± SD. $P < 0.05$ indicated statistically significant differences.

RESULTS

SLC17A9 Is Highly Expressed in LIHC Tissues And Is Related to Gender, DSS, and PFI

We analyzed the expression level of SLC17A9 in TCGA pan-cancer dataset (**Figure 1A**). The results showed that SLC17A9 was highly expressed in 12 cancer types, including breast cancer, colonic adenocarcinoma, and LIHC. Low SLC17A9 expression was found in 21 cancers, including cervical cancer and cholangiocarcinoma. Analysis of SLC17A9 expression in LIHC vs. normal tissues in paired and unmatched samples revealed that SLC17A9 expression was significantly higher in LIHC tissues than in normal tissues ($p < 0.001$; **Figures 1B, C**). ROC analysis showed that the area under the ROC curve was 0.812. The sensitivity and specificity of predicting

SLC17A9 expression in liver cancer were 63.6% and 96%, respectively (**Figure 1D**). Correlation analysis revealed that high SLC17A9 expression correlated with poor prognosis (**Figure 1E**). Relative to patients with low SLC17A9 expression, those with high SLC17A9 expression had significantly shorter survival ($p = 0.015$). Correlation analysis of TCGA data revealed correlation between SLC17A9 expression and some clinical features. High SLC17A9 expression correlated positively with gender, disease-specific survival (DSS), and progression-free interval (PFI) ($p = 0.015$, 0.006, and 0.023, respectively; **Table 2**). To confirm this finding, we carried out IHC analysis and found that SLC17A9 is mainly localized in the cytosol, with modest presence in the nucleus. IHC results showed that the protein level of SLC17A9 in tumor tissues was significantly higher than that in adjacent normal tissues (**Figure 1F**). These results indicate that SLC17A9 has a potential carcinogenic effect on the progression of LIHC.

Co-Expressed Genes of SLC17A9 in LIHC

Analysis of genes' co-expression with SLC17A9 in LIHC on LinkedOmics found that SLC17A9 expression positively correlated with 4,084 genes and negatively correlated with 3,702 genes (**Figure 2A**). Heatmaps were used to visualize the top 50 genes that positively or negatively correlated with SLC17A9 expression, respectively (**Figures 2B, C**). GO/KEGG functional enrichment analysis ($p < 0.05$) of SLC17A9 identified 2,462 items related to biological process (GO-BP), 351 items related to cell component (GO-CC), 234 items related to molecular function (GO-MF), and 184 KEGG. KEGG pathway analysis showed that SLC17A9 co-expression was mainly associated with PI3K/Akt signaling pathway, neuroactive ligand-receptor interaction, Human Papillomavirus infection (HPV) infection, MAPK signaling, passive transmembrane transporter activity, and channel activity (**Figure 2D**). The bubble map GO function analysis showed that SLC17A9 co-expression was mainly associated with neuronal cell body, presynapse, and axonogenesis (**Figure 2E**).

SLC17A9 -Related Hub Genes

To understand the relationship between SLC17A9 expression in LIHC, a PPI network consisting of 20 nodes was constructed on the basis of the STRING database (**Figure 3A**). The nodes in the network show that genes were related to SLC17A9 in terms of physical interactions, co-expression, predicted, co-localization, genetic interactions, pathway, and shared protein domains. The gene with the most significant correlation with SLC17A9 was MYO5A, followed by GSDMB, NF2, ATP7B, and GALT. Prediction analysis showed that GSDMB and GALT genes were co-expressed and co-localized with SLC17A9. In addition, NF2 shared protein domains with SLC17A9, whereas ATP7B is co-expressed with SLC17A9.

PPI network analysis of SLC17A9 and related proteins was performed using the STRING webserver (**Figure 3B**). The results indicated that SLC17A9 was associated with SLC18A3 (vesicular acetylcholine transporter), PANX1 (pannexin-1), PANX3 (pannexin-3), MYO5A (unconventional myosin-Va), GID8 (glucose-induced degradation protein 8 homolog), ABCG4 (ATP-binding cassette sub-family G member 4), UNC13B (protein unc-13 homolog B), WDTC1 (WD and tetratricopeptide repeat protein 1), SLC37A1 (glucose-6-phosphate transporter member 1), and SLC37A2 (glucose-6-phosphate transporter member 2). The correlation coefficients were 0.947, 0.555, 0.518, 0.508, 0.506, 0.557, 0.551, 0542, 0.553, and 0.675, respectively.

Effects of SLC17A9 Knockdown on the Function and ATP Levels of Hepatoma Cells

Expression of SLC17A9 in HepG2 cells was down regulated by treatment of the cells with siRNA. Effectiveness of SLC17A9 knockdown in liver cancer cell line was determined by Western blot and RT-qPCR analysis that showed stable siSLC17A9 (**Figures 4A, B**). There was a significant difference in SLC17A9 expression level ($P = 0.0083$ and 0.002273) between siSLC17A9-related HepG2 cells and control HepG2 cells. Immunofluorescence assays showed that SLC17A9 was localized in the cell cytoplasm, and the expression level in the siSLC17A9 group was significantly lower relative to the expression level of SLC17A9 in the control group (**Figure 4C**). The colony-forming ability of cells after SLC17A9 knockdown showed a significant decrease relative the colony-forming ability of the control group ($P = 0.0007$; **Figure 4D**). Wound healing assay showed that the cell migration ability of the siSLC17A9 group was significantly reduced compared with the migration ability of the control group ($P = 0.0069$; **Figure 4E**). The results showed significantly lower HepG2 cell ATP content in the siSLC17A9 group relative to the ATP content in the control group ($P < 0.0001$; **Figure 4F**). Moreover, cells in the siSLC17A9 group showed a significant decrease in cell proliferation ability compared with the proliferate rate of cells in the control group ($P < 0.05$; **Figure 4G**).

SLC17A9 Expression Level Is Correlated With Infiltration of Tumor Immune Cells

The relationship between SLC17A9 and various immune cells in LIHC was explored using TIMER database. The findings showed that the expression level of SLC17A9 was correlated with infiltration of B cells ($r = 0.094$, $P = 8.06E-02$), $CD4^+$ T cells ($r = 0.184$, $P = 5.95E-04$), macrophages ($r = 0.137$, $P = 1.15E-02$), neutrophils ($r = 0.145$, $P = 7.12E-03$), and $CD8^+$ T cells ($r = 0.027$, $p = 6.05$) (**Figure 5A**). In addition, analysis using date retrieved from GEPIA database showed that SLC17A9 expression level was correlated with levels of immune marker genes of Tfh, Th1, Th17, M1 macrophage, M2 macrophage, Tumor associated macrophage (TAM), and natural killer cell (NK) cells (**Table 3**). Furthermore, TCGA LIHC analysis showed that SLC17A9 expression level was positively correlated with the infiltration level of $CD4^+$ T cells and macrophages (**Figure 5B**). Patients were assigned to high and low expression groups to explore differences in immune infiltration levels under different SLC17A9 expression levels. The findings showed that infiltration of naive B cells ($P = 0.015$), naive CD4 T cells ($P = 0.023$), memory resting CD4 T cells ($P = 0.033$), T-cell regulatory (Tregs) cells ($P = 0.036$), and monocytes ($P < 0.001$) were significantly different between the high and low expression groups (**Figure 5C**).

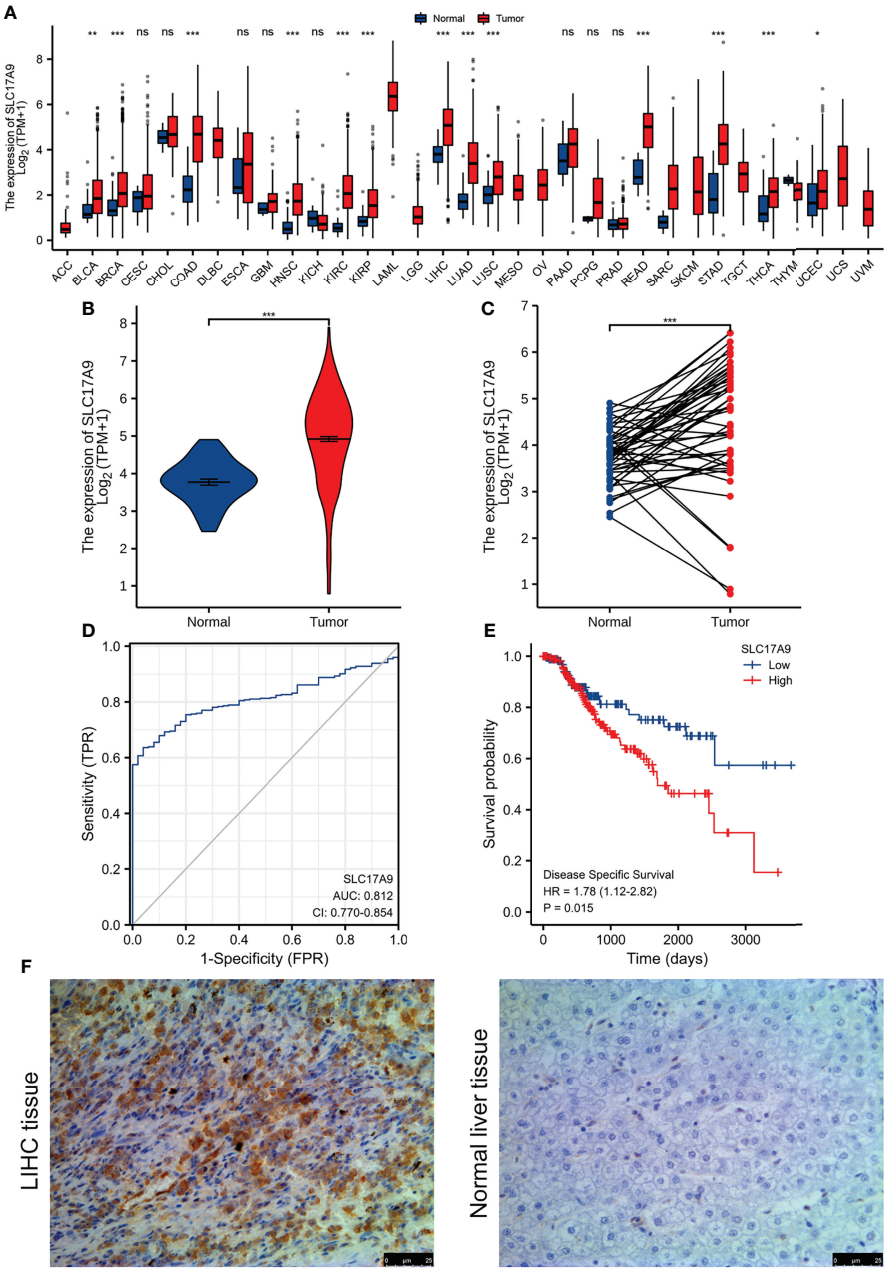

FIGURE 1 | The expression of SLC17A9 in hepatocellular carcinoma (LIHC) and pan-carcinoma. **(A)** The TCGA database shows the SLC17A9 mRNA expression levels in different tumor types (Sample information: normal group, N = 730; and tumor group, N = 10,363). [The sample data of **(B–E)** are from TCGA-LIHC RNA-seq platform. Sample information: normal group, N = 50; and tumor group, N = 374]. **(B)** R software package was used to analyze SLC17A9 expression in non-paired samples between LIHC and normal tissues. **(C)** R software package was used to analyze the difference of SLC17A9 expression in paired samples between LIHC and normal tissues. **(D)** Receiver operating characteristic curve analysis showed that in predicting the outcome of normal and tumor groups, the predictive ability of variable SLC17A9 has a certain accuracy (AUC = 0.812; CI = 0.770–0.854). Sensitivity and specificity for the prediction of SLC17A9 expression were 63.6% and 96.0%, respectively. **(E)** R software package graph to show the survival analyses of patients with LIHC based on SLC17A9 expression. **(F)** Immunohistochemical staining for SLC17A9 in LIHC tissue and adjacent normal liver tissues. *p < 0.05; **p < 0.01; ***p < 0.001; ns, no significance.

Expression of SLC17A9 Is Correlated With m6A Methylation Regulator in LIHC

m6A modification is a potential target for designing drugs for tumor treatment. Therefore, the correlation between expression level of SLC17A9 and levels of m6A-related genes was explored using TCGA LIHC datasets (**Figures 6A, B**). The results showed that SLC17A9 expression was significantly correlated with level of METTL3 (r = 0.181, P < 0.001), WTAP (r = 0.134, P =

TABLE 2 | Correlation between SLC17A9 expressions and different clinicopathological characteristics in LIHC.

Characteristic	Levels	SLC17A9 Expression		P-Value
		Low (%)	High (%)	
Age	≤60	83 (22.3%)	94 (25.2%)	0.323
	>60	103 (27.6%)	93 (24.9%)	
Gender	Female	49 (13.1%)	72 (19.3%)	**0.015**
	Male	138 (36.9%)	115 (30.7%)	
T stage	T1	90 (24.3%)	93 (25.1%)	0.561
	T2	51 (13.7%)	44 (11.9%)	
	T3	36 (9.7%)	44 (11.9%)	
	T4	8 (2.2%)	5 (1.3%)	
N stage	N0	130 (50.4%)	124 (48.1%)	0.059
	N1	0 (0%)	4 (1.6%)	
M stage	M0	134 (49.3%)	134 (49.3%)	0.622
	M1	1 (0.4%)	3 (1.1%)	
Pathologic stage	Stage I	84 (24%)	89 (25.4%)	0.285
	Stage II	49 (14%)	38 (10.9%)	
	Stage III	39 (11.1%)	46 (13.1%)	
	Stage IV	1 (0.3%)	4 (1.1%)	
Histologic grade	G1	36 (9.8%)	19 (5.1%)	0.094
	G2	88 (23.8%)	90 (24.4%)	
	G3	57 (15.4%)	67 (18.2%)	
	G4	5 (1.4%)	7 (1.9%)	
OS event	Alive	125 (33.4%)	119 (31.8%)	0.587
	Dead	62 (16.6%)	68 (18.2%)	
DSS event	Alive	154 (42.1%)	133 (36.3%)	**0.006**
	Dead	28 (7.7%)	51 (13.9%)	
PFI event	Alive	107 (28.6%)	84 (22.5%)	**0.023**
	Dead	80 (21.4%)	103 (27.5%)	
Age, median (IQR)		62 (52, 69)	60 (51, 68)	0.286

Bold values indicate P < 0.05.

0.009), RBM15B (r = 0.144, P = 0.005), YTHDC1 (r = 0.158, P = 0.002), YTHDC2 (r = 0.157, P = 0.002), YTHDF1 (r = 0.267, P < 0.001), HNRNPC (r = 0.223, P < 0.001), IGF2BP1 (r = 0.214, P < 0.001), IGF2BP2 (r = 0.319, P < 0.001), RBMX (r = 0.156, P = 0.003), and HNRNPA2B1 (r = 0.153, P = 0.003) genes. The datasets were assigned into high and low expression groups to determine the expression differences between m6A modification–related genes at different SLC17A9 expression levels. The SLC17A9 high expression group showed significantly high expression levels of METTL3 (P = 0.006), WTAP (P = 0.003), RBM15B (P = 0.011), YTHDC1 (P = 0.006), YTHDC2 (P = 0.011), YTHDF1 (P < 0.001), HNRNPC (P = 0.001), IGF2BP1 (P = 0.002), IGF2BP2 (P < 0.001), IGF2BP3 (P < 0.001), RBMX (P = 0.009), and HNRNPA2B1 (P = 0.003) genes relative to the low expression group (**Figure 6C**). **Figure 6D** shows that m6A regulators expression change in tumor and normal tissues. On the basis of the above data, we screened two genes, METTL3 and YTHDF1, which not only increased expression in esophageal cancer, but also had the closest relationship with SLC17A9. Next, we used Western blots and RT-qPCR approaches to validate the functions of METTL3 and YTHDF1 genes at RNA and protein levels. The findings from Western blots showed significantly lower protein expression levels of METTL3 and YTHDF1 in the siSLC17A9 group compared with the expression levels in the control group (P < 0.0001, P = 0.03942; **Figures 6E, F**). RT-qPCR results showed significantly lower mRNA expression levels of METTL3 and YTHDF1 in the siSLC17A9 group compared with the expression levels in the control group (P = 0.038579, P = 0.002157; **Figures 6G, H**).

SLC17A9 Is Strongly Associated With Expression Levels of Iron Deficiency-Related Genes in LIHC

Further, the correlation between SLC17A9 and ferroptosis gene was explored using TCGA LIHC dataset (**Figures 7A, B**). The results showed that SLC17A9 expression level was significantly correlated with expression levels of HSPA5 (r = 0.240, p < 0.001), SLC7A11 (r = 0.180, p < 0.001), FANCD2 (r = 0.280, p < 0.001), CISD1 (r = 0.320, p < 0.001), SLC1A5 (r = 0.210, p < 0.001), AT1 (r = 0.210, p < 0.001), TFRC (r = 0.250, p < 0.001), LPCAT3 (r = 0.250, p < 0.001), GLS2 (r = 0.170, p = 0.001), DPP4 (r = 0.170, p = 0.001), ATP5MC3 (r = 0.130, p = 0.012), ALOX15 (r = 0.200, p < 0.001), and ACSL4 (r = 0.370, p < 0.001) genes. Moreover, the TCGA LIHC dataset was grouped into high and low expression groups to determine the expression difference in iron deficiency-related genes at different SLC17A9 expression levels. The findings showed that the expression levels of HSPA5 (p = 0.006), FANCD2 (p = 0.003), SLC1A5 (p = 0.011), SAT1 (p = 0.006), TFRC (p = 0.011), LPCAT3 (p < 0.001), GLS2 (p = 0.001), DPP4 (p = 0.002), CARS (p < 0.001), ATP5MC3 (p < 0.001), ALOX15 (p = 0.009), and ACSL4 (p = 0.003) were significantly higher in the SLC17A9 high expression group, relative to levels in the SLC17A9 low expression group (**Figure 7C**). ACSL4, CISD1, and ATP5MC3 genes were chosen for validation of these

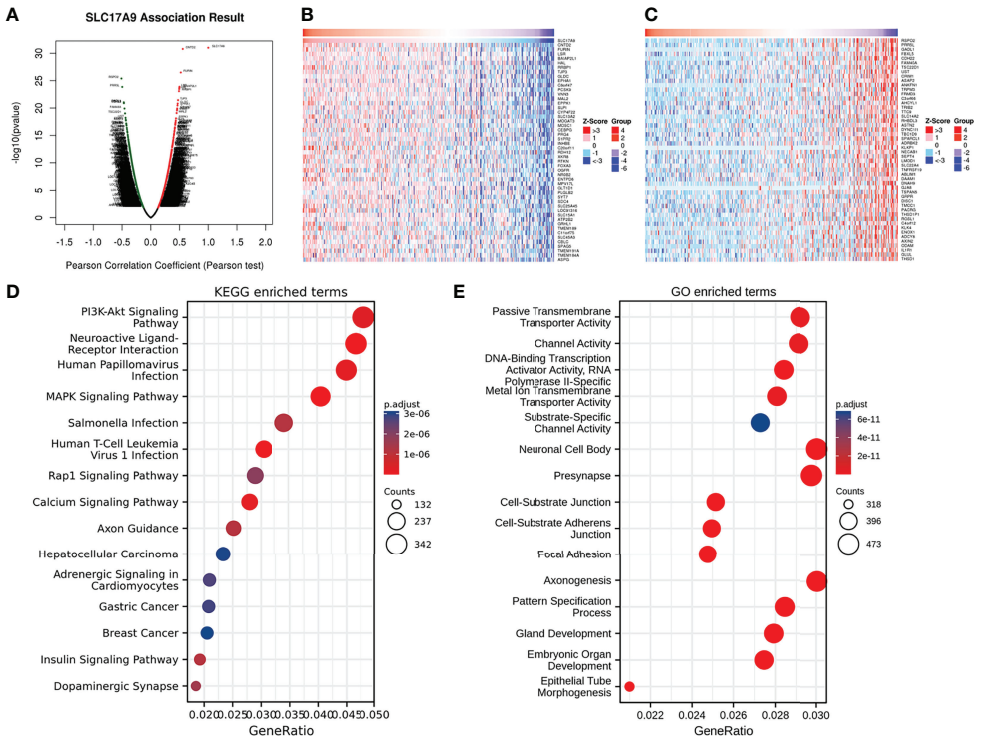

FIGURE 2 | Enrichment analysis of SLC17A9 gene co-expression network in LIHC. **(A)** The volcano map showed co-expression genes associated with SLC17A9 expression in the TCGA LIHC data set. **(B)** Heatmaps showed the top 50 co-expression genes positively correlated with SLC17A9 expression in the LIHC. **(C)** Heatmaps showed the top 50 co-expression genes negatively correlated with SLC17A9 expression in the LIHC. **(D)** Enrichment of Gene Ontology (GO) SLC17A9 co-expression genes. **(E)** Enrichment of Kyoto Encyclopedia of Genes and Genomes (KEGG) terms for SLC17A9 co-expression genes.

results using RT-qPCR analysis. The mRNA expression levels of ACSL4, CISD1, and ATP5MC3 in the siSLC17A9 group were significantly lower relative to the mRNA expression levels in the control group ($P = 0.0481$, $P < 0.0001$, $P = 0.0048$; **Figures 7D–F**).

DISCUSSION

SLC17A9 is a vesicle nucleotide transporter involved in ATP transport and is highly localized on lysosomes (25). Reduced SLC17A9 levels cause lysosomal ATP accumulation, lysosomal function impairment, and cell death. Mounting evidence has associated the lysosome with cancer. During tumorigenesis, the lysosome location and lysosomal membrane permeability change, releasing vast amounts of cathepsin into the cytoplasm, which, together with matrix metalloproteinases and blood plasminogen activation system, promotes tumorigenesis by degrading the extracellular matrix. Thus, SLC17A9 expression directly or indirectly affects tumorigenesis. Past studies have implicated SLC17A9 upregulation in gastric (26), liver (27), and colon cancer (28). However, its expression and function in liver cancer have not been determined. Using IHC, we show that SLC17A9 upregulated in LIHC and further knocked out the SLC17A9 gene for *in vitro* experiments. We find that SLC17A9 silencing HepG2 markedly suppressed ATP production as well as cell proliferation, migration, and colony formation. In LIHC, SLC17A9 expression significantly correlated with sex, DSS, and PFI, indicating that it may have prognostic value in LIHC. ROC curve analysis highlighted the diagnostic value of SLC17A9 expression in LIHC. Second, we find that patients with LIHC expressing high SLC17A9 levels had worse prognosis than those with low SLC17A9 levels, indicating that SLC17A9 has potential diagnostic and prognostic value in LIHC.

KEGG pathway enrichment analysis showed that SLC17A9 expression was mainly associated with PI3K/Akt signaling pathway, neuroactive ligand-receptor interaction, HPV infection, MAPK signaling, passive transmembrane transporter activity, and channel activity. It is reported that LLGL2 drives carcinogenic PI3K/AKT signaling in LIHC to promote LIHC (29). In addition, TMOD3 thought to promote liver cancer progression *via* MAPK/ERK signaling (30). These metabolic pathways can directly or indirectly affect tumorigenesis and highlight potential multi-target and multi-pathway synergistic treatment for LIHC. We speculate that SLC17A9 may interact with these pathways to promote liver cancer progression.

GO term enrichment analysis showed that SLC17A9 expression is associated with many aspects of BP, CC, and MF and are mainly associated with neuronal cell body, presynapse, and axonogenesis, indicating that SLC17A9 may be involved in protein binding,

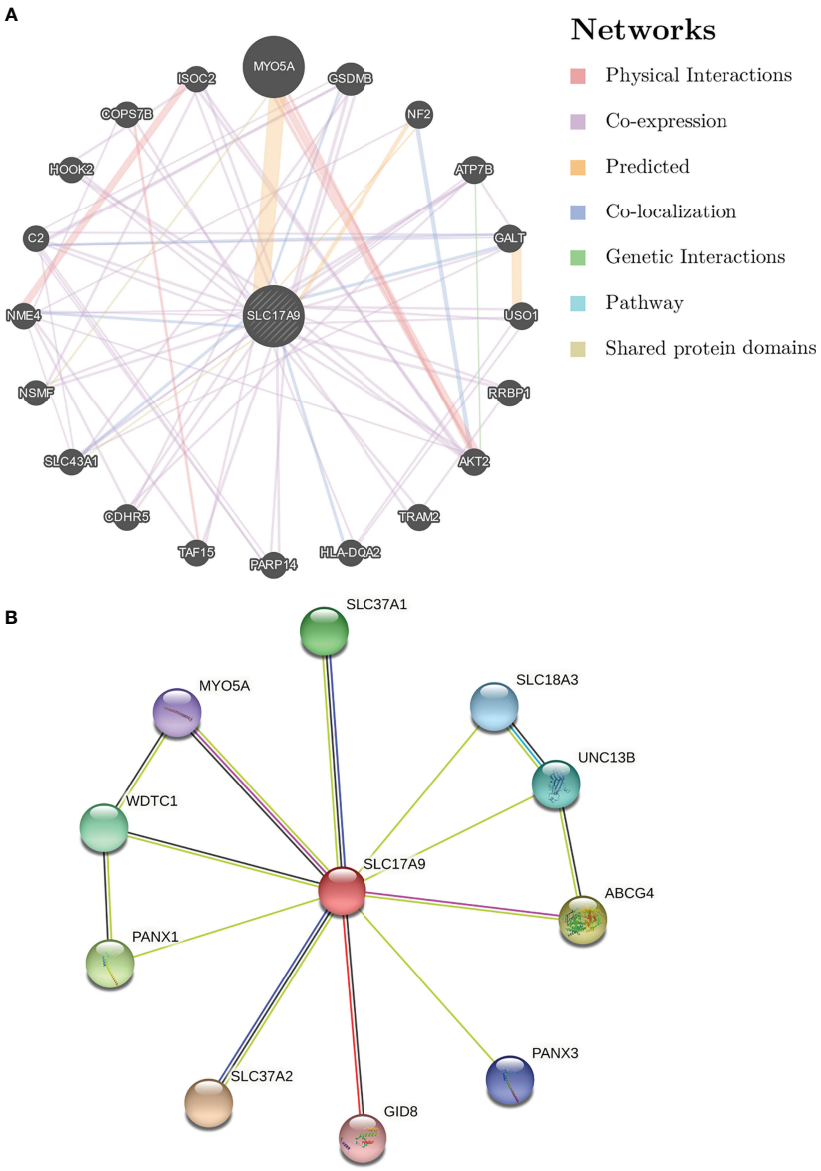

FIGURE 3 | Analysis of gene–gene interaction (GGI) and protein–protein interaction (PPI) of SLC17A9. **(A)** GGI network of SLC17A9. **(B)** PPI interaction network of SLC17A9.

plasma membrane, membrane composition, nucleus, and other biological functions.

GGI and PPI analysis of co-expressed genes revealed the strongest correlation to be between MYO5A, SLC18A3, and SLC17A9. MYO5A is a key component of the myosin V family, which participates in transport vesicle formation, protein transcription, and tumor progression (31). Studies have implicated MYO5A in laryngeal squamous cell carcinoma and esophageal squamous cell carcinoma (32, 33). SLC18A3 belongs to the family of vesicular acetylcholine transporters. Various acetylcholine signaling pathways can regulate a range of cellular functions, including proliferation, differentiation, and cytoskeleton integrity (34). L cells from small cell lung cancer are reported to secrete acetylcholine and promote tumor proliferation (35). These results suggest that the expression of MYO5A and SLC18A3 affects tumorigenesis, which provide a theoretical basis in treatment of liver cancer.

Analysis of the relationship between SLC17A9 and immune cell infiltration in LIHC revealed that SLC17A9 expression correlates with B cells, $CD4^+$ T cells, macrophages, neutrophils, and immune marker genes for Tfh, Th1, Th17, M1 macrophage, M2 macrophage, TAM, and NK cells. It was also positively associated with the degree of infiltration by infiltration $CD4^+$ T cells and macrophages. CiberSort analysis showed that naive B cells, naive

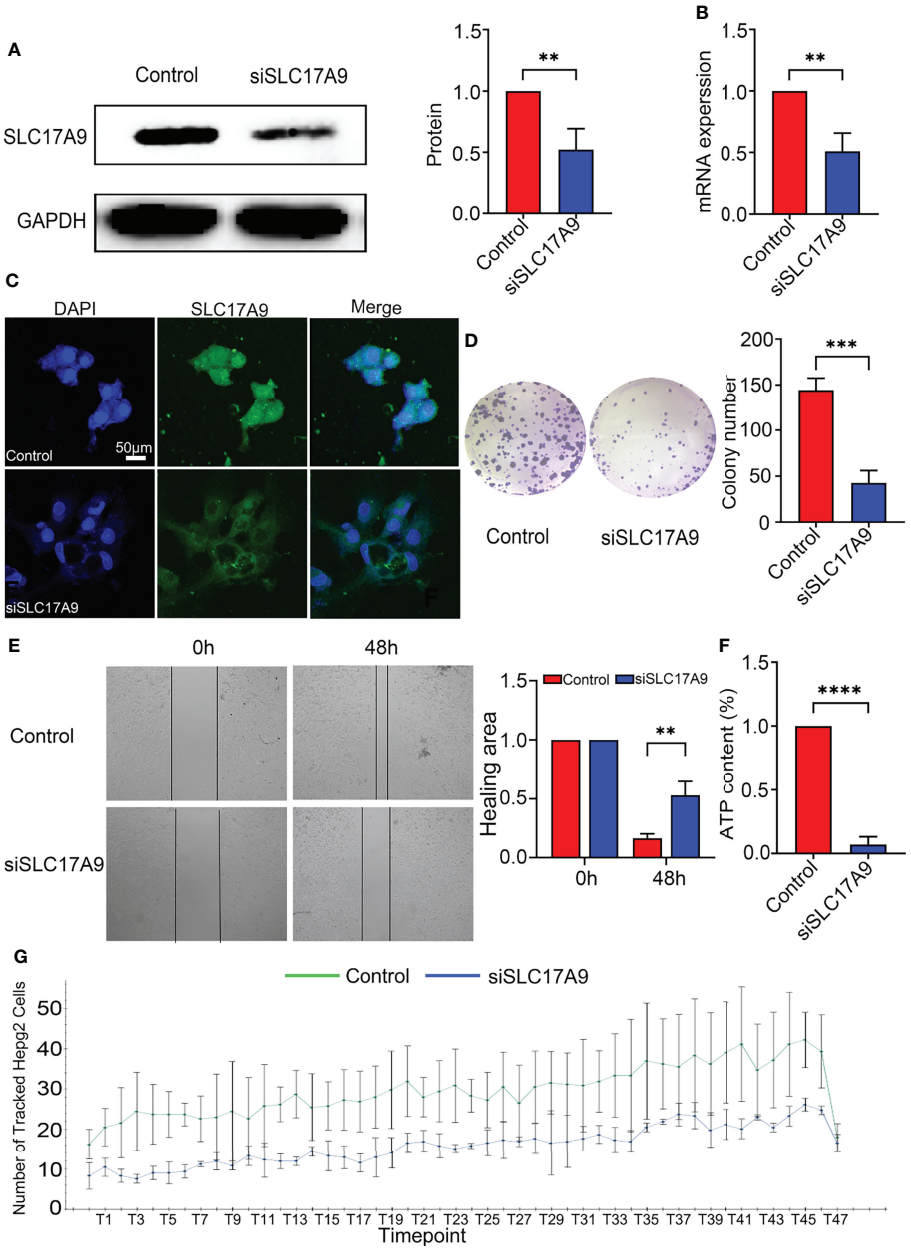

FIGURE 4 | Silencing of SLC17A9 reduced malignant phenotypes of liver cancer. **(A)** Western blot showed the knockdown efficacy of SLC17A9 siRNA. **(B)** SLC17A9 mRNA expression level in control and siSLC17A9 groups. **(C)** Immunofluorescence detection of proliferation rate. **(D)** Colony formation assay results in control and siSLC17A9 groups. **(E)** Wound healing assay after transfection with SLC17A9 siRNA or control siRNA. **(F)** ATP levels were measured in the control and siSLC17A9 groups. **(G)** Using high-content imaging to detect the increment rate of cells in different periods. *p < 0.05; **p < 0.01; ***p < 0.001; ****p <0.0001.

$CD4^+$ T cells, memory resting $CD4^+$ T cells, regulatory T cells (Tregs), and monocytes differed significantly with SLC17A9 expression. Together, these results confirmed that SLC17A9 was associated with tumor infiltration by immune cells in LIHC, especially B cells, $CD4^+$ T cells, and macrophages. Macrophages have been associated with immunosuppression and angiogenesis, which provides sufficient nutrition for tumor proliferation (36). SLC17A9 expression and vesicular ATP exocytosis by macrophages can activate the P2 receptors and participate in macrophage activation expression (37). We speculate that high SLC17A9 expression in LIHC may activate macrophages, which influence LIHC proliferation.

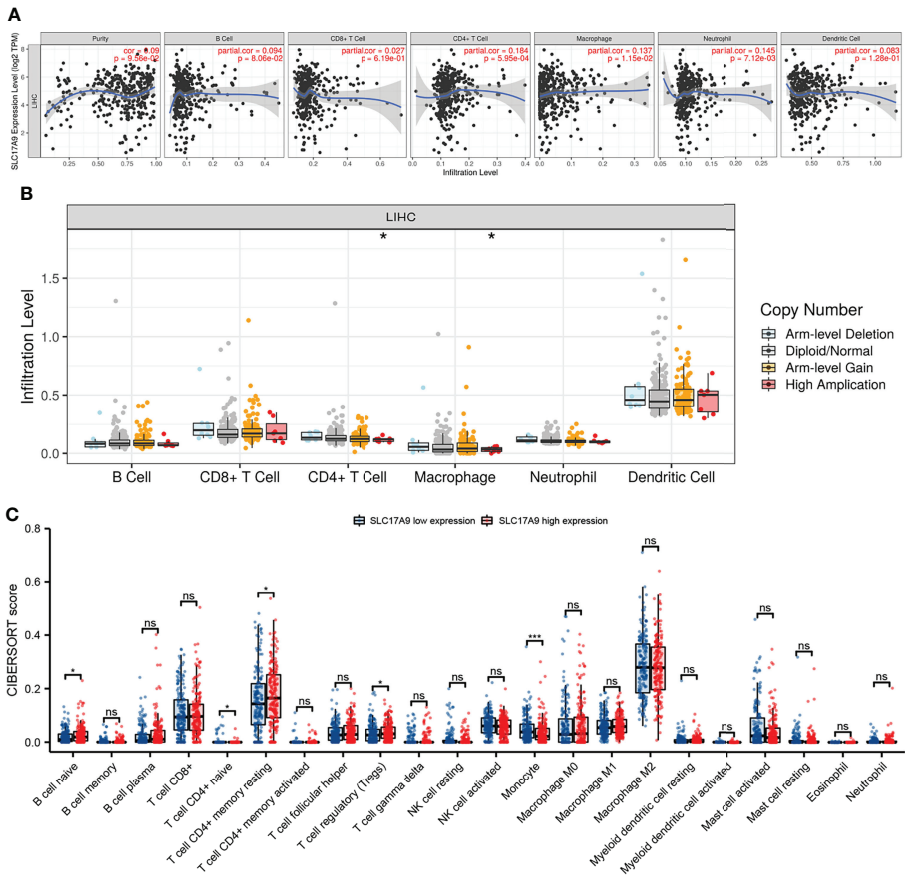

FIGURE 5 | Analysis of the correlation between SLC17A9 and immune cells and genetic copy number variations (CNV) of SLC17A9 with the relative abundance of tumor-infiltrating cells and CIBERSORT analysis. **(A)** Correlation between SLC17A9 and tumor immune infiltrating cells **(B)** SLC17A9 CNV affects the infiltrating levels of CD4$^+$ T cell and neutrophil cells in LIHC. **(C)** The change ratio of 22 immune cell subtypes in the high and low SLC17A9 expression groups in LIHC. *p < 0.05; **p < 0.01; ***p < 0.001; ****p < 0.0001.

TABLE 3 | Correlation analysis between SLC17A9 and immune cell marker gene in GEPIA database.

Description	Gene Markers	GEPIA	
		Tumor	
		Correlation	P-Value
B cell	CD19	0.02	0.69
	MS4A1	−0.012	0.81
	CD79A	−0.028	0.57
CD8$^+$ T cell	CD8A	−0.068	0.17
	CD8B	−0.048	0.32
	IL2RA	−0.03	0.53
Tfh	CXCR3	−0.009	0.85
	CXCR5	0.21	**2.20E-05**
	ICOS	−0.0026	0.96
Th1	IL12RB1	−0.065	0.18
	CCR1	−0.14	**0.0039**
	CCR5	−0.043	0.38
Th2	CCR4	0.00023	1
	CCR8	0.034	0.48
	IL21R	−0.045	0.36
Th17	IL23R	0.02	0.69

(Continued)

TABLE 3 | Continued

Description	Gene Markers	GEPIA	
		Tumor	
		Correlation	P-Value
	CCR6	0.15	**0.0025**
	FOXP3	0.0098	0.84
Treg	NT5E	0.09	0.065
	IL7R	–0.019	0.7
	PDCD1	0.088	0.071
T-cell exhaustion	CTLA4	0.045	0.36
	LAG3	–0.024	0.62
	CD68	–0.049	0.32
M1 macrophage	ITGAM	–0.039	0.43
	NOS2	–0.0044	0.93
	IRF5	0.27	**2.30E-08**
M2 macrophage	CD163	–0.16	**0.00084**
	MRC1	–0.026	0.6
	CCL2	–0.1	**0.041**
TAM	CD86	–0.069	0.16
	CD14	–0.054	0.27
	CD33	–0.094	0.054
Monocyte	B3GAT1	–0.0096	0.84
	KIR3DL1	–0.085	0.081
	CD7	0.15	**0.0024**
Natural killer cell	FCGR3A	–0.094	0.054
	CD55	0.035	0.48
	CD1C	–0.0014	0.98
Neutrophil	THBD	–0.035	0.47
	CD19	0.02	0.69
	MS4A1	–0.012	0.81
Dendritic cell	CD79A	–0.028	0.57
	CD8A	–0.068	0.17
	CD8B	–0.048	0.32

Bold values indicate P < 0.05.

m6A methylation is the most common mRNA modification in eukaryotes, and it influences proliferation and migration of tumors. Here, analysis on various databases found that SLC17A9 expression positively correlated with METTL3, YTHDF1, and WTAP expression. Western blot analysis and RT-qPCR analysis revealed that siSLC17A9 silencing reduced the expression of METTL3 and YTHDF1 significantly relative the control group. RNA-seq analysis revealed that HNNPC was specifically upregulated in LIHC. It is reported that METTL3 overexpression promotes LIHC growth *in vivo* and *in vitro* (38) and that this correlates with poor prognosis in LIHC. On the basis of these findings, we point out that the SLC17A9 modification by m6A enhances its mRNA stability, thereby promoting LIHC growth.

Iron cell death is reported to play an important role in tumorigenesis. Here, database analysis showed that SLC17A9 expression correlated with the expression of various genes, including lACSL4, CISD1, and ATP5MC3. These observations were verified by RT-qPCR analysis, which showed that ACSL4, CISD1, and ATP5MC3 expression was significantly lower in siSLC17A9 cells relative to the controls. ACSL4 is an enzyme that regulates lipid composition. It can also promote ferroptosis. It is reported that ACSL4 promotes LIHC *via* the ERK/FBW7/c-Myc axis (39). Numerous studies have reported CISD1 expression in LIHC. ATP5MC3 has been associated with colon cancer (40). We speculate whether SLC17A9 interaction with other genes like ACSL4, CISD1, and ATP5MC3 affects iron-dependent cell death in LIHC.

The core of our article is to discuss the expression of SLC17A9 in hepatocellular carcinoma and further transfect siRNA to verify it by *in vivo* experiments. Some information related to immune infiltration, m6A, and iron death were added, and several m6A-related factors with strong correlation were screened to verify the protein expression level and RNA expression level. Our results do show that the expression levels of METTL3 and YTHDF1 in the siSLC17A9 group are lower than those in the control group, but our results are only superficial and only validate individual factors, and no batch in-depth research has been done, which is one of our defects and deficiencies.

To our knowledge, this is the first study to comprehensively analyze SLC17A9 expression in LIHC with regards to cellular function. SLC17A9 upregulation in LIHC correlates with poor prognosis and has a significant correlation with biology, highlighting its potential therapeutic and diagnostic potential.

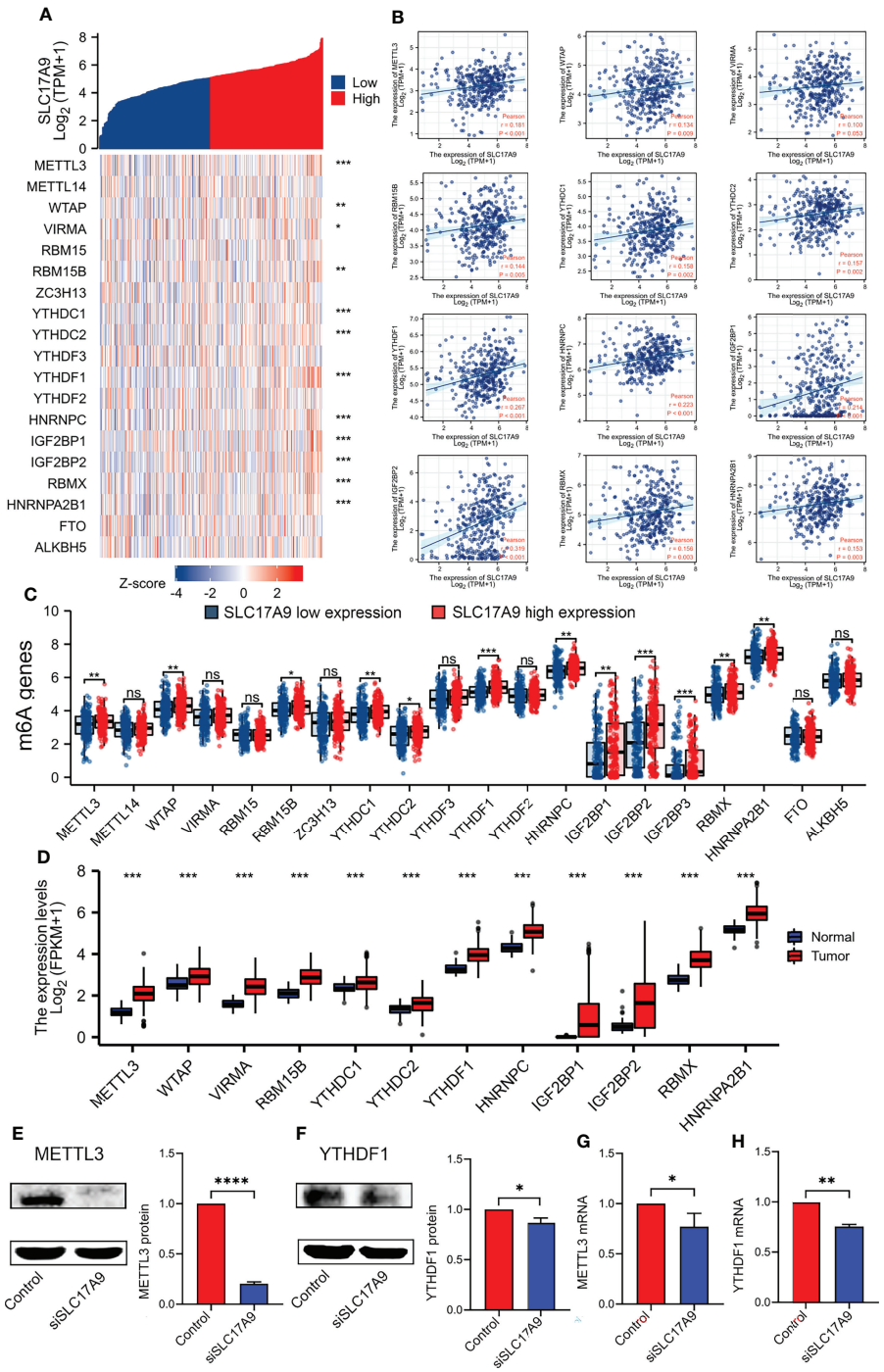

FIGURE 6 | Correlations of SLC17A9 expression with m6A-related genes in LIHC. **(A)** Thermography shows the correlation between the expression of SLC17A9 and m6A-related genes. **(B)** The scatter plot shows the correlation between the expression of SLC17A9 and m6A-related genes. **(C)** Expression of m6A-related genes in the high and low SLC17A9 expression groups in LIHC. **(D)** m6A regulators expression in tumor and normal tissues. **(E, F)** METTL3 (left) and YTHDF1 (right) protein expression level in control and siSLC17A9 groups. **(G, H)** METTL3 (left) and YTHDF1 (right) mRNA expression level in control and siSLC17A9 groups. *p < 0.05; **p < 0.01; ***p < 0.001; ****p < 0.0001.

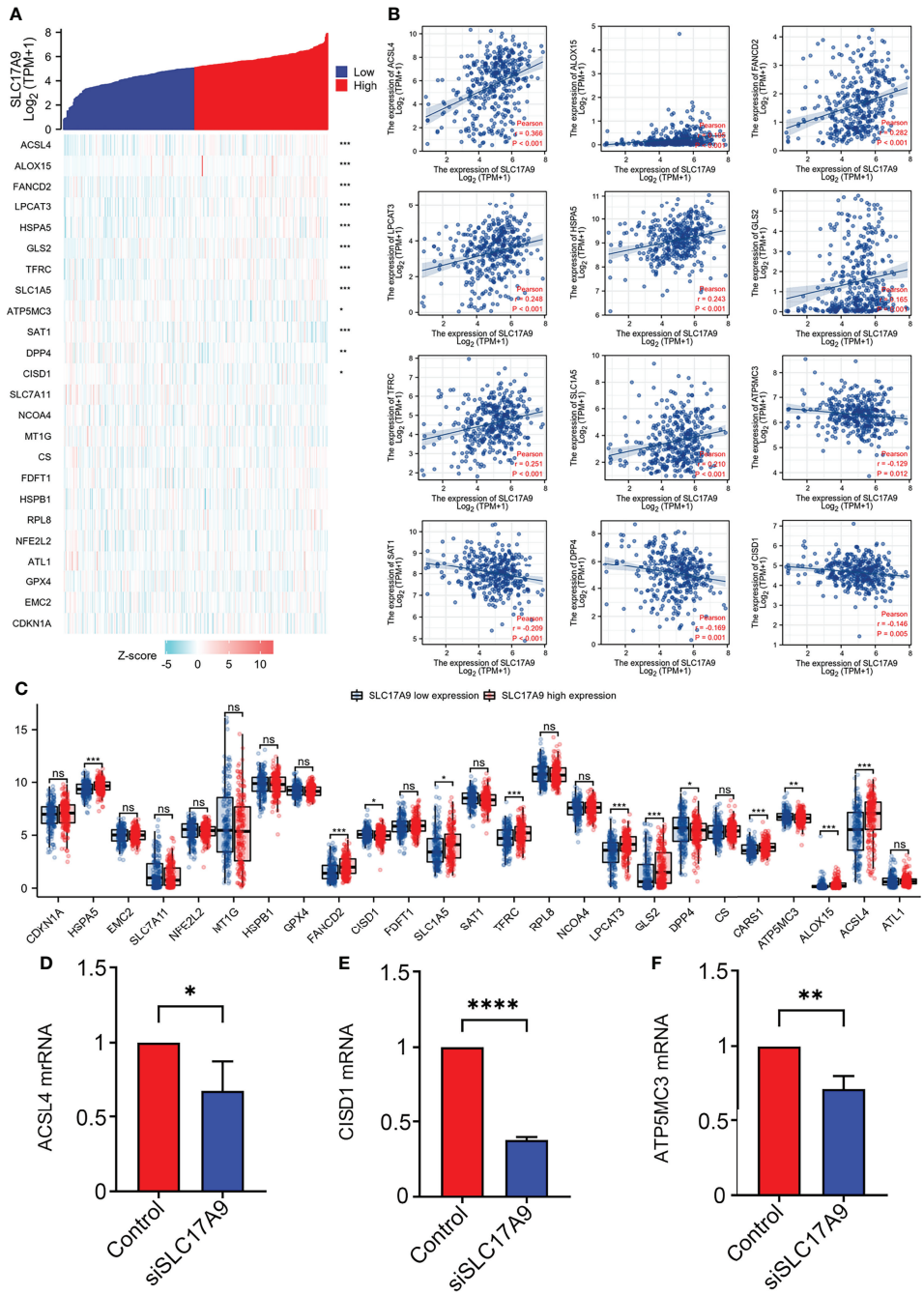

FIGURE 7 | Correlations of SLC17A9 expression with Fe deficiency-related genes in LIHC. **(A)** Thermography shows the correlation between the expression of SLC17A9 and Fe deficiency-related genes. **(B)** The scatter plot shows the correlation between the expression of SLC17A9 and Fe deficiency-related genes. **(C)** Expression of Fe deficiency-related gene in the high and low SLC17A9 expression groups in LIHC. **(D)** ACSL4 mRNA expression level in control and siSLC17A9 groups. **(E)** CISD1 mRNA expression level in control and siSLC17A9 groups. **(F)** ATP5MC3 mRNA expression level in control and siSLC17A9 groups. *p < 0.05; **p < 0.01; ***p < 0.001; ****p <0.0001.

DATA AVAILABILITY STATEMENT

The original contributions presented in the study are included in the article/supplementary materials. Further inquiries can be directed to the corresponding author.

ETHICS STATEMENT

The studies involving human participants were reviewed and approved by Ethics Committee of Taihe Hospital Affiliated of Hubei University of Medicine. Written informed consent for

participation was not required for this study in accordance with the national legislation and the institutional requirements.

AUTHOR CONTRIBUTIONS

X-YK and YG conceived the project and wrote the manuscript. X-YK, JZ, J-WY, and X-SL participated in data analysis. X-YK, YG, L-MZ, and X-YL participated in the discussion and language editing. Z-JP reviewed the manuscript. All authors contributed to the article and approved the submitted version.

FUNDING

This work was supported by the Hubei Province's Outstanding Medical Academic Leader program, the Foundation for Innovative Research Team of Hubei Provincial Department of Education (No. T2020025), the general project of Hubei Provincial Department of Education (No. B2021160), the HuBei Provincial Department of Science and Technology Innovation Group Programme (grant no. 2019CFA034), Innovative Research Program for Graduates of Hubei University of Medicine (grant nos. YC2020011 and YC2021018), and the Key Discipline Project of Hubei University of Medicine.

REFERENCES

1. Bray F, Ferlay J, Soerjomataram I, Siegel RL, Torre LA, Jemal A. Global Cancer Statistics 2018: GLOBOCAN Estimates of Incidence and Mortality Worldwide for 36 Cancers in 185 Countries. *CA Cancer J Clin* (2018) 68 (6):394–424. doi: 10.3322/caac.21492
2. Torre LA, Bray F, Siegel RL, Ferlay J, Lortet-Tieulent J, Jemal A. Global Cancer Statistics, 2012. *CA Cancer J Clin* (2015) 65(2):87–108. doi: 10.3322/caac.21262
3. Mani S, Andrisani O. Interferon Signaling During Hepatitis B Virus (HBV) Infection and HBV-Associated Hepatocellular Carcinoma. *Cytokine* (2019) 124:154518. doi: 10.1016/j.cyto.2018.08.012
4. Zhong XZ, Cao Q, Sun X, Dong XP. Activation of Lysosomal P2X4 by ATP Transported Into Lysosomes *via* VNUT/SLC17A9 Using V-ATPase Generated Voltage Gradient as the Driving Force. *J Physiol* (2016) 594 (15):4253–66. doi: 10.1113/JP271893
5. Frye M, Harada BT, Behm M, He C. RNA Modifications Modulate Gene Expression During Development. *Science* (2018) 361(6409):1346–9. doi: 10.1126/science.aau1646
6. Cao Q, Zhao K, Zhong XZ, Zou Y, Yu H, Huang P, et al. SLC17A9 Protein Functions as a Lysosomal ATP Transporter and Regulates Cell Viability. *J Biol Chem* (2014) 289(33):23189–99. doi: 10.1074/jbc.M114.567107
7. Dou Y, Wu HJ, Li HQ, Qin S, Wang YE, Li J, et al. Microglial Migration Mediated by ATP-Induced ATP Release From Lysosomes. *Cell Res* (2012) 22 (6):1022–33. doi: 10.1038/cr.2012.10
8. Zhang Z, Chen G, Zhou W, Song A, Xu T, Luo Q, et al. Regulated ATP Release From Astrocytes Through Lysosome Exocytosis. *Nat Cell Biol* (2007) 9(8):945–53. doi: 10.1038/ncb1620
9. Sathe MN, Woo K, Kresge C, Bugde A, Luby-Phelps K, Lewis MA, et al. Regulation of Purinergic Signaling in Biliary Epithelial Cells by Exocytosis of SLC17A9-Dependent ATP-Enriched Vesicles. *J Biol Chem* (2011) 286 (28):25363–76. doi: 10.1074/jbc.M111.232868
10. Inoue A, Nakao-Kuroishi K, Kometani-Gunjigake K, Mizuhara M, Shirakawa T, Ito-Sago M, et al. VNUT/SLC17A9, a Vesicular Nucleotide Transporter, Regulates Osteoblast Differentiation. *FEBS Open Bio* (2020) 10(8):1612–23. doi: 10.1002/2211-5463.12918
11. Haanes KA, Kowal JM, Arpino G, Lange SC, Moriyama Y, Pedersen PA, et al. Role of Vesicular Nucleotide Transporter VNUT (SLC17A9) in Release of ATP From AR42J Cells and Mouse Pancreatic Acinar Cells. *Purinergic Signal* (2014) 10(3):431–40. doi: 10.1007/s11302-014-9406-7
12. Schizas D, Charalampakis N, Kole C, Mylonas KS, Katsaros I, Zhao M, et al. Immunotherapy for Esophageal Cancer: A 2019 Update. *Immunotherapy-Uk* (2020) 12(3):203–18. doi: 10.2217/imt-2019-0153
13. Li L, Song X, Lv Y, Jiang Q, Fan C, Huang D. Landscape of Associations Between Long non-Coding RNAs and Infiltrating Immune Cells in Liver Hepatocellular Carcinoma. *J Cell Mol Med* (2020) 24(19):11243–53. doi: 10.1111/jcmm.15690
14. Yu J, Chen M, Huang H, Zhu J, Song H, Zhu J, et al. Dynamic M6a Modification Regulates Local Translation of mRNA in Axons. *Nucleic Acids Res* (2018) 46(3):1412–23. doi: 10.1093/nar/gkx1182
15. Deng X SRWH. RNA N6-Methyladenosine Modification in Cancers: Current Status and Perspectives. *Cell Res* (2018) 5(28):507–17. doi: 10.1038/s41422-018-0034-6
16. Capelletti MM, Manceau H, Puy H, Peoc'H K. Ferroptosis in Liver Diseases: An Overview. *Int J Mol Sci* (2020) 21(14). doi: 10.3390/ijms21144908
17. Tang D, Chen X, Kang R, Kroemer G. Ferroptosis: Molecular Mechanisms and Health Implications. *Cell Res* (2021) 31(2):107–25. doi: 10.1038/s41422-020-00441-1
18. Liang C, Zhang X, Yang M, Dong X. Recent Progress in Ferroptosis Inducers for Cancer Therapy. *Adv Mater* (2019) 31(51):e1904197. doi: 10.1002/adma.201904197
19. Wang C, Yang S, Jin L, Dai G, Yao Q, Xiang H, et al. Biological and Clinical Significance of GATA3 Detected From TCGA Database and FFPE Sample in Bladder Cancer Patients. *Onco Targets Ther* (2020) 13:945–58. doi: 10.2147/OTT.S237099
20. Liu XS, Gao Y, Wu LB, Wan HB, Yan P, Jin Y, et al. Comprehensive Analysis of GLUT1 Immune Infiltrates and ceRNA Network in Human Esophageal Carcinoma. *Front Oncol* (2021) 11:665388. doi: 10.3389/fonc.2021.665388
21. Warde-Farley D, Donaldson SL, Comes O, Zuberi K, Badrawi R, Chao P, et al. The GeneMANIA Prediction Server: Biological Network Integration for Gene Prioritization and Predicting Gene Function. *Nucleic Acids Res* (2010) 38(Web Server issue):W214–20. doi: 10.1093/nar/gkq537
22. Szklarczyk D, Gable AL, Nastou KC, Lyon D, Kirsch R, Pyysalo S, et al. The STRING Database in 2021: Customizable Protein-Protein Networks, and Functional Characterization of User-Uploaded Gene/Measurement Sets. *Nucleic Acids Res* (2021) 49(D1):D605–12. doi: 10.1093/nar/gkaa1074
23. Chen W, Chen X, Li S, Ren B. Expression, Immune Infiltration and Clinical Significance of SPAG5 in Hepatocellular Carcinoma: A Gene Expression-Based Study. *J Gene Med* (2020) 22(4):e3155. doi: 10.1002/jgm.3155
24. Yang JW, Yuan LL, Gao Y, Liu XS, Wang YJ, Zhou LM, et al. (18)F-FDG PET/CT Metabolic Parameters Correlate With EIF2S2 Expression Status in Colorectal Cancer. *J Cancer* (2021) 12(19):5838–47. doi: 10.7150/jca.57926
25. Tokunaga A, Tsukimoto M, Harada H, Moriyama Y, Kojima S. Involvement of SLC17A9-Dependent Vesicular Exocytosis in the Mechanism of ATP Release During T Cell Activation. *J Biol Chem* (2010) 285(23):17406–16. doi: 10.1074/jbc.M110.112417
26. Li J, Su T, Yang L, Deng L, Zhang C, He Y. High SLC17A9 Expression Correlates With Poor Survival in Gastric Carcinoma. *Future Oncol* (2019) 15 (36):4155–66. doi: 10.2217/fon-2019-0283
27. Wu J, Yang Y, Song J. Expression of SLC17A9 in Hepatocellular Carcinoma and its Clinical Significance. *Oncol Lett* (2020) 20(5):182. doi: 10.3892/ol.2020.12043
28. Yang L, Chen Z, Xiong W, Ren H, Zhai E, Xu K, et al. High Expression of SLC17A9 Correlates With Poor Prognosis in Colorectal Cancer. *Hum Pathol* (2019) 84:62–70. doi: 10.1016/j.humpath.2018.09.002
29. Leng S, Xie F, Liu J, Shen J, Quan G, Wen T. LLGL2 Increases Ca(2+) Influx and Exerts Oncogenic Activities *via* PI3K/AKT Signaling Pathway in Hepatocellular Carcinoma. *Front Oncol* (2021) 11:683629. doi: 10.3389/fonc.2021.683629
30. Jin C, Chen Z, Shi W, Lian Q. Tropomodulin 3 Promotes Liver Cancer Progression by Activating the MAPK/ERK Signaling Pathway. *Oncol Rep* (2019) 41(5):3060–8. doi: 10.3892/or.2019.7052
31. Velvarska H, Niessing D. Structural Insights Into the Globular Tails of the Human Type V Myosins Myo5a, Myo5b, And Myo5c. *PLoS One* (2013) 8(12): e82065. doi: 10.1371/journal.pone.0082065
32. Liang X, Wu Z, Shen S, Niu Y, Guo Y, Liang J, et al. LINC01980 Facilitates Esophageal Squamous Cell Carcinoma Progression *via* Regulation of miR-190a-

5p/MYO5A Pathway. *Arch Biochem Biophys* (2020) 686:108371. doi: 10.1016/j.abb.2020.108371
33. Zhao X, Zhang W, Ji W. MYO5A Inhibition by miR-145 Acts as a Predictive Marker of Occult Neck Lymph Node Metastasis in Human Laryngeal Squamous Cell Carcinoma. *Onco Targets Ther* (2018) 11:3619–35. doi: 10.2147/OTT.S164597
34. Lau JK, Brown KC, Thornhill BA, Crabtree CM, Dom AM, Witte TR, et al. Inhibition of Cholinergic Signaling Causes Apoptosis in Human Bronchioalveolar Carcinoma. *Cancer Res* (2013) 73(4):1328–39. doi: 10.1158/0008-5472.CAN-12-3190
35. Brown KC, Perry HE, Lau JK, Jones DV, Pulliam JF, Thornhill BA, et al. Nicotine Induces the Up-Regulation of the Alpha7-Nicotinic Receptor (Alpha7-Nachr) in Human Squamous Cell Lung Cancer Cells *via* the Sp1/GATA Protein Pathway. *J Biol Chem* (2013) 288(46):33049–59. doi: 10.1074/jbc.M113.501601
36. Wenes M, Shang M, Di Matteo M, Goveia J, Martin-Perez R, Serneels J, et al. Macrophage Metabolism Controls Tumor Blood Vessel Morphogenesis and Metastasis. *Cell Metab* (2016) 24(5):701–15. doi: 10.1016/j.cmet.2016.09.008
37. Tatsushima K, Hasuzawa N, Wang L, Hiasa M, Sakamoto S, Ashida K, et al. Vesicular ATP Release From Hepatocytes Plays a Role in the Progression of Nonalcoholic Steatohepatitis. *Biochim Biophys Acta (BBA) - Mol Basis Dis* (2021) 1867(3):166013. doi: 10.1016/j.bbadis.2020.166013
38. Chen M, Wei L, Law CT, Tsang FH, Shen J, Cheng CL, et al. RNA N6-Methyladenosine Methyltransferase-Like 3 Promotes Liver Cancer Progression Through YTHDF2-Dependent Posttranscriptional Silencing of SOCS2. *Hepatology* (2018) 67(6):2254–70. doi: 10.1002/hep.29683
39. Chen J, Ding C, Chen Y, Hu W, Lu Y, Wu W, et al. ACSL4 Promotes Hepatocellular Carcinoma Progression *via* C-Myc Stability Mediated by ERK/FBW7/c-Myc Axis. *Oncogenesis* (2020) 9(4):42. doi: 10.1038/s41389-020-0226-z
40. Nie J, Shan D, Li S, Zhang S, Zi X, Xing F, et al. A Novel Ferroptosis Related Gene Signature for Prognosis Prediction in Patients With Colon Cancer. *Front Oncol* (2021) 11:654076. doi: 10.3389/fonc.2021.654076

Conflict of Interest: The authors declare that the research was conducted without any commercial or financial relationships that could be construed as a potential conflict of interest.

Publisher's Note: All claims expressed in this article are solely those of the authors and do not necessarily represent those of their affiliated organizations, or those of the publisher, the editors and the reviewers. Any product that may be evaluated in this article, or claim that may be made by its manufacturer, is not guaranteed or endorsed by the publisher.

frontiers | Frontiers in Oncology

TYPE Review
PUBLISHED 04 August 2022
DOI 10.3389/fonc.2022.867670

OPEN ACCESS

EDITED BY
Hernandes F. Carvalho,
State University of Campinas, Brazil

REVIEWED BY
Juan Li,
Zhengzhou University, China
Giovanni Blandino,
Hospital Physiotherapy Institutes (IRCCS), Italy

*CORRESPONDENCE
Dajin Chen
zju2001@zju.edu.cn

SPECIALTY SECTION
This article was submitted to Molecular and Cellular Oncology, a section of the journal Frontiers in Oncology

RECEIVED 01 February 2022
ACCEPTED 11 July 2022
PUBLISHED 04 August 2022

CITATION
Yao Q, Zhang X and Chen D (2022) The emerging potentials of lncRNA DRAIC in human cancers. *Front. Oncol.* 12:867670. doi: 10.3389/fonc.2022.867670

The emerging potentials of lncRNA DRAIC in human cancers

Qinfan Yao[1,2,3,4], Xiuyuan Zhang[1,2,3,4] and Dajin Chen[1,2,3,4]*

[1]Kidney Disease Center, the First Affiliated Hospital, College of Medicine, Zhejiang University, Hangzhou, China, [2]Key Laboratory of Kidney Disease Prevention and Control Technology, Hangzhou, China, [3]National Key Clinical Department of Kidney Diseases, Institute of Nephrology, Zhejiang University, Hangzhou, China, [4]Zhejiang Clinical Research Center of Kidney and Urinary System Disease, Hangzhou, China

Long non-coding RNA (lncRNA) is a subtype of noncoding RNA that has more than 200 nucleotides. Numerous studies have confirmed that lncRNA is relevant during multiple biological processes through the regulation of various genes, thus affecting disease progression. The lncRNA DRAIC, a newly discovered lncRNA, has been found to be abnormally expressed in a variety of diseases, particularly cancer. Indeed, the dysregulation of DRAIC expression is closely related to clinicopathological features. It was also reported that DRAIC is key to biological functions such as cell proliferation, autophagy, migration, and invasion. Furthermore, DRAIC is of great clinical significance in human disease. In this review, we discuss the expression signature, clinical characteristics, biological functions, relevant mechanisms, and potential clinical applications of DRAIC in several human diseases.

KEYWORDS

DRAIC, lncRNA, biological function, mechanism, application

Introduction

Long non-coding RNA (lncRNA) is a type of non-protein-coding RNA that is longer than 200 nucleotides (1–5). With the advancement of genomics technology during the past few decades, several lncRNAs have become the focus of clinical research and were

discovered to be closely associated with the progression of human diseases (5–8). There is growing evidence that lncRNA can actively participate in the regulation of a variety of biological functions mainly through the modification of gene expression levels (9–13). These functions include cell proliferation, apoptosis, autophagy, metabolism, invasion, and migration.

The lncRNA DRAIC (Downregulated RNA In Cancer) is a 1.7 kb lncRNA located on the human chromosome 15q23 (14). lncRNA DRAIC was first discovered to act as a tumor suppressor in prostate cancer, but it appears to exert varied biological activity in different diseases. Increasing evidence has indicated that an imbalance in lncRNA DRAIC expression is involved in many diseases especially cancers, including prostate cancer (14–18), lung cancer (19–21), glioma (22–24), breast cancer (25–27), colorectal cancer (28), esophageal cancer (29), gastric cancer (30), nasopharyngeal carcinoma (31), retinoblastoma (32), in addition to Hirschsprung's disease (33, 34) and omphalocele (35). Abnormal expression levels of DRAIC have also been associated with clinicopathological features of patients, such as lymph node metastasis, neoplasm stage, overall survival and progression-free survival. More notably, lncRNA DRAIC exhibited a vital influence on the modulation of abnormal cellular processes and tumorigenesis progression through cell proliferation, invasion, migration, and autophagy. Mechanistic investigations have further prompted major advances in the clinical applications of lncRNA DRAIC, including its potential for diagnosis, prognosis, and treatment. In this review, we first focus on the biological functions, relevant mechanisms, and future clinical applications of lncRNA DRAIC, and summarize available knowledge on the expression profiles and clinical characteristics of lncRNA DRAIC in disease processes.

The role of the lncrna draic in cancers

LncRNA DRAIC was shown to be aberrantly expressed in several types of human disease, including prostate cancer, lung cancer, glioma, breast cancer, colorectal cancer, esophageal cancer,

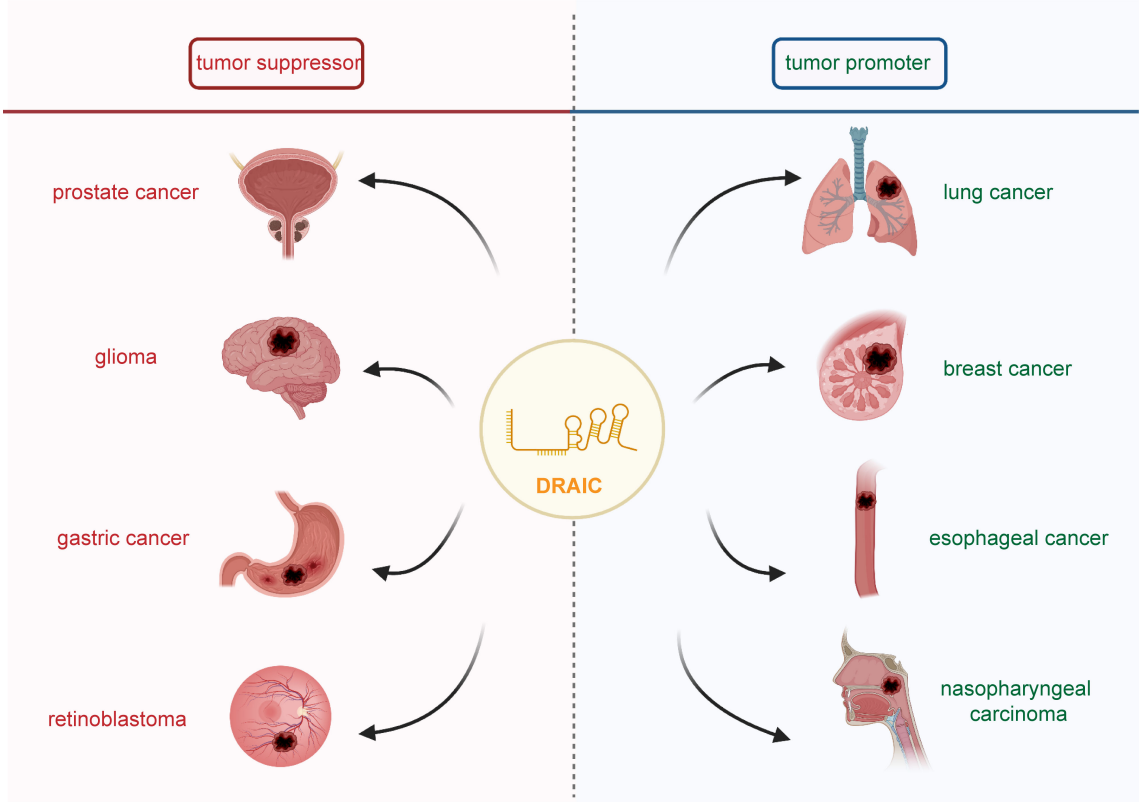

FIGURE 1
The role of lncRNA DRAIC in human cancers. It has been shown that lncRNA DRAIC acts as a tumor suppressor in prostate cancer, glioma, gastric cancer, and retinoblastoma. DRAIC also functioned as an oncogene in lung cancer, breast cancer, esophageal cancer and nasopharyngeal carcinoma.

TABLE 1 lncRNA DRAIC expression and clinical characteristics in human diseases.

Disease type	Expression	Clinical characteristics	Refs
prostate cancer	downregulated	overall survival, and disease-free survival	33430890,31900260, 28241429,27562825,25700553
lung cancer	upregulated	TNM stage, lymph node metastasis, and poor prognosis	34764698,34306024,33771173
glioma	downregulated	overall survival, and progression-free survival	34746949,33767991,33336743
breast cancer	upregulated	overall survival, and disease specific survival	34645975,30872794,30544991
esophageal cancer	upregulated	/	32659236
gastric cancer	downregulated	lymph node metastasis	32351584
nasopharyngeal carcinoma	upregulated	advanced clinical stage	31497998
retinoblastoma	downregulated	/	31058073
Hirschsprung's disease	upregulated	/	34471485,31647312
Omphalocele	downregulated	/	30538881

gastric cancer, nasopharyngeal carcinoma, retinoblastoma, Hirschsprung's disease, and omphalocele (Figure 1). Indeed, lncRNA DRAIC expression was shown to have a significant association with patient clinicopathological features (Table 1). LncRNA DRAIC also exerts key roles in multiple cellular processes *via* diverse mechanisms (Table 2).

The tumor-suppressor role of DRAIC in cancers

Prostate cancer

Prostate cancer (PCa) is the most frequent malignant tumor and accounts for the second leading cause of cancer-related deaths in men (36–40). The androgen receptor (AR) plays a crucial role in the pathogenesis of PCa and is considered a clinically validated target for the treatment of PCa (41–44). Unfortunately, long-term androgen deprivation can ultimately lead to castration-resistant PCa (CRPC), which favors metastasis and poor prognosis (45–47). Although much effort has been made to improve PCa treatment, it is still needed to identify more sensitive biomarkers to guide early diagnosis and treatment (37, 48, 49). Several studies have shown that lncRNA DRAIC is dysregulated in PCa LNCaP and C4-2B cells as well as in 7 PCa tumor biopsies by androgens in a dose and time-dependent manner (14–18). Moreover, lncRNA DRAIC was considered to be a tumor suppressor by preventing the transformation of cuboidal epithelial cells to fibroblast-like morphology as well as cell migration and invasion. *In vivo*, lncRNA prevents the growth of xenograft tumors.

Glioma

Glioma is one of the most prevalent primary malignant tumors in the central nervous system, accounting for about 81%

TABLE 2 Functions and mechanisms of lncRNA DRAIC in cancers.

Disease type	Cell lines	Functions	Related mechanisms	Refs
prostate cancer	LNCaP, and C4-2B cells	cell migration, and invasion	FOXA1, NKX3-1, IKK, and NF-κB	33430890,31900260, 28241429,27562825, 25700553
lung cancer	Calu-3, HCC827, NCI-H441, and NCI-H1975 cells	cell proliferation, migration, and invasion	miR-3940-3p	34764698,34306024, 33771173
glioma	U251, A172, U87, and U373 cells	cell proliferation, migration, invasion, and autophagy	AMPK, NF-κB, mTOR, S6K1, H3K4me3, SET7/9, and miR-18a-3p	34746949,33767991, 33336743
breast cancer	HeLa, T47D, MCF-7, SKBR3, MDA-MB-361, and MDA-MB-231 cells	cell proliferation, migration, invasion, autophagy, and apoptosis	FOXP3, miR-432-5p, and SLBP	34645975,30872794, 30544991
esophageal cancer	Eca-109, TE-1, EC9706, and OE19 cells	cell proliferation, invasion, apoptosis, and autophagy	miR-149-5p, and NFIB	32659236
gastric cancer	HGC-27, SGC-7901, BGC-823, AGS, and MKN45 cells	cell proliferation, migration, and invasion	UCHL5, and NFRKB	32351584
nasopharyngeal carcinoma	CNE-1, and C666-1 cells	cell proliferation, migration, and invasion	miR-122, and SATB1	31497998
retinoblastoma	Y79 cells	cell proliferation	/	31058073

of malignant brain tumors (50–52). lncRNA DRAIC has been shown to be downregulated in glioma tissues and cell lines (U251, A172, U87, and U373 cells) (22–24). Survival analysis has indicated that a high lncRNA DRAIC expression was associated with a remarkably favorable overall survival and progression-free survival of lower-grade glioma patients who had been submitted to radiotherapy (23). lncRNA DRAIC repressed cell proliferation, migration, invasion, and *in vivo* xenograft tumor growth, as well as induced cell autophagy in U251, A172, and U87 cells (22, 24).

Gastric cancer

Gastric cancer is one of the most frequent digestive tract cancers, which accounts for a large proportion of cancer-related morbidity and mortality worldwide (53–57). Although advances have been made in the treatment of patients with gastric cancer over the past few years, their 5-year survival rate is still lower than 25% (58–61). Of note, novel biomarkers should be identified to improve the early diagnosis and survival rates of gastric cancer patients (61–63). The expression of lncRNA DRAIC was downregulated according to tumor progression in 67 primary gastric cancer patients who were submitted to surgical resection as well as in HGC-27, SGC-7901, BGC-823, AGS and MKN45 cell lines (30). A high lncRNA DRAIC level was significantly associated with lymph node metastasis, while the downregulation of DRAIC inhibited cell proliferation and metastasis in HGC-27, MKN45, and SGC-7901 cells.

Pediatric retinoblastoma

Retinoblastoma is the most common intraocular tumor in children and is initiated by the biallelic inactivation of the retinoblastoma 1 (RB1) gene (64–68). A recent a study revealed that lncRNA DRAIC was dysregulated in retinoblastoma Y79 cells and 7 retinoblastoma tissues. This lncRNA was involved in the modulation of Y79 cell growth and proliferation (32).

The tumor-promoting role of DRAIC in cancers

Lung cancer

Lung cancer is the most commonly diagnosed malignancy worldwide and lung adenocarcinoma (LUAD) represents the most common histological type of lung cancer (69–73). A late diagnosis of LUAD contributes to high metastasis and mortality rates, emphasizing the urgency for better identification of sensitive biomarkers during lung cancer progression (69, 74–76). High expression of lncRNA DRAIC was recently observed in LUAD tissues and cell lines (Calu-3, HCC827, NCI-H441, and NCI-H1975 cells) and was positively correlated with TNM stage, lymph node metastasis, and a poor prognosis (19–21). lncRNA DRAIC has been proved to exhibit tumorigenic effects through the regulation of cell proliferation, migration, and invasion of Calu-3 and HCC827 cells.

Breast cancer

Breast cancer is a common malignancy with high incidence and morbidity rates in females (77–81). Therefore, establishing an effective biomarker is essential to decrease mortality and improve the survival rate for breast cancer patients (81–84). lncRNA DRAIC expression was distinctly upregulated in 828 breast cancer specimens and cell lines (HeLa, T47D, MCF-7, SKBR3, MDA-MB-361, and MDA-MB-231 cells). Kaplan–Meier plots and log-rank tests have shown that a high expression of lncRNA DRAIC was correlated with a poorer overall survival and disease specific survival, especially in ER-positive breast cancer patients (27). In addition, lncRNA DRAIC stimulated tumor progression through the promotion of cell proliferation, migration, and invasion, as well as the inhibition of cell autophagy and apoptosis in SKBR3, MCF-7 and MDA-MB-231 cells (25, 26).

Esophageal cancer

Esophageal cancer is a common upper gastrointestinal malignancy that ranks eighth in the world among cancer incidence, especially in China (85–89). High levels of DRAIC were found in esophageal cancer cells Eca-109, TE-1, EC9706, and OE19 (29). Moreover, DRAIC played an oncogene role since it facilitated cell proliferation and invasion, and repressed cell apoptosis and autophagy in Eca-109 and EC9706 cells.

Nasopharyngeal carcinoma

Nasopharyngeal carcinoma is an epithelial carcinoma generated within the nasopharyngeal mucosal lining (90–94). lncRNA DRAIC was highly expressed in nasopharyngeal carcinoma cell lines CNE-1 and C666-1 as well as in 32 biopsy tissues (31). Moreover, a high expression level of lncRNA DRAIC showed a close relationship with higher clinical stages. In addition, lncRNA DRAIC acted as an oncogene and enhanced cell proliferation, migration and invasion in CNE-1 and C666-1 cells.

Accumulating evidence has reported that the differential expression of DRAIC in prostate cancer, lung cancer, glioma, breast cancer, colorectal cancer, esophageal cancer, gastric

cancer, nasopharyngeal carcinoma, and retinoblastoma. And its abnormal expression was significantly related to many clinicopathological features, notably the patient's prognosis. Furthermore, DRAIC was implicated as a regulator of a wide variety of cellular processes and then participated in the pathogenesis and progression of numerous human disorders. Therefore, elucidating the underlying molecular mechanisms of DRAIC in cancer progression has been proven to hold promise to support its clinical application significance.

Regulatory mechanisms of lncrana draic

Several studies have reported that lncRNA DRAIC actively participates in crucial biological processes of many diseases, such as cell proliferation, apoptosis, autophagy, invasion and migration. Here, we discuss the main biological functions and molecular mechanisms of lncRNA DRAIC during disease progression.

Cell proliferation

It is well known that cells proliferate excessively which ultimately results in tumor progression (95–98). In glioma, lncRNA DRAIC has been demonstrated to suppress the proliferation of U251 cells by targeting miR-18a-3p (24). And lncRNA DRAIC was activated by FOXP3 in breast cancer and promoted cell proliferation in SKBR3 and MDA-MB-231 cells *via* sponging miR-432-5p to increase SLBP levels (25). lncRNA DRAIC was also found to improve MCF-7 cell proliferation in an autophagy-independent manner by regulating the activity of ULK1 and enhancing LC3B expression (26). Similarly, lncRNA DRAIC led to cell proliferation in esophageal cancer Eca-109 and EC9706 cells through the miR-149-5p/NFIB axis (29). In gastric cancer, lncRNA DRAIC has also been indicated to inhibit the proliferation of SGC-7901, HGC-27, and MKN45 cells by binding to UCHL5 and accelerating the ubiquitination of NFRKB (30). Additionally, lncRNA DRAIC increased the proliferation of nasopharyngeal carcinoma CNE-1 and C666-1 cells *via* an interaction with miR-122 and up-regulation of SATB1 (31).

Cell migration and invasion

Metastasis, also termed invasion-migration cascade, is a multistep process that involves the dissemination of tumor cells from the primary tumor site to distant organs and subsequent formation of secondary tumors (99–103). As the major reason behind most cancer-related deaths, metastasis is a current challenge to improve the survival of cancer patients (99, 104–107).

DRAIC was shown to positively regulate FOXA1 and NKX3-1 and to block the transformation of LNCaP prostate cancer cuboidal epithelial cells to a fibroblast-like morphology. This subsequently hindered cell migration and invasion through an interaction with IKK that inactivated NF-κB (Figure 2) (14, 16). In glioma cells, lncRNA DRAIC also exerted pro-migratory and invasive roles *via* the repression of NF-κB, coupled with increases in AMPK phosphorylation and thus inhibition of mTOR activity and phosphorylation of key substrates like S6K1 (22). Moreover, the interaction between the H3K4me3 protein and the lncRNA DRAIC promoter was mediated by SET7/9 and increased the association of DRAIC with miR-18a-3p. These mechanisms were shown to improve the metastasis of U251 cells (24). And in breast cancer cell lines, lncRNA DRAIC was up-regulated by FOXP3 and promoted cell migration and invasion *via* the miR-432-5p/SLBP axis (25).Moreover, lncRNA DRAIC improved esophageal cancer Eca-109 and EC9706 cell invasion through binding to miR-149-5p, which regulated NFIB levels (29). lncRNA DRAIC also hindered cell metastasis through its interaction with UCHL5 and repression of NFRKB deubiquitination in gastric cancer (30). In nasopharyngeal carcinoma cells, lncRNA DRAIC boosted cell migration and invasion through its interaction with miR-122 and the consequent increase of SATB1 levels (31). Furthermore, lncRNA DRAIC facilitated the migration of HSCR 293T and SH-SY5Y cells by sponging miR-34a-5p, which positively modulated ITGA6 expression (33).

Cell autophagy

Autophagy is a process of intracellular component degradation that maintains cellular homeostasis (26, 108–111). Its dysfunction contributes to a series of pathophysiological processes of various diseases, including cancer. Studies have identified that numerous lncRNAs regulate autophagy through various mechanisms (112–115). lncRNA DRAIC has been reported modeulate autophagy in glioblastoma A172 and U87 cells by downregulating the NF-κB target gene GLUT1, increasing AMPK levels, and thus inhibiting mTOR (22, 116). lncRNA DRAIC also suppressed cell autophagy in breast cancer MCF-7 cells through the activation of ULK1 (26). Similarly, lncRNA DRAIC was found to inhibit cell autophagy in esophageal cancer Eca-109 and EC9706 cells acting as ceRNAs to modulate the expression of NFIB by quenching miR-149-5p (Figure 3) (29). Take together, DRAIC was involved in the multiple biological process of cancers through interaction with diverse molecules (Figure 4).

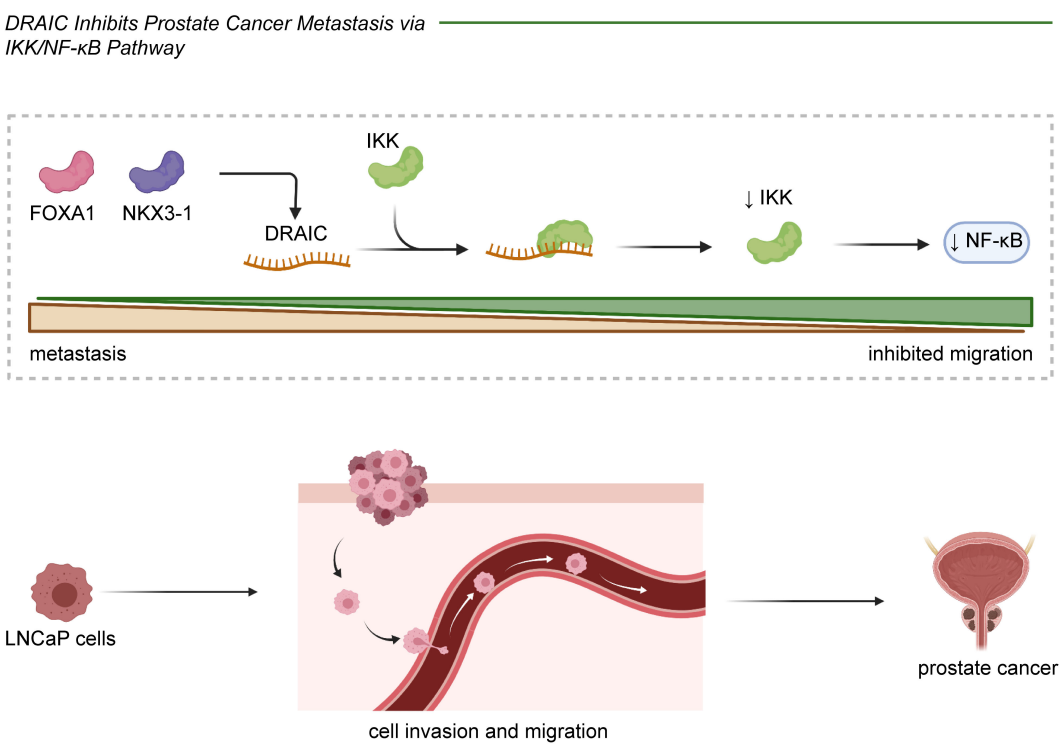

FIGURE 2
In prostate cancer, lncRNA DRAIC played a tumor suppressive role through inhibiting cell migration and invasion. DRAIC was activated by FOXA1 and NKX3-1 and interacts with IKK to further decrease NF-κB expression in LNCaP cells.

Prospects for the clinical applications of draic in disease management

In recent years, numerous studies have shown the significance of lncRNAs in clinical applications for human disease, especially in cancer (117–121). lncRNA DRAIC is a newly identified lncRNA involved in multiple human diseases. Previous evidence suggests that DRAIC is extensively involved in the modulation of numerous biological functions and intimately associated with pathological characteristics, which may be valuable for clinical diagnosis, prognosis, and treatment. In this section, we address the promising significance of lncRNA DRAIC in human disease.

DRAIC as a diagnostic and prognostic biomarker

The expression levels of lncRNA DRAIC in a diverse array of tissues and cell lines were observed to be differentially regulated depending on the disease state, which reveals that lncRNA DRAIC expression can be used to distinguish between normal and diseased tissues. Therefore, assessing lncRNA DRAIC concentration may effectively act as a method for the early diagnosis of diseases. Besides, increasing data supports that lncRNA DRAIC expression is significantly associated with a variety of clinicopathological features, demonstrating the promising potential for prognosis prediction. For example, lower levels of DRAIC were observed as PCa progressed from AD to CR. This was associated with a lower disease-free-survival rate of patients verified by the Kaplan-Meier plot (14). lncRNA DRAIC was overexpressed at a higher level in high malignancy breast cancers when compared to low malignancy cases, suggesting its diagnostic and prognostic value (27). In low-grade glioma, DRAIC was shown to reflect the prognosis of radiotherapy treatment (27). Additionally, lncRNA DRAIC was perceived as a novel prognosis biomarker for risk evaluation of HSCR (34). In LUAD, lncRNA DRAIC was regarded as an immune-related RNA and incorporated into the 5-lncRNA-based model and 5-lncRNA risk signature, which has been shown to accurately predict the prognosis of patients (20, 21). However, lncRNA DRAIC was mainly measured in cell lines and tissues, which must be optimized to a more accessible and convenient approach. Tissue biopsy has several drawbacks, such

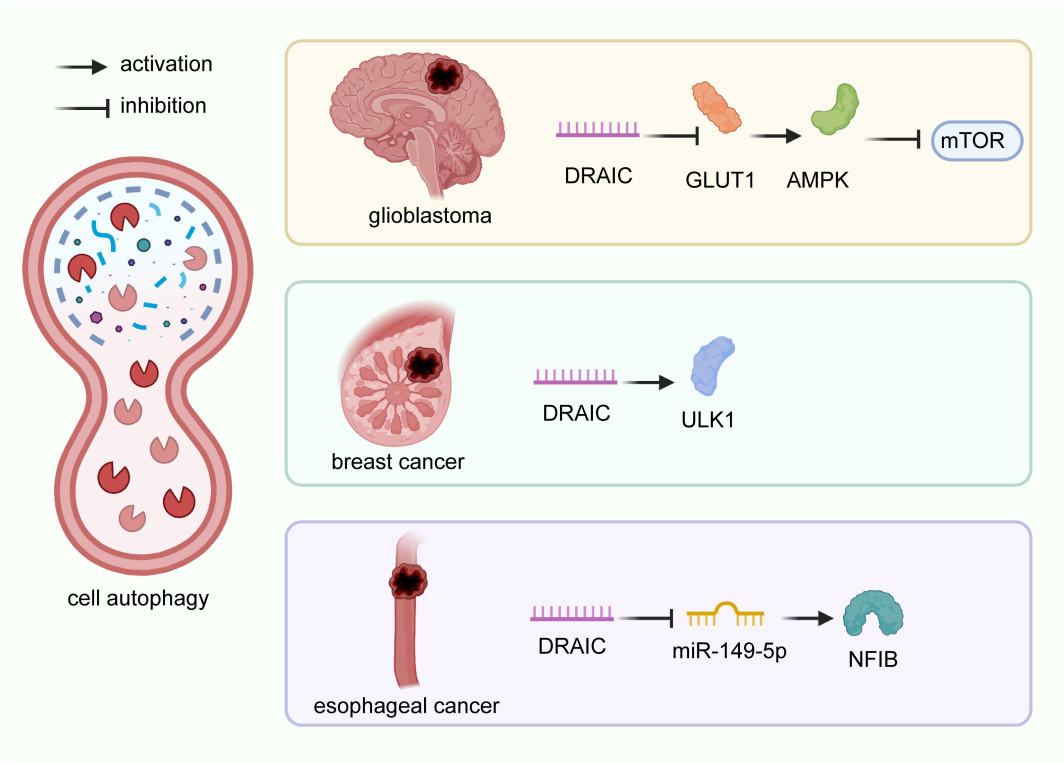

FIGURE 3
Regulatory mechanisms of DRAIC on cell autophagy in cancers. In glioblastoma A172 and U87 cells, lncRNA DRAIC induced autophagy by downregulating the NF-κB target gene GLUT1, which activated AMPK, and blocked the expression of mTOR. In breast cancer MCF-7 cells, DRAIC enhanced ULK1 expression and inhibited cell autophagy. In esophageal cancer, lncRNA DRAIC suppressed cell autophagy through its interaction with miR-149-5p and up-regulation of NFIB.

as invasiveness, complicated manipulation, high cost, bleeding complications, poor reproducibility, and sampling variability. Minimally invasive (e.g., saliva, urine, and blood) detection of lncRNA DRAIC expression and sensitivity is an increasing research interest for its diagnostic and prognostic applications.

LncRNA DRAIC as a treatment target

The abnormal expression of lncRNA DRAIC in disease also provided novel insights for disease treatment. Alterations of lncRNA DRAIC expression may be developed as a therapeutic target for the inhibition of disease progression. Furthermore, the molecular mechanisms through which DRAIC regulates the pathogenesis of diseases also resulted in an effective therapy target. Knockdown or activation of lncRNA DRAIC and relevant molecules, as well as the regulation of intramolecular interactions, may also serve as potential targeting candidates for novel pharmaceutical development and molecular-targeted therapies (122). Indeed, lncRNA DRAIC knockout was confirmed to suppress the tumorigenesis of PCa PC3M cells by inhibiting the NF-κB pathway in nude mice. Moreover, lncRNA DRAIC expression was shown to reflect the sensitivity of tumor cells to chemotherapy or radiotherapy. For example, lncRNA DRAIC expression was demonstrated to predict patient response to radiosensitivity in lower-grade glioma (23). In breast cancer, the expression level of lncRNA DRAIC can reflect the efficacy of chemotherapy drugs, such as paclitaxel, FEC, and lapatinib, which may contribute to guiding more sensitized and individualized treatment options for patients (27). In addition, existing research on DRAIC has mainly been concentrated on the cellular level with a deficiency of *in vivo* studies. lncRNA DRAIC was currently explored in only a small portion of human diseases, and there is little known about the multifaceted role and functional mechanisms of DRAIC in other types of disease. Further *in vivo* experiments are required to determine whether the molecular mechanisms of lncRNA DRAIC on disease progression discovered by *in vitro* studies are consistent. Besides, more mechanistic insights of lncRNA DRAIC in other diseases probably also contribute to the development of better-targeted therapeutics.

In general, lncRNA DRAIC was proved to be a potential diagnostic and prognosis biomarker, together with a treatment target for human cancers. Further investigation is needed to determine the expression profile, sensitivity and stability of

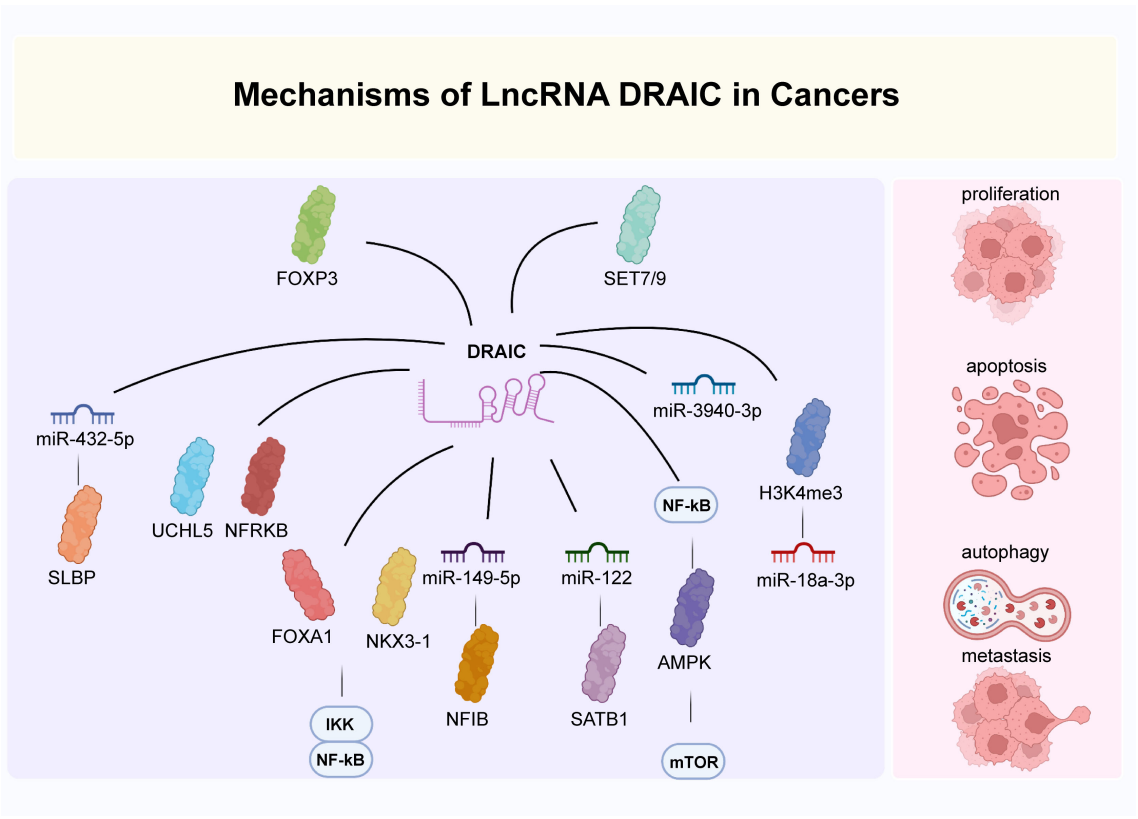

FIGURE 4
The main mechanisms of DRAIC in cancers. DRAIC participated in the regulation of biological processes of cancers through interaction with diverse molecules.

lncRNA DRAIC in non-invasive samples. This could improve disease diagnosis and prognosis as well as the efficiency and safety of lncRNA DRAIC-targeted treatment.

Conclusion

Numerous reports have shown that lncRNA DRAIC is abnormally expressed in PCa, lung cancer, glioma, breast cancer, colorectal cancer, esophageal cancer, gastric cancer, nasopharyngeal carcinoma, retinoblastoma, HSRC, and omphalocele. Moreover, lncRNA DRAIC exhibited a significant association with patient clinicopathological characteristics, especially immune cell infiltration, tumor stage, lymph node metastasis, overall survival and progression-free survival. lncRNA DRAIC was demonstrated to exert momentous roles in multiple cellular process, such as cell proliferation, invasion, migration, and autophagy. Functional assays have revealed a series of molecular mechanisms of lncRNA DRAIC in the development of diseases. These features can be exploited for various medicinal applications, including diagnosis, prognosis and treatment of human diseases.

Extensive research has been undertaken to explore the clinical application of lncRNAs in the past few years (123). The majority of non-invasive biopsy biomarkers are currently being investigated for diagnostic and prognostic purposes (124). The detection of lncRNA DRAIC expression can be used as a promising clinical biomarker for early diagnosis and prognosis. Additional studies are necessary to validate whether lncRNA DRAIC can be detected in non-invasive samples and further verify the stability and specificity of its expression in non-invasive samples. Moreover, lncRNA DRAIC and the relevant molecular pathways may also be applied as new candidates for targeted treatment of several diseases. However, the available studies mainly focus on the expression of lncRNA DRAIC on clinical tissue samples and *in-vitro* cell lines, lacking enough *in vivo* animal studies. The follow-up animal experiments and prospective studies are needed to confirm the efficacy and safety of lncRNA DRAIC-targeted therapy. And the roles and mechanisms of lncRNA DRAIC have merely been explored in a

comparably small number of diseases. It is necessary to further probe the role of lncRNA DRAIC in other disease types.

Author contributions

DC provided a source of ideas for this review. XZ collected the related paper. QY drafted and reviewed the manuscript. All authors have contributed substantially to the original research and approved the submitted version.

Funding

This work was funded by the National Nature Science Foundation (81802085).

Conflict of interest

The authors declare that the research was conducted in the absence of any commercial or financial relationships that could be construed as a potential conflict of interest.

Publisher's note

All claims expressed in this article are solely those of the authors and do not necessarily represent those of their affiliated organizations, or those of the publisher, the editors and the reviewers. Any product that may be evaluated in this article, or claim that may be made by its manufacturer, is not guaranteed or endorsed by the publisher.

References

1. Huang X, Sun L, Wen S, Deng D, Wan F, He X, et al. RNA Sequencing of plasma exosomes revealed novel functional long noncoding RNAs in hepatocellular carcinoma. *Cancer Sci* (2020) 9:3338–49. doi: 10.1111/cas.14516

2. Zhou Q, Hou Z, Zuo S, Zhou X, Feng Y, Sun Y, et al. LUCAT1 promotes colorectal cancer tumorigenesis by targeting the ribosomal protein L40-MDM2-p53 pathway through binding with UBA52. *Cancer Sci* (2019) 4:1194–207. doi: 10.1111/cas.13951

3. Braicu C, Zimta AA, Harangus A, Iurca I, Irimie A, Coza O, et al. The function of non-coding RNAs in lung cancer tumorigenesis. *Cancers (Basel)* (2019) 5:605. doi: 10.3390/cancers11050605

4. Lu W, Cao F, Wang S, Sheng X, Ma J. LncRNAs: The regulator of glucose and lipid metabolism in tumor cells. *Front Oncol* (1099) 2019). doi: 10.3389/fonc.2019.01099

5. Pan H, Ding Y, Jiang Y, Xia X, Ji Y. LncRNA LIFR-AS1 promotes proliferation and invasion of gastric cancer cell *via* miR-29a-3p/COL1A2 axis. *Cancer Cell Int* (2021) 1:7. doi: 10.1186/s12935-020-01644-7

6. Yang YT, Wang YF, Lai JY, Ming X, Tu YF, Tian J, et al. Long non-coding RNA UCA1 contributes to the progression of oral squamous cell carcinoma by regulating the WNT/β-catenin signaling pathway. *Cancer Sci* (2016) 11:1581–9. doi: 10.1111/cas.13058

7. Sun W, Nie W, Wang Z, Zhang H, Li Y, Fang X, et al. Lnc HAGLR promotes colon cancer progression through sponging miR-185-5p and activating CDK4 and CDK6 *in vitro* and in vivo. *Onco Targets Ther* (2020) 13:5913–25. doi: 10.2147/OTT.S246092

8. Parfenyev S, Singh A, Fedorova O, Daks A, Kulshreshtha R, Barlev NA, et al. Interplay between p53 and non-coding RNAs in the regulation of EMT in breast cancer. *Cell Death Dis* (2021) 1:17. doi: 10.1038/s41419-020-03327-7

9. Hu X, Goswami S, Qiu J, Chen Q, Laverdure S, Sherman BT, et al. Profiles of long non-coding RNAs and mRNA expression in human macrophages regulated by interleukin-27. *Int J Mol Sci* (2019) 24:6207. doi: 10.3390/ijms20246207

10. Prensner JR, Chinnaiyan AM. The emergence of lncRNAs in cancer biology. *Cancer Discov* (2011) 5:391–407. doi: 10.1158/2159-8290.CD-11-0209

11. Ulitsky I, Bartel DP. lincRNAs: genomics, evolution, and mechanisms. *Cell* (2013) 1:26–46. doi: 10.1016/j.cell.2013.06.020

12. Wang LQ, Zheng YY, Zhou HJ, Zhang XX, Wu P, Zhu SM. LncRNA-fendrr protects against the ubiquitination and degradation of NLRC4 protein through HERC2 to regulate the pyroptosis of microglia. *Mol Med (Cambridge Mass)* (2021) 1:39. doi: 10.1186/s10020-021-00299-y

13. Li X, Wu Z, Fu X, Han W. lncRNAs: insights into their function and mechanics in underlying disorders. *Mutat Res Rev Mutat Res* (2014) 762:1–21. doi: 10.1016/j.mrrev.2014.04.002

14. Sakurai K, Reon BJ, Anaya J, Dutta A. The lncRNA DRAIC/PCAT29 locus constitutes a tumor-suppressive nexus. *Mol Cancer Res* (2015) 5:828–38. doi: 10.1158/1541-7786.MCR-15-0016-T

15. Videira A, Beckedorff FC, daSilva LF, Verjovski-Almeida S. PVT1 signals an androgen-dependent transcriptional repression program in prostate cancer cells and a set of the repressed genes predicts high-risk tumors. *Cell Commun Signal* (2021) 1:5. doi: 10.1186/s12964-020-00691-x

16. Saha S, Kiran M, Kuscu C, Chatrath A, Wotton D, Mayo MW, et al. Long noncoding RNA DRAIC inhibits prostate cancer progression by interacting with IKK to inhibit NF-κB activation. *Cancer Res* (2020) 5:950–63. doi: 10.1158/0008-5472.CAN-19-3460

17. Smolle MA, Bauernhofer T, Pummer K, Calin GA, Pichler M. Current insights into long non-coding RNAs (LncRNAs) in prostate cancer. *Int J Mol Sci* (2017) 2:473. doi: 10.3390/ijms18020473

18. Colditz J, Rupf B, Maiwald C, Baniahmad A. Androgens induce a distinct response of epithelial-mesenchymal transition factors in human prostate cancer cells. *Mol Cell Biochem* (2016) 1-2:139–47. doi: 10.1007/s11010-016-2794-y

19. Liu Z, Yang S, Zhou S, Dong S, Du J. Prognostic value of lncRNA DRAIC and miR-3940-3p in lung adenocarcinoma and their effect on lung adenocarcinoma cell progression. *Cancer Manage Res* (2021) 13:8367–76. doi: 10.2147/CMAR.S320616

20. Wu G, Wang Q, Zhu T, Fu L, Li Z, Wu Y, et al. Identification and validation of immune-related LncRNA prognostic signature for lung adenocarcinoma. *Front Genet* (2021) 12:681277. doi: 10.3389/fgene.2021.681277

21. Mu L, Ding K, Tu R, Abounader R, Dutta A. Identification of 4 immune cells and a 5-lncRNA risk signature with prognosis for early-stage lung adenocarcinoma. *J Trans Med* (2021) 1:127. doi: 10.1186/s12967-021-02800-x

22. Saha S, Zhang Y, Wilson B, Abounader R, Dutta A. The tumor-suppressive long noncoding RNA DRAIC inhibits protein translation and induces autophagy by activating AMPK. *J Cell Sci* (2021) 24:jcs259306. doi: 10.1242/jcs.259306

23. Li Z, Cai S, Li H, Gu J, Tian Y, Cao J, et al. Developing a lncRNA signature to predict the radiotherapy response of lower-grade gliomas using Co-expression and ceRNA network analysis. *Front Oncol* (2021) 11:622880. doi: 10.3389/fonc.2021.622880

24. Li C, Feng SY, Chen L. SET7/9 promotes H3K4me3 at lncRNA DRAIC promoter to modulate growth and metastasis of glioma. *Eur Rev Med Pharmacol Sci* (2020) 23:12241–50. doi: 10.26355/eurrev_202012_24016

25. Li S, Jia H, Zhang Z, Wu D. DRAIC promotes growth of breast cancer by sponging miR-432-5p to upregulate SLBP. *Cancer Gene Ther* (2021) 29:951–60. doi: 10.1038/s41417-021-00388-4

26. Tiessen I, Abildgaard MH, Lubas M, Gylling HM, Steinhauer C, Pietras EJ, et al. A high-throughput screen identifies the long non-coding RNA DRAIC as a regulator of autophagy. *Oncogene* (2019) 26:5127–41. doi: 10.1038/s41388-019-0783-9

27. Zhao D, Dong JT. Upregulation of long non-coding RNA DRAIC correlates with adverse features of breast cancer. *Noncoding RNA* (2018) 4:39. doi: 10.3390/ncrna4040039

28. Zhang C, Wang Y, Wang P, Jiang L, Xiao X. LncRNA DRAIC promotes apoptosis and inhibits proliferation of colorectal cancer *via* regulating MiR-223. *Minerva Med* (2021) 10.23736:S0026–4806. doi: 10.23736/S0026-4806.21.07605-9

29. Li F, Zhou X, Chen M, Fan W. Regulatory effect of LncRNA DRAIC/miR-149-5p/NFIB molecular network on autophagy of esophageal cancer cells and its biological behavior. *Exp Mol Pathol* (2020) 116:104491. doi: 10.1016/j.yexmp.2020.104491

30. Zhang Z, Hu X, Kuang J, Liao J, Yuan Q. LncRNA DRAIC inhibits proliferation and metastasis of gastric cancer cells through interfering with NFRKB deubiquitination mediated by UCHL5. *Cell Mol Biol Lett* (2020) 25:29. doi: 10.1186/s11658-020-00221-0

31. Liao B, Wang Z, Zhu Y, Wang M, Liu Y. Long noncoding RNA DRAIC acts as a microRNA-122 sponge to facilitate nasopharyngeal carcinoma cell proliferation, migration and invasion *via* regulating SATB1. *Artif Cells Nanomed Biotechnol* (2019) 1:3585–97. doi: 10.1080/21691401.2019.1656638

32. Rajasekaran S, Nagarajha Selvan LD, Dotts K, Kumar R, Rishi P, Khetan V, et al. Non-coding and coding transcriptional profiles are significantly altered in pediatric retinoblastoma tumors. *Front Oncol* (2019) 221. doi: 10.3389/fonc.2019.00221

33. Sun C, Xu B, Wang L, Su Y. LncRNA DRAIC regulates cell proliferation and migration by affecting the miR-34a-5p/ITGA6 signal axis in hirschsprung's disease. *Ups J Med Sci* (2021) 126:10.48101. doi: 10.48101/ujms.v126.7895

34. Niu X, Xu Y, Gao N, Li A. Weighted gene coexpression network analysis reveals the critical lncRNAs and mRNAs in development of hirschsprung's disease. *J Comput Biol* (2020) 7:1115–29. doi: 10.1089/cmb.2019.0261

35. Zhou HF, O'Conor CJ, Gangahar C, Dehner LP. 15q23 gain in a neonate with a giant omphalocele and multiple Co-occurring anomalies. *Case Rep Pediatr* (2018) 2018:8702568. doi: 10.1155/2018/8702568

36. Masato M, Miyata Y, Kurata H, Ito H, Mitsunari K, Asai A, et al. Oral administration of e-type prostanoid (EP) 1 receptor antagonist suppresses carcinogenesis and development of prostate cancer *via* upregulation of apoptosis in an animal model. *Sci Rep* (2021) 1:20279. doi: 10.1038/s41598-021-99694-y

37. Zhou J, Wang H, Cannon V, Wolcott KM, Song H, Yates C, et al. Side population rather than CD133(+) cells distinguishes enriched tumorigenicity in hTERT-immortalized primary prostate cancer cells. *Mol Cancer* (2011) 10:112. doi: 10.1186/1476-4598-10-112

38. Torre LA, Siegel RL, Ward EM, Jemal A. Global cancer incidence and mortality rates and trends–an update. *Cancer Epidemiol Biomarkers Prev* (2016) 1:16–27. doi: 10.1158/1055-9965.EPI-15-0578

39. Conte A, Kisslinger A, Procaccini C, Paladino S, Oliviero O, de Amicis F, et al. Convergent effects of resveratrol and PYK2 on prostate cells. *Int J Mol Sci* (2016) 9:1542. doi: 10.3390/ijms17091542

40. T JMC, Arif M, Niessen WJ, Schoots IG, Veenland JF. Automated classification of significant prostate cancer on MRI: A systematic review on the performance of machine learning applications. *Cancers (Basel)* (2020) 6:1606. doi: 10.3390/cancers12061606

41. Li Q, Deng Q, Chao HP, Liu X, Lu Y, Lin K, et al. Linking prostate cancer cell AR heterogeneity to distinct castration and enzalutamide responses. *Nat Commun* (2018) 1:3600. doi: 10.1038/s41467-018-06067-7

42. Baumgart SJ, Nevedomskaya E, Lesche R, Newman R, Mumberg D, Haendler B, et al. Darolutamide antagonizes androgen signaling by blocking enhancer and super-enhancer activation. *Mol Oncol* (2020) 9:2022–39. doi: 10.1002/1878-0261.12693

43. Shiota M, Fujimoto N, Kashiwagi E, Eto M. The role of nuclear receptors in prostate cancer. *Cells* (2019) 6:602. doi: 10.3390/cells8060602

44. Schneider JA, Craven TW, Kasper AC, Yun C, Haugbro M, Briggs EM, et al. Design of peptoid-peptide macrocycles to inhibit the β-catenin TCF interaction in prostate cancer. *Nat Commun* (2018) 1:4396. doi: 10.1038/s41467-018-06845-3

45. Song J, Chen W, Zhu G, Wang W, Sun F, Zhu J, et al. Immunogenomic profiling and classification of prostate cancer based on HIF-1 signaling pathway. *Front Oncol* (2020) 1374. doi: 10.3389/fonc.2020.01374

46. Ma Y, Fan B, Ren Z, Liu B, Wang Y. Long noncoding RNA DANCR contributes to docetaxel resistance in prostate cancer through targeting the miR-34a-5p/JAG1 pathway. *Onco Targets Ther* (2019) 12:5485–97. doi: 10.2147/OTT.S197009

47. Takayama KI, Kosaka T, Suzuki T, Hongo H, Oya M, Fujimura T, et al. Subtype-specific collaborative transcription factor networks are promoted by OCT4 in the progression of prostate cancer. *Nat Commun* (2021) 1:3766. doi: 10.1038/s41467-021-23974-4

48. Abou D, Benabdallah N, Jiang W, Peng L, Zhang H, Villmer A, et al. Prostate cancer theranostics - an overview. *Front Oncol* (2020) 884. doi: 10.3389/fonc.2020.00884

49. Qian Y, Zhang L, Cai M, Li H, Xu H, Yang H, et al. The prostate cancer risk variant rs55958994 regulates multiple gene expression through extreme long-range chromatin interaction to control tumor progression. *Sci Adv* (2019) 7:eaaw6710. doi: 10.1126/sciadv.aaw6710

50. Louis DN, Ohgaki H, Wiestler OD, Cavenee WK, Burger PC, Jouvet A, et al. The 2007 WHO classification of tumours of the central nervous system. *Acta Neuropathol* (2007) 2:97–109. doi: 10.1007/s00401-007-0243-4

51. Weller M, Wick W, Aldape K, Brada M, Berger M, Pfister SM, et al. Glioma. *Nat Rev Dis Primers* (2015) 1:15017. doi: 10.1038/nrdp.2015.17

52. Ostrom QT, Cioffi G, Gittleman H, Patil N, Waite K, Kruchko C, et al. CBTRUS statistical report: Primary brain and other central nervous system tumors diagnosed in the united states in 2012-2016. *Neuro Oncol* (2019) Suppl 5:v1–v100. doi: 10.1093/neuonc/noz150

53. Sun J, Wang X, Zhang Z, Zeng Z, Ouyang S, Kang W, et al. The sensitivity prediction of neoadjuvant chemotherapy for gastric cancer. *Front Oncol* (2021) 11:641304. doi: 10.3389/fonc.2021.641304

54. Maruyama R, Akino K, Toyota M, Suzuki H, Imai T, Ohe-Toyota M, et al. Cytoplasmic RASSF2A is a proapoptotic mediator whose expression is epigenetically silenced in gastric cancer. *Carcinogenesis* (2008) 7:1312–8. doi: 10.1093/carcin/bgn060

55. Yang Y, Wu F, Zhang J, Sun R, Li F, Li Y, et al. EGR1 interacts with DNMT3L to inhibit the transcription of miR-195 and plays an anti-apoptotic role in the development of gastric cancer. *J Cell Mol Med* (2019) 11:7372–81. doi: 10.1111/jcmm.14597

56. Bray F, Ferlay J, Soerjomataram I, Siegel RL, Torre LA, Jemal A, et al. Global cancer statistics 2018: GLOBOCAN estimates of incidence and mortality worldwide for 36 cancers in 185 countries. *CA Cancer J Clin* (2018) 6:394–424. doi: 10.3322/caac.21492

57. Van Cutsem E, Sagaert X, Topal B, Haustermans K, Prenen H. Gastric cancer. *Lancet (Lond Engl)* (2016) 10060:2654–64. doi: 10.1016/S0140-6736(16)30354-3

58. Hayakawa Y, Fox JG, Gonda T, Worthley DL, Muthupalani S, Wang TC. Mouse models of gastric cancer. *Cancers (Basel)* (2013) 1:92–130. doi: 10.3390/cancers5010092

59. Zhao CM, Hayakawa Y, Kodama Y, Muthupalani S, Westphalen CB, Andersen GT, et al. Denervation suppresses gastric tumorigenesis. *Sci Trans Med* (2014) 250:250ra115. doi: 10.1126/scitranslmed.3009569

60. Fu DJ, Wang L, Chouairi FK, Rose IM, Abetov DA, Miller AD, et al. Gastric squamous-columnar junction contains a large pool of cancer-prone immature osteopontin responsive Lgr5(-)CD44(+) cells. *Nat Commun* (2020) 1:84. doi: 10.1038/s41467-019-13847-2

61. Ye D, Li Y, Zhang H, Zhou Z, Tang Y, Wu P, et al. Silencing PRSS1 suppresses the growth and proliferation of gastric carcinoma cells *via* the ERK pathway. *Int J Biol Sci* (2021) 4:957–71. doi: 10.7150/ijbs.52591

62. Cao G, Li P, He X, Jin M, Li M, Chen S, et al. FHL3 contributes to EMT and chemotherapy resistance through up-regulation of slug and activation of TGFβ/Smad-independent pathways in gastric cancer. *Front Oncol* (2021) 11:649029. doi: 10.3389/fonc.2021.649029

63. Yang X, Zhang Z, Zhang L, Zhou L. MicroRNA hsa-mir-3923 serves as a diagnostic and prognostic biomarker for gastric carcinoma. *Sci Rep* (2020) 1:4672. doi: 10.1038/s41598-020-61633-8

64. Wei R, Ren X, Kong H, Lv Z, Chen Y, Tang Y, et al. Rb1/Rbl1/Vhl loss induces mouse subretinal angiomatous proliferation and hemangioblastoma. *JCI Insight* (2019) 22:e127889. doi: 10.1172/jci.insight.127889

65. Xie C, Lu H, Nomura A, Hanse EA, Forster CL, Parker JB, et al. Co-Deleting pten with Rb in retinal progenitor cells in mice results in fully penetrant bilateral retinoblastomas. *Mol Cancer* (2015) 14:93. doi: 10.1186/s12943-015-0360-y

66. Simeonova I, Lejour V, Bardot B, Bouarich-Bourimi R, Morin A, Fang M, et al. Fuzzy tandem repeats containing p53 response elements may define species-specific p53 target genes. *PloS Genet* (2012) 6:e1002731. doi: 10.1371/journal.pgen.1002731

67. Chen S, Chen X, Luo Q, Liu X, Wang X, Cui Z, et al. Retinoblastoma cell-derived exosomes promote angiogenesis of human vesicle endothelial cells through microRNA-92a-3p. *Cell Death Dis* (2021) 7:695. doi: 10.1038/s41419-021-03986-0

68. Shields CL, Shields JA. Retinoblastoma management: advances in enucleation, intravenous chemoreduction, and intra-arterial chemotherapy. *Curr Opin Ophthalmol* (2010) 3:203–12. doi: 10.1097/ICU.0b013e328338676a

69. Yu Y, Wang Z, Zheng Q, Li J. GREB1L overexpression correlates with prognosis and immune cell infiltration in lung adenocarcinoma. *Sci Rep* (2021) 1:13281. doi: 10.1038/s41598-021-92695-x

70. Kim C, Xi L, Cultraro CM, Wei F, Jones G, Cheng J, et al. Longitudinal circulating tumor DNA analysis in blood and saliva for prediction of response to osimertinib and disease progression in EGFR-mutant lung adenocarcinoma. *Cancers (Basel)* (2021) 13:3342. doi: 10.3390/cancers13133342

71. Gong WJ, Liu JY, Yin JY, Cui JJ, Xiao D, Zhuo W, et al. Resistin facilitates metastasis of lung adenocarcinoma through the TLR4/Src/EGFR/PI3K/NF-κB pathway. *Cancer Sci* (2018) 8:2391–400. doi: 10.1111/cas.13704

72. Kim C, Giaccone G. Precision oncology in non-small-cell lung cancer: opportunities and challenges. *Nat Rev Clin Oncol* (2018) 6:348–9. doi: 10.1038/s41571-018-0008-0

73. Stahel RA. Adenocarcinoma, a molecular perspective. *Ann Oncol* (2007) 18: ix147–9. doi: 10.1093/annonc/mdm310

74. Zong S, Jiao Y, Liu X, Mu W, Yuan X, Qu Y, et al. FKBP4 integrates FKBP4/Hsp90/IKK with FKBP4/Hsp70/RelA complex to promote lung adenocarcinoma progression *via* IKK/NF-κB signaling. *Cell Death Dis* (2021) 6:602. doi: 10.1038/s41419-021-03857-8

75. Bouzidi A, Magnifico MC, Paiardini A, Macone A, Boumis G, Giardina G, et al. Cytosolic serine hydroxymethyltransferase controls lung adenocarcinoma cells migratory ability by modulating AMP kinase activity. *Cell Death Dis* (2020) 11:1012. doi: 10.1038/s41419-020-03215-0

76. Cheung CHY, Juan HF. Quantitative proteomics in lung cancer. *J BioMed Sci* (2017) 1:37. doi: 10.1186/s12929-017-0343-y

77. Yin J, Lang T, Cun D, Zheng Z, Huang Y, Yin Q, et al. pH-sensitive nano-complexes overcome drug resistance and inhibit metastasis of breast cancer by silencing akt expression. *Theranostics* (2017) 17:4204–16. doi: 10.7150/thno.21516

78. Gomes LR, Rocha CRR, Martins DJ, Fiore APZP, Kinker GS, Bruni-Cardoso A, et al. ATR mediates cisplatin resistance in 3D-cultured breast cancer cells *via* translesion DNA synthesis modulation. *Cell Death Dis* (2019) 6:459. doi: 10.1038/s41419-019-1689-8

79. Early Breast Cancer Trialists' Collaborative Group (EBCTCG). Effects of chemotherapy and hormonal therapy for early breast cancer on recurrence and 15-year survival: an overview of the randomised trials. *Lancet (Lond Engl)* (2005) 9472:1687–717. doi: 10.1016/S0140-6736(05)66544-0

80. Gerber B, Freund M, Reimer T. Recurrent breast cancer: treatment strategies for maintaining and prolonging good quality of life. *Dtsch Arztebl Int* (2010) 6:85–91. doi: 10.3238/arztebl.2010.0085

81. Kast K, Rhiem K. Familial breast cancer - targeted therapy in secondary and tertiary prevention. *Breast Care (Basel Switzerland)* (2015) 1:27–31. doi: 10.1159/000380756

82. Cardoso F, Harbeck N, Fallowfield L, Kyriakides S, Senkus E. Locally recurrent or metastatic breast cancer: ESMO clinical practice guidelines for diagnosis, treatment and follow-up. *Ann Oncol* (2012) 23:vii11–9. doi: 10.1093/annonc/mds232

83. Qian D, Zheng Q, Wu D, Ye B, Qian Y, Zhou T, et al. Integrated analysis of ceRNA network reveals prognostic and metastasis associated biomarkers in breast cancer. *Front Oncol* (2021) 11:670138. doi: 10.3389/fonc.2021.670138

84. Groza IM, Braicu C, Jurj A, Zanoaga O, Lajos R, Chiroi P, et al. Cancer-associated stemness and epithelial-to-Mesenchymal transition signatures related to breast invasive carcinoma prognostic. *Cancers (Basel)* (2020) 10:3053. doi: 10.3390/cancers12103053

85. Zha W, Li X, Tie X, Xing Y, Li H, Gao F, et al. The molecular mechanisms of the long noncoding RNA SBF2-AS1 in regulating the proliferation of oesophageal squamous cell carcinoma. *Sci Rep* (2021) 1:805. doi: 10.1038/s41598-020-80817-w

86. Vrána D, Matzenauer M, Neoral Č, Aujeský R, Vrba R, Melichar B, et al. From tumor immunology to immunotherapy in gastric and esophageal cancer. *Int J Mol Sci* (2018) 1:13. doi: 10.3390/ijms20010013

87. Siegel RL, Miller KD, Jemal A. Cancer statistics, 2019. *CA Cancer J Clin* (2019) 1:7–34. doi: 10.3322/caac.21551

88. Chen JL, Lin ZX, Qin YS, She YQ, Chen Y, Chen C, et al. Overexpression of long noncoding RNA LINC01419 in esophageal squamous cell carcinoma and its relation to the sensitivity to 5-fluorouracil by mediating GSTP1 methylation. *Ther Adv Med Oncol* (2019) 11:1758835919838958. doi: 10.1177/1758835919838958

89. Xue Y, Zhou X, Xue L, Zhou R, Luo J. The role of pretreatment prognostic nutritional index in esophageal cancer: A meta-analysis. *J Cell Physiol* (2019) 11:19655–62. doi: 10.1002/jcp.28565

90. Yang SS, Guo JG, Liu JN, Liu ZQ, Chen EN, Chen CY, et al. Effect of induction chemotherapy in nasopharyngeal carcinoma: An updated meta-analysis. *Front Oncol* (2020) 591205. doi: 10.3389/fonc.2020.591205

91. Zhao Y, Zhou Q, Li N, Shen L, Li Z. Paranasal sinus invasion should be classified as T4 disease in advanced nasopharyngeal carcinoma patients receiving radiotherapy. *Front Oncol* (2020) 10:01465. doi: 10.3389/fonc.2020.01465

92. Li Z, Zhou Z, Wu X, Zhou Q, Liao C, Liu Y, et al. LMP1 promotes nasopharyngeal carcinoma metastasis through NTRK2-mediated anoikis resistance. *Am J Cancer Res* (2020) 7:2083–99.

93. Li HP, Huang CY, Lui KW, et al. Combination of epithelial growth factor receptor blockers and CDK4/6 inhibitor for nasopharyngeal carcinoma treatment. *Cancers (Basel)* (2021) 12:2954. doi: 10.3390/cancers13122954

94. Yu MC, Yuan JM. Epidemiology of nasopharyngeal carcinoma. *Semin Cancer Biol* (2002) 6:421–9. doi: 10.1016/S1044579X02000858

95. Wang X, Liang H, Xu W, Ma X. Wallenda-nmo axis regulates growth *via* hippo signaling. *Front Cell Dev Biol* (2021) 9:658288. doi: 10.3389/fcell.2021.658288

96. Zhao F, Feng Y, Zhang X, Liu X, Li A. Kinesin superfamily member 18B (KIF18B) promotes cell proliferation in colon adenocarcinoma. *Cancer Manag Res* (2020) 12:12769–78. doi: 10.2147/CMAR.S261894

97. Collins K, Jacks T, Pavletich NP. The cell cycle and cancer. *Proc Natl Acad Sci U S A* (1997) 7:2776–8. doi: 10.1073/pnas.94.7.2776

98. Kar S. Unraveling cell-cycle dynamics in cancer. *Cell Syst* (2016) 1:8–10. doi: 10.1016/j.cels.2016.01.007

99. Wan L, Pantel K, Kang Y. Tumor metastasis: moving new biological insights into the clinic. *Nat Med* (2013) 11:1450–64. doi: 10.1038/nm.3391

100. Mitra P, Kalailingam P, Tan HB, Thanabalu T. Overexpression of GRB2 enhances epithelial to mesenchymal transition of A549 cells by upregulating SNAIL expression. *Cells* (2018) 8:97. doi: 10.3390/cells7080097

101. Giubellino A, Burke TRJr., Bottaro DP. Grb2 signaling in cell motility and cancer. *Expert Opin Ther Targets* (2008) 8:1021–33. doi: 10.1517/14728222.12.8.1021

102. Steeg PS. Targeting metastasis. *Nat Rev Cancer* (2016) 4:201–18. doi: 10.1038/nrc.2016.25

103. Massagué J, Obenauf AC. Metastatic colonization by circulating tumour cells. *Nature* (2016) 7586:298–306. doi: 10.1038/nature17038

104. Zhang Z, Li J, Ou Y, Yang G, Deng K, Wang Q, et al. CDK4/6 inhibition blocks cancer metastasis through a USP51-ZEB1-dependent deubiquitination mechanism. *Signal Transduct Target Ther* (2020) 1:25. doi: 10.1038/s41392-020-0118-x

105. Turajlic S, Swanton C. Metastasis as an evolutionary process. *Science (New York N Y)* (2016) 6282:169–75. doi: 10.1126/science.aaf2784

106. Nan X, Wang J, Liu HN, Wong STC, Zhao H. Epithelial-mesenchymal plasticity in organotropism metastasis and tumor immune escape. *J Clin Med* (2019) 5:747. doi: 10.3390/jcm8050747

107. Popeda M, Stokowy T, Bednarz-Knoll N, Jurek A, Niemira M, Bielska A, et al. NF-kappa b signaling-related signatures are connected with the mesenchymal phenotype of circulating tumor cells in non-metastatic breast cancer. *Cancers (Basel)* (2019) 12:1961. doi: 10.3390/cancers11121961

108. Yao H, Han B, Zhang Y, Shen L, Huang R. Non-coding RNAs and autophagy. *Adv Exp Med Biol* (2019) 1206:199–220. doi: 10.1007/978-981-15-0602-4_10

109. Onorati AV, Dyczynski M, Ojha R, Amaravadi RK. Targeting autophagy in cancer. *Cancer* (2018) 16:3307–18. doi: 10.1002/cncr.31335

110. Kim KH, Lee MS. Autophagy–a key player in cellular and body metabolism. *Nat Rev Endocrinol* (2014) 6:322–37. doi: 10.1038/nrendo.2014.35

111. Parzych KR, Klionsky DJ. An overview of autophagy: morphology, mechanism, and regulation. *Antioxid Redox Signal* (2014) 3:460–73. doi: 10.1089/ars.2013.5371

112. Morris BJ. Human renin protein and gene structures: present and future targets for renin blockade in treatment of hypertension. *J Hypertens Suppl* (1989) 2: S9–14. doi: 10.1097/00004872-198904002-00003

113. Frankel LB, Lubas M, Lund AH. Emerging connections between RNA and autophagy. *Autophagy* (2017) 1:3–23. doi: 10.1080/15548627.2016.1222992

114. Zhang J, Wang P, Wan L, Xu S, Pang D. The emergence of noncoding RNAs as heracles in autophagy. *Autophagy* (2017) 6:1004–24. doi: 10.1080/15548627.2017.1312041

115. Yang L, Wang H, Shen Q, Feng L, Jin H. Long non-coding RNAs involved in autophagy regulation. *Cell Death Dis* (2017) 10:e3073. doi: 10.1038/cddis.2017.464

116. Zou Z, Yuan Z, Zhang Q, Long Z, Chen J, Tang Z, et al. Aurora kinase a inhibition-induced autophagy triggers drug resistance in breast cancer cells. *Autophagy* (2012) 12:1798–810. doi: 10.4161/auto.22110

117. Wang K, Ma L, Tang J, Yu Q, Shen Y, Wei Y, et al. LncRNA00518 promotes cell proliferation through regulating miR-101 in bladder cancer. *J Cancer* (2020) 6:1468–77. doi: 10.7150/jca.35710

118. Vitamin e supplementation of premature infants. *Nutr Rev* (1988) 3:122–3. doi: 10.111/j.1753-4887.1988.tb05397.x

119. Yin H, Wang X, Zhang X, Wang Y, Zeng Y, Xiong Y, et al. Integrated analysis of long noncoding RNA associated-competing endogenous RNA as prognostic biomarkers in clear cell renal carcinoma. *Cancer Sci* (2018) 10:3336–49. doi: 10.1111/cas.13778

120. Wang QF, Wang QL, Cao MB. LncRNA PITPNA-AS1 as a potential diagnostic marker and therapeutic target promotes hepatocellular carcinoma

progression via modulating miR-448/ROCK1 axis. *Front Med (Lausanne)* (2021) 8:668787. doi: 10.3389/fmed.2021.668787

121. Simion V, Zhou H, Haemmig S, Pierce JB, Mendes S, Tesmenitsky Y, et al. A macrophage-specific lncRNA regulates apoptosis and atherosclerosis by tethering HuR in the nucleus. *Nat Commun* (2020) 1:6135. doi: 10.1038/s41467-020-19664-2

122. Fichtner AS, Karunakaran MM, Gu S, Boughter CT, Borowska MT, Starick L, et al. Alpaca (Vicugna pacos), the first nonprimate species with a phosphoantigen-reactive Vγ9Vδ2 T cell subset. *Proc Natl Acad Sci U S A* (2020) 12:6697–707. doi: 10.1073/pnas.1909474117

123. Yao ZT, Yang YM, Sun MM, He Y, Liao L, Chen KS, et al. New insights into the interplay between long non-coding RNAs and RNA-binding proteins in cancer. *Cancer Commun (Lond Engl)* (2022) 2:117–40. doi: 10.1002/cac2.12254

124. Toden S, Goel A. Non-coding RNAs as liquid biopsy biomarkers in cancer. *Br J Cancer* (2022) 3:351–60. doi: 10.1038/s41416-021-01672-8

Frontiers in Oncology

Advances knowledge of carcinogenesis and tumor progression for better treatment and management

The third most-cited oncology journal, which highlights research in carcinogenesis and tumor progression, bridging the gap between basic research and applications to imrpove diagnosis, therapeutics and management strategies.

Discover the latest Research Topics

See more →

Frontiers

Avenue du Tribunal-Fédéral 34
1005 Lausanne, Switzerland
frontiersin.org

Contact us

+41 (0)21 510 17 00
frontiersin.org/about/contact